

A.M. Kooijman
L.H. Cammeraat
A.C. Seijmonsbergen *Editors*

The Luxembourg Gutland Landscape

The Luxembourg Gutland Landscape

A.M. Kooijman · L.H. Cammeraat
A.C. Seijmonsbergen
Editors

The Luxembourg Gutland Landscape

 Springer

Editors

A.M. Kooijman
Institute of Biodiversity and Ecosystem
Dynamics (IBED)
University of Amsterdam
Amsterdam
The Netherlands

A.C. Seijmonsbergen
Institute of Biodiversity and Ecosystem
Dynamics (IBED)
University of Amsterdam
Amsterdam
The Netherlands

L.H. Cammeraat
Institute of Biodiversity and Ecosystem
Dynamics (IBED)
University of Amsterdam
Amsterdam
The Netherlands

ISBN 978-3-319-65541-3 ISBN 978-3-319-65543-7 (eBook)
<https://doi.org/10.1007/978-3-319-65543-7>

Library of Congress Control Number: 2017949115

© Springer International Publishing AG 2018

This work is subject to copyright. All rights are reserved by the Publisher, whether the whole or part of the material is concerned, specifically the rights of translation, reprinting, reuse of illustrations, recitation, broadcasting, reproduction on microfilms or in any other physical way, and transmission or information storage and retrieval, electronic adaptation, computer software, or by similar or dissimilar methodology now known or hereafter developed.

The use of general descriptive names, registered names, trademarks, service marks, etc. in this publication does not imply, even in the absence of a specific statement, that such names are exempt from the relevant protective laws and regulations and therefore free for general use.

The publisher, the authors and the editors are safe to assume that the advice and information in this book are believed to be true and accurate at the date of publication. Neither the publisher nor the authors or the editors give a warranty, express or implied, with respect to the material contained herein or for any errors or omissions that may have been made. The publisher remains neutral with regard to jurisdictional claims in published maps and institutional affiliations.

Printed on acid-free paper

This Springer imprint is published by Springer Nature
The registered company is Springer International Publishing AG
The registered company address is: Gewerbestrasse 11, 6330 Cham, Switzerland

Preface

This book is a tribute to the Luxembourg Cuesta landscape that inspired so many researchers. It integrates more than 50 years of study on the long and short-term evolution and functioning of the cuesta landscape in central Luxembourg. A landscape that reveals large contrasts in lithology, geomorphology, soils and forest vegetation over short distances. An attractive landscape with a high biodiversity and geodiversity that entices many tourists. It is a showcase for education, both students and laymen. By presenting a scientific overview of the knowledge obtained over these past decades we hope to attract more scientific attention for the area and to inspire students and scientists to explore new pathways of research.

The area of study is part of the north-eastern margin of the Paris Basin, a characteristic cuesta landscape. A beautiful landscape with wide, slightly undulating plateaus under grassland and agriculture, deep river incisions, forested rims and steep sandstone cliffs. In the lower parts of the cuesta, marly strata give rise to more gentle slopes, a rolling landscape with numerous small brooks and mixed land-use.

The area did not only attract the attention of researchers from Luxembourg, such as geologists, soil scientists and hydrologists. It also has been a key study area for physical geographers and landscape ecologists of the University of Amsterdam for more than five decades. The geological diversity and tectonic history of the area provide excellent opportunities to study the interactions between landscape development, hydrology, geomorphological processes, soil formation and forest vegetation at multiple scales. Numerous scientific papers, Ph.D. dissertations and students reports have been published that highlight the cuesta landscape. Over the years, the focus has shifted from the use of traditional field methods and descriptive techniques, towards more quantitative approaches, including field monitoring and digital mapping. Modern research and information techniques, such as remote sensing data in combination with computer modelling, field observations and laboratory measurements, make it possible to maintain high standards in educational and research programs.

The book is organized around three themes that are closely interrelated. The first theme (Chapters 1–5) addresses the *long-term geological, geomorphological and hydrological development* of the Luxembourg cuesta landscape, as well as the scientific historical perspective of research in this area. The second theme (Chapters 6–8) focusses on *the geo-ecological system functioning of the landscape*, including soil development, nutrient

availability and forest ecology. The third theme (Chaps 9 and 10) illustrates the *biological and physico-chemical control of natural erosion processes*, including the impact of fauna and vegetation and the substrate on soil erosion processes. Chapter 11 is a showcase of how *obtained knowledge can be applied*. Chapter 12 presents *impressions of students* whom have been working in the area. In several chapters student work is integrated in the scientific results.

Finally, we would like to thank the forestry departments and local communities for their permission and support and all those that in one way or another contributed to this book.

Amsterdam, The Netherlands

A.M. Kooijman
L.H. Cammeraat
A.C. Seijmonsbergen

Contents

1	Geological and Geomorphological Evolution of Luxembourg and Its Cuesta Landscape	1
	B. Kausch and R. Maquil	
2	Historical Perspective of Dutch Geomorphological Research in the Gutland Region in Luxembourg	21
	P.D. Jungerius	
3	Palynological Reconstruction of the Effects of Holocene Climatic Oscillations and Agricultural History on Soils and Landforms in Luxembourg	39
	J.M. van Mourik and R.T. Slotboom	
4	Contrasting Hydrologic Response in the Cuesta Landscapes of Luxembourg	73
	L. Pfister, C. Hissler, J.F. Iffly, M. Coenders, R. Teuling, A. Arens and L.H. Cammeraat	
5	Hybrid Geomorphological Mapping in the Cuesta Landscape of Luxembourg	89
	A.C. Seijmonsbergen and L.W.S. de Graaff	
6	Soils of the Luxembourg Lias Cuesta Landscape	107
	L.H. Cammeraat, J. Sevink, C. Hissler, J. Juilleret, B. Jansen, A.M. Kooijman, L. Pfister and J.M. Verstraten	
7	Alternative Strategies for Nutrient Cycling in Acidic and Calcareous Forests in the Luxembourg Cuesta Landscape	131
	A.M. Kooijman, K. Kalbitz and A. Smit	
8	Relationships Between Forest Vegetation, Parent Material and Soil Development in the Luxembourg Cuesta Landscape	153
	A.M. Kooijman and A. Smit	
9	Steinmergelkeuper Forest Soils in Luxembourg: Properties and Pedogenesis of Soils with an Abrupt Textural Contrast	177
	L.H. Cammeraat, T.M.W. van den Broek and J.M. Verstraten	

-
- 10 Soil Animals and Litter Quality as Key Factors to Plant Species Richness, Topsoil Development and Hydrology in Forests on Decalcified Marl** 231
A.M. Kooijman, L.H. Cammeraat, C. Cusell, H. Weiler
and A.C. Imeson
- 11 Applications of Physiotope Mapping in the Cuesta Landscape of Luxembourg** 253
A.C. Seijmonsbergen, L.H. Cammeraat and A.M. Kooijman
- 12 Twenty-Five Years of Life Lessons.** 269
Annemieke Smit, Luuk Dorren, Hans van Noord, Josja Veraart,
Casper Cusell and Henk Pieter Sterk

About the Editors

A.M. Kooijman received her Ph.D. in Biology in 1993 at the University of Utrecht on changes in nutrient availability and vegetation in rich fens due to environmental stress. She has been working at the University of Amsterdam as a landscape ecologist, currently at the Ecosystem and Landscape Dynamics Department of the Institute for Biodiversity and Ecosystem Dynamics at the University of Amsterdam, The Netherlands. She works on interactions between soils and biota in ecosystems with gradients in geology and pH, such as semi-terrestrial wetlands, coastal dune grasslands and Luxembourg forests, with particular focus on ecosystem nutrition. For the Luxembourg forests, she has published a number of studies about the impact of geology and litter quality on ecosystem functioning. She has been teaching (field) courses on soils and landscape ecology in various ecosystems for more than 25 years.

L.H. Cammeraat received his Ph.D. in Environmental Sciences in 1992 at the University of Amsterdam on work in hydro-geomorphological processes in a forested marl catchment in Luxembourg. He worked next as a postdoc and PI on EU- and Dutch-funded projects related to Mediterranean desertification and degradation remediation. Currently he is appointed as Associate professor in geomorphology and land degradation at the Ecosystem and Landscape Dynamics Department of the Institute for Biodiversity and Ecosystem Dynamics at the University of Amsterdam, The Netherlands. He works on soil-geomorphology-vegetation interactions in both humid and dryland areas, as well as on degradation remediation strategies using ecoengineering approaches, and on the fate of carbon in soils. He has been teaching (field) courses on geomorphology, soils, landscape ecology, and hydrology for more than 20 years.

A.C. Seijmonsbergen was born in 1961 in Amsterdam (The Netherlands) and studied Physical Geography at the University of Amsterdam. During his Master- and Ph.D. research he developed methods for the evaluation of natural hazards based on detailed geomorphological mapping in Austria. He has over 30 years of experience in teaching field courses, remote sensing and GIS tools and techniques.

Currently his research in the Theoretical Computational Ecology group at the University of Amsterdam is focusing on the functioning of Geo-Ecosystems by analyzing the 3D structure of both the landscape and the vegetation cover using air-borne and terrestrial LiDAR-based high resolution elevation data as well as geodiversity mapping at multiple scales.

Geological and Geomorphological Evolution of Luxembourg and Its Cuesta Landscape

1

B. Kausch and R. Maquil

Abstract

Two different regions in Luxembourg are characterized by different substrates and landscapes. In the north, the plateaus with deeply incised valleys of the Eislek have developed in folded Devonian rocks. These rocks constitute the geological basement of the country. In the southern Gutland region, the Devonian basement is covered by a succession of Mesozoic sedimentary formations, gently dipping to the southwest. This succession of sedimentary rocks is expressed by an alternation of hard and soft rocks, which is responsible for the characteristic geomorphology of the cuesta landscape of the Gutland. The hard relief-building rocks are pervious, while the soft rocks of impervious nature form gentle slopes. The latter are of clayey and marly constitution and are sensible to variation in water content. Differential uplift and climatic changes have influenced the landscape development and fluvial incision processes since the Tertiary. The epigenetically developed drainage network has sculptured the present landscape. Generally, slope evolution is largely controlled by soil erosion and mass movements, rock fall in hard rocks and landslides in soft rocks. The intensity of landscape forming processes depends on the local climatic and hydrogeological conditions. Nowadays man's influence is not negligible any more, as expressed by the displacement of soil and rocks, as well as in triggering mass movements and agricultural induced soil erosion. This chapter introduces the general geological evolution of Luxembourg and surroundings, as well as the various geomorphological processes acting during the Tertiary and Quaternary. This will be illustrated by examples from the present landscape, which is the result of the interplay between geology, geomorphology, climate and the relatively recent influence by man.

B. Kausch (✉)
Service Géologique du Luxembourg/Geological
Survey Luxembourg, 23, Rue du Chemin de Fer,
8057 Bertrange, Luxembourg
e-mail: b.kausch@web.de

R. Maquil
Now: 91, Rue Clairefontaine, 9220 Diekirch,
Luxembourg
e-mail: robert.maquil@pt.lu

1.1 Geology and Geomorphology of Luxembourg

1.1.1 Geological Overview

Two distinct geologic-geomorphologic regions dominate the landscape of Luxembourg.

The northern part, the Eislek, is part of the Belgian Ardennes and the Rhenish Massif in Germany (Fig. 1.1). It is built of folded lower Devonian rocks of Pragian (Siegenian) and Emsian age. The marine sediments were

originally deposited in the Devonian seas as weathered material of the Old-Red-continent, a part of which is still exposed in the Stavelot Massif, located just a couple of kilometres north of Luxembourg. Marine sediments with a thickness of several ten thousand metres were successively deposited, lithified and then folded during the Hercynian Orogeny. The Eislek substrate is built of schists, quartzites, sandstones and locally slates. The different proportions of rocks vary locally, schists being the dominant lithology. The central part of the Eislek is formed

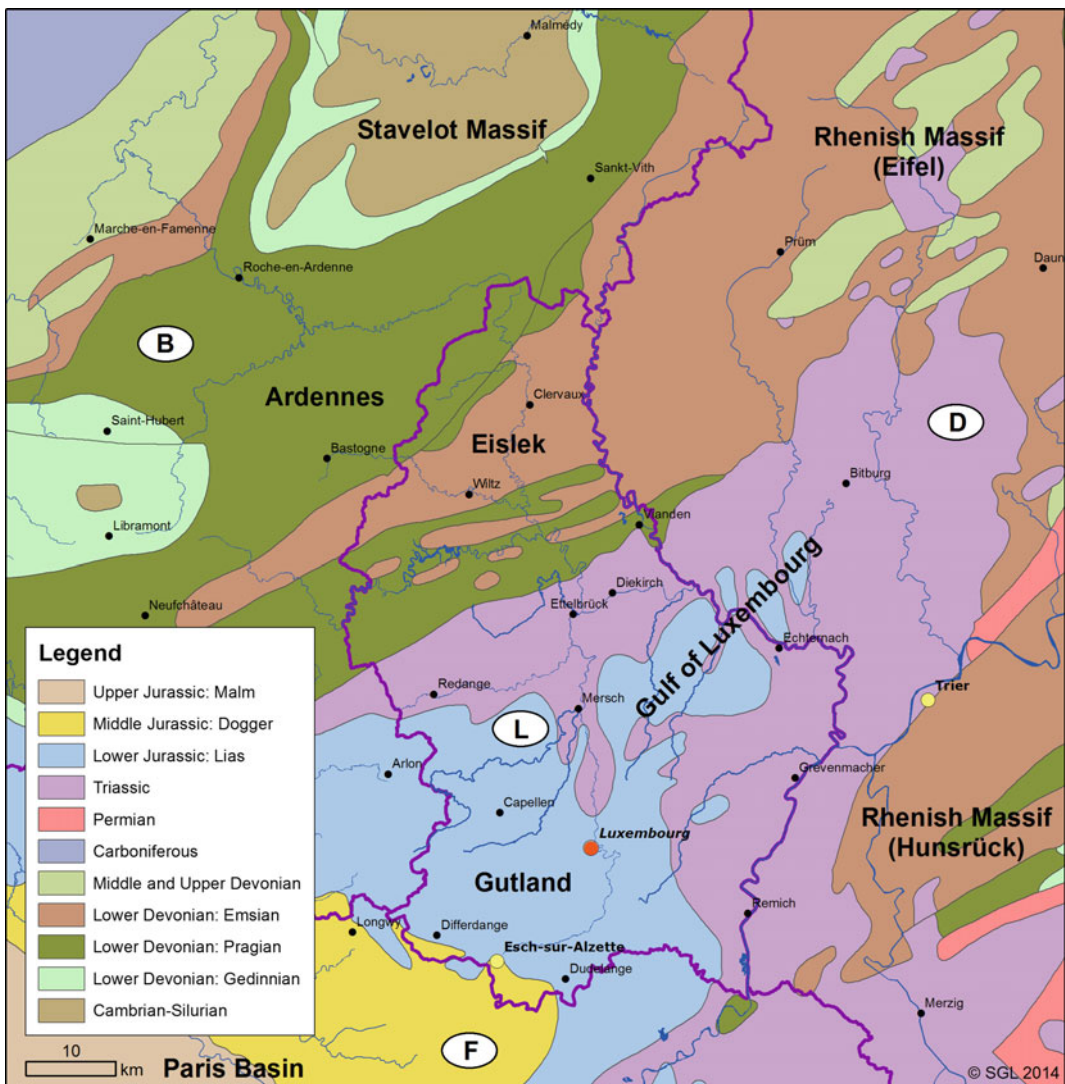


Fig. 1.1 General overview of the regional geology, with geological and geographical subdivisions, © SGL 2014

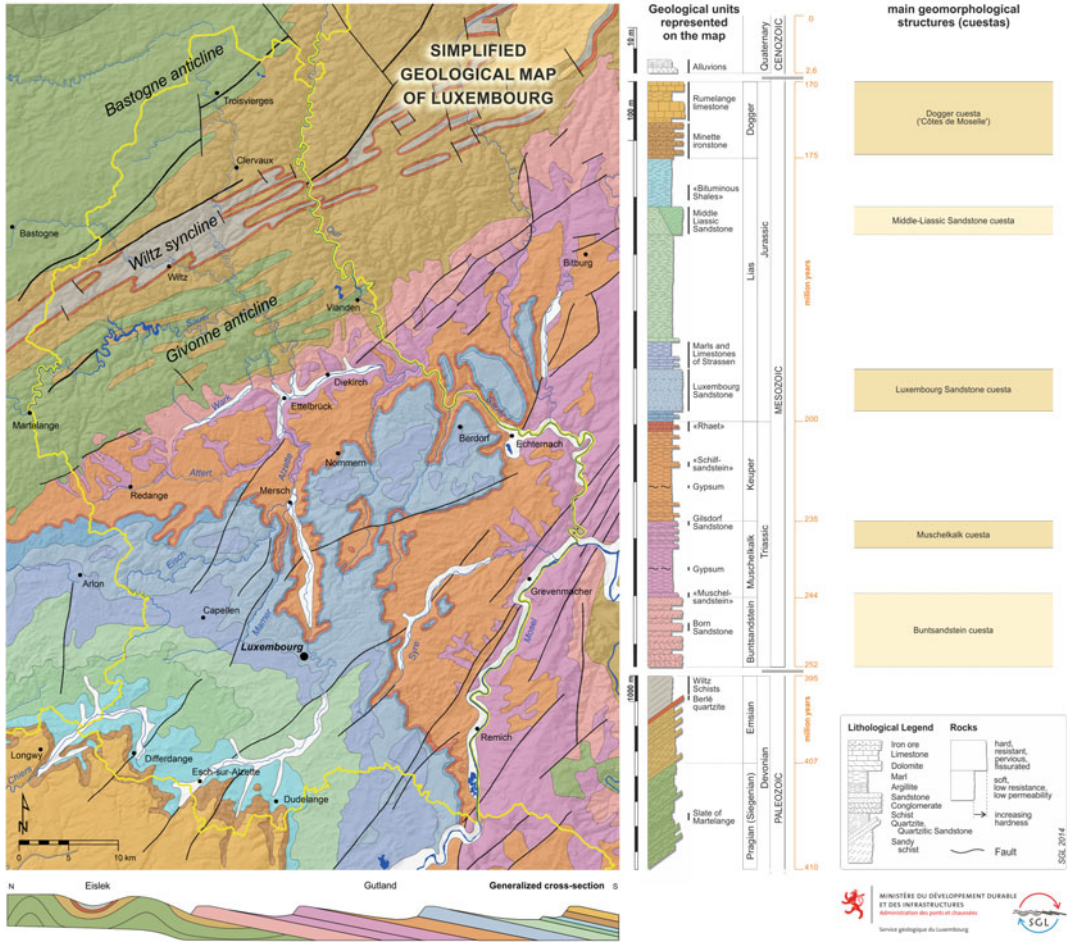


Fig. 1.2 Geological map of Luxembourg, © SGL 2014

by the Wiltz syncline, which is essentially composed of shales, with well-expressed schistosity. The shales are more erodible than the surrounding quartzite dominated rocks and thus form large topographical low-lying areas. To the north and south, the anticlines of Bastogne (N) and Givonne (S) are formed by rocks with a more quartzitic nature (Lucius 1950). Due to intense folding, schistosity is very well developed and oriented parallel to the axial planes of the folds. In the southwestern part of the Eislek, in the Martelange region (Fig. 1.2), more fine grained, clayey, pelitic rocks are present in a slate facies, which have been exploited extensively (Maquil et al. 1984).

By the end of the Perm, the Hercynian massif in this region had been largely eroded, forming the so-called pre-triassic peneplain (Lucius 1950). During the lower Trias, the Buntsandstein seas transgressed over the eroded Hercynian massif and coarse-grained fluvial material was deposited in an arid environment (Mader 1982; Guillocheau et al. 2002), forming a lithological (angular) unconformity. The coastlines of the following and transgressing Mesozoic seas moved progressively to the west, covering the flooded areas with new sediments. The area, forming the Gulf of Luxembourg, belongs to the north-eastern rim of the Paris Basin (Fig. 1.1). These sediments, starting at the Buntsandstein,

dip slowly to the central part of the Basin (Fig. 1.2, cross section). Due to the sedimentation history, the lower strata are not developed beneath the entire basin. This can nicely be seen in Fig. 1.2 west of Redange, in Belgium, where only sediments of Keuper age rest discordantly on Devonian rocks. The Mesozoic sediments are characterized by an alternation of hard rocks of sandy, dolomitic or calcareous nature, and of soft rocks of clayey nature like (clayey) marls and claystones. Due to new uplift processes, probably in relation with alpine orogeny by lithospheric buckling as well as a mantle plume beneath the Eifel (Demoulin 2005), the Hercynian basement and its Mesozoic cover was incorporated in the continental environment and erosion processes started again. In the Eislek, the Mesozoic sediments have been eroded since. In today's Gutland, one observes in its most southern part a maximum thickness of 1000 m (Fig. 1.2).

The lithological log in Fig. 1.2 shows the succession of sediments, the hard-soft property is emphasized. The main mineralogical components of the rocks are quartz, clay minerals and carbonates. Important accessory minerals are gypsum and pyrite. All the rocks are of the consolidated type. The hard ones are resistant to weathering, fractured and pervious to water. The soft ones are much less resistant to weathering, not very fractured and quite impervious to water. Soft rocks like marls and claystones consist of different proportions of clay minerals and carbonates. The latter ones are also soluble in water and dissolution leaves residual clays. Gypsum veins ($\text{CaSO}_4 \cdot 2 \text{H}_2\text{O}$) of variable thickness occur in the marly Trias formations of Muschelkalk and Keuper age. They were largely exploited in underground quarries. Dissolution of gypsum induces higher permeability in the substrate and the sensibility to landsliding is largely increased. Weathering processes form rocks of an unconsolidated type, which can be coarse (sand and gravel) or fine grained, the latter being of clayey nature, cohesive and quite impervious to water. Hard rock formations form steep slopes and are expressed in the landscape as *cuestas*. The soft rocks are sensitive to variations in water content, form shallow slopes and are, in case of extreme

meteorological conditions, very prone to landslides.

At the Mesozoic, due to the disposition of the coast lines, large variations in facies and thickness may occur. Close to the former coast lines, the sediments are often very coarsely grained (sandy and conglomeratic), becoming more and more marly and clayey to the open sea (Lucius 1948). This facies variation is seen on the map of Fig. 1.2 in the Middle-Liassic rocks, the sandstone changing from west to east to a more marly facies.

Jurassic and Triassic rocks differ in the type of carbonates of their marls. The carbonate of the Jurassic rocks is calcite (CaCO_3), while the carbonate building the Triassic rocks is dolomite ($\text{CaMg}(\text{CO}_3)_2$). The solubility of the two carbonates is very different. The solubility of calcite is much larger than that of dolomite, which induces different weathering rates. On marly (dolomitic) sediments of Keuper age, the thickness of the regolith is often just a couple of centimetres, while it might be several metres thick on Jurassic (calcitic) marls, due to different weathering and erosion rates. The dissolution of carbonates and gypsum gives the groundwater a very typical hydrochemical signature. The Ca/Mg-ratio allows to distinguish groundwater from Triassic (dolomitic) and Jurassic (calcareous) rocks, while high concentrations of sulphates (SO_4^{2-}) characterize groundwater from substrates rich in gypsum.

The tectonic structure of the Gutland is characterized by a NE-SW oriented succession of undulations, building the Gulf of Luxembourg (Figs. 1.1 and 1.2) submerging from the Eifel region to the centre of the Paris Basin. The local dip of the strata towards the axis of the undulations, combined with the presence of faults, determine the topographical features and the main direction of groundwater flow. Groundwater emerges as springs at the surface of the underlying impervious rocks, such as marls. The discharge rate depends essentially on the thickness of the strata as well as the type and size of the catchment area. A simple calculation allows to evaluate discharge rates for the Luxembourg Sandstone (outcrop area: about 300 km^2). By

admitting an infiltration rate of 25% of a mean annual rainfall of 800 mm, one square kilometre produces about 550 m³ per day.

1.1.2 Geomorphological Overview

The Eislek and Gutland can be discriminated on Fig. 1.3, clearly showing the correspondence of the geological structure (Figs. 1.1 and 1.2) with the general geomorphology of the landscape.

The rivers of Luxembourg belong with the Alzette, Sauer and Mosel to the catchment of the river Rhine. The Chiers in the southwest, as well as a small river in the north, flow to the west and are part of the drainage network of the river Meuse. The relief of Luxembourg spans heights from 129 m at the confluence of Sauer and Mosel to 559 m at Buerglplatz north-east of Troisvierges (Fig. 1.2).

The Eislek is formed by broad plateaus at about 500 m altitude dipping gently to the south and by deeply incised V-shaped valleys. In the north-western Eislek, the plateaus at higher altitudes are covered by a much thicker weathering mantle than in the south, as these surfaces are believed to correspond to one of the older erosion surfaces (Lucius 1950; Demoulin 1995). In the Wiltz syncline, heights of 350–450 m dominate, which correspond to a younger erosion surface (Lucius 1950; Demoulin 1995). Locally, as in the region of Vian-den, in front and below today's outcrop of the Buntsandstein rocks at the border of Gutland and Eislek (Fig. 1.3), one might observe residues of the oldest pre-Triassic weathering mantle.

Due to the domination of surface or near surface runoff on the largely impervious substrate of the Eislek, the plateaus were dissected by a dense network of small streams (Fig. 1.4a), following often hercynian structural directions (NE-SW). The valley heads mostly are trough-shaped valleys, whereas the slopes at the lower sections of the rivers are V-shaped and have frequently inclinations of more than 70° (Désiré-Marchand 1985). The valleys often have an asymmetrical cross section with steep cliffs at one side, which are subject to undercutting and denudation by rock fall.

In the Gutland, the slightly sloping alternation of resistant hard and non-resistant soft sedimentary strata, with differences in weathering and soil erosion rates (Jungerius 1980; see also Chap. 2), led to the formation of three important cuestas (Figs. 1.2 and 1.3). They developed in different stratigraphic units, running from north to south. The Muschelkalk cuesta follows the geological outcrop of the Muschelkalk dolomites to the east, and passes into Germany, surrounding the Gulf of Luxembourg. The cuesta of the Luxembourg Sandstone is the most important one, the sandstone having generally a thickness varying from 60 to 80 m. The topography is influenced by the large synclinal structure of the Gutland sediments, as well as the dipping and local undulations of the Gulf of Luxembourg strata. Secondary undulations induce the formation of numerous buttes in front of the cuesta (Fig. 1.4b), separated from the cuesta by the regressive erosion of smaller rivers. The Dogger cuesta (Fig. 1.3), facing north-east, is formed in the youngest Mesozoic rocks of Luxembourg, the iron ore Minette and its overlying limestones. It passes to France and there it forms the north-south-oriented Côtes de Moselle. Also here, several buttes are developed. Two smaller escarpments are observed: the Buntsandstein cuesta is developed in the north-east. To the west, it merges with the Muschelkalk one, the facies of both units becoming mostly sandy and conglomeratic and grouped as 'Trias in border facies'. The Middle-Liassic Sandstone cuesta is developed only in the southwest of Luxembourg, in the more sandy facies of the unit. Numerous secondary steps may be observed locally in thicker strata of more weathering and erosion resistant harder rocks, their importance varying with the thickness of the strata.

The top of the main escarpments culminates at altitudes of about 400 m, independent of their stratigraphic position. The lower lying, undulating and less resistant marls associated with the escarpments lie at about 300 m (Fig. 1.5).

The density of the drainage network depends on the permeability of the substrate. It is less dense but much more accentuated on permeable rocks than on impervious ones, where surface

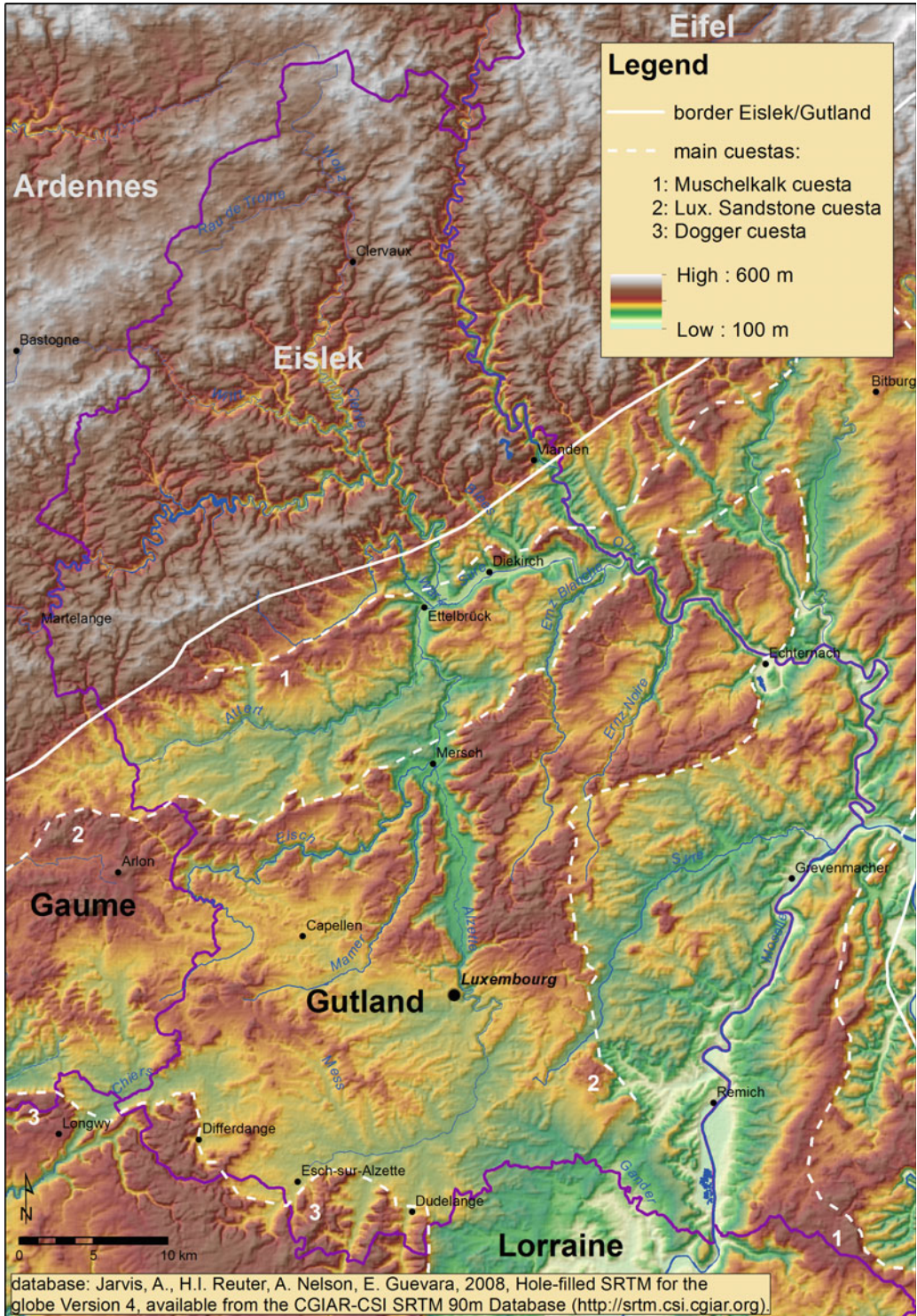


Fig. 1.3 Relief map of the Luxembourg region with its geographical subdivisions and main cuestas, © SGL 2014

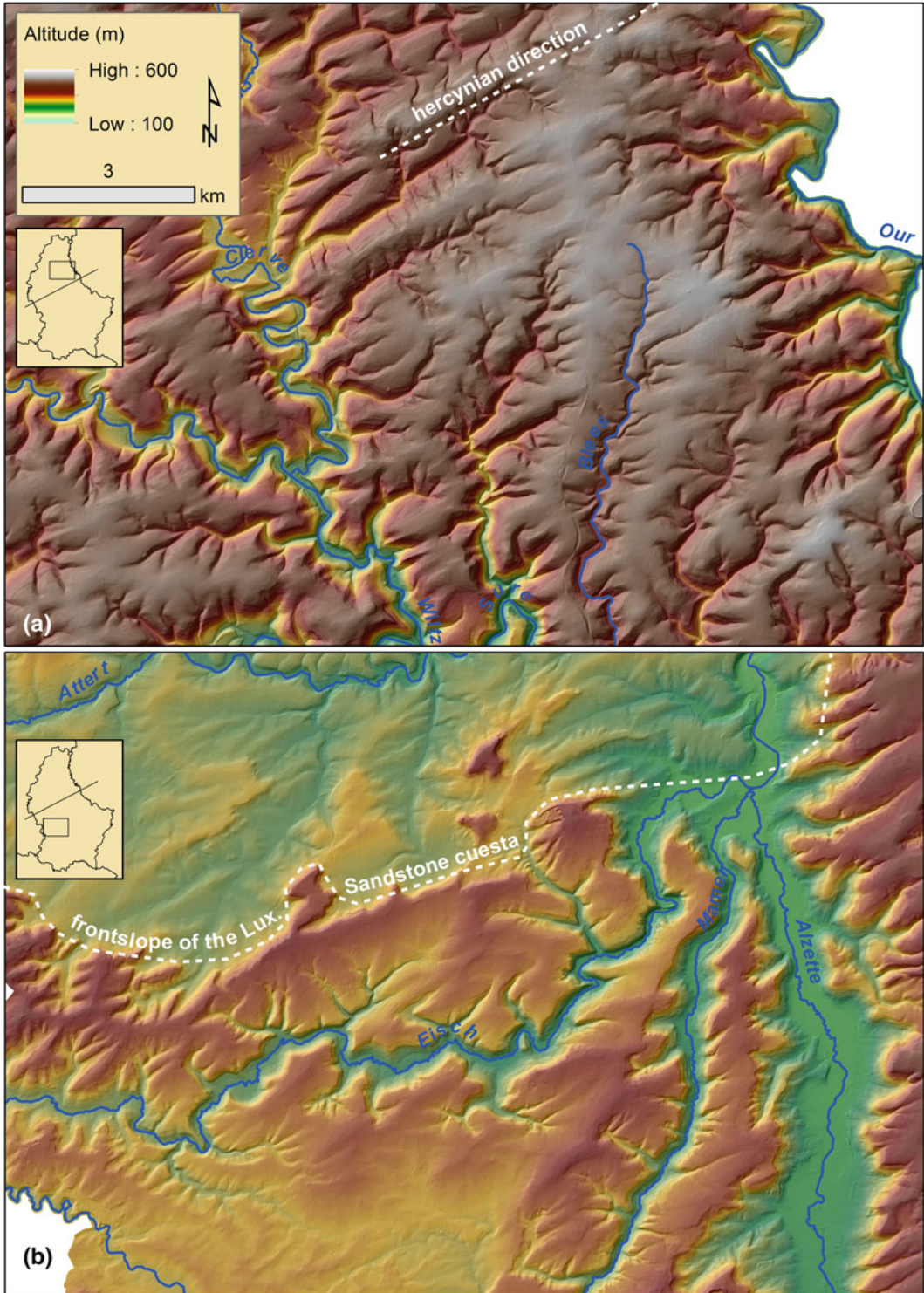


Fig. 1.4 Typical details of the two contrasting landscapes in Luxembourg (shaded DEM, © ATC 2014). **a** The plateaus of the Eislek, dissected by deeply incised rivers, with preferred hercynian (NE–SW) directions of

the small streams. **b** The Gutland with the cuesta of the Luxembourg Sandstone, with the deeply incised main rivers and the dense drainage network of the small streams on the marls e.g. north of the cuesta, flowing to the north



Fig. 1.5 The stepped cuesta landscape at the border of Luxembourg and Germany, viewed from the foot of the Luxembourg Sandstone cuesta to the east beyond the Sauer valley on the Muschelkalk cuesta (photo BK)

runoff dominates (Fig. 1.4b). The drainage pattern of the Gutland is, however, independent of the geological structures. Particular observations support this: the Alzette flows to the north and cuts through the Lias plateau, the Sauer flows to the south-east to Echternach. It dissects the Lias plateau into the Mullerthal region in Luxembourg and the Ferschweiler Plateau in Germany. In the Ferschweiler Plateau, developed in the northern outcrop of the south dipping Sandstone, the dissection is largely completed. The south flowing Prüm river has, as have the other rivers, created nicely developed escarpments on both sides of the valleys. The Eisch river flows from the region of Arlon to the east and flows on the back of the cuesta, the Attert flows quite parallel, but in front of the cuesta (Figs. 1.2 and 1.4b). The Wark River west of Ettelbrück shows an even more complicated pattern with an incursion into Devonian substrate.

1.2 General Landscape Evolution

Landscape evolution started at the moment, when the freshly formed, compacted and lithified Mesozoic sediments emerged from the sea and were integrated in the landmass. Weathering and geomorphological processes have been active since. It is commonly admitted that the depositional area of the youngest strata of Dogger age, nowadays limited to the southern border of Luxembourg, may have covered large parts of the Gutland (Siehl and Thein 1989). There are

not many relicts of ancient landscape evolution from the Mesozoic. They start to become more abundant from Tertiary to Quaternary times. The compiled Fig. 1.6 shows the time scale, in which landscape evolution, tectonic movements, eustatic sea level changes and climatic change took place.

The Palaeogene was characterized by a tropical warm-humid climate, inducing a deep chemical weathering of the bedrock. The alteration is essentially characterized by dissolution of carbonates and oxidation of iron minerals, in function of the rock types and their mineralogical composition. This produced several tens of metres of regolith with typical red and brown colours forming a planation surface. Thick deposits of altered material in the north-west and some relicts on other plateaus of the Eislek are interpreted as remnants of this alteration. In the Gutland, only relicts might be observed on top of the erosional surfaces of the cuesta plateaus. In the late Eocene, an up to 200 m deep incised drainage network developed on the new land surface in the Eifel, flowing to the north and triggered by tectonic uplift, forming the Buntsandstein cuesta in this region. In the later Eislek and Gutland, the general direction of surface water flow was probably still to the Paris Basin (Löhnertz 1994; Löhnertz et al. 2011).

During Eocene and Oligocene times, the Eifel valleys refilled partially by ingressions due to eustatic sea level rises, forming a flat relief of less than 200 m differences in altitude, known as the great valley filling (Louis 1953; Löhnertz 2003).

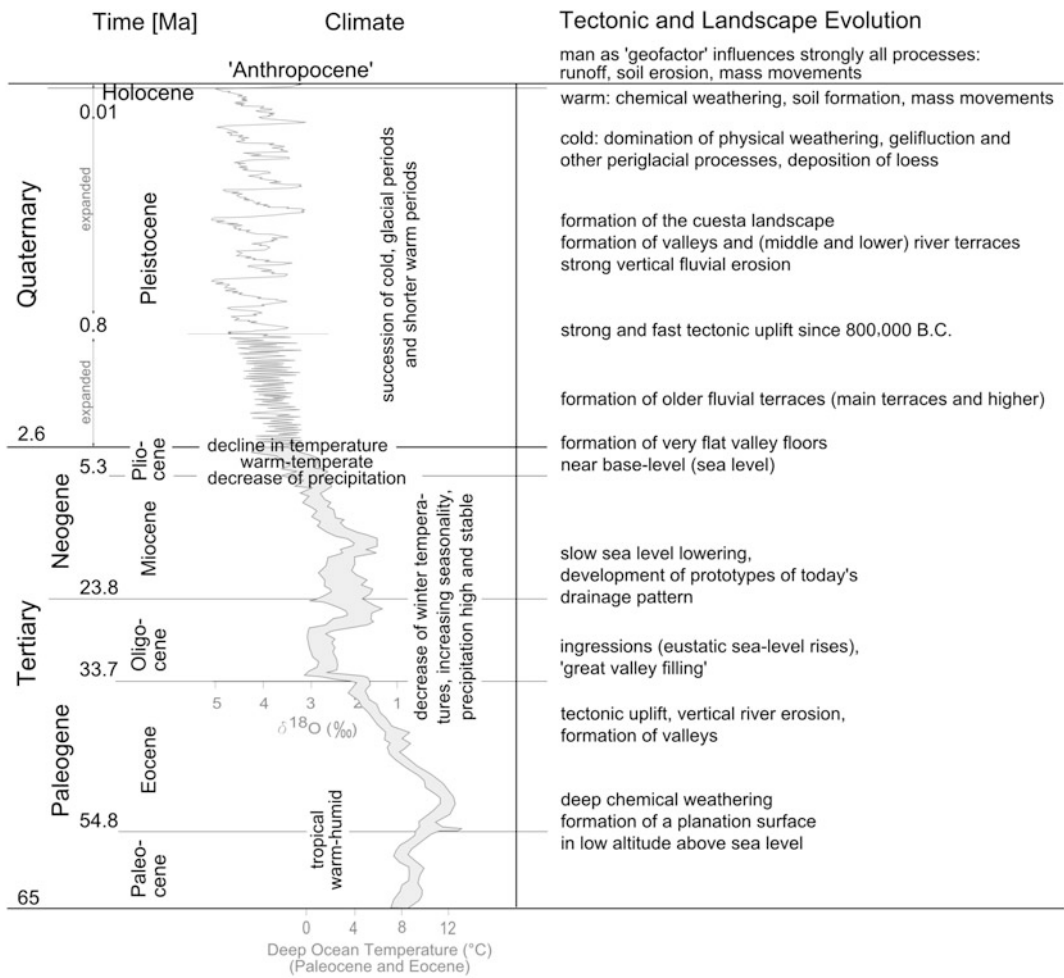


Fig. 1.6 Tertiary and Quaternary evolution of climate, tectonic and landscape (climate modified according to Jansen et al. (2007) (Fig. 6.1), Lisiecki and Raymo

(2005), Moosbrugger et al. (2005), tectonic and landscape evolution according to Löhnertz (1994, 2003), Löhnertz et al. (2011), time: STDKe 2012) (compilation BK)

In a slightly different geological setting, Le Roux and Harmand (2014) describe a polygenetic infra-cretaceous surface in the eastern Paris Basin, from which today’s landscape developed. As a consequence of sea level lowering during the late Oligocene and Neogene, the predecessor of the present-day drainage system incised epigenetically and independent from the nature and structure of the underlying basement, partially in the old river beds. At the beginning, the cuestas were not yet exposed respectively buried under Tertiary sediments. According to Löhnertz (2003) and Löhnertz et al. (2011), the slow

lowering of the base level led to the development of vast valley floors in different altitudes. These are marked by relicts of gravel deposits, currently located at high topographical terrain positions.

The first Luxembourg river system, evolved in the central part of the Luxembourg Gulf area, may have been less accentuated, due to the proximity to the water divide, and a greater distance to the base level in the central Paris Basin. A general cooling of the climate took place since the mid-Eocene. This became more pronounced at the end of Pliocene (Moosbrugger et al. 2005), followed in the Pleistocene by a succession of

cold, glacial periods and shorter warmer periods, and leading to a warm climate in the Holocene. An abrupt change in evolution took place in the Pleistocene, about 800,000 years ago, with a strong and fast tectonic uplift (Meyer and Stets 1998). This uplift was caused by an active mantle plume under the Eifel region (Garcia-Castellanos et al. 2000; van Balen et al. 2000), and induced an accelerated vertical fluvial erosion and formation of deeper and narrower valleys in both the Eislek and the cuesta landscape of the Gutland (Löhnertz et al. 2011). Differential uplift processes of the Eislek and Gutland (Lucius 1948) accelerated the river incision and sculptured the present relief. At that time, the different resistance of rocks to weathering became important. Physical weathering and mass transport were active on slopes under periglacial cold conditions, while under temperate conditions chemical weathering and soil formation were predominant. Newly formed regolith was removed, the landscape evolved, locally strongly influenced by groundwater flow, determined by the geological structure and lithological properties.

Today's position of the main escarpments developed progressively on the boundary of two different rock types, the more resistant hard one like sandstone or dolomite formations and the less resistant soft marls (Figs. 1.2 and 1.3). There is consensus that the position of the main cuesta escarpments has moved slightly since their formation, as described by Busche et al. (2005) and Tricart (in Liedtke et al. 2010). Jungerius et al. (1970, 1982) showed that the surface lowering of the Steinmergelkeuper landscapes was about 50 cm during the Holocene if compared to the top of the Luxembourg sandstone plateau, and about 100 m maximum for the whole of the Quaternary (see also Chap. 2). Rivers cut in function of the nature of the substrate, and also in relation with the tectonic setting and the time available for development. One observes narrow valleys in resistant rocks, while the valleys are wider in marly strata. A nice example is seen in Hesperange south of Luxembourg city (Figs. 1.2 and 1.3), where an important fault, even seen on satellite images, separates a narrow-incised

valley less than 150 m wide and 40 m deep in the Luxembourg Sandstone (N) from an almost 1 km wide shallow valley in the Liassic marls (S).

Holocene landscape evolution can also be derived from palynological reconstruction (see also Chap. 3). This showed that, before the Subatlantic, denudation and fluvial processes were in balance. However, this balance was disturbed after the arrival of man, as evidenced by colluvial slope deposits and alluvial beds in first order catchments.

Geomorphological relicts of the Quaternary landscape evolution are abundant in the actual landscape. Section 1.3 shows several regional examples, differentiated by processes and forms.

1.3 Geomorphological Processes and Landforms

1.3.1 Introduction

The principal geomorphological processes are dominated by fluvial erosion and mass movements. The intensity of the geomorphological processes varied during the Quaternary, largely in relation to cold glacial and relatively warm interglacial conditions, and more recently by human impact (Fig. 1.6).

During glacial periods, the region was affected by periglacial conditions and permafrost. Rocks were fractured due to frost weathering by the freezing of water in cracks and pores, and subsequently disintegrated into fragments of different sizes. Mechanical weathering and mass movements reworked the produced regolith. Gelifluction and solifluction or faster mass movements transported hillslope material downhill. The typical coarse-grained debris deposits with large blocks occurring along major escarpments and valley slopes are thought to be relicts of this periglacial degradation. Weathered material was transported to the valley bottoms, where it accumulated in the floodplain because of the reduced discharge rate of the rivers. Tectonic uplift and incision of the rivers, following increase of discharge during climatic transition

phases, deepened the valleys and left behind fluvial terraces in now higher topographical positions. Winds in the cold and dry pleniglacial climate transported fine-grained particles, which were deposited locally as loess.

While physical weathering was most intensive during the cold phases of the Pleistocene, the chemical weathering was more dominant in the warmer and wetter interglacial periods such as the Holocene. At that time, dissolution of carbonates and sulphates played an important role in the Gutland, by transforming marly substrates to a clayey regolith. Oxidation of iron and manganese minerals changed the initially grey and bluish colours to brownish. Carbonates in the limestones, dolomites and marls were dissolved by infiltrated rainwater, which subsequently was also enriched in CO₂ by root respiration. Many small closed natural depressions called *Mardellen* have developed through this processes on marly Keuper and Lias substrate. However, some of the sinkholes on the Keuper are also man made (see also Chap. 3).

The geomorphologic position and the processes acting on the plateaus or slopes dictate the nature and thickness of the weathering mantle that covers the substrate. On the plateaus, the weathering mantle is still in a large part in situ and reflects the composition of the original substrate. On the slopes, however, the regolith is transported at different speeds as a function of the inclination and moisture conditions and reflects the composition of the upslope available substrates. This regolith material has different geotechnical properties, such as the angle of internal friction and cohesion, as a function of its clay and water content. The disposition of the regolith can be homogenous or formed by a layered mixture of different materials. The speed of regolith movement, through creep or slide processes, is strongly influenced by shallow groundwater circulation within regolith layers of variable permeability.

The regolith observed below escarpments is often formed by an alternation of pervious coarse textured layers and impervious clay lenses. Groundwater emerges from the hard rocks at variable rates, as a function of prevailing

meteorological conditions and infiltration rates. Rainwater infiltrates directly into the ground or might be introduced locally into open joints. In that last case, it is incorporated rapidly into the groundwater, which leads to increased hydraulic pressure in the pervious layers and reduction of shear strength. The triggering occurs in natural conditions during extreme rainfall periods, and/or reduced down-flow in the pervious layers of the regolith, e.g. due to frozen ground.

Taking the period of the late Quaternary and the variation of meteorological and hydrological conditions into account, it is likely that all sensitive slopes have been affected by different types of mass movements. Today, a first localization of regions sensitive to mass movements is done by considering the geological map with respect to lithology, in combination with field observations (Fig. 1.2). Geological areas sensitive to landslides lie on clayey or marly strata below pervious hard rocks. The slope angle has to be generally less than 20° to be stable. Stability then depends largely on the angle of internal friction of the clayey regolith material and on the quantity of water controlled by the dip of the pervious strata towards or away from the slope.

In the floodplains, Holocene alluvium of up to 8 m valley fill occur, e.g. in the Mosel valley. Valley fill accumulated as a result of agricultural induced soil erosion in the watersheds, but nowadays stabilizes the foot of the slopes against mass wasting in large areas. Slopes are generally stable under the prevailing meteorological conditions, but this might change in the future, as extreme meteorological conditions are predicted to occur more frequently.

Currently, but effectively since the beginning of the Anthropocene (Fig. 1.6), man plays an important role as geofactor, when considering the rapid development of settlements and construction of transport roads, and also by the effects of land use change and deforestation. The valleys of the Gutland were preferred settlement areas, and the influence of man on triggering mass movements is growing since its first active presence. Some dormant Pleistocene landslides have already been reactivated in the valleys by deep excavations.

Man's influence on the water cycle is increasing, and affects also fluvial erosion and deposition processes.

1.3.2 Fluvial Processes and Landforms

Fluvial terraces have developed during the Pleistocene along the larger river valleys in Luxembourg. Numerous publications deal with the development of these valleys. Generally, they distinguish between high, main, middle and lower terraces (e.g. de Ridder 1957; Verhoef 1966; Wiese 1969). The latest research by Cordier (2005) distinguishes six middle and two lower terraces in the Mosel valley of France, Luxembourg and Germany. Terraces in catchments of smaller tributary rivers are occasionally observed in temporary road outcrops or construction sites. An example is described by Kausch and Maquil (2006) from the Syre river. Duijsings (1987) described in detail the current processes of a small stream, which is currently incising itself in Keuper marls including fine scale terraces.

In the river systems of the Attert and the Wark, there is evidence for a stream capture east of Redange, which took place during the Pliocene (Verhoef 1966). In the Sauer valley at Echternach (Fig. 1.2), a meander cut-off took place at the end of the last glacial period (Würm-Dryas). This is dated by pollen analysis, leaving the Thull hill as meander core (Coûteaux 1970). The Sauer river shows more abandoned meanders, such as those near Bettendorf (e.g. Fig. 5.6 in Chap. 5). Also, the Alzette river started to connect to the Sauer not earlier than the late Pliocene, as on the older terraces sediments containing Raseneisenerze (Riezebos et al. 1990) are completely absent, whereas they start to appear lower down the slope at the high and main terraces (level T9 of Verhoef 1966). This difference indicates the establishment of a connection of the Alzette to the Sauer, bringing material originating from the southern part of Luxembourg to the north. At the edge of the Luxembourg Sandstone plateaus, numerous

small and actual dry valleys are observed. They are filled with ancient alluvial deposits.

1.3.3 Periglacial Landforms and Processes

Loess deposits are present as isolated relicts of primary aeolian deposits on nearly all plateaus of the Gutland, while they are very rare in the Eislek. Loess is frequently found on slopes as an important constituent in material reworked by gelifluction processes, and the thickness of primary loess is normally only 1–2 metres (Storoni 1980). Some reworked loess deposits have been mostly accumulated on the foot of the slopes.

On the Merscherberg (near Mersch, Fig. 1.2), an exceptionally, up to 12 m thick layer of loess, lying on the level of the middle terrace, is preserved and has been investigated (Maquil and Postolache 2005). At its base, lacustrine sediments show initial deposition on a more or less flat, partially inundated surface. In these layers, one finds locally reworked grains of Raseneisenerz of Tertiary origin (Riezebos et al. 1990). The loess accumulation took place in the shadow of the Lias cuesta, showing that the escarpment had probably at that time its present-day position.

On the slope of the Merscherberg, reworked loess deposits have been exploited in pits (Heuertz 1969; Heyart 1964). Similar sediments were observed in a temporary outcrop in the Mosel valley at Remerschen (south of Remich, Fig. 1.2). There, one finds lenticular shaped layers of weathered marls, included in an up to 4 m thick loess-like regolith. The marls crop out on the upper part of the slope, and its presence within the loess is interpreted as the result of pull-out of marls flakes by solifluction and earth flow. These deposits are nowadays still prone to sliding.

One particular observation can be made on the site of the 'Champignon' north-east of Nommern (Fig. 1.2). The huge sandstone block is wind shaped, and rests as a regular sculpture on a large surface of rounded sandstone, lying below and a



Fig. 1.7 An outcrop of about 2 m in height showing bending of sedimentary layers, interpreted as the result of periglacial creep (near Remerschen, south of Remich, *photo* BK)

couple of hundreds of metres in front of the Lias cuesta.

Evidence of Pleistocene permafrost conditions like creep, earth flow, gelifluction, patterned ground, ice wedges exist. Such evidence, however, is seldom visible on the surface and is usually observed in small, short-lived outcrops, on building sites, in road cuts or in quarries.

Periglacial creep on slopes has often affected and deformed the underlying substrate. On the Mosel slopes near Remerschen, a large outcrop has been opened during a land consolidation project. The slope on Keuper marls was largely affected by ancient and recent slides, and the authors surveyed, planned and attended the numerous drainage and consolidation works. The slope shows undulations and shearing deformation of the marly and dolomitic strata of Keuper age, covered by a thin cover of Holocene regolith (Fig. 1.7). The slight original dipping of the strata has been dragged and folded by gelifluidal movements. Movements of this kind might pull out fragments of the substrate including it into the regolith. This phenomenon has also been described by Cammeraat for Keuper marls in a much flatter landscape in the Stegen-Schrodweiler region (Cammeraat 1992).

A similar process is known from the Devonian shale of the Eislek (Fig. 1.8). The original schistosity is broken up and bent parallel to the slopes by creep (bended outcrop; Hakenschlagen). The thickness of the deformed layer can be one to several metres and depends on the

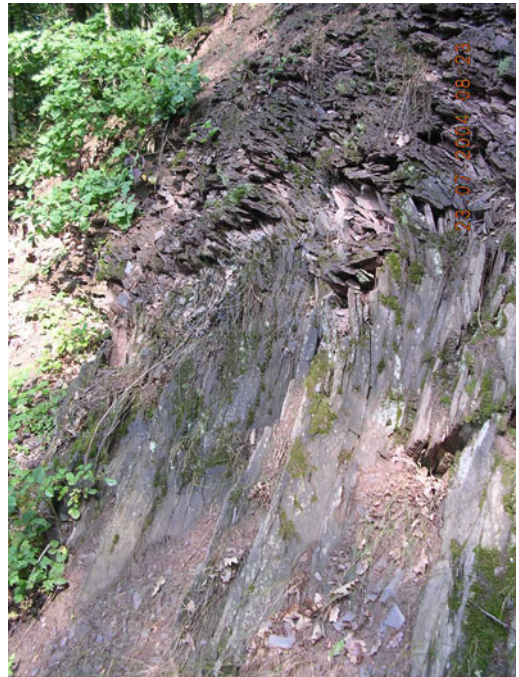


Fig. 1.8 Bending of the schistosity by creep in the Eislek near Michelau (*photo* SGL)

steepness of the slope. This phenomenon is still active today, but at a much slower intensity than by periglacial creep (Wiese 1969). Intense fracturing as a result of frost weathering simultaneously affected the schists, leading to thin and elongated fragments of a few centimetres in size in well sorted sediments, called grèze-lithée (Riezebos 1987). Nice outcrops might be observed in the Our valley south of Vianden



Fig. 1.9 Up to 5 m deep incised active gully in a sandy valley fill near Kopstal (west of Luxembourg city) as a consequence of concentrated discharge of surface water, the front part of the concrete tube itself is eroded (photo BK)

(Fig. 1.2). This material, transported by gelifluccion processes, has extensively filled up small and dry valleys in the Eislek. Some of these deposits were exploited in gravel pits.

The shallow valley heads, observed in the Eislek as well as on the Luxembourg sandstone plateau, are nowadays characterized by the absence of water flow. Introduction of additional surface water in these valleys by man will induce intense gully formation downslope, especially in the sandstone substrate (Fig. 1.9), transporting fine-grained material to the river system.

Cryoturbation structures are observed locally as well. This process was active in places characterized by the alternation of rocks of different permeability and water contents (Fig. 1.10). The observed structure in the outcrop near

Frisange (south of Luxembourg city) can be explained by the local freezing of water in the altered marls, lifting up thin overlying limestone strata.

Fossil ice wedge polygons can be seen on numerous places in the Gutland on aerial images. An example is shown on the hill Thull on the meander core of the Sauer at Echternach, where patterns of darker colours, induced by soil moisture and vegetation, indicate a system of fossil ice wedge polygons in the terrace sediments (Fig. 1.11).

Asymmetric valleys are very common all over the landscape. In the Eislek, the small valleys are often oriented parallel to the geological structures of the Devonian bedrock (Fig. 1.4a). They show asymmetrical cross sections due to structural characteristics of the bedrock, such as the dip of the stratification or orientation of the schistosity, as well as to the topographical exposition. On south to east exposed slopes, melting and freezing was more active under periglacial conditions, inducing more freeze-thaw-induced fracturing and faster transport of the regolith to the valley bottom. Slopes exposed from north to west received less energy from the sun and were more stable (Wiese 1969).

In the Gutland, asymmetric valleys are developed in relation to the structural disposition. The local dip of the strata affects largely water circulation. Groundwater emerges rather on one side of the valley while it infiltrates on the other side. Slopes rich in groundwater, emerging as springs or as diffuse exfiltration, evolve more rapidly than the opposite ones. This might lead on one side to active slope movements, while the other side is relatively stable.

1.3.4 Mass Movement and Hillslope Processes and Landforms

Gravitational mass movements are strongly influenced by the geological structure of the Gutland. Landslides dominate in soft and impermeable clayey rocks, rockfalls in hard and



Fig. 1.10 Cryoturbation structures in a new road cut in the altered Marls and Limestones of Strassen (li3). Three layers of dislocated limestones can be observed. (photo SGL)

permeable rocks, and one process might affect the other one. Several examples of mass movements have been observed and studied by the authors in different geological positions.

Sliding is a particular movement observed in many parts of the cuesta of the Luxembourg Sandstone (Fig. 1.3), e.g. in the region around Berdorf (Fig. 1.2). Fracturing during regional uplift, inducing a pattern of joints, has broken up the sandstone strata in rock monoliths with sections varying from 25 to 400 m² in plan surface, often with an almost rectangular pattern. The Marls of Elvange (li1) and especially the Rhät-claystone (ko2), underlying the Luxembourg sandstone, are incompetent and particularly sensitive to deformation. About 70% of the actual landslides, mostly influenced by man, were active on these two formations. Sliding at the

base of larger sandstone monoliths, over these marly beds, might occur if stratification is dipping towards the topographical slope, or by pressure release after erosion of the rock face. Different movements of the monoliths are observed, depending on the localization of the sliding plane, relative to the base or the centre of gravity of the monoliths. Toppling of a sandstone block will occur when the slide surface is located close to its outer edge. Sliding at its base will occur when a large part of the base is affected. The latter movement opens joints to narrow caves, as nicely seen in Fig. 1.12.

A recent example of man-induced mass movements is that of Deysermillen (Fig. 1.13), south of Grevenmacher (Fig. 1.2), where an about 50 m thick dolomite package of the upper Muschelkalk forms an impressive escarpment.



Fig. 1.11 Fossil patterned ground near Echternach, © SGL 2014

Gypsiferous marls of the middle Muschelkalk are underlying the dolomitic unit. This unit is, due to its clayey character and the presence of gypsum veins, very sensitive to landsliding. Local dissolution of gypsum develops a secondary permeability, inducing progressively new groundwater circulation paths in a normally quite impervious material. In the winter of 1964–1965, a very large movement has been triggered, affecting progressively the entire slope, destroying several buildings and pushing the valley road into the river. Works on the Mosel waterway have been done since the beginning of the 1960s. The water level of the Mosel had been raised up to 4 m by the Grevenmacher lock gate. The higher water table reduced the groundwater down-flow rate, and raised hydraulic pressure at the toe of the slope. At the same time, earthworks at the new Mosel road reduced the load on the toe. A first slope slice started to move towards the Mosel. This affected the upper parts of the

slope by reducing the retaining forces. A second destabilized slope slice of about 200 m length (2 in Fig. 1.13) moved very rapidly to the river, up to 20 m during one night. The movement progressed uphill over a couple of months up to the dolomitic escarpment, dragging down even some dolomite monoliths.

A couple of hundreds of metres north of this site, the historical landslide of Longkaul is located in a similar position. Its contours can nicely be seen on the 1:25,000 topographical map (Grevenmacher). A thick cover of marly Keuper sediments (ku on Fig. 1.13), overlying the dolomitic cuesta, regularly glides over the escarpment and falls on the regolith below. This progressively loads the top of the regolith below the escarpment, thereby reducing its stability. A first natural movement is believed to have started off in medieval times, and it has been reactivated numerous times by extreme meteorological conditions.



Fig. 1.12 A sandstone block slid at its base on the underlying marls and is vertically displaced by several metres and now leans against the Lias escarpment (Raiberhiel near Berdorf) (photo BK)

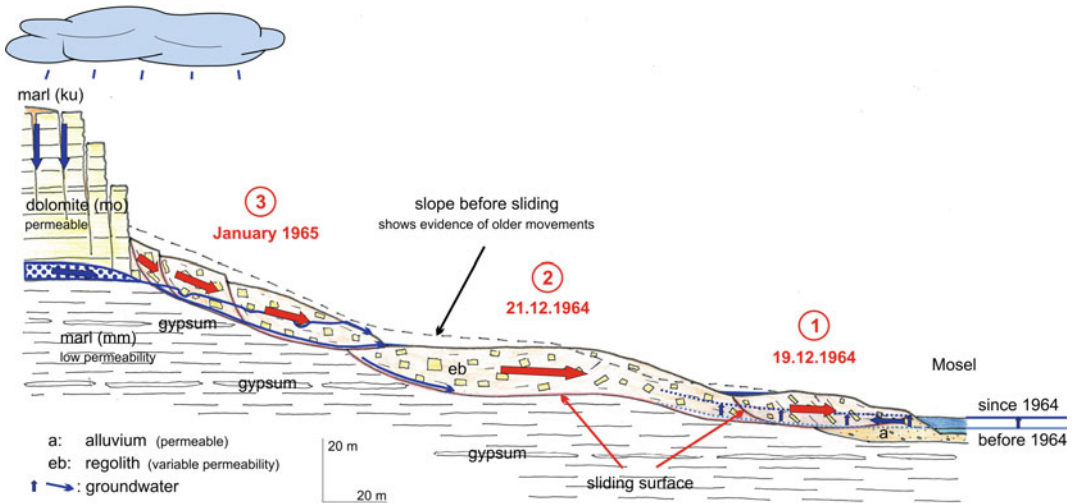


Fig. 1.13 The movement of Deysermillen south of Grevenmacher in winter 1964/65 (cross-section BK)

1.3.5 Anthropogenic Processes

Evidence for **soil erosion processes** is documented by truncated soil profiles on erosion sites, as well as by sediment traps like colluvial deposits on (the foot of) slopes (see also Chap. 6) floodplains or small closed depressions such as *Mardellen* (e.g. Poeteray et al. 1984). A relation between the history of soil erosion and the history of land use is shown on different sites on arable land and under forest (see also Chap. 3). A compendium of soil erosion studies in Luxembourg is given by Cammeraat (2006) and in Chap. 2.

Besides the Lias cuesta, man has also intensely affected the appearance of the Dogger cuesta (Fig. 1.3) that developed in the south of Luxembourg in the iron ore *Minette* and the overlying limestones. The iron ore has been largely exploited, dissecting the natural cuesta front towards the south, and exposing local large bedrock cliffs in the quarries. The new escarpments are now exposed to natural processes, such as weathering and rock fall. With time, these cliffs and the slopes below will become even more stable than before, since the influence of water has also been strongly reduced. Before exploitation, groundwater flow was to the north, to the *Alzette* basin. However, mine drainage changed the groundwater circulation, and waters are now conducted underground to the south-east into the basin of the *Mosel*. This reduces the discharge to, or dry out the small streams initially flowing down the slopes in front of the cuesta.

Chapter 3 discusses the human impact on the *Gutland* landscape, which becomes visible in sedimentological records from the late Holocene. In Chap. 5, examples of the complex nature of the Luxembourgian landscape are shown for some sample areas along the cuesta landscape near *Diekirch* (Fig. 1.2). For these landscapes, the complex spatio-temporal evolution and interaction between different geomorphological processes is illustrated. The described processes were active and sculptured the landscape under changing climatic conditions. Since the Holocene, some of the processes are still active on a finer scale. Nowadays man's influence is more

and more visible. Also, the predicted more extreme climatic conditions might influence the intensity of the processes.

References

- Busche D, Kempf J, Stengel I (2005) *Landschaftsformen der Erde. Bildatlas der Geomorphologie*, Wissenschaftliche Buchgesellschaft, Darmstadt
- Cammeraat ELH (1992) Hydro-geomorphologic processes in a small forested sub-catchment: preferred flow-paths of water. Thesis University, Amsterdam
- Cammeraat ELH (2006) Luxembourg. In: Boardman J, Poesen J (eds) *Soil erosion in Europe*. Wiley, Chichester, pp 427–438
- Cordier S (2005) Middle and upper pleistocene fluvial evolution of the *meurthe* and *moselle* valleys in the *paris* basin and the *rhenish* massif. *Quaternaire* 16:201–215
- Coûteaux M (1970) Etude palynologique des dépôts quaternaires de la Vallée de la *Sûre* à *Echernach*, et à *Berdorf*, et de la *Moselle* à *Mertert*. *Arch Sci* 34:297–336
- De Ridder NA (1957) Beiträge zur Morphologie der Terrassenlandschaft des luxemburgischen Moselgebietes. Thesis University, Utrecht
- Demoulin A (1995) L'Ardenne des plateaux, heritage des temps. Surfaces d'érosion en Ardenne. In: Demoulin A (ed) *L'Ardenne. Essai de géographie physique*. Université de Liège, pp 68–93
- Demoulin A (2005) Tectonic evolution, geology, and geomorphology. In: Koster EA (ed) *The physical geography of Western Europe*. Oxford University Press, Oxford, pp 3–24
- Désiré-Marchand J (1985) Notice de la carte géomorphologique du Grand-Duché de Luxembourg. *Publ Serv Géol Lux* 13. Luxembourg
- Duijsings JJHM (1987) A sediment budget for a forested catchment in Luxembourg and its implications for channel development. *Earth Surf Proc Land* 12:173–184
- García-Castellanos D, Cloetingh S, van Balen R (2000) Modelling the middle pleistocene uplift in the Ardennes/Rhenish Massif: thermo-mechanical weakening under the Eifel? *Glob Planet Change* 27:39–52
- Guillocheau F, Péron S, Bourquin S, Dagallier G, Robin C (2002) Les sédiments fluviaux (facies *Buntsandstein*) du Trias inférieure et moyen de l'est du Bassin de Paris. *Bull Inf Bass Paris* 39:5–12
- Heuertz M (1969) Documents préhistoriques du territoire luxembourgeois, Le milieu naturel l'homme et son œuvre, Fascicule I. Publications du musée d'histoire naturelle et de la Société naturalistes luxembourgeois, Luxembourg
- Heyart H (1964) Etude d'un dépôt loessique sur le territoire du Grand-Duché de Luxembourg. *Arch Sci* 30:73–105
- Jansen E, Overpeck J, Briffa KR, Duplessy J-C, Joos F, Masson-Delmotte V, Olago D, Otto-Bliesner B,

- Peltier WR, Rahmstorf S, Ramesh R, Raynaud D, Rind D, Solomina O, Villalba R, Zhang D (2007) Palaeoclimate. In: Solomon S, Qin D, Manning M, Chen Z, Marquis M, Averyt KB, Tignor M, Miller HL (eds) *Climate Change 2007: The Physical Science Basis. Contribution of Working Group I to the Fourth Assessment Report of the Intergovernmental Panel on Climate Change*. Cambridge University Press, Cambridge, United Kingdom and New York, NY, USA
- Jungerius PD (1980) Holocene surface lowering in the Lias cuesta area of Luxembourg as calculated from the amount of volcanic minerals of Allerod age remaining in residual soils. *Z Geomorph NF* 24:192–199
- Jungerius PD, Mücher HJ (1970) Holocene slope development in the Lias cuesta area, Luxembourg, as shown by the distribution of volcanic minerals. *Z Geomorph NF* 14:127–136
- Jungerius PD, van Zon HJM (1982) The formation of the Lias cuesta (Luxembourg) in the light of present da erosion processes operating on forest soils. *Geogr Ann* 64/A:127–140
- Kausch B, Maquil R (2006) Eine pleistozäne Terrasse der Syre bei Oetrange—ein Beispiel für die Hangentwicklung im südlichen Luxemburg (Gutland). *Bull Soc Nat luxemb* 106:167–180
- Le Roux J, Harmand D (2014) Les enseignements du relief de côtes dans l'est du Bassin Parisien. *Bull Inf Géol Bass Paris* 51:20–35
- Liedtke H, Deshaies M, Gamez P, Harmand D, Preusser H (2010) Die Oberflächenformen in der Grenzregion Saarland – Lothringen – Luxemburg, Les formes de relief dans la région frontalière Sarre – Lorraine – Luxembourg. *Forschungen zur deutschen Landeskunde* 259, Leipzig
- Lisiecki LE, Raymo ME (2005) A Pliocene-Pleistocene stack of 57 globally distributed benthic $\delta^{18}\text{O}$ records. *Paleoceanography* 20, PA1003, doi:[10.1029/2004PA001071](https://doi.org/10.1029/2004PA001071)
- Löhnertz W (1994) Grudzüge der morphologischen Entwicklung der südlichen Eifel im ältesten Tertiär. *Mainz naturwiss Arch Beih* 16:17–38
- Löhnertz W (2003) Eocene paleovalleys in the Eifel: mapping, geology, dating and implications for the reconstruction of the paleosurfaces and vertical movements of the lithosphere at the edges of the Rhenish shield. *Géol de la France* 2003:57–62
- Löhnertz W, Lutz H, Kaulfuß U (2011) Eifel – Mosel - Hunsrück. In: *Deutsche Stratigraphische Kommission (ed) Stratigraphie von Deutschland IX, Tertiär, Teil 1. Schriftenreihe der Deutschen Gesellschaft für Geowissenschaften* 75:376–415
- Louis H (1953) Über die ältere Formenentwicklung im Rheinischen Schiefergebirge, insbesondere im Moselgebiet. *Münchner Geographische Hefte* 2, München
- Lucius M (1948) Erläuterungen zu der geologischen Spezialkarte Luxemburgs, Geologie Luxemburgs. *Das Gutland Publ Serv Géol Lux V, Luxembourg*
- Lucius M (1950) Erläuterungen zu der geologischen Spezialkarte Luxemburgs, Geologie Luxemburgs. *Publ Serv Géol Lux VI, Luxembourg, Das Oesling*
- Mader D (1982) Petrographie und Diagenese fluviatiler Sedimente im Buntsandstein der Westeifel. *Z Geol Wiss* 10:181–205
- Maquil R, Postolache T (2005) Etude stratigrapho-morpho-micromorphologique de sédiments meubles provenant du forage de reconnaissance n° SGL-94-05, Merscherbiert, Grand-Duché de Luxembourg. In: *Centre Pierre Werner d'études et documentation. Ambassadeur de Roumanie au Grand-Duché de Luxembourg*, pp 187–200
- Maquil R, Mosar J, Thein J (1984) Unterdevon-Stratigraphie und variskischer Gebirgsbau im Eislek/Nord Luxembourg (Exkursion D am 26. und 27. April 1984). *Jber Mitt Oberrhein Geol Ver* 66:57–75
- Meyer W, Stets J (1998) Junge Tektonik im Rheinischen Schiefergebirge und ihre Quantifizierung. *Z dt Geol Ges* 149:359–379
- Moosbrugger V, Utescher T, Dilcher DL (2005) Cenozoic continental climatic evolution of Central Europe. *PNAS* 102:14964–14969
- Poeteray FA, Riezebos PA, Slotboom RT (1984) Rates of subatlantic surface lowering calculated from mardel-trapped material (Gutland, Luxembourg). *Z. Geomorph. N.F.* 28:467–481
- Riezebos PA (1987) Relic stratified screes occurrences in the Oesling (Grand-Duchy of Luxembourg), approximate age and some fabric properties. *Travaux Scientifiques du Musee d'Histoire naturelle de Luxembourg XII, Luxembourg*
- Riezebos PA, Ten Kate WGHZ, De Bruin M (1990) Eluvial Derivation of Rasenerz Concretions from the Minette Formation (Luxembourg), Evidence based on Numerical Classification of geochemical data. *Publ Serv Géol Lux* 15, Luxembourg
- Siehl A, Thein J (1989) Minette-type ironstones. In: *Young TP, Taylor WEG (eds) Phanerozoic ironstones. Geol Soc Spec Publ*, 46:175–193
- STDKe (2012) *Deutsche Stratigraphische Kommission (ed, Coordination and Layout: Menning M, Hendrich A) (2012) Stratigraphic Table of Germany Compact 2012 (STDKe 2012)*, Potsdam
- Storoni A (1980) Etat actuel de la recherche sur le loess au Luxembourg. *Bull Soc Préhist Lux* 2:8–12
- Van Balen RT, Houtgast RF, van der Wateren FM, Vandenberghe J, Bogaart PW (2000) Sediment budget and tectonic evolution of the Meuse catchment in the Ardennes and the Roer Valley Rift System. *Glob Planet Change* 27:113–129
- Verhoef P (1966) Geomorphological and pedological investigations in the Redange-sur-Attert area (Grand-Duchy of Luxembourg). *Thesis University, Amsterdam*
- Wiese B (1969) Die Terrassen des Ourtals. *Publ Serv Géol Lux* 18, Luxembourg

Historical Perspective of Dutch Geomorphological Research in the Gutland Region in Luxembourg

2

P.D. Jungerius

Abstract

In the 1950s, geomorphological research by the University of Amsterdam broke with the traditional way of studying landforms by introducing laboratory research. Starting with *grain size analysis* and *standard chemical analysis*, it gradually extended to *clay mineralogy*, *heavy mineral analysis*, *palynology* and *micromorphology*. These methods were also used in Luxembourg, where research concentrated on past conditions: tropical weathering during the Tertiary and periglacial phenomena during the Pleistocene. In the 1970s, the emphasis in Luxembourg swung to present-day processes. This was a major parameter shift again requiring new research methods such as soil profile analysis for geomorphological reconstructions, and setting up hydrological field stations. Prevailing research subjects included cuesta formation by differential soil erosion, soil erosion in agricultural lands, and soil formation and erosion under forest with the role of rodents and earthworms. It was a prelude to the last decades, in which the role of litter quality and differences in pH, decomposition and mineralization of nutrients have been addressed.

2.1 Introduction and Aim

Luxembourg has always attracted Dutch geomorphologists. There are several explanations for this popularity: the characteristic European

mountainous relief which is not found in the Netherlands, the absence of a Luxembourg University where earth sciences were taught, and the presence of a cooperative geological survey.

Geomorphologists of the University of Utrecht were among the first to produce valuable studies of the geomorphology of Luxembourg, mainly on the development of river terraces as a response to tectonic uplift. Their promotor was prof.dr. Jacoba Hol whose Ph.D. thesis was devoted to the hydrology of the Ardennes. The

P.D. Jungerius (✉)
Institute for Biodiversity and Ecosystem Dynamics,
University of Amsterdam, Science Park, Po box
94248, 1090 GE Amsterdam, The Netherlands
e-mail: jungerius@geomland.nl

University of Amsterdam followed in the 1960s. Over the years, their research developed into two methodological directions, the *bio-geomorphological approach* based on soil studies which is examined in this chapter, and the *hydro-geomorphological approach* dealt with in later chapters.

The aim of this chapter is twofold:

- Presentation of a number of methods developed by the University of Amsterdam for investigating the many past and present processes active in a characteristic European cuesta landscape.
- The contribution of these processes to the geomorphological development of European secondary mountain chains ('Mittelgebirge').

2.2 The Setting

The Grand-Duchy of Luxembourg can be subdivided into two main regions (Fig. 2.1): the Oesling, which is the northern part with a substratum of Devonian rocks (Lucius 1950) and the southern Gutland, which has a substratum of diverse Mesozoic sedimentary rocks (Lucius 1948). The Gutland is situated at the NE border of the Paris basin and is a characteristic cuesta landscape surrounding a major tectonic basin. A sequence of cuesta steps that is present is related to outcrops of Triassic and Jurassic sedimentary strata, which slightly dip inwards towards the centre of the Paris Basin. In between the outcropping dolomite, limestone and sandstone formations, marls and claystones are present of which the Keuper marls proved to be particularly important. The marls underlie one of the most prominent cuestas, the Luxemburger Sandstone or Lias cuesta, which is developed in the Lower Lias. The highest parts of the cuesta landscape rise to altitudes of about 420 m and cover large slightly sloping plateau-like areas. The lowest parts are adapted to the level of the Mosel river which is about 140 m at the confluence with the Sauer.

The Gutland of Luxembourg has a temperate humid climate with an annual rainfall ranging from less than 700 mm in the east to 1000 mm in the utmost southwest (Atlas du Luxembourg 1971). Average annual temperature is around 9 °C. Evapotranspiration rates are typically about 400–500 mm year⁻¹ depending on land use. Rainfall intensities over 60 mm h⁻¹ are relatively rare (Lahr 1964). From recent data, it is becoming clear that rainfall amounts increase through time, especially under the prevailing westerly winds (Pfister et al. 2000).

The Gutland has a miscellaneous land use, which is strongly related to substrate and slope. The steep slopes of the cuestas are mainly covered with deciduous forests. Important tree species are beech (*Fagus sylvatica* L.) and hornbeam (*Carpinus betulus* L.) because they regulate geomorphological processes, either directly such as by stem flow, or indirectly through the palatability of their leaves for earthworms. The dip slopes in between the cuesta escarpments are now under different types of crops, but grasslands are becoming more common. Conversely, the former grassland on heavy marl soils is increasingly used for the cultivation of maize.

2.3 Historic Overview, in the Footsteps of Davis

To appreciate the scope of the geomorphological and soil research of the University of Amsterdam in Luxembourg, it is necessary to put this research in a historical perspective. Starting point is the maxim of Davis (1899), who was the founder of geomorphology as a systematic discipline:

$$\text{Landform} = \int (\text{structure, process, stage})$$

Each of the terms on the right side of this equation has its own aficionados, to the extent that the main aim of the equation—explaining the landform—often recedes to the background.

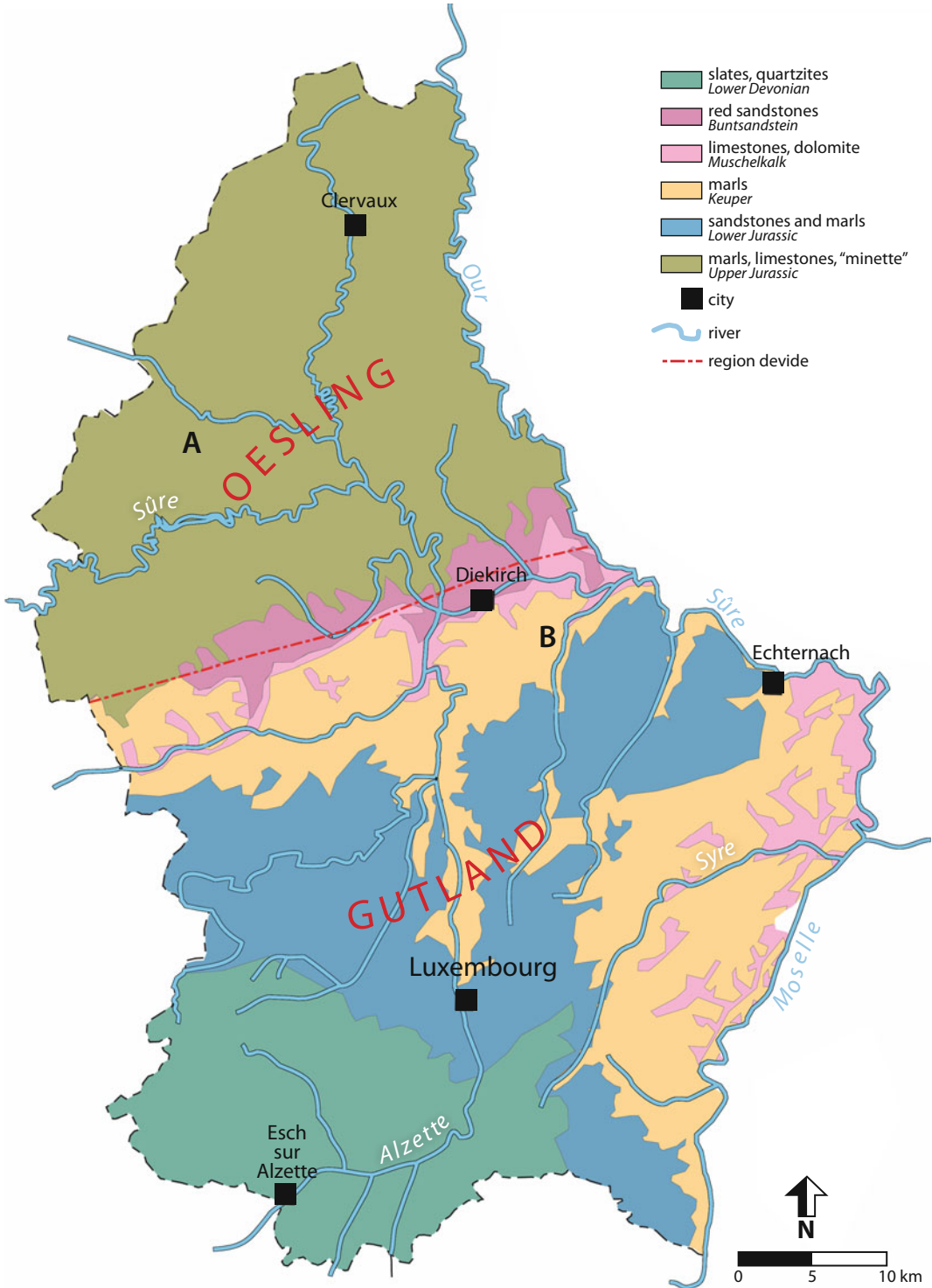


Fig. 2.1 The two main regions of Luxembourg, Oesling and Gutling and the main geological subdivision of the country

2.3.1 Stage \approx Time

Davis, a geologist himself, emphasized the role of time in the explanation of landforms. He brought order in the apparently chaotic appearance of the Earth's landforms by postulating a time sequence and subdividing the landforms in sequential developments stages (Davis 1899). Starting with uplift in the juvenile stage, a mountain range reaches maximum relief during maturity, and ends up as a gently undulating peneplain in the old age. This approach dominated geomorphological research in Europe for the next five decades. Especially German geomorphologists went out of their way to show that Davis' model was much too simple. They argued that the sequential development could be interrupted at any time by tectonic movements or by climate change. They coined the terms *Morphotektonics* and *Klimamorphologie*, respectively, for the two specializations that emerged from their research. With their studies of stream terraces, the geomorphologists of the University of Utrecht contributed to morphotektonics. The University of Amsterdam emphasized the climatic control of the Klimamorphology.

2.3.2 Structure \approx Materials

Jan Pieter Bakker was the founder of geomorphology at the University of Amsterdam in the 1930s. He gave geomorphological research a drastic twist by expanding the significance of the first independent term of Davis' conceptual equation. He discovered that earth materials reveal much more of the origin of the landforms than geological structure alone. Also, these materials contain a wide diversity of information that is not visible in the field but can be extracted from samples in the laboratory. In 1951, he established the Laboratory of Physical Geography and Soil Science and started with applying to geomorphology the sedimentological methods then in use for soil research in the newly established Dutch polders (Jungerius 2002). It started with *grain size analysis* and *standard chemical*

analysis, to be extended later to *clay mineralogy* and *heavy mineral analysis*.

Bakker introduced laboratory studies not to explain landforms, but to support his 'Klimamorphological' theory, in his case by detecting past tropical and subtropical climates in weathering profiles. Clay mineralogy was used to study the changes in the Tertiary climate which had influenced the development of the European low mountain ranges ('Mittelgebirge'). Climate in that period shifted from warm-humid to relatively dry periods (Bakker and Levelt 1964). In the first case, strong chemical weathering led to the development of the Tertiary plateau loams investigated by Levelt (1965). The dry climates affected the higher parts of the landscape through denudation in the absence of an uninterrupted vegetation cover. Hermans (1955) extended the concept of 'denudative altiplanation' to the Oesling, the crystalline northern part of Luxembourg. He argued that the relatively level summits were not remnants of a peneplain as was the current theory at the time, but the result of periglacial denudation processes affect the higher parts of the relief. This was what Bakker taught his pupils: being critical of established theories often opens exciting new avenues of research.

Our realization of the importance of soil profiles began when we followed a course in soil survey methods with the soil survey of Belgium, which was part of the obligatory curriculum of the study physical geography at the University of Amsterdam. All geomorphological research of physical geographers that followed the line of Bakker in Luxembourg started by making a soil map of their fieldwork area. It makes students familiar with the pattern of erosion (=down wearing) and colluviation (=raising). Soil erosion cum colluviation is, therefore, a process that has direct consequences for the geomorphological dynamics of a terrain: it links soil science to geomorphology (Jungerius 1958). Formal training in geomorphological methods and remote sensing started years later when the Vorarlberg group shifted their field practicals to Luxembourg (see also Chap. 5). More than 60 years ago, in the Soil Survey Manual of the US Department of

Agriculture of 1951, soil erosion in need of conservation was called *accelerated soil erosion*, to distinguish this anthropogenic variety of the process from natural soil erosion. Natural soil erosion was defined on page 251 of the Soil Survey Manual as *a constructive as well as destructive process, geologically speaking responsible for wearing down higher points and elevating lower points*. Admittedly this two-pronged effect of the erosion process is confusing, but it is familiar to most members of the European Society of Soil Conservation (SSSC) with a geomorphological background because they are aware that erosion processes include downwearing as well as raising parts of the landscape. Deposition of colluvium is the agricultural counterpart of elevating the land as part of the natural erosion process.

Unfortunately, in applied soil science and agriculture generally, the term soil erosion is now used in the restricted, anthropogenic sense. This overlooks the fact that natural soil erosion has formed most landscapes that are affected by accelerated soil erosion, and continues to do so, because natural erosion never stops as long as there is relief. Even where the accelerated soil erosion processes are dramatically visible as gullies or rills, the natural erosion processes that have shaped the relief in the course of geologic time usually remain evident in the shape of the land. Moreover, the total output of waste from watersheds is often more dependent on natural processes than on agricultural activities.

2.3.3 Process

The concern for processes, the second term in Davis' equation, began in the USA in the middle of the twentieth century, with the hydrogeomorphological studies of Leopold, Wolman and Schumm, soon to be adopted in the UK. In Amsterdam, this methodological turn came in the early 70s of last century, when Anton Imeson joined the staff and introduced in Luxembourg the

methods of process research developed in the UK. It involved a further shift from laboratory to field research. Adopting the drainage basin approach, Amsterdam geomorphologists established a number of hydrological and meteorological stations (Duijsings 1985; Cammeraat 1992). These stations served to obtain data on discharge of water and sediments, needed to test hypotheses of the effect of various geomorphological processes in the drainage basin. Research concentrated on forests, which have been the most common vegetation type since the formation of the Luxembourg landscape, with arable land and grassland as derivatives. In contrast to the proliferation of erosion studies elsewhere in Europe, emphasis was not on the production of output figures for models developed elsewhere, such as the widely used Wischmeier equation, but on understanding the processes involved. This necessitated the concentration of the research on the smallest spatial units of the drainage basin, the first- and second-order watersheds.

This meant that all three dependent parameters of Davis' equation were investigated in one integrated research programme. And not only that: Davis' essentially physical method was supplemented with a biological approach to determine the geomorphological and pedological significance of plant growth and soil life. The appointment of Annemieke Kooijman filled in the biological gap. The wide range of specialists and methods available made it possible to embark upon the classical quest of geomorphology, the explanation of the landform, which is the quintessence of Davis' equation. The research gave answers to a number of hitherto unsolved questions in geomorphology. These questions included cuesta formation, dating of Holocene soil erosion and the role of soil fauna in the erosion process. In this chapter, we discuss these subjects as they emerged in the early years. Together they contribute to a consistent picture of the development of a typical Western-European cuesta landscape since its origin in the middle of the Tertiary, that will be amplified in other chapters.

2.4 The Formation of a Cuesta by Differential Soil Erosion

The role that is traditionally ascribed to qualities of the underling rock is in point of fact, often due to the response of soil material at the surface to subaerial erosion processes. Where concordant sedimentary rocks dip gently—which they do over enormous expanses of the earth's surface—they give rise to asymmetric hill ridges known as cuestas. It is the stubborn belief of authors of geological and geomorphological textbooks that these landforms are due to differences in 'hardness' of the underlying beds. They fail to realize that rocks are seldom exposed on the dip slope or in the foreland of cuesta landscapes, with the exception of the steep front which is not subject to downwearing but to backwearing and plays a passive role in the development of the cuesta. If there has been any differentiating process at work in carving out the cuesta, it is much more plausible to hold the resistance of the weathering and soil materials responsible, because they are exposed to the subaerial erosion processes. **In other words, a cuesta is shaped by differential soil erosion.**

The significance of this principle is evident in situations where a 'weak' rock develops into a soil which resists erosion. The escarpment in the soft Upper Coal Measures in Nigeria is a case in point (Fig. 2.2). The resistance is due to a protective armour formed in the soil of the Upper Coal Measures by plinthite that hardened on exposure into ironstone concretions. The concretions make the soil over the soft rock more resistant to erosion than the sandy soil of the false-bedded sandstones underneath. The layer of ironstone concretions is the result of the poor drainage of the subsoil (Jungerius 1964, 2011). Termites bring the clay in between the ironstone concretions to the surface where it is removed by the prevailing slope wash processes, leaving the concretions behind. In the course of geologic time, this protective ironstone cap turns the originally soft rock into a 30 m high cuesta front.

The origin of the Lias cuesta in Luxembourg is in a way comparable. This impressive cuesta has been attributed to the 'hard' Luxembourg

sandstone consisting mainly of quartz sand embedded in calcium carbonate which provides the 'hardness'. This explanation is questionable, in view of the fact that the Lias cuesta continues across the border with Germany where the sandstone is not impregnated with calcium carbonate and has a rather loose consistency (R. Hansen, pers. comm.).

The Laacher See explosion

A great help for dating the eroded slope materials in Luxembourg proved to be the ash produced by the explosion of the Laacher See in the Eastern Eifel at the transition of the Pleistocene to the Holocene (12,000–11,000 B.P.). At that time, a layer of these minerals covered all the land for thousands of square kilometres around the Laacher See with a characteristic heavy mineral assemblage of brown amphibole, poxene and sphene. The original deposit was found to be 4 cm thick in peat deposits in and around Luxembourg (Jungerius et al. 1968). The present distribution of these minerals reflects the pattern of the Holocene soil erosion: where soil erosion removed much of the surface soil, the volcanic minerals are scarce or absent. For the same reason, colluvial deposits of Holocene age contain these minerals and can, therefore, be separated from Pleistocene slope deposits in which they are absent (Jungerius 1964).

Jungerius and Mücher (1970) tested the hypothesis that the Lias cuesta is formed by differential erosion of the surface soils. They analysed the erosion rates of the various slope elements of the cuesta by studying the remaining concentration of volcanic minerals left behind in the surface soil by the Laacher See eruption (Laacher see explosion 2.1). Compared to the Sandstone on top of the cuesta, the soils of the marly Steinmergelkeuper at the base of the escarpment slope showed highest erosion rates (Fig. 2.3). In a later paper, Jungerius (1980)

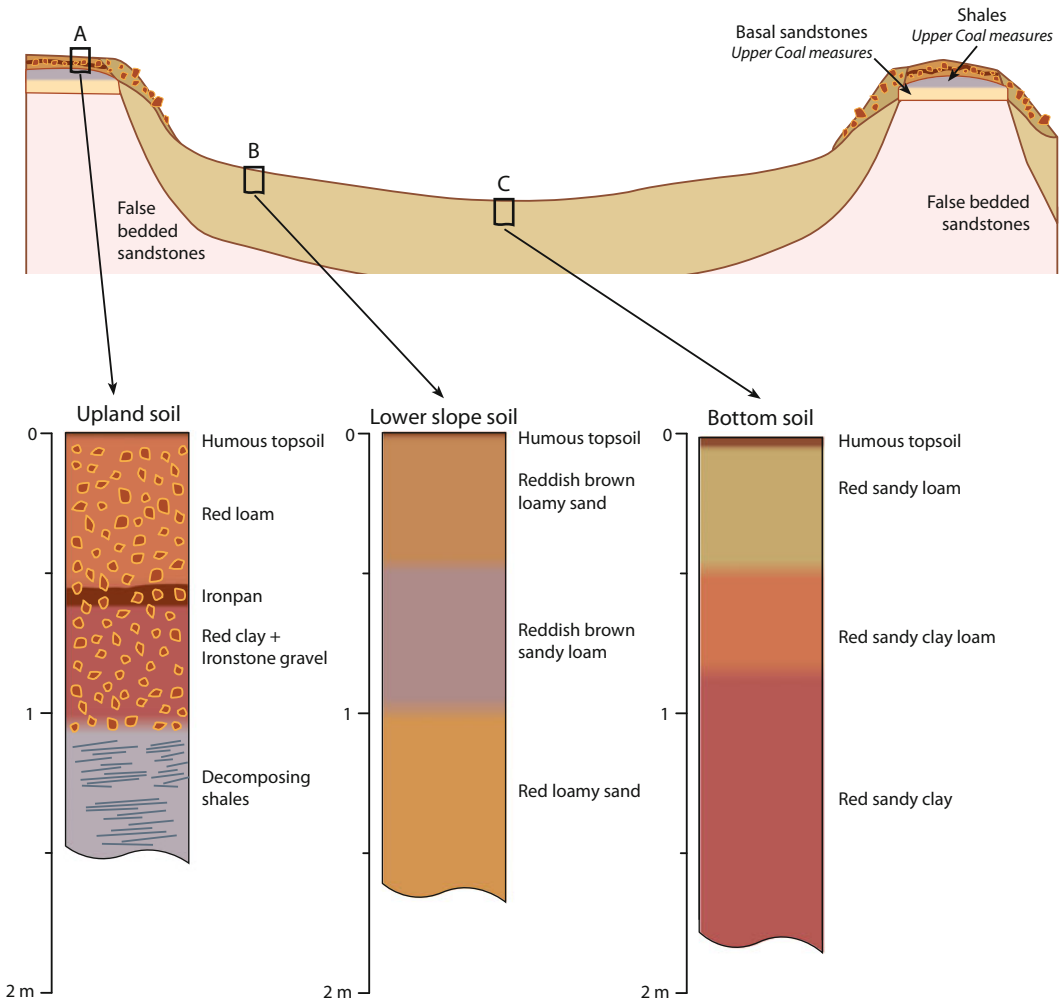


Fig. 2.2 Upper Coal Measures cuesta in Nigeria (after Jungerius 1964)

refined these results by quantifying the Holocene surface lowering with a simulation model using the amount of volcanic minerals left in the surface soil as a measure of soil erosion. Relative to the soils in the Luxembourg sandstone on top, the soils of the Steinmergelkeuper marls were lowered 44–57 cm (Fig. 2.3). Extrapolating this for the whole 2.8 million years long Quaternary, this would amount to 116 m. This amount is of the same order of magnitude as the approximately 100 m difference in elevation actually found. The surplus is presumably due to the fact that the calculated Holocene lowering includes

the effects of soil erosion on bare agricultural lands during the last two or three millennia.

Several authors presented current erosion rates for small catchments on the forested Keuper marl areas (Van Hooff and Jungerius 1984; Imeson and Vis 1984a; Duijsings 1987). According to these authors, the small watersheds under forest in question show suspended solid outputs to be a factor 2–5 lower than the agricultural watersheds on the same substratum. However, the influence of land use on sediment production in Luxembourg is ambiguous. Imeson and Vis (1984b) found that soil erodibility, determined by rainfall

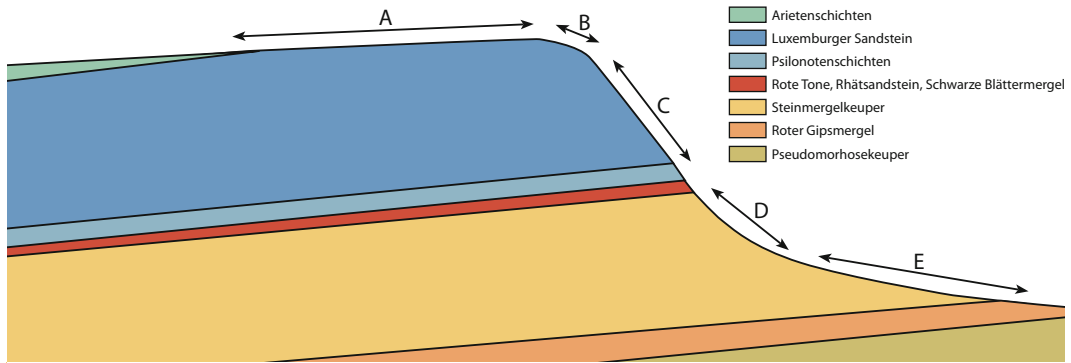


Fig. 2.3 Relative Holocene surface lowering across the Lias cuesta calculated from the frequency of Laacher See minerals of Allerød age remaining in residual soils. After Jungerius (1970)

simulator experiments, aggregate stability and splash erosion measurements, was largest for arable farmland, followed by forest colluvium and undisturbed forest topsoil, and that pasture was least erodible. They further found that erodibility showed a strong seasonal variation.

For these reasons, the erosion processes under agriculture and under forest are discussed separately in the following sections.

2.5 Soil Erosion in Agricultural Lands (Current Erosion Rates)

At the time, every student of the University of Amsterdam started his or her field work in Luxembourg by preparing a soil map of the allocated field work area from soil profile descriptions. There is hardly a better way to get acquainted with the ‘population’, to use a statistical term. In the second year, they were free to study a preferred process. As most field work areas included forest and agricultural areas, the maps provided much insight in the role of land use.

The general presence in the farmland of truncated soil profiles and associated colluvial deposits, with no sign of soil development, indicates ongoing soil erosion resulting from agricultural practices such as vegetation removal and tillage. Erosion processes on farmed land include splash, rill and gully erosion. Generally, these features are found on slopes with low

vegetation cover, such as recently ploughed, fallow fields and fields with maize crops. Figure 2.4 shows the result of gully formation in a fallow agricultural field on marls near the village of Nommern that was subjected to an extreme rainstorm in June 2003, with rainfall intensity of approximately 9 mm in 30 min. The sediment yield of this event was approximated at 15–18 tonne ha⁻¹ (Cammeraat 2006).

Soil profile truncation under agricultural land use is common in the marl areas, especially on Steinmergelkeuper. Whereas soil profiles under forest are typically developed with a clear B horizon (see Chap. 6), the profiles on agricultural fields with the same gentle slopes often show no more than a thin Ap horizon directly on top of the C material, or even directly on the weathered bedrock. Evidence of soil erosion is also seen in the occurrence of colluvial deposits on foot slopes and in the dry valleys, and the deposition of alluvium along the stream of third and higher order catchments. The influence of human occupation is clearly demonstrated by the presence of charcoal in the colluvial and alluvial sediments. Holocene fluvial sedimentation in the valley bottoms may reach a depth of several metres and is still continuing these days, as is demonstrated by the presence of a well-layered level of 75 cm thickness depth deposited on a paved road dating from the 1960s near Reisdorf.

To quantify surface lowering by soil erosion, Van Hooff and Jungerius (1984) combined data on extent and depth of soil truncation of 11 first



Fig. 2.4 Fresh gully developed in slope deposits on marls in a fallow field as generated during an intense storm on 10th of June 2003, near the village of Nommern. Reproduced with permission from Wiley Cammeraat (2006)

order watersheds in the Gutland with marl substratum, as shown on detailed soil maps prepared by the students, and compared the results with extent and thickness of nearby colluvial deposits shown on the same maps. This study covered an area of nearly 40 km². Only 6% of the area showed complete soil profiles, 44% of the area truncated profiles, 46% colluvial deposits and 4%

alluvial deposits. They calculated an average soil truncation of 55 cm for the whole area. This is a conservative measure, as in places where the whole solum was lost, the total degree of truncation could not be established. The figure agrees fairly well with the 44–57 cm value calculated from the presence of volcanic minerals (Jungerius 1980). It appeared that roughly 60% of the

eroded material left the second-order catchments, and 40% stayed behind. Similar results were obtained in the USA (Beer et al. 1966; Piest et al. 1975). The material that stayed behind in the catchments filled up the depressions as colluvium and raised the valley bottom with alluvium.

The dating of erosion by pollen analysis

Poeteray et al. (1984) used pollen analysis to date the colluvial deposits in closed depressions. A colluvial layer on slopes in northern Luxembourg which we initially interpreted as a periglacial deposit proved by them to be Subatlantic. They investigated the content of several closed depressions, which have been acting as traps for sediment and pollen. Several cores were analysed, some of which date back as far as the Roman period, based on palynological dating. From these deposits, the surface lowering rates were calculated, showing two clear peaks between 1200–1350 AD (0.086–0.215 mm year⁻¹) and between 1460–1600 AD (0.100–0.279 mm year⁻¹). In the first period, many forest areas were converted to arable land to provide food for the rapidly growing population of the many newly founded cities. This course of events is not restricted to Luxembourg: according to Bork and Lang (2003), extreme soil loss occurred in Germany during the first half of the fourteenth century and—less pronounced—in the second half of the eighteenth century.

The intervening period of recovery of the forest and decrease of soil erosion is probably the effects of outbreaks of pest and the thirty-year war, reducing the intensity of agriculture. It is interesting to note that the sudden enormous supply of eroded material that fed the streams in the hinterland coincides with the palynologically dated formation of the Younger Dunes between the eleventh and fourteenth century (Jelgersma et al. 1970). The rivers transported the eroded material from the

catchments to the sea, longshore drift spread it out along the coast, surf deposited it on the beach and the wind blew it inward to dunes. The latest method of sand suppletion is based on the postulated course of events: the so-called Zandmotor mimics the output of a river mouth from where longshore drift, surf and wind take over to bring the sand to the required location.

After the sixteenth century, sedimentation rates declined to 0.055–0.156 mm year⁻¹ from 1600–1800 AD. After 1800 AD, this rate declined further to 0.020–0.054 mm year⁻¹, as a result of decreased land use due to the introduction of potatoes, which have a higher calorific yield per ha. This led to land abandonment and reforestation (Poeteray et al. 1984). In the Chap. 3, this technique is applied to new records of Holocene sediments to disentangle the landscape evolution in the Holocene and the impact of man on the landscape.

In general, it can be concluded that the soil erosion levels in Luxembourg are low to moderate for natural areas. For the agricultural areas, this also seems to be the case, except for some problem areas. The low to moderate erosion rates are consistent with the results provided by Kirkby et al. (2000), for adjoining France.

2.6 Soil Erosion Under Forest, the Bio-Geomorphological Approach

For the development of the cuesta landscape, the rate of soil erosion under woodland is geomorphologically more meaningful than accelerated erosion by agriculture. This type of vegetation, mostly deciduous forest, has dominated the Gutland over long geological time spans, and largely controlled the development of the present landforms. The study of soil erosion under forest was, therefore, one of the focal points of the

University of Amsterdam. Two approaches can be distinguished, depending on the methods used. The *bio-geomorphological* approach maps and monitors slope-forming processes and studies soil profiles, highlighting the role of soil fauna, mainly rodents and earthworms (see also Chaps. 10). The biotic factor, with its manifold effects on soil and landscape development in Luxembourg, was introduced as a major research theme in the early 1970s (Imeson 1976, 1977). The *hydro-geomorphological* approach collects data from instrumented catchments on partial areas (shallow depressions), piping and the role of forest trees such as beech and hornbeam. The methodology was worked out by Cammeraat (1992) and is further dealt with in Chaps. 9 and 10.

In the absence of overland flow, the most important process of sediment supply in forests is splash erosion (Kwaad 1977). Splash impact is particularly heavy in forest because rainwater drips from the leaves in large drops. Measurements showed these drops to have diameters of up to 6 mm. When they fall on the ground from the tree crowns, which are often more than 10 m high, they have reached their theoretical terminal velocity. Splash erosion is confined to areas of exposed mineral soil, produced mainly by the activity of burrowing animals. The amount of splashed material reflects not only burrowing, but also the yearly cycle of litter-fall and decay because splash erosion is impeded by the protection of the soil surface by low vegetation as well as by litter. Two types of animals contributed directly to sediment production and slope formation: burrowing rodents and earthworms. Cammeraat and Kooijman elaborated on this (Cammeraat 2002; Cammeraat and Kooijman 2009; Kooijman and Cammeraat 2010) by coupling forest tree community to dominant bio-geo-hydrological processes (see also Chap. 10).

2.6.1 Rodents

Burrowing rodents, mostly moles, enhance the erodibility of slopes by bringing material with a

loose structure and often low organic matter content to the surface. They also play an important role in enhancing hydrological connectivity by connecting soil shrinkage cracks, creating semi-permanent pipes and enabling the transfer of water and sediment downslope to the streams (Imeson 1986; Cammeraat 2002). The effects of splash erosion on bare soil material were extensively studied in experimental plots on a 22° upper slope in a representative valley of the Luxembourg Ardennes, about 15 m from the river, grading abruptly to a 30–35° lower slope (Imeson and Kwaad 1976). The area was completely forested. It is noted that most of the bare soil was found within 10 m or so from the river and that 95% of the bare soil was the result of animal activity, predominantly moles and voles. These animals apparently prefer to live in the moist soils near the river bed and in shallow depressions. The splashed material is the main source of the suspended load in the river.

Aggregate stability was investigated with micromorphological techniques (Imeson and Jungerius 1974). The aggregate stability of the crumb structure of the mounds is low. Splash removed preferentially the particles <2 mm. With longer exposure, the stoniness of the exposed soil increased from 25–50% to 100% when the erosion stopped. Erosion was measured with erosion pins and splash boards. By combining the measurements of soil exposure with those of splash erosion for the same period, the lowering of the slopes by splash erosion was estimated to be 0.33 mm per 1000 years ($330 \text{ kg km}^{-2} \text{ year}^{-1}$), near the river increasing to 91.6 mm per 1000 years (Imeson and Kwaad 1976). The geomorphological implications are quite interesting: the convexity of the break in the lower slope is in proportion to the rate of lowering due to the activity of the rodents. A timespan of about 18,000 years would be required to explain the difference in elevation between the projection of the straight slope above the break of slope to a point above the river bed and the present river bed.

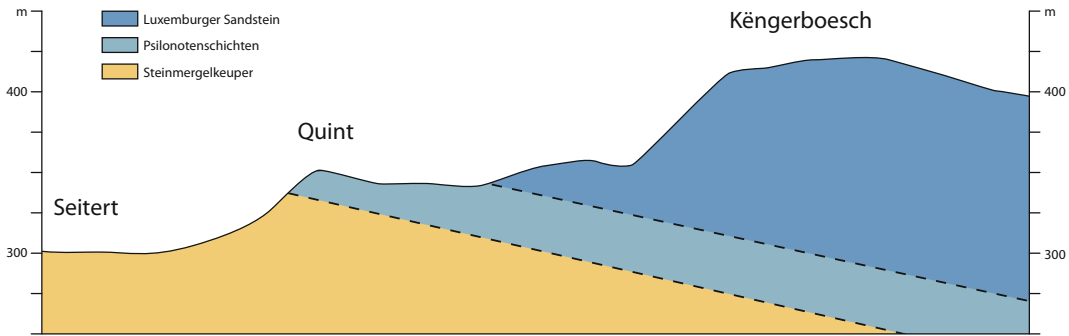


Fig. 2.5 One of the five investigated sections. The names refer to the topographical map 1:20,000. Administration du Cadastre de G.D. de Luxembourg.

LS = Luxembourg Sandstone, PM = Psilonoten marls, KM = Keuper marls. After Jungerius and van Zon (1982)

2.6.2 Earthworms

A leading part in the biotic factor of the Gutland is played by earthworms, mainly *Lumbricus terrestris* L. and to a lesser extent *Allolobophora longa* L. They are significant in two respects. First, they are responsible for much of the bioturbation in the surface soils. In this way, they contribute to the contrast between the surface soil and the subsoil, which is characteristic for the soils of the Steinmergelkeuper Formation. Second, they are responsible for removing litter (Satchell 1961, see also Chap. 10), which results in the forest floor being bare and exposed to splash erosion and occasional overland flow.

To investigate the long-term effects of these two earthworm activities, two research projects were set up in Luxembourg. The first of these projects ran from 1980 to 1987 and investigated the area of bare forest floor exposed by earth worms, along five transects across the level parts of the three main steps of the Lias escarpment: Luxembourg sandstone which forms the main escarpment, Psilonoten marls which forms a secondary step and the Keuper marls at the base (Fig. 2.5). The beginning of each transect was marked on the topographical map 1:25,000 and in the field.

Each year before the new leaf fall, estimates of the percentage soil cover were made in squares of 4 m², 10 m apart along each transect's length of 400 m, numbering a total of 600 observations each year. The beginning and end of each

transect were marked; deviations from the line between successive years were random but never more than a few metres. Leaf consumption by earth worms was the main cause of the observed differences in exposure, which in turn depended on ecological conditions of the soil: sand and moisture content (Jungerius and Van Zon 1982, 1984; Jungerius et al. 1989). The experiment was stopped after 1987 because local deforestation, heavy storms and a road building project had spoiled the experimental design. Over the measuring period, forest floor exposure in summer averaged over 40% on the Keuper marls, 11% on the somewhat more sandy Psilonoten marls and 0–3% on the sandy soil of the Luxembourg Sandstone. These results support the hypothesis that the cuesta formation is a function of the activity of earth worms, which in turn is controlled by the geological conditions.

2.6.3 Soil Creep

The second project focused on soil creep. On slopes in the Keuper marls, there is evidence of soil creep affecting the surface soil, which appears to shift slowly downslope as a result of the continuous bioturbation by worms in combination with gravitational forces (see Chap. 10). An important factor is the abrupt textural contrast between the AE and B horizon (see Chap. 9). The reason is that the soil material is easy to disperse, due to the presence of swelling and dispersible smectite in

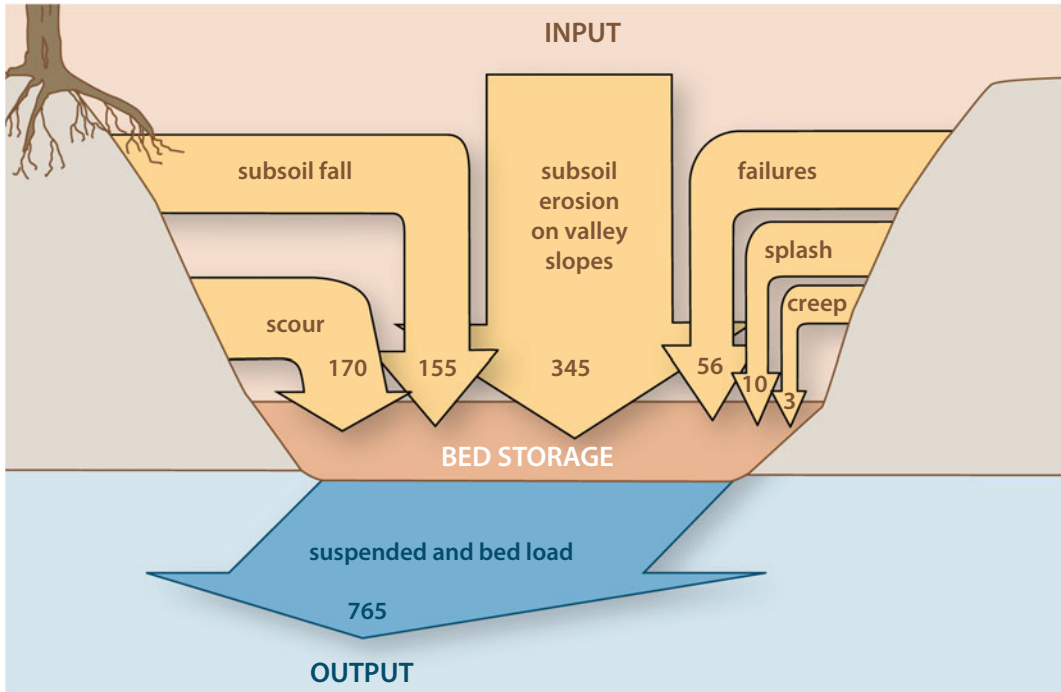


Fig. 2.6 Sediment budget for the Schrondweilerbaach catchment 1979–1981. Numbers are in kg ha⁻¹ year⁻¹. Reproduced with permission from Wiley after Duijsings (1985)

the fine clay fraction and the relatively high pH, in combination with a complex saturation of divalent cations (no active Al³⁺).

Soil creep was studied in the Schrondweiler catchment with so-called Rudberg pillars (Jungerius et al. 1989). At five locations along a catenary sequence of 200 m length, from the upper slope across the 2° slope to the bottom, small boreholes 50 cm deep and 2 cm wide were filled with contrasting yellow sand in April 1981. With this method, downward creep of the surface soil can be detected by dislocation of the sand columns. Two columns were dug up after 14 months. Both columns showed definite bending in the upper 15 cm indicating downslope movement varying between 2 and 8 mm. More columns were excavated after 6 years. Bioturbation in that period had been so intensive that the sand columns could no longer be detected in any of the surface horizons, and the experiment had to be terminated. Vestiges of the soil in the lowest member of the transect suggested a downslope displacement of 22 mm since the start of the experiment 7 years

before. The type of mass movements was classified as seasonal creep which is produced by the combined action of gravity stresses and expansion or contraction stresses due to changing moisture content (Carson and Kirkby 1972). Part of the clay minerals in the Keuper are particularly prone to swelling and shrinking as could be shown by the presence of slickensides in thin sections, and produced movement on slopes as low as 2°. The exerted forces were manifest from the way an aluminium weir from an abandoned experiment, dug into the soil to collect surface runoff, became more and more distorted (Photo 1 in Jungerius et al. 1989).

2.6.4 Outline of the Erosion Processes on the Keuper Marls

The natural erosion here is due to the specific nature of the substratum, especially the swell and shrink properties of the soil, the type of

Table 2.1 Sediment budget for the Schrondweilerbaach catchment 1979–1981.

		Process	Sediment supply kg (2 years) ⁻¹	%
Input	Stream banks	Lateral corrasion	20,650	22.9
		Subsoil fall	18,860	21.0
		Mass movements	6850	7.6
		Rainsplash erosion	1240	1.4
		Soil creep	400	0.4
		Overland flow	–	–
		Streambank total	48,000	53.3
	Valley slopes	Splash detachment + overland flow	38,000	42.2
		Throughflow	4000	4.5
		Slopes total	42,000	46.7
		Total sediment input	90,000	
	Output	Suspended load	86,300	92.8
		Bed load	6700	7.2
Total sediment output		93,000		
Net dissolved output		180,400		

From Duijsings (1985)

Figures in bold denote totals

vegetation and soil faunal activity and the hydrological regime (Hazelhoff et al. 1981; Van den Broek 1989; Cammeraat 2002). Apart from splash, overland flow and creep on soils with burrowing animals, there are a number of other processes active on the forest-covered slopes of Luxembourg. After 2 years of monthly measurements in a 60.8 ha catchment, Duijsings (1985, 1987) found that sediment transfer from the Schrondweilerbaach on Keuper marls was determined by three types of processes active on the valley slope and six types of processes active on the streambank (Fig. 2.6 and Table 2.1). Valley slope processes such as splash erosion and overland flow contributed with 46.7% of the sediment budget of the Schrondweilerbaach, but throughflow with 4.5%. This process is controlled by the texture difference between the AE and B horizon of the Keuper soil, which promotes the process of subsurface erosion of dispersive clay (see Chap. 9). The streambanks contributed 53.3% to the supply of sediment, with lateral corrasion and subsoil fall being the main bank processes contributing, respectively, 22.9 and 21.0%. Each process could be related to

a specific condition: lateral corrasion and splash erosion to summer thunderstorms, subsoil fall to frost periods, soil creep to biological activity. In terms of surface lowering, the output of 0.765 tonne ha⁻¹ (Duijsings 1987; Table 2.1) approximates 0.05 mm year⁻¹. This value agrees with the average rates of slope denudation given by Poeteray et al. (1984) for the last 200 years: 0.020–0.054 mm year⁻¹.

2.6.5 Erosion Processes on the Luxembourg Sandstone

By comparison, erosion of the sandy soils of the Luxemburger Sandstone is relatively low, but not absent. Van Zon (1980) gives denudation rates for a small forested catchment on the Luxemburg sandstone on the scarp slope. Measured denudation was found to be very low: only 0.010 tonne ha⁻¹ year⁻¹. An important factor is the presence of bare spots where the sandy soil was subject to splash erosion. Unexpectedly, he found that about a quarter of the amount was

transported by the leaves of the forest floor, which may well be an important factor in the explanation of the presence of colluvium on forest slopes covered with litter (Van Zon 1978).

Although soil life is practically non-existent in the sandy soils of the Luxemburg sandstone, especially those under the widespread beech forests, but soil formation is not without interest. At a depth of 50–70 cm in beech forest on almost level dipslopes, the soil is often compacted to a mottled *fragipan*, which restricts water flow and root penetration (Jungerius 1980). True to theory current at the time, this fragipan was attributed to periglacial conditions during the last glaciation (Van Vliet and Langohr 1981), but the close relationship with beech trees indicates that it is related to the beech forest. The even distribution of volcanic minerals of the Laacher See above the fragipan shows that the profile layer above the fragipan is completely homogenized, whereas roots and volcanic minerals are absent below the fragipan. In the absence of worms, this distribution must have been caused by the roots of the trees. It is apparently a slow process because the formation of a brown B2 horizon above the fragipan can outpace the effects of the homogenization. The cause of the abrupt increase in density is open to debate. It is possible that it is caused by fluctuating pressure exercised by the horizontal root mat during storms, but that would need further research.

2.7 Back to Davis, the Explanation of the Landforms

We can now see how far our research can explain the morphology of cuesta landscape, which was Davis' ultimate goal. Van Zon (1980) gives current denudation rates for a forested catchment on the Luxemburg sandstone on top of the scarp slope. Measured denudation after 2 years was found to be very low, in total only $0.010 \text{ tonne ha}^{-1} \text{ year}^{-1}$, which means 5 m in 1 million years. Several authors presented current denudation rates for small catchments on the forested Keuper marls. The most

detailed catchment study, the Schrondweilerbaach, showed values of $0.765 \text{ tonne ha}^{-1} \text{ year}^{-1}$, equaling approximately 0.05 mm of annual soil surface lowering, equivalent to 50 m in 1 million years (Duijsings 1987). There is local variation: in Keuper forests, estimated denudation rates are 1.46–2.0 $\text{tonne ha}^{-1} \text{ year}^{-1}$ in areas where the forest floor is bare in summer, in contrast to 0.13–0.26 $\text{tonne ha}^{-1} \text{ year}^{-1}$ in areas with full litter cover under beech, which may lead to local development of shallow depressions and ridges (see Chap. 10). However, the difference in lowering of forest soils on the Luxemburg Sandstone on top of the escarpment and on the Steinmergelkeuper at the bottom is at least 45 m in 1 million years. The experiments in the forests on the Luxemburg sandstone were carried out where the cuesta has a height of 416 m, those in the forests of the Schrondweilerbaach at the base had an average height of 310–318 m. This means an altitude difference of roughly 100 m. When we apply Lyell's concept that the present is the key to the past and assume that forests have existed as long as the Keuper has been exposed in Luxemburg, worms would need about 2 million years to bring about this relief configuration. This brings us back to the early Pleistocene. There are indications that the environment of the geomorphological processes in this area has not much changed since the Pliocene and even the Miocene (Frenzel 1967; Van Hooff and Jungerius 1984).

It is a mental quantum leap from 2 years monitoring the sediment production by slope processes to extrapolating the results over millions of years. All the more admiration deserves Darwin (1881), who concluded the experiments with earthworms in his garden with the statement: *'...if a small fraction of the layer of fine earth, 0.2 of an inch in thickness ($\pm 5 \text{ mm}$), which is annually brought to the surface by worms, is carried away, a great result cannot fail to be produced within a period of time which no geologist considers extremely long'* Or, in the words of Jose Rubio (2009) past president of the ESSC: *'we can interpret the history of the world through the observation of minuscule processes, that largely*

pass unnoticed but have the enormous dimension of time to originate major changes'.

Acknowledgements Jan van Arkel is thanked for providing the graphical work in this chapter.

References

- Atlas du Luxembourg (1971) Ministère de l'Education Nationale, Imprimerie Saint-Paul
- Bakker JP, Levelt ThWM (1964) An inquiry into the probability of a polyclimatic development of peneplains and pediments (etchplains) in Europe during the Senonian and Tertiary Period. Lucius Gedenkbuch, Geologische Dienst Luxemburg
- Beer CE, Farnham CW, Heinemann HG (1966) Evaluating sedimentation prediction techniques in western Iowa. *Trans Am Soc Agric Engineers* 9:828–831
- Bork H-R, Lang A (2003) Quantification of past soil erosion and land use/land cover changes in Germany. Springer, Heidelberg
- Cammeraat LH (1992) Hydro-geomorphological processes in a small forested catchment: Preferred flow paths of water. Ph.D.-thesis University of Amsterdam, Amsterdam
- Cammeraat LH (2002) A review of two strongly contrasting geomorphological systems within the context of scale. *Earth Surf Proc Land* 27:1201–1222
- Cammeraat LH (2006) Luxembourg. In: Boardman J and Poesen J (eds) *Soil Erosion in Europe*. Wiley, pp 427–438
- Cammeraat LH, Kooijman AM (2009) Biological control of pedological and hydro-geomorphological processes in a deciduous forest ecosystem. *Biologia* 64:428–432
- Carson MA, Kirkby MJ (1972) *Hillslope*. Cambridge University Press, Form and Process
- Darwin C (1881) The formation of vegetable mould through the action of worms, with observations on their habits. Reprint Faber & Faber Ltd. 1945
- Davis WM (1899) *The Geographical Cycle*. *Geogr J* XIV: 481–504. (Reprinted as *Geographical essays*. Dover Publications Inc. New York 1954, Chapter XIII: 249–278)
- Duijsings JJHM (1985) Streambank contribution to the sediment budget of a forest stream. Ph.D. Thesis, University of Amsterdam, Amsterdam
- Duijsings JJHM (1987) A sediment budget for a forested catchment in Luxembourg and its implications for channel development. *Earth Surf. Proc. and Landforms* 12:173–184
- Frenzel B (1967) Die Klimaschwankungen des Eiszeitalters. Die Wissenschaft 129, Vieweg, Braunschweig
- Hazelhoff H, van Hooff PPM, Imeson AC, Kwaad FJPM (1981) The exposure of forest soil to erosion by earthworms. *Earth Surf Proc Landforms* 6:235–250
- Hermans WF (1955) Description et genèse des dépôts meubles de surface et du relief de l'Oesling. Thesis University of Amsterdam, Amsterdam
- Imeson AC (1976) Some effects of burrowing animals on slope processes in the Luxembourg Ardennes; The excavation of animal mounds in experimental plots. *Geogr Ann* 58 A:115–125
- Imeson AC (1977) Splash erosion, animal activity and sediment supply in a small forested Luxembourg catchment. *Earth Surf Processes* 2:153–160
- Imeson AC, (1986) Investigating volumetric changes in clayey soils related to subsurface water movement and piping. *Z Geomorph N.F. Suppl.-Bd.* 60:115–130
- Imeson AC, Jungerius PD (1974) Landscape stability in the Luxembourg Ardennes as exemplified by hydrological and (micro) pedological investigations of a catena in a experimental watershed. *CATENA* 1:273–295
- Imeson AC, Kwaad FJPM (1976) Some effects of burrowing animals on slope processes in the Luxembourg Ardennes: the erosion of animal mounds by splash under forest. *Geogr Ann* 58 A:317–328
- Imeson AC, Vis M (1984a) The output of sediments and solutes from forested and cultivated clayey drainage basins in Luxembourg. *Earth Surf Proc Land* 9:585–594
- Imeson AC, Vis M (1984b) Seasonal variation in soil erodibility under different land-use types in Luxembourg. *J Soil Sci* 35:323–331
- Jelgersma S, De Jong J, Zagwijn WH, Van Regteren Altena JF (1970) The coastal dunes of the western Netherlands, geology, vegetational history and archaeology. *Meded Rijks Geol Dienst Nieuwe Ser* 21:93–167
- Jungerius PD (1958) Zur Verwitterung. Bodenbildung und Morphologie der Keuper-Liaslandschaft bei Moutfort in Luxemburg. *Publ, Service Géologique du Luxembourg*, p 13
- Jungerius PD (1964) The upper coal measures cuesta in Eastern Nigeria. *Z Geomorph NF Suppl* 5:167–176
- Jungerius PD (1980) Holocene surface lowering in the Lias cuesta area of Luxembourg as calculated from the amount of volcanic minerals of Allerød age remaining in residual soils. *Z Geomorph NF* 242:192–199
- Jungerius PD (2002) De fysisch-geografische traditie. In: Knippenberg, H and Schendelen Mvan (eds) *Alles heeft zijn plaats: 125 jaar geografie en planologie aan de Universiteit van Amsterdam, 1877–2002* Aksant pp 457–481
- Jungerius PD (2011) Soil erosion and conservation in natural and semi-natural landscapes. Guest editorial Newsletter 2011/1. European Society for Soil Conservation (ESSC)
- Jungerius PD, Mücher HJ (1970) Holocene slope development in the Lias cuesta area, Luxembourg, as shown by the distribution of volcanic minerals. *Z Geomorph NF* 14:127–136
- Jungerius PD, van Zon HJM (1982) The formation of the Lias cuesta (Luxembourg) in the light of present day erosion processes operating on forest soils. *Geogr Ann* 64A:127–140
- Jungerius PD, van Zon HJM (1984) Sources of variation of soil erodibility in wooded drainage basins in

- Luxembourg. In: Burt TP and Walling DE (Eds): Catchment experiments in fluvial geomorphology. Geobooks Norwich 13:235–246
- Jungerius PD, Riezebos PA, Slotboom RT (1968) The age of Eifel maars as shown by the presence of Laacher See ash of Allerød age. *Geol Mijnbouw* 47: 199–205
- Jungerius PD, Van den Ancker JAM, Van Zon HJM (1989) Long term measurements of forest soil exposure and creep in Luxembourg. *CATENA* 16:437–447
- Kirkby MJ, Le Bissonais Y, Coulthard TJ, Daroussin J, McMahon MD (2000) The development of land quality indicators for soil degradation by water erosion. *Agr Ecosyst Environ* 81:125–135
- Kooijman AM, Cammeraat ELH (2010) Species richness under beech and hornbeam on decalcified marl: disentangling litter quality effects on organic layer, pH and soil moisture characteristics. *Funct Ecol* 24:469–477
- Kwaad FJPM (1977) Measurements of rainsplash erosion and the formation of colluvium beneath deciduous woodland in the Luxembourg Ardennes. *Earth Surf Processes* 2:161–173
- Lahr E (1964) Temps et climat au Grand-Duché de Luxembourg. *Publ Min de l'Agriculture, Luxembourg*
- Levelt ThWM (1965) Die Plateaulehme Süd-Luxemburgs und ihre Bedeutung die morphogenetische Interpretation der Landschaft. Thesis University of Amsterdam, Amsterdam
- Lucius M (1948) *Geologie Luxemburgs: Das Gutland, Luxembourg, Publ Serv Geol de Luxembourg, Erläuterungen zu der geologische Spezialkarte Luxemburgs*
- Lucius M (1950) *Geologie Luxemburgs: Das Oesling, Luxembourg, Publ Ser Geol de Luxembourg, Erläuterungen zu der geologische Spezialkarte Luxemburgs*
- Pfister L, Humbert J, Hoffmann L (2000) Recent trends in rainfall-runoff characteristics in the Alzette River Basin. *Clim Change* 45:323–337
- Piest RF, Kramer LA, Heinemann HG (1975) Sediment movement from loessial watersheds. In: Present and prospective technology for predicting sediment yield and sources. *USDA Agric Res Serv ARS-S 40:130–141*
- Poeteray FA, Riezebos PA, Slotboom R (1984) Rates of subatlantic surface lowering calculated from mardel-trapped material (Gutland, Luxembourg) *Z Geomorph NF* 28:467–481
- Rubio J (2009) Darwin's worms. *ESSC Newsletter* 3–2009:8–11
- Satchell JE (1961) Lumbricidae. In: Burges A, Raw F (eds) *Soil biology*, Academic Press, London and NY pp 259–322
- Soil Survey Division Staff (1951) *Soil survey manual*. Soil Conservation Service. U.S. Department of Agriculture Handbook 18
- Van den Broek TMW (1989) Clay dispersion and pedogenesis of soils with an abrupt contrast in texture. Ph.D. Thesis, University of Amsterdam, Amsterdam
- Van Hooff PPM, Jungerius PD (1984) Sediment source and storage in small watersheds on the Keuper marls in Luxembourg, as indicated by soil profile truncation and the deposition of colluvium. *CATENA* 11:133–144
- Van Vliet B, Langohr R (1981) Correlation Between Fragipans and Permafrost with Special Reference to Silty Weichselian Deposits in Belgium and Northern France. *CATENA* 8:137–153
- Van Zon HJM (1978) Litter transport as a geomorphic process (a case study in the Grand-Duchy of Luxembourg). Thesis University of Amsterdam, Amsterdam
- Van Zon HJM (1980) The transport of leaves and sediment over a forest floor. *CATENA* 7:97–110

Palynological Reconstruction of the Effects of Holocene Climatic Oscillations and Agricultural History on Soils and Landforms in Luxembourg

J.M. van Mourik and R.T. Slotboom

Abstract

Holocene deposits in valleys and mardels contain valuable pollen records for the reconstruction of the Holocene Landscape evolution, driven by climatic oscillations, forest development and agriculture. Before the Subatlantic, denudation and fluvial discharge were in balance. The Late Holocene displacement of the *Quercetum mixtum* into a *Fageto-Quercetum* and the introduction of sedentary agriculture at the expense of forests since the Celtic/Roman Time, stimulated soil erosion. Accelerated soil erosion in the Subatlantic caused deposition of colluvial covers on foot slopes and alluvial beds in primary catchments. In addition, the colluvial deposits in mardels on the Gutland plateau are the result of Subatlantic soil erosion. The pollen records of the deposits on valley floors and in mardels show correlations of Subatlantic climatic oscillations with denudation rate and agricultural management. In particular the Little Ice Age stands out as a period with increased denudation and temporally extension of arable land.

3.1 Introduction

The present geomorphology of the landscapes in the Eislek and the Gutland is inherited from Tertiary and Quaternary landscape evolution,

which was initiated by the Pliocene mantle plume uplift of the entire Luxembourg region (see also Chap. 1). The uplift was more pronounced in the Eislek than in the Gutland. As a result, the Mesozoic cover was completely eroded in the north. The Eislek landscape is now characterized by wide open plateaus on Devonian rock, with an average elevation of 450 m, dissected by valleys. The present Gutland is a cuesta landscape, underlain by alternating tilted sedimentary rock formations with different resistance to weathering and erosion.

R.T. Slotboom—Deceased

J.M. van Mourik (✉) · R.T. Slotboom
Institute for Biodiversity and Ecosystem Dynamics,
University of Amsterdam, Science Park, PO box
94062, 1090 GB Amsterdam, The Netherlands
e-mail: J.M.vanMourik@uva.nl

During the Pleistocene, the landscape has been subjected to several cycles of weathering and erosion by the alternation of glacial and interglacial periods (Lucius 1948; Verhoef 1966). During glacial periods, landscape development was dominated by erosion and denudation under periglacial conditions. During interglacial periods, the landscape became vegetated, denudation was reduced and soil profiles could develop. Pleistocene landforms and deposits are scarcely available in the present landscape. Verhoef (1966) has described fossil ice wedges and traces of periglacial cryoturbation and ascribes asymmetrical valley development to periglacial conditions (see also Chap. 1). Riezebos (1987) reported the occurrence of typical periglacial deposits such as grèze lithee in the Eislek.

The Holocene landscape evolution started in a landscape with thin regolithic slope covers and pre-Holocene gravelly deposits on the valley floors (Heuertz and Heyart 1964; Verhoef 1966). Plant growth, weathering and soil formation were dominant processes in the Early Holocene. Holocene sediment cores on valley floors and in mardels turned out to be valuable soil archives for palynological reconstruction of the Holocene landscape development. During the last 50 years, results of palynological case studies of such sediment cores have been published in different papers and congress abstracts (Slotboom 1963; Riezebos and Slotboom 1974; Kwaad and Mùcher 1976; Riezebos and Slotboom 1978; Poeteray et al. 1984; van Mourik et al. 2012; van Mourik et al. 2013).

In this chapter we assemble the available palynological information to a reconstruction of the effects of the Holocene climatic oscillations and the agricultural history on soils and landforms in Luxembourg. Three of the selected records concern peat deposits (Elteschmuer, Roudbaach and Boeckenwiesen), the other records concern alluvial and colluvial deposits. Compared with pollen records of peat profiles, the interpretation of pollen records of alluvial and colluvial deposits are complicated (van Mourik 2001, 2003). The pollen content is a mix of the

regular aeolian pollen influx with colluvial transported pollen.

Pollen records of peat deposits are appropriate for the reconstruction of the Holocene vegetation development, records of colluvial and alluvial deposits are appropriate for the reconstruction of environmental conditions, resulting in erosion and sedimentation. Based on the combination of these records we reconstructed the regional effects of climatic oscillations and agricultural history on denudation, colluviation and alluvial deposition.

3.2 Materials and Methods

3.2.1 Pollen Analysis

For the reconstruction of the impact of climatic oscillations and historical land use on soils and landforms in the Luxembourg landscape, we selected pollen diagrams from various studies, realized by IBED staff and students (Table 3.1). The soil determination of the sampled profiles was based on the World Reference Base (ISRIC-FAO 2006). In Fig. 3.1, the profile sites are denoted on a fragment of the map of the Roman road network (Thill 1977), showing the relatively intensive land use during Roman Time. Samples from soft sediments (peat, loamy peat and humic clay) were taken with a peat sampler; samples from more resistant sediments (loam, sand and gravel) were taken with an 'Edelman' soil auger. Pollen extractions were carried out using the tufa extraction method (Moore et al. 1998). For the identification of pollen grains, the pollen key of Moore et al. (1998) was applied. Pollen scores were based on the total pollen sum of arboreal and non-arboreal plant species (minimal 200, maximal 400). The pollen extractions were performed in the Laboratory for Palynology of the University of Amsterdam.

The pollen diagrams, presented in this chapter, show the headlines of the original diagrams; curves of species with incidental scores were excluded.

Table 3.1 Selection of records from previous publications

Site	Site name	Landform	Soil/Sediment	Publication
1	Roudbaach	Wide valley floor	Histosol/Peat	R&S 1974
2	Boeckenwiesen	Wide valley floor	Histosol/Peat	M et al. 2013
2	Eisbaach	Valley floor	Regosol/Alluvium	M 2013
3	Husterbaach	Valley floor	Regosol/Alluvium	R&S 1978
4	Dirbaach 1	Valley floor	Regosol/Alluvium	R&S 1974
4	Dirbaach 2	Valley floor	Regosol/Alluvium	R&S 1974
5	Birkbaach	Valley floor	Regosol/Alluvium	M&S 2012
6	Elteschmuer	Mardel	Histosol/Peat	M&S 2012
7	Brasert	Mardel	Regosol/Colluvium	P et al. 1984
8	Kalefeld	Mardel	Regosol/Colluvium	P et al. 1984

For site numbers, see also Fig. 3.1. R&S 1974 = Riezebos and Slotboom (1974); R&S 1978 = Riezebos and Slotboom (1978); P et al. 1984 = Poeteray et al. (1984); M&S 2012 = Van Mourik and Slotboom (2012); M et al. 2013 = Van Mourik et al. (2013)

3.2.2 Radiocarbon Dating

The geochronology of the pollen records is based on the palyno-zonation, introduced by Firbas (1949). However, a reliable geochronology cannot be based on pollen zones alone. Sometimes clear palynological reflections of historical events can be observed, such as the appearance of *Fagopyrum* or *Picea*. Characteristic peaks of *Fagus sylvatica* L. can also be used for palyno-dating. A robust chronological control is supplied by absolute dating techniques. For that purpose, 14 samples have been radiocarbon dated in the Centre for Isotope Research of the University of Groningen.

3.2.3 Water Analysis

The reliability of radiocarbon dates of organic matter from closed depressions as mardels can be affected by reservoir effects (Mook and Streurman 1983). Subsurface dissolution of calcium carbonate and gypsum (present in the Keuper formations) can result in increased concentrations of Ca, SO₄ and HCO₃ in water, stagnating in mardels. Inorganic carbon, derived from dissolved evaporate rock may affect the reliability of radiocarbon dates. We took water samples in the mardels to test pH, EC and the concentrations of

Mg, SO₄, HCO₃. The analysis have been performed in the IBED soil chemistry laboratory.

3.3 Results

3.3.1 Radiocarbon Dating and Water Analysis

The results of radiocarbon dating are summarized in Table 3.2. The reliability of radiocarbon dates is affected by the quality of the organic samples. Radiocarbon dates of wood and peat samples are considered as reliable. The dates of samples of loamy valley deposits are also reliable, because valleys are open systems with a continues water flow. The $\delta^{13}\text{C}$ values (<-29) indicate soil organic carbon originating from (local) wetland species (Osmond et al. 1981). The radiocarbon dates of samples from colluvial deposits in closed depressions as mardel probably overestimate the true age due to the reservoir effects, above all by high concentrations of older inorganic carbonates (Mook and Streurman 1983).

Table 3.3 summarizes the results of water analysis of samples from mardels. A second effect that causes overestimating of the real age is the contamination of the organic carbon fraction with older redeposited soil organic carbon originating from the eroded forest soils. The $\delta^{13}\text{C}$

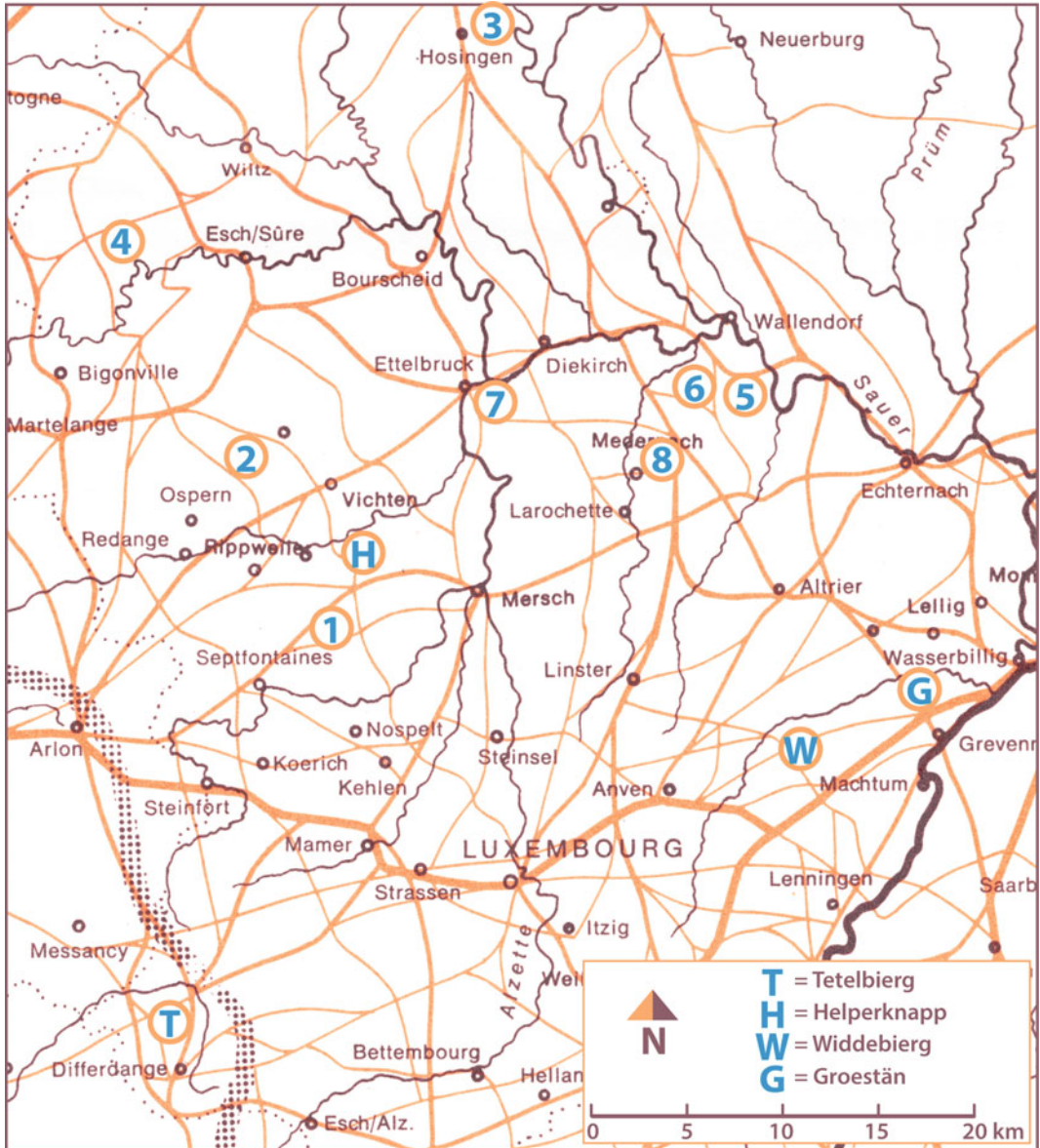


Fig. 3.1 Fragment of the map of the Roman road network and some important Roman sites (Thill 1977). The research sites are indicated with numbers:

1 Boeckenwiesen, Eisbaach; 2 Roudbaach; 3 Husterbaach; 4 Dirbaach; 5 Birkbaach; 6 Elteschmuier; 7 Brasert; 8 Kalefeld

values (≈ -27) point to soil organic matter from eroded forest soils, not to decomposed organic matter of a local wetland vegetation (Osmond et al. 1981). Due to these effects, the radiocarbon ages of the samples Brasert and Kalefeld are not in line with the palynological ages, expressed in the Firbas zoning.

The samples of the Elteschmuier mardel, situated in a mixed forest on Luxembourg sandstone (li2), have the characteristics of slightly buffered rain water, stagnating on (impermeable) sandstone. The low percentages of ashes indicate a low input of clastic sediments with the drain water. In the Brasert mardel, situated

Table 3.2 Radiocarbon dates of Luxembourger valley and CD deposits

Sample	Substrate	GrN	%OM	%Ash	$\delta^{13}\text{C}$	Year BP	Calendric age ^a	Firbas zone
Roudbaach 65 cm	Peaty loam	6944	28.2	56.2	-29.0	2815 ± 55	BC 985 ± 70	VIII
Roudbaach 165 cm	Peaty loam	6933	40.2	38.3	-29.7	9235 ± 86	BC 8467 ± 110	IV
Boeckenwiesen 272 cm	Wood	11,285	54.4	0.0	-26.7	8810 ± 180	BC 7939 ± 236	IV
Husterbaach 55 cm	Humic loam	7465	16.1	67.1	-29.6	390 ± 45	AD 1527 ± 71	X
Husterbaach 65 cm	Humic loam	7464	15.0	69.7	-29.6	430 ± 45	AD 1498 ± 63	X
Husterbaach 95 cm	Humic loam	7466	12.9	76.0	-29.6	680 ± 45	AD 1325 ± 47	X
Dirbaach-2 50 cm	Wood	6946	57.5	0.0	-27.4	1175 ± 45	AD 853 ± 67	IX
Birkbaach 130 cm	Peaty loam	26,048	46.3	2.3	-29.1	2040 ± 100	BC 301 ± 58	IX
Elteschmuer 34 cm	Peat	26,045	56.1	2.8	-28.1	1850 ± 60	AD 84 ± 18	IX
Elteschmuer 38 cm	Peat	26,046	50.7	9.3	-28.8	2560 ± 50	BC 799 ± 19	VIII
Elteschmuer 60 cm	Peat	26,047	49.2	16.6	-28.4	3790 ± 100	BC 2091 ± 36	VIII
Brasert 150 cm	Humic loam	11,797	27.7	43.2	-27.0	1300 ± 70	AD 739 ± 71	X
Brasert 215 cm	Humic loam	11,796	23.5	54,0	-27.0	1750 ± 90	AD 272 ± 108	IX
Kalefeld 125 cm	Humic loam	11,795	23.2	50,0	-27.0	2200 ± 140	BC 245 ± 163	X

^aCalibrated with online CalPal, quickcal 2007 version 1.5

Table 3.3 Results of analysis of water samples from mardels

Mardel	Substrate	pH	EC $\mu\text{S cm}^{-1}$	HCO_3 $\mu\text{mol l}^{-1}$	Ca $\mu\text{mol l}^{-1}$	Mg $\mu\text{mol l}^{-1}$	SO4 $\mu\text{mol l}^{-1}$
Elteschmuer-1	li2	5.85	162	549	227	111	126
Elteschmuer-2	li2	5.89	144	297	205	129	179
Brasert	km3	6.39	225	728	480	218	286
Kalefeld	li3	7.42	521	3363	3027	175	97

in a *Fagus* forest on Keuper (km3), and the Kalefeld mardel, situated in a pasture on the Lias (li3), water stagnates on Subatlantic colluvial clay deposits. The water samples show increased concentrations of Ca and HCO_3 ,

which indicates dissolution of carbonates in the feeding drain water. The carbonates may originate from the calcareous parent materials of the surrounding soils in the Luxembourger sandstone and Keuper. The Mg and SO_4

concentrations seem not to be raised by active dissolution of gypsum.

3.3.2 Pollen Records of Valley Floor Deposits

3.3.2.1 Roudbaach Valley Mire

Sample point Roudbaach is situated in a wide part of the Roudbaach valley with mire conditions (Figs. 3.2 and 3.3). The Roudbaach valley deposits contain valuable soil archives for the reconstruction of the Holocene vegetation and landscape development (Fig. 3.4). It is a sequence of peat and loamy layers, deposited on the Late Glacial valley floor (Verhoef 1966). The sampled profile is classified as a Gleyic Humic Regosol, overlying a Sapric Histosol. The pollen content of the gravelly loamy basic layer (Zone III) is affected by post sedimentary infiltration. This means that the palynological age of this layer is younger than the sedimentary age (van Mourik 2001). Around 1980, the drainage of the valley was improved by the construction of subsurface drains. Drainage of peat deposits

promotes bio-oxidation and land surface lowering, but the peat profile is still well preserved.

The pollen diagram (Fig. 3.4) indicates that the sedimentation started in the Preboreal with the deposition of loamy peat (zone IV, characterized by high percentages of the non-arboreal pollen) on the gravelly basement. In the valley, an open wetland vegetation (Zone III, IV; Cyperaceae) was gradually replaced by an Alnetum (zones VI, VII, VIII). The sequence of the arrival of trees in the surroundings is well recorded; *Pinus* and *Betula* in the Late Glacial, *Corylus* in the Boreal, *Quercus* and *Tilia* in the Atlantic, *Fagus* and *Carpinus* in the course of the Subboreal.

The pollen record indicates the start of the deforestation and the appearance of *Cerealia* in the Subatlantic. The composition of the deposits changed from loamy peat to (peaty) loam. There is no palynological evidence of human landscape disturbance before the Roman Time. The arrival of the Romans is expressed by the start of deforestation and the extension of agriculture (55–45 cm). The Dark Ages, a period with lower temperatures, mass migrations of people and



Fig. 3.2 Roudbaach valley and sample site on Google Earth



Fig. 3.3 Picture of the Roudbaach valley (from the sample site to the west)

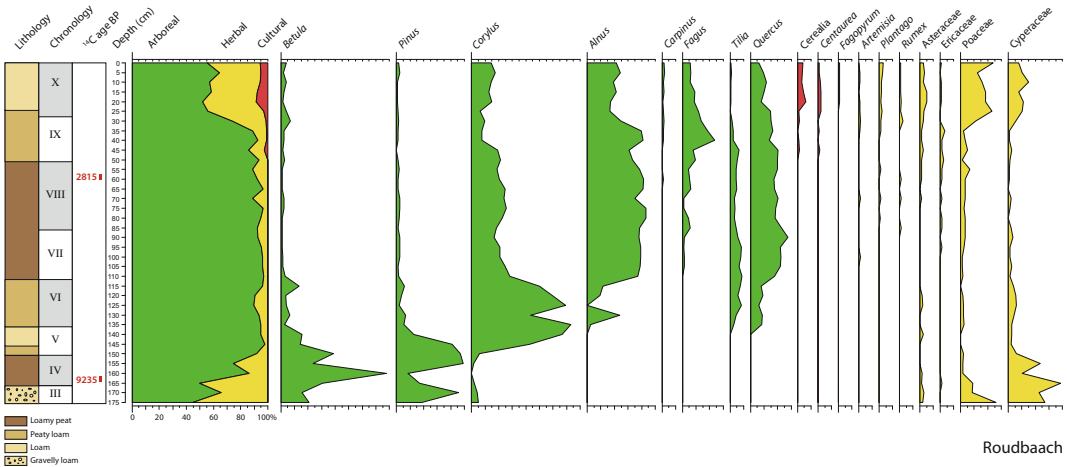


Fig. 3.4 Pollen diagram Roudbaach

forest recovery are expressed in the temporal recovery of the Alnetum (45–53 cm). In the Late Middle Ages, forest was replaced by arable land. This is also lithologically expressed in the sediment core. During the Atlantic and the Subboreal, peat was deposited with a low content of loam. In the Subatlantic, the clastic fraction

increased: peaty loam during zone IX and humic loam during zone X.

3.3.2.2 Boeckenwiesen Valley Mire

The Boeckenwiesen (Figs. 3.5 and 3.6) is situated between the Lias cuesta and the Eisbaach. The central part of this basis was a mire, until

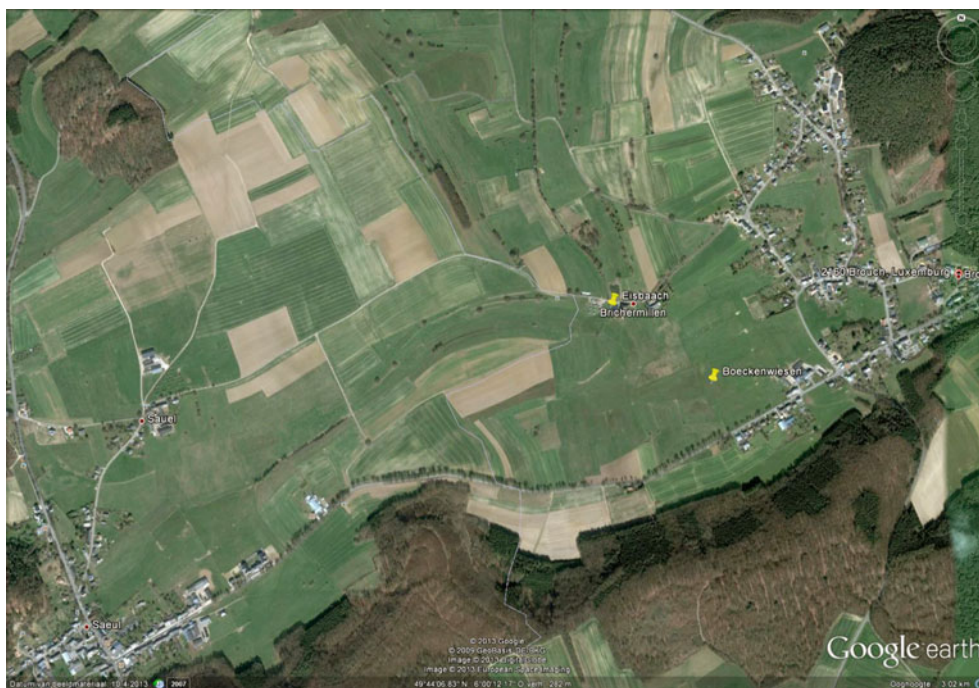


Fig. 3.5 The sample sites Boeckenwiesen and Eisbaach on Google earth



Fig. 3.6 Picture of the Boeckenwiesen from sample point Boeckenwiesen to the south

people improved the drainage of this area by underground drains around 1980. Bio-oxidation and land surface subsidence started, the soils in the Eisbaach valley lost their fluvic properties and transformed into Humic Regosols. Below a young anthropogenic sand cover, the peat profile of the previous mire was well preserved. The present profile was classified as a Sapric Histosol.

The physiographic map (Fig. 3.7) of the surrounding of Boeckenwiesen shows the impact of historical land use (deforestation, agriculture) on the Late Holocene soil development. On the Lias plateau, well developed and intact soils still occur, but due to continuous water infiltration and harvesting they became more acidic (see also Chap. 6). Soil erosion and mass movement dominate the upper slopes of the cuesta front. The lower slopes are covered with colluvial deposits, and the rivers (as the Eisbaach) are no longer able to transport the sediments supplied by accelerated soil erosion. This resulted in Subatlantic deposition of colluvial/alluvial sediments on foot slopes and valley bottoms (see also Chap. 2).

The diagram Boeckenwiesen shows a complete Holocene pollen record. The accumulation of humic sediments on a gravelly surface started in the Late Glacial (zone III). The pollen spectra are dominated by herbs, *Betula* and *Pinus*. The accumulation of peat started in the Preboreal (zone IV). The pollen spectra are dominated by *Pinus* and *Betula*. During the Boreal (V) and the

Atlantic (VI, VII), a deciduous forest developed (spectra dominated by *Corylus*, *Alnus* and *Quercus*). During the Subboreal (VIII) arboreal pollen still dominate the spectra, but the first traces of deforestation appear, followed by culture indicators. The curve of culture indicators is based on an association of weeds, growing on arable land or pasture such as *Artemisia*, *Centaurea*, *Cerealia*, *Fagopyrum*, *Linum*, *Rumex*, *Papilionaceae*, *Plantago* (Behre 1980), and starts in Roman Times. In the beginning of the Subatlantic (IX), the first extension of *Fagus* is visible. At the end of zone IX, the spectra show evidently the deforestation and the extension of culture indicators as *Cerealia*. *Fagopyrum* appears during zone X.

Compared with the Early Holocene (Preboreal till Subboreal), the accumulation rate increased during the Late Holocene (Subboreal and Subatlantic). Deforestation in the uplands caused acceleration of water infiltration and wetting of basins and valley bottoms. The intercalated loamy beds in the peat deposits were considered as streambed deposits of the original meandering peat brook, transporting an increasing sediment load in the Subatlantic. This brook disappeared in underground drains after the improvement of the drainage and the reclamation of the former wetland to pasture around 1980.

Figure 3.9 shows the Subatlantic increase of sediment supply. Before the start of the Subatlantic (IX, X), the Eisbaach was an eroding River, and the valley bottom was covered with

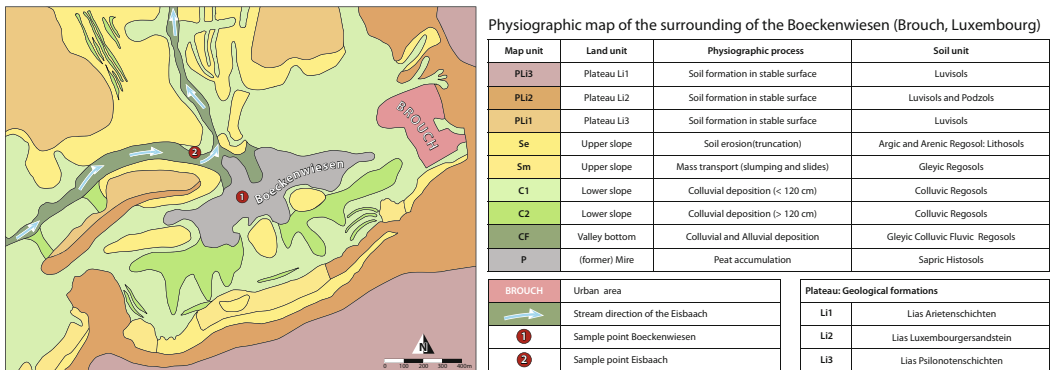


Fig. 3.7 Physiographic map of the Boeckenwiesen and surroundings

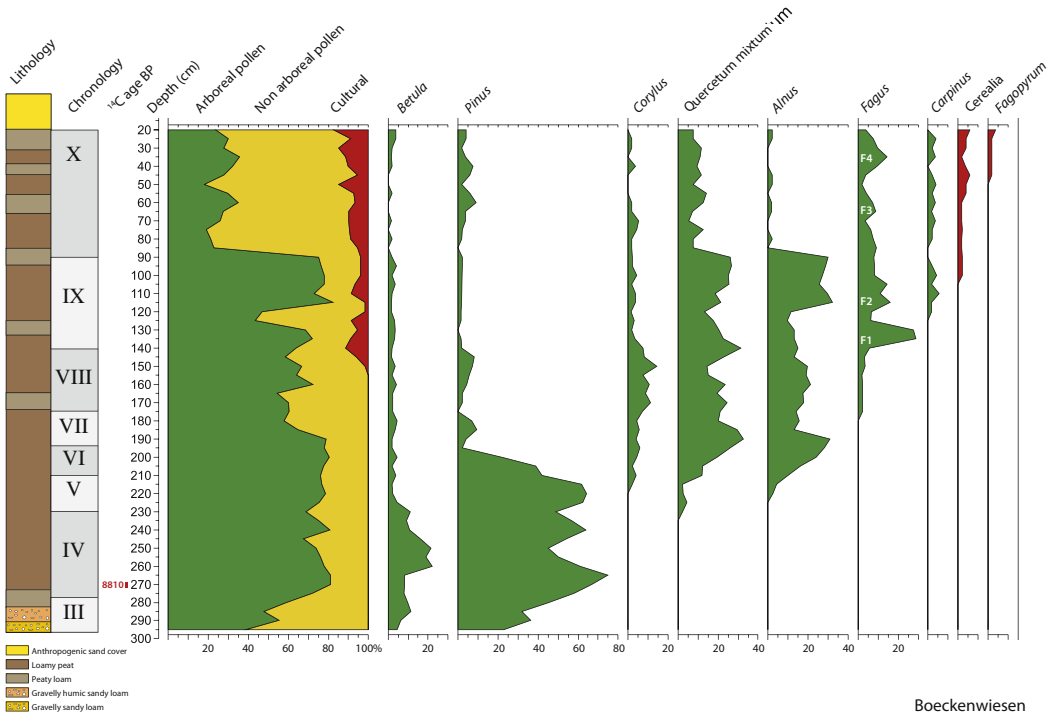


Fig. 3.8 Pollen diagram Boeckenwiesen

gravelly sediment. The infill with colluvial/alluvial sediments started in the beginning of the Subatlantic. All the spectra are dominated by *Alnus*, *Fagus* and culture indicators, pointing to a Subatlantic age of the sediments. Before the beginning of the Subatlantic, the Eisbaach was able to transport the sediment load, supplied by slope process. Deforestation and extension of agriculture caused accelerated soil erosion and deposition of foot slope colluvium and valley alluvium. The properties of colluvium and alluvium deposits are rather similar, which makes it difficult to distinguish a precise field boundary between them. Moreover, due to the improvement of the drainage of the Eisbaach valley, the soil lost its fluvic properties and is now classified as Humic Regosol.

3.3.2.3 Husterbaach Valley Alluvium

The Husterbaach is located in the Eislek near Hosingen (Fig. 3.10). Deposition of peaty clay on Late Glacial gravelly loam (probably with a post sedimentary pollen content) started around

1200 AD. The pollen record (Fig. 3.11) shows some headlines of the agricultural development in a deforested landscape. The presence of *Linum* pollen reflects the development of the culture of flax. It is known that during the fifteenth century the cultivation of flax in the Mosel region strongly increased (Slicher van Bath 1960). Also Schmithusen (1940) records a prosperous textile industry which ended with the Thirty Years War (1618–1648). The similar values of arboreal and non-arboreal pollen in all spectra of the pollen diagram indicate a stable distribution of agricultural area and forest. Consequently, variation in arable and pasture indicators correlate with changes in land use, visible in the sub-diagram arable land use. The selection of arable indicators (*Cerealia*, *Fagopyrum*, *Rumex*, *Centaurea*, *Artemisia* and *Linum*) and pasture indicators (*Poaceae*, *Papilionaceae* and *Plantago*) is based on Behre (1980).

Before 1500 AD, the high percentages of pasture indicators suggest that a great part of this area has been used for grazing. The high

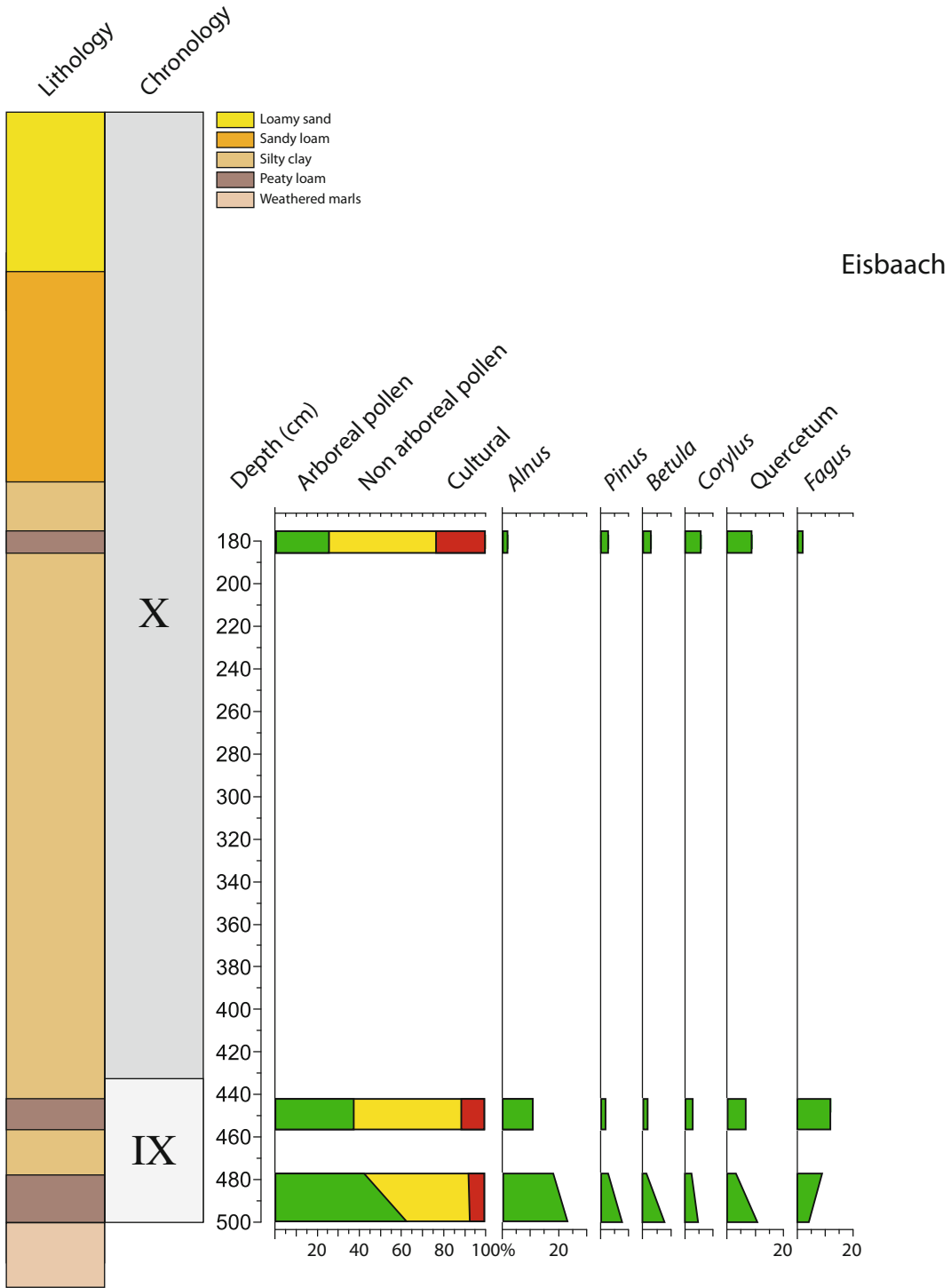


Fig. 3.9 Pollen diagram Eisbaach

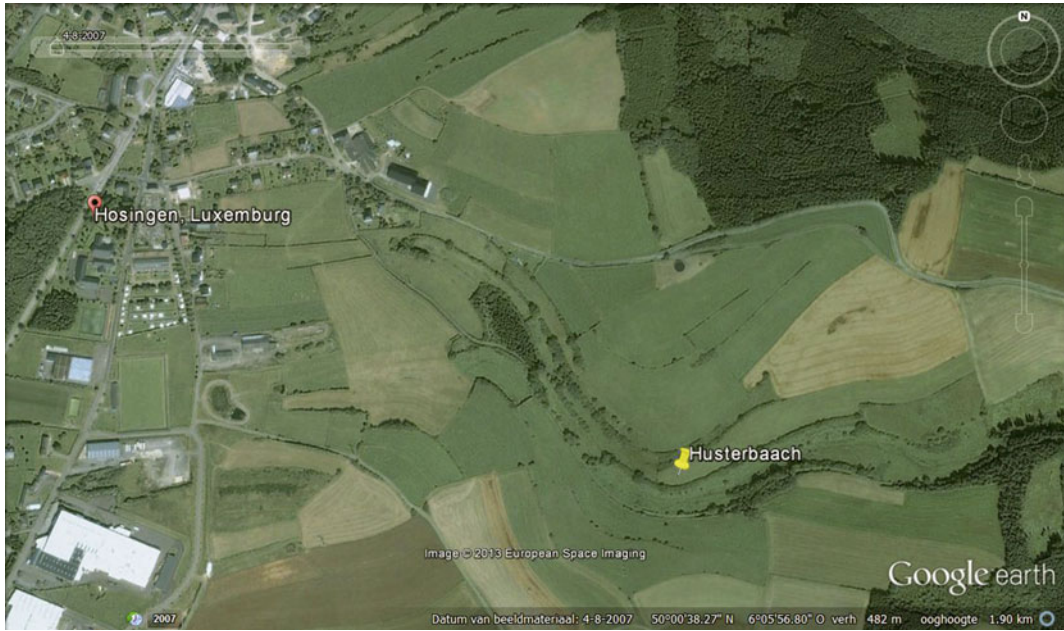


Fig. 3.10 Husterbaach valley and sample site on Google Earth

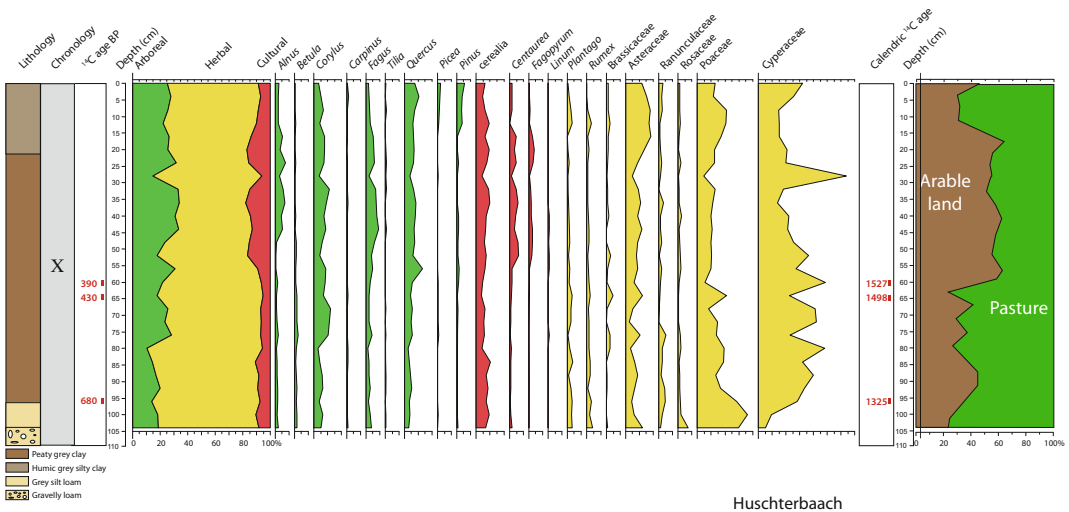


Fig. 3.11 Pollen diagram Husterbaach

percentages of *Plantago* and Poaceae, below 60 cm in particular, indicate that extensive grasslands were present. *Plantago* was one of the most important plants on ancient rough pastures. But also arable indicators are present, indicating

that a part of the surface was used for the cultivation of cereals.

After 1500 AD the texture of the valley floor sediments changed from peaty clay to humic clay, due to increasing soil erosion. The land use

diagram shows an increase of the arable indicators on the expense of the pasture indicators between 1500 and 1800 AD. Also, the cultivation of buckwheat started around 1500 AD. Most likely, arable land extended on the slopes, and pasture confined to the valleys, which is in agreement with the low values of *Plantago*.

The remarkable decline in the arable land/pasture since 1800 is probably associated with introduction of the potato, which rapidly became an important food supplier. In contrast to pollen grains of cereals, grains of the potato cannot fossilize and are absent in pollen spectra.

3.3.2.4 Dirbaach Valley Alluvium

Profile Dirbaach-1 is situated in the upper catchment of the Dirbaach valley, at altitude 375 m (Fig. 3.12). This profile is a sequence of peaty and loamy beds, deposited on the gravelly basement. The protected position in the upper part of the Dirbaach catchment made it possible that the peaty deposits have not been disturbed

during the Subboreal and Subatlantic. The pollen record of Dirbaach-1 (Fig. 3.13) fits in the upper part of the Roudbaach diagram (Fig. 3.2) between 55 cm depth and the surface. The spectra of zone VIII (post sedimentary pollen, infiltrated in the gravelly basement) show high percentages arboreal pollen, especially *Quercus*, *Tilia* and *Corylus*, the latter species probably occurring especially at the borders of the forest and the clearings. The spectra of Zone IX show increasing percentages of herbal pollen, which reflects the start of deforestation and agriculture. Also, *Tilia* disappears and *Fagus* appears, which reflects the transition of the Quercetum mixtum into the Fageto-Quercetum. Profile Dirbaach-2, with altitude 355 m (Fig. 3.12), is situated 800 m downstream from Dirbaach-1. In this profile, the deposition of alluvial sediments started on the gravelly basement around 850 AD. At that time, the flow of colluvial/alluvial sediments, due to the progress of human land management, reached this part of the valley bottom.

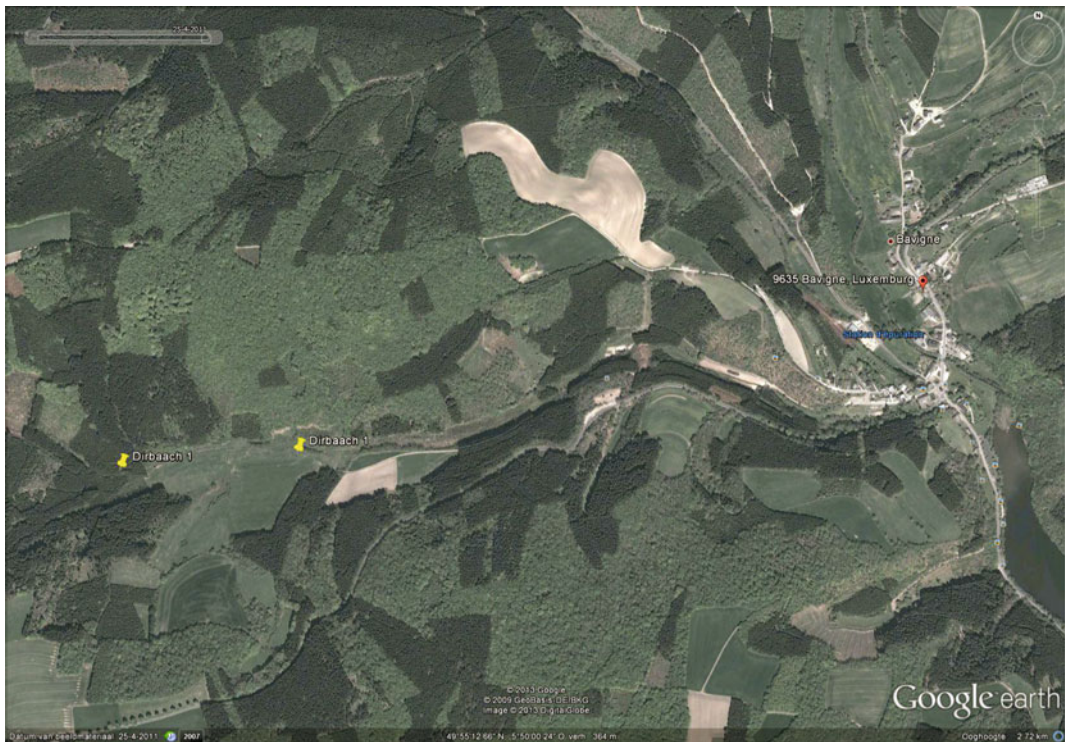
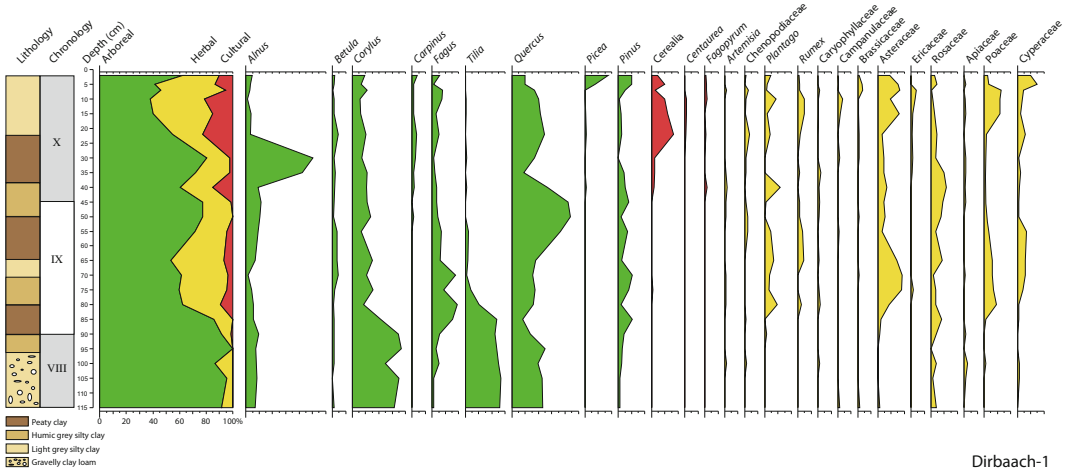
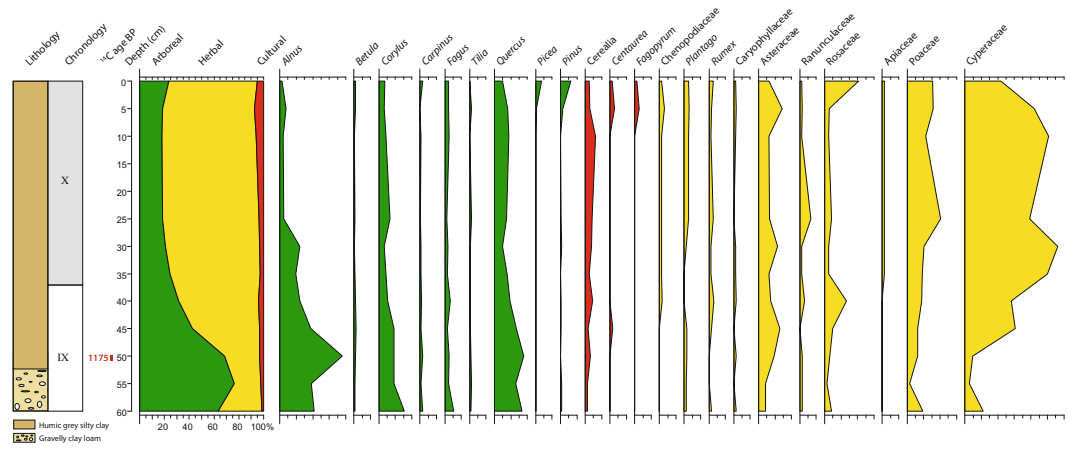


Fig. 3.12 Dirbaach valley on Google Earth with the two sample locations



Dirbaach-1

Fig. 3.13 Pollen diagram Dirbaach-1



Dirbaach-2

Fig. 3.14 Pollen diagram Dirbaach-2

The pollen record of Dirbaach-2 fits in Dirbaach-1 from 55 cm depth and the surface (Fig. 3.14).

3.3.2.5 Birkbaach Valley Deposits

The Birkbaach valley (Figs. 3.15 and 3.16) is an incision in the Lias cuesta, north of Beaufort. Deforestation resulted in an increase of soil erosion and deposition on the valley bottom. It is difficult to accurately estimate the amounts of sediment deposited on the valley bottom and transported by the water. It is thus not possible to

estimate the lowering of the land surface in the feeding area, associated with agricultural land management. But the evolution of the valley bottom can still be reconstructed (Fig. 3.17): absence of older sediments, fluvial incision during the Early Holocene, and deposition due to human impact during the Late Holocene as recorded in the pollen diagram Birkbaach (Fig. 3.18). Based on radiocarbon dating, the colluvial/alluvial deposition on the valley bottom started around 2040 BP (300 BC). The pollen diagram Birkbaach lacks a clear zoning, which is

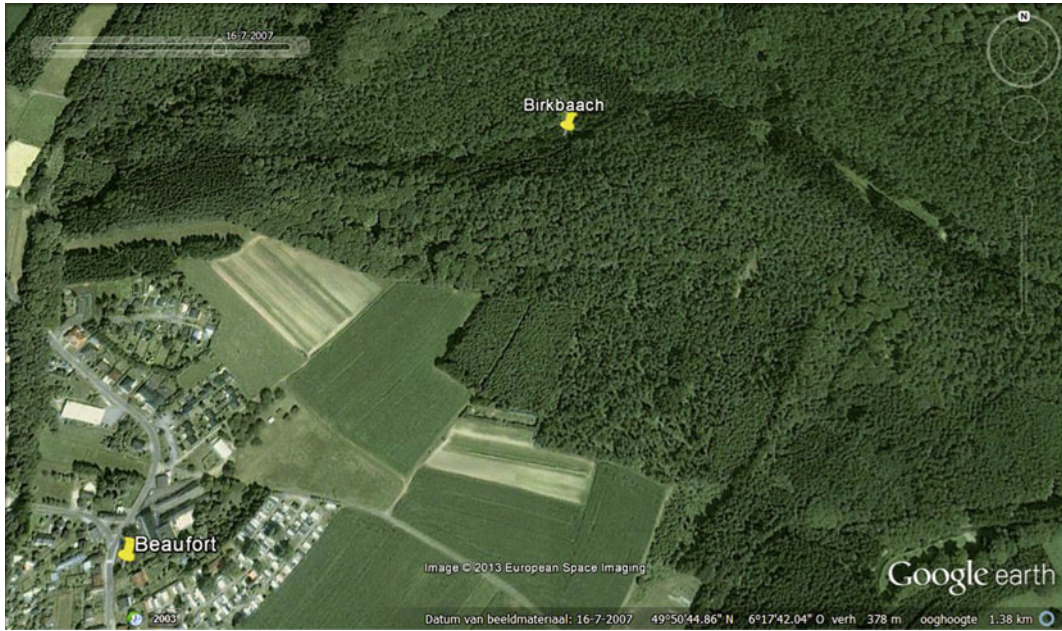


Fig. 3.15 Birkbaach valley with sample point Birkbaach on Google maps

caused by the mix of the normal pollen influx and pollen provided by slope processes. At the sample site, the altitude of the valley floor before the Roman Time was 1.5 m below the present level. Similar results have been reported from catchments in Germany (Zolitschka et al. 2003).

3.3.3 Pollen Records of Mardel Deposits

The occurrence of mardels is characteristic for the geomorphology of the Gutland Plateau, which can be defined as small closed depressions (diameter 10–40 m; depth 1–3 m). The genesis of mardels has been discussed in various studies. In older publications, the development of mardels is ascribed to natural evolution under periglacial conditions or karst processes (Lucius 1941, 1948; Slotboom 1963; Braque 1966; Barth 1996; Thoen and Hérault 2006). In more recent publications, mardels were interpreted as anthropogenic excavations (Etienne et al. 2011).

In the Gutland, mardels occur on the Steinmergelkeuper (km1) and Pseudomorphosenkeuper (km3). Slotboom (1963) interpreted these depressions as natural mardels in subsidence basins, caused by the subsurface dissolving of gypsum veins in the Keuper formations. However, mardels were also found on the Strassen marls (li3), a formation without gypsum veins (Schmalen 2002). These mardels are probably historical clay quarries. Finally, some natural mardels occur in shallow elongated depression on crevasses in the Luxembourg Sandstone (li2), as shown in Slotboom and van Mourik (2015).

In the present landscape, mardels are filled with clayey colluvium with a Stagnosol (clayic, colluvic), and they contribute as wetlands significantly to the biodiversity of the landscape. The age of the mardel deposits is Post-Roman. Clay has been extracted in Celtic and Roman Time for the production of pottery, as confirmed by the finds in the neighborhood of mardels (Schmidt 1995; Jacoby 2011). Most of the



Fig. 3.16 Picture of the Birkbaach valley bottom

mardels on the km1 and km3 are probably also abandoned quarries. It is now assumed that they developed as shallow depressions with moist soils, and have been selected as favorite sites for clay extraction in Roman Time or later.

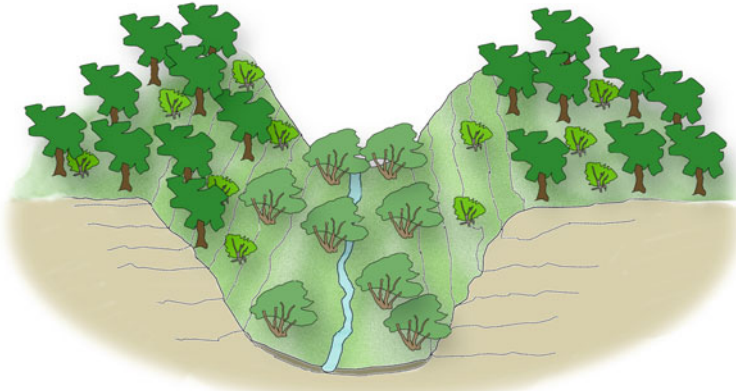
The development of mardels on the Keuper marls started in the Early Holocene, and it is noticeable that the investigated colluvial sediments in them have been dated as Post Roman (Etienne et al. 2011; Slotboom and van Mourik 2015). It is very likely that Pre Roman clayey colluvial deposits have been extracted in Celtic and Roman Time, together with the loamy topsoil in mardels, developed on the km1 and km3. Under deciduous forest, the controlling soil process was lateral leaching of clay (Cammeraat and Kooijman 2009) and depressions in the slope of the plateau were sediment traps (see also Chap. 10). An archaeometrical test of the composition of mardel clay and local roman pottery

of the Biischtert archaeological site (Jacoby 2011) showed that Romans really used mardel clay (van Mourik and Braekmans 2016). Figure 3.19 show a typology of mardels, occurring on the Gutland plateau (Fig. 3.20).

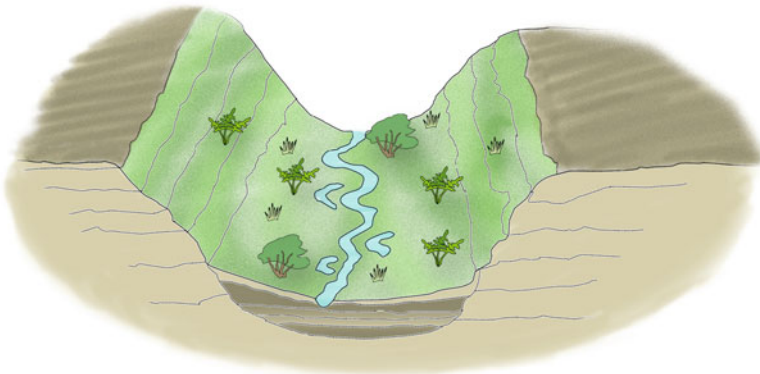
3.3.3.1 Elteschmuer Mardel

The Elteschmuer mardel is an alder carr on the Luxembourg Sandstone, 400 m east of the cuesta front (Fig. 3.21). A range of wetlands has developed in an elongated basin parallel to the cuesta front. Considering the vicinity of the cuesta front, it is likely that the shape is associated with patterns of tectonic crevices. The wetland vegetation is now dominated by *Betula* trees, *Molina caerulea* (L.) Moench and *Sphagnum* spp. (Fig. 3.22). Peat accumulated since around 3800 BP (Late Subboreal) on a medium fine humic sand. The water in the pond is mainly stagnating, and has a low alkalinity. The vertical

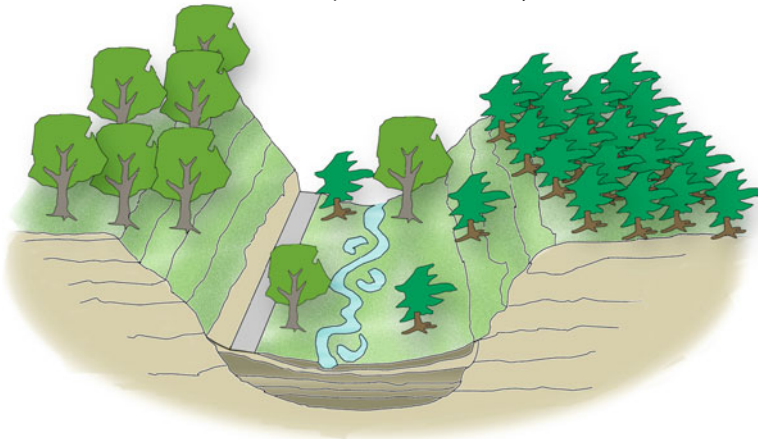
Human impact on the development of Birkbaach Valley



Cross section before deforestation; *Quercetum mixtum* on the plateau, *Alnetum* in the valley floor



Deforested landscape during Roman Time with accelerated denudation and alluvial deposition in the valley



Cross section of the present situation after reforestation with *Pinus* and *Fagus*

Fig. 3.17 Late Holocene valley evolution in a primary catchment

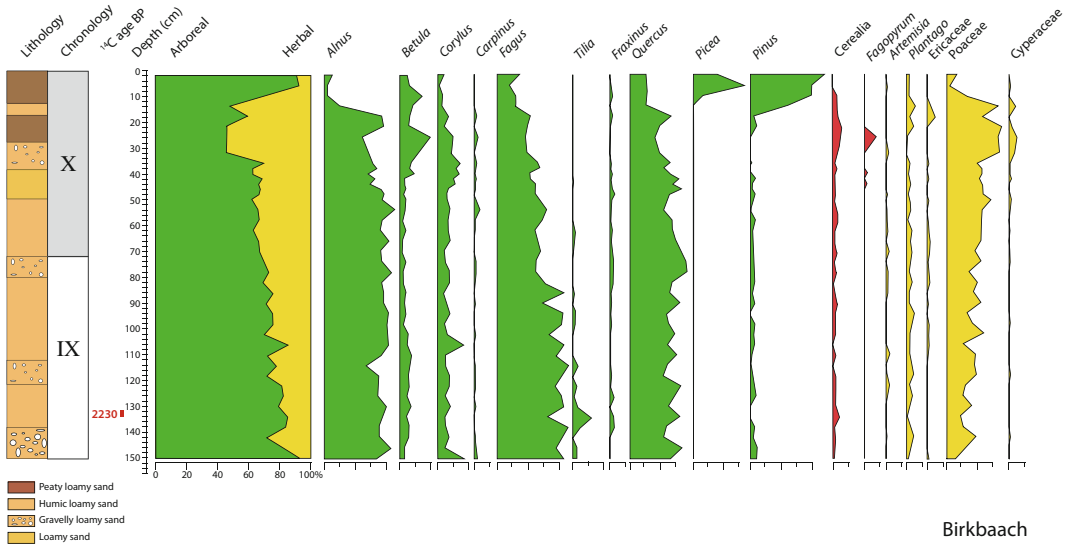


Fig. 3.18 Pollen diagram Birkbaach

drainage is probably limited by an impermeable bed of silicon-cemented sandstone. The low concentration inorganic carbonate (Table 3.3) indicates that the radiocarbon dates of the peat samples have not been seriously affected by reservoir effect.

The pollen spectra of Zone VIII are dominated by arboreal pollen: *Quercus*, *Corylus* and *Tilia* (Fig. 3.23). It is likely that the pollen content of the sandy substrate was the result of soil pollen infiltration (van Mourik 2001). Rejuvenation of the pollen composition could continue till the start of the peat accumulation around 3800 BC. Likely, the lowering of the temperature and subsequently the decrease of evapotranspiration by forest at the end of the Atlantic was responsible for soil wetting at that time. The oldest peat layer has sapric properties and consists of strongly decomposed plant tissues, indicating seasonal ground water level oscillations. *Betula*, not present in the sandy substrate, appears in the sapric peat horizon. Between 2560 and 1850 BP, the character of the sediment changed from sapric into fibric peat, and the increase of herbal

pollen reflected deforestation. Zone IX is characterized by decrease of *Tilia* and *Quercus* and increase of *Fagus*, which reflects the transformation of the Quercetum mixtum to Fageto-Quercetum.

The palynological registration of human impact on the landscape development is clearly expressed in the Subatlantic pollen. The diagram shows the Roman deforestation, in combination with the extension of *Cerealia* (35–30 cm), recovery of forest (*Quercus*, *Fagus*, *Betula*) during the Dark Ages (30–25 cm), Medieval extension of agriculture and the appearance of *Fagopyrum* (25–15 cm) and finally the extension of *Pinus* and the appearance of *Picea* (15–0 cm).

The *Fagus* curve in this record clearly shows four maxima in the Subatlantic, the first during the Roman Time from 0 to 200 AD (F1), the second from 700 to 800 AD (F2), the third around 1200 AD (F3) and the last from 1700 to 1900 AD (F4). These four maxima were also reported by Slotboom (1963), Persch (1950) and Daniels (1964) and usable as palynological chronomarkers.

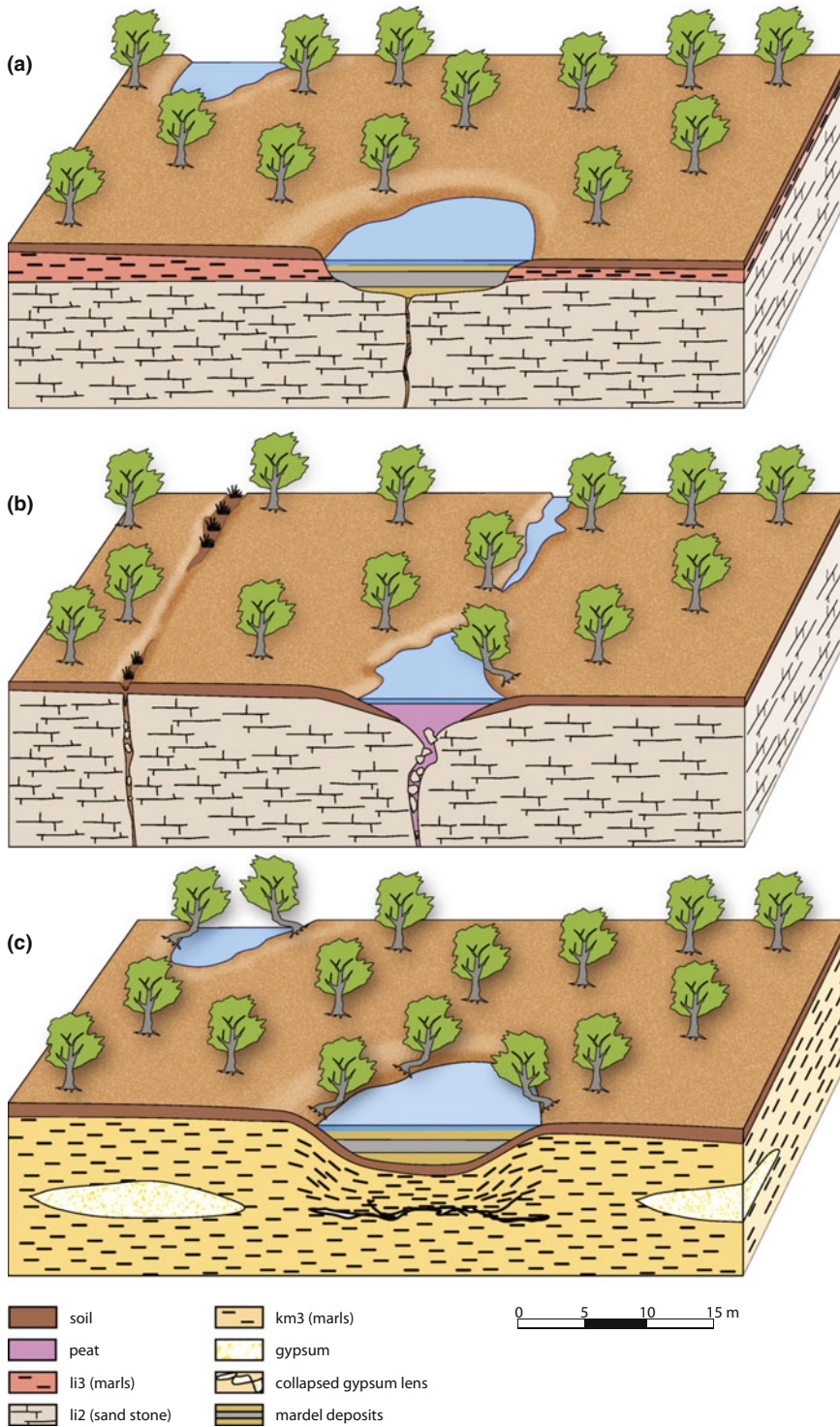
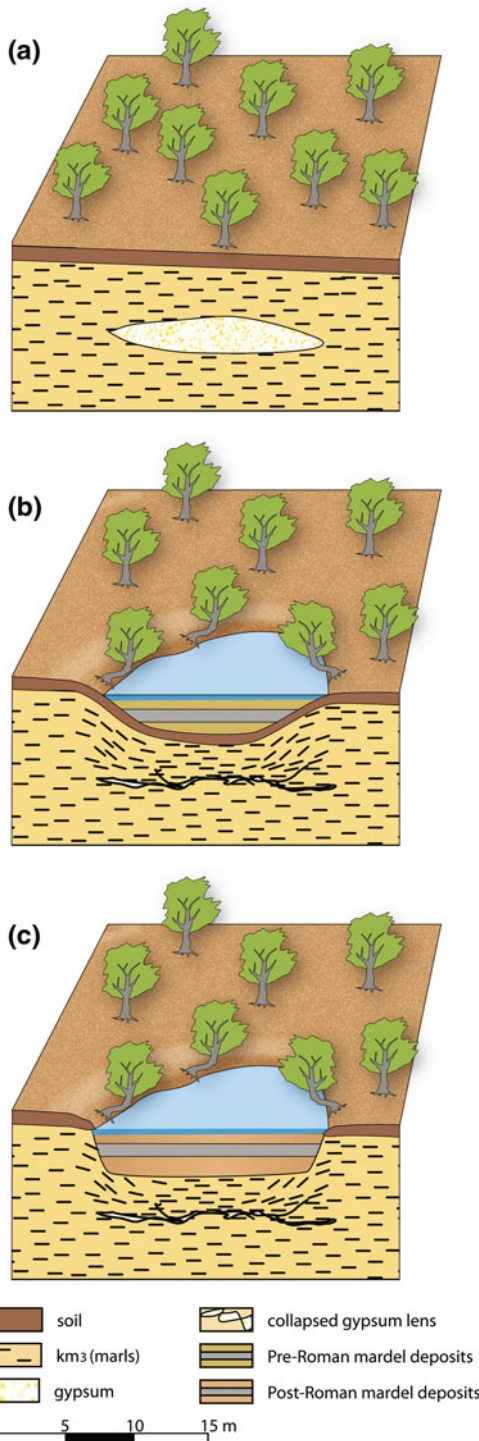


Fig. 3.19 Typology of mardels on the Gutland plateau. **a** Mardels on the Strassen marls (li3), historical quarries (clay excavations), filled with clayey colluvium. **b** Mardels on the Luxembourg Sandstone (li2), depressions determined by faults or joints, filled with

sandy colluvium and peat. **c** Mardels on the Steinmergelkeuper (km3), subsidence basins caused by sub-surface solution of gypsum lenses, filled with clayey colluvium



◀ **Fig. 3.20** The development of mardels on the Steinmergelkeuper. **a** Initial landscape on the Steinmergelkeuper (li3), with a subsurface gypsum lens. **b** The development of a subsidence basis, caused by dissolution of the gypsum lens, filled with pre-Roman clayey colluvium, burying the descended palaeosol. **c** Mardel after Roman clay excavation, filling with post-Roman clayey colluvium, burying the quarry floor

3.3.3.2 Brasert Mardel

The Brasert mardel (Fig. 3.24) is situated on the Steinmergelkeuper under Fageto-Quercetum, on a concave slope segment at 100 m distance from the local watershed. The soil around the mardel is a Gleyic Alisol, developed in a 140 cm thick clayey layer of weathered Keuper marls. The dominating soil process is the combination of surficial and subsurface (piping) leaching of clay (Cammeraat 2006). In the soils around the mardel, the weathering front in the (calcareous) Keuper marls was found at 140 cm below the surface level. The corresponding weathering front in the mardel was found 220 cm lower, suggesting a corresponding subsidence of the original surface, according to Lucius (1948) and Slotboom (1963), caused by the solution of a gypsum lens in the Steinmergelkeuper (km3). The mardel is filled with 270 cm colluvial beds, deposited on a dark grey gravelly basal layer. Based on the palynochronology (*Fagus maxima*), the deposition of colluvium started around 100 AD (Fig. 3.25). Older colluvial beds are not present. Most probably they have been excavated. A mardel is a trap for clayey sediments on a slope with active soil erosion. An explanatory process for the clay transport on the slope under Fageto-Quercetum is lateral erosion of dispersed clay and silt in the subsurface water flow, due to the combination of soil acidification and bioturbation by earthworms and moles (Cammeraat 2006; Cammeraat and Kooijman 2009; see also Chap. 10).

In general, the chronology of sediments in closed depressions allows estimation of the rate of surface lowering in the related feeding areas, if the accumulated volume and surface of the feeding area can be assessed. Applied to the

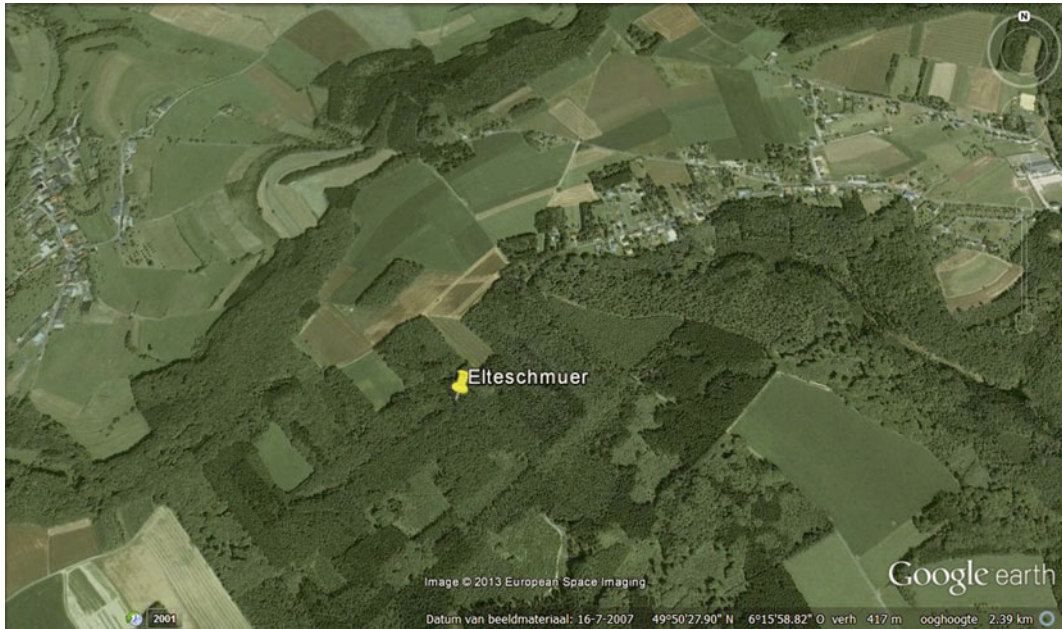


Fig. 3.21 Elteschmuer on Google earth

Brasert mardel, this reveals that the average rate of denudation at that particular site has been fluctuating considerably during the Subatlantic (Poeteray et al. 1984). The sedimentation rate was largest during the Little Ice Age between 1500 and 1800 AD (Fig. 3.26). This is most probably related to lower mean temperatures (Loehle 2007) and heavy winter precipitation (Buisman 1995, 2006) during this period. Based on the ratio arable/pasture indicators, the pollen record suggest, just as in the Husterbaach record, a temporal increase of arable land between 1500 and 1800 AD, outside the forest where Brasert is located.

3.3.3.3 Kalefeld Mardel

The Kalefeld mardel is situated on the Strassen marls (li3) in pasture on a smooth slope of 3% at a distance of 150 m to the local watershed (Figs. 3.27 and 3.28). Kalefeld borders in the east on the Oustert forest, where several dry mardels occur with an anthropogenic origin. Romans excavated clay from the li3, but also in historical time farmers extracted clay (Schmidt 1995).

Based on the palynochronology, the sedimentation of grey silty clay on a floor of resistant sandstone started around 1200 AD (F3). The absence of soil erosion and mardel deposition before 1200 AD can be explained by the youth of this depression. The pollen diagram Kalefeld shows two periods of forest recovery (Fig. 3.29). The lower tree-dominated part of the record reflects recovery of the forest between 1200 and 1500 AD. Around 1500 AD, *Fagopyrum* appeared, the synanthropic indicators increased and the arboreal pollen content diminished. This reflects a short period with extension of arable land during the Little Ice Age. The color of the deposited silty clay changed from grey to light grey, indicating a lower humus content. After a relatively short period dominated by arable land use, the forest recovered again. The *Fagus* curve shows the F4 maximum (1700 AD) at 30 cm depth. The color of the deposited silty clay changed from light grey to grey. Because *Picea* appears at a depth of 10 cm, simultaneously with an increase in *Pinus* percentages, this level may be dated as 1800 AD.



Fig. 3.22 Elteschmuer mardel on the Li2. **a** Wetland vegetation in the Elteschmuer mardel. **b** Crooked trees at the edge of the Elteschmuer mardel, indicating still active mass movement

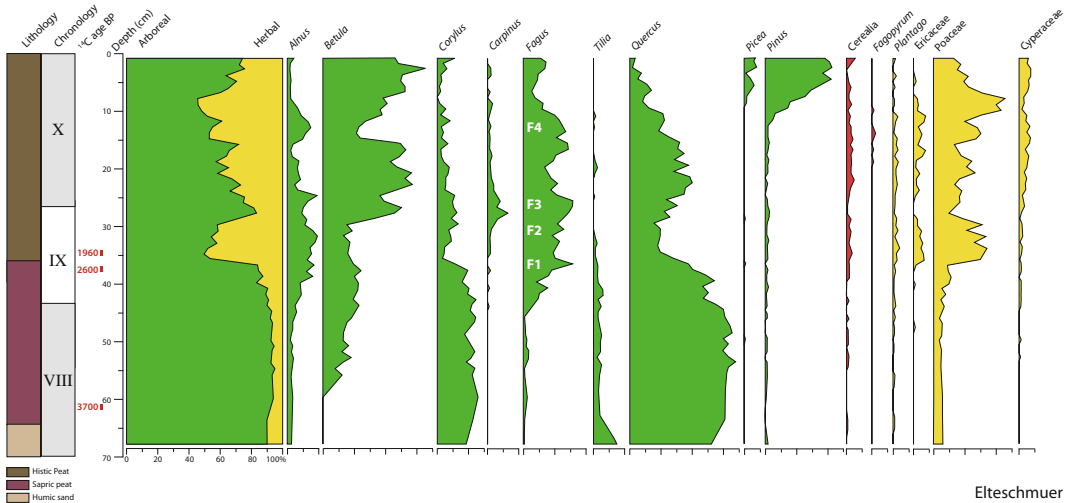


Fig. 3.23 Pollen diagram Elteschmuier

3.4 Discussion

The aim of this palynological study was to reconstruct the Holocene vegetation development of the Gutland and the changes in environmental conditions, resulting in the deposition of alluvial and colluvial sediments. Comparison of the pollen records with Holocene and Subatlantic temperature records (Schönwiese 1995; Loehle 2007) and historical data made it possible to reconstruct the effects of climatic oscillations and agriculture on the Subatlantic landscape development as well.

3.4.1 Interpretation Aspects of Pollen Spectra from Valley Floor and Mardel Deposits

The interpretation of pollen records of peat, colluvial and alluvial deposits is complicated by several factors. The pollen content of peaty deposits is supposed to be syn-sedimentary and the palynochronology is underpinned by reliable ^{14}C dates (van Mourik 2001). Still, there are some complications in the translation from pollen scores to vegetation types (Faegry and Iversen 1989). It is known that wind-pollinated species

are overrepresented and that insect-pollinated species are underrepresented in pollen spectra. Some species, such as potato, are even absent because the pollen grains do not fossilize. Also, the pollen production of a monoculture of *Quercus* is $\approx 35 \times 10^6 \text{ a}^{-1}$, and of *Fagus* $\approx 20 \times 10^6 \text{ ha}^{-1}$ (Andersen 1970). Consequently, a displacement of *Fagus* by *Quercus* inside a forest stand will result in increase of the arboreal pollen score, but this cannot be translated in forest extension (Faegry and Iversen 1989). Optimal environmental conditions for the Fageto-Quercetum are relatively base-rich substrates, a mean annual temperature of 7–9 °C, an annual precipitation of 600–800 mm and a topographical altitude of 200–550 m. Fluctuations in temperature and precipitation affected the ratio between *Quercus* and *Fagus* trees. A colder and wetter climate during the Dark Ages and the Little Ice age promoted the extension of *Quercus* trees at the expense of *Fagus*, while warmer and moister conditions during the Roman Time and Middle Ages promoted the extension of the *Fagus* trees (Firbas 1949; Fanta 1995).

Forest management can also affect the pollen production of tree species, and disturb the ratio between pollen scores and presence in the vegetation. A good example is the recovery of pollen production of *Alnus* trees with a factor 18 after a



Fig. 3.24 Brasert mardel. **a** Brasert mardel on Google earth. **b** The sampled Mardel on the Km1 under Fageto-Quercetum. **c** Second mardel on the Km1, 500 m west of the sampled mardel; on the foreground erodible clayey castings of soil inhabiting animals



Fig. 3.24 (continued)

period of coppice management (Faegry and Iversen 1989). Probably, the high scores of *Alnus* in Diagram Dirbaach-1 (Fig. 3.13) at 35–30 cm reflect the recovery of Alder trees during the Dark Ages.

The interpretation of pollen records of colluvial and alluvial loamy deposits is subjected to additional problems (van Mourik 2001). Firstly, the pollen content of the basal layer (the Late Glacial gravelly basement in the valleys or palaeosols in mardels) is post sedimentary. Under stable and vegetated conditions, pollen will infiltrate by bioturbation and survive decay in protecting soil aggregates (van Mourik 2003). Consequently, the real age of the sediments is older than the palynological. Secondly, the pollen composition of the sediment is a mix of the regular aeolian pollen influx, and pollen present in eroded and transported material. Consequently, species occurring on eroded slopes can

be overrepresented in pollen extractions of colluvial and alluvial deposits.

3.4.2 Reconstruction of the Holocene Environmental Development

The reconstruction of the Holocene vegetation development (Fig. 3.30) is based on the pollen records of Roudbaach and Boeckenwiesen. The same trends in the vegetation development have been reported by Coûteaux (1970) and Schwenninger (1989). In the Late Glacial (III) and Preboreal (IV), the vegetation had an open character. The pollen spectra show high scores of herbal pollen, and *Betula* and *Pinus* are the dominant arboreal pollen species. During the Boreal (V), the development of deciduous forest started. The spectra show low scores of herbal pollen, and

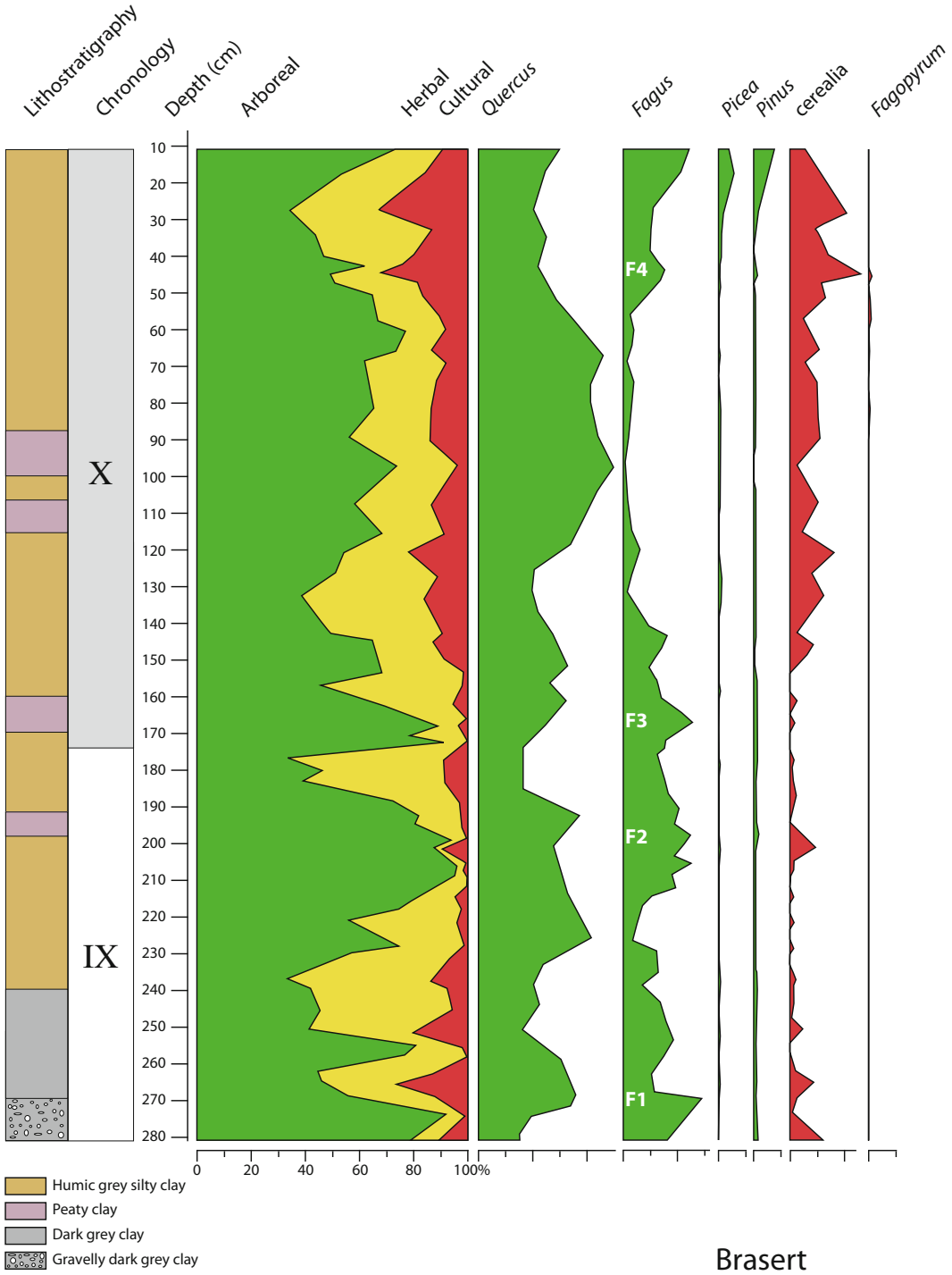


Fig. 3.25 Pollen diagram Brasert

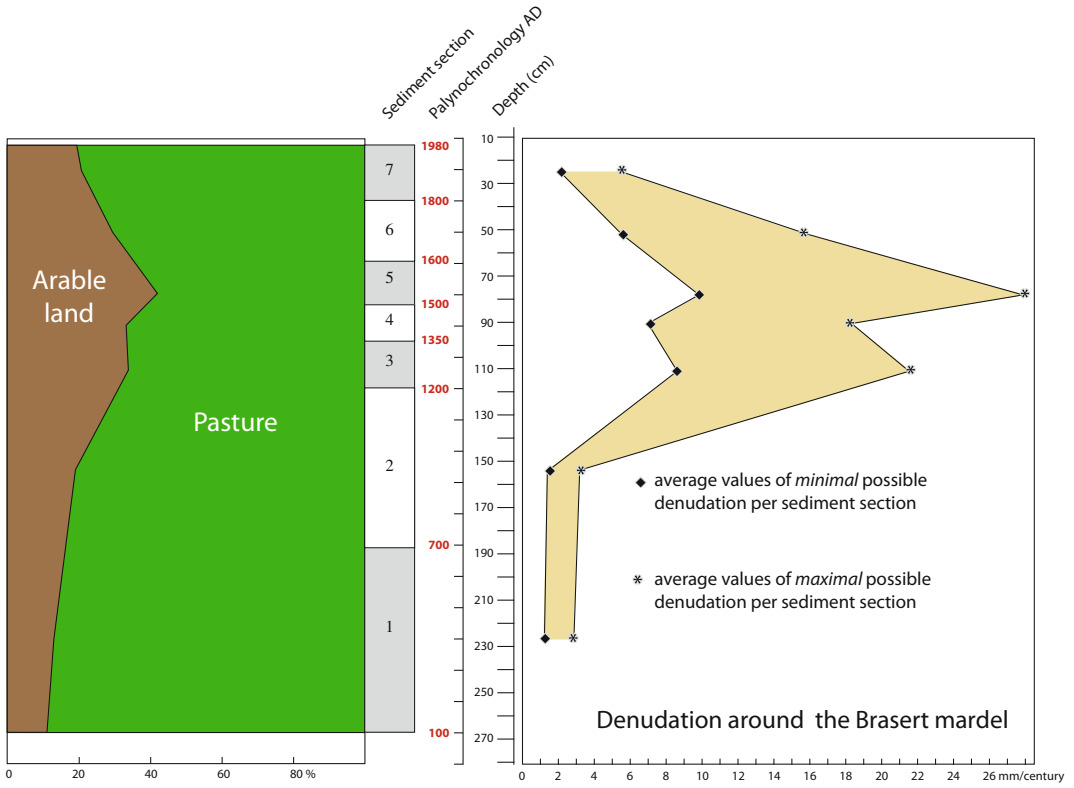


Fig. 3.26 Diagram of the pasture/arable ratio and the estimation of denudation rates

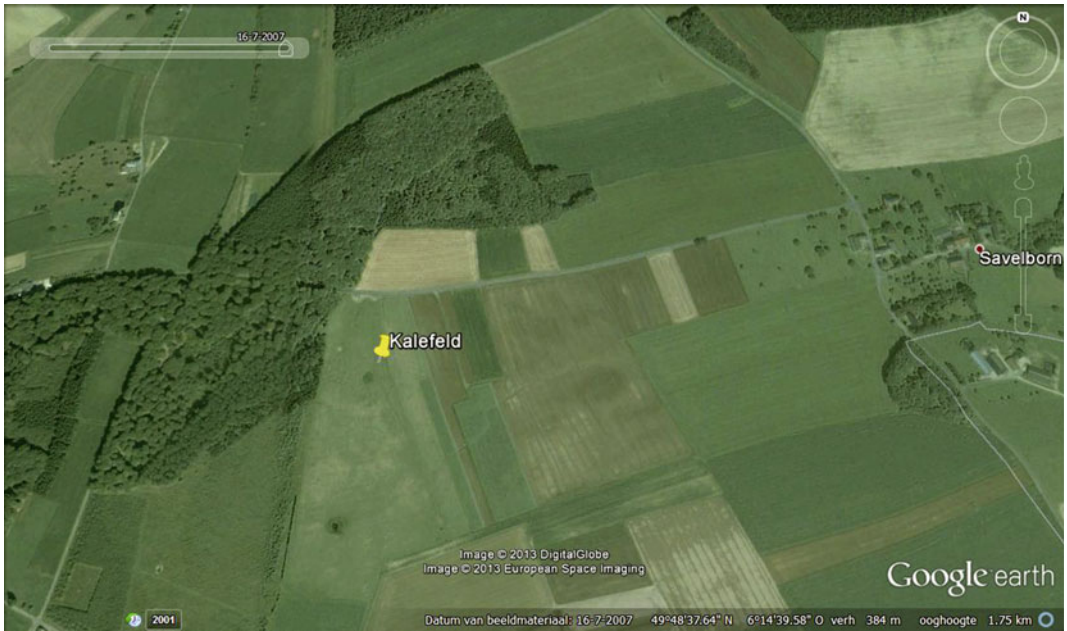


Fig. 3.27 Kalefeld on Google Earth



Fig. 3.28 a Picture of the Kalefeld mardel on the Li3 in pasture; b Picture of one of the mardels in the Oustert forest, 150 m east of the Kalefeld mardel

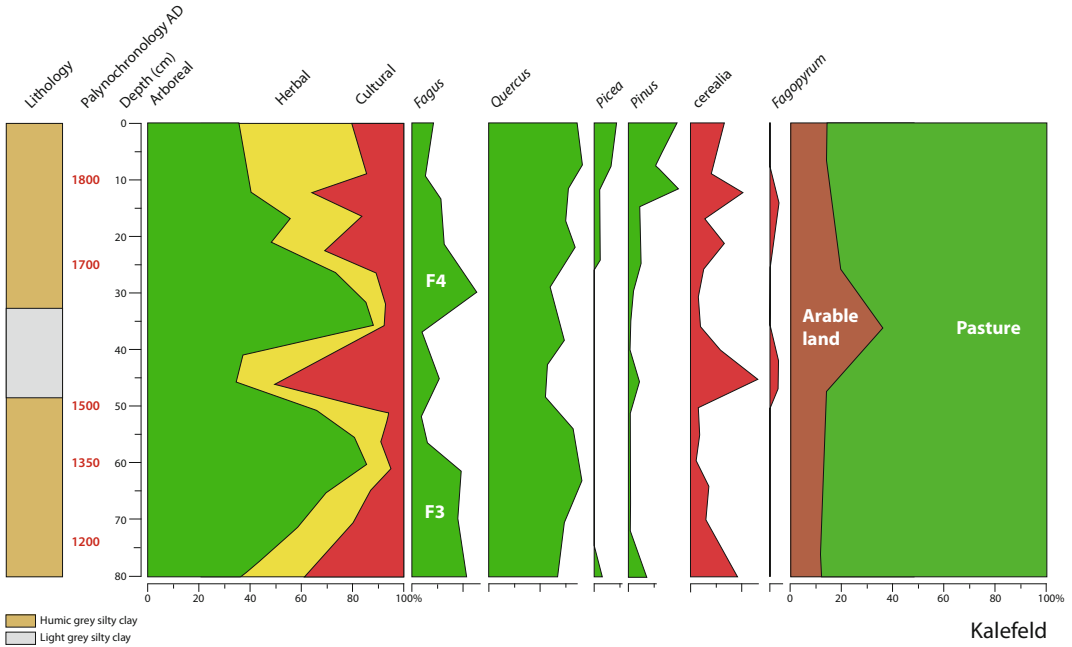


Fig. 3.29 Pollen diagram Kalefeld

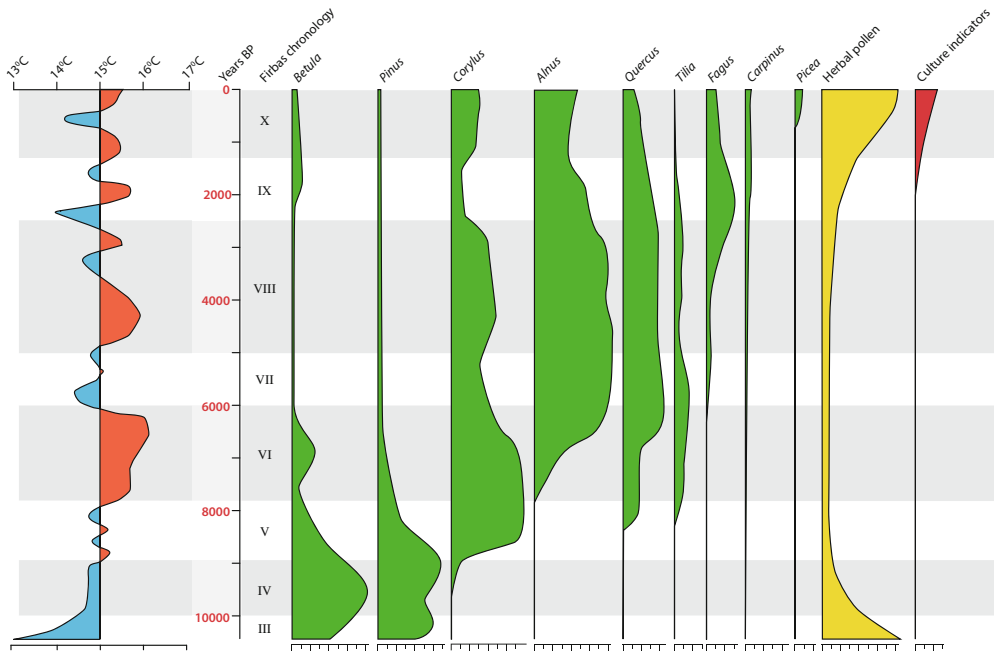


Fig. 3.30 The Holocene vegetation development in the Gutland based on the pollen records Roudbaach (Fig. 3.4) and Boeckewiesen (Fig. 3.8) combined with the average near surface temperatures of the northern hemisphere (Schönwiese 1995)

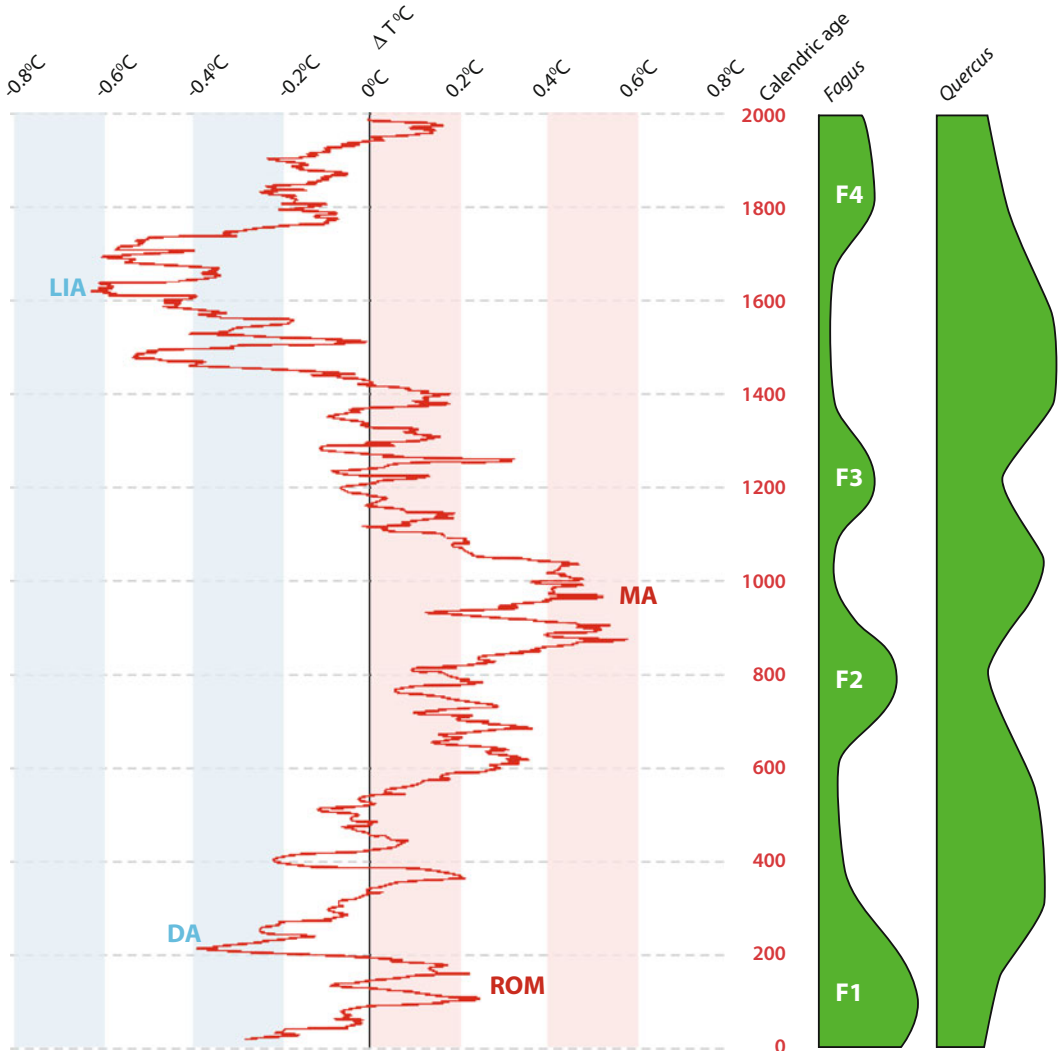


Fig. 3.31 Deviations of the mean temperature of the northern hemisphere from 16 to 1980 AD (Loehle 2007) compared with the *Fagus* chronology as recorded in the

pollen diagrams Elteschmuer (Fig. 3.25) and Brasert (Fig. 3.29). ROM Roman Time, DA Dark Ages; MA Middle Ages; LIA Little Ice Age

within the arboreal pollen, *Betula* and *Pinus* are decreasing and *Corylus* increasing. During the Atlantic (VI, VII), a deciduous forest developed. The pollen spectra are dominated by *Alnus*, *Quercus* and *Tilia*. In palynological studies, the Atlantic forest is indicated as Quercetum mixtum, characterized by the sum of the pollen species *Quercus*, *Tilia*, *Ulmus*, *Fraxinus* and *Acer* (Feagri and Iversen 1989). In the course of the Subboreal (VIII), *Tilia* decreases, while *Fagus* and *Carpinus* appear. The forest

transformed from Quercetum mixtum into Fageto-Quercetum. The Subatlantic (IX, X) is characterized by deforestation (decrease of arboreal pollen) and extension of agriculture (appearance of culture indicators). Finally *Picea* appeared and *Pinus* extended in the pollen records after 1800 AD due to forest plantations, started by the administration of Maria Theresia (Riezebos and Slotboom 1974).

The Subboreal arrival of *Fagus* and *Carpinus* in the Gutland is supposed to be the effect of

natural migration (Feagri and Iversen 1989), but during this period, the start of human impact on the vegetation was also registered. There is no consensus in the literature on the question whether the decline of *Tilia* in the Quercetum mixtum during the Subboreal is the consequence of human activities, or of the 2–3 °C decline in summer temperatures, but Firbas (1949) suggested a crucial role of the climate. Fanta (1995) suggested that, in the northwestern lowlands, *Fagus* arrives in the Subboreal by natural migration. The decline of *Tilia* and extension of *Fagus* during the Celtic/Roman Time (F1) was promoted by a moister soil regime and increasing temperature, but in addition, the Neolithic population contributed to the decline of *Tilia* by tree cutting and using the leaves, bark and wood. Consequently, the Subboreal and Subatlantic forest development must have been triggered by both natural and cultural forces (Zolitschka et al. 2003).

Based on the pollen record, we can conclude that before the Subatlantic, the rivers were able to transport the sediment load, supplied by the geological rate of weathering and denudation. In this period, geomorphological stability dominated the landscape evolution. The pollen records of alluvial valley floor deposits pointed to an acceleration of soil erosion and alluvial deposition in the Subatlantic. It is difficult to separate the impact of natural forest dynamics from anthropogenic deforestations and extension of agriculture. There are no references available to estimate the rate of soil erosion before the arrival of *Fagus* and the fall of *Tilia*, but possibly the change from Quercetum Mixtum to Fageto-Quercetum has been responsible for increased soil erosion to some extent. The valley floor profiles show that the deposition rate of alluvium was very low before the arrival of *Fagus* and *Carpinus* in the Gutland, indicating a low rate of soil erosion under the Quercetum mixtum. It is assumed that the *Fagus* and *Carpinus* trees in the Fageto-Quercetum promote soil acidification, clay dispersion and soil erosion (Cammeraat 2006; Cammeraat and Kooijman 2009; see also Chap. 10). Data about soil acidification and erosion under the former Quercetum

mixtum are however not available, which makes it complicated to ascribe the increase of soil erosion to the changing forest composition, climatic oscillations, land use or a combination of these triggers (Zolitschka et al. 2003).

The increased denudation in the Subatlantic resulted in colluvial slope covers and alluvial fills of valleys (Riezebos and Slotboom 1974; Kwaad and Mûcher 1976). Jungerius (1980) estimated the Holocene denudation rate of the Gutland cuestas by comparing the actual concentrations of Eifel minerals in the soil horizon, subjected to bioturbation, with the original concentrations short after the Eifel eruption (12,920 CalBP; Lucius 1961; Jungerius and Riezebos 1976). The mean Holocene surface lowering of the Lias cuesta was estimated at 4–5 cm per 1000 year (see also Chap. 2). However, these estimations concern the whole Holocene, without differentiation in periods with lower and accelerated rates of denudation. The results of the Brasert record (Poeteray et al. 1984) show an estimated mean Subatlantic surface lowering in the feeding area (under Fageto-Quercetum) of 6 cm per 1000 year. However, the mean estimated surface lowering during the relative cold and wet period between 1400 and 1700 AD amounts to 18 cm per 1000 year. In this period, a maximal extension of arable land surface was interpreted (Fig. 3.26). Based on this information, it can be concluded that the denudation rate during the Subatlantic was variable, with a maximum in the period between 1400 and 1700 AD.

Special attention deserves the Subatlantic *Fagus* curve as recorded in the mardels Elteschmuer (Fig. 3.25) and Brasert (Fig. 3.29). The *Fagus* maxima in pollen records can be used as palynological chronomarkers. Slotboom (1963) distinguished four *Fagus* peaks during the Subatlantic. Other researchers found similar results in pollen records of Aamsveen, Eastern Netherland (Daniels 1964) and Hohen Venn, Belgium (Persch 1950). The *Fagus* minima and maxima correlate with the Subatlantic climatic oscillations (Loehle 2007; Fig. 3.31). Maxima occurred in the warmer periods from 0 to 200 AD (F1), 700–800 AD (F2), around 1200 AD (F3) and from 1700 to 1900 AD (F4). Slotboom

(1963) and Daniels (1964) pointed to the correlation of the decline of *Fagus* during the intermediate cooler phases with a more oceanic character of the climate.

The climatic oscillations affected not only the forest composition, but also the geomorphological processes. The accelerated soil erosion between 1300 en 1700 AD must be ascribed to the effects of the Little Ice Age, with its maximal expression between 1551 en 1621 AD (Buisman 1995–2006). The lower winter temperatures and the increase of precipitation were responsible for soil erosion under the barren trees of the Fageto-Quercetum. Buisman (1995–2006) describes documents, pointing to extreme cold and winters with increased snowfall in the northwest European lowlands during the seventeenth century. Especially the abundant spring melt water streams must have been responsible for accelerated denudation, and deposition of colluvic loam on foot slopes and valley bottoms and in closed depressions.

Since Celtic/Roman Time, deforestations and extension of agriculture contributed to the denudation as well. The first settlements in the area date from the second century BC (Thill 1977). Between 58 and 51 BC, the Romans conquered Luxembourg and brought a turning point into the relation between man and landscape. They contributed to the development of public houses, shops, temples, settlements and large farms, known as *Villae*. They introduced also ‘modern’ agricultural techniques, resulting in the extension of pasture and arable land. They created a dense road network, still visible in the landscape, to connect agricultural areas, the local markets and military camps (Thill 1977). The Roman Time is clearly recorded in the pollen diagrams Roudbaach (Fig. 3.4), Boeckenwiesen (Fig. 3.8), Dirbaach (Fig. 3.13) and Elteschmuer (Fig. 3.23).

During the Dark Ages from 400 to 800 AD, a turbulent unsettling took place. The Roman Empire collapsed and the society transformed. Mass migration occurred and the population growth stagnated. The Dark Ages are climatically characterized by a cold oscillation (Figs. 3.30 and 3.31). Lowering of the mean

temperatures during the Dark Ages is also expressed in records of alluvial valley deposits in Germany (Zolitschkaa et al. 2003) and the Alpine region (Patzelt 1975). The Dutch coastal area was subjected to a transgression (Duinkerken-2), indicating increasing oceanic climatic conditions (Berendsen and Stouthamer 2001). Probably climatic deterioration affected agricultural harvesting, and contributed to stagnation or even decline of the population in Luxembourg. In some pollen records, the Dark Ages are expressed by forest recovery as visible in the diagrams Roudbaach (Fig. 3.4), Boeckenwiesen (Fig. 3.8), and Dirbaach (Fig. 3.13).

During the tenth to fourteenth century, the climate was warmer than in the preceding period (Fig. 3.31). Pollen records show changing land use: forests was cleared and agriculture expanded into the hills. Palynologically, this period is clearly recorded in the pollen diagrams Roudbaach (Fig. 3.4) and Boeckenwiesen (Fig. 3.8).

The Mediaeval and Post Mediaeval agricultural history is clearly registered in pollen diagram Husterbaach (Fig. 3.11). Striking is the extension of arable land at the expense of pasture in a deforested landscape, from 1500 to 1800 AD. Palynologically, the Little Ice Age is, in contrast to the Dark Ages, not expressed by decline of agricultural activities and forest recovery. Farmers continued with the development of the cultural landscape, but probably they switched to crops resistant to colder and wetter climatic circumstances (Slicher van Bath 1960). The records of Husterbaach (Fig. 3.11), Brasert (Fig. 3.25) and Kalefeld (Fig. 3.29) show a clear palynological registration of the temporally increase of arable land during the Little Ice Age.

3.5 Conclusions

The pollen records of the valley deposits document the development of a deciduous forest (*Quercetum mixtum*) from the Early Holocene till the Subboreal. During this period, the fluvial discharge was in balance with the sediment load, supplied by natural slope processes. Fluvial incision took place in the primary catchments.

Downstream, the sedimentation of peaty loam started, but the sedimentation rate was relatively low. This balance was disturbed in the course of the Subboreal due to three factors:

1. During the Subboreal, *Fagus* and *Carpinus* arrived in the area, and the Quercetum mixtum transformed into Fageto-Quercetum. Clay dispersion and erosion in the soils below this forest type may have contributed to the deposition of colluvial covers on foot slopes and alluvial sediments on valley bottoms.
2. In the course of the Subboreal, the first culture indicators appeared. Deforestation and extension of agriculture contributed to the acceleration of soil erosion.
3. Climatic oscillations, in particular the Dark Ages and the Little Ice age, are responsible for changes in precipitation, land use and soil erosion.

In contrast to valley floor deposits, deposits in the closed depressions of the mardels are suitable for the reconstruction of the sedimentation rate. In particular the Little Ice Age was recorded as a period with accelerated sedimentation. In mardels on slopes under forest, the increasing precipitation and clay dispersion was the main trigger, and in mardels under agriculture the temporal extension of arable land. Comparison of the denudation rate in the feeding area of the Brasert mardel with the estimated Holocene regional denudation on the Lias cuesta indicates that the denudation accelerated in the Subatlantic, with a maximum in the Little Ice Age.

Acknowledgements This chapter is honourably dedicated to the late Dr. Ruud Slotboom. The first results of the research of the Gutland mardels have been published by him in his Ph.D. thesis (Slotboom 1963). Fifty years later, triggered by the contrasting results of researchers as Etienne et al. (2011), we decided to return to the Gutland to find new data to contribute to the controversial issue of natural vs anthropogenic mardel genesis. Some preliminary results concerning the mardels on the Strassen marls (pointing to anthropogenic genesis) have been published (Slotboom and van Mourik 2015) short before Ruud passed away in February 2015. The first author of this chapter decided to finish the Gutland mardel study with new diagrams of the mardels on the Keuper marls and to apply archaeometrical tests to correlate mardel deposits

and Roman pottery.

We express gratitude to the master students Hubert Mettievier Meijer, Frans Poeteray and Gijs Rering for the realization of their research master projects dedicated to the palynological studies of Luxembourg. We are grateful to Robert Colbach (Geological Service of Luxembourg), Tom Scholtes (forestry Medernach) and Marc Hoffman (forestry Beaufort) for their scientific advices about mardel genesis. Finally we like to thank Jan van Arkel (IBED, University of Amsterdam) for the production of the digital illustrations.

References

- Andersen ST (1970) The relative pollen productivity and pollen representation of North European trees. *Denmarks Geol Unders* R2(96):1–99
- Barth B (1996) Mardellen im Lotharingischen Gipskeuper. *Delatinnia* 22:7–60
- Behre KE (1980) The interpretation of anthropogenic indicators in pollen diagrams. *Pollen Spores* 23:225–245
- Berendsen HJA, Stouthamer E (2001) Palaeogeographic development of the Rhine-Meuse delta. The Netherlands, Van Gorcum, Assen, Netherlands
- Braque R (1966) Observation sur les mardelles du plateau nivernais. *Bulletin de l'Association française pour l'étude du quaternaire* 3(3):167–179.
- Buisman J (1995–2006) Duizend jaar weer, wind en water in de lage landen, vol 1–5. KNMI, Netherlands
- Cammeraat LH (2006) Luxembourg. In: Boardman J, Poesen J (eds) *Soil erosion in Europe*. Wiley, Chichester, pp 427–438
- Cammeraat LH, Kooijman AM (2009) Biological control of pedological and hydro-geomorphological processes in a deciduous forest ecosystem. *Biologia* 64:428–432
- Coüteaux M (1970) Etude palynologique des dépôts quaternaires de la vallée de la Sûre à Echternach et à Berdorf, et de la Moselle à Mertert. *Archives Sect Sc nat phys et math Inst Gr-Ducal de Luxembourg* 34:297–336
- Daniels AGH (1964) A contribution to the investigation of the Holocene history of the Beech in the Eastern Netherlands. *Acta Bot Neerl* 1:66–74
- Etienne D, Ruffaldi P, Goepf S, Ritz F, Georges-Leroy M, Pollier B, Dambrine E (2011) The origin of closed depressions in Northeastern France: a new assessment. *Geomorphology* 126:121–131
- Faegri K, Iversen J (1989) *Textbook of pollen analysis*, 4th edn. Wiley, Chichester
- Fanta J (1995) *Beuk (Fagus sylvatica) in het Nederlandse deel van het NW-Europees diluvium*. *Nederlands Bosbouw Tijdschr* 1995:225–234
- Firbas F (1949) *Spät und nacheiszeitliche Waldgeschichte Mitteleuropas nördlich der Alpen*. Band 1: *Allgemeine Waldgeschichte*. Gustav Fischer, Jena, Germany
- Heuertz AJ, Heyart H (1964) *Le alluvions de l'Alsette entre Pettange et Moesdorf et leur contenance préhistorique*. *Institut Grand-Ducal de Luxembourg, section des Sciences*. *Arch Nouv Série*, Tome XXX:271–296

- ISRIC-FAO (2006) World Reference Base for Soil Recourses 2006. World soil resources reports 103
- Jacoby R (2011) Chronologie der Aktivitäten in der Biischtert. *De Viichter Geschitsfrënd* 10:7–10
- Jungerius PD (1980) Holocene surface lowering in the Lias cuesta area of Luxemburg as calculated from the amount of volcanic minerals of Allerød age remaining in residual soils. *Z für Geomorphol N.F* 24:192–199
- Jungerius PD, Riezebos PA (1976) The distribution of Laacher See ash west of the Eifel region. *Geol Mijnbouw* 55:159–162
- Kwaad FJPM, Mücher HJ (1976) The evolution of soils and slope deposits in the Luxembourger Ardennes near Wiltz. *Geoderma* 17:1–37
- Loehle C (2007) A 2000-year global temperature reconstruction based on non-treering proxies. *Energy Environ* 18 No. 7 + 8
- Lucius M (1941) Beiträge zur Geologie von Luxemburg: Die Ausbildung der Trias am Südrande des Eisleks. *Veröff Lux Geol Landesaufnahm.* B III
- Lucius M (1948) Geologie Luxemburgs; Erläuterungen zu der Geologischen Spezialkarte Luxemburgs, band V Service Géologique de Luxembourg
- Lucius M (1961) La présence de loess, de minéraux dense et de minéraux volcanique dans les dépôts meubles de plateaux de notre pays (Luxembourg). *Extrait du bulletin 1958 n° 63 de la Société des Naturalistes Luxembourgeois*
- Mook WG, Streurman HJ (1983) Physical and chemical aspects of radiocarbon dating. *First Symposium on ¹⁴C and Archaeology.* Groningen, *PACT* 8:31–55
- Moore PD, Webb JA, Collinson ME (1998) *Pollen Analyses.* Blackwell Scientific Publications, Oxford
- Osmond CB, Valaane N, Haslam SN, Uotila P, Roksandic Z (1981) Comparisons of $\delta^{13}\text{C}$ values in leaves of aquatic macrophytes from different habitats in Britain and Finland. *Oecologia* 50:117–124
- Patzelt G (1975) Unterinntal - Zillertal - Pinzgau - Kitzbühel. *Spät- und postglaziale Landschaftsentwicklung.* *Innsbrucker Geogr Stud Bd.2* 1975:309–329
- Persch F (1950) Zur postglazialen Wald- und Morentwicklung im Hohen Venn. *Decheniana* 104
- Poeteray FA, Riezebos PA, Slotboom RT (1984) Rates of Subatlantic lowering calculated from mardel-trapped material (Gutland, Luxembourg). *Z für Geomorphol* 1984:467–4821
- Riezebos PA (1987) Relic stratified screes occurrences in the Eislek (Grand-Dutchy of Luxembourg), approximate age and some fabric properties. *Travaux Scientifiques du Musée d'Histoire de Luxembourg XII*
- Riezebos PA, Slotboom RT (1974) Palynology in the study of present day hill slope development. *Geol Mijnbouw* 5:436–448
- Riezebos PA, Slotboom RT (1978) Pollen analysis of the Husterbaach peat (Luxembourg): its significance for the study of sub recent geomorphological events. *Boreas* 7:75–82
- Schmalen C (2002) Einige Mardellen Luxemburgs auf den Keuper-und Liasschichten des Forstamtbezirks Zentrum. *Diplomarbeit in Studiengang Umweltplanung an der Fachhochschule Trier, Standort Birkenfeld,* p 2002
- Schmidt G (1995) *Cartographie de biotopes de Medernach; le plateau des fermes de Savelborn.* *Oeko Fonds,* juin 1995
- Schmithusen J (1940) *Das Luxemburger Land; Landesnatur. Volkstum und bäuerliche Wirtschaft,* Leipzig
- Schönwiese C (1995) *Klimaänderungen: Daten, Analysen, Prognosen.* Springer, Heidelberg
- Schwenninger JL (1989) Pollen analysis and community structure of Holocene forests: a regional palynological study of the Middle and Upper Postglacial from semi-subhydric alder carr sediments at Berdorf (Luxembourg). *Bull Soc Nat Luxembourg* 89:157–196
- Slicher van Bath BH (1960) *De agrarische geschiedenis van West Europa.* Uitgave Spectrum, Aula 32
- Slotboom RT (1963) Comparative geomorphological and palynological investigation of the pingos (Viviers) in the Haute Fagnes (Belgium) and the Mardellen in the Gutland (Luxembourg). *Z für Geomorphol* 7:193–231
- Slotboom RT, van Mourik JM (2015) Pollen records of mardel deposits; the effects of Subatlantic climatic oscillations and land management on soil erosion in Gutland, Luxembourg. *CATENA* 132:72–88
- Thill G (1977) *Vor- und Frühgeschichte Luxemburgs.* Editions Bourg-Bourger, Luxembourg, p 1977
- Thoen D, Hérault B (2006) Flore, groups socio-écologique et typologie de mardelles forestières de Lorraine belge et luxembourgeoise. *Bull Soc luxemb* 107:3–25
- van Mourik JM (2001) Pollen and spores, preservation in ecological settings. In: Briggs EG, Crowther PR (eds) *Palaeobiology II.* Blackwell, Oxford, pp 315–331
- van Mourik JM (2003) Life cycle of pollen grains in mormoder humus forms of young acid forest soils: a micromorphological approach. *CATENA* 54:651–663
- van Mourik JM, Braekmans DJG (2016) *Mardellen Geografie* 2016:31–43
- van Mourik JM, Slotboom RT (2012) Palyno-ecological reconstruction of the impact of historical land use on soils and landforms. *EGU General Assembly Conference Abstracts* 2012/12575
- van Mourik JM, Slotboom RT, Mettievier Meijer H (2013) Palyno-ecological reconstruction of the impact of historical land use on soil erosion and colluviation in the basin of Brouch, Luxembourg. *EGU General Assembly Conference Abstracts* 2013/5954
- Verhoef P (1966) *Geomorphological and pedological investigations in the Redange-sur-Atter Area (Luxembourg).* *Publicaties van het Fysisch Geografisch en Bodemkundig Laboratorium van de Universiteit van Amsterdam*
- Zolitschka B, Behre KE, Schneider J (2003) Human and climatic impact on the environment as derived from colluvial, fluvial and lacustrine archives examples from the Bronze Age to the Migration Period, Germany. *Quatern Sci Rev* 22:81–110

Contrasting Hydrologic Response in the Cuesta Landscapes of Luxembourg

4

L. Pfister, C. Hissler, J.F. Iffly, M. Coenders, R. Teuling,
A. Arens and L.H. Cammeraat

Abstract

The Attert River basin in Luxembourg is characterised by a large variety of clean and mixed physiogeographical settings (i.e. topography, soil types, land use, bedrock geology, etc.). This in turn generates manifold configurations of rainfall-runoff transformation processes. Here, we provide experimental data from more than a decade of hydro-meteorological observations carried out in a nested catchment set-up, and develop on past and ongoing research on fundamental hydrological functions of catchments: water collection, storage and release. In a first section, we detail the characteristics of the Attert River basin and a set of 9 nested sub-catchments. The second section provides insights into the seasonal and spatial variability of hydrological responses along a wide range of landuse, soil and bedrock settings. The analysis of double-mass curves between precipitation and discharge provided insights into how certain physiogeographic characteristics control hydrological responses. In the third section, we develop on dynamic catchment storage and how it differs between catchments with contrasted landuse and lithology. The fourth section provides insights into the spatial and temporal variability of forest canopy and forest floor storage capacity. Given the considerable amount of precipitation that is intercepted at annual scale, the process is likely to have a substantial influence on catchment storage dynamics.

L. Pfister (✉) · C. Hissler · J.F. Iffly
Catchment and Eco-Hydrology Group,
Environmental Research and Innovation
Department, Luxembourg Institute of Science and
Technology, 41 Rue Du Brill, 4422 Belvaux,
Luxembourg
e-mail: laurent.pfister@list.lu

M. Coenders
Water Resources Section, Faculty of Civil
Engineering and Geosciences, Delft Technical
University, Stevinweg 1, 2628 CN Delft,
The Netherlands

R. Teuling · A. Arens
Department of Environmental Sciences, Hydrology
and Quantitative Water Management Group,
Wageningen University, Droevendaalsesteeg 3,
6708PB Wageningen, The Netherlands

L.H. Cammeraat
University of Amsterdam, Institute for Biodiversity
and Ecosystem Dynamics, Science Park 904,
1098XH Amsterdam, The Netherlands

4.1 Introduction

In the early 1990s, the main floodplains of Luxembourg were struck by three successive major inundations that eventually caused substantial damage to local infrastructures. In the aftermath of these natural disasters, there were rising concerns about the potential first signs of an ongoing climate change and/or the impacts of an urbanisation that had been galloping for decades. At that time, little was known about the factors and processes that control and drive the rainfall–runoff transformation in the river basins of Luxembourg. For nearly half a century, meteorological and hydrological monitoring programmes had been restricted to daily measurements within a relatively coarse observation network.

Here, we provide an overview of hydrological processes research that has been carried out more specifically in the cuesta landscapes of Luxembourg since the mid-1990s. Our developments will focus on the Attert River basin. Due to its complex physiogeographic characteristics, this basin is representative of the geological, topographical and land use contexts in Luxembourg. During this pioneering period for hydrology in Luxembourg, numerous complementary research activities have rapidly grown from the initial implementation of a modern hydro-climatological observatory in the Attert River basin: hydrological processes studies (e.g. runoff generation, rainfall interception, etc.), hydrological modelling, climate variability/change and its implications on the hydrological cycle at regional scale, exploration of new measurement techniques of hydro-climatological variables (e.g. satellite-borne remote sensing, thermal IR imagery, eco-hydrological tracers).

In this chapter, we develop on the past and ongoing research in the Attert River basin on fundamental hydrological functions of catchments: water collection, storage and release (as per Black 1997). In a first section, we detail the physiogeographic characteristics of the Attert River basin. The second section provides insights into the seasonal and spatial variability of hydrological responses along a wide range of

clean and mixed landuse, soil and bedrock settings. In the third section, we develop on dynamic catchment storage and how it is controlled through physiographic characteristics. The fourth section provides insights into a specific and yet important aspect of water storage: the spatial and temporal variability of forest canopy and forest floor storage capacity.

4.2 The Attert River Basin

Paleozoic and Mesozoic substrata are characterising the geology of Luxembourg. The Attert River basin is located in the contact zone of these very distinct geological entities. The so-called Oesling region in the northern half of the country is dominated by Devonian bedrocks and deeply cut V-shaped valleys, while in the southern Gutland region deep valleys cut into the Luxembourg sandstone alternate with large valleys located in the Keuper marls—eventually characterising the typical cuesta landscapes.

Altitudes range from 225 to 559 m.a.s.l. in the Oesling and from 140 to 440 m.a.s.l. in the Gutland. Landuse in the Oesling is dominated by forests and agricultural lands, while in the Gutland, agricultural lands, forests and urban areas alternate.

4.2.1 Physiogeographic Context

The Attert basin is located in the mid-western part of Luxembourg and has a total surface area of 288 km² at the outlet in Bissen (Fig. 4.1). Lying in the contact zone between the schistous Ardennes massif (northern part, called Oesling) and the sedimentary Paris Basin (southern part, called Gutland) (Pfister et al. 2009), the Attert River basin is representative of the wider physiogeographic setting of Luxembourg. The Oesling covers 24% of the total Attert basin area. It is a high sub-horizontal plateau with average altitudes ranging between 450 and 500 m. The lithology of the Oesling mainly consists of schists and phyllades. The schistous bedrock can be considered as being rather impermeable, even

though a weathered zone with a considerable variance in depth can store large amounts of water. Landuse is dominated by forests, while soils consist of Cambisols and Regosols (IUSS working group 2014). The soil texture is mainly silty and mixed with gravels.

The Gutland represents 76% of the total area and extends through the middle and southern part of the Attert River basin. It can be divided into two distinctive physiogeographic units (Fig. 4.1). The so-called marly depression in the center of the Attert river basin represents 68% of the total basin area. The very clayey soils (Stagnosols, Planosols, Vertisols and Cambisols) of the marly depression support mainly grassland and forests. The topography is marked by gently sloping hills. The second unit, called the Luxembourg plateau, is located in the southern part of the Attert basin and represents 8% of the total basin area. It mainly consists of a plateau made of permeable Luxembourg sandstone locally covered by marls and supports sandy to clayey soils such as Podzols, Cambisols, Luvisols, Regosols and Stagnosols (Juilleret et al. 2012).

4.2.2 The Nested Catchment Set-up in the Attert River Basin

A nested system of nine sub-catchments ranging from 0.47 to 249.61 km² has been implemented since 2002 in the Attert River basin (Fig. 4.1). It includes micro-basins equipped with an instrument network operating at a very high spatio-temporal resolution (Pfister et al. 2006). Via this network various meteorological, hydrological and hydro-geochemical processes are monitored in the framework of long-term environmental monitoring programmes (e.g. Pfister et al. 2005; Gerrits et al. 2007; Martínez-Carreras et al. 2010a, 2010b; Pfister et al. 2009; Zehe et al. 2014).

The Weierbach (0.47 km²) and the Colpach-Haut (19.21 km²) sub-catchments, mainly characterised by periglacial slope deposits on Devonian schists (Juilleret et al. 2011), are located in the northwest of the Attert River basin. The Roubach sub-catchment (43.32 km²), located in the north-eastern part of the Attert River basin is mainly characterised by red

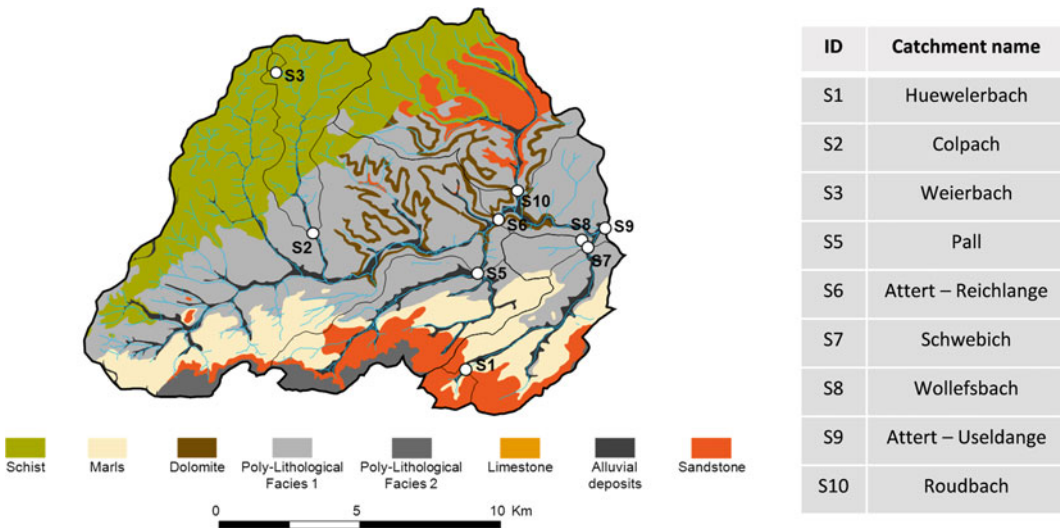


Fig. 4.1 The Attert experimental basin—geology, river network and streamgauge stations. This figure has partly been reproduced from Pfister et al. (2017) in Hydr Proc.31:1828-1845 DOI:10.1002/hyp.11134

sandstone (Buntsandstein) and is almost equally covered by forest, grassland and cultivated land.

The bedrock of the Wollefsbach (4.61 km²) and Pall (37.14 km²) sub-catchments in the center of the Attert basin is predominantly Keuper sandy marl. The landuse is primarily characterised by grassland and cultivated land.

The Schwebich sub-catchment (30.16 km²) includes the Huewelerbach and the Wollefsbach sub-catchments in the southern part of the Attert basin, and thus represents intermediate physiogeographic characteristics. The Huewelerbach sub-catchment (2.76 km²) is characterised predominantly by the Luxembourg sandstone. While it is mainly covered by forests, grassland dominates in the alluvial part.

In addition, the gauging stations Reichlange (160.2 km²) and Useldange (249.61 km²) are located along the main reach of the Attert River.

Hydrological stations are equipped with electronic pressure sensors to measure water depths. Readings are collected every 15 min with data loggers. Rainfall data from eight recording rain gauges located within and in the close vicinity of the Attert River basin are available (+20 manual raingauges available for approx. 30 years). The recorders are tipping bucket rain gauges, normally installed as a part of a meteorological station. The gauges have a resolution of 0.1 mm per tip, an area of 200 cm² and are not operational during frost, snow or hail. Readings are also collected every 15 min with a data logger.

4.3 Hydrological States Revealed Through Streamflow Coefficients

Double-mass curves of aggregated precipitation versus aggregated discharge provide highly valuable information on a given catchment's hydrological regime (Pfister et al. 2002). Seasonal patterns in the rainfall-runoff response will translate into strong differences between summer and winter slopes of the double-mass plots. Likewise, these responses may also exhibit a

spatial variability and can be related to specific physiogeographic characteristics.

Here, we present the precipitation-discharge transformation process for six sub-catchments of the Attert River basin, as expressed through their individual double-mass curves of aggregated precipitation versus aggregated discharge (Fig. 4.2). For all plots, the double-mass slopes start on 1 October and end on 30 September of the following year. At the beginning of the hydrological year (i.e. 1 October), most catchments respond to precipitation inputs in a very moderate way, as suggested by the predominantly flat slopes of the double-mass curves. With the onset of the dormant season, temperatures drop and losses through evapotranspiration decrease, leading to a gradual increase in streamflow response. Consequently, the slope of the double-mass curve between precipitation and discharge rises—eventually stabilising at a level that is largely controlled by the catchment's specific physiogeographic characteristics. In early spring, with rising temperatures and growing vegetation evapotranspiration losses setting back in, streamflow response gradually decreases—causing the double-mass curve between precipitation and discharge to flatten.

Even though this general seasonal pattern can be observed in most catchments, it nonetheless shows a strong spatial variability. While in some catchments the seasonal cycle is reflected very strongly (e.g. in the marly Wollefsbach catchment), it is almost totally absent in others (e.g. in the sandstone dominated Huewelerbach catchment). Larger catchments, such as the Roudbach or the Attert in Useldange, present intermediate behaviours.

Winter stormflow coefficients, as inferred from the precipitation-discharge double-mass curves, were regionalised for the Alzette River basin (Pfister et al. 2002; Hellebrand et al. 2007), as well as for the Nahe basin—located in Rhineland-Palatinate, Germany (Hellebrand et al. 2007). Simple linear models gave the best results in describing the spatial variability of the winter stormflow coefficients, mainly relying on

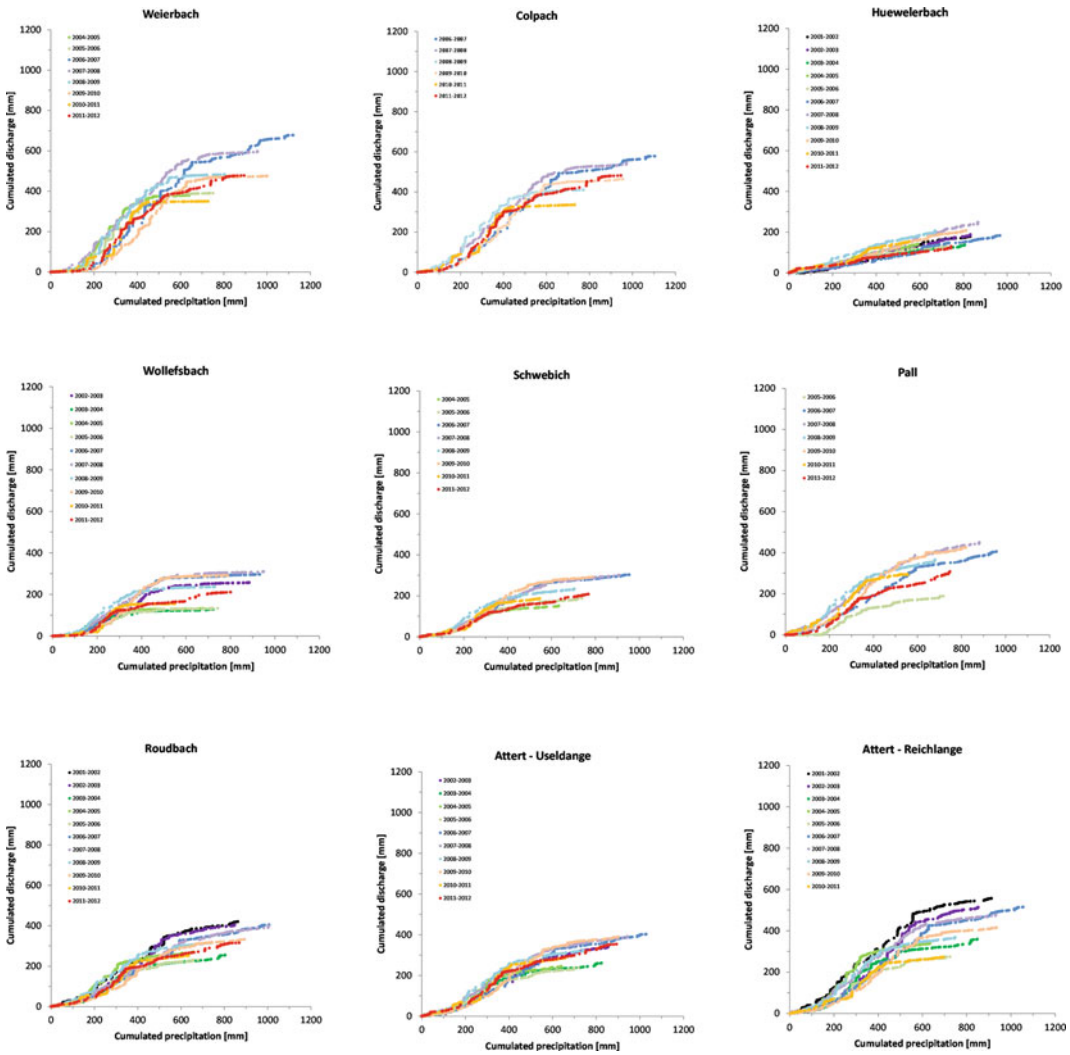


Fig. 4.2 Precipitation-discharge double-mass curves for individual hydrological years (Weierbach 0.4 km²—schists, Colpach 19.21 km²—schists, Huewelerbach 2.7 km²—sandstone, Wollefsbach 4.5 km²—marls, Schwebich 30.1 km²—sandstone & marls, Pall 37.14 km²—

sandstone & marls, Roudbach 44 km²—schists, sandstone & marls, Attert-Useldange 247 km²—sandstone, marls & schists, Attert-Reichlange 160.2 km²—sandstone, marls & schists)

substrate permeability and key runoff generation processes (e.g. saturation excess overland flow).

The analysis of double-mass curves between precipitation and discharge provided insights into how certain physiogeographic characteristics control hydrological responses in our set of nested catchments. However, this approach only provides integrative or lumped information on what is actually the result of manifold processes that operate at various spatial and temporal

scales. In the following section, we develop more specifically on the catchment storage function.

The kind of analysis of discharge and precipitation series, as well as of runoff coefficients, as described here above only provides integrative or averaged information on what actually is the result of a plenitude of processes that operate at numerous spatial and temporal scales. In the next section, we develop more specifically on individual catchment storage dynamics and how they

are controlled by physiogeographic characteristics.

4.4 Spatial and Temporal Variability of Catchment Storage

The state of a hydrological system is expressed through the volume of water stored in a catchment as snow, soil moisture, groundwater and surface water (McNamara et al. 2011). To date, we still lack understanding of how flow processes and wetness conditions in catchments are related to the spatial and temporal variability of streamflow age components (Hrachowitz et al. 2013; Heidbüchel et al. 2013).

Recent hydrological process research focussed on how much water a catchment can store and how these catchments store and release water (Sayama et al. 2011). Storage can be a valuable metric for catchment description, inter-comparison and classification. Furthermore, storage controls catchment mixing, non-linearities in rainfall-runoff transformation and eco-hydrological processes. Various methods exist to determine catchment storage (e.g. natural tracer, soil moisture and groundwater data, hydrological models). Today, it remains unclear what parts of the catchment storage are measured with the different models.

4.4.1 Catchment Dynamic Storage

We have computed catchment dynamic storage changes for each winter season over the period 2002–2012 (based on precipitation as input; discharge and evapotranspiration as output). We determined dynamic storage changes for each winter semester (October–March) in all nine nested catchments of the Aart River basin over the period 2002–2012 (see Fig. 4.3 as an example for 2006–2007). At the beginning of each hydrological winter season, all catchments showed similar trends in storage change (Fig. 4.3). A few weeks into the winter season, catchments with the lowest permeability (e.g.

marls) started to plateau. The highest storage values were reached only several months later in catchments dominated by permeable substrate (e.g. sandstone).

4.4.2 A Perceptual Model of Catchment Storage

Here, we propose a perceptual model that resumes on our findings proposing geology as a dominating control on catchment water mixing, storage and release. We relied on the concept of dynamic storage introduced by Sayama et al. (2011), where catchments exhibit distinct phases of storage increase during the wetting-up phase, followed by clear geologically controlled storage limits.

Figure 4.4 shows our perceptual models for two major contrasted geological settings within our region of interest, namely sandstone and marls. The diagrams present groundwater tables in the permeable bedrock and/or regolith layers at the beginning of the winter season (i.e. prior to wet-up). With vegetation entering the dormant season, losses through evapotranspiration rapidly decline, and precipitation starts infiltrating the soils and eventually percolates to the permeable bedrock. The rising groundwater tables translate into increasing catchment dynamic storage. The substantially larger permeable bedrock layer (several tens of metres) that characterises the sandstone allows for considerable rises of the groundwater table. Consequently, total storage change through the wet-up phase is considerably larger in catchments dominated by sandstone. In the shallow regolith (~ 1 m) that characterises marly catchments (Juilleret et al. 2012), the amplitude of groundwater table fluctuations is very limited, causing the total storage changes in the wet-up period to be small.

In the high relief sandstone catchments, groundwater seepage is limited to spring lines at the intersection with impermeable substrata. The steep slopes that characterise the schist catchments trigger seepage area dynamics essentially limited to the riparian zones. The largest seepage

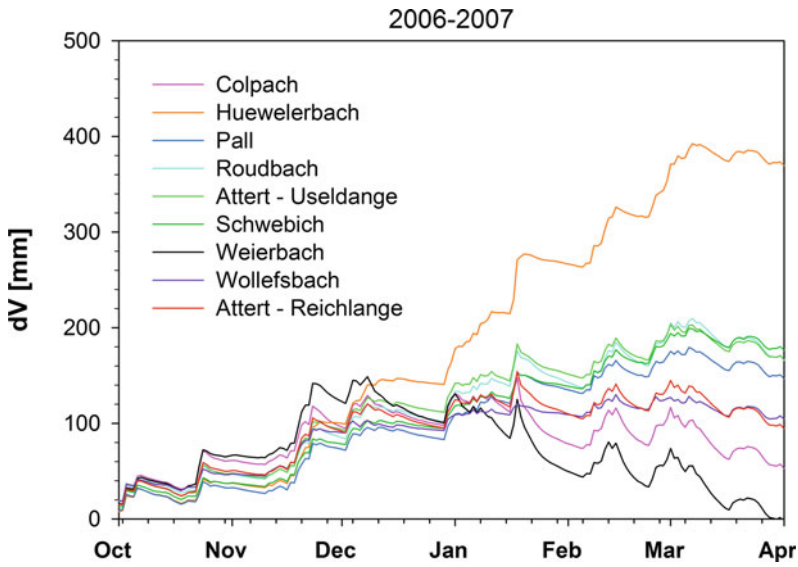


Fig. 4.3 Temporal evolution of total storage changes (dV) during the winter season for 9 catchments (example of the hydrological year 2006–2007)

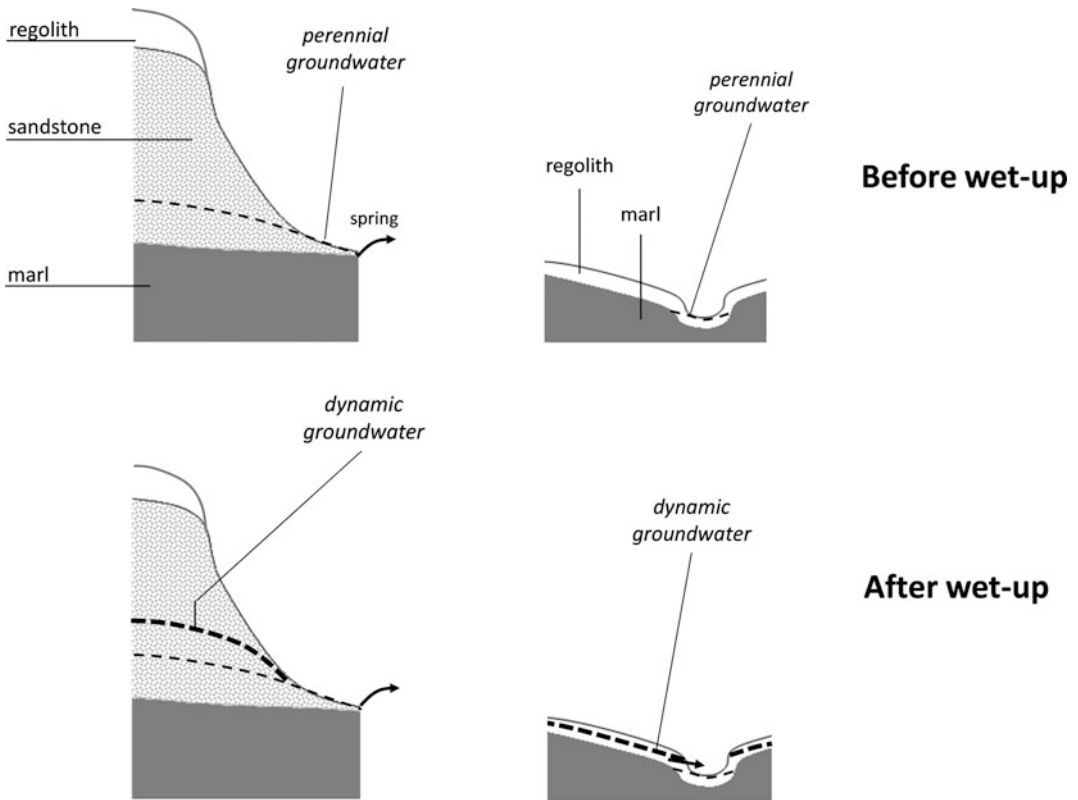


Fig. 4.4 Perceptual model of geological control on catchment storage, mixing and release (*left* sandstone dominated; *right* marls dominated). Weathered and fractured sandstone expands through several tens of metres (e.g. Huewelerbach)

and offers a wide amplitude of groundwater table fluctuations, translating into large dynamic storage. The shallow regolith that characterises marly catchments (e.g. Wollefsbach) generates limited dynamic storage potential

areas develop in the low relief marly catchments at the option of rapidly rising groundwater tables within the shallow regolith. Eventually, saturated area dynamics will translate into time variant contributions to streamflow from various sources (ground-, soil- and surface water) and geological settings.

4.5 Seasonal and Spatial Dynamics of the Interception Process

Interception concerns about 10–50% of the total incoming precipitation in forests of the temperate humid latitudes (Rutter et al. 1975; Aussenac 1981; Viville et al. 1993; Hörmann et al. 1996; Savenije 1997; Gerrits et al. 2010). The interception process actually consists of two parts, with rain drops first hitting the forest canopy before eventually falling to the floor, where they will again be intercepted by litter. Leaves and litter then gradually dry-out by evaporation. Since the intercepted and evaporated water is lost for the forest soils, the interception process is of highest importance for the water balance in forests. The evaporated water will not contribute to filling the soil reservoirs and will thus also not be available for the vegetation. Besides this loss effect, the interception process also plays an important role as a redistributor of rainfall in space. Throughfall and stemflow often are at the origin of important concentrations of water under the forest canopy (Germer et al. 2006; Gerrits et al. 2009). These spatial and temporal redistributions of rainfall under the canopy underline the important role of the forest on soil moisture patterns and the water balance at a given location (Bouten et al. 1992).

The interception process is characterised by a large spatio-temporal variability that is controlled by stand density, age, tree height, storage capacity, etc. The percentages of intercepted precipitation generally represent average values issued from observation periods that integrate rainfall events of different amounts and intensities (Petit and Kalombo 1984). Thus, the interception loss can exceed 50% during periods where rainfall events were scarce (up to 15 mm in a week for example),

but it can also be less than 25% during periods where precipitation was particularly abundant (more than 100 mm in a week).

Hereafter, we refer to both forest canopy interception (I_c) and forest floor interception (I_{ff}), which equals the sum of the change in interception storage ($S_i^c + S_i^{ff}$) and evaporation from this storage ($E_i^c + E_{ii}^{ff}$):

$$I = I_c + I_{ff} = E_i^c + \frac{dS_i^c}{dt} + E_i^{ff} + \frac{dS_i^{ff}}{dt} \quad (4.1)$$

To date, most studies on interception found in the literature refer to events or short durations (e.g. Kittredge 1948; Zinke 1967; Breuer et al. 2003). Here, we explore both the event and seasonal variability of interception—a process that is largely driven by potential evaporation, as well as canopy storage capacity in case of deciduous trees. The transition in interception between seasons is rarely described in the literature, with at best a distinction being made between leaf-on and leaf-off states (Rutter et al. 1975; Rowe 1983; Hörmann et al. 1996; Zhang et al. 2006; Fenicia 2008; Herbst et al. 2008).

4.5.1 The Huewelerbach Experimental Plot

The study area is located in the 2.76 km² Huewelerbach catchment. Exposed to the South-East, the experimental beech stand (120 years of age) has a total area of 0.0596 ha and is located at an altitude of 380–382 m. The density of the stand is of approximately 168 trees/ha, while the tree height varies from 30–40 m (Fig. 4.5).

Incident precipitation was measured at the meteorological station, located in the middle of the Huewelerbach catchment. Precipitation measurements were recorded at a 15-min time-step. An additional pluviometer collected incident precipitation. Cumulated rainfall in the pluviometer was read at a weekly time-step and helped validating the recording pluviograph.

In the experimental plot, throughfall was measured both continuously and at a weekly

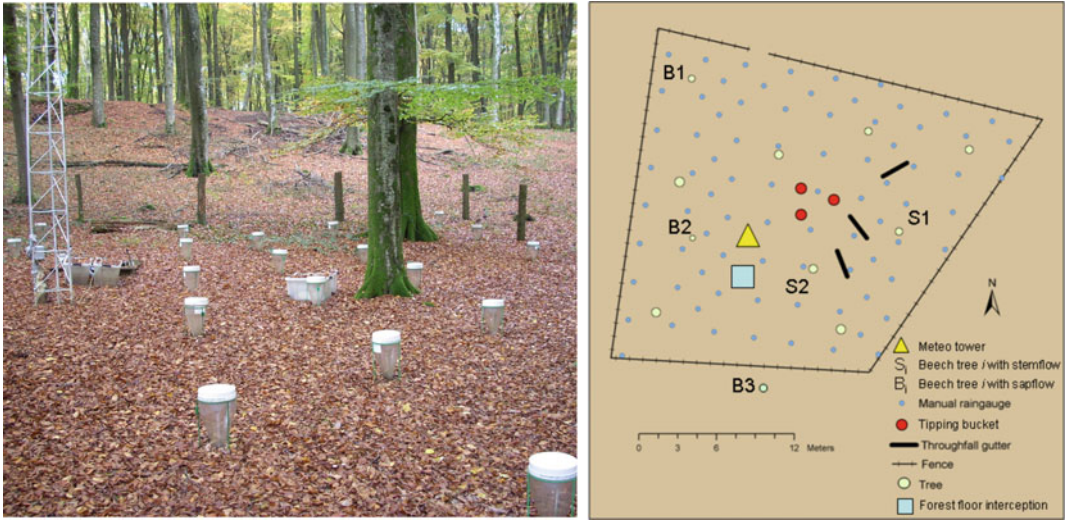


Fig. 4.5 The Huewelerbach experimental plot (beech stand). Reproduced with permission from Wiley Gerrits et al. (2010)

time-step. In the experimental plot, a network of three gutters had been built (total collecting area of 1.07 m²). The gutters were connected to tipping bucket pluviometers and a recording device, so to provide the temporal structure of throughfall below the canopy (recording time-step of 5 min). Since the representativity of these gutters is extremely difficult to assess, because of the high spatial variability of the canopy density, an additional network of pluviometers had been dispatched inside the experimental stand. More than 80 pluviometers were dispatched in this network and were equidistant of 3 m.

The pluviometers gave both an indication of the spatial variability of throughfall, as well as a precise measurement of the amount of throughfall at a weekly time-step. The weekly throughfall amounts were then disaggregated via the measurements obtained by the tipping bucket gauges that were connected to the gutters and were installed below the canopy.

Stemflow along the trees can represent an important fraction of the total water amount that reached the soil. This can thus lead to an important modification of the hydrologic balance around the trees. The measurement of stemflow was done via plastic gutters that were

fixed with silicone around three tree stems (Fig. 4.6).

Stemflow was determined via Eq. 4.2:

$$S_F = \left(\frac{S_f}{n} \cdot N \right) \cdot A^{-1} \quad (4.2)$$

with

- S_F stemflow (mm/15 min)
- S_f stemflow (L/15 min)
- n number of trees equipped with gutters in the experimental plot ($n = 3$)
- N number of trees in the experimental plot ($N = 9$)
- A experimental plot area (m²)

The stemflow that was collected by the experimental device was directed towards a tipping bucket pluviograph. Recordings of stemflow took place at a 15-min time-step.

To measure forest floor interception, a special device was developed (Gerrits et al. 2007) that consists of two aluminium basins that are mounted above each other (Fig. 4.7). The upper basin contains the forest floor material, has a permeable bottom and is weighed every 5 min. The lower basin collects the infiltrated



Fig. 4.6 Throughfall (*left*) and stemflow (*right*) collection systems in the Huewelerbach experimental plot

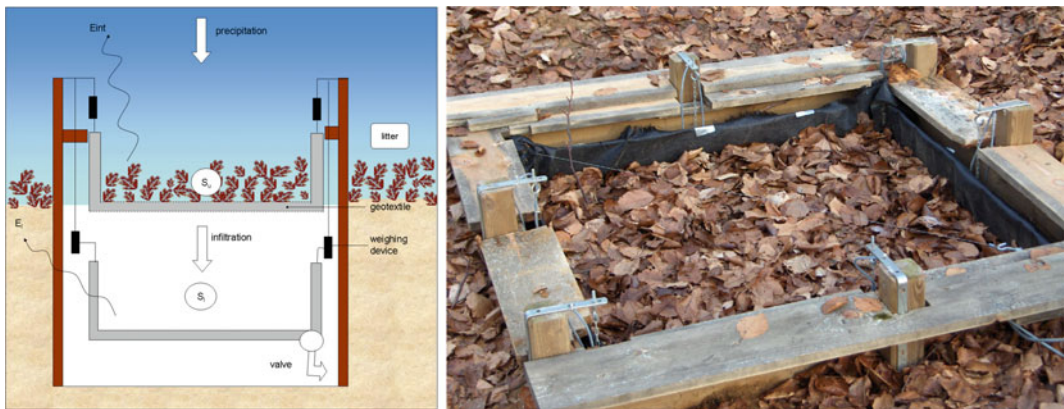


Fig. 4.7 Forest floor interception device filled with beech litter. Reproduced with permission from Wiley Gerrits et al. (2010)

water and is emptied every day by an electronic valve.

4.5.2 Temporal Variability of Canopy Hydrological Variables

In most studies on rainfall interception by forest canopies, indirect techniques are used to determine canopy hydrological variables. Those indirect techniques rely either on observations from multiple storms, or on measurements of a high temporal resolution recorded during a single storm event.

According to Hutchings et al. (1988), the interception capacity of spruce stands is not a

fixed parameter, since it varies with rainfall intensity, as well as with canopy architecture. It is thus a dynamic storage, with its contribution to the losses due to interception being probably low, except for those events where the evaporation rate is very high.

Here, we present interception data that spans over six hydrological years in the experimental plot of the Huewelerbach (2004–2009). All phenological phases of the beech stand have thus been incorporated in the study of the spatio-temporal variability of the interception process. The results described hereafter are focusing on the seasonal variability of the phenomenon.

4.5.2.1 Interception Rates

Canopy interception rates showed a high seasonal variability (Fig. 4.8a): while the average interception loss of total rainfall from 2004 to 2009 mounted up to 12%, winter interception (leaves off) only reached 7% of total incoming precipitation and summer interception rate was 15% (leaves on). However, the interception process was also characterised by a strong annual variability. In certain years (e.g. 2004 and 2006) the canopy interception rate mounted up to ~60%, while in other years (e.g. 2007) it would reach ~20% at best. The positive and negative outliers in Fig. 4.8 coincide with small rainfall episodes or with snow events, where measurement errors became substantial.

Due to problems with the newly developed device, large gaps exist in forest floor interception data series (Fig. 4.8b). Nonetheless, the (limited) data shows that on average 22% of throughfall (=19% of gross rainfall) evaporated

from the forest floor. Unlike with canopy interception, the seasonal effect of forest floor interception is much smaller: forest floor evaporation reached 19% of incident precipitation in summer and 20% in winter, respectively.

The high interseasonal variability of the canopy interception process in the experimental plot of the Huewelerbach was due to both the seasonal variability of evaporation (changing with average seasonal temperatures) and the phenological phases of the vegetation, regulating the transpiration process. During summer, the canopy density is much higher and thus the rate of intercepted rainfall increases accordingly. During winter months, the canopy is much more permeable to incoming precipitation, since no leaves are on the tree branches. However, these leaves are now stored on the forest floor. Combined with more radiation that is able to penetrate through the canopy, the evaporation from the forest floor becomes significant. Hence, if one considers the total interception

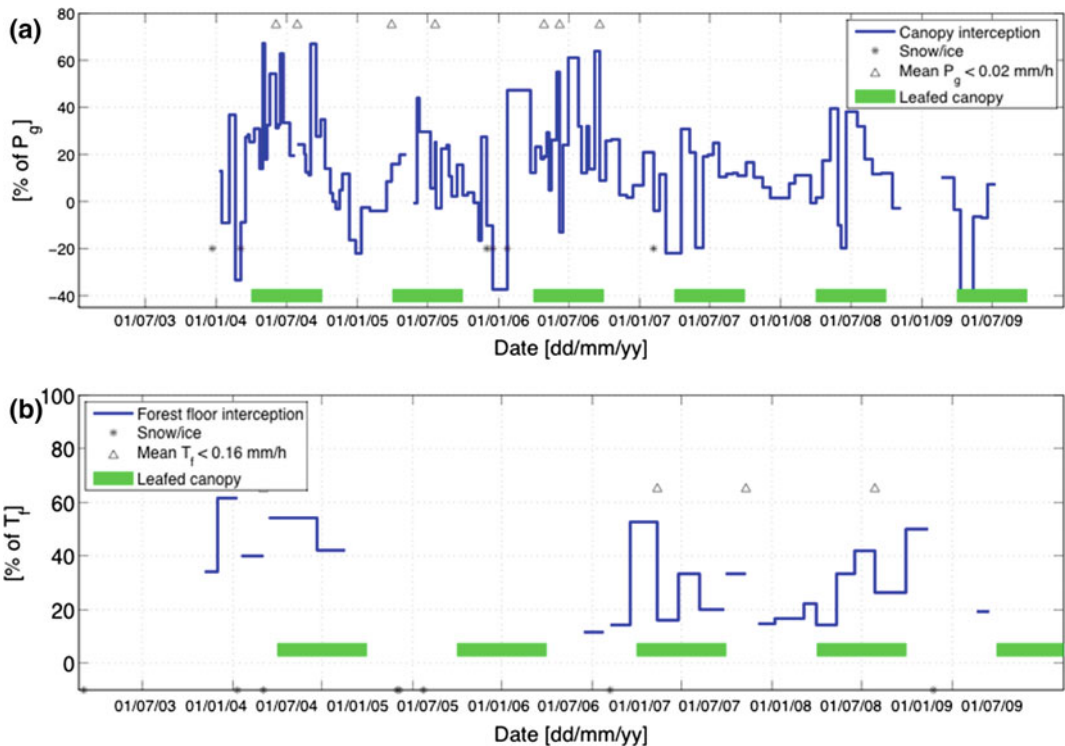


Fig. 4.8 a Temporal variation of: a canopy interception as percentage of gross rainfall (P_g); b forest floor interception as percentage of throughfall. Reproduced with permission from Wiley Gerrits et al. (2010)

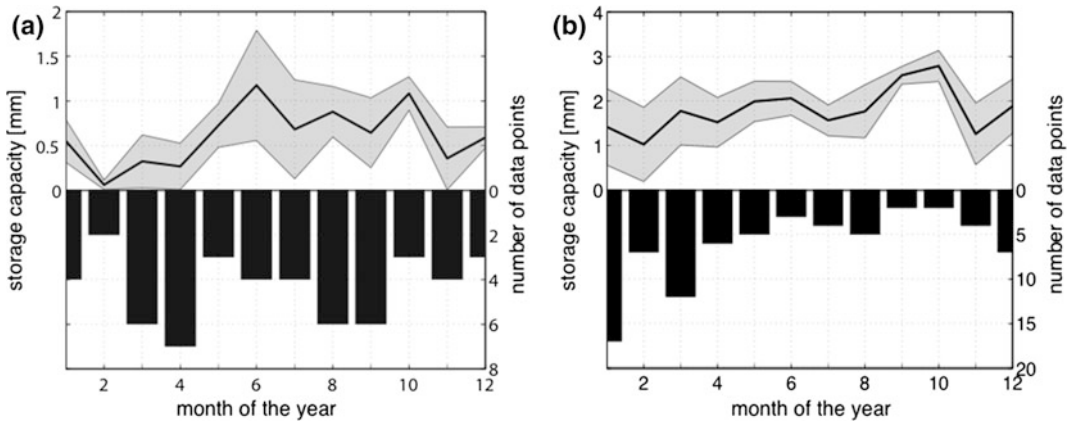


Fig. 4.9 Variability of storage capacity of: **a** forest canopy and **b** forest floor. *Black line* average value from all events for a given month; *Grey area* standard

deviation; *Bars* number of selected events. Reproduced with permission from Wiley (Gerrits et al. (2010))

process of the canopy and forest floor, 34% of incident precipitation can evaporate in summer and 27% in winter.

Stemflow appeared to play only a minor role in the interception process (3.3% of total incoming precipitation in summer and 6.6% in winter).

4.5.2.2 Canopy and Forest Floor Storage Capacity

Between 2004 and 2009, 52 rainfall events had been selected for the determination of the canopy storage capacity of the beech stand in the experimental plot of the Huewelerbach and 74 events for the forest floor storage capacity. Selection criteria for these rainfall events were mainly based on the condition that prior to the rainfall event the canopy was dry for at least two days and that the event was large enough to saturate the storage capacity.

To determine the canopy storage capacity we used the ‘mean method’ of Klaassen et al. (1998), where the storage capacity is the negative intercept with the y-axis of the linear regression line of accumulated gross rainfall versus accumulated throughfall of an event. The mean method thus takes evaporation during the event into account, since the slope of the regression line can be less than the 1:1 line. For determining the forest floor storage capacity we relied on the

same method—however, we used accumulated throughfall *versus* accumulated infiltration instead.

The analysis of canopy hydrological variables for 52 individual rainfall events between 2004 and 2006 revealed that canopy storage capacity is characterised by a high seasonal variability (Fig. 4.9a). The highest values (up to 0.9 ± 0.5 mm) were observed in mid-summer, when canopy density was largest. The canopy storage capacity dropped to 0.4 ± 0.2 mm during winter months, before rising again progressively with the onset of the vegetation period during spring. Likely the high standard deviation (especially in summer time) is related to wind speed and rainfall intensity during the events, but in the literature there is no consensus on how this might be related.

The storage capacity of the forest floor shows much less seasonality (Fig. 4.9b). Both in winter and summer the average capacity is 1.8 mm with only a momentarily peak during early fall at 2.8 mm. The latter can be explained by the freshly fallen leaves that dry-out quickly and provide curly shaped dry leaves which act as multiple small water reservoirs. However, this curly shape can disappear quickly after rain or snow events.

Furthermore, Fig. 4.9b shows that the standard deviation of forest floor storage capacity in summer is smaller: 0.4 mm *versus* 0.8 mm in

winter. The relatively high variation in winter is likely caused by alternating periods with and without snow cover. A snow pack flattens the forest floor and thus lowers its storage capacity.

4.5.3 Conclusion on the Interception Process

The experiments that have been carried out in the beech stand of the Huewelerbach have helped quantifying the interception process, as well as its components. The interaction between the canopy and forest floor was not studied before for such a long time and revealed new insights. Frequently, the interception process is considered as being important solely in summer, essentially due to tree phenology. This has turned out to be an overly simplified conceptualisation, completely ignoring the role of forest litter.

While the forest canopy has a relatively small storage capacity (0.9 ± 0.5 and 0.4 ± 0.2 mm for summer and winter, respectively), the evaporative power (i.e. availability of radiation and moisture deficit in the atmosphere) is much higher. The opposite is true for the forest floor, where the average storage capacity is large (1.8 ± 0.4 and 1.8 ± 0.8 mm for summer and winter, respectively), the evaporative power is lower, due to lower radiation and wind speed underneath the canopy.

Overall, the storage capacity of the beech stand in the Huewelerbach experimental plot can be considered as being close to the values cited in the literature. The same statement holds also for the amount of rainfall that is intercepted by the beech forest, with 30% of incoming rainfall being intercepted on average by both the canopy and forest floor. Duijsings (1985) and Cammeraat (1992) found annual intereception rates for a beech-hornbeam-oak forest near Diekirch (Luxembourg) of 32–36% and 29–31%, respectively.

As shown in our investigations, as well as previous research by Duijsings (1985) and Cammeraat (1992), the interception process is characterised by a considerable event-scale and seasonal variability, depending on prevailing meteorological conditions (rainfall intensity,

wind speed, air temperature, etc.), as well as tree species. Given the considerable amount of precipitation that is intercepted at annual scale, the process is likely to have a substantial influence on catchment storage dynamics.

4.6 Follow-up Investigations

To date, our investigations have been essentially motivated by the need for reducing measurement approximations, increase our process knowledge and thereby eventually improve our perceptual models of streamflow generation. Pappenberger et al. (2006) have indeed criticised that it is commonly assumed that approximations are correct or only subject to negligible errors, and that the methodology and model are a valid representation of the real physical system. These assumptions are generally considered as being very questionable, given the numerous potential error and uncertainty sources, such as input uncertainty (e.g. rainfall), parameter uncertainty and model uncertainty. Our research in experimental hydrology is complementary to other research avenues in hydrological modelling that have recently been introduced for reducing the difficulties in model calibration.

Fencia et al. (2007) have shown the potential of multiobjective calibration strategies applied to hydrological models run on river basins in the Grand Duchy of Luxembourg. Following a concept of iterative model improvement, new measurement techniques, such as isotopic tracers (Fencia et al. 2007) and microwave remote sensing of soil moisture (Matgen et al. 2007), illuminated new aspects of catchment behaviour and contributed to model improvements. By providing new high-resolution data for flooded areas, remote sensing techniques, such as synthetic aperture radar (SAR) applied to the floodplains of the Alzette and Sûre rivers (not shown here), have shown considerable potential to increase the performances of flood inundation models (Matgen et al. 2006, 2007; Schumann et al. 2007).

Even though the new observation techniques that we have been exploring in recent years have shown very promising results, they nonetheless

also suffer from limitations. One common limitation of both conventional and new monitoring techniques lies in the fact that their implementation is often still cumbersome in that samples must be taken in the field and measured in the lab—resulting in very coarse sampling intervals. What is needed now is an approach to make these measurements directly in the field at high frequency. Such new measurement potential would allow for fundamental new insights into hydrological processes controlling rainfall-runoff transformation.

Acknowledgements Data and results presented in this chapter have been partially obtained through research projects funded in the framework of FNR (Fonds National de la Recherche du Luxembourg) programmes (CYCLEAU, STORE-AGE, CAOS-1, CAOS-2, SOWAT, BIGSTREAM, ECSTREAM). We acknowledge support during multiple field campaigns to Cyrille Taillez and Jérôme Juilleret at LIST.

References

- Aussenac G (1981) L'interception des précipitations par les peuplements forestiers. *La Houille Blanche* 7 (8):531–536
- Black PE (1997) Watershed functions. *J Am Water Resour Assoc* 33:1–11
- Bouten W, Heimovaara TJ, Tiktak A (1992) Spatial patterns of throughfall and soil water dynamics in a Douglas fir stand. *Water Resour Res* 28. doi:10.1029/92WR01764
- Breuer L, Eckhardt K, Frede HG (2003) Plant parameter values for models in temperate climates. *Ecol Model* 169:237–293
- Cammeraat LH (1992) Hydro-geomorphological processes in a small forested catchment: preferred flow paths of water. PhD-thesis, Amsterdam
- Duijsings JJHM (1985) Streambank contribution to the sediment budget of a forest stream, PhD. University of Amsterdam, Amsterdam
- Fenicia F (2008) Understanding catchment behaviour through model concept improvement. PhD thesis. Delft Technical University, The Netherlands. 138 pp
- Fenicia F, Savenije HHG, Matgen P, Pfister L (2007) A comparison of alternative multiobjective calibration strategies for hydrological modelling. *Water Resour Res* 43:W03434. doi:10.1029/2006WR005098
- Germer S, Elsenbeer H, Moraes JM (2006) Throughfall and temporal trends of rainfall redistribution in an open tropical rainforest, south-western Amazonia (Rondonia, Brazil). *Hydrol Earth Syst Sci* 10:383–393
- Gerrits AMJ, Savenije HHG, Hoffmann L, Pfister L (2007) New technique to measure forest floor interception—an application in a beech forest in Luxembourg. *Hydrol Earth Syst Sci* 11:695–701
- Gerrits AMJ, Savenije HHG, Pfister L (2009) Canopy and forest floor interception and transpiration measurements in a mountainous beech forest in Luxembourg. *IAHS Redbook* 326:18–24
- Gerrits AMJ, Pfister L, Savenije HHG (2010) Spatial and temporal variability of canopy and forest floor interception. *Hydrol Proc* 24:3011–3025. doi:10.1002/hyp.7712
- Heidbüchel I, Troch PA, Lyon SW (2013) Separating physical and meteorological controls of variable transit times in zero-order catchments. *Water Resour Res* 49:7644–7657
- Hellebrand H, Hoffmann L, Juilleret J, Pfister L (2007) Assessing winter stormflow generation by means of permeability of the lithology and dominating runoff production processes. *Hydrol Earth Syst Sci* 11:1673–1682
- Herbst M, Rosier PT, McNeil DD, Harding RJ, Gowing DJ (2008) Seasonal variability of interception evaporation from the canopy of a mixed deciduous forest. *Agric For Meteorol* 148:1655–1667
- Hörmann G, Branding A, Clemen T, Herbst M, Hinrichs A, Thamm F (1996) Calculation and simulation of wind controlled canopy interception of a beech forest in Northern Germany. *Agric For Meteorol* 79:131–148
- Brachowitz M, Savenije HHG, Blöschl G, McDonnell JJ, Sivapalan M, Pomeroy JW, Arheimer B, Blume T, Clark MP, Ehret U, Fenicia F, Freer JE, Gelfan A, Gupta HV, Hughes DA, Hut RW, Montanari A, Pande S, Tetzlaff D, Troch PA, Uhlenbrook S, Wagener T, Winsemius HC, Woods RA, Zehe E, Cudennec C (2013) A decade of Predictions in Ungauged Basins (PUB)—a review. *Hydrol Sci J* 58:1198–1255
- Hutchings NJ, Milne R, Crowther JM (1988) Canopy storage capacity and its vertical distribution in a sitka spruce canopy. *J Hydrol* 104:161–171
- IUSS Working Group WRB (2014) World Reference Base for Soil Resources 2014: international soil classification system for naming soils and creating legends for soil maps. *World Soil Resources Reports* 106. Rome, FAO
- Juilleret J, Iffly JF, Pfister L, Hissler C (2011) Remarkable pleistocene slope deposits in Luxembourg (Oesling): pedological implication and geosite potential. *Bull Soc Nat Luxemb* 112:125–130
- Juilleret J, Iffly JF, Hoffmann L, Hissler C (2012) The potential of soil survey as a tool for surface geological mapping: a case study in a hydrological experimental catchment (Huewelerbach, grand-duchy of Luxembourg). *Geol Belgica* 15:36–41
- Kittredge J (1948) *Forest influences*. McGraw-Hill Book Co, New York

- Klaassen W, Bosveld FC, de Water E (1998) Water storage and evaporation as constituents of rainfall interception. *J Hydrol* 36–50:212–213
- Martínez-Carreras N, Krein A, Udelhoven T, Gallart F, Iffly JF, Hoffmann L, Pfister L, Walling DE (2010a) A rapid spectral reflectance-based fingerprinting approach for documenting suspended sediment sources during storm runoff events. *J Soils Sediments*. doi:10.1007/s11368-009-0162-1
- Martínez-Carreras N, Udelhoven T, Krein A, Gallart F, Iffly JF, Ziebel J, Hoffmann L, Pfister L, Walling DE (2010b) The use of sediment colour measured with diffuse reflectance spectrometry to determine sediment sources: application to the Attert river basin (Luxembourg). *J Hydrol*. doi:10.1016/j.jhydrol.2009.12.017
- Matgen P, Henry J-B, Hoffmann L, Pfister L (2006) Assimilation of remotely sensed soil saturation levels in conceptual rainfall-runoff models. In: IAHS Red Book Series. Prediction in ungauged basins: promise and progress, IAHS Publication 303: 226–234
- Matgen P, Schumann G, Henry J-B, Hoffmann L, Pfister L (2007) Integration of SAR-derived river inundation areas, high-precision topographic data and a river flow model toward near real-time flood management. *Int J Appl Earth Obs Geoinf* 9:247–263
- McNamara JP, Tetzlaff D, Bishop K, Soulsby Ch, Seyfried M, Peters NE, Aulenbach BT, Hooper R (2011) Storage as a metric of catchment comparison. *Hydrol Proc* 25:3364–3371
- Pappenberger P, Matgen P, Beven K, Henry J-B, Pfister L, De Fraipont P (2006) Influence of uncertain boundary conditions and model structure on flood inundation predictions. *Adv Water Resour* 29:1430–1449
- Petit F, Kalombo K (1984) L'interception des pluies par différents types de couverts forestiers. *Bull Soc Géogr Liège* 20:99–127
- Pfister L, Humbert J, Iffly JF, Hoffmann L (2002) Use of regionalized stormflow coefficients in view of hydro-climatological hazard mapping. *Hydrol Sci J* 47:479–491
- Pfister L, Wagner C, Vansuypeene E, Drogue G, Hoffmann L (2005) Atlas climatique du grand-duché de Luxembourg. In: Ries C (ed) Musée National d'Histoire Naturelle, Soc Nat Luxemb, Centre de Recherche Public—Gabriel Lippmann, Administration des Services Techniques de l'Agriculture, Luxembourg, 79 p
- Pfister L, Hoffmann L, Iffly JF, Matgen P, Moquet A, Tailliez C, Vansuypeene E, Schoder R, Buchel D, Lepesant P, Wiltgen C, Ernst P, Kipgen R, Ripp C, Schleich G (2006) Atlas hydro-climatologique du Grand-Duché de Luxembourg 2005. Ministère de l'Agriculture, de la Viticulture et du Développement Rural, Ministère de l'Intérieur, Centre de Recherche Public-Gabriel Lippmann, 464 p
- Pfister L, McDonnell JJ, Wrede S, Hlúbíková D, Matgen P, Fenicia F, Ector L, Hoffmann L (2009) The rivers are alive: on the potential for diatoms as a tracer of water source and hydrological connectivity. Invited commentary. *Hydrol Proc* 23:2841–2845
- Pfister et al. (2017) *Hydr Proc* 31:1828–1845 doi:10.1002/hyp.11134
- Rowe L (1983) Rainfall interception by an evergreen beech forest, Nelson, New Zealand. *J Hydrol* 66:143–158
- Rutter AJ, Morton AJ, Robins PC (1975) A predictive model of rainfall interception in forests. II Generalization of the model and comparison with observations in some coniferous and hardwood stands. *J Appl Ecol* 12:367–380
- Savenije HHG (1997) Determination of evaporation from a catchment water balance at a monthly time scale. *Hydrol Earth Syst Sci* 1:93–100
- Sayama T, McDonnell JJ, Dhakal A, Sullivan K (2011) How much water can a watershed store? *Hydrol Proc* 25:3899–3908
- Schumann G, Matgen P, Hoffmann L, Hostache R, Pappenberger F, Pfister L (2007) Deriving distributed roughness values from satellite radar data for flood inundation modelling. *J Hydrol* 344:96–111
- Viville D, Biron P, Granier A, Dambrine E, Probst A (1993) Interception in a mountainous declining spruce stand in the Strengbach catchment (Vosges, France). *J Hydrol* 144:273–282
- Zehe E, Ehret U, Pfister L, Blume T, Schröder B, Westhoff M, Jackisch C, Schymanski SJ, Weiler M, Schulz K, Allroggen N, Tronicke J, van Schaik L, Dietrich P, Scherer U, Eccard J, Wulfmeyer V, Kleidon A (2014) HESS Opinions: From response units to functional units: a thermodynamic reinterpretation of the HRU concept to link spatial organization and functioning of intermediate scale catchments. *Hydrol Earth Syst Sci* 18:4635–4655
- Zhang G, Zeng GM, Jiang YM, Huang GH, Li JB, Yao JM, Tan W, Xiang RJ, Zhang XL (2006) Modelling and measurement of two layer-canopy interception losses in a subtropical mixed forest of central-south China. *Hydrol Earth Syst Sci* 10:65–77
- Zinke PJ (1967) Forest interception studies in the United States. In: Sopper WE, Lull HW (eds) *Forest hydrology*. Pergamon Press, Oxford, pp 137–161

Hybrid Geomorphological Mapping in the Cuesta Landscape of Luxembourg

5

A.C. Seijmonsbergen and L.W.S. de Graaff

Abstract

A method to prepare hybrid geomorphological maps of the cuesta landscape in Luxembourg is presented. A hybrid geomorphological map is a combination of a classical geomorphological map and digital geomorphological information layers. The classical maps are hand drawn, utilize symbol-based legends and are printed as paper maps on a 1:10.000 scale. Digital information layers carry geospatial information that is stored in a geodatabase which is managed in a Geographic Information System (GIS). The digital geomorphological information layers include attributes that describe additional information on genesis of landforms, materials composition, process type and process activity, or other conditions. The geomorphological geodatabase serves as a repository for environmental information, which can flexibly be consulted by the end-user, e.g., for planning, land management, hazard assessment, or geoconservation purposes. Two types of geomorphological maps are presented. The first is an overview map on the landscape scale which comprises main units belonging to the cuesta (cuesta plateau and cuesta front), and to the fluvial, mass movement, periglacial, organic, aeolian and the anthropogenic environment. The second type are hybrid geomorphological maps, which here are used to show three detailed characteristic landscapes. These concern a former meander of the Sûre near Bettendorf, the transition from the cuesta front to the fluvial landscape near Reisdorf, and a mass movement area along the cuesta front near Wallendorf.

A.C. Seijmonsbergen (✉)
Institute for Biodiversity and Ecosystem Dynamics,
University of Amsterdam, Science Park 904,
1098 XH Amsterdam, The Netherlands
e-mail: a.c.seijmonsbergen@uva.nl

L.W.S. de Graaff
Research Foundation for Alpine and Subalpine
Environments, Stern 6, Broek op Langedijk
The Netherlands
e-mail: leowsdegraaff@kpnmail.nl

5.1 Introduction

Geomorphological mapping as a scientific discipline has been modernized drastically over the past 15 years, mainly due to technological advances, such as Geographic Information Systems (GIS), the increasing detail of Digital

Elevation Models (DEMs), and field mapping tools such as Global Positioning Systems (GPS) and mobile GIS. Whereas classical geomorphological maps depict the landscape using a variety of symbol- and color-based legends (e.g., Barsch and Liedtke 1980; de Graaff et al. 1987; Klimaszewski 1990; Gustavsson et al. 2006; Seijmonsbergen et al. 2011), modern geomorphological maps use GIS-based mapping for presenting and analysis of the landscape (Seijmonsbergen 2013). This means that a modern geomorphological map has nowadays become a repository of digital geomorphological information layers, stored and managed in a digital platform such as a GIS (Gustavsson et al. 2006, 2008).

Digital information can easily be combined into new information layers by using spatial analysis and/or modeling tools. Therefore, classical mapping is gradually being challenged by digital mapping procedures. Such mapping includes the analysis of digital elevation models (DEMs), the use of mobile GIS devices equipped with GPS for field inventories and (3D) visualization in a GIS.

Expert knowledge of the experienced earth scientist remains especially important for interpreting unclear field conditions. For example, the study of sediment sequences may be required for the interpretation of complex landforms which must be carried out in the field. Less effort can be put into drawing of field boundaries, a procedure that, to a large extent, can be done in a (semi-) automated way from digital data sources, which also reduces subjectivity in selecting landform boundaries.

In Luxembourg, geomorphological landforms and processes have been documented in the ‘Carte Géomorphologique Du Grand-Duché De Luxembourg’, at a scale 1:100.000, published by the Ministère des Travaux Publics du Luxembourg—Service Géologique (1984), but detailed (digital) geomorphological maps do not exist for the whole country. Modern digital geomorphological maps include a variety of attribute information such as process type and activity and material properties. Such attributes can be

weighted and ranked to produce digital derivative maps.

We present a geomorphological inventory method, which combines both the classical and the modern geomorphological mapping approach. The hybrid geomorphological maps include an overview map of part of the cuesta landscape near Diekirch-Reisdorf and three detailed maps in the area. The maps can be consulted as printed versions or as digital information layers. These layers can be queried in a flexible way by the end-user in a GIS or as a GeoPdf document that allows georeferenced scrolling and consulting of attribute information, or in a web-based server interface such as the ‘GeoPortal’ of the University of Amsterdam (see: <http://geodata.science.uva.nl:8080/geoportal/>).

First, a brief overview of the main geomorphological environments that occur in the wider surroundings of the study area is presented. The hybrid mapping method is explained in Sect. 5.2. A geomorphological overview map and three detailed case studies are presented in Sect. 5.4 and ends with general remarks in Sect. 5.5. The aim of this study is to present a new hybrid geomorphological mapping method for the cuesta landscape of Luxembourg.

5.2 Geomorphological Overview

The geomorphology of the cuesta near Diekirch-Reisdorf (Fig. 5.1) has been the subject of interest for three decades of bachelor students, under guidance of staff members from the University of Amsterdam. The cuesta landscape is part of the ‘Gutland’ region of southern Luxembourg, which is underlain by a sequence of Mesozoic sedimentary rock formations of Jurassic and Triassic age, being part of the NE-edge of the Paris Basin (Demoulin 2005; Chap. 1). This rock sequence consists of a contrasting bedrock sequence comprising dolomites, limestone, marl and sandstone that overlies a folded and faulted Devonian-Silurian basement, which geologically is part of the Ardennes. This basement is also exposed over the entire northern part of

Luxembourg, the ‘Oesling’ (Lucius 1948, 1950 see also the overview in Chap. 1).

The geomorphological development of Luxembourg is closely related to the geotectonic history, the variations in bedrock, and responses of the hydrological network to uplift and climatic changes since the Pliocene. For example, relicts of former fluvial deposits have been preserved on various paleosurfaces, that are nowadays present at various altitudes in the landscape along the rim of the Paris basin, varying in age from Jurassic to the Tertiary (DeWolf and Pomerol 2005). The youngest surface is a typical polygenetic surface that extended over the whole basin as the result of several erosion phases under varying climatic conditions. Isolated relicts of coarse fluvial deposits are still present on the plateau, while loamy deposits have been interpreted as fluvial deposits as well. These should not be confused with löss, which was deposited during glacial periods, or inherited as weathering residue from

overlying formations such as the Ariëtschichten Formation (li3) (Levelt 1965). In this polygenetic surface of more or less uniform altitude, the hydrological network was formed. During uplift, the surface was affected by the uprising Vosges, and was warped irregularly (DeWolf and Pomerol 2005). Additional overview information on the geology and geomorphology of Luxembourg is presented in Chap. 1 in this book.

In the following sections, the focus is on long-term landscape development, on the present geomorphology and on the occurrence and changes in the intensity of geomorphological processes.

5.2.1 The Cuesta

The cuesta landscape in eastern Gutland is dominated by a sequence of structurally determined cuestas, which developed on top of slightly tilted alternating resistant and non-resistant Mesozoic sedimentary rocks (DeWolf and Pomerol 2005). A cuesta is an asymmetric ridge built of dipping sedimentary rocks of alternating resistance against weathering and erosion, and elongated along the strike of strata (Goudie 2006). The cuestas in the study area (Fig. 5.1) developed on top of slightly tilted resistant and less-resistant underlying rock formations from the Muschelkalk, Keuper and Lias. During the Pliocene, a planation surface has been formed that obliquely cuts through the tilted Mesozoic rock formations, as the result of fluvial and denudational processes. Following the tectonic uplift, the soft rocks, mainly marls of Keuper age, have preferentially been dissected by the Mosel, the pre-Sûre and its tributaries, the Ourthe and Ernzt Blanche Rivers. The uplift has accelerated during the second half of the Quaternary as the result of active volcanism (Van Balen et al. 2000) Adaptation of these rivers to the local strike and dip directions of the underlying formations resulted in a trellis drainage pattern.

In places, broad and open, low gradient valleys, which are supposed to have formed under



Fig. 5.1 Location of the study area (red box) near Diekirch in the north of the Gutland in Luxembourg

periglacial conditions during the Pleistocene (Verhoef 1966) occur on the cuesta plateau. During interglacial periods, forest cover and soil formation protected the slopes from substantial erosion. The 'retreat' of the cuesta front in the area through degradation processes, in fact, is rather slow (Levelt 1965). The position of former river terraces reveals that natural gravity-driven processes have contributed only slightly to cuesta front retreat. Other studies dealing with the natural development of the Lias cuesta by Jungerius and Mûcher (1970), Jungerius (1980), Jungerius and van Zon (1982), and Poeteray et al. (1984), confirm this observation.

The relative importance of fine-scale geomorphological processes along the cuesta front, such as creep and soil erosion changed, due to the interference of man, mainly through deforestation and agricultural land use, which locally increased the degradation rates of the cuesta front.

5.2.2 The Fluvial Environment

Regional uplift during the Plio-Pleistocene and the general lowering of sea level initiated the formation of deeply incised valleys into the former peneplain, a process during which river terraces were formed at various topographic levels. These terraces have been used in previous studies by De Ridder (1957), Lucius (1948), Verhoef (1966) and Wiese (1969) in the confluence areas of the rivers Sûre, Ourthe and Ernzt Blanche, in order to reconstruct former river courses in space and time. However, new data on mantle plume activity below the Vosges, may well have influenced former relative age correlations of terraces (DeWolf and Pomerol 2005), which is hardly an issue when correlating over short distances. Pleistocene terrace relicts in smaller tributary streams have scarcely been described (Kausch and Maquil 2006), although they probably do occur east of Medernach within the study area.

On a detailed scale, quantitative erosion studies, e.g., Duysings (1985), Van den Broek (1989), Cammeraat (1992, 2002), Hendriks

(1993), and Hooff and Jungerius (1984), focused on the measurement of detailed geomorphological and soil forming processes in the areas underlain by (forested) marls (Keuper) of the Gutland, which shed light on the hydrological behavior of small catchments under forest cover (see also Chap. 2). In particular, the supply of sediments to first-order streams revealed interesting data on erosion/sedimentation rates from both surficial and subsurface processes as well as the influence of burrowing animals (Imeson 1977; Imeson and Vis 1984; Hooff 1983; Jungerius and van Zon 1984). Cammeraat (2006) noted that mechanical and chemical erosion in such areas is strongly related to truncation of soil profiles, dispersion of clays, dissolution and to biological subsurface activity, leading from low to moderate natural erosion rates.

5.2.3 Mass Movement Environment

As a consequence of the increase in relief and of changing climatic conditions, mass movement processes became gradually more active during the Middle and Upper Pleistocene. Important is the strong impact of periglacial conditions during glacial cycles (ice ages), and periods of absence of a full vegetation cover. Gelifluction or congelifluction coincided also with an increase of other types of active mass movements, such as cambering, toppling and rock fall along the cuesta front and along major river slopes. Though less active, the last-mentioned processes are still continued today.

Landforms and deposits resulting from flow-type mass movements have been mapped mainly along the foot of the cuesta front, and comprise mudflow, debris flow and solifluction deposits. Solifluction here includes all flow-type processes able to transport a weathering mantle including the formed soils by flowage of (partially) water-saturated material. Flowage frequently occurs on the transition of the base of the Luxembourg Sandstone (li2) to the underlying Pilonotenschiefer (li1) and Steinmergel Marls (km3). Numerous niches occur along the cuesta front and on the slopes and at the heads of fluvial

valleys. Such niches often originate from a combination of processes which are triggered by exfiltration of groundwater, leading to erosion, solifluction, soil creep, and surficial sliding.

Palynological and soil records from mardels, small closed depressions in the landscape, have been studied in Chap. 3. They concluded that mardels result either from dissolution of gypsum bearing layers that occur within marls from the Keuper, collapse along joint patterns in the Luxembourg Sandstone or from excavations. In some cases, the mardels are ponded or partially filled by colluvium and or peat.

Fine-scale mass movement processes along small meandering streams such as subsoil fall, bank failures and creep (Duysings 1985), and the effect of litter transport (van Zon 1978) have not been addressed in the presented maps. Such processes need to be measured and monitored to be able to quantify their distribution in time and space. They can potentially be mapped, but additional inventories at a detailed scale, and preferably using high resolution LiDAR-based DEMs, are necessary.

5.2.4 Periglacial, Organic and Aeolian Environment

The so-called dells, the shallow, broad open asymmetric valleys on the cuesta plateau, are regarded as relicts of the periglacial environment during which flow-type (solifluction) processes were dominant on the cuesta plateau. At present, many dells are still influenced by flow-type processes, therefore most of them have been categorized as solifluction niches. Peat and organic deposits have been locally formed and preserved in mardels (Chap. 3) and in poorly drained upper valley sections in areas underlain by marly rocks. Remnants of Tertiary duricrust formation on the sandstone cuesta may also lead to local peat formation (Cammeraat et al. Chap. 6). Löss, often found as transported and re-deposited

slope and colluvial deposits, is locally found in former lee side areas of undulating flat-topped plateau areas and fluvial terraces and divides, such as the Zëpp, Koop, and Eebierg and document former cold climatic conditions.

5.2.5 Human Impact on the Landscape

Deforestation, intensified land use and climatic changes have caused the rate of geomorphological processes to change over time, the effect being different on different substrata. As a counter measure against accelerated soil erosion, farmers started to construct obstructions, such as stone rows, hedges, and lynchets, more or less parallel to contour lines in the landscape. Countless lynchets have been erected, transforming the local slope geometry into a stepped terraced landscape. Lynchets are frequent in the areas underlain by marl, mainly along the cuesta front and along foot slopes of river valleys, where they function as colluvial sediment traps. These lynchets are mostly depicted on the 1:20.000 topographical sheets of Luxembourg (Table 5.1), maps that formed the basis for geomorphological mapping of these important features.

The increase in sediment transport and deposition as the result of human interference is also observed in numerous first-order streams, in which small stream terraces locally had formed, a possible effect of short-time disturbance in the steady state balance between erosion, transport, and sedimentation. However, natural causes, e.g., the presence of a resistant sandstone layer, may trigger local terrace formation until the local stream has cut through this protective layer. Landscape elements such as quarries, pits, and infrastructure are examples of anthropogenic influence that may irreversibly disturb natural landforms and processes.

Table 5.1 Spatial data used for preparation of the hybrid geomorphological maps

Data	Source/Date	Scale/Cell size	Use
Topographical maps 1:20.000 sheets 9, 12, 13 and 1:5.000, sheets 75–77 and 109–119	Cadastral and Topographical Administration Luxembourg 1987 and 1999	1:50.000/1:20.000/1:5.000	Field mapping/location and orientation
Historic air photos, panchromatic	Cadastral and Topographical Administration Luxembourg 1987 and 1999	1:20.000, High resolution panchromatic photo-prints	Land use change/3D stereo landscape interpretation and mapping
Satellite image	France/Spot 3 MS 1997	25 m	Historic land use
Geological maps	Geological map sheets 6, Diekirch (1949) and 7. Echternach (1949) by M. Lucius and map sheet Beaufort (1981) by M. Geister-Frantz	1:25.000	Distribution of lithology and materials, relation to landforms/landscape genesis
Regional literature	e.g., Verhoef (1966), Levelt (1965)	Not applicable	Background information of case study areas
Google Earth/Bing aerial	GE Version 6, various dates: 2002, 2005, 2009, 2010	Recent high resolution true color air photos	As backdrop images, for mapping and location purposes.
Historical maps	Bibliothèque Royal de Belgique/Ferraris (1777)	Approx. 1:25.000	Land cover change
Digital Elevation Map (DEM), slope angle map	Cadastral and Topographical Administration Luxembourg Topographic map 1:20.000 sheet 9, 12, 13	Contour interval 5 m, cell size 5 m	Visualization/analysis/digital mapping

5.3 Geomorphological Mapping Method

Thorough understanding of all landforms and former and present processes forms the basis for a geomorphological inventory. The geomorphological map is a hybrid map, in which a classical geomorphological map is combined with a digital geomorphological map. The workflow in Fig. 5.2 presents five steps which are necessary to make the hybrid geomorphological map: (1) Data/fieldwork preparation, (2) Fieldwork, (3) Classical Geomorphological Map, (4) Digital Geomorphological Map, and (5) Hybrid Geomorphological Map. The legends of the classical geomorphological map are shown in Fig. 5.3, the digital geomorphological legend in Table 5.2. In the following paragraphs, each of these steps will be described.

5.3.1 Data/Fieldwork Preparation

For the classical and digital mapping, multiple datasets with from different sources have been used. An overview of these source data and their metadata information is listed in Table 5.1. All datasets have been imported in an ArcGIS file geodatabase. For that, all available paper maps and historic panchromatic air photos have been scanned and georeferenced into the GCS_Luxembourg_1930 geographic coordinate system using the D_Luxembourg_1930 datum from the ArcGIS projection toolset. After all data have been collected and properly stored and structured in a file geodatabase, a preliminary concept geomorphological map has been prepared by extracting geomorphological information from 3D aerial photographs under a mirror stereoscope in combination with 3D drapes of historic aerial

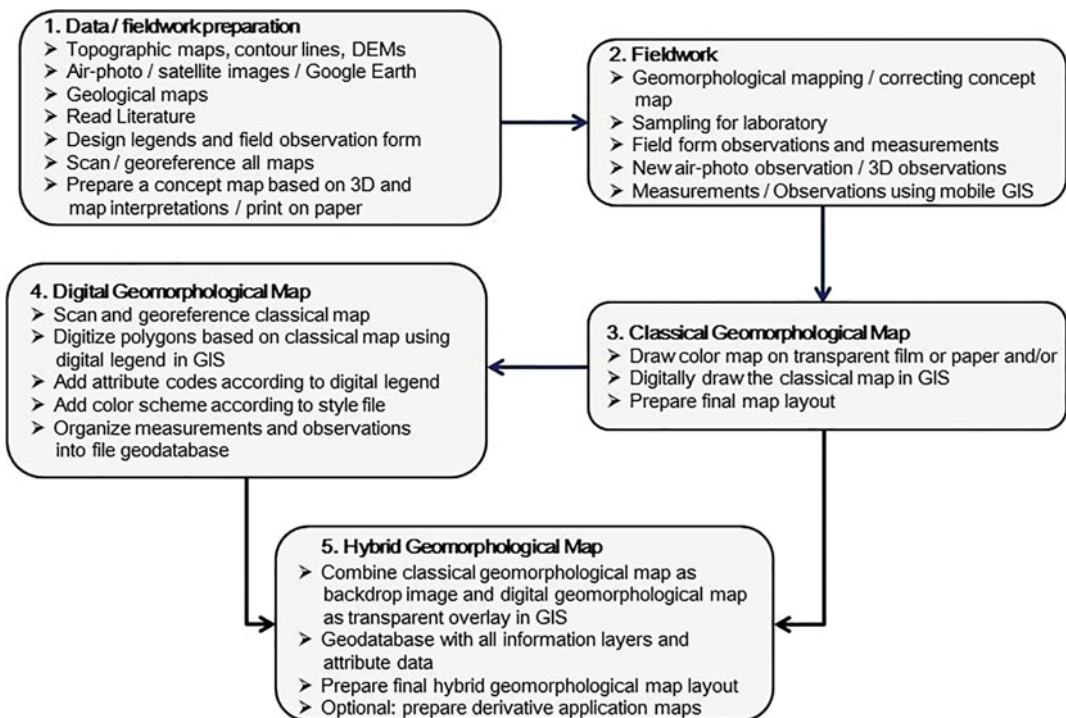


Fig. 5.2 Workflow for the preparation of the hybrid geomorphological map

Legend geomorphological symbol map Luxembourg

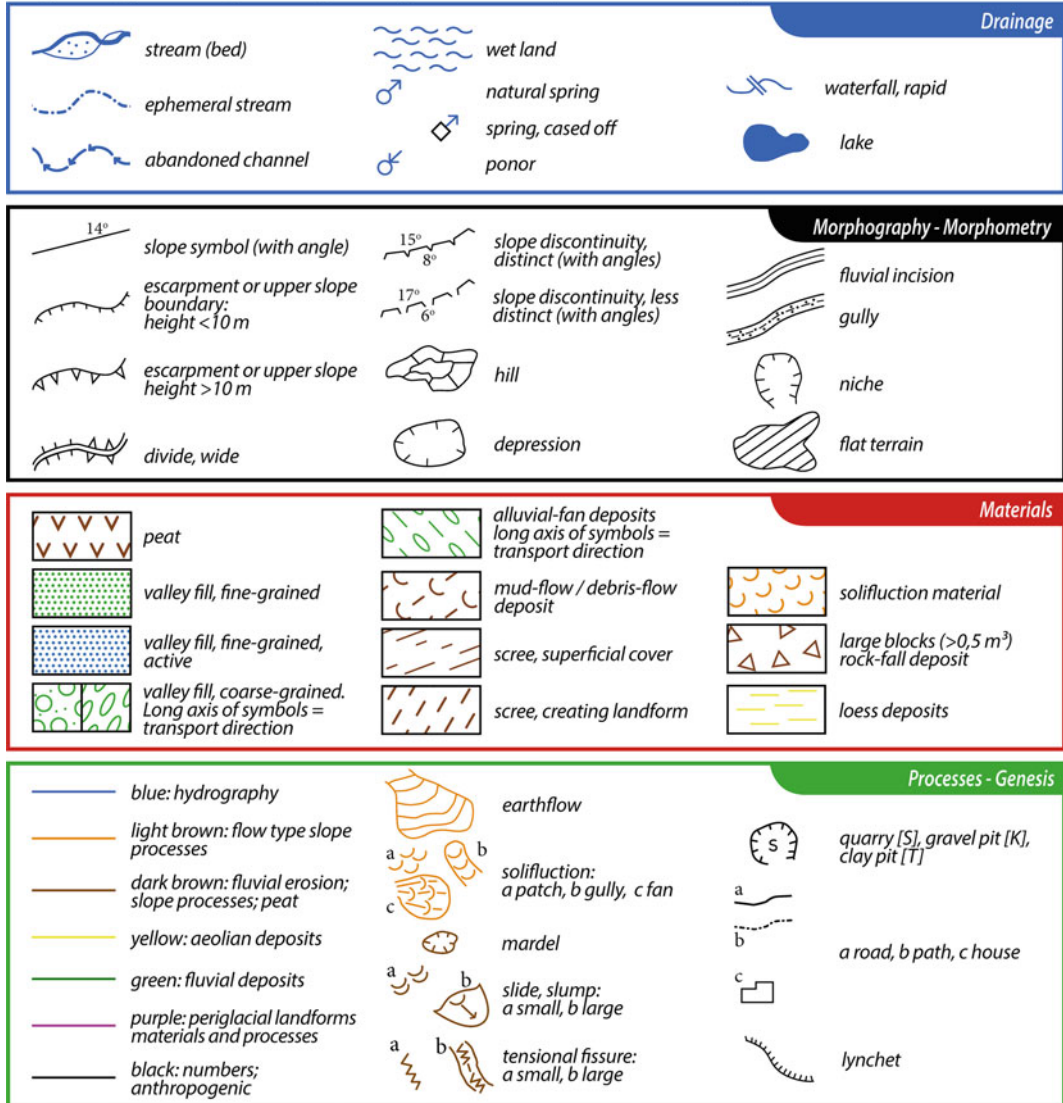


Fig. 5.3 Symbol-based classical geomorphological legend used in Luxembourg

photographs over a 5 m resolution DEM in ArcScene in combination with the recent imagery available in the Google Earth virtual globe environment. The concept map, including its legend is then utilized as a paper copy in the field, in combination with a field form.

The field form contains six attributes, which, together, describe the geomorphological situation in a landscape, namely (1) The geomorphological main unit, (2) The geomorphological subunit,

(3) Process I, (4) Process II, (5) Unconsolidated material, and (6) Process activity. On the field form, labels or GIS codes are marked that correspond to the legend items of Table 5.2 for the geomorphological main- and subunits, and to the GIS codes in Table 5.3 for the additional attribute information. In many complex, landscapes more than one process is or has been active. Therefore at first, predominant process is selected and an optional second active or fossil process

Table 5.2 Legend for polygon-based digital geomorphological mapping

Main units		Landforms and deposits	GIS code	Color
Cuesta 100	Plateau 110	Horizontal, <3°	111	
		Sloping, >3°	112	
		Relic hill, butte	113	
	Front 120	Cliff	121	
		Slope, covered by dispersed slope deposits	122	
		Foot slope with accumulation of slope deposits	123	
Fluvial 200	Erosion 210	Rock terrace, horizontal <3°	211	
		Rock terrace, sloping >3°	212	
		Abandoned channel	213	
		Gully/small valley	214	
		Steep valley slope	215	
		Low-angle valley slope	216	
		Divide	217	
	Accumulation 220	Terrace, horizontal <3°	221	
		Terrace, sloping >3°	222	
		Alluvial fan	223	
		Valley floor	224	
	Open water 230	Wide river	231	
		Lake	232	
		Artificial basin	233	
	Mass movement 300	Denudation/transport 310	Erosional niche	311
Solifluction niches			312	
Complex niches			313	
Slope affected by landslides			314	
Mardel			315	
Accumulation 320		Slope underlain by slide deposits	321	
		Landforms underlain by fall deposits	322	
		Landform underlain by flow deposits	323	
Periglacial 400	Dell	410		
Organic 500	Landform underlain by peat deposits	510		
Aeolian 600	Landform underlain by löss deposits	610		
Anthropogenic 700	Urban area	710		
	Leveled terrain	711		
	Pit, quarry	712		
	Other	713		

5.3.2 Fieldwork

code can be added in a separate column. A final attribute field is added to document the current process activity in the landscape, in five categories. The activity classes are based on field evidence observed in the field, such as occurrence of tilted trees, disturbed fences, cracks in buildings and roads, exfiltration of water, cracks in the grass cover, absence of vegetation cover, and presence of mosses/lichens, evaluated within the specific geomorphological setting for each geomorphological subunit.

Fieldwork offers the opportunity to collect all data necessary to prepare the classical geomorphological map and to collect attribute information for storage in the various digital geomorphological information layers. In practice, this means that the area is visited by walking efficiently to characteristic areas recognized in the concept map and adapting unit boundaries and adding cartographic symbols on drainage, morphography/morphometry, materials and

Table 5.3 List of GIS codes and attributes legend for process/conditions, materials and process activity

GIS code	Processes I and/or II	GIS code	Materials	GIS code	Process activity
1	Human influence	40	Waste material	80	Not active
5	Weathering	45	Peat, organic-rich material	81	Fossil activity
10	Soil saturation/ponding	50	Fine grained fluvial deposits	82	Low activity
15	Fluvial erosion	51	Coarse-grained fluvial deposits	83	Moderate activity
16	Fluvial deposition	52	Alluvial fan deposits	84	High activity
20	Solifluction/soil creep	53	Fine grained deposits (solifluction and löss)		
21	Debris flow/mudflow	60	Dispersed slope deposits forming a thin cover on rock		
22	Sliding/slumping	61	Slope deposits, determining landform		
23	Fall	62	Solifluction (mixed slope deposits)		
24	Rock disintegration (fissuring, toppling, rock creep)	63	Solifluction material, mixed with fluvial deposits		
25	Subsidence	64	Blocks, coarse/fine rock fall deposits		
30	Periglacial	70	Water		
35	Aeolian				

processes/genesis (Fig. 5.3). Field comparison with historic air photos and geological maps is useful to train the geomorphologist, so that similar field situations can be recognized elsewhere. A hand-held GPS devices and/or mobile GIS is used to mark waypoints, such as observation points to register the field form information, and to add photo locations, to record optional sampling sites and rock and/or sediment exposures, that are important to understand landscape genesis.

5.3.3 Classical Geomorphological Map

Once the 1:10.000 scale classical geomorphological map boundaries and cartographic symbols have been finished on a transparent drawing film in the field, a final version was prepared. In our method, we first prepared a transparent

“black & white” version during field mapping, which was subsequently drawn in colors using the standard palette presented in Fig. 5.3 under “Processes-Genesis,” which has been adapted after de Graaff et al. (1987). Subsequently, the colored version was scanned, and redrawn as a new vector layer by using a drawing tablet coupled to the Adobe Illustrator software. The following step was to export the map as a raster layer to ArcMap and add a coordinate system. Examples of these maps are presented and explained in detail in Sect. 5.4.

5.3.4 Digital Geomorphological Map

The digital geomorphological legend (Table 5.2) has a hierarchical structure, which means that the main geomorphological environment can be divided into finer units—comprising landforms and deposits—that together build a higher order

legend unit. This legend is used to convert the scanned and georeferenced classical geomorphological map into a polygon-based geomorphological information layer through manual definition and digitalization of polygons using the classical map as a backdrop image in ArcGIS. Each polygon has been assigned attribute codes for the 'main units' and 'landforms and deposits' (see Table 5.2). A color scheme is added by using a 'style file', that holds the color definitions and transparency information for each unit (Table 5.2). Additional attributes derived from the field form observations (Table 5.3) are added to the digital geomorphological map to further complete the geomorphological geodatabase, which is structured according to the original design by Gustavsson et al. (2006).

5.3.5 Hybrid Geomorphological Map

The hybrid map is a visual combination of the classical and the digital geomorphological map. The final map shows the classical geomorphological map as a backdrop image of the digital geomorphological map, the latter displayed with 50% transparency. In such a way, the original symbols can still be evaluated, while the boundaries and categorization of the digital layer is also visible.

The final layout depends on the requirements of the end-user. A classical map is normally printed on paper and displays all possible information in one static layer. The modern hybrid geomorphological map can be visualized on-screen in 2D or in 3D bird's eye view, in combination with tabular content. Another option is to view the maps via a web-service interface, on mobile and/or remote devices, or to disseminate the maps in GeoPdf format. GeoPdf maps display attribute information and coordinates while scrolling over the screen (Otto et al. 2011). These new possibilities provide the end-user with the freedom to extract and present information according to particular needs, just in a single layer or in combination with other layers, and in formats suitable for storage, analysis, presentation, and communication.

5.4 Geomorphological Map Examples

5.4.1 Overview Map

The geomorphological overview map is shown in Fig. 5.4. A hillshade map is displayed as a backdrop image with 50% transparency to enhance topographic expression. A contour layer (interval 10 m) has been added, as well as a 'Rivers' and a 'Roads' layer. The map covers the transition of the Lias cuesta to the fluvial landscape of the Ern Blance, Ourthe and Sûre rivers. A note to the legend has to be made here. The occurrence of peat and löss in this area is fragmented and patches are small on the displayed map scale. In the digital environment of a GIS, where the smallest mapping scale is less important, visibility is more flexible and can be adapted by the individual user by zooming. In addition, attribute information on materials (Table 5.3) allows for differentiation of materials and processes.

The eastern half of the map is largely underlain by the Luxembourg Sandstone (Lias) and covers the cuesta, which is subdivided into two main units: the plateau and the cuesta front. The plateau between Beaufort and Haller is dissected by a widely spaced pattern of steep-sided valleys, in general draining towards the southeast, which reflects the general dip direction of the underlying strata. The head of these valleys often continues into shallow and relatively inactive niches or broad valleys, which have been formed by a combination of periglacial flow processes such as (con)gelifluction, and by recent shallow ongoing flow processes. Occasionally, for example, east of Bigelbach (Fig. 5.4), a coarse-grained scatter of fluvial rounded quartzite cobbles at relatively high altitude on the plateau in combination with the loam-rich material, may indicate fluvial deposition of the former Sûre/Ourthe-Ernz-Blanche river floodplain, parts of which were already recognized by Verhoef (1966). The slope angles along the cuesta front generally range between 10° and 35°, although vertical cliffs in the Luxembourg Sandstone locally may predominate. The length of the local

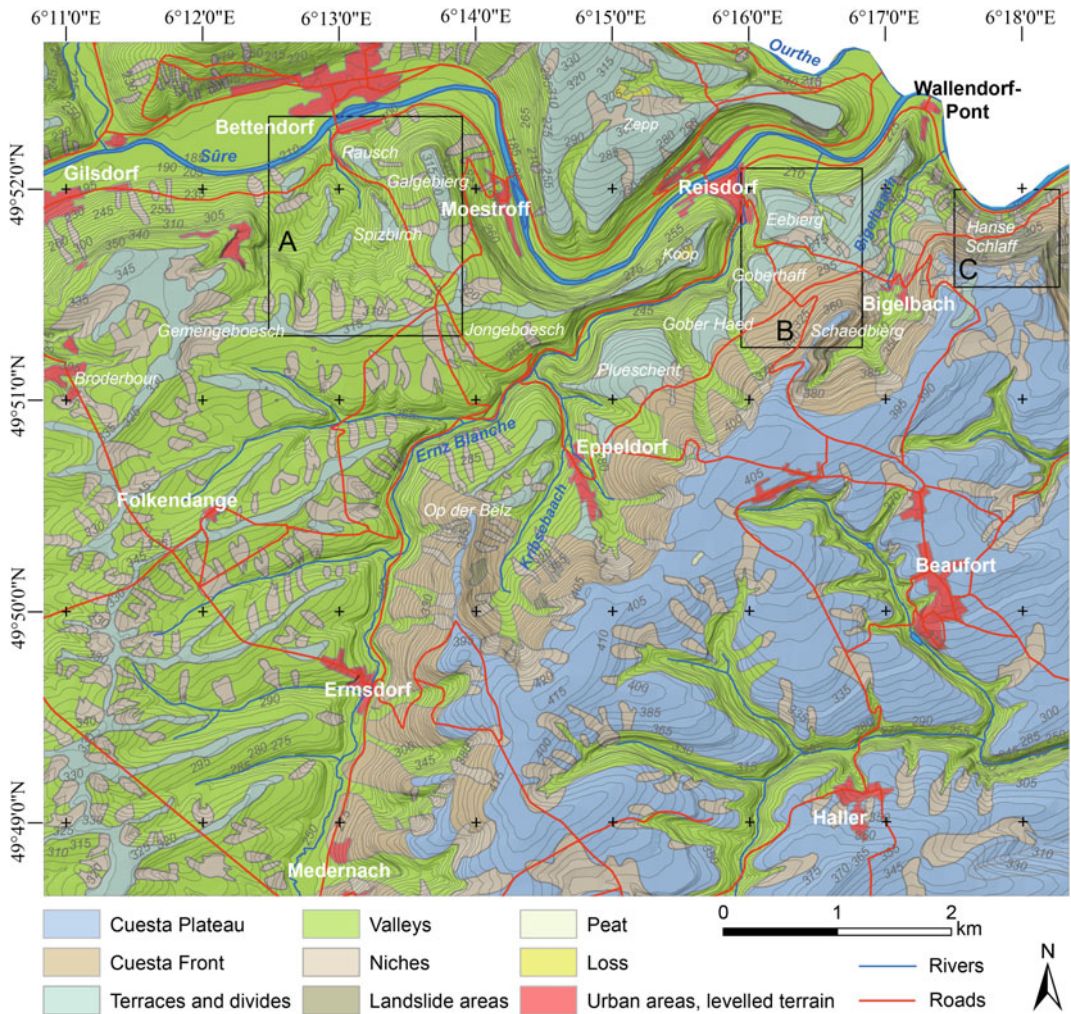


Fig. 5.4 Digital geomorphological overview map (location see Fig. 5.1). The inset frames A, B and C correspond to the maps of Figs. 5.5, 5.6 and 5.8

cuesta front slope can exceed 1 km, although northeast of Bigelbach the valley of the Sûre ‘meets’ the cuesta front (Fig. 5.4). Undercutting of the River Sûre has over-steepened the cuesta front slopes, in which, over a short distance, the stratigraphic sequence of ‘sandstone - marl - dolomite’ is crossed. Between Ermsdorf and Eppeldorf and southwest of Bigelbach some mesa and butte-like landforms have developed at the front of the cuesta resulting from differential escarpment retreat. Landsliding occurs and is expressed by rotational slides, rockfall, tensional

fissuring and local springs (see detailed description of case area C: Hanse Schlaff).

The western half of the map is underlain by formations belonging to the Keuper and Muschelkalk and the geomorphology is dominated by fluvial valleys, erosional and depositional terraces, interrupted by flat-topped local divides. The altitude of the landscape varies between 195 and 340 m, which is lower compared to altitudes of the cuesta plateau (320–420 m). Striking landforms are the abandoned and entrenched meander curve near Bettendorf

(see for detailed map and description case area 'A') and a sequence of fluvial terraces Between Eppeldorf and Bigelbach. The sub-horizontal surfaces of Pluschent, Gober Haed, and Goberhaff are erosional in nature, their position reflects the gradual migration and incision of the meandering rivers in the uplifted landscape at various topographic levels. Therefore, spatial distribution of fluvial landforms and deposits in the region emphasizes that the long-term retreat of the cuesta front is primarily controlled by fluvial processes and locally by mass movement processes that may preferentially use geological faults and/or joints. Some of the tributary streams, such as the Kribsebaach and the Bigelbaach, have managed to develop small catchments after further incision of the main rivers. Nowadays, their discharge is low, which is due to relatively low precipitation regimes, local process activity, and capturing of surface drainage.

5.4.2 Detailed Maps

Detailed geomorphological maps are presented to describe three case studies (for locations see Fig. 5.4). Example 'A' is part of an abandoned *meander curve near Bettendorf* and illustrates the adaptation of the incising Sûre river to a lower base level (cf. Verhoef 1966). The second area 'B' covers an area near the *Eebierg*, close to the cuesta front, highlighting former fluvial deposition. These deposits later became gradually eroded by various processes. The third area near the *Hanse Schlaff* presents a transition of the cuesta plateau to a contrasting landslide complex along the cuesta front, which is triggered by a combination of environmental factors.

Case study A: Meander curve near Bettendorf

In Fig. 5.5 (upper half), the classical geomorphological map is presented (for a legend, consult Fig. 5.3), the hybrid geomorphological map is also shown in Fig. 5.5 (lower half). The area is fully a part the fluvial landscape (see Fig. 5.2). The label numbers refer to the GIS codes that are used for the 'Landforms and deposits' units of the polygon-based legend (Table 5.2).

The shape of the former meander of the Sûre River (compare Fig. 5.2), seen in the upper left corner of the map of Fig. 5.5, is reflected in the shape of the local surrounding water divides (code 217) in the southern and eastern section of the map. Inside this former meander both rock terraces (code 211) and accumulation terraces (code 221) have been mapped, some of them matching Verhoef's (1966) terrace levels T6, T5, and T4, while others could not be verified or were interpreted differently after field observations. As a consequence of the meander contraction, the younger tributary streams show a drainage pattern drainage network, perpendicular to the former course of the Sûre River. The lower slope west of the Galgebjerg is covered with a mixture of gravel and cobbles of fluvial origin, and flow-type slope deposits. The original fluvial terrace has been largely eroded and as such, has not been mapped. On the Galgebjerg and other water divides fragmented covers of fluvial gravel have been preserved, which supports evidence for former fluvial deposition. A remarkable man-made valley fills with domestic waste (code 713) has blocked the drainage of the sharply, up to 20 m deeply incised local valley (code 214) in the central western part of the map. Review of the geological map of the area, and given the valleys geomorphological position indicates that fluvial incision on a fault could be a reason for the relatively straight surface expression. Although flow-type processes and fluvial processes still continue, their impact has decreased substantially, due to artificial subterranean drainage and the construction of lynchets.

Case study B: Eebierg

The 'Eebierg' is the local name for a flat-topped fluvial terrace level at 266 m altitude, which corresponds in the work of Verhoef (1966) to his T6 Terrace level. The preservation potential of the gravel of the Eebierg is relatively high, since the Eebierg is well protected against erosion by a resistant underlying dolomite layer of the Grenzschichten (mo3-dolomite/limestone alternations), acting as a caprock which supports the up to 5 m thick cover of gravel deposits of the Eebierg. Furthermore, degradational processes, such as gullying, erosion, flowage, and

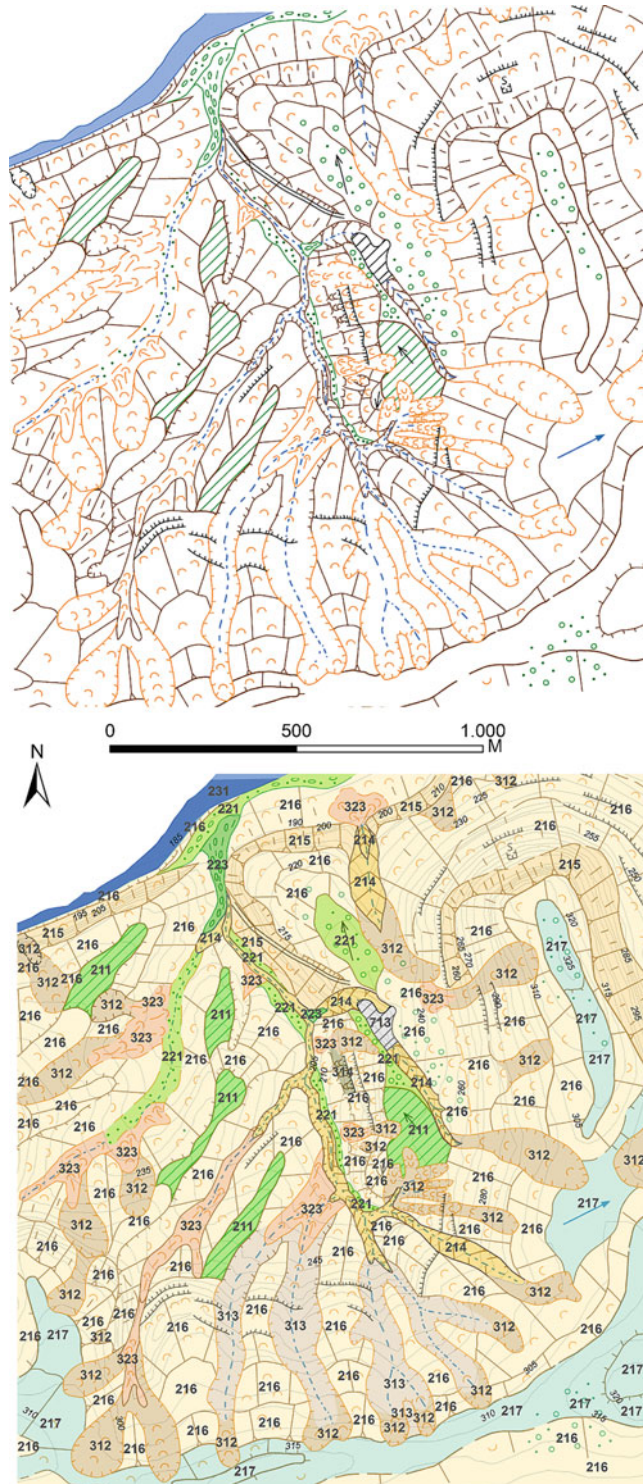


Fig. 5.5 *Upper half* Classical symbol-based geomorphological map of the abandoned meander curve near Bettendorf. For location see Fig. 5.4, for corresponding legend see Fig. 5.3. *Lower half* Hybrid geomorphological map, in which the classical symbol-based geomorphological and modern geomorphological map of the abandoned meander curve near Bettendorf are combined. For location see Fig. 5.4, for corresponding legends see Fig. 5.3 and Table 5.2

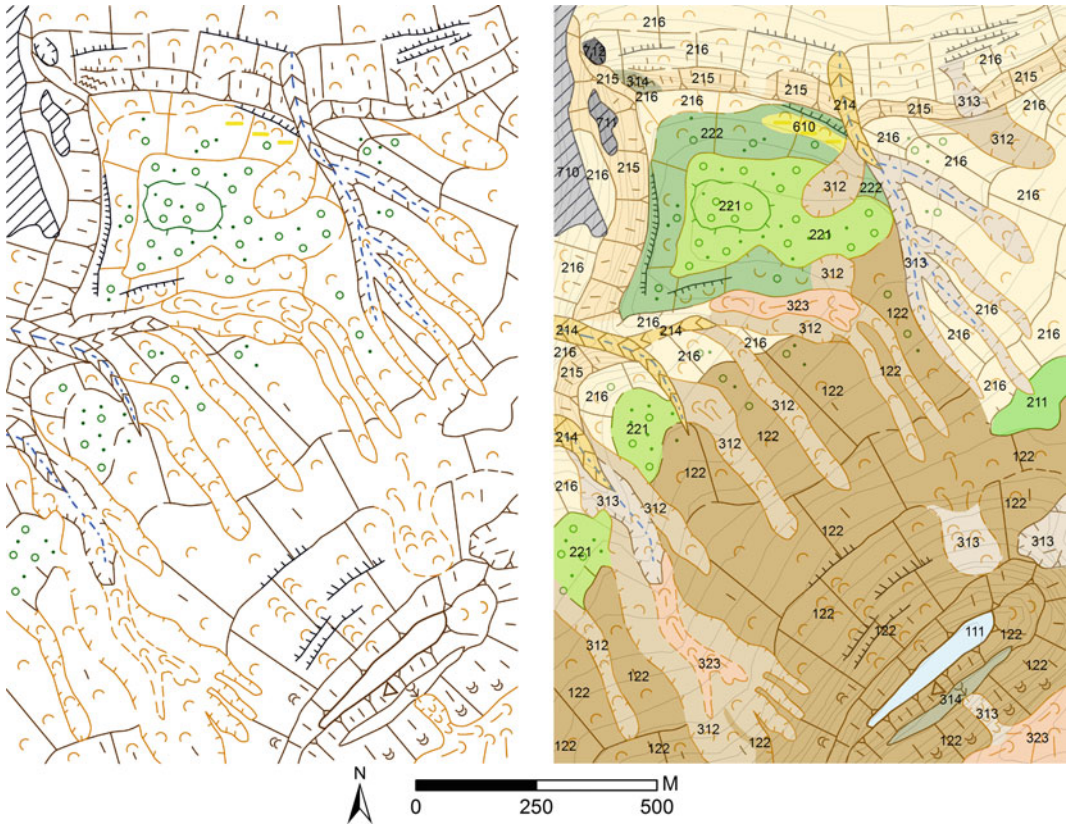


Fig. 5.6 Classical symbol-based geomorphological map (left) and the corresponding hybrid polygon-based geomorphological map of the Eebierg and surroundings. For legends see Fig. 5.3 and Table 5.2

mass wasting developing from the slopes NW of the ‘Schaeferberg’ (Fig. 5.2), a local butte which is hardly attached to the Luxemburg Sandstone plateau, cannot reach the Eebierg. The latter takes an isolated position which enhances its preservation potential, in contrast to, for example, the Pluschent and Goberheed rock terraces (Fig. 5.2). The gravel content of the Eebierg contains a high content of iron-ore pebbles (‘Rasenerz’), proving that at least part of the gravel stems from the ‘Minette’ (Riezobos et al. 1990), an area in the south of Luxembourg, and as such, cannot be of local origin. The map fragment (Fig. 5.6) shows the diverse geomorphology in a section from the Schaeferberg butte, along the cuesta front slopes and the Eebierg terrace to the village of Reisdorf (for names: refer to Fig. 5.4). This coincides with the geological transition from the Luxemburg Sandstone, passing marl

from the Keuper and ending with the Muschelkalk Formation. In his sequence of terrace levels, Verhoef (1966) notes a decrease in Rasenerz percentages from above the Eebierg terrace (called T6-terrace), falling down to almost zero at the T9 terrace level. At the same time, he explains the high percentages of quartzite cobbles above the T9 level as the result of prolonged weathering, which has eliminated relatively non-resistant components. For a landscape overview photo of this area, see Fig. 5.7.

The two maps of Fig. 5.8 present the classical symbol-based map (left) and the hybrid geomorphological map (right). The steep-sided incised valley of the river Sûre has undercut the cuesta front, which led to active deep-reaching and surficial mass movements. The morphology of the plateau is undulating, controlled by differences in resistance within the Luxemburg



Fig. 5.7 Overview of cuesta landscape from Bigelbach to the east, showing the frontal part of the Schaedberg butte (outlier of Lias cuesta), the escarpment of the Muschelkalk cuesta (*upper right*) and in between the terrace landscape of Eebierg, Koop and Zépp

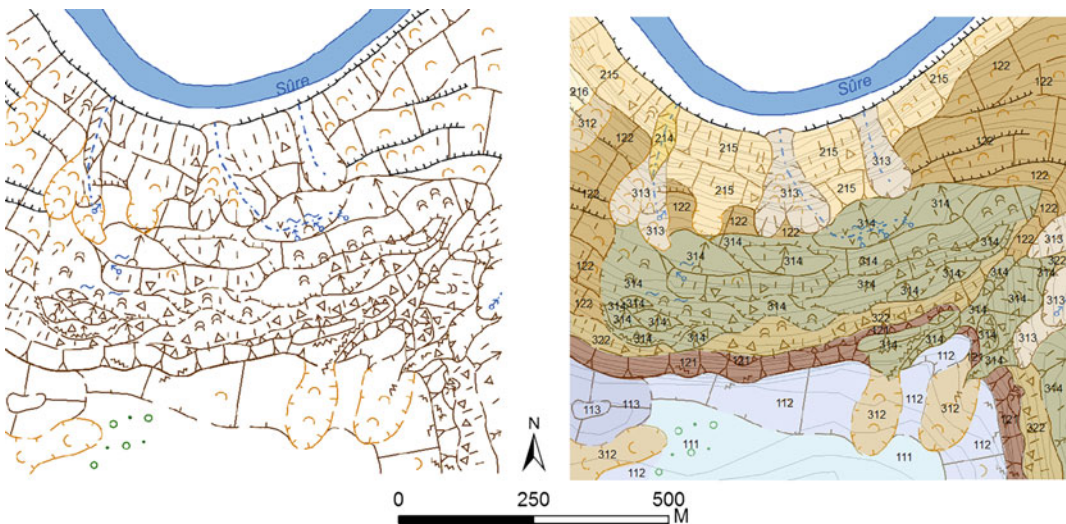


Fig. 5.8 Classical symbol-based geomorphological map (*left*) and hybrid geomorphological map (*right*) of the Hansche Schlaff area. For legends see Fig. 5.3 and Table 5.2

sandstone, often reflecting variations in calcium carbonate content and fracture density variations. Local deposits of coarse rounded quartzite gravel at heights of 400 m.a.s.l. indicate former floodplains of the major rivers. Along the cuesta front, the sandstone layers have been destabilized by a combined influence of the undercutting power of the River Sûre and exfiltration of groundwater on top of the marl/clay rich formations belonging to the Keuper and Pilonotenschiefer. The sandstone is fragmented into rotational slide units. Further disintegration is also leading to extensive rockfalls along the

upper part of the cuesta front. According to Colbach (2005), vertically discontinuous short fractures with decimetric spacing, and fractured zones, cutting through the whole formation may occur. The abrupt change in direction of movement along the northern and eastern exposed slopes illustrate the effect of tension release. The increased downslope surface water availability in combination with relatively steep slopes underlain by marls is marked by the transition to flow-type mass movement (solifluction and creep), although the steeper slopes suffer from scree fall as well.

5.5 Concluding Remarks

Geomorphological mapping has evolved from a pure paper-based inventory into a digital GIS-based inventory. One result of this development is the production of hybrid geomorphological maps, which are combinations of classical symbol-based and digital geomorphological information layers. The geodatabase, in which the hybrid maps are stored, can easily be extended with supplementary information. The presentation and visualization of hybrid geomorphological maps are not fixed, but can be adapted by the end-user, depending on its use. The hybrid maps contain science-based information that can be interpreted by an environmental scientist for use in landscape reconstructions over time, and for the preparation of GIS-based derivative maps, for example a hazard map. The geomorphological geodatabase, including its attribute data, may further be used as input for scenario models of potential soil erosion, climate change studies, and land use change.

Acknowledgements Jan van Arkel (digital illustrator at IBED) is kindly thanked for preparing Figs. 5.3, 5.5, 5.6 and 5.8. The GIS-studio (www.GIS-studio.nl) of IBED is thanked for computational and software support. The work builds on decades of mapping in the region by students of the University of Amsterdam. We are really indebted to them.

References

- Barsch D, Liedtke H (1980) Principles, scientific value and practical applicability of the geomorphological map of the Federal Republic of Germany at the scale of 1:25 000 (GMK 25) and 1:100 000 (GMK 100). *Z Geomorphol*, N.F. Supplement Band 36:296–313
- Cadastral and Topographical Administration Luxembourg (2015) Topographical maps and historic aerial photos of Luxembourg. <http://map.geoportail.lu/?lang=en>. Accessed 21 May 2015
- Cammeraat LH (1992) Hydro-geomorphologic processes in a small forested sub-catchment: preferred flow-paths of water. PhD-thesis, University of Amsterdam
- Cammeraat LH (2002) A review of two strongly contrasting geomorphological systems within the context of scale. *Earth Surf Proc Land* 27:1201–1222
- Cammeraat LH (2006) Luxembourg. In: Boardman J, Poesen J (eds) *Soil erosion in Europe*. Wiley, Chichester, pp 427–438
- Colbach R (2005) Overview of the geology of the Luxembourg sandstone(s). *Ferrantia* 44:155–160
- de Graaff LWS, De Jong MGG, Rupke J, Verhofstad J (1987) A geomorphological mapping system at scale 1:10.000 for mountainous areas. (Austria). *Z Geomorphol* 31:229–242
- De Ridder NA (1957) *Beiträge zur Morphologie des Terrassenlandschaft des Luxemburgischen Mosel-Gebietes*. PhD-thesis, University Utrecht
- Demoulin A (2005) Tectonic evolution, geology, and geomorphology. In: Koster EA (ed) *The physical geography of Western Europe*. Oxford University Press, New York, pp 3–24
- DeWolf Y, Pomerol C (2005) The Parisian Basin. In: Koster EA (ed) *The physical geography of Western Europe*. Oxford University Press, New York, pp 251–265
- Duysings JJHM (1985) Streambank contribution to the sediment budget of a forest stream. PhD-thesis, University of Amsterdam, 190 pp
- Ferraris CD (1777) *Carte de cabinet Pais Bas Autrichiens*. (Reprint 1965–1970) Bruxelles, Bibliotheque Royal de Belgique
- Goudie AS (2006) *Encyclopedia of geomorphology*. Routledge, London and New York
- Gustavsson M, Kolstrup E, Seijmonsbergen AC (2006) A new symbol-and-GIS based detailed geomorphological mapping system: renewal of a scientific discipline for understanding landscape development. *Geomorphology* 77:90–111
- Gustavsson M, Seijmonsbergen AC, Kolstrup E (2008) Structure and contents of a new geomorphological GIS database linked to a geomorphological map—with an example from Liden, central Sweden. *Geomorphology* 95:335–349
- Hendriks MR (1993) Effects of lithology and land use on storm run-off in East Luxembourg. *Hydrol Process* 7:213–226
- Hooff PV (1983) Earthworm activity as a cause of splash erosion in Luxembourg forest. *Geoderma* 31:195–204
- Hooff PPM, Jungerius PD (1984) Sediment source and storage in small watersheds on the Keuper Marl in Luxembourg, as indicated by soil profile truncation and the deposition of colluvium. *Catena* 11:133–144
- Imeson AC (1977) Splash erosion, animal activity and sediment supply in a small forested Luxembourg catchment. *Earth Surf Proc* 2:153–160
- Imeson AC, Vis M (1984) The output of sediments and solutes from forested and cultivated clayey drainage basins in Luxembourg. *Earth Surf Proc Land* 9:585–594

- Jungerius PD (1980) Holocene surface lowering in the Lias cuesta area of Luxembourg as calculated from the amount of volcanic minerals of Allerod age remaining in residual soils. *Z Geomorphol* 24(2):192–199
- Jungerius PD, Mûcher HJ (1970) Holocene slope development in the Lias cuesta area, Luxembourg, as shown by the distribution of volcanic minerals. *Z Geomorphol* 14(2):127–136
- Jungerius PD, van Zon HJM (1982) The formation of the Lias-cuesta in the light of present-day erosion processes operating on forest soils. *Geogr Ann* 64A(3–4):127–146
- Jungerius PD, van Zon HJM (1984) Sources of variation of soil erodibility in wooded drainage basins in Luxembourg. In: Burt T, Walling DE (eds) *Catchment experiments in fluvial geomorphology*. Geo Books, Norwich, pp 235–245
- Kausch B, Maquil R (2006) Eine pleistozäne Terrasse der Syre bei Oetrange – ein Beispiel für die Hangentwicklung im südlichen Luxemburg (Gutland). *Bull Soc Nat Luxemb* 106:167–180
- Klimaszewski M (1990) Thirty years of geomorphological mapping. *Geographia Pol* 58:11–18
- Levelt ThWM (1965) Die Plateaulehne Süd-Luxemburgs und ihre Bedeutung für die morphogenetische Interpretation der Landschaft. PhD-thesis, University of Amsterdam
- Lucius M (1948) Das Gutland. Erläuterungen zu der Geologische Spezialkarten Luxembourgs, Bd5
- Lucius, M. (1950). Das Oesling. Erläuterungen zu der Geologische Spe-zialkarten Luxembourgs, Bd6
- Ministère des Travaux Publics du Luxembourg—Service Géologique (1984) *Carte Géomorphologique du Grand-Duché de Luxembourg*
- Otto J-C, Geilhausen M, Gustavsson M (2011) Cartography: design, symbolization and visualization of geomorphological maps. In: Smith MJ, Paron P, Griffiths J (eds) *Geomorphological mapping: a professional handbook of techniques and applications*. Elsevier, London
- Poeteray FA, Riezebos PA, Slotboom RT (1984) Rates of subatlantic surface lowering calculated from mar-del-trapped material (Gutland, Luxembourg). *Z Geomorphol* 28(4):467–481
- Riezebos PA, Ten Kate WGHZ, De Bruin M (1990) Eluvial derivation of Rasenerz concretions from the Minette Formation (Luxembourg). Evidence based on numerical classification of geochemical data. *Bull Service Géol Luxemb* 15:1–34
- Seijmonsbergen AC (2013) The modern geomorphological map. In: Schroder J, Switzer AD, Kennedy DM (eds) *Treatise on geomorphology—methods in geomorphology*, 14.4. Elsevier, San Diego, pp 35–52
- Seijmonsbergen AC, Hengl T, Anders NA (2011) Semi-automated identification and extraction of geomorphological features using digital elevation data. In: Smith MJ, Paron P, Griffiths J (eds) *Geomorphological mapping: a professional handbook of techniques and applications*. Elsevier, London, pp 297–335
- Van Balen RT, Houtgast RF, Van der Wateren J, Vandenberghe J, Boogaart PW (2000) Sediment budget and tectonic evolution of the Meuse catchment in the Ardennes and the Roer valley Rift System. *Global Planet Change* 27:113–129
- Van den Broek TMW (1989) Clay dispersion and pedogenesis of soils with an abrupt contrast in texture: a hydro-pedological approach on subcatchment scale. PhD-thesis, University of Amsterdam
- van Zon HJM (1978) Litter transport as a geomorphic process (a case study in the G.D. of Luxembourg). PhD-thesis, University of Amsterdam
- Verhoef P (1966) Geomorphological and pedological investigations in the Rédange-sûr-Attert area. (Grand-Duchy of Luxembourg). PhD-thesis, University of Amsterdam
- Wiese B (1969) Die Terrassen des Ourtals. *Publications du Service Géologique de Luxembourg, XVIII*. Service Géologique de Luxembourg, Luxembourg

Soils of the Luxembourg Lias Cuesta Landscape

6

L.H. Cammeraat, J. Sevink, C. Hissler, J. Juilleret,
B. Jansen, A.M. Kooijman, L. Pfister and J.M. Verstraten

Abstract

The soil pattern of the Lias cuesta landscape in central Luxembourg is strongly related to lithology, land cover and land use. On a short distance, many of the major soil types of the temperate zone can be found, as the substrates show a clear distinction and gradient from acidic to more neutral conditions in both fine and coarser textured materials. This makes the area an interesting showcase of soils for both researchers and students. In separate sections, the various soils are described per landscape unit, and in relation to lithology, landscape position, geomorphological dynamics and land use. It starts with the soils of the highest plateau landscape with soils developed in the Liassic strata, including the Luxembourg sandstone, with dominantly Brunic Arenosols and also Podzols, and on the marls Regosols and Luvisols. Descending the steep cuesta front, the soils developed on the Liassic and Keuper strata in a face slope cuesta position are presented, with dominantly Arenosols, Regosols or Leptosols. Further down the cuesta, soils in the Muschelkalk strata in steep positions are discussed, and which show dominantly Leptosols and Regosols. Also soils developed in younger deposits occur, such as loess and Tertiary and Quaternary river sediments, that are present in various altitudinal positions, with dominantly Stagnosols, Luvisols or Alisols. Finally, the Keuper soils present in a dip slope or rolling landscape position are presented, with mainly Stagnosols or Planosols under forest and Regosols under agriculture. Furthermore, the described trends in soil development were corroborated by an independent statistical test on soil properties and soil types as found in relative undisturbed forests along the described landscape gradient.

L.H. Cammeraat (✉) · J. Sevink · B. Jansen ·
A.M. Kooijman · J.M. Verstraten
Institute for Biodiversity and Ecosystem Dynamics,
University of Amsterdam, Science Park,
PO Box 94240, 1090GE Amsterdam,
The Netherlands
e-mail: l.h.cammeraat@uva.nl

C. Hissler · J. Juilleret · L. Pfister
Catchment and Eco-hydrology Group,
Environmental Research and Innovation
Department, Luxembourg Institute of Science
and Technology, 41 rue du Brill, 4422 Belvaux,
Luxembourg

6.1 Introduction

The soils of the Luxembourg Cuesta Landscape show a wide range in type and composition, as well as in their genesis. In fact, within a very limited area, most soils characteristic for the temperate zone can be encountered, mainly due to the large variation in geomorphology and parent material.

The objective of this chapter is to describe the main soil types related to this cuesta landscape, that are developed on the geological formations of the Liassic cuesta in Luxembourg. The lithology of this landscape includes from top to bottom the calcareous Liassic “Strassen marls”, as well as sandstones of the Luxembourg Sandstone, Keuper strata that are dominated by marls, and the dolomitic Muschelkalk (Fig. 6.1). Furthermore, also soils have developed in Tertiary and Quaternary sediments, including fluvial and mass wasting deposits and loess.

The most important lithological units encountered in this landscape are given in Table 6.1. The various soil types and their typical setting are described in accordance with their catenary position, of which a schematic overview is given in Fig. 6.1.

The description will start with the soils developed on the stratigraphically highest and youngest Mesozoic formations, beginning with the relatively level landscapes of the Strassen formation and Luxembourg Sandstone on the dip slope of the Liassic cuesta (right in Fig. 6.1). Descending the cuesta with typical slope deposits will be described, finally arriving at the alluvial valley bottom of the Sauer. Climbing out of the valley, passing slope deposits again, as well as ancient river terraces, the rolling Keuper landscape will be entered (left in Fig. 6.1). The outline of this chapter follows this landscape gradient. Each soil type will be described with regard to profile characteristics and physico-chemical composition. Soil classification is based on the system ‘World Reference Base for Soil Resources’ (IUSS Working Group WRB 2015; referred to in the text as IUSS 2015), which is one of the two globally used classification systems, the Soil Taxonomy of the USA being the other one (Soil Survey Staff 2014). In addition, the ect-/endorganic profile classification according to Green et al. (1993) is used.

For the European temperate climate zone, trends in soil genesis as a function of parent

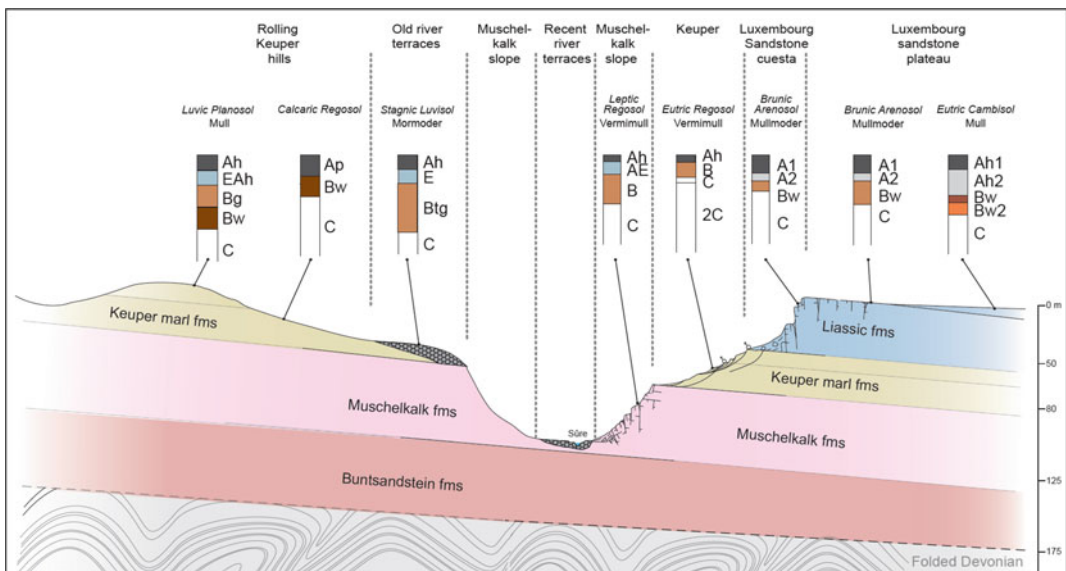


Fig. 6.1 Major geological formations, geomorphological units, typical soil profiles and associated humus type that occur in the Luxembourg sandstone cuesta landscape along a representative transect. *fms* = formations

Table 6.1 Chrono- and lithostratigraphy of the Gutland rock strata

Chronostratigraphy		Lithostratigraphy		
		Lithostratigraphical name ^a	Code ^b	Lithology ^c
Jurassic	Liassic	Mergel und Kalke von Strassen	li3	Marl (limestone)
		Luxemburger Sandstein	li2	Sandstone (sand)
		Pylonoten-schichten	li1	Marl (calcarenite)
Triassic	Rhaetian	Rote Tone	ko2	Red clay
		Sandstein und Schwarzer Blättermergel	ko1	Sandstone and black marl
	Keuper	Steinmergelkeuper	km3	Variegated marl (dolomite)
		Gipsmergelkeuper	km2	Red marl (gypsiferous)
		Schilfsandstein	km2s	Sandstone (conglomerate)
		Pseudomorphosenkeuper	km1	Marl, (sandstone, conglomerate)
	Muschelkalk	Grenzdolomit und Bunte Mergel	ku	Dolomite, variegated marl
		Grenzschiefer und Nodosus-schichten	mo2	Dolomite (marl)
		Trochiten-schichten	mo1	Dolomite
		Gipsmergel	mm1	Dolomite
		Linguladolomit	mm2	Marl (dolomite, gypsum)
		Muschelsandstein	mu	Dolomite, sandstone (marl)
	Upper Buntsandstein	Voltziensandstein	so2	Sandstone (clay)
		Zwischenschichten	so1	Sandstone (clay, conglomerate)
Devonian	Emsian/Siegenian			Quartzites, schists, phyllites, slates

^aThe official German nomenclature is followed as used by Lucius (1948, 1950) and the Luxembourg Geological Survey and after the Geological Map of Luxembourg, sheet 6 (1981)

^bLithostratigraphical code applied on the geological maps of Luxembourg (Lucius 1948, 1950)

^cDominant rock type and thinner intercalations between brackets

material and time are well established, largely based on classic soil chronosequence studies in Germany (e.g. Blume et al. 2016), and France (Jamagne 2011; Duchaufour 2012). General trends can be summarized as follows:

In soils in parent materials with higher acid-neutralizing capacity, such as loess, fluvial terraces (if not too coarse textured), marls and loamy sandstones, *clay translocation (lessivage)* is the dominant process. Clay translocation will occur after an initial stage of Cambisols and similar soils with a Bw-horizon, and lead to textural differentiation between the topsoil and the argic horizon below (Luvisols, Alisols). In relatively sandy soils, impoverishment of clay and associated free iron(hydr)oxides may go so

far that podzolization starts (Retisols, IUSS 2015; Podzoluvisols or Albiluvisols in other classification systems). In more clayey soils, water stagnation on the argic B horizon may lead to, first, saturation and reduction of the horizon showing stagnic to gleyic properties (stagnogley or pseudogley) and acidification, in which case bleached surface horizons develop and vertical drainage is minimal (e.g. Luvisols, Stagnosols and Planosols). The development of pseudogley and eventually stagnogley is primarily dependent on the local geomorphological conditions. A special soil of relatively level terrain and truly clayey parent materials (e.g. Keuper marls) is the so-called Pelosol (Duchaufour 2012), which is marked by strongly restricted vertical drainage

and leaching, and in which lateral transport of clay and other fines prevails. Since seasonal contrasts between wet and dry periods are too small to produce Vertisols, they are generally classified (IUSS 2015) as Stagnic Cambisols, Luvic Stagnosols, Stagnic Luvisols or Planosols, the latter especially under forest. However, such a classification does not properly reflect its genesis, which is by lateral rather than vertical transport of clay particles ('appauvrissement').

Podzolization is a dominant process on acid silicate rocks, with soils developing in time from decalcified Arenosols, over time becoming increasingly acid and exhibiting slight transport of Al-(Fe)-DOM compounds, towards fully developed Podzols with prominent eluvial (albic material) and illuvial (spodic horizon) characteristics. The nature of the latter (Bs/Bh or only Bh) depends very much on the drainage, with poorly drained soils generally developing a stagnating Bh horizon with complete removal of free iron (hydr)oxides, and distinct accumulation of a surficial organic layer and, eventually, peat. Rates of the podzolisation process depend on the (low) acid buffering capacity of the parent material and the vegetation (promoted by coniferous and ericaceous vegetation types).

6.2 Soils of the "Lias Strata" Plateau

6.2.1 Soils on the Strassen Formation

Starting from the dip slope part (plateau) of the Lias cuesta, one crosses the youngest geological formation, which consists of marly calcareous strata (li3). The soils are developed in weathered material of the Strassen formation. The clay content of the substratum favours the development of soils having stagnic properties (Stagnic Cambisol to Stagnosol). Generally, cambic or argic horizons occur (IUSS 2015). When no signs of clay illuviation are found, Eutric or Calcareous Regosols are common, mostly where soil development is influenced by erosion processes or tillage. In the deeper horizons, close to the

substratum, where the clay content is high (Table 6.2), slickensides can be observed. At many places, the Strassen strata are overlain by younger loamy to clayey deposits ("Plateau-lehme" or "plateau loams" of Jungerius (1958) and Levelt (1965)). Grassland and maize culture are the principal current land use types on these soils.

6.2.2 Soils on the Luxembourg Sandstone Plateau Area

Much of the variability among the sandy soils, which today are present on the plateau of the Luxembourg sandstone (li2) can be related to (1) the origin and variability in the parent material; (2) the presence of weathering products, rock induration or Plio-Pleistocene (fluvial) sediments, (3) historical and current land use, and (4) the associated erosion/sedimentation processes.

6.2.2.1 Soils Developed on Luxembourg Sandstone

In the Luxembourg sandstone, most of the rocks consist of sandstone with well sorted, rounded grains, but sometimes very thin intercalations of loam occur, and more rarely sandy strata with few isolated small pebbles or shell breccias in a conglomeratic facies. The Luxemburger sandstone (li2) becomes also loamier from the east (Echternach-Diekirch region) to the west (Arlon-Redangen and Gaume region in Belgium; Bouezmarni et al. 2009).

In the eastern part of the cuesta landscape, between Diekirch and Echternach, by far the most profiles are developed in a very porous sandstone that was originally cemented by CaCO₃ (van den Brill and Swennen 2008). In the upper metres of the weathered sandstone, the parent material is free of carbonates and the weathered material normally consists of loamy sand with very low pH (<4; see also Table 6.3). In this environment, Leptosols, Arenosols and Podzols prevail, depending on soil texture, soil depth, soil age and land use. In Fig. 6.2, a typical

Table 6.2 Soil profile from the Strassen formation near Beaufort (coordinates: 49.8399°N; 6.3087°E) under deciduous forest

A. Texture of the different soil horizons (weight % on absolute dry base)													
Horizon	Depth (cm)	2–1 mm	1–0.5 mm	0.5–0.25 mm	0.25–0.125 mm	125–63 µm	63–16 µm	16–2 µm	<2 µm	Sand	Silt	Clay	
Ah1	0–4	0.1	0.3	0.9	1.7	5.6	43.5	27.5	20.5	8.4	71.1	20.5	
Ah2	4–9	0.1	0.2	0.9	1.8	5.1	44.2	26.8	21.0	8.0	71.0	21.0	
Ah3	9–20	0.0	0.2	0.9	1.7	4.9	43.0	28.6	20.7	7.7	71.6	20.7	
Bw	20–27	0.0	0.2	0.8	1.6	4.8	40.9	28.5	23.2	7.4	69.4	23.2	
Bg1	27–40	0.0	0.3	1.0	1.9	5.4	46.1	22.8	22.5	8.7	68.8	22.5	
Bg2	40–51	0.1	0.2	0.6	1.2	5.2	44.9	19.5	28.4	7.2	64.4	28.4	
2C	>51	0.0	0.1	0.0	0.1	2.9	40.8	17.2	38.8	3.2	58.0	38.8	

B. pH, electrical conductivity, organic matter, nitrogen and total amorphous & organic amorphous iron, aluminium and manganese concentrations on total absolute dry base													
Horizon	Depth (cm)	pH (CaCl ₂) ^a	EC ₂₅ (µScm ⁻¹) ^a	Org matter (%) ^b	N (%) ^c	Fe am _{tot} (mmol/kg) ^d	Mn am _{tot} (mmol/kg) ^d	Al am _{tot} (mmol/kg) ^d	Fe am _{org} (mmol/kg) ^e	Mn am _{org} (mmol/kg) ^e	Al am _{org} (mmol/kg) ^e		
Ah1	0–4	6.2	332	8.8	0.3	70	7.6	30	32.0	5.2	16.9		
Ah2	4–9	5.8	117	5.7	0.2	77	7.9	31	37.3	3.8	18.6		
Ah3	9–20	5.9	104	4.1	0.2	82	7.9	32	39.4	2.6	18.9		
Bw	20–27	6.0	82.5	2.3	0.1	77	7.0	32	34.4	1.6	15.5		
Bg1	27–40	6.2	52	1.7	0.1	64	7.0	30	26.7	1.2	12.5		
Bg2	40–50	6.3	44	1.6	0.1	53	2.9	32	25.6	0.5	13.3		
2C	>50	–	41	1.8	0.1	40	0.1	33	15.2	0.3	19.1		

Eutric Cambisol with a mull ectorganic horizon

org Organic; *am* Amorphous; *tot* Total^aDetermined in 1:2.5 (w/v) soil water suspension after 24 h^bDetermined by loss of ignition at 375 °C^cTotal nitrogen by CNS analyser^dNH₄-oxalate extracted^eNa-pyrophosphate extracted

Table 6.3 Physico-chemical characteristics of a Brunic Arenosol developed in the Luxembourg Sandstone (I12), with a mormoder ecotorganic horizon developed near Befortrehead/Tinnes (coordinates: 49.8414°N; 6.2581°E) under beech (*Fagus sylvatica*) with spruce (*Picea abies*) undergrowth

A. Grain size distribution (weight % on absolute dry base)												
Horizon	Depth (cm)	2–1 mm	1–0.5 mm	0.5–0.25 mm	0.25–0.125 mm	125–63 µm	63–16 µm	16–2 µm	<2 µm	Sand	Silt	Clay
AEh	0–3	0.2	0.6	5.6	53.3	22.6	7.1	5.8	4.8	82.3	13.0	4.8
EA	3–5	0.1	0.4	5.0	55.6	21.9	6.7	5.5	4.8	83.0	12.2	4.8
Bw	5–15	1.1	1.4	1.1	53.7	25.9	7.6	4.1	5.1	83.1	11.8	5.1
C1	15–42	0.2	0.4	4.5	53.5	24.1	7.4	4.6	5.1	82.8	12.1	5.1
C2	46–70	0.3	0.5	4.5	52.5	26.2	6.8	4.3	4.9	84.0	11.1	4.9

B. pH, electrical conductivity, organic carbon, nitrogen, total amorphous & organic amorphous iron, aluminium and manganese concentrations (on abs. dry base)												
Horizon	Depth (cm)	pH (CaCl ₂) ^a	EC ₂₅ (µS cm ⁻¹) ^a	Org. matter (%) ^b	N (%) ^c	Fe am _{tot} (mmol/kg) ^d	Mn am _{tot} (mmol/kg) ^d	Al am _{tot} (mmol/kg) ^d	Fe am _{org} (mmol/kg) ^e	Mn am _{org} (mmol/kg) ^e	Al am _{org} (mmol/kg) ^e	
AEh	0–3	3.0	227	10.9	0.32	18.2	0	10.7	17.2	0	9.7	
EA	3–5	3.1	127	5.8	0.18	18.8	0.2	10.2	14.9	0	6.3	
Bw	5–15	3.3	80	2.6	0.08	27.1	1.7	13.6	21.7	0	8.5	
C1	15–42	4.0	42	1.3	0.04	17.4	1.5	33.2	15.7	0	30.2	
C2	46–70	4.0	40	0.9	0.03	12.7	0.8	18.9	8.2	0	15.0	

^aDetermined in 1:2.5 (w/v) soil water suspension after 24 h

^bLoss of ignition (375 °C)

^cTotal nitrogen by CNS analyser

^dNH₄-oxalate extracted

^eNa-pyrophosphate extracted

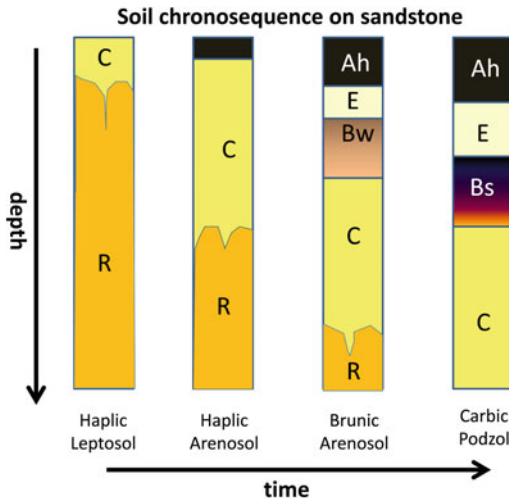


Fig. 6.2 A typical chronosequence of soils developed on sandstones. *R* bedrock, *C* weathered parent material, *Bw* weathering horizon, *Bs* spodic horizon (carbic), *E* eluviation horizon (albic material), *Ah* horizon with accumulation of organic matter in the topsoil

chronosequence is given for the development of an undisturbed profile from a shallow Leptosol towards a Podzol on a sandy substratum. Where Podzols occur, the sandstone does not contain carbonates or loam, and is often cemented with silica. In these areas, soils are often shallow and not suitable for agriculture, and were mostly planted with pine forests (*Pinus sylvestris*). In these locations, the Podzols are preserved by afforestation and absence of ploughing. Undergrowth often also reflects acid soil conditions with typically heather (*Calluna vulgaris*) and blueberry (*Vaccinium myrtillus*). In recently felled forests, that have been converted into arable land, the border between the old agricultural fields with Brunic Arenosols and the recently deforested areas with Podzols can sometimes directly be recognized.

Within the Arenosols, Brunic Arenosols are often found under forest and Haplic Arenosols under cultivation, as the soils are disturbed by ploughing. In Table 6.3 an overview is given of the most important physico-chemical properties of a typical Brunic Arenosol under deciduous forest. Although there is some Fe and Al translocation visible in the chemical analysis of

the Bw horizon, it is not sufficient to classify as a spodic (Podzol B) horizon (IUSS 2015).

Going to the western region of the sandstone cuesta, the substratum becomes loamier and Regosols and Luvisols occur under arable land (Hissler et al. 2015). However, Podzols may be preserved under Pine (*Pinus sylvestris*) dominated forests.

6.2.2.2 Soils Developed in Plateau Loam

In many locations on the Luxembourg Sandstone plateau, also loamy soils occur. The origin of the loamy material can be related to various processes and sources. First of all, the surface of the plateau has been under a long period of weathering and geomorphological development. Periglacial processes during glacial periods such as solifluction have been important, and may have relocated and mixed surface materials, which changed their original superposition and also affected local topography.

In addition, various sources of material can be identified, related to (1) local occurrence of loamy intercalations of the Luxembourg sandstone formation; (2) remnants of weathering residue of the Strassen strata (li3); (3) remnants of weathered fine-grained alluvial deposits of the Sauer and its tributaries, deposited on the Luxembourg sandstone in the period before the main incision of the Sauer; (4) a very old weathering residue of various origin (plateau loams) and (5) remnants of loess deposits.

The first option is less likely, as the lithological intercalations in the Luxembourg sandstone are very thin (5–10 cm) in the Beaufort area, whereas the actual thickness of the loamy material in the soil is often much larger. The second origin is discussed by Jungerius (1958), but the Strassen strata now occur further away from the cuesta rim, and not directly along the cuesta itself. The third alluvial origin is mentioned in Verhoef (1966), although he does not differentiate between sedimentary and erosion terraces. The latter origins for loamy plateau soils are mentioned by Levelt (1965).

Occurrences of soils with a loamy soil on a part of the plateau near Beaufort are given in

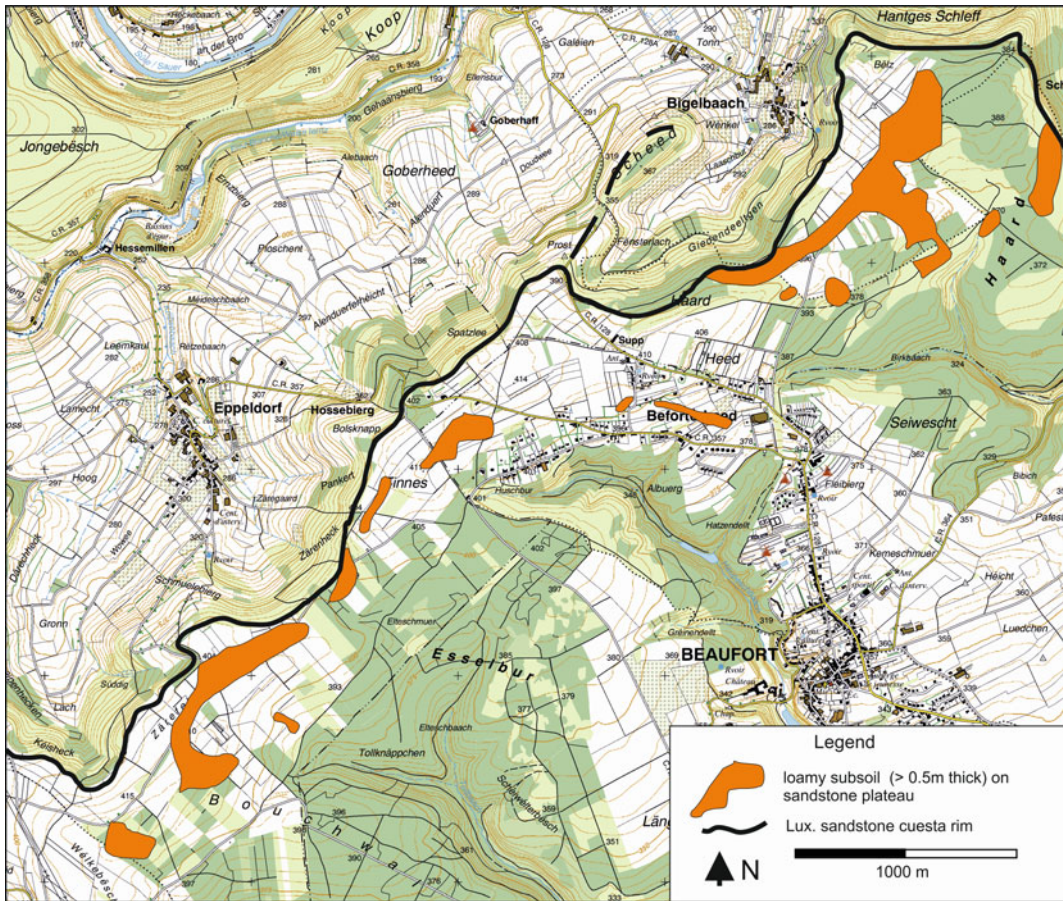


Fig. 6.3 Map showing the occurrence of soils with a loamy soil (“plateau loam”) on the cuesta front near Beaufort, based on a field map by D. Balders (on background of the topographical map of Luxembourg, www.geoportal.lu)

Fig. 6.3. Their presence just along the cuesta front is striking, but their actual elevation could not be related to the current topography. These loamy deposits can be up to 3 m thick and can also include gravel layers. The fluvial origin is corroborated by the occurrence of coarse gravelly material nearby, with a provenance from the Ardennes as large quartz pebbles, as well as the presence of fluvial gravel beds at greater depth, intercalating with the loamy material. They should be seen as remnants of old river deposits with a long history of soil development, that have been eroded and disconnected during the (later stages of the) Quaternary.

The soils on these deposits are generally classified as Stagnic Alisols or Alic Stagnosols.

They have a clear argic horizon, show stagnic properties in varying intensities and have a low base saturation together with a high exchangeable Al content (>50%) at the adsorption complex. This indicates that these soils, present in Pliocene deposits (Verhoef 1966), have developed over very long time spans, resulting in high leaching and low base saturation. A profile in such thick loamy deposits is described in more detail in Table 6.4, which shows a clear sequence of a loamy topsoil, argic horizons with clayloam texture and again loamy deeper soil layers.

This particular soil is classified as an Alic Stagnosol, with low base saturation and high aluminium saturation of the exchange complex in the upper part of the profile, and high base

Table 6.4 Analytical results of an Alic Stagnosol with a mormoder ectorganic horizon developed in loamy plateau deposits near Beaufort/Kazebuer (coordinates: 49.8577°N, 6.2964°E) under deciduous forest

<i>A. Grain size distribution per soil horizon (in weight % on absolute dry base)</i>													
Horizon	Depth (cm)	2000–210 µm	210–105 µm	105–63 µm	63–32 µm	32–16 µm	16–8 µm	8–4 µm	4–2 µm	<2 µm	Sand	Silt	Clay
Ah	0–12	11.5	26.9	8.6	8.8	17.1	9.7	4.8	3.5	9.2	47	43.8	9.2
E	12–20	9.7	29.6	8.6	9.4	17.3	9.4	5.2	2.9	7.9	48	44.1	7.9
Btg1	20–47	8.1	23.2	6.8	8.8	18.9	11.3	5.9	3.5	13.5	38	48.5	13.5
2Btg1	47–75	5.7	19.4	5.4	7.5	18.8	10.7	5.8	3.2	23.5	30.5	46	23.5
2Btg2	75–100+	4.4	21.7	8.6	8.6	11.8	9.1	5.5	2.9	27.3	34.7	37.9	27.3
	170	0.8	4.7	12.9	13.7	8.5	8.8	5.8	4.6	40.3	18.4	41.3	40.3
	200	0.2	1.2	17.6	17.2	8.6	7.8	6.4	3.7	37.2	19.1	43.7	37.2
	280	2.5	25.2	24.1	6.1	3.9	5	4.3	2.8	26	51.8	22.2	26
	300	18.1	13.8	19.3	8.6	5.2	4.9	4.2	3.3	22.6	51.2	26.2	22.6

<i>B. pH, organic matter, CEC and base saturation and Al saturation of the exchange complex</i>									
Horizon	Depth (cm)	pH H ₂ O ^a	pH CaCl ₂ ^b	Org matter (%) ^b	CaCO ₃ (%) ^c	CEC f.e. (cmolc kg ⁻¹) ^c	CEC clay (cmolc/kg ⁻¹ clay) ^c	Base Sat. (%)	Al-sat. AC (%)
Ah	0–12	4.2	3.5	22	0	11.2		21	77
E	12–20	4.44	3.89	1.5	0	1.9		8.4	90
Btg1	20–47	4.71	3.96	0.4	0	2.5	18.5	39	57
2Btg1	47–75	4.8	3.88	0.2	0	7.7	32.8	45	54
2Btg2	75–100+	4.52	3.58	0.2	0	9.6	35.2	44	56
	170	5	3.81	0.2	0	12.6	46.2	74	26
	200	5.18	3.86	0.2	0	12.2	30.3	77	23
	280	5.42	4.23	0.1	0	8.3	31.9	89	4.5
	300			0.1	4.47	7.6	33.6	96	2

CEC Effective cation exchange complex; f.e. Fine earth; CEC/clay CEC of clay fraction; Base Sat. Base saturation; Al-sat. AC Aluminium saturation of adsorption complex

^aDetermined in 1:2.5 (w/v) soil water suspension after 24 h

^bLoss of ignition

^cDetermined with Wesemael method

^dDetermined with NH₄-acetate at pH7. Weight % and concentrations on abs. dry base

saturation in the deeper part of the profile. This clearly indicates intensive leaching and weathering of the upper part of the soil.

6.2.2.3 Hydromorphic Soils on the Plateau

In the sandstones, also indurated layers occur on which water stagnates and small fens occur on the plateau near the cuesta front. The Elteschmuer wetland close to Beaufort is a good example of such a fen that recently has been restored after the previous drainage. Currently, this fen is protected under national law. The impermeability of the sandstone layers is related to silica cementation, which occurred at or very near the soil surface. This silica cementation is possibly a remnant of Tertiary weathering and soil formation. Under the more tropical conditions of that period, silica dissolved and was translocated in the parent material, thus cementing and filling the pore space in between the sand grains. This led to the formation of impermeable duricrust or silcrete. The occurrence of remnant parts of the Tertiary silcretes—also called “Pierre de Stonne”—is known in Luxembourg (Baeckeroot 1929; Voisin 1988) and adjacent areas (Demoulin 1990). Because of the permanent presence of stagnating water, organic matter has accumulated and Histosols can be found in these locations. Podzols may occur in the direct surroundings of these wet zones.

6.2.2.4 Colluvial Deposits on the Sandstone Plateau

Additional differentiation can be made in shallow depressions on the plateau, where soils are covered by darker coloured loamy or sandy colluvium with varying thickness. The underlying Bw horizons are quite discontinuous over the area, according to either lithological changes in the parent material, erosion and sedimentation processes and tillage in the shallower soils. Tree uprooting, which took place in the Holocene due to natural or historical land use changes, could also have destroyed the continuity of underlying Bw horizons.

6.3 Soils of the Lias Sandstone Cuesta Front

The Lias Cuesta escarpment is characterized by the presence of slope deposits derived from soils and rocks present in the cuesta front. The underlying strata follow the stratigraphic sequence of Mesozoic rocks which starts with the Luxembourger Sandstone, having vertical rock cliffs, permeated with joints, and in descending order, the more marly strata of the Pilonoten-schichten (li1), Rote Tone (Red clays, ko1), Schwarzer Blättermergel (marls with leafs, ko2), Steinmergelkeuper (km3), Schilfsandstein (km2s) and Pseudomorphosenkeuper (km1). They all have a different weathering sensitivity and permeability, and generally downwards the slope a more concave profile (Fig. 6.4; see also Chap. 2). Geomorphologically, these slopes are very active. At the very top of the cuesta, rockfall and toppling of the sandstone cliffs predominate, by which the disintegrating sandstone fragments move downwards over the slope. Lower on the slope, solifluction, slumping and creep phenomena are more important. Locally, this process is accelerated by undermining due to fluvial erosion or erosion in spring areas. In lower positions, slope or colluvial deposits can occur, such as in the valley floors of the small erosion niches that start in the cuesta front. These erosion niches continue downslope and are feeding small alluvial fans. The high geodynamics in this landscape zone hamper soil formation as the erosion and transport rate of (parent) material is generally much faster than the soil formation rate. This means that the properties of many soils are directly linked to the material derived from the strata present upslope.

6.3.1 Soils of the Upper Part of the Lias Cuesta Front

This section describes the upper part of the Lias cuesta front, especially the part underlain by the Lias strata of the Luxembourger sandstone and the Pilonoten-Schichten (blue strata in Fig. 6.1). First, the parent material and geomorphology of



Fig. 6.4 Cuesta in the Kribsebaach valley near Eppeldorf, showing differences in slope angle

the three main sub-units of this landscape unit will be described and next their associated soils.

The upper part of the cuesta front is dominated by sandy and gravelly material, and normally covered by various forests, such as Luzulo-Fagetum Beech forests and plantations of Pine and Spruce.

The upper part of this landscape unit (“zone 1”) is dominated by very steep slopes with outcrops of sandstone of the Luxembourger Sandstone (li2), and slopes covered with sandstone debris and weathered silty, sandy and gravelly material. Finer material may occur, originating from loamy intercalations within the Luxembourger sandstone as well as from the plateau. Hillslope processes are dominated by dry mass wasting such as rock fall and toppling. Lower on the slope, the slope angle declines and sandstone debris become less frequent.

Where the slope shows a clear break to more moderate slope angles (“zone 2”), the material at

the surface becomes more and more mixed with finer materials derived from the marls of the Psilonoten layers (Li1) which directly underlie the Luxembourg Sandstone. Because of the much finer texture of these marls, water that infiltrated in the overlying porous sandstone stagnates on the impervious marls. As a consequence, springs and wet zones start to appear at, and just below this contact zone.

This water stagnation induces more water-dominated mass wasting processes such as slumping, solifluction or even earthflows (“zone 3”). These mass wasting processes are very variable in occurrence, and major spring zones give rise to the development of large erosion niches in the cuesta (e.g. spring zone of the Kribsebaach near Eppeldorf). Mass wasting processes and transport of materials can be active on a local scale over some metres, but also be present on major parts of the cuesta slopes. Earth flows, initiated in zone 2, may even reach

Table 6.5 Textures of the horizons of a Eutric Colluvic Regosol, developed in a hillslope deposit in the upper part of the cuesta front near Nommern, with incorporation of both material derived from the Strassen formation (li3) and the Luxembourger Sandstone (li2) (in % of total) (coordinates: 49° 46'N, 6° 09'E)

Horizon	Depth (cm)*	2.0–0.42 mm	0.42–0.3 mm	0.3–0.25 mm	0.25–0.125 mm	125–50 µm	50–32 µm	32–16 µm	16–8 µm	8–4 µm	4–2 µm	<2 µm	Sand	Silt	Clay
Ah	10	3.9	8.6	18.6	26.2	12.1	7.1	7.9	5.7	2.6	1.8	5.6	69.4	25.0	5.6
1C	45	0.4	4.4	17.1	19.8	19.6	10.4	11.1	6.9	4.4	3.1	10.0	54.1	35.9	10.0
2C	105	0.6	3.6	14.6	15.2	8.4	12.5	11.7	8.3	4.7	3.2	17.4	42.2	40.4	17.4
3C	170	2.8	6.7	6.7	23.1	10.3	9.4	5.6	4.7	3.1	2.5	25.3	49.4	25.3	25.3

Adapted from Van Zon (1978). Weight % on absolute dry base

Depth (cm)*: sampling depth only, not horizon thickness

towards the Sauer valley bottom, and threat local infrastructure, such as on the steep slopes of the Hantges Schleff between the Sandstone plateau and the Sauer river. In combination with the variability in origin and hence type of material, all these processes give rise to a very variable composition of materials in which the soils are developing. This is expressed in both a fast lateral change in textural composition of soil materials, as well as in a high variability in soil depth and variation in the presence of layered slope deposits.

In “zone 1”, on the upper part of the cuesta front, most soils are Arenosols. Soil types range from Nudilithic Leptosols where the bedrock cliffs are present, via Lithic and Haplic Leptosols, Haplic Arenosols to Brunic Arenosols at the more stable places. They often show a very variable profile development depending on the type of material, and finer and coarse grained layers may alternate within one profile, as also shown in Table 6.5. In the lower zones 2, large differences in soil types can be observed, with patchy distribution of Arenosols and Regosols in areas with more sandy or loamy parent materials (Juilleret et al. 2012). For instance, in areas where slumping occurs, Brunic Arenosols can be found on the slumps themselves as the surface of the slump itself is a rather stable environment. This contrasts to the back scar of the slump and its immediate surrounding areas, where the active geomorphological processes hinder soil development and Regosols occur. In these places, even small fens occur at places where water exfiltrates, which have Gleysol or Histosol profile development. In “zone 3”, soil types are predominantly Regosols. However, in more stable or protected areas, also Cambisols may occur.

6.3.2 The Middle and Lower Part of the Lias Cuesta Front

This section describes the middle and lower part of the cuesta front, which is underlain by Keuper substrates, such as the Steinmergelkeuper (km3), Schilfsandstein (km2s) and Gipsmergelkeuper



Fig. 6.5 Extreme creep of marly soils in apple orchard near Bigelbach

(km²) and Pseudomorphosenkeuper (km¹), and is represented by the yellowish zone in Fig. 6.1.

6.3.2.1 Shallow Soils on Marly Substratum and Steep Slopes

At the lower part of the cuesta front, steep slopes can still be present. In this slope section, agricultural land use has or had a big impact on the soil. Creep, solifluction and other mass wasting processes, surface erosion after deforestation, as well as tillage have resulted in quite shallow soils (Fig. 6.5). Situations occur where the marly bedrock is quite close to the surface without any colluvial or slope deposit cover. In areas with steep slopes, even gullies occur. In such positions, poorly developed shallow soils are found, with no B horizon or at best a starting Cambic horizon, giving rise to either Calcareous Colluvic Leptic Regosols or Cambisols respectively. Within 50 cm, the weathered shards of the dolomitic or calcareous Steinmergelkeuper marls

start to appear. In such situations, where agricultural land use is strongly reduced, chalk grasslands may occur with high biodiversity and presence of many orchids.

6.3.2.2 Colluvial Soils at the Middle and Lower Slopes

Often the substrate consists of different parent materials, which form evidence of various episodes of mass wasting processes, during which sheets of sandy or marly material were transported and deposited, and even buried paleosoils occur. At the most stable sites, Cambisols can occur, but otherwise Colluvic Regosols are present (Fig. 6.6). In cases where the slope angle declines below 20°–15° the common land use changes from forest into grassland, where we generally find Regosols and Cambisols. In some grasslands, colluvial deposits, rich in organic matter due to high root litter input, may even have a mollic epipedon, which would classify as a (Cambic) Phaeozem.



Fig. 6.6 Soil in typical colluvial material on Steinmergelkeuper substratum on a sloping meadow near Bigelbach (photo by K. Kalbitz). The soil does not exhibit clear soil formation features, and is classified as a Colluvic Regosol. The *white spots* are fragments of rock, either transported from upslope (in the colluvial upper 70 cm of profile) or in situ (in the Steinmergelkeuper lower part of the profile, starting with banded layers)

6.3.2.3 Soils on the Lower Part of the Cuesta Landscape

Below the steep upper part of the Cuesta front, the slope angle is often much lower, and large flat areas occur. These areas can often be related to the emergence of sandstones and conglomerates of the Schilfsandstein formation (km2s). These red or green sandstones are only a few metres thick, but can be followed for hundreds of metres on low angle sloping terrain. A good example is the relatively flat landscape step around 260–280 m altitude that can be followed from Eppeldorf to Bigelbach, which is located between Reisdorf in the Sauer Valley and Beaufort on the Luxembourgger Sandstone plateau. Slightly lower in the stratigraphical section, in the Pseudomorphosenkeuper (km1), conglomerate beds occur that are also expressed as

flatter areas in the landscape (e.g. Galgebierg, over Bettendorf in the Sauer valley).

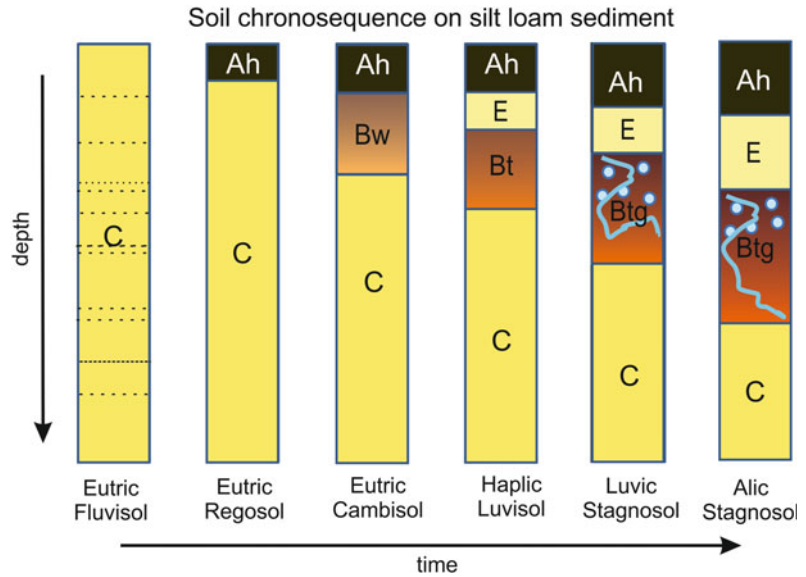
As the slope angle strongly reduces, colluvial deposits originating from the cuesta front run out over the flatter areas below, sometimes feeding dry valleys (Juilleret et al. 2012) and generally showing Regosols or Cambisols on the more protected locations. Further downslope, gravelly fluvatile terrace material is present and in shielded places even loess deposits can be found. In this zone of the cuesta landscape, small brooks appear more frequently and can be associated with Gleysols.

The diversity of materials in this landscape section is also expressed in the soils that are encountered. The Pseudomorphosenkeuper is characterized by red marls, but also contains dolomitic and calcareous beds, as well as conglomerates. Soil types related to these different materials are Regosols, Cambisols, Luvisols or Stagnosols, also depending on their age and their geomorphic position. In parts dominated by colluvial processes, at and just below the slope break, Regosols can be found. Soils occurring in the often red Schilfsanstein or Pseudomorphosenkeuper, can inherit these red colours also in their profiles, especially in the Bt(g) and C horizons. This may lead to the addition of the qualifier Chromic. Strictly spoken, these red colours are not related to soil formation processes, but the IUSS soil classification only uses a colour criterion for this qualifier, and not a process related criterion.

The fluvatile terraces, however, show well-developed, deep Luvisols, Stagnosols and even Alisols with clear argic horizons, or truncated remnants of those soils. In Fig. 6.7, an idealized scheme is represented showing the development of Luvic Stagnosol in fluvatile deposits. The well-developed Luvisols and especially Alisols have been formed over long time spans, as the fluvatile materials have been deposited at various moments during the Pleistocene (Verhoef 1966).

Below terrace level 9 of Verhoef (1966), at approximately 300 m altitude in the area around Reisdorf, fluvatile influence from the Alzette tributary can be proven by the presence of

Fig. 6.7 Soil chronosequence on fluvatile sediment with silt loam texture under temperate humid climate in areas with low relief (diagnostic horizons: *Bw* cambic horizon, *Bt* argic horizon, *Btg* argic horizon with stagnic properties. Other: *E* eluvial horizon or Albic material, *C* C-horizon (weathered parent material without soil formation)



‘Rasenerz’, i.e. iron containing concretions derived from the Minette formation south of Luxembourg city (Riezebos et al. 1990). The Alzette tributary was not connected to the Sauer system until the end of the Pliocene, which corresponds to the sudden occurrence of iron stones in terrace level 9 of Verhoef (1966) and which are increasingly present on the lower terraces.

The soils of the fluvatile terraces have been preserved, as they are located at places with relatively low impact of geomorphic processes, due to the small slope angles. The prolonged soil formation has resulted in deep soils with well-developed argic horizons, commonly also showing clear stagnic properties (Table 6.6). The E horizon can be present, but is often truncated by water- or tillage erosion, or has been mixed with the plough layer (*Ap*) in agricultural fields. In case of very gravelly material (skeletal soil), the clayey material in the argic horizon is present in the voids between the gravel, giving these soils a very compact nature.

During and after clay illuviation processes, which took place over long time spans, also acidification of the soils occurred. Under forest, soils now have low base saturation, because Ca and Mg, that initially constituted the major part of the base cations at the exchange complex, were replaced by mainly Al (Table 6.4). When

the base saturation drops below 50%, Luvisols develop into Alisols (IUSS 2015). However, under agriculture, base saturation is (much) more than 50%, because it is common practice to supply lime to the soil, resulting in higher base saturation of the exchange complex.

6.4 Muschelkalk Soils

Under the Keuper beds the Muschelkalk strata appear (ku, mm and mo), i.e. the pink strata in Fig. 6.1. They are also high in carbonates but are dominated by resistant dolomite. The strata can occur either in dip slope or face slope positions and have a different soil development in the two geomorphological positions. In places where the Muschelkalk strata have been incised by the Sauer or one of its tributaries, steep to very steep slopes have developed in dolomite bedrock. This gives rise to shallow and stony soils. The soil profile is also influenced by colluvial material from upslope.

The Ah-horizons are relatively thin (<20 cm, but very dark, porous and mulched, and rich in organic matter (Fig. 6.8). The Ah horizons generally have pH values around 7.1–7.2 (Chap. 7), but the soil sampled for this study was free of calcium carbonates in the fine earth fraction and

Table 6.6 Texture of a soil (Stagnic Alisol) with vermimull ectorganic horizon, from the Jongebësch, developed in slightly gravelly to gravelly clay loam fluvialite material, under deciduous forest (coordinates: 49° 51.47'N; 6° 13.96'E)

A. Grain size distribution per soil horizon (weight % on absolute dry base)												
Horizon	Depth (cm)	2000–425 µm	425–212 µm	212–63 µm	32–63 µm	16–32 µm	8–16 µm	4–8 µm	2–4 µm	<2 µm	Sand	Clay
Ah	0–3	3.3	5.3	3.7	12.2	20.9	14.2	11	17.6	11.8	12.3	11.8
E	3–9	3.1	5.4	2.3	12.1	21.3	14.1	11.3	7.2	23.2	10.8	23.2
Btg1	9–27	2.3	3.7	2.9	15	19.2	12.4	10.5	7	26.9	8.9	26.9
Btg21	27–60	1.8	1.5	1.8	4.7	9.3	9.2	11.4	7.8	52.5	5.1	42.4
Btg22	60+	0.1	0.3	1.7	5	6.3	8.1	10.2	6	62.2	2.1	62.2

B. pH, organic carbon, nitrogen and effective CEC of the Jongebësch profile (weight % and CEC on abs. dry base)									
Horizon	Depth (cm)	pH (CaCl ₂) ^a	Corg (%) ^b	N (%) ^b	Corg/N ^b	CEC (cmolc/kg ⁻¹ clay) ^c			
Ah	0–3	4.0	5.6	0.4	15.1	31.3			
E	3–9	3.7	1.6	0.1	17.7	28.0			
Btg1	9–27	3.7	0.9	0.1	12.6	25.9			
Btg21	27–60	3.7	0.4	0.1	5.8	29.6			
Btg22	60+	3.9	0.3	0.1	5.0	34.5			

^aDetermined in 1:2.5 (w/v) soil water suspension after 24 h

^bTotal carbon and nitrogen by CNS analyser

^cDetermined with NH₄-acetate method at pH7



Fig. 6.8 Shallow soil in steep Muschelkalk slopes (Leptic Colluvic Dolomitic Regosol)

had relatively low pH levels (Table 6.7). In the C and R horizons, carbonates derived from the dolomitic substratum are generally present. On these steep slopes B horizons rarely occur, but even argic horizons, as indicated by clay skins (cutans), can be found occasionally. At places, only colluvial material is present directly on the bedrock material. Leptosols and Regosols frequently occur in this landscape zone and sometimes Cambisols or Luvisols. The forests on these Muschelkalk slopes generally have a very high biodiversity (Hordelymo-Fagetum and Carici-Fagetum; see also Chap. 8). Near some of the villages, remnants of abandoned narrow terraces occur, fully overgrown by mature forest vegetation.

On dip slope positions, the soils on the Muschelkalk can be very thick, but locally also loess or fluvatile deposits occur. Luvisols are the common soil type. However, soil depth and development is very variable due to local soil erosion, or the presence of resistant limestone or dolomite with Leptosols close to the surface. The

Table 6.7 Texture (in weight % on absolute dry base), pH, Electrical conductivity (EC), Organic carbon content and lime content of a Leptic Colluvic Dolomitic Regosol (vermicull ectorganic horizon) on a steep Muschelkalk slope near Moestroff (Sauer valley) (coordinates: 49° 51.95'N; 6° 14.50'E)

Horizon	Depth (cm)	pH (CaCl ₂) ^a	pH (H ₂ O) ^a	EC ₂₅ (μS/cm) ^a	C _{org} (%) ^b	CaCO ₃ (%) ^c	2–1 mm	1–0.5 mm	0.5–0.25 mm	0.25–0.125 mm	125–63 μm	63–16 μm	16–2 μm	<2 μm	Sand	Silt	Clay
Ah1	0–6	4.6	5.2	209	5.7	0	0.1	0.4	1.8	8.6	11.7	23.7	25.5	28.2	22.6	49.2	28.2
Ah2	6–15	3.7	4.6	51	2.1	0	0.1	0.5	1.9	8.6	11.8	24.4	24.3	28.5	22.8	48.7	28.5
Bw	15–35	6.1	6.6	121	1.8	0	0.4	0.6	1.8	8.5	11.3	24.6	19.6	33.2	22.6	44.2	33.2

^aDetermined in 1:2.5 (w/v) soil water suspension after 24 h

^bCalculated from loss of ignition at 375 °C

^cDetermined with Wesemael method

topsoil material often has a silty character, possibly also containing a loess component.

6.5 Soil Developed in (Sub)Recent Fluvial Deposits

In the valley bottom (sub)recent fluvial deposits can be quite extensive. Along the larger streams as the Sauer and Ernztal, the rivers are occasionally flooding the lower alluvial plains and terraces. Depending on the texture of the deposited material and time since deposition, Fluvisols, Regosols and Arenosols prevail. Fluvisols are found if fluvial material prevails, Regosols when the texture is sandy loam or finer, and Arenosols when the texture is loamy sand or coarser textured material. In many cases, the biological activity in the deposits is so high that the individual layers of the fluvial material are obliterated very quickly. In the field, the distinction between the Regosols and Arenosols can be quite difficult, as most sediments have a texture near the sandy loam–loamy sand boundary, or show a vertical alternation of loamy and sandy material, except for the sandier natural levees and the active channels where gravel beds are prominent. Technosols are also regularly occurring in the case of recently buried constructions along active river courses.

6.6 Soils Developed in Loess

Loess soils developed in deposits of the last ice age, and locally occur in sheltered places in depressions or leeward sides of valleys. In many cases the loess is containing coarser fragments, indicating that the loess has been redeposited (Dittrich 1984). Loess deposits of over 6 metres thickness can be present, often on top of Steinmergelkeuper, Pseudomorphosenkeuper or the Grenzschichten. If not truncated, Stagnic Luvisols or Luvisols are found. The upper soil is characterized by low base saturation and high exchangeable acidity dominated by aluminium, especially in the E horizon (Table 6.8). However, in the Btg2 and C horizons, base

Table 6.8 Soil chemical and texture characteristics of Loess profile (Luvisc Stagnosol, vermimull) under beech forest (Seitert) near the N. Derfebaach deposited on Steinmergelkeuper (not shown in table) (coordinates: 49° 49.25'N; 6° 12.60'E)

Horizon	Depth (cm)	org. C (%)	pH H ₂ O	pH CaCl ₂	Eff. CEC f. e. (cmolekg ⁻¹)	Base sat. (%)	Al sat. AC (%)	CEC clay (cmole kg ⁻¹ clay)	2000–63 µm	63–32 µm	32–16 µm	16–8 µm	8–4 µm	4–2 µm	<2 µm	Sand	Silt	Clay
Ah	0–5	7.4	5.2	3.9	6.8	44	48	–	5.9	14.0	33.3	19.0	8.6	4.3	14.8	5.9	79.3	14.8
EA	5–11	3.3	4.8	3.7	4.5	23	74	–	5.6	13.3	34.8	18.8	8.3	4.8	14.5	5.6	80.0	14.5
E	11–22	2.2	4.6	3.6	4.1	16	82	28	5.2	14.9	33.2	18.7	8.7	4.6	14.6	5.2	80.1	14.6
Btg1	22–45	0.0	4.7	3.7	6.7	38	62	29	3.6	12.5	34.5	15.6	7.2	3.8	22.9	3.6	73.5	22.9
Btg2	45–110	0.0	5.0	4.1	13.0	84	16	39	1.4	7.7	36.3	13.7	4.9	2.3	33.8	1.4	64.8	33.8

The profile was totally decalcified. (weight % on absolute dry base) For abbreviations and methods see Table 6.4

Fig. 6.9 Cored profile (length 1.2 m) of a Stagnic Luvisol developed in loess deposited on Grenzschichten (ko). The Ap, E, Btg, C (all developed in loess, on the right-hand side) and 2C (red marls) are clearly visible



saturation is much higher. This is due to the relatively young age of the loess soil, compared to the Alisols on the older Plio-Pleistocene fluvial terraces in the area. Figure 6.9 shows a cored profile with a Stagnic Luvisol from the rim of the plateau between Bigelbach and Reisdorf, developed on weathered red marly Grenzschichten. The surface of the loess soil shows also the typical sensitivity of loess to slaking and crust formation, inducing overland flow and erosion processes.

6.7 Soils Developed on the Keuper Dip slopes and the Rolling Keuper Landscape

Large areas exist with a rolling landscape in Keuper marl strata, especially developed in the Steinmerkeuper and Pseudomorphosenkeuper. Such landscapes exist in the area between the Sauer main valley and the Luxembourg Sandstone cuesta front, approximately between Ettelbrück and Reisdorf. The morphological expression of the two Keuper formations in a dip slope position is quite different from those exposed in the face slope of the cuesta front. Consequently, the soils are also different, as the

slope angles on the dip slope are far smaller, reducing the impact of geomorphological processes and leaving room for a more mature pedological development, although human activity also has a large impact on the soil profiles encountered.

The development of soil profiles in Steinmergelkeuper strata under more or less undisturbed forested conditions and their hydrology has been studied extensively in the past by various researchers (Imeson and Jungerius 1977; Hazelhoff et al. 1981; Bonell et al. 1984; van den Broek 1989; Cammeraat 2002; Cammeraat and Kooijman 2009; Kooijman and Cammeraat 2010) and is described in detail in Chap. 9.

Under semi-natural forest, Luvic Planosols are found in stable, slightly sloping areas, and Luvic Stagnosols in less stable colluvial positions, where soils are younger and the textural difference between the eluvial silty topsoil and clay-rich B horizons consequently smaller. Lateral eluviation of easily dispersible clay from the top of the Bg horizon leads to a strong and abrupt contrast in texture between the shallow AEh/EAh and Bg horizons. The AEh and EAh horizons can be perceived as a highly bioturbated (geological) erosion remnant of the original soil material, strongly depleted in (fine) clay, and with

Table 6.9 Texture, org carbon, C/N and CaCO₃ for a soil profile in the Schrondweilerbusch, near Stegen under semi-natural deciduous forest on Steinmergelkeuper strata (Luvic Planosol; vermimull; coordinates: 49° 49' 16"N, 6° 10' 50"E; from van den Broek 1989), (weight % on absolute dry base)

Horizon	Depth (cm)	pH (H ₂ O) ^a	pH (CaCl ₂) ^a	org. C (%) ^b	C/N ratio ^c	CaCO ₃ (%) ^d	CEC f.e. (cmolc kg ⁻¹) ^e	Base. sat (%)	2 mm–50 µm	50 µm–2 µm	<2 µm
AEh	0–10	5.87	5.44	4.0	11.7	0	13.8	95.9	14	63	23
EAh	10–20	5.75	5.14	2.2	10.8	0	10.4	96.3	17	59	24
Bwg	20–34	6.20	5.51	0.8	6.9	0	21.6	93.4	12	38	50
Bw	34–50	6.48	5.83	0.4	4.4	0	31.0	93.0	10	52	38
C1	50–58	7.14	6.57	0.3	5.5	0	29.0	100	13	64	24

^aDetermined in 1:2.5 (w/v) soil water suspension after 24 h

^bDetermined by Allison method (wet oxidation by dichromate)

^cN determined by Kjeldahl method

^dDetermined with Wesemael method

^eDetermined by 0.01 M Ag-thiourea

extremely high internal drainage (Cammeraat 1992; Hendriks 1993). In contrast, the Bg and Bw are dense, clay-rich sub-horizons originating from the underlying weathered (and decalcified) marls (Table 6.9). Note that the high clay content in the Bg horizon is a result of weathering and not of illuviation (van den Broek Broek 1989).

However, under agriculture or grassland, the soil profiles on Steinmergelkeuper (km3) are very different. Especially, the characteristic abrupt textural difference is lacking (Table 6.10), due to deforestation, topsoil erosion and tillage in these physically very fragile soils. The A(p) horizons have a similar (silty) clayey texture as the B horizons, with a much lower internal drainage, and both contain lime. Generally, they can be classified as Calcaric Regosols or sometimes Cambisols. On Steinmergelkeuper, vertic properties such as slickensides and wedge shapes aggregates can be observed when the clay content is higher than 45%, and the clay contains 20–25% of an interstratification of chlorite-vermiculite. Regosols are also very common on the gentle sloping agricultural soils of the Pseudomorphosenkeuper. In this slightly undulating area, loess deposits or fluvial deposits with Luvisols can also be found (see earlier section).

6.8 Trends in Soil Development Under Forest: A Statistical Approach

To test the above-mentioned overview of soil development under forest over the landscape gradient, soil characteristics were described in 198 forest plots. The soil descriptions were produced by five groups of students, each group studying an area of approximately 5 km² adjacent to each other along the cuesta landscape. The plots consisted of 10 × 10 m², and were randomly selected from the plateau and upper part of the cuesta in Luxembourg sandstone (li2), in colluvial deposits of at least 1 m thickness in the lower cuesta, in Keuper marl (km1–km3), in Plio-Pleistocene fluvial deposits and loess, and in Muschelkalk (mo1–mo3; mm1–mm3). In each plot, the humus form and profile were described

Table 6.10 Texture, organic carbon, C/N and CaCO₃ contents for a profile near Gilcher (Stegen) under grassland on Steinmergelkeuper substrate (Protostagnic Calcaric Regosol; coordinates: 49° 49.473N, 6° 11.399E); (weight % on absolute dry base)

Horizon	Depth (cm)	pH (H ₂ O) ^a	pH (CaCl ₂) ^a	org. C (%) ^d	C/N ratio ^b	CaCO ₃ (%) ^c	Sand (%)	Silt (%)	Clay (%)
Ap	0–8	7.06	6.71	5.0	8.9	13.2*	6.9	38.3	54.8
Ap2	8–12	7.17	6.85	2.2	7.8	14.8*	8.1	40.2	51.9
Bw	12–22	7.56	7.14	1.2	6.8	19.4*	6.7	40.6	52.7
B1g	25–32	7.93	7.3	0.2	5.0	71.3*	1.2	39.4	59.4
B2g	32–47	7.95	7.36	0	–	50.8*	1.4	36.9	61.7
C1	47+	7.98	7.36	0	–	45.7*	1.3	40.9	57.9

*Including dolomite, but calculated as CaCO₃.

^aDetermined in 1:2.5 (w/v) soil water suspension after 24 h

^bTotal carbon and nitrogen by CNS analysator

^cDetermined by Wesemael method

^dC_{org} is calculated by subtracting inorganic carbon from total carbon

according to Green et al. (1993). Soil profiles were cored to 120 cm depth (if possible), described and classified according to IUSS (2015). All soil descriptions were regularly checked, and students sent back to the field, if deemed necessary by the staff. The associated vegetation patterns are discussed in Chap. 8 in this book. For the present chapter, a number of soil parameters were selected. Thickness of L, F, H and Ah horizons were used as proxy for litter decomposition and development of the organic profile, and humus forms were characterized as Mull or Mormoder. Slopes were characterized as steep (>6°) or gentle (<6°). Soils were further characterized according to the presence or absence of hard rock and/or carbonates within 120 cm depth, the latter determined with 2M HCL-solution. Also, clear signs of pseudogley mottles, clay eluviation or podzolisation were used to distinguish soil groups, and diagnostic horizons such as albic, spodic and argic horizons.

As expected, the parent materials over the landscape gradient clearly differed in soil characteristics. Bedrock was encountered within 120 cm depth in most of the Luxembourg sandstone soils, both on the plateau and the upper cuesta, and on Muschelkalk (Table 6.11). Bedrock was much deeper in soils with colluvial parent material in the lower cuesta, in Keuper marls, in Plio-Pleistocene fluvial terraces and in loess deposits. Steep slopes were especially

encountered in the upper part of the cuesta and in Muschelkalk, and lime was present in the first 120 cm of the soil especially in colluvial soils of the lower cuesta, Keuper marls and Muschelkalk.

The humus profile also differed along the landscape gradient. Thick ectorganic layers with distinct F and H horizons were mainly found on Luxembourg sandstone, both on the plateau and in the upper parts of the cuesta front (Table 6.12). Mormoder was the prominent humus form here, which reflects the low rates of decomposition in the relatively dry, sandy soils with low biological activity. In Plio-Pleistocene river terraces, about half of the humus forms were Mormoder, especially in the older ones located in higher landscape positions. On the other parent materials, Mull humus forms predominated, which points to higher rates of decomposition in the loamier soils, which have more impeded drainage and higher biological activity than sandy soils (see also Chaps. 7, 8 and 10).

The landscape gradient also affected characteristics of the mineral soil. The thickness of the solum was relatively limited on the Luxembourg sandstone plateau with bedrock within 120 cm of the soil surface, but also along the cuesta and on Muschelkalk with their steep slopes, where transport processes prevail over in situ soil forming processes (Table 6.13). Albic material and spodic horizons, indicative for the podzolization process, only occurred on Luxembourg sandstone, on the plateau, but also in the upper cuesta slope, such as

Table 6.11 Site and soil characteristics of forest soils over a landscape gradient in the area around Diekirch-Beaufort, Luxembourg ($n = 198$)

	n	Bedrock present (%)	Bedrock depth (cm)	Steep slope (%)	Slope angle (°)	Carbonates present (%)	Carbonate depth (cm)
Luxembourg sandstone plateau (li2)	37	78	72 (38)	0	1 (1)	0	–
Luxembourg sandstone upper cuesta	31	87	59 (33)	90	15 (7)	0	–
Colluvial soils lower cuesta	13	31	90 (53)	46	10 (11)	85	30 (46)
Keuper marls (km1–km3)	39	13	116 (23)	38	6 (6)	77	54 (45)
Plio-Pleistocene river terraces	12	0	–	0	2 (1)	0	–
Loess deposits	12	0	–	8	2 (1)	8	114 (31)
Muschelkalk (mo1–mo2, mm1–mm2)	57	96	34 (24)	95	20 (8)	96	17 (27)

Differences between parent materials are significant for all factors (one-way Anova; $p < 0.05$). Values are averages, and where indicated with standard deviations in brackets

Table 6.12 Characteristics of the humus forms in forest soils over a landscape gradient in the area around Diekirch-Beaufort, Luxembourg ($n = 198$)

	n	Thickness organic layer (cm)	FH-horizon (cm)	Ah-horizon (cm)	Mormoder profiles (%)	Mull profiles (%)
Luxembourg sandstone plateau (li2)	37	5.7 (2.5)	3.2 (2.1)	13 (9)	89	11
Luxembourg sandstone upper cuesta	31	5.9 (2.7)	3.5 (2.0)	11 (8)	84	16
Colluvial soils cuesta front	13	2.2 (1.7)	1.0 (1.0)	24 (19)	31	69
Keuper marls (km1–km3)	39	3.4 (1.4)	1.6 (1.2)	12 (9)	23	77
Plio-Pleistocene river terraces	12	4.5 (2.3)	1.8 (1.0)	9 (7)	50	50
Loess deposits	12	4.3 (1.6)	1.7 (1.2)	6 (3)	25	75
Muschelkalk (mo1–mo2, mm1–mm2)	57	2.4 (1.5)	0.8 (0.6)	23 (13)	2	98

Differences between parent materials are significant for all factors (one-way Anova; $p < 0.05$). Values are averages, and where indicated with standard deviations in brackets

on the flat surface of slumps. Argic horizons, characteristic of clay translocation, were found in Keuper marls, Plio-Pleistocene fluvial terraces and loess deposits with shallow slopes and deep soils. These soils were also characterized by pseudogley mottles, formed by water stagnation on the clay-rich argic horizon, which leads to seasonally alternating wet and dry conditions.

Along the landscape gradient, different parent materials have thus given rise to different soil forming processes. In the Luxembourg sandstone group, both on plateau and the upper cuesta soils, Arenosols prevailed with 62 and 68%, respectively, but Podzols were also found there, and accounted for 38 and 32% of the soil profiles described. The colluvial lower cuesta mainly

Table 6.13 Soil properties of forest soils over a landscape gradient in the area around Diekirch-Beaufort, Luxembourg ($n = 198$)

	<i>n</i>	Depth A-B horizons (cm)	Albic material (%)	Spodic horizon (%)	Argic horizon (%)	Pseudogley (%)
Luxembourg sandstone plateau (li2)	37	37 (24)	38	38	0	8
Luxembourg sandstone upper cuesta	31	17 (14)	32	32	0	0
Colluvial soils cuesta front	13	32 (32)	0	0	0	15
Keuper marls (km1–km3)	39	40 (26)	0	0	62	62
Plio-Pleistocene river terraces	12	60 (42)	0	0	100	100
Loess deposits	12	88 (33)	0	0	100	100
Muschelkalk (mo1–mo2, mm1–mm2)	57	22 (14)	0	0	0	0

Differences between parent materials are significant for all factors (one-way Anova; $p < 0.05$). Values are averages, and where indicated with standard deviations in brackets

consisted of (Colluvic) Regosols. In Keuper marls, both Regosols (44%) and Planosols (56%) occurred. On Plio-Pleistocene river terraces and loess deposits, soils primarily consisted of (Luvic/Alic) Stagnosols. On Muschelkalk, 39% of the soils could be classified as Leptosol, while the other 61% consisted of (Leptic) Regosols.

6.9 Conclusion

The soil pattern of the Lias cuesta landscape is strongly related to lithology, local geomorphological conditions, land cover and land use. On a very short distance many of the major soil types of the temperate zone can be found as the substrates show a clear distinction and gradient from more acidic conditions to more neutral conditions in both coarse and finer textured materials. Within this large-scale pattern, a more complex heterogeneous “soilscape” exist, due to the large spatial variety in geodynamics, such as water erosion, mass wasting and colluviation. The result is a highly dynamic landscape with strong gradients in soils, hydrology, vegetation and biodiversity.

Acknowledgements The laboratory of IBED, and especially Leo Hoitinga, Leen de Lange, and Bert de Leeuw are thanked for their help with carrying out the soil physical and chemical data presented in this book. Jan van Arkel is thanked for his graphical work on Fig. 1. Furthermore, also David Balders is thanked for his work on the spatial distribution of loamy soils on the cuesta plateau in the surrounding of Beaufort. The authors would like to thank Mark Bokhorst, Ricardo van Dijk, Martijn Heuff, Gertrud Houkes, Vincent Kalkman, Robert Kuiper, Christiaan Kwakkestein, Maartje van Meteren, Marieke Nonhebel, Inka de Pijper, Ceciel Rip, Kasper de Rooy, Vincent Simons, Jeroen Timmers, Femke Tonneijck, Floris van der Valk, Mirjam Vriend†, Riekje Wiersma and Sybren Ydema for collecting the student dataset. We also would like to thank the communities and farmers of Beaufort, Bettendorf, Bigelbach, Eppeldorf, Ermsdorf, Folkendange, Medernach, Reisdorf and Stegen for allowing us to work on their lands for so many years. Also, the cooperation with the forestry service of Beaufort and Stegen is highly appreciated.

References

- Baeckeroot G (1929). Sur l'existence de la Pierre de Stonne entre la Meuse et la Moselle (Grand Duché de Luxembourg). *Ann Soc Géol Nord LIV:88–94*
- Blume HP, Brümmer GW, Horn R, Kandeler E, Kögel-Knabner I, Kretschmar R, Stahr R, Wilke B-M (2016) Scheffer/Schachtschabel soil science, 16th edn. Springer, Berlin, Heidelberg

- Bonell M, Hendriks MR, Imeson AC, Hazelhoff L (1984) The generation of storm runoff in a forested clayey drainage basin in Luxembourg. *J Hydrol* 71:53–77
- Bouezmarni M, Denne P, Debbaut V (2009) Notice explicative carte hydrogéologique de Wallonie; Meix-Devant-Virton. Université de Liège—Campus d’Arlon
- Cammeraat LH (1992) Hydro-geomorphological processes in a small forested catchment: preferred flow-paths of water. Unpublished PhD thesis, University of Amsterdam, Amsterdam, 146 pp
- Cammeraat LH (2002) A review of two strongly contrasting geomorphological systems within the context of scale. *Earth Surf Proc Land* 27:1201–1222
- Cammeraat LH, Kooijman AM (2009) Biological control of pedological and hydro-geomorphological processes in a deciduous forested ecosystem. *Biologia* 64(3):428–432
- Demoulin A (1990) Les silicifications tertiaires de la bordure nord de L’Ardenne et du Limbourg meridional. *Z Geomorphol NF* 34:179–197
- Dittrich D (1984) Erläuterungen zur Geologischen Karte von Luxembourg, Blatt Nr. 8 Mersch. Publications du Service Geologique du Luxembourg, XXV. Service Geologique du Luxembourg, Luxembourg
- Duchaufour R (2012) *Pedology: pedogenesis and classification*. Springer Science & Business Media
- Green RN, Trowbridge RL, Klinka K (1993) Towards a taxonomic classification of humus forms. Society of American Foresters, Bethesda, MD
- Hazelhoff H, van Hoof P, Imeson AC, Kwaad FJPM (1981) The exposure of forest soil to erosion by earthworms. *Earth Surf Proc Land* 6:235–250
- Hendriks MR (1993) Effects of lithology and land use on storm run-off in East Luxembourg. *Hydrol Process* 7:213–226
- Hissler C, Gourdol L, Juilleret J, Marx S, Leydet L, Flammang F (2015) *Projet BDSOL3: inventaire des sols luxembourgeois et évolution de l’application BDSOL – partie 3: fonctions de pédotransfert pour la prédiction des caractéristiques hydriques des sols au Luxembourg. Rapport d’étude ASTA/LIST*
- Imeson AC, Jungerius PD (1977) The widening of valley incisions by soil fall in a forested Keuper area, Luxembourg. *Earth Surf Proc* 2:141–152
- IUSS Working Group WRB (2015) *World Reference Base for Soil Resources 2014, update 2015. International soil classification system for naming soils and creating legends for soil maps. World Soil Resources Reports No. 106*. FAO, Rome
- Jamagne M (2011) *Grands paysages pédologiques de France*. Éditions Quae
- Juilleret J, Ifly JF, Hoffmann L, Hissler C (2012) The potential of soil survey as a tool for surface geological mapping: a case study in a hydrological experimental catchment (Huewelerbach, Grand-Duchy of Luxembourg). *Geol Belg* 15(1–2):36–41
- Jungerius PD (1958) Zur verwitterung, bodenbildung und morphologie der Keuper-Liaslandschaft bei Moutfort in Luxembourg. *Publications du Service Geologique de Luxembourg Vol XIII*
- Kooijman AM, Cammeraat E (2010) Biological control of beech and hornbeam affects species richness via changes in the organic layer, pH and soil moisture characteristics. *Funct Ecol* 24(2):469–477
- Levelt ThWM (1965) *Die Plateaulehme Süd-Luxemburgs und ihre Bedeutung für die morphogenetische Interpretation der Landschaft*. Publication of the Laboratory of Physical Geography of the University of Amsterdam, nr. 6, Amsterdam
- Lucius M (1948) *Das Gutland. Erläuterungen zu der Geologische Spezialkarten Luxemburgs, Bd5*
- Lucius L (1950) *Das Oesling. Erläuterungen zur geologischen Spezialkarten Luxemburgs. Band 6*. Publications of the Luxembourg Geological Survey
- Riezebos PA, Ten Kate WGHZ, De Bruin M (1990) Eluvial derivation of Rasenerz concretions from the Minette Formation (Luxembourg). Evidence based on numerical classification of geochemical data. *Bull Serv Géol Luxemb* 15:1–34
- Soil Survey Staff (2014) *Keys to soil taxonomy*. United States Department of Agriculture and Natural Resources Conservation Service
- van den Bril K, Swennen R (2008) Sedimentological control on carbonate cementation in the Luxembourg Sandstone Formation. *Geol Belg* 12:3–23
- van den Broek TMW (1989) Clay dispersion and pedogenesis of soils with an abrupt contrast in texture. Unpublished PhD thesis, University of Amsterdam, Amsterdam
- Van Zon JM (1978) Litter transport as a geomorphic process (a case study in the G.D. of Luxembourg). Unpublished PhD-thesis, University of Amsterdam
- Verhoef P (1966) *Geomorphological and pedological investigations in the Redange-sur-Attert area (Grand-Duchy of Luxembourg)*. PhD-thesis. Laboratory of Physical Geography and Soil Science, UvA, Amsterdam
- Voisin L (1988) *Introduction à l’étude de la Pierre de Stonne et des formations siliceuses associées au sud-ouest de l’Ardenne. Mémoire hors-série Société d’Histoire Naturelle des Ardennes*

Alternative Strategies for Nutrient Cycling in Acidic and Calcareous Forests in the Luxembourg Cuesta Landscape

7

A.M. Kooijman, K. Kalbitz and A. Smit

Abstract

In the forests of the Luxembourg cuesta landscape, nutrient cycling is affected by parent material, but in a different way than usually assumed. We challenge the ‘conventional wisdom’ that net N-mineralization is higher in calcareous than in acidic soils, due to higher biological activity and gross N-mineralization. In four separate laboratory incubation experiments, net N-mineralization was higher in acidic than in calcareous soil. Experiments with different tree species showed that soil type was even more important than litter quality. In acidic forests, high net N-mineralization may be due to dense organic layers, but also to differences in soil communities, which are dominated by fungi at low pH versus bacteria at high pH. Fungi have lower N-demand than bacteria, and may thus mitigate low activity and gross N-release. Model studies suggested that microbial immobilization was below 20% in acidic soil, and above 80% in calcareous soil, in both organic layer and mineral topsoil. Differences between fungi and bacteria were supported by selective inhibition. Microbial immobilization significantly decreased with the bactericide *streptomycin*, while respiration increased with the fungicide *cycloheximide*. This further supports that bacteria and fungi, and with them calcareous and acidic soils, show different strategies for N-nutrition. For P-nutrition, differences between calcareous and acidic soils are also important, as net P-mineralization mainly occurred in the organic layer,

A.M. Kooijman (✉) · K. Kalbitz · A. Smit
Institute for Biodiversity and Ecosystem Dynamics,
University of Amsterdam, Science Park,
PO Box 94248, 1090 GE Amsterdam,
The Netherlands
e-mail: a.m.kooijman@uva.nl

K. Kalbitz
e-mail: karsten.kalbitz@tu-dresden.de

A. Smit
e-mail: annemieke.smit@wur.nl

K. Kalbitz
Technische Universität Dresden, Bodenressourcen
und Landnutzung, University of Amsterdam,
Pianner Straße 19, 01737 Tharandt, Germany

A. Smit
Alterra, PO Box 47, 6700 AA Wageningen
Wageningen, The Netherlands

due to chemical sorption in the mineral soil. As a result, in the Luxembourg cuesta landscape, availability of both N and P may be higher in acidic than calcareous forests.

7.1 Introduction

The geological gradients in the Luxembourg cuesta landscape, from Luxembourg sandstone, Keuper marls and Muschelkalk formations to local Pleistocene river terraces and Loess deposits, may not only lead to differences in soil formation (see also Chap. 6) and vegetation (see also Chap. 8), but also to differences in nutrient cycling. Since the early studies of Swift et al. (1979), it is clear that soil conditions affect carbon and nutrient cycling (e.g. Aerts and Chapin 2000; Schimel and Bennett 2004; Booth et al. 2005; Parton et al. 2007). Acidic soils are generally associated with low litter turnover and low N-availability to the vegetation, while calcareous soils show high decomposition and supposedly high nutrient availability.

Differences between acidic and calcareous soils in nutrient cycling are associated with differences in microbial communities, which generally shift from fungal-dominated systems at low pH to bacteria-dominated systems at high pH (Blagodatskaya and Anderson 1998; Bååth and Anderson 2003; Högberg et al. 2007; Rousk et al. 2010). Fungi are associated with slow and highly conservative nutrient cycling, and are assumed to have higher immobilization of N than bacterial-dominated systems (Schimel and Bennett 2004; de Vries et al. 2011). In contrast, calcareous soils are generally dominated by earthworms and bacteria, and show higher biological activity than acidic soils (Pop 1997; Ponge 2003; Rousk et al. 2010). Calcareous soils may thus be expected to have higher rates of depolymerization and net N-mineralization (Aerts and Chapin 2000; Schimel and Bennett 2004).

Yet, despite this being the ‘conventional wisdom’, there seem to be surprisingly few

studies from natural ecosystems to support such an increase in net N-mineralization with high pH (e.g. Ruess and Seagle 1994; Bayley et al. 2005). In contrast, Ellenberg (1977) found no clear increase from acidic to calcareous soils, even within the same type of ecosystem. Also, Hart et al. (1994) and Campell and Gower (2000) showed that gross and net N-release were not actually correlated. Several authors even published a decrease rather than increase in net N-mineralization from low to high pH. In forest studies, net N-mineralization was higher in acidic than calcareous soils in Zöttle (1960) and Davy and Taylor (1974). In wetlands and coastal dune grasslands, net N-mineralization generally decreased from low to high pH (Verhoeven et al. 1988, 1990; Veer 1997; Kooijman and Besse 2002; Kooijman and Hedenäs 2009; Mettrop et al. 2014). Also, in natural grasslands subjected to simulated atmospheric N-deposition, N-storage in the soil was higher in calcareous than in acidic soil (Phoenix et al. 2003).

Shifts in net N-mineralization can thus not be explained by litter decay rates and gross N-mineralization alone. Possibly, differences in microbial N-demand play a role. Fungi may have lower N-demand than bacteria, due to their higher C:N ratio (Hassink 1994; Moore et al. 2005), lower rates of cell division, and use of carbohydrates rather than amino acids for osmoregulation (e.g. Measures 1975; Kuehn et al. 1998; Cleveland and Liptzin 2007). In acidic soil, low microbial N-demand by fungi may thus lead to low immobilization, and perhaps also to relatively high net N-mineralization, even though gross N-mineralization is relatively low.

The Luxembourg cuesta landscape, with its mild climate, clear gradients in parent material (see also Chaps. 1 and 6) and semi-natural forest

areas (see also Chap. 8), offers the opportunity to test differences in N-nutrition over a geosequence. It is also possible to test whether differences between soil types are altered by differences in litter quality, which is an important factor to forest ecology as well (Swift et al. 1979; Parton et al. 2007). In the area, beech (*Fagus sylvatica* L.) and hornbeam (*Carpinus betulus* L.) are common trees on acidic and calcareous soils, but clearly differ in litter quality and N-content (Swift et al. 1979; Laskowski et al. 1995; Aubert et al. 2003). In addition, spruce (*Picea abies* (L.) H. Karts.), which has more recalcitrant litter than deciduous trees, has been planted on various substrates.

Shifts in N-nutrition over geosequences are important, but adequate nutrient supply to the vegetation is also dependent on the availability of P (Lang et al. 2016). Phosphorus has become a limiting factor in many European beech forests, due to high atmospheric N-deposition (Jonard et al. 2014). In contrast to N, availability of P is not only regulated by decomposition of organic matter, but also by chemical sorption processes (Lindsay and Moreno 1966; Walker and Seyers 1976; Shen et al. 2011; Turner and Condron 2013). Under a wide range of soil chemical conditions, P is either precipitated as Ca-, Fe-, and Al-P minerals, adsorbed by sesquioxides, or bound within the soil organic matter (Lang et al. 2016).

In this chapter, a synthesis is given of the work on nutrient cycling in the Luxembourg cuesta landscape in the past decade, over a range of forest types and parent materials (Kooijman et al. 2008; Kooijman and Martinez-Hernandez 2009; Kooijman and Smit 2009; Kooijman et al. 2009, 2016; A.M. Kooijman unpublished records). We want to challenge the ‘conventional wisdom’ that net N-mineralization is higher in calcareous than in acidic soil, due to high biological activity and gross N-mineralization. The main questions are: (1) Does net N-mineralization increase or actually decrease from acidic to calcareous soil? (2) Is the relationship between net N-mineralization and parent material affected by litter quality? (3) Can differences in net N-mineralization be explained by

differences in microbial communities? (4) Is net P-mineralization also affected by the gradient in parent materials?

7.2 Methods

7.2.1 Study Area

The study sites are located in the Luxembourg cuesta landscape, mostly in the area south of Diekirch. The area has a temperate humid climate and rainfall in all months. Mature forests were selected on Luxembourg sandstone (li2), Pleistocene river terraces and Loess deposits, Keuper marls (km) and/or dolomitic limestone of the Muschelkalk formation (mm and mo), depending on the particular study. On Luxembourg sandstone and Muschelkalk limestone, spruce plantations were also sampled. Most forests were dominated by beech and hornbeam, intermixed with summer oak (*Quercus robur* L.), except on Luxembourg sandstone, where hornbeam does not occur. Deciduous forests on Luxembourg sandstone and Pleistocene deposits were probably planted 150 years ago, with beech as planted and hornbeam as spontaneous species. On Keuper marl, however, many forests were oldgrowth (Ferraris le Comte de 1777), and on limestone, many have spontaneously developed after Roman times. The forests are relatively undisturbed, and management is restricted to occasional removal of large trees.

Different parent materials were characterized by different humus forms, soil profiles and forest communities. Luxembourg sandstone was characterized by acidic soils with Mormoder humus forms (Green et al. 1993), Ah-E-Bs-Bw-C soil profile and Podzol-Arenosol soil type (IUSS 2015), and Luzulo-Fagetum forest type (Niemeyer et al. 2010). Pleistocene river terraces and loess deposits had acidic soils with Mormoder-Mullmoder humus forms, Ah-E-Bt-C profile, Luvic Stagnosol soil type and Galio odorati-Fagetum forest type. On the gentle dip-slope, Keuper marls of the Steinmergelkeuper formation were characterized by decalcified soils with intermediate pH values (Kooijman and

Cammeraat 2010), Vermimull humus forms, AEh-EAh-Bwg-C profile, Stagnosol-Planosol soil type and Galio-Carpinetum forest type. On the steep face slope, however, Keuper marls remained calcareous due to erosion, and soils were characterized by Vermimull humus profiles, Ah-Bw-C profile, Cambisol soil type and Hordelymo-Fagetum forest type. The dolomitic limestone of the Muschelkalk formation (mainly Trochitenkalk) was characterized by calcareous soils with Vermimull humus forms, Ah-C-R profiles with bedrock often within 25 cm and Leptosol of Leptic Regosol soil type, and Hordelymo-Fagetum or Carici-Fagetum forest type.

7.2.2 Field Surveys

Field surveys were conducted in different forests and (parts of the) years, depending on the particular study. In general, representative beech, hornbeam and/or spruce plots were selected in the forest interior, according to stratified random sampling procedures. In one experiment, four mono-specific beech stands were selected on Luxembourg sandstone, Pleistocene river terrace, decalcified Keuper dipslope, and calcareous Keuper face slope (Kooijman et al. 2008, 2009). In a second experiment, spruce, beech and hornbeam stands were selected on Luxembourg sandstone, Keuper dipslope and/or Muschelkalk limestone (Kooijman and Smit 2009). In a third experiment, beech and hornbeam stands were selected in seven mixed forests on Pleistocene river terrace, Loess deposits, Keuper dipslopes and Muschelkalk limestone (Kooijman and Martinez-Hernandez 2009). In a fourth experiment, beech stands were selected on Luxembourg sandstone and calcareous Keuper face slope (Kooijman et al. 2016). Sampling localities only occasionally overlapped, and 22 different forest stands were selected in total. In mono-specific beech and spruce stands, plots were 10 × 10 m, but in mixed beech-hornbeam forests, plots were approximately 7 × 7 m, and surrounded by at least three mature trees of the required species. The number of replicates

differed between particular studies from 4–9. In all plots, the organic layer was sampled within 25 × 25 cm squares and stored at 4 °C until further analysis. In each square, the mineral topsoil was sampled in metal rings of 5 or 10 cm depth, and 100 or 200 ml volume. This generally comprised the entire Ah. In all study sites except spruce plantations, litter input was determined from 2003–2005 at the end of November, just after leaf fall. Fresh litter was collected in 25 × 25 cm², dried and weighed. Fresh and mature beech and hornbeam leaves were collected on Luxembourg sandstone, Keuper dipslope and/or Muschelkalk in July, for determination of total nutrient contents.

7.2.3 Incubation Experiments

Fresh weight and gravimetric moisture content of the organic layer and the mineral topsoil were determined, and dry weight and bulk density calculated. After homogenization by hand, pH values were determined in water, using a 1:2.5 weight:volume ratio for mineral samples and 1:10 weight:volume ratio for organic layer. After drying (48 h at 70 °C for organic and 105 °C for mineral samples) and grinding of subsamples, C and N contents of the samples were determined with a CNS analyzer (Westerman 1990). C and N content were also measured of the fresh litter samples of November, and of the mature beech and hornbeam leaves of July. Of the latter, P-content was also determined, with HNO₃-digestion in the microwave (Westerman 1990).

In all experiments, net N-mineralization and respiration were determined with 4–7 week incubation under laboratory conditions, for organic layer and mineral topsoil separately. Fresh samples were homogenized by hand, put into large petri dishes and stored at optimal gravimetric moisture levels (300% for organic layer and 50% for mineral topsoil; Tietema 1992) at 20 °C in the dark. Moisture content was checked and replenished when necessary. Ammonium, nitrate, DON and DOC concentrations of fresh and incubated samples were extracted with 50 ml 0.5 M K₂SO₄ solution,

using the equivalent of 1.5 and 4.5 g dry material for organic and mineral samples respectively, and measured on a continuous-flow analyzer (Westerman 1990). In two of the four experiments (Kooijman and Martinez-Hernandez 2009; Kooijman et al. 2016), ortho-P was also measured. Net N-mineralization, and if measured, net P-mineralization, were calculated from differences between incubated and fresh samples. Nitrification was calculated as net release of nitrate, and expressed as percentage of total net N-mineralization.

In all incubation experiments except Kooijman and Smit (2009), microbial C and N were measured at the start and end of the incubation period, with the chloroform fumigation and extraction procedure (Brooks et al. 1985). Fumigated samples were flushed for 24 h with chloroform and extracted with 0.5 M K_2SO_4 immediately afterwards, to prevent microbial regrowth. Ammonium, nitrate, DON and DOC were measured in fumigated and non-fumigated samples using a continuous-flow analyzer. Microbial C and N concentrations were calculated as differences between fumigated and non-fumigated samples. Microbial C and N in incubated samples were not included in further analyses, since they generally did not differ from fresh ones, indicating that populations remained more or less stable.

In all experiments except Kooijman and Martinez-Hernandez (2009), respiration was measured at the start and end of the incubation period, and also in between in Kooijman and Smit (2009). Fresh or incubated material from the petri dishes used for net N-mineralization was placed in open glass jars during one night, with the equivalent of 5 g dry for organic and 10–15 g dry for mineral samples. During measurements, the jars were closed and air samples were extracted by needle. CO_2 -concentrations were measured three times by injecting the air sample into a Carlo Erba Varian gas chromatograph (Tietema 1992). CO_2 - production rates were calculated from the increase in CO_2 - concentration during the day, the volume of the head space and sample dry weight. Total CO_2 - production over the incubation period was

calculated, based on its duration and CO_2 - production at start and end of the experiment.

7.2.4 Model Estimates of Gross N-Mineralization and Immobilization

To test whether potential shifts in net N-mineralization along the geological gradient could be explained by existing theoretical models, equations of C and N dynamics of Berendse et al. (1989) and Tietema and Wessel (1992) were reformulated. When respiration, net N-mineralization and N:C ratios of substrate and micro-organisms are known, microbial growth efficiency (e_C) can be estimated according to Equation 3 (Table 7.1). Microbial growth efficiency is the fraction of gross C-release used for microbial assimilation, and a key parameter in the allocation of C and N from organic matter to micro-organisms (Schimel 1988; Tietema and Wessel 1992). With the model, gross N-mineralization and immobilization can be calculated over longer periods, in contrast to the short-term ^{15}N pool dilution method (Schimel 1988; Hart et al. 1994; Fisk and Fahey 2001). The use of C:N ratios however assumes homogeneous substrates (which is not likely), so the model should be seen as explorative rather than absolute. Microbial growth efficiency was calculated for litter, organic layer and mineral topsoil, using the measured values for respiration, net N-mineralization and C:N ratios of substrate and microbes. Using the estimated e_C values, gross C-release and microbial assimilation were estimated according to Equations 6 and 7. In combination with substrate or microbial C:N ratios, gross N-release and immobilization were estimated according to Equations 8 and 9, and microbial immobilization efficiency (e_N) according to Equation 11. In Kooijman et al. (2008), mean values and standard deviations of gross N-mineralization and immobilization were based on direct model outcomes. In Kooijman and Smit (2009), a four-factor perturbation experiment was used ($n = 16$; Henderson-Sellers and Henderson-Sellers 1993), with measured mean

Table 7.1 List of symbols and equations derived from literature (Berendse et al. 1989; Tietema and Wessel 1992) and adapted by Kooijman et al. (2008)

Symbols and equations		
<i>Measured symbols</i>		<i>Value</i>
NM	Net N-mineralization	$\text{g N m}^{-2} \text{ day}^{-1}$
Q	Respiration	$\text{g C m}^{-2} \text{ day}^{-1}$
NC_M	N-to-C ratio in microbes	$\text{g N g}^{-1} \text{ C}$
NC_S	N-to-C ratio in substrate	$\text{g N g}^{-1} \text{ C}$
<i>Calculated symbols</i>		
e_C	Microbial growth efficiency	$\text{g C g}^{-1} \text{ C}$
GC	Gross C-release	$\text{g C m}^{-2} \text{ day}^{-1}$
A	C-assimilation	$\text{g C m}^{-2} \text{ day}^{-1}$
GN	Gross N-release	$\text{g N m}^{-2} \text{ day}^{-1}$
I	N-immobilization	$\text{g N m}^{-2} \text{ day}^{-1}$
e_N	Microbial immobilization efficiency	$\text{g N g}^{-1} \text{ N}$
<i>Equations in literature</i>		<i>Source</i>
1	$\text{NM} = \text{GN} - \text{I}$	By definition
2	$\text{NM} = ((\text{NC}_S * \text{Q}) / (1 - e_C)) - ((e_C * \text{NC}_M * \text{Q}) / (1 - e_C))$	Berendse et al. (1989), Tietema and Wessel (1992)
<i>Derived equations of C transformations</i>		
3	$e_C = ((\text{NC}_S * \text{Q}) - \text{NM}) / ((\text{NC}_M * \text{Q}) - \text{NM})$	Different expression of (2)
4	$e_C = \text{A} / \text{GC}$	By definition
5	$\text{GC} = \text{Q} + \text{A}$	By definition
6	$\text{GC} = (1 / (1 - e_C)) * \text{Q}$	Substitution of (4) and (5)
7	$\text{A} = (e_C / (1 - e_C)) * \text{Q}$	Substitution of (4) and (5)
<i>Derived equations of N transformations</i>		
8	$\text{GN} = (1 / (1 - e_C)) * \text{NC}_S * \text{Q}$	Different expression of GN based on (1) and (2)
9	$\text{I} = (e_C / (1 - e_C)) * \text{NC}_M * \text{Q}$	Different expression of I based on (1) and (2)
10	$e_N = \text{I} / \text{GN}$	By definition
11	$e_N = e_C * (\text{NC}_M / \text{NC}_S)$	Substitution of (8) and (9) into (10)

C = carbon; N = nitrogen. Respiration, net N-mineralization and N/C ratios of substrate and microbes were measured independently, and used to estimate microbial growth efficiency. In turn, gross C and N release and microbial assimilation and immobilization were estimated

values plus or minus one standard deviation of respiration, net N-mineralization and C:N ratios of substrate and microbes.

7.2.5 Microbial Analyses

Bacteria and fungi were measured in four beech forests on Luxembourg sandstone, Pleistocene river terrace, Keuper dipslope and Keuper face slope (Kooijman et al. 2008), with standard plate

count methods (ICMSF 2000). Bacterial and fungal colonies were measured in litter, organic matter and mineral topsoil samples ($n = 5$). For each sample, duplicate subsamples of 10 g were extracted with sterile phosphate tamponed water in six steps of dilution, and cultivated on sterile plates. For bacteria, plates with Plate Count Agar were incubated for 48 h at 30 °C. For fungi, plates with Sabouraud Oxytetracycline Agar were incubated for 6 days at 25 °C. Values were expressed in 10^6 CFU (colony forming unit)

ml⁻¹, and ratios between fungal and bacterial colonies calculated as fungi/(fungi + bacteria).

In the same four forests, undisturbed samples of the upper soil were collected in Kubiena boxes for micromorphological analysis (Kooijman et al. 2009). Analyses were conducted with an Olympus polarization microscope. To distinguish bacteria, which are rarely more than a few μm in length, high magnification (1000 \times) and reflected light rather than transmitted were used. Soil micromorphological characteristics, related to soil organic matter, ped characteristics, soil fauna and micro-organisms, were semi-quantitatively expressed on a scale from 0 to 3 (0 = not detected; 1 = low amounts or activity; 2 = moderate amounts or activity; 3 = high amounts or activity).

Selective inhibition of bacteria and fungi was applied during a one month incubation experiment with samples of the organic layer and mineral topsoil (0–10 cm) of two beech forests on Luxembourg sandstone and Keuper face slope (Kooijman et al. 2016). For selective inhibition, the bactericide *streptomycin* and the fungicide *cycloheximide* were used, according to Bååth and Anderson (2003). *Streptomycin* was applied as 4 mg g⁻¹ dry weight in the organic layer and mineral topsoil of the calcareous site, and 2 mg g⁻¹ in the acidic site, because bacteria were less abundant in the latter. *Cycloheximide* was applied as 3 mg g⁻¹ in calcareous soil, and 6 mg g⁻¹ in acidic soil. To prevent regrowth, antibiotics were applied weekly during the one month incubation experiment. Respiration and net N-mineralization were measured according to Sect. 7.2.3.

7.2.6 Statistical Analyses

In all experiments, the potential effect of parent material or soil type on soil and microbial characteristics was tested for organic layer and mineral topsoil separately. For each horizon, differences between parent materials were tested with one or two-way Analysis of variance, with parent material and, if relevant, sampling period or tree species as independent factors (Cody and Smith 1987). Differences between individual mean values were generally tested with post hoc LSmeans tests.

7.3 Results and Discussion

7.3.1 Respiration and Net N-Mineralization

Soil characteristics clearly differed between beech forests on acidic Luxembourg sandstone, acidic Pleistocene river terrace, decalcified Keuper dipslope and calcareous Keuper face slope (Table 7.2). Over this gradient, pH values of the mineral topsoil increased from 3.7 to 7.0. Mass of the organic layer clearly decreased from 1.1 kg C m⁻² on acidic soil to only 0.4 kg m⁻² on calcareous soil, which reflect different rates of litter decomposition. Earthworms, which are rare in acidic but common in calcareous soil (Pop 1997), consume a lot of litter, especially anecic species such as the common *Lumbricus terrestris* L. (e.g. Marhan and Scheu 2005; Pulleman et al. 2005). The amount of C in the mineral topsoil thus increased from 2.3 m⁻² in acidic soil to 3.5 kg m⁻² in calcareous soil.

Soil N showed similar patterns, with a clear decrease in the organic layer from acidic to calcareous soil, and increase in the mineral topsoil. In the organic layer, C:N ratio increased from acidic to calcareous soil, because organic material was older and more decomposed in the first, and consisted of relatively fresh litter in the latter (Swift et al. 1979; Berg and Ekbohm 1983; Berg 2000). In the mineral topsoil, however, C:N ratios decreased from acidic to calcareous soil, which reflects higher biological activity and loss of C in the latter.

Respiration in the organic layer decreased from acidic to calcareous soil (Fig. 7.1). This was mainly due to differences in mass of the organic layer, because respiration rates per g C did not differ (Kooijman et al. 2008). In the mineral topsoil, however, respiration increased from acidic to calcareous soils, due to higher biological activity. As a result, total respiration of organic layer and mineral topsoil combined was more or less the same.

Total net N-mineralization, however, showed a clear decrease from acidic to calcareous soils. This was mainly due to the decrease in the organic layer over this gradient. In acidic sites, the organic layer

Table 7.2 Soil pH H₂O, carbon and nitrogen content of litter, organic layer and upper 5 cm of the mineral topsoil in four Luxembourg beech forests with different soil types

	Luxembourg sandstone	Pleistocene terrace	Keuper dipslope	Keuper face slope
pH				
Organic layer	4.7 (0.4) ^a	4.8 (0.2) ^a	5.4 (0.3) ^b	6.4 (0.7) ^c
Mineral topsoil	3.7 (0.1) ^a	4.0 (0.3) ^a	4.7 (0.4) ^b	7.0 (0.5) ^c
Organic matter				
Litter input (kg C m ⁻² year ⁻¹)	0.23 (0.05) ^a	0.21 (0.04) ^a	0.22 (0.01) ^a	0.23 (0.04) ^a
Organic layer (kg C m ⁻²)	1.11 (0.45) ^b	0.57 (0.14) ^{ab}	0.40 (0.09) ^a	0.42 (0.10) ^a
Mineral topsoil (kg C m ⁻²)	2.32 (0.11) ^b	1.78 (0.27) ^a	2.16 (0.32) ^{ab}	3.49 (0.81) ^c
Nitrogen				
Litter input (g m ⁻² year ⁻¹)	5.9 (1.0) ^b	4.9 (0.6) ^{ab}	6.1 (0.8) ^b	4.2 (0.3) ^a
Organic layer (g m ⁻²)	73 (30) ^c	43 (12) ^b	25 (6) ^a	24 (6) ^a
Mineral topsoil (g m ⁻²)	128 (35) ^{ab}	95 (17) ^a	141 (12) ^b	216 (56) ^c
C:N ratio				
Fresh litter	43 (7) ^{ab}	47 (6) ^{ab}	40 (5) ^a	53 (4) ^b
Organic layer	22 (2) ^a	24 (3) ^b	26 (3) ^b	28 (4) ^c
Mineral topsoil	19 (1) ^b	19 (2) ^b	16 (2) ^a	17 (2) ^a

Mean values and standard variations are based on two sampling periods, and derived from Kooijman et al. (2008). Different letters indicate significant differences between soil types for a particular parameter ($p < 0.05$), values significantly increase from a to c

had higher mass, more decomposed material and higher N-content. In more decomposed litter, supply of easily degradable substrate may decrease, and C become a limiting factor (Swift et al. 1979; Berg and Ekbohm 1983; Berg 2000). In that case, N is no longer used for microbial growth, but becomes available for plant uptake. In calcareous sites, however, the organic layer consisted of relatively fresh litter, in which N is still a limiting factor, and net N-mineralization did not yet occur. In the mineral topsoil, differences between soil types were less pronounced, but due to the low contribution of the organic layer, total net N-mineralization was significantly lower in calcareous than in acidic soil.

Although laboratory experiments yield potential rather than actual rates of net N-mineralization in the field, low N-availability in calcareous soils was supported by significantly lower N-input in fresh litter (Table 7.2). Over a three year period, fresh litter input ranged around 230 g C m⁻² in both acidic and calcareous beech forests, but N-input was 5.9 g N m⁻² in the first, and only 4.2 g N m⁻² in the latter.

7.3.2 Potential Effects of Litter Quality

Spruce, beech and hornbeam clearly differed in mass of the organic layer (Table 7.3), which reflects their differences in litter quality (Swift et al. 1979; Laskowski et al. 1995; Aubert et al. 2003; Kooijman and Martinez-Hernandez 2009). However, parent material was also important. Over the gradient from Luxembourg sandstone to Keuper marl and/or Muschelkalk limestone, all three species showed a clear increase in pH, decrease in mass of the organic layer and higher amounts of C in the mineral topsoil. Also, C:N ratio of the mineral topsoil slightly decreased from spruce to beech and hornbeam, in accord with differences in litter quality, but the change in C:N ratio with parent materials was much larger.

For soil respiration, litter quality was more important than parent material (Fig. 7.2). Total soil respiration, for organic layer and topsoil combined, was significantly higher for spruce than for beech and hornbeam, due to higher mass of the organic layer. However, for each tree species, total respiration remained more or less the same over the

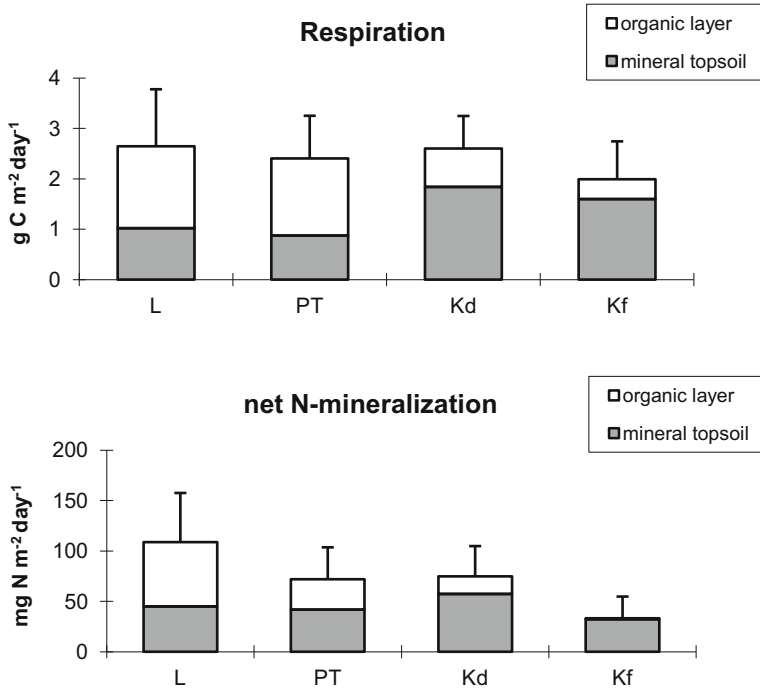


Fig. 7.1 Soil respiration and net N-mineralization in the organic layer and upper 5 cm of the mineral topsoil in four Luxembourg beech forests on different parent materials, measured in 4–6 week laboratory incubation experiments. *L* Luxembourg sandstone, *PT* Pleistocene river terrace, *Kd* decalcified Keuper dipslope, *Kf* calcareous Keuper face slope. Mean values ($n = 9$) and standard variations are based on two sampling periods, and derived from Kooijman et al. (2008)

Table 7.3 Soil characteristics in the organic layer and upper 5 cm of the mineral topsoil in Luxembourg spruce, beech and hornbeam stands on different parent materials, measured in a laboratory incubation experiment

		pH-KCl		Soil C (kg m ⁻²)		C:N ratio (g g ⁻¹)	
		Organic layer	Mineral topsoil	Organic layer	Mineral topsoil	Organic layer	Mineral topsoil
Spruce	L	3.2 (0.1) ^a	3.2 (0.1) ^a	4.0 (0.6) ^c	1.8 (0.4) ^a	26 (2) ^b	26 (5) ^b
	M	5.5 (0.4) ^c	5.9 (0.7) ^b	1.7 (0.6) ^b	2.6 (0.3) ^b	26 (2) ^b	16 (2) ^a
Beech	L	4.1 (0.1) ^b	3.4 (0.1) ^a	0.7 (0.4) ^b	2.2 (0.7) ^{ab}	21 (1) ^a	24 (7) ^b
	Kd	4.9 (0.3) ^a	4.1 (0.3) ^a	0.4 (0.2) ^b	2.2 (0.7) ^{ab}	34 (1) ^b	17 (2) ^b
Hornbeam	M	5.7 (0.1) ^c	5.8 (0.7) ^b	0.3 (0.1) ^{ab}	2.5 (0.3) ^b	39 (3) ^c	15 (2) ^a
	Kd	4.7 (0.1) ^a	4.3 (0.4) ^{ab}	0.3 (0.2) ^{ab}	2.0 (0.3) ^a	29 (3) ^a	15 (2) ^{ab}
	M	5.2 (0.5) ^{ab}	5.3 (0.9) ^{bc}	0.1 (0.1) ^a	2.0 (0.3) ^a	41 (3) ^c	13 (1) ^a

L Luxembourg sandstone, *Kd* decalcified Keuper dipslope, *M* Muschelkalk limestone. Mean values ($n = 4$) and standard deviations are derived from Kooijman and Smit (2009). Different letters indicate significant differences between species and/or parent materials for a particular soil parameter ($p < 0.025$, due to Bonferoni corrections)

Values significantly increase from a to c

gradient in parent materials, although contributions of organic layer and mineral topsoil shifted.

In contrast, for net N-mineralization, parent material was more important than litter quality. Spruce and beech showed a similar decrease in

total net N-mineralization from sandstone to limestone, mainly due to smaller contributions of the organic layer. For hornbeam, net N-mineralization showed a similar trend, although differences between parent materials were smaller, because

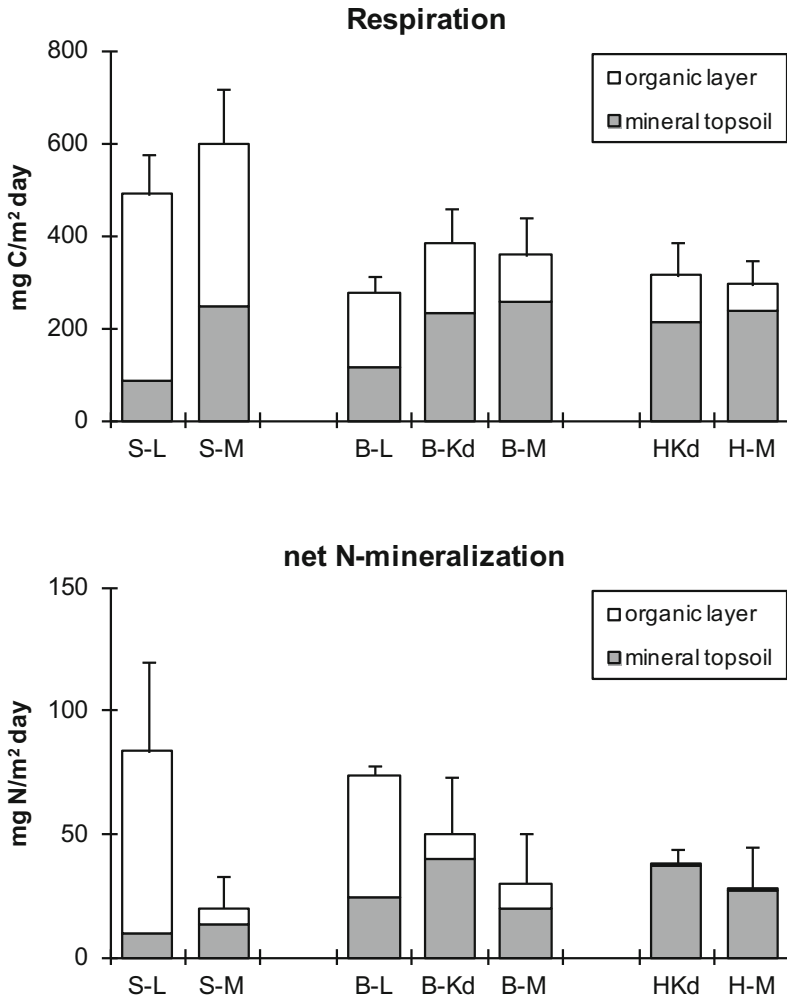


Fig. 7.2 Soil respiration and net N-mineralization in the organic layer and upper 5 cm of the mineral topsoil in Luxembourg spruce, beech and hornbeam stands on different parent materials, measured in a one month laboratory incubation experiment. *S* spruce, *B* beech, *H* hornbeam; *L* Luxembourg sandstone, *Kd* decalcified Keuper dipslope, *M* Muschelkalk limestone. Mean values ($n = 4$) and standard deviations are derived from Kooijman and Smit (2009)

marl and limestone were both relatively base-rich. These response patterns were supported by a study in seven beech and hornbeam forests (Kooijman and Martinez-Hernandez 2009). In this study, net N-mineralization clearly decreased from acidic to calcareous soils, but beech and hornbeam plots did not differ at all, despite clear initial differences in N-content of the litter.

The lack of response in net N-mineralization to litter quality was unexpected (Scheu 1997; Högberg et al. 2006; Parton et al. 2007). Possibly, differences in initial N-content were not large enough. In our studies, initial N-content of

beech and hornbeam ranged from 9 to 14 mg g⁻¹. However, in Scheu (1997) and Högberg et al. (2006), net N-mineralization significantly increased when litter contained 43 mg g⁻¹ and 29 mg g⁻¹ N respectively, while values ranged from 4 to 20 mg g⁻¹ N in Parton et al. (2007). Also, effects of initial N-content on net N-mineralization may be evident in litter bags (Parton et al. 2007), but overruled by soil characteristics under actual field conditions (Reich et al. 1997; Campbell and Gower 2000). In any case, in the Luxembourg cuesta landscape, litter quality effects (if present) on net

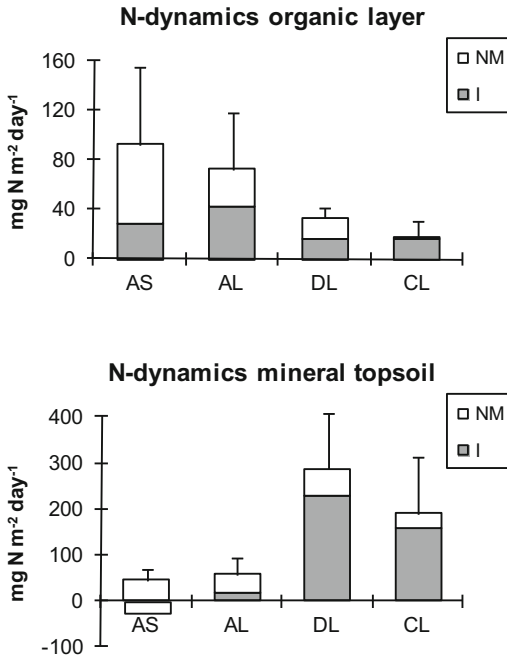


Fig. 7.3 N-dynamics in the organic layer and upper 5 cm of the mineral topsoil in four Luxembourg beech forests on different parent materials. *L* Luxembourg sandstone, *PT* Pleistocene river terrace, *Kd* decalcified Keuper dipslope, *Kf* calcareous Keuper face slope. *NM* net N-mineralization and *I* immobilization; $NM + I =$ gross N-mineralization. Gross N-mineralization and immobilization are calculated with a theoretical model (Table 7.1, Kooijman et al. 2008), based on a.o. measured values of respiration and net N-mineralization in 4–6 weeks laboratory incubation experiments. Standard deviations are those of (estimated) gross N-mineralization

N-mineralization are clearly overruled by different soil conditions.

7.3.3 Gross N-Mineralization and Microbial Immobilization

In the traditional view, gross N-mineralization is supposedly low in acidic soils, and high in calcareous soils, due to increased biological activity of earthworms and bacteria (Aerts and Chapin 2000; Ponge 2003; Schimel and Bennet 2004). Also, microbial immobilization would be higher in acidic, fungal-dominated soils, than in bacteria-dominated soils, due to their extensive hyphal networks (de Vries et al. 2011).

In the study with four mono-specific beech forests, simulated gross N-mineralization, based on the model equations with respiration and C:N ratios of substrate and micro-organisms, indeed increased from acidic to calcareous soil (Fig. 7.3). In the organic layer, gross N-mineralization was higher in acidic than in calcareous soil, due to its higher mass. However, in the mineral topsoil, gross N-mineralization was much higher in calcareous than acidic soil. For translation of gross to net N-mineralization, microbial immobilization is also important. In the organic layer, simulated immobilization ranged from 19% of gross N-release in acidic soil to 96% in calcareous soil, which may explain why net N-mineralization was relatively high in the first and non-existent in the latter. In the mineral topsoil, immobilization showed similar patterns, with values of –23% of gross N-release in acidic to 80% in calcareous soil. This may explain why differences in net N-mineralization were lower than expected. In acidic soils, net N-mineralization may be higher than expected from the low gross N-mineralization, because immobilization is also low. In calcareous soils, however, net N-mineralization was much lower than expected from the high gross N-mineralization, because immobilization is high as well.

In the experiment with spruce, beech and hornbeam on different parent materials, more or less similar patterns in N-dynamics were found (Fig. 7.4). In the organic layer, gross N-mineralization was high for spruce on sandstone and limestone, and for beech on sandstone, due to high mass. However, immobilization was only low on sandstone, and very high on marl and limestone. This explained why spruce and beech showed substantial net N-mineralization only on the acidic Luxembourg sandstone, and low values on the calcareous Muschelkalk. For hornbeam, the organic layer did not contribute to net N-mineralization, because immobilization was too high. In the mineral soil, gross N-mineralization increased from sandstone to marl and limestone for all tree species, but immobilization did so as well, and net N-mineralization only slightly differed between soil types or trees.

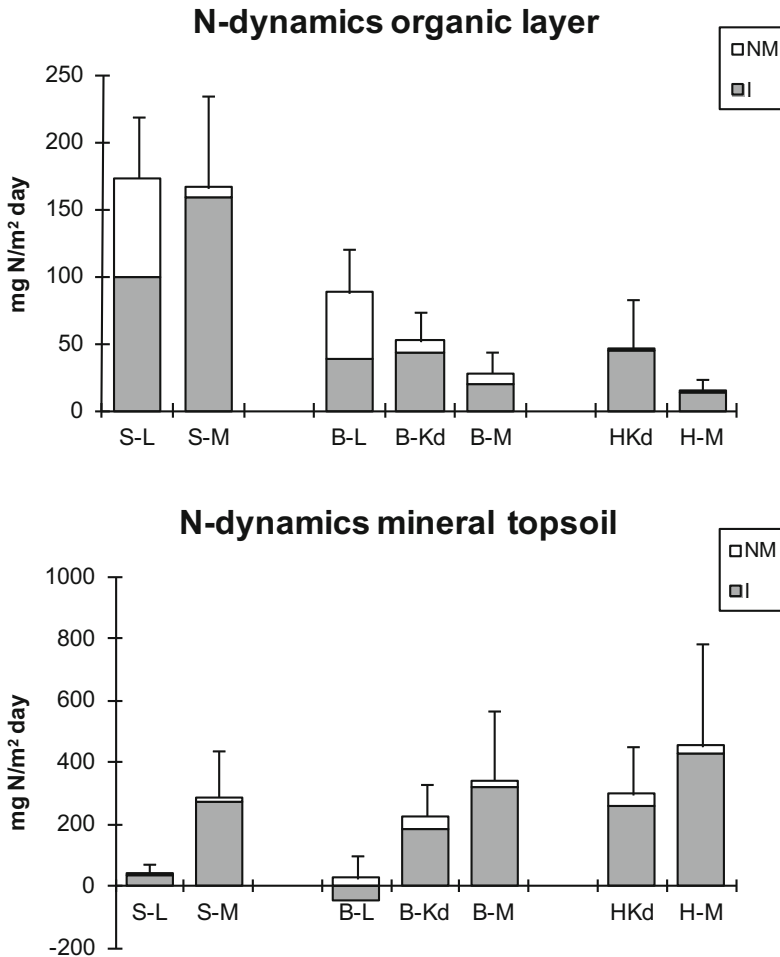


Fig. 7.4 N-dynamics in the organic layer and upper 5 cm of the mineral topsoil in Luxembourg spruce, beech and hornbeam stands on different parent materials. *S* spruce, *B* beech, *H* hornbeam; *L* Luxembourg sandstone, *Kd* decalcified Keuper dipslope, *M* Muschelkalk limestone. *NM* net N-mineralization and *I* immobilization; $NM + I$ = gross N-mineralization. Gross N-mineralization and immobilization are calculated with a theoretical model (Table 7.1), based on a.o. measured values of respiration and net N-mineralization in a one month laboratory incubation experiment, derived from Kooijman and Smit (2009). Standard deviations are those of (estimated) gross N-mineralization

7.3.4 Microbial Communities

In the experiment with four mono-specific beech stands, microbial N generally increased from acidic to calcareous soil (Fig. 7.5). Distribution of microbial N over different layers also changed. In acidic soil, 41–59% of total microbial N was present in the organic layer, but in calcareous soil, the mineral topsoil was much more important. Similar patterns were found in seven forests with beech and hornbeam (Kooijman and Martinez-Hernandez 2009). In this study,

microbial N increased from Pleistocene river terraces to Muschelkalk limestone, and the importance of the organic layer generally decreased. Also, microbial C:N ratio shifted from 9.6 in the mineral topsoil on Pleistocene river terrace to 3.8 on Muschelkalk parent materials. These values come close to literature C:N ratios of 10 for fungi and 4 for bacteria (Moore et al. 2005).

The thin sections of the four mono-specific beech stands showed that soil communities indeed change over the gradient from

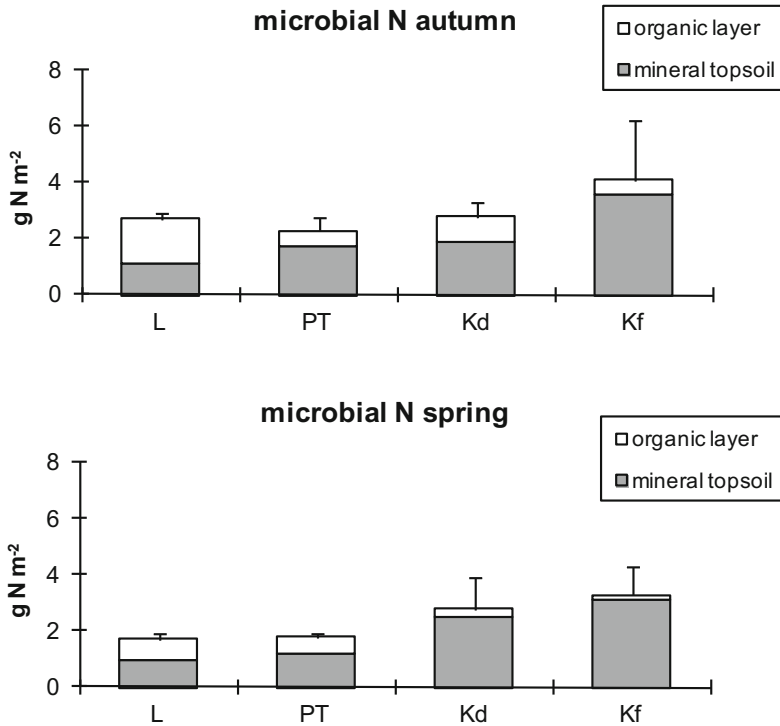


Fig. 7.5 Microbial *N* in the organic layer and upper 5 cm of the mineral topsoil in four Luxembourg beech forests on different parent materials, measured in a laboratory incubation experiment in autumn and spring. *L* Luxembourg sandstone, *PT* Pleistocene river terrace, *Kd* decalcified Keuper dipslope, *Kf* calcareous Keuper face slope. Mean values ($n = 4-5$) and standard variations are based on Kooijman et al. (2008)

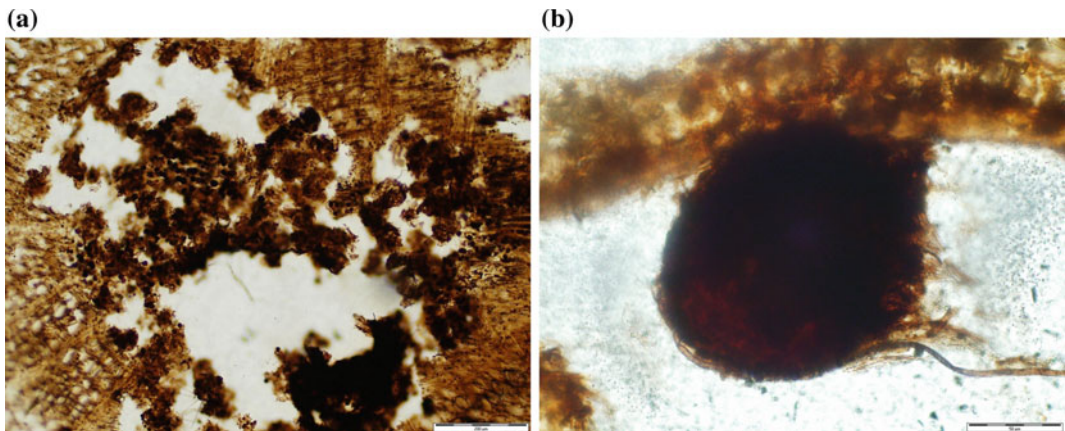


Fig. 7.6 Selection of micromorphological characteristics in thin sections. **a** Faecal pellets within a root structure, F-layer acid sandy site (scale bar indicates 500 μm).

b Secondary fungi attack on a faecal pellet, F-layer acid loamy site (scale bar indicates 50 μm)

Luxembourg sandstone to Muschelkalk. As expected, the soil microbial community was dominated by fungi in acidic soil (Fig. 7.6 and Table 7.4). Fungi play an important role in litter

decay, and attack numerous substrates by growing hyphae (Coleman and Crossley 1996). In calcareous soil, however, earthworms and bacteria prevailed. The latter generally consume

Table 7.4 Micromorphological analysis of four Luxembourg beech forests on different soil

	Luxembourg sandstone	Pleistocene terrace	Keuper dipslope	Keuper face slope
pH mineral topsoil	3.7 (0.1)	4.0 (0.3)	4.7 (0.4)	7.0 (0.5)
Earthworm channels	1	2	3	3
Earthworm chambers	0	2	0	3
Microarthropod activity in litter layer	1	1	3	3
Microarthropod activity in F-layer	3	3	2	2
Microarthropod activity in mineral topsoil	1	1	3	3
Bacteria	0	0	3	3
Primary fungi in litter layer	3	3	2	1
Primary fungi in F-layer	3	3	2	1
Secondary fungi in F-layer	3	3	1	0
Secondary fungi in mineral topsoil	3	3	1	0
Fungal hyphae in peds mineral topsoil	3	3	1	0
Mycorrhiza	1	1	1	1

Data are based on Kooijman et al. (2009)

easily degradable food, such as simple sugars and proteins, and can be found around roots, faecal pellets and mucus secretions in the burrows of earthworms. Microarthropods such as springtails and mites were found in all soil types, but in different layers. In acidic soil, microarthropod activity was relatively high in the F-layer, the more decomposed part of the organic layer, and in calcareous soil in the mineral topsoil.

Relationships between fungi, bacteria and N-cycling were further tested by microbial culture experiments with samples of the four beech stands (Fig. 7.7). The actual fungal contribution is probably underestimated by the colony growth method, but the results corroborate with the thin sections, which showed that fungi were prominent in acidic soils, and bacteria in more calcareous soils. Net N-mineralization per unit C respired, a proxy for the efficiency of the N-mineralization process and indicator of microbial immobilization, clearly decreased from low to high F:B ratio. When fungi were rare or absent, N-mineralization per unit C respired was very low, which points to high immobilization. When fungi were more common, however, N-mineralization per unit C respired became

much higher, and immobilization lower. This suggests that microbial N-demand can be rather high when bacteria predominate, but low when fungi become more important.

These findings are supported by selective inhibition of bacteria and fungi (Fig. 7.8). In both organic layer and mineral topsoil, net N-mineralization significantly increased with application of antibiotics, due to higher substrate availability, partly of dead microbes (Kooijman et al. 2016). However, with fungicide, when fungi were inhibited and bacteria stimulated, increase in net N-mineralization was associated with a significant increase of respiration in both organic layer and mineral topsoil. This suggests that dominance of bacteria indeed leads to high microbial activity. However, when bactericide was applied, bacteria were inhibited and fungi became the dominant microbes, respiration did not increase. In this case, net N-mineralization per unit C respired significantly increased, which point to lower microbial immobilization. These results suggest that bacteria are characterized by high activity, but also high N-demand, while fungi may show lower activity, but also lower microbial immobilization. This further supports that acidic, fungi-dominated soil can have high

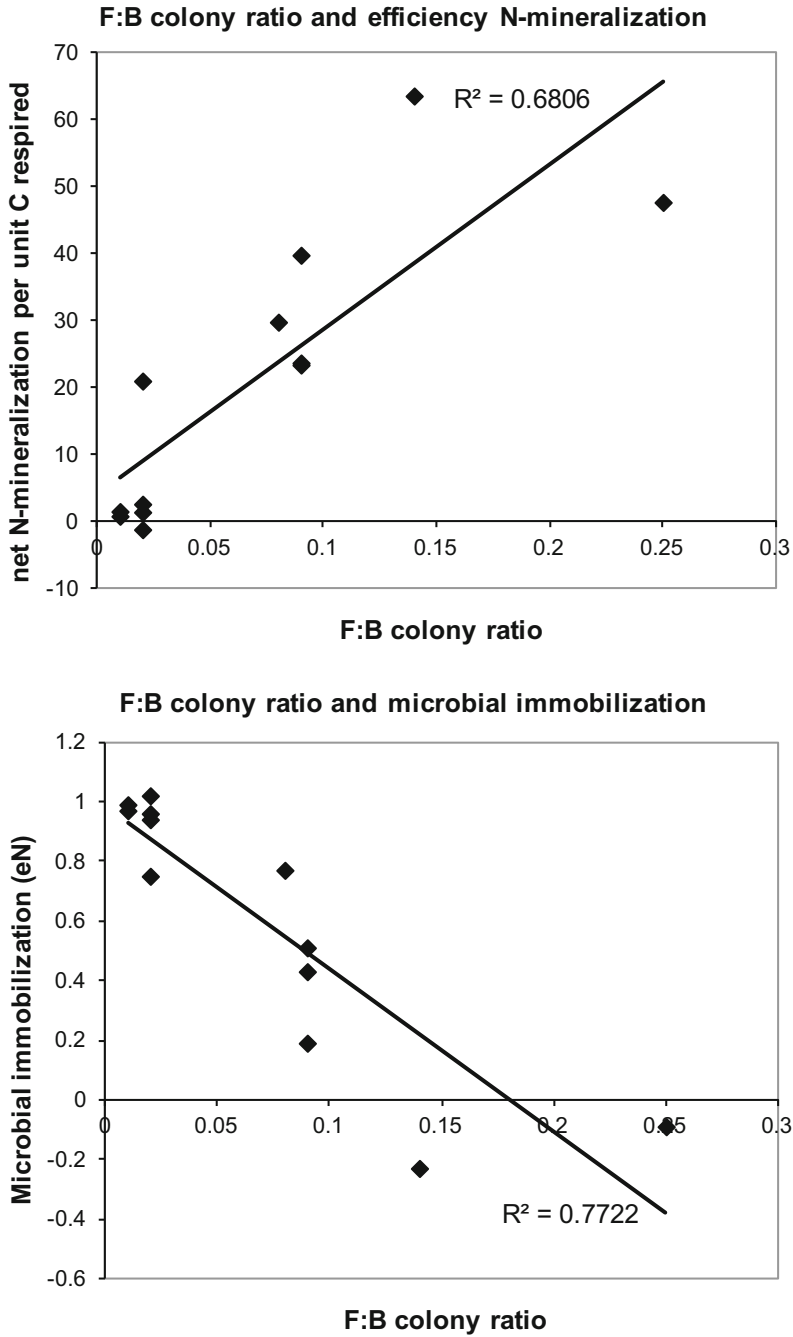


Fig. 7.7 Fungal/bacterial colony ratio in litter, organic layer and mineral topsoil of four Luxemburg beech forests with different parent materials, in relation to net N-mineralization per unit C respired (mg N per g C), and microbial immobilization efficiency in a four week laboratory incubation experiment. Since microbial behavior and amount of colonies were measured in different years, the correlation was based on mean values per site (Kooijman et al. 2008). Both correlations were significant ($p < 0.05$)

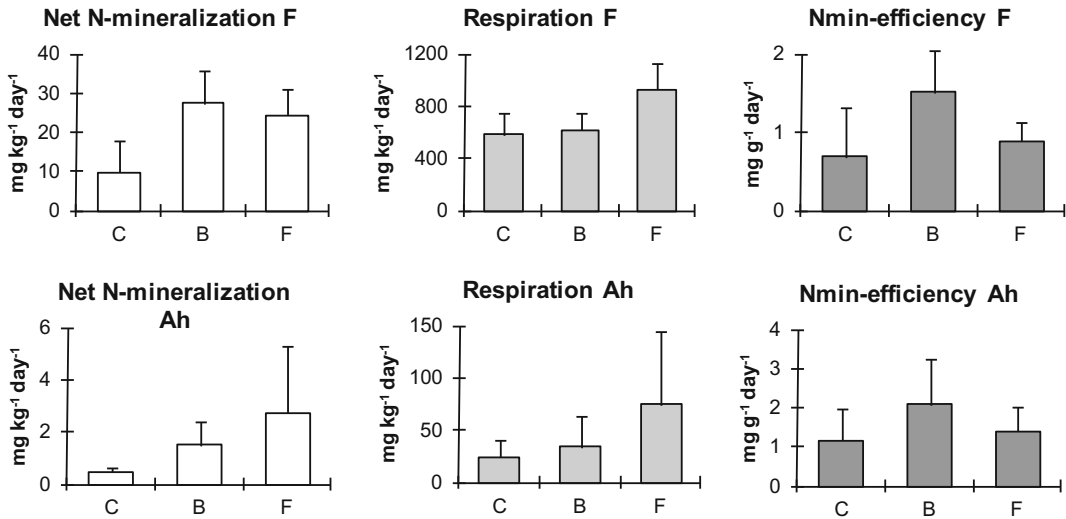


Fig. 7.8 Effect of selective inhibition of bacteria and fungi on net N-mineralization and respiration rates and efficiency of N-mineralization per unit C respired in a one month incubation experiment in **a** the organic layer and **b** the mineral topsoil (0–10 cm) of two Luxembourg beech forests. Because antibiotic treatment was more important than parent material, values of Luxembourg sandstone and Keuper face slope were combined. *C* control treatment; *B* bactericide treatment; *F* fungicide treatment. Mean values ($n = 10$) and standard deviations. Different letters indicate significant differences for a particular parameter between antibiotic treatments. Data are based on Kooijman et al. (2016)

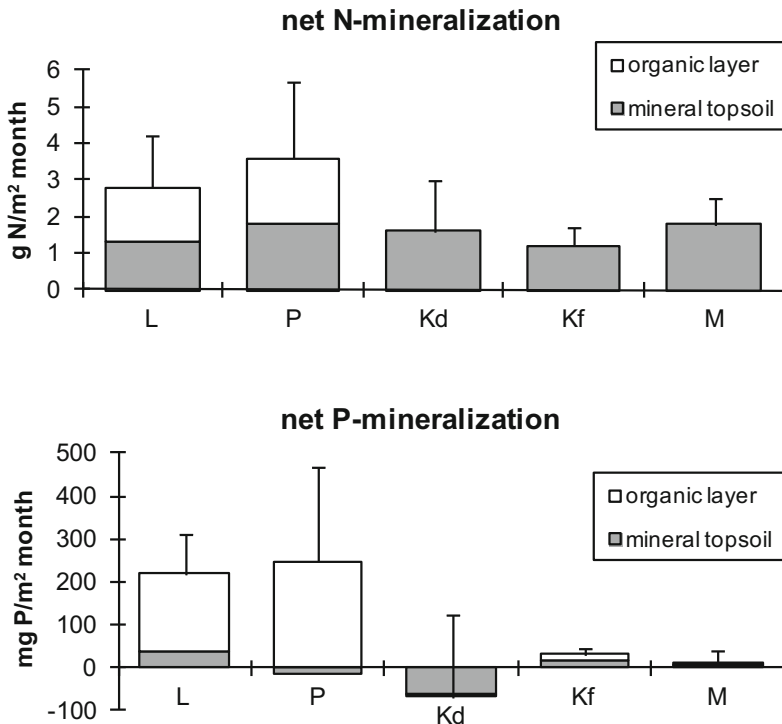


Fig. 7.9 Net N- and P-mineralization in the organic layer and upper 10 cm of the mineral topsoil in four Luxembourg beech forests on different parent materials, measured in 4–7 weeks laboratory incubation experiments. *L* Luxembourg sandstone, *P* Pleistocene deposits, *Kd* decalcified Keuper dipslope, *Kf* calcareous Keuper face slope, *M* Muschelkalk limestone. Mean values ($n = 4–6$) and standard variations are based on two separate experiments, with samples on *L* and *Kf* collected in October, and samples of *P*, *Kd* and *M* collected in March

net N-mineralization despite low gross N-release, due to low immobilization. In contrast, in calcareous, bacteria-dominated soil, net N-mineralization may be lower than expected, because biological activity is high, but microbial immobilization as well.

7.3.5 Net P-Mineralization

Apart from N, availability of P may also be an important ecosystem factor, and many beech forests may have low P-availability (Talkner et al. 2009; Jonard et al. 2014; Lang et al. 2016). Net P-mineralization was measured in beech forests on five different parent materials, but in two different periods and incubation experiments. The samples on Luxembourg sandstone and calcareous Keuper face slope were collected in October, and samples on Pleistocene deposits, decalcified Keuper dipslopes and Muschelkalk in March. Nevertheless, the incubation experiments showed similar response patterns along the geological gradients, and the results were combined in the same figure (Fig. 7.9).

Like in earlier experiments, net N-mineralization was significantly higher on acidic Luxembourg sandstone and Pleistocene deposits than on the more calcareous Keuper marls and Muschelkalk. Also, differences in total net N-mineralization were primarily due to the organic layer. Under laboratory conditions, the mineral topsoil

accounted for 1.2–1.8 g N m⁻² month⁻¹, more or less independent of parent material. In acidic soils, this amount was doubled by the contribution of the organic layer, but in calcareous soils, the organic layer was unimportant.

For net P-mineralization, the organic layer was even more important than for N, especially on the acidic Luxembourg sandstone and Pleistocene deposits. Almost all net release of P occurred in the organic layer. Also, in all organic layers, microbial N:P ratios ranged from 2.2 to 5.7, which is around the balance value of 3.1 (Cleveland and Liptzin 2007). In the mineral topsoil, however, net P-mineralization was very low, even though the total amount of P is probably much larger than in the organic layer (Talkner et al. 2009; Lang et al. 2016). This is due to high chemical sorption to Ca, Fe or Al (Lindsay and Moreno 1966; Shen et al. 2011; Lang et al. 2016). On Luxembourg sandstone, net P-mineralization was slightly positive, because P sorption to iron and aluminium oxides is probably relatively low, as most of the sand grains consist of quartz. On Pleistocene deposits and decalcified Keuper marl, however, net P-mineralization was strongly negative, probably due to sorption to clay particles and/or precipitation with Al and Fe at low pH (Shen et al. 2011). In the calcareous soils of Muschelkalk and the Keuper face slope, net P-mineralization was also low, possibly due to (re)precipitation of P in calcium diphosphates (Shen et al. 2011).

Table 7.5 Foliar N and P concentrations and N:P ratios of beech and hornbeam on Luxembourg sandstone, Keuper dipslope and Muschelkalk limestone

		Plant N (mg g ⁻¹)	Plant P (mg g ⁻¹)	N:P ratio (g g ⁻¹)
Beech	Luxembourg sandstone	25.3 (2.4) ^a	2.4 (0.3) ^b	10.5 (0.9) ^a
	Keuper dipslope	23.8 (1.7) ^a	1.4 (0.1) ^a	16.4 (0.3) ^c
	Muschelkalk	25.2 (1.5) ^a	2.1 (0.1) ^b	12.1 (1.2) ^b
Hornbeam	Keuper dipslope	25.4 (1.6) ^a	1.1 (0.2) ^a	18.0 (1.1) ^d
	Muschelkalk	23.3 (1.5) ^a	2.4 (0.1) ^b	9.7 (1.0) ^a

Mean values ($n = 4$) and standard deviations are given. Different letters indicate significant differences between mean values for a particular parameter ($p < 0.05$), values significantly increase from a to d

However, calcareous soils showed intermediate values for net P-mineralization compared to acidic sandy and acidic loamy soils. Net P-mineralization showed a significant negative correlation with microbial C:P and N:P ratios ($R = -0.57$ and -0.60 respectively). Microbial C:P ratios ranged from 2.1 in acidic sandy soil to 266 in acidic loamy soil, the latter indicating strong P-limitation (Cleveland and Liptzin 2007). Microbial C:P ratios ranged from 25 to 261, which also suggests a shift towards P-limited conditions.

Net mineralization of N and P in laboratory incubation experiments reflect only part of the ecosystem nutrition, as the role of e.g. earthworms, mycorrhiza and deep roots is disregarded. Nevertheless, the changes in net P-mineralization and microbial C:P and N:P ratios over the geosequence are to some extent reflected in the N:P ratios of beech and hornbeam leaves (Table 7.5). For plant leaves, N:P ratios below 14 usually indicate N-limitation, while values above 16 are characteristic for P-limitation (Koerselman and Meuleman 1996; Güsewell 2004). On Luxembourg sandstone, foliar N:P ratios were around 10, which suggest that P is not at all a limiting factor, due to the extensive organic layers and relatively low sorption compared to more clayey soils. Nitrogen seemed to be the main limiting nutrient, which is surprising, because net N-mineralization was also high on this parent material. Probably, low N:P ratios reflect high P-availability rather than real N-limitation. On decalcified Keuper marl, however, foliar N:P ratios were relatively high, with values above 16 for both beech and hornbeam. This corresponds with the negative net P-mineralization and high microbial C:P and N:P ratios, and suggests that P is indeed a limiting factor, due to lack of organic layers, and high P-sorption in the mineral soil. In contrast, on Muschelkalk, foliar N:P ratios were low again, with values of 10–12 for both beech and hornbeam. In calcareous soils, N may really be a limiting factor, because net P-mineralization was low as well, and microbes clearly P-limited. This is in accord with the low net N-mineralization in all four incubation experiments, and low N-content of fresh beech litter found in this study.

7.3.6 N and P Nutrition in Luxembourg Forests

Ecosystem nutrition is more than net mineralization of N and P, but this process forms an important source of nutrients in forest ecosystems, and its regulation by bacteria and fungi is highly relevant. In all four incubation experiments, with samples from 22 different forest stands, net N-mineralization was higher in acidic than in calcareous soil, in contrast to the common view. These differences between soil types were not affected by litter quality, which was also contrary to expectations.

Differences in net N-mineralization between acidic and calcareous soils could partly be explained by differences in microbial communities. Acidic soils were dominated by fungi, and calcareous soils by bacteria, in accord with other studies (Blagodatskaya and Anderson 1998; Bååth and Anderson 2003; Rousk et al. 2010). Fungi and bacteria differed in behaviour, with low respiration and N-immobilization for fungi and high values for bacteria. High immobilization by bacteria may be due to lower C:N ratios than for fungi (Hassink 1994; Moore et al. 2005), high rates of cell division, and use of amino acids for osmoregulation rather than carbohydrates (e.g. Measures 1975; Kuehn et al. 1998; Cleveland and Liptzin 2007).

Despite differences in microbial communities, in the mineral topsoil, net N-mineralization did not differ between acidic and calcareous soils. In acidic soil, low gross N-mineralization was compensated for by low immobilization, while high immobilization counteracted the effect of high gross N-mineralization in calcareous soil. In the field, net N-mineralization in calcareous soils may be higher than expected from the laboratory experiments, because earthworms were excluded. Earthworms clearly increase N-availability by bacterial grazing and excretion of N in urine, mucoproteins and dead tissue (e.g. Scheu 1997). Nevertheless, high bacterial immobilization should be taken into account, as it may counteract the positive effect of high biological activity.

While differences in the mineral topsoil were relatively low, acidic and calcareous soils highly

differed in the organic layer. In calcareous sites, the organic layer played no role in net N-mineralization, because it mainly consists of relatively fresh litter due to high earthworm activity. In acidic sites, however, net N-mineralization in the organic layer was at least as high as in the mineral topsoil, due to its higher mass, more advanced stage of decomposition and dominance by fungi. For P-nutrition, the organic layer is even more important, as most net P-mineralization takes place here, and even microbes showed high P-stress in the mineral soil, especially in loamy soils with high P-sorption.

7.4 Concluding Remarks

The geological gradient in the Luxembourg cuesta landscape is one of the most important factors in ecosystem nutrition, which affects soil communities, decomposition of organic matter and cycling of nutrients. On acidic parent materials, low earthworm activity leads to accumulation of litter, which is slowly but gradually decomposed by fungi. Microbial immobilization is low, and decomposition of organic matter may be C-limited, which leads to relatively large net release of N and P. On calcareous parent materials, however, high earthworm activity prevents development of a substantial organic layer, and nutrient availability is mainly regulated by the mineral soil. High biological activity leads to high gross N-mineralization, but as bacterial N-demand is also high, net N-mineralization may be lower than expected. As net P-mineralization is reduced as well, calcareous soils may have low availability of both N and P. This may restrict growth of trees, but favour undergrowth diversity.

Acknowledgements The authors would like to thank Bas van Dalen, Greet Kooijman-Schouten, Benito Martinez-Hernandez, Jan van Mourik and Madeleine Schilder for their contribution to fieldwork and data collection, and Leo Hoitinga, Leen de Lange, Piet Wartenbergh and Joke Westerveld for their support in the laboratory.

References

- Aerts MAPA, Chapin FS (2000) The mineral nutrition of wild plants revisited: a re-evaluation of process and patterns. *Adv Ecol Res* 30:1–67
- Aubert M, Hedde M, Decaens T, Bureau F, Margerie P, Alard D (2003) Effects of tree canopy composition on earthworms and other macro-invertebrates in beech forests of Upper Normandy (France). *Pedobiologia* 47:904–912
- Bååth E, Anderson TH (2003) Comparison of soil fungal/bacterial ratios in a pH gradient using physiological and PLFA-based techniques. *Soil Biol Biochem* 35:955–963
- Bayley SE, Thormann MN, Szumigalski AR (2005) Nitrogen mineralization and decomposition in western boreal bog and fen peat. *Ecoscience* 12:455–465
- Berendse F, Bobbink R, Rouwenhorst G (1989) A comparative study on nutrient cycling in wet heathland ecosystems. II. Litter decomposition and nutrient mineralization. *Oecologia* 78:338–348
- Berg B (2000) Litter decomposition and organic matter turnover in northern forest soils. *For Ecol Manage* 133:13–22
- Berg B, Ekbohm G (1983) Nitrogen immobilisation in decomposing needle litter at variable carbon:nitrogen ratios. *Ecology* 64:63–67
- Blagodatskaya EV, Anderson TH (1998) Interactive effects of pH and substrate quality on the fungal-to-bacterial ratio and qCO₂ of microbial communities in forest soils. *Soil Biol Biochem* 30:1269–1274
- Booth MS, Stark JM, Rastetter E (2005) Controls of nitrogen cycling in terrestrial ecosystems: a synthetic analysis of literature data. *Ecol Monogr* 75:139–157
- Brooks PC, Landman A, Pruden G, Jenkinson DS (1985) Chloroform fumigation and the release of soil nitrogen: a rapid direct extraction method to measure microbial biomass nitrogen in soil. *Soil Biol Biochem* 17:837–842
- Campbell JL, Gower ST (2000) Detritus production and soil N transformations in old-growth eastern hemlock and sugar maple stands. *Ecosystems* 3:185–192
- Cleveland CC, Liptzin D (2007) C:N:P stoichiometry in soil: is there a “Redfield ratio” for the microbial biomass? *Biogeochemistry* 85:235–252
- Cody RP, Smith JK (1987) Applied statistics and the SAS programming language. Elsevier Science Publishers Co. Int., Amsterdam, p 280
- Coleman DC, Crossley DA jr (1996) Fundamentals of soil ecology. Academic Press Inc, San Diego
- Davy AJ, Taylor K (1974) Seasonal patterns of nitrogen availability in contrasting soils in the chiltern hills. *J Ecol* 62:793–807
- de Vries FT, van Groenigen JW, Hoffland E, Bloem J (2011) Nitrogen losses from two grassland soils with

- different fungal biomass. *Soil Biol Biochem* 43:997–1005
- Ellenberg H (1977) Stickstoff als Standortfaktor, insbesondere für mitteleuropäische Pflanzengesellschaften. *Oecologia Plant.* 12:1–22
- Ferraris le Comte de (1777) Reissued in 1965–1970. *Carte de Cabinet des Pays-Bas Autrichiens*. Bibliothèque Royale de Belgique, Bruxelles
- Fisk MC, Fahey TJ (2001) Microbial biomass and nitrogen cycling responses to fertilization and litter removal in young northern hardwood forests. *Biogeochemistry* 53:201–223
- Green RN, Trowbridge RL, Klinka K (1993) Towards a taxonomic classification of humus forms. Supplement to *Forest Science*, vol 39
- Güsewell S (2004) N: P ratios in terrestrial plants: variation and functional significance. *New Phytol* 164:243–266
- Hart SC, Nason GE, Myrold DD, Perry DA (1994) Dynamics of gross nitrogen transformations in an old-growth forest: the carbon connection. *Ecology* 75:880–891
- Hassink J (1994) Effects of soil texture and grassland management on soil organic C and N and rates of C and N mineralization. *Soil Biol Biochem* 26:1221–1231
- Henderson-Sellers B, Henderson-Sellers A (1993) Factorial techniques for testing environmental model sensitivity. In: Beck MB, McAleer MJ, Jakeman AJ (eds) *Modelling change in environmental systems*. Wiley, Chichester, England
- Högberg MN, Myrold DD, Giesler R, Högberg P (2006) Contrasting patterns of soil N-cycling in model ecosystems of Fennoscandian boreal forests. *Oecologia* 147:96–107
- Högberg MN, Högberg P, Myrold DD (2007) Is microbial community composition in boreal forest soils determined by pH, C-to-N ratio, the three, or all three? *Oecologia* 150:590–601
- ICMSF (2000) *Microorganisms in Foods I, their significance and methods of enumeration*, 2nd edn. University of Toronto Press, Toronto
- IUSS (2015) *World Reference Base for Soil Resources 2014, update 2015*. International soil classification system for naming soils and creating legends for soil maps. *World Soil Resources Reports No. 106*. FAO, Rome
- Jonard M, Fuerst A, Verstraeten A, Thimonier A, Timmermann V, Potocic N, Waldner P, Benham S, Hansen K, Merila P, Ponette Q, de la Cruz AC, Roskams P, Nicolas M, Croise L, Ingerslev M, Matteucci G, Decinti B, Bascietto M, Rautio P (2014) Tree mineral nutrition is deteriorating in Europe. *Glob Change Biol* 21:418–430
- Koerselman W, Meuleman AFM (1996) The vegetation N:P ratio: a new tool to detect the nature of nutrient limitation. *J Appl Ecol* 33:1441–1450
- Kooijman AM, Besse M (2002) On the higher availability of N and P in lime-poor than in lime-rich coastal dunes in the Netherlands. *J Ecol* 90:94–403
- Kooijman AM, Hedenäs L (2009) Changes in nutrient availability from calcareous to acid wetland habitats with closely related brown moss species: increase instead of decrease in N and P. *Plant Soil* 324:267–278
- Kooijman AM, Martinez-Hernandez GB (2009) Effects of litter quality and parent material on organic matter characteristics and N-dynamics in Luxembourg beech and hornbeam forests. *For Ecol Manag* 257:1732–1739
- Kooijman AM, Smit A (2009) Paradoxical differences in N-dynamics between Luxembourg soils: litter quality or parent material? *Eur J Forest Res* 128:555–565
- Kooijman AM, Kooijman-Schouten MM, Martinez-Hernandez GB (2008) Alternative strategies to sustain N-fertility in acid and calcareous beech forests: low microbial N-demand versus high biological activity. *Basic Appl Ecol* 9:410–421
- Kooijman AM, van Mourik J, Schilder MLM (2009) The relationship between N mineralization or microbial biomass N with micromorphological properties in beech forest soils with different texture and pH. *Biol Fertil Soils* 45:449–459
- Kooijman AM, Cammeraat E (2010) Biological control of beech and hornbeam affects species richness via changes in the organic layer, pH and soil moisture characteristics. *Funct Ecol* 24:469–477
- Kooijman AM, Bloem J, van Dalen BR, Kalbitz K (2016) Differences in activity and N demand between bacteria and fungi in a longer-term incubation experiment with selective inhibition. *Appl Soil Ecol* 99:26–39
- Kuehn KA, Churchill PF, Suberkropp K (1998) Osmoregulatory responses of fungi inhabiting standing litter of the freshwater emergent macrophyte *Juncus effusus*. *Appl Environ Microbiol* 64:607–612
- Lang F, Bauhus J, Frossard E, George E, Kaiser K, Kaupenjohann M, Krueger J, Matzner E, Polle A, Prietzel J, Rennenberg H, Wellbrock N (2016) Phosphorus in forest ecosystems: new insights from an ecosystem nutrition perspective. *J Plant Nutr Soil Sci* 179:129–135
- Laskowski R, Niklinska M, Maryanski M (1995) The dynamics of chemical elements in forest litter. *Ecology* 76:1393–1406
- Lindsay WL, Moreno EC (1966) Phosphate phase equilibria in soils. *Proceedings of the SSSA* 24:177–182
- Marhan S, Scheu S (2005) Effects of sand and litter availability on organic matter decomposition in soil and in casts of *Lumbricus terrestris* L. *Geoderma* 128:155–166
- Measures JC (1975) Role of amino acids in osmoregulation of non-halophilic bacteria. *Nature* 257:398–400
- Mettrop IS, Cusell C, Kooijman AM, Lamers LPM (2014) Nutrient and carbon dynamics in peat from rich fens and Sphagnum-fens during different gradations of drought. *Soil Biol Biochem* 68:317–328
- Moore JC, McCann K, de Ruiter PC (2005) Modelling trophic pathways, nutrient cycling, and dynamic stability in soils. *Pedobiologia* 49:499–510

- Niemeyer T, Ries C, Härdtle W (2010) Die Waldgesellschaften Luxemburgs. Vegetation, Standort, Vorkommen und Gefährdung. Ferrantia 57, Musée national d'histoire naturelle, Luxembourg, 122 pp
- Parton WP, Silver WL, Burke IC, Grassens L, Harmon ME, Currie WS, King JY, Adair EC, Brandt LA, Hart SC, Fath B (2007) Global-scale similarities in nitrogen release patterns during long-term decomposition. *Science* 315:361–364
- Phoenix GK, Booth RE, Leake JR, Read DJ, Grime JP, Lee JA (2003) Effects of enhanced nitrogen deposition and phosphorus limitation on nitrogen budgets of semi-natural grasslands. *Glob Change Biol* 9:1309–1321
- Ponge JF (2003) Humus forms in terrestrial ecosystems: a framework to biodiversity. *Soil Biol Biochem* 35:935–945
- Pop V (1997) Earthworm-vegetation-soil relationships in the Romanian Carpathians. *Soil Biol Biochem* 29:223–229
- Pulleman MM, Six J, van Breemen N, Jongmans AG (2005) Soil organic matter distribution and microaggregate characteristics as affected by agricultural management and earthworm activity. *Eur J Soil Sci* 56:453–467
- Reich PB, Grigal DF, Aber JD, Gower ST (1997) Nitrogen mineralization and productivity in 50 hardwood and conifer stands on diverse soils. *Ecology* 78:335–347
- Rousk J, Bååth E, Brookes PC, Lauber CL, Lozupone C, Caporaso JG, Knight R, Fierer N (2010) Soil bacterial and fungal communities across a pH gradient in an arable soil. *Int Soc Microb Ecol J* 4:1340–1351
- Ruess RW, Seagle SW (1994) Landscape patterns in soil microbial processes in the Serengeti National Park, Tanzania. *Ecology* 75:892–904
- Scheu S (1997) Effects of litter (beechness and stinging nettle) and earthworms (*Octolasion lacteum*) on carbon and nutrient cycling in beech forests on a basalt-limestone gradient: a laboratory experiment. *Biol Fertil Soils* 24:384–393
- Schimel DS (1988) Calculation of microbial growth efficiency from ^{15}N immobilization. *Biogeochemistry* 6:239–243
- Schimel JP, Bennett J (2004) Nitrogen mineralization: challenges of a changing paradigm. *Ecology* 85:591–602
- Shen J, Yuan L, Zhang J, Li H, Bai Z, Chen X, Zhang W, Zhang Z (2011) Phosphorus dynamics: from soil to plant. *Plant Physiol* 156:997–1005
- Swift MJ, Heal OW, Anderson JM (1979) Decomposition in terrestrial ecosystems. University of California Press, Berkeley
- Talkner J, Jansen M, Beese FO (2009) Soil phosphorus status and turnover in central-European beech forest ecosystems with differing tree species diversity. *Eur J Soil Sci* 60:338–346
- Tietema A (1992) Abiotic factors regulating nitrogen transformations in the organic layer of acid forest soils: moisture and pH. *Plant Soil* 147:69–78
- Tietema A, Wessel WW (1992) Gross nitrogen transformations in the organic layer of acid forest ecosystems subjected to increased atmospheric nitrogen input. *Soil Biol Biochem* 24:943–950
- Turner BL, Condon LM (2013) Pedogenesis, nutrient dynamics, and ecosystem development: the legacy of T.W. Walker and J.K. Syers. *Plant Soil* 367:1–10
- Veer MAC (1997) Nitrogen availability in relation to vegetation changes resulting from grass-encroachment in Dutch dry dunes. *J Coast Conserv* 3:41–48
- Verhoeven JTA, Kooijman AM, van Wirdum G (1988) Mineralization of N and P along a trophic gradient in a freshwater mire. *Biogeochemistry* 6:31–43
- Verhoeven JTA, Maltby E, Schmitz MB (1990) Nitrogen and phosphorus mineralization in fens and bogs. *J Ecol* 78:713–726
- Walker TW, Syers JK (1976) The fate of phosphorus during pedogenesis. *Geoderma* 15:1–19
- Westerman RL (1990) Soil testing and plant analysis, 3rd edn. Soil Science Society America, Madison, Wisconsin
- Zöttle H (1960) Dynamik der Stickstoffmineralisation im Waldbodenmaterial III. pH-wert und Mineralstickstoff-Nachlieferung. *Plant Soil* 13:207–223

Relationships Between Forest Vegetation, Parent Material and Soil Development in the Luxembourg Cuesta Landscape

8

A.M. Kooijman and A. Smit

Abstract

In the cuesta landscape, the natural forest vegetation is affected by the clear gradients in parent material. Most forests belong to the alliances *Fagion sylvaticae*, *Luzulo-Fagion* and *Carpinion betuli*. Forest associations show a clear shift in species composition from calcareous to acidic soils. The species-rich *Carici-Fagetum* and *Hordelymo-Fagetum* occur on steep slopes on Muschelkalk, with shallow Leptosols and Leptic Regosols, and pH values around 7. *Galio-Carpinetum*, with many wet-tolerant species, occurs on gentle slopes in Keuper marl, with Luvic Stagnosols and Planosols, pH around 5–6, and perched water tables during part of the year. The relatively species-poor *Galio odorati-Fagetum* is found on acidic loamy soils, such as the marls of the upper cuesta, Pleistocene river terraces and Loess deposits. Soil types range from Colluvic Regosols to Luvic Stagnosols, with pH values around 4. The species-poor *Luzulo-Fagetum* is found on plateau and upper cuesta of the Luxembourg sandstone, but also on the oldest river terraces. Soil types range from (Leptic) Arenosols and Podzols to Alic Stagnosols, and pH values are around or below 4. In forests plots on Keuper and Muschelkalk with base-rich, loamy topsoils, parent material was more important to species composition than litter quality. Calcicole species predominated on Muschelkalk, and wet-tolerant species on Keuper, although diversity was lower under beech than under hornbeam. The clear decrease in plant species richness from calcareous to acidic soil is discussed in terms of toxicity, nutrient availability and tolerance to wet conditions, but also in relation to landscape history and regional species pool.

A.M. Kooijman (✉) · A. Smit
Institute for Biodiversity and Ecosystem Dynamics,
University of Amsterdam, Science Park, 94248,
1090 GE Amsterdam, The Netherlands
e-mail: a.m.kooijman@uva.nl

A. Smit
e-mail: annemieke.smit@wur.nl

A. Smit
Alterra, 6700 AA Wageningen, 47, Wageningen,
The Netherlands

8.1 Introduction

The landscape of the Luxembourg Lias cuesta is clearly reflected in landforms, hydrology and soil development (see also Chaps. 1, 4, 5 and 6). The cuesta landscape also forms an outstanding area to study the semi-natural forest vegetation. In the agricultural landscape, natural relationships between parent material, soil and plant species composition have largely disappeared, due to the conversion of forest to arable land and increased fertilization. However, in the area between Diekirch, Beaufort and Medernach, many forests still exist, such as on the steep slopes of the Muschelkalk and the Luxembourg sandstone cuesta, and the vast forest on the Keuper dipslopes between Sure and Ernzt Blanche. Fragmentation may have reduced dispersal of particular diaspores (e.g., Bossuyt et al. 1999; Graae et al. 2003), especially in isolated patches. However, many Luxembourg forests still consist of more or less natural plant communities, which clearly differ in species composition along gradients in parent material and pH (e.g., Ellenberg 1988; van der Werf 1991; Niemeyer et al. 2010). In some places, old-growth forest has remained (Ferraris le Comte de 1777; Cammeraat 2002), with human impact restricted to small scale cutting. Apart from parent material, undergrowth species composition may also be affected by litter quality (van Oijen et al. 2005; van Calster et al. 2008; Kooijman and Cammeraat 2010). In the natural forests of the Luxembourg Gutland, beech (*Fagus sylvatica* L.) and hornbeam (*Carpinus betulus* L.) are both common and often intermixed species, which clearly differ in litter quality (e.g., Swift et al. 1979; Laskowski et al. 1995; Aubert et al. 2003). Hornbeam has leaf litter with a higher initial N-content than that of beech, and often disappears in a few months, whereas beech litter remains on the forest floor all year long (see also Chap. 10). Within a particular type of parent material, such as Keuper marls, biodiversity of the undergrowth is clearly affected by dominance of beech or hornbeam (Kooijman and Cammeraat 2010). It is however not clear whether such litter quality effects also

emerge when other parent materials are considered.

The aim of this study was to investigate relationships between forest vegetation, parent material and soil characteristics in the area between Diekirch, Beaufort and Medernach, which was also one of the aims of the student fieldwork in the past decades. In this part of the cuesta landscape, the geological gradient is very clear, and many different parent materials and soil types are well-represented. The first research question was whether forest communities were in accord with Niemeyer et al. (2010), and indeed changed with parent material. This was tested with a dataset of 68 relevés on Luxembourg sandstone, Keuper marl, Muschelkalk, Pleistocene fluvial terraces and Loess deposits. The second question was whether soil characteristics and development indeed differed between forest communities. This was tested with a dataset of 200 descriptions of vegetation and soil, based on student surveys. The third question was whether abiotic control of plant diversity would be more important than biotic factors such as differences in litter quality. This was tested with a dataset of 60 relevés on Keuper marl and Muschelkalk, based on Kooijman (2010), in plots dominated by beech and hornbeam.

8.2 Methods

8.2.1 Study Area

The study area is located in the Luxembourg Gutland, roughly between Diekirch, Beaufort and Medernach, along the rivers Sure and Ernzt Blanche. The climate is mesic, with mean temperatures of 0.8 °C in January and 17.2 °C in July and annual rain fall of 788 mm with precipitation in all months, and the growing season is approximately 180 days.

The cuesta landscape basically consist of the geological formations Muschelkalk (ku, mm and mo), Keuper (km) and Lias (Luxembourg) sandstone (li2), deposited on top of each other and slightly tilted (see also Chaps. 1 and 5). The

upper part of the landscape consists of the Luxembourg sandstone plateau, cut at the edge to form the steep upper cuesta slopes. The middle part of the landscape consists of Keuper marls, which form part of the middle cuesta slope south of the major rivers, at the face slope of the tilted formations. However, between Sure and Ernzy Blanche, large undulating Keuper plateaus have developed on the gentle dip slope. The lower part of the landscape generally consists of Muschelkalk, with steep slopes of dolomitic limestone. Across the main geological gradient, Pliocene, but mostly Pleistocene parent materials occur in the form of river terraces (Verhoef 1966). These fluvial terraces generally consist of poorly sorted sediments from clay to gravel, and have known long periods of soil formation, due to their relatively stable position in the landscape. Also, loess deposits from the last glacial period may occur.

8.2.2 Forest Communities Distinguished by Niemeyer, Ries and Härdtle (2010)

Niemeyer et al. (2010) gave an overview of natural and semi-natural forest associations in Luxembourg, with their characteristic plant species and associated habitat conditions related to climate and soil. Nomenclature of plant species and communities is according to this publication. Most deciduous forests are dominated by beech (*F. sylvatica*), which has a wide habitat amplitude, and may occur under various soil conditions from lime-rich to lime-poor (Ellenberg et al. 1974; Kooijman and Martinez-Hernandez 2009). Forests dominated by hornbeam (*C. betulus*) also occur, in places which are too wet or dry for beech (Bolte et al. 2007), but on calcareous soil they may also develop from logging and over-exploitation of beech forests. In the area, five forest associations seem to be most prominent in the forests with a deep permanent groundwater table, ranging from calcareous to acidic habitats: Carici-Fagetum, Hordelymo-Fagetum, Galio-

Carpinetum, Galio odorati-Fagetum and Luzulo-Fagetum (Fig. 8.1).

The Carici-Fagetum belongs to the alliance *F. sylvaticae*, with *F. sylvatica* as dominant tree species. In the shrub layer, character species are *Lonicera xylosteum*, *Viburnum lantana*, *Daphne mezereum* and *Ligustrum vulgare*. In the herb layer, character species are *Bromus ramosus* agg., *Neottia nidus-avis*, *Carex montana*, *Carex digitata*, *Platanthera bifolia*, *Cephalanthera damasonium*, *C. rubra* and *C. longifolia*. This forest community is mainly found on calcareous and relatively exposed and sunny habitats. Organic layers mainly consist of fresh litter, due to high biological activity and decomposition.

The Hordelymo-Fagetum is closely related to the former association, and also belongs to the alliance *F. sylvaticae*, with *F. sylvatica* as the dominant tree species. In the herb layer, character species are *Arum maculatum*, *Vicia sepium*, *Primula elatior*, *Geum urbanum*, *Stachys sylvatica*, *Brachypodium sylvaticum*, *Mercurialis perennis*, *Sanicula europaea*, *Adoxa moschatellina* and *Hordelymus europaeus*. This association is also mainly found on calcareous soil, but in general, soils are deeper and moisture content is higher than in the *Carici-Fagetum*. Organic layers are also not extensive, due to high biological activity and decomposition.

In contrast to the first two associations, the Galio-Carpinetum belongs to the alliance Carpinion betuli, with *C. betulus* as major tree species. Other characteristic trees are *Quercus petraea* and *Q. robur*. *F. sylvatica* may also occur. In the shrub and herb layer, character species are *Prunus avium*, *Rosa arvensis*, *Stellaria holostea*, *Potentilla sterilis*, and *Galium sylvaticum*. This association is mainly found on base-rich, clayey soil, with water stagnation in winter and relatively dry conditions in summer. In natural stands, dominance of beech is restricted by the clay-rich soil and seasonal variation in soil moisture availability. The Galio-Carpinetum may however also develop on limestone slopes, due to logging and overexploitation of calcareous beech forests such as Carici-Fagetum and Hordelymo-Fagetum.



Fig. 8.1 Different forest communities of the Luxembourg cuesta landscape. *Top*: Luzulo-Fagetum on the *upper part* of the Lias sandstone cuesta near Eppeldorf. *Bottom*: Galio odorati-Fagetum on Pleistocene river terrace near Reisdorf. Photographs are made by Jan van Arkel

Fig. 8.1 (continued)

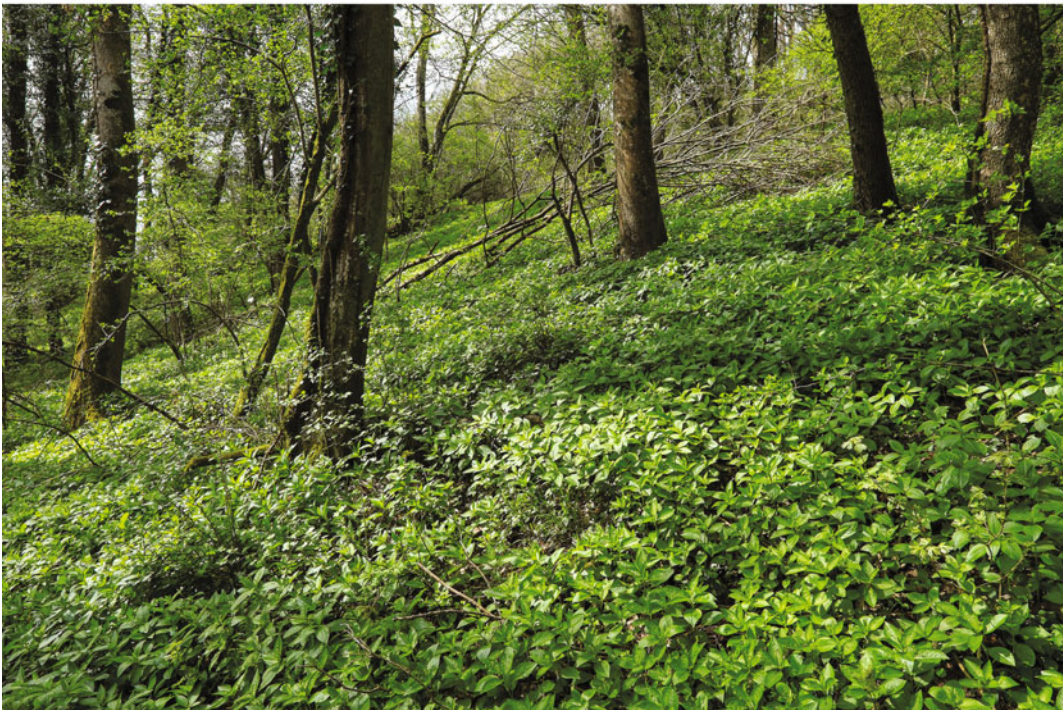


Fig. 8.1 (continued) *Top*: Galio-Carpinetum with transition to Galio odorati-Fagetum on Keuper marl near Schrondweiler. *Bottom*: Hordelymo-Fagetum on Muschelkalk limestone near Reisdorf



Fig. 8.1 (continued) *Top*: Carici-Fagetum on Muschelkalk limestone near Wallendorf. *Bottom*: selection of spring flowers in deciduous forests of the Luxembourg cuesta landscape: *left*, from top to bottom: *Oxalis acetosella*, *Cardamine pratense* and *Arum maculatum*. *Middle*, from top to bottom: *Anemone nemorosa*, *Viola riviniana* and *Primula veris*. *Right*, from top to bottom: *Primula elatior*, *Mercurialis perennis* and *Euphorbia amygdaloides*

The Galio odorati-Fagetum belongs again to the alliance *F. sylvaticae*, with *F. sylvatica* as the dominant tree species. This association is relatively species-poor and has no real character species, although character species of the alliance may occur, such as *Galium odoratum*, *Festuca altissima* and *Melica uniflora*. This association can be found on base-rich to base-poor loamy soil, and in its optimal phase typically looks like a ‘Hallenwald’, an open forest of tall trees without shrub layer.

The Luzulo-Fagetum belongs to the alliance Luzulo-Fagion, with *F. sylvatica* as the dominant tree species. Character species in the herb layer, which is usually species-poor, are *Luzula luzuloides*, *Oxalis acetosella*, *F. altissima* and *Luzula sylvatica*. The association is one of the most base-poor beech forests, and mainly found in acid loamy-sandy habitats, often with podzolic soils. Organic layers become more extensive, due to decrease in biological activity, and contain most of the fine roots.

8.2.3 Methods

To answer the first question about the relationship between parent material and forest communities, 68 vegetation relevés of 10×10 m were made by the first author in May. Plots were randomly selected in deciduous forests throughout the area, on parent materials such as Luxembourg sandstone, Keuper marls, Muschelkalk dolomitic limestone, and Pleistocene sediments such as river deposits and loess. Holocene alluvial areas were excluded from this study, because they only form narrow strips along rivers and brooks, and are generally highly disturbed. In each plot, all plant species including mosses were recorded, and cover values were estimated as percentage. Nomenclature is according to van der Meijden (2005) and van Tooren and Sparrius (2007). The relevés were analyzed with Twinspan (Hill 1979). The distribution of particular vegetation types over the various parent materials was tested with Chi-Square tests, with $p < 0.05$, and expected frequency based on the number of relevés on a particular parent material.

To answer the second question about forest communities and soil development, 200 descriptions of vegetation and soil in forest plots were produced by five groups of students, in areas of approximately five km² adjacent to each other. Vegetation relevés and soil descriptions were made in May. In this part of the study, apart from deciduous forests, coniferous stands with spruce (*Picea abies*) and Scots pine (*Pinus sylvestris*) were also included. The plots consisted of 10×10 m², and were randomly selected on Luxembourg sandstone, Keuper marl, Muschelkalk, Pleistocene river terraces and Loess deposits. In each plot, all phanerogam species were recorded, and their cover estimated as percentage. In each plot, the humus profile was described according to Green et al. (1993). Soil profiles were cored to 120 cm depth (if possible), described and classified according to IUSS (2015). All species lists, identifications and soil descriptions were regularly checked, and students sent back to the field if necessary. Vegetation relevés were analyzed with Twinspan (Hill 1979). For the purpose of this study, a number of soil parameters was selected. Thickness of L, F, H and Ah horizons were used as proxy for litter decomposition and development of the organic profile, and humus forms were characterized as Mull or Mormoder. Slopes were characterized as steep ($>6^\circ$) or gentle ($<6^\circ$). Soils were further characterized according to the presence or absence of hardrock and/or lime within 120 cm depth, the latter determined with 2 M HCL-solution. Also, clear signs of pseudogley mottles, clay eluviation or podzolization were used to distinguish soil groups. The distribution of vegetation types over particular parent materials and soil groups was tested with Chi-Square tests, with $p < 0.05$, and expected frequency based on the number of relevés on a particular parent material or soil type.

To answer the third question about parent material versus litter quality, 60 vegetation relevés on Keuper marl and Muschelkalk limestone were used, based on Kooijman (2010). On each parent material, five mixed forests with beech and hornbeam were selected. In each forest, six 7×7 m plots were selected according to

stratified random sampling procedures, with three plots dominated by beech, and three dominated by hornbeam. In each plot, all plant species were recorded, and cover values estimated as percentages. In each plot, mass of the organic layer was determined in $25 \times 25 \text{ cm}^2$, and soil characteristics such as pH and soil moisture content in samples of the mineral topsoil (0–5 cm), collected with metal rings. Vegetation relevés were analyzed with Twinspan (Hill 1979) and Correspondence Analysis, as implemented in the program Canoco (CJF ter Braak 1988). Differences in organic layer and mineral topsoil were tested with two-way Anova, with tree species and parent material as independent factors (Cody and Smith 1987).

8.3 Results and Discussion

8.3.1 Species Composition, Forest Communities and Parent Material

Forest communities and species composition

The 68 forest relevés in the study area were clustered in five plant communities, which largely coincide with the associations described by Niemeyer et al. (2010). The relevés were first separated in a species-rich group with many calcicole species characteristic of calcareous habitats, and a species-poor group with species of more acidic habitat conditions (Fig. 8.2). The species-poor group showed many characteristics of the forest association Luzulo-Fagetum and was not further separated (Table 8.1). The undergrowth contained character species of the association such as *L. luzuloides* and *Oxalis acetosella*, but also species of more acidic soils such as *Deschampsia flexuosa* and *Vaccinium myrtillus*.

The species-rich group with many calcicole species contained four subgroups. The first division was between a group with calcicole species, such as *Ribes alpinum* and *Corylus avellana*, and one without them. The group with calcicole species was further separated into two groups, resembling the forest associations Carici-Fagetum and Hordelymo-Fagetum. The Carici-Fagetum group

contained character species of the association such as *Viburnum lantana*, *D. mezereum*, *Cephalanthera damasonium*, and *N. nidus-avis*, but also other orchids, such as *Orchis purpurea*. These species may be relatively common in Luxembourg, but in the Netherlands all belong to the Red List (van der Meijden 2005). In the Hordelymo-Fagetum, character species such as *M. perennis* were found, but also species of calcareous, but relatively humid conditions, such as *Paris quadrifolia* and *Actaea spicata*. Many species in the Hordelymo-Fagetum group belong to the Dutch Red List as well.

The species-rich group without calcicole species was further separated into two groups, resembling the forest associations Galio-Carpinetum and Galio odorati-Fagetum. In the Galio-Carpinetum group, as suggested by the name, *C. betulus* was a characteristic species in the tree layer, even though *F. sylvatica* was more abundant. The Galio-Carpinetum group further contained character species of the association, such as *Quercus robur*, *Rosa arvensis* and *P. sterilis*, but also *Crataegus laevigata* and *Viburnum opulus*. Other common species were *Anemone nemorosa*, *Deschampsia cespitosa* and *Circaea lutetiana*, the latter two indicating relatively moist soil conditions. In the other group, resembling the Galio odorati-Fagetum, species richness was relatively low. Also, this association does not have particular character species. However, common species such as *Galium odoratum*, *Hedera helix* and *A. nemorosa* were still characteristic of relatively base-rich soil conditions, in contrast to the species of Luzulo-Fagetum, which was placed in an entirely different branch of the Twinspan-analysis.

Forest communities and parent materials

The distribution of forest communities was significantly affected by the gradient in parent materials (Table 8.2). The Carici-Fagetum was only found on Muschelkalk. This forest association indeed contained many species characteristic for calcareous conditions. The Hordelymo-Fagetum was also mainly found on Muschelkalk, which is in accordance with the calcareous habitat preferences of its characteristic species. This forest association also occurred on Keuper marl, Loess deposits and even Luxembourg sandstone. Keuper marl and Loess

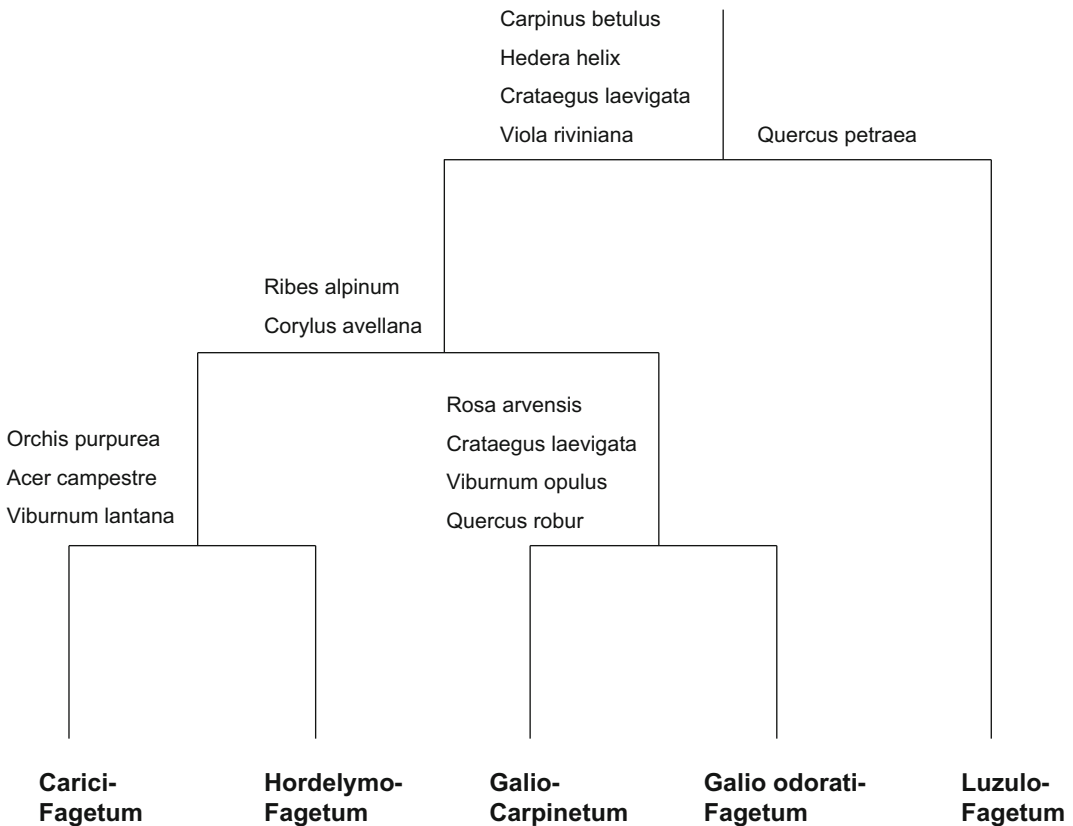


Fig. 8.2 Plant species composition of different forest communities in the Luxembourg cuesta landscape, based on the 68 relevés made by the first author

deposits initially contain calcium carbonates, and may still be calcareous when erosion is strong enough to counteract decalcification. Also, a small part of the Luxembourg sandstone is still calcareous, such as in the area south of Ermsdorf and Medernach, in the upper parts of the cuesta landscape and even on the plateau.

The Galio-Carpinetum had a strong preference for Keuper marl. Almost all plots were found on the gentle Keuper dip slope, with relatively low rates of erosion, and more stable conditions for soil formation. The soil generally shows clay eluviation in the topsoil, which results in a relatively porous upper layer, on top of an impermeable clay-rich subsoil (van den Broek 1989; Cammeraat 1992, see also Chaps. 9 and 10). This stagnant layer accounts for relatively moist conditions during part of the year, and explains the presence of species with a tolerance for wet soil, such as *D. cespitosa* and *C. lutetiana*.

The Galio odorati-Fagetum was found on all parent materials except Muschelkalk. This forest association showed particularly high affinity with Loess deposits. This parent material was not very common in the study area, but when present, it was almost always covered with Galio odorati-Fagetum. Plant species such as *Galium odoratum*, *Hedera helix* and *A. nemorosa* indicate relatively base-rich conditions, but species of calcareous conditions, such as *C. avellana* and *M. perennis*, did not occur anymore.

The Luzulo-Fagetum showed a clear preference for Luxembourg sandstone. On this parent material, acid sandy soils prevail, except in the more calcareous areas above Ermsdorf and Medernach. This forest association, with species such as *L. luzuloides* and *Oxalis acetosella*, was found on the Luxembourg plateau, but also on the upper cuesta slopes. The forest association also occurred on Plio-Pleistocene river terraces. In this case, it was

Table 8.1 Plant species composition of different forest communities in the Luxembourg cuesta landscape

	Carici-Fagetum	Hordelymo-Fagetum	Galio-Carpinetum	Galio odorati-Fagetum	Luzulo-Fagetum
nr of relevés	15	10	14	8	21
Tree layer					
<i>Fagus sylvatica</i>	IV	V	V	V	V
<i>Carpinus betulus</i>	IV	IV	IV	III	–
<i>Fraxinus excelsior</i>	I	IV	–	II	–
<i>Quercus robur</i>	IV	II	IV	I	–
<i>Quercus petraea</i>	–	–	II	II	V
<i>Pinus sylvestris</i>	–	–	–	–	II
Moss layer					
<i>Eurynchium striatum</i>	V	IV	IV	II	–
<i>Ctenidium molluscum</i>	III	I	–	I	–
<i>Rhytidiadelphus triquetrus</i>	II	I	I	–	–
<i>Polytrichum commune</i>	–	–	III	III	III
<i>Dicranum scoparium</i>	–	–	–	II	III
Herb layer					
<i>Hedera helix</i>	V	IV	V	IV	I
<i>Ribes alpinum</i>	V	IV	–	–	–
<i>Corylus avellana</i>	V	III	–	–	–
<i>Virburnum lantanum</i>	V	I	–	–	–
<i>Acer campestre</i>	V	I	I	–	–
<i>Orchis purpurea</i>	IV	I	–	–	–
<i>Euonymus europaeus</i>	IV	III	–	–	–
<i>Rosa arvensis</i>	IV	II	IV	–	I
<i>Arum maculatum</i>	IV	II	III	–	–
<i>Vicia sepium</i>	IV	I	II	I	–
<i>Cephalanthera damasonium</i>	III	–	–	–	–
<i>Cornus sanguinea</i>	III	III	–	–	–
<i>Prunus spinosa</i>	III	–	II	–	–
<i>Neottia nidus-avis</i>	III	I	I	–	–
<i>Daphne mezereum</i>	III	I	I	–	–
<i>Crataegus monogyna</i>	III	I	I	I	I
<i>Viola riviniana</i>	III	IV	IV	I	–
<i>Melica uniflora</i>	III	IV	I	III	I
<i>Galium odoratum</i>	II	V	III	V	I
<i>Mercurialis perennis</i>	II	IV	–	I	–
<i>Carex sylvatica</i>	–	IV	IV	I	I
<i>Galium luteum</i>	II	III	I	II	I
<i>Milium effusum</i>	I	III	I	II	I
<i>Dryopteris filix-mas</i>	I	III	–	II	I

(continued)

Table 8.1 (continued)

	Carici-Fagetum	Hordelymo-Fagetum	Galio-Carpinetum	Galio odorati-Fagetum	Luzulo-Fagetum
<i>Paris quadrifolia</i>	I	III	I	–	–
<i>Actaea spicata</i>	I	III	–	–	–
<i>Crataegus laevigata</i>	IV	IV	V	–	I
<i>Viburnum opulus</i>	III	II	V	–	I
<i>Anemona nemorosa</i>	–	I	V	IV	II
<i>Deschampsia cespitosa</i>	–	I	V	II	I
<i>Rubus</i> sp.	I	II	V	III	II
<i>Circaea lutetiana</i>	I	II	IV	II	I
<i>Brachypodium sylvaticum</i>	II	I	III	–	–
<i>Carex flacca</i>	II	–	III	–	I
<i>Cardamine pratensis</i>	–	I	II	–	–
<i>Phyteuma spicatum</i>	–	I	II	I	–
<i>Convallaria majalis</i>	–	I	III	II	–
<i>Potentilla sterilis</i>	I	–	III	–	–
<i>Ranunculus ficaria</i>	–	I	III	–	–
<i>Poa nemoralis</i>	II	I	I	III	I
<i>Luzula luzuloides</i>	–	I	I	II	I
<i>Oxalis acetosella</i>	–	I	I	II	II
<i>Deschampsia flexuosa</i>	–	–	–	II	III
<i>Dryopteris dilatata</i>	–	I	–	I	II
<i>Majanthemum bifolium</i>	–	–	–	I	II
<i>Vaccinium myrtillus</i>	–	–	–	–	II

The frequency of individual species is given in classes: I = 1–20%; II = 20–40%; 3 = 40–60%; IV = 60–80% and Y = 80–100%. Only species with frequency of at least II in one of the communities are listed

Table 8.2 The distribution of forest types over parent materials, given as percentage

	F _e	CF	HF	GC	GoF	LF
Muschelkalk	32	100	60	7	–	–
Keuper	25	–	10	86	25	5
Loess deposits	6	–	10	–	38	–
Pleistocene river terraces	9	–	–	7	13	19
Luxembourg sandstone	28	–	20	–	25	76

The total number of relevés was 68. F_e expected frequency, based on the total number of plots on each parent material, also given as percentage. *CF* Carici-Fagetum, *HF* Hordelymo-Fagetum, *GC* Galio-Carpinetum, *GoF* Galio odorati-Fagetum, *LF* Luzulo-Fagetum. The distribution over particular parent materials was significantly different from the expected distribution ($p < 0.05$) for all five forest types

restricted to the oldest T16-terraces (Verhoeff 1966), with the most acid soils.

8.3.2 Relationships Between Vegetation and Soil

With the 200 student relevés, the forest communities were slightly different from before, because not only deciduous forests, but also coniferous tree plantations were included. Also, recognition of the more than 200 species occurring in the area may be a problem for students. The authors have taken great care to minimize misidentifications, but could not prevent that some of the plant species present may not have been observed at all, especially in more diverse plots. Nevertheless, the distribution of relevés over vegetation types more or less resembles the forest communities as described by Niemeyer et al. (2010), and gives valuable additional information of the relationships between vegetation and soil.

Forest communities and species composition

The total dataset was first separated in deciduous forests with *F. sylvatica* and in coniferous stands with *P. abies* and *P. sylvestris* (Fig. 8.3). The beech forests were further separated in a species-rich and a species-poor group. The species-rich beech forests contained three subgroups, all representing some kind of forest association: (1) Hordelymo-Fagetum with (planted) stands of *P. abies*, (2) Hordelymo-Fagetum in a more proper sense, and (3) Galio-Carpinetum. The species-poor beech forests also contained three subgroups: (4) Galio odorati-Fagetum, (5) Luzulo-Fagetum and (6) Luzulo-Fagetum with (planted) stands of *P. sylvestris*. The coniferous tree plantations contained two subgroups: (7) stands with *P. abies* and (8) stands with *P. sylvestris*.

Community (1), Hordelymo-Fagetum with *P. abies*, had a understorey with calcicole species such as *Cornus sanguinea*, *M. perennis* and *C. avellana* (Table 8.3). This forest community was

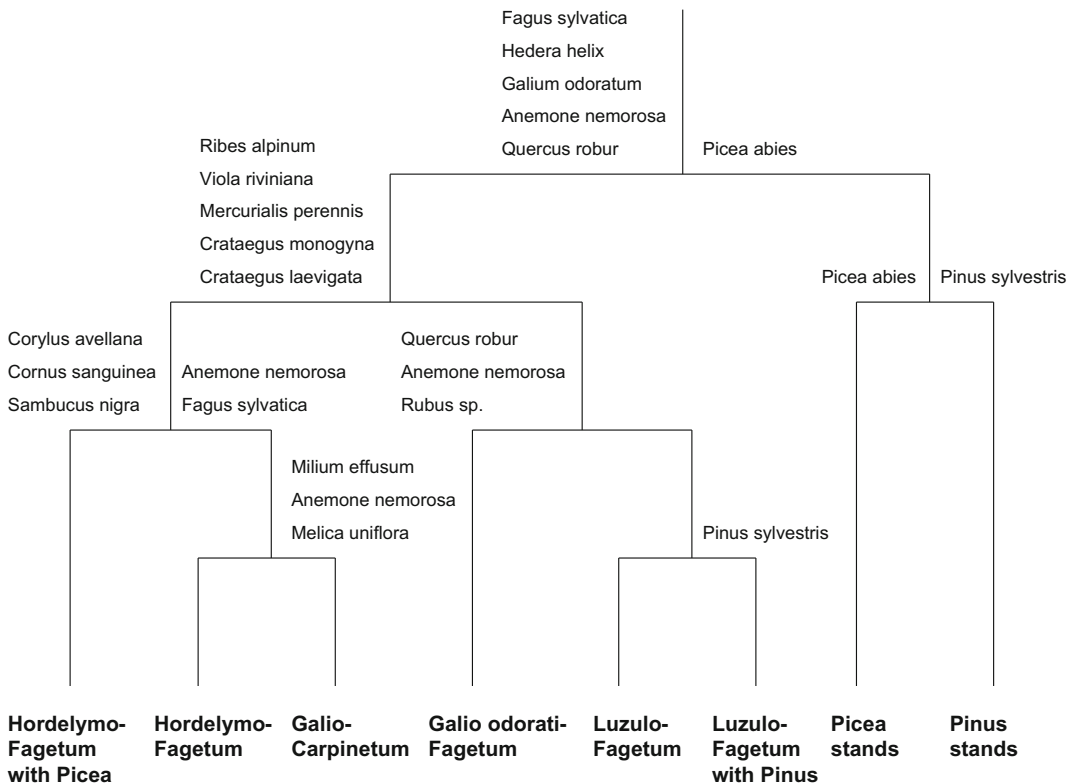


Fig. 8.3 Plant species composition of different forest communities in the Luxembourg cuesta landscape, based on the 200 relevés made by students

Table 8.3 Plant species composition of different forest communities in the Luxembourg cuesta landscape

	HF-Picea	HF	GC	GoF	LF	LF-Pinus	Picea	Pinus
nr of relevés	25	35	27	22	45	14	22	10
<i>Tree layer</i>								
<i>Fagus sylvatica</i>	II	V	V	V	V	IV	I	I
<i>Carpinus betulus</i>	II	III	III	–	–	–	–	–
<i>Fraxinus excelsior</i>	IV	III	–	–	–	–	–	–
<i>Quercus robur</i>	II	II	IV	IV	I	–	–	–
<i>Quercus petraea</i>	–	I	I	II	III	II	I	I
<i>Picea abies</i>	II	I	–	I	–	–	V	II
<i>Pinus sylvestris</i>	II	I	–	–	I	V	I	V
<i>Herb layer</i>								
<i>Cornus sanguinea</i>	IV	I	I	–	–	–	–	–
<i>Sambucus nigra</i>	IV	I	I	I	I	I	I	–
<i>Mercurialis perennis</i>	III	III	II	–	–	–	–	–
<i>Corylus avellana</i>	III	I	I	–	–	–	–	–
<i>Daphne mezereum</i>	II	I	I	–	–	–	–	–
<i>Paris quadrifolia</i>	I	II	I	–	–	–	–	–
<i>Arum maculatum</i>	II	II	II	I	–	–	–	–
<i>Acer campestre</i>	III	II	II	I	I	–	I	–
<i>Ribes alpinum</i>	III	IV	III	–	I	I	I	–
<i>Galium odoratum</i>	III	IV	V	II	II	II	I	–
<i>Viola riviniana</i>	III	III	IV	I	I	I	I	–
<i>Anemone nemorosa</i>	–	I	IV	IV	II	–	–	–
<i>Vicia sepium</i>	I	I	III	–	I	–	I	–
<i>Deschampsia cespitosa</i>	I	I	II	I	I	–	–	–
<i>Luzula luzuloides</i>	–	–	I	–	II	–	–	–
<i>Maianthemum bifolia</i>	–	–	–	I	I	–	–	I
<i>Vaccinium myrtillus</i>	–	–	–	–	I	I	I	III
<i>Deschampsia flexuosa</i>	–	–	–	–	II	–	–	IV

The frequency of individual species is given in classes: I = 1–20%; II = 20–40%; 3 = 40–60%; IV = 60–80% and V = 80–100%. Only species with frequency of at least II in one of the communities are listed. HF Hordelymo-Fagetum, GC Galio-Carpinetum, GoF Galio odorati-Fagetum, LF Luzulo-Fagetum. Picea = *Picea abies*; Pinus = *Pinus sylvestris*

again mainly found on Muschelkalk, but to some extent also on Keuper marl (Table 8.4). In community (2), Hordelymo-Fagetum, calcicole species prevailed as well, among which *M. perennis*, *P. quadrifolia*, and *Ribes alpinum*. It is likely that the Hordelymo-Fagetum also contained relevés belonging to the Carici-Fagetum, but this was not distinguished as a separate community in the analysis. Like before, the Hordelymo-Fagetum showed high affinity with Muschelkalk. Community (3),

Galio-Carpinetum, was found on both Muschelkalk and Keuper, and to some extent on Loess deposits. This community contained undergrowth species such as *Galium odoratum*, *A. nemorosa* and *Viola riviniana* + *reichenbachiana*, while *C. betulus* was abundant in the tree layer. It is possible that some of the relevés grouped under Galio-Carpinetum reflect species-poor forms of the Hordelymo-Fagetum, especially on Muschelkalk. However, the presence of *D. cespitosa*, a species of relatively wet

Table 8.4 The distribution of forest types over parent materials, given as percentage

	F_e	HF-Picea	HF	GC	GoF	LF	LF-Pinus	Picea	Pinus
Muschelkalk	34	80	86	52	5	2	–	14	–
Keuper	20	20	14	44	23	18	–	18	–
Loess deposits	6	–	–	4	23	13	–	–	–
Pleistocene river terraces	6	–	–	–	32	9	–	5	–
Luxembourg sandstone	34	–	–	–	18	58	100	64	100

The total number of relevés was 200. F_e expected frequency, based on the total number of plots on each parent material, also given as percentage. HF *Hordelymo-Fagetum*, GC *Galio-Carpinetum*, GoF *Galio odorati-Fagetum*, LF *Luzulo-Fagetum*. Picea = *Picea abies*; Pinus = *Pinus sylvestris*. The distribution over the parent materials was significantly different from the expected distribution ($p < 0.05$) for all eight forest types

conditions, as well as the common occurrence on Keuper marls are indicative for *Galio-Carpinetum*.

In the species-poor beech forests, community (4), the *Galio odorati-Fagetum*, had an undergrowth with *A. nemorosa* and to some extent *Galium odoratum*. Like in the first part of the study, this forest association may occur on almost all parent materials, but seemed to have a preference for Loess deposits and Pleistocene river terraces. In these parent materials, the loamy soils are not calcareous any more, but still relatively base-rich. Community (5), *Luzulo-Fagetum*, was even poorer in species, and undergrowth was usually very sparse. Characteristic species were again *A. nemorosa* and *G. odoratum*, but now also *D. flexuosa*, an indicator of more acid conditions. Like before, this forest association was mainly found on Luxembourg sandstone, but also on some of the other parent materials. Community (6), *Luzulo-Fagetum* with *P. sylvestris*, was only found on Luxembourg sandstone, however. This community was generally very poor in species.

Of the stands dominated by coniferous trees, community (7) with *P. abies* was also very species-poor, probably due to a lack of light. The community was found over a range of parent materials, from Muschelkalk and Keuper to Luxembourg sandstone. Community (8), with *P. sylvestris*, was however only found on Luxembourg sandstone. In this community, with relatively open tree cover, undergrowth was sometimes rather extensive, and consisted of *V. myrtillus* and *D. flexuosa*.

Forest communities and soil characteristics

The eight forest communities differed significantly with respect to the presence of hardrock in the soil profile (Fig. 8.4). In the two *Hordelymo-Fagetum* communities, mainly found on Muschelkalk, 72–80% of the plots had hardrock within 120 cm depth. These two communities also had relatively steep slopes, due to the competent parent material in the river valleys. Shallow soils with hardrock within 120 cm were also often found in *Luzulo-Fagetum*, especially in the community with scots pine. This was due to their preference for Luxembourg sandstone. However, because the Luxembourg sandstone occurs on the cuesta topslope, but also on the plateau, both steep and shallow slopes were found. The intermediate forest communities, *Galio-Carpinetum* and *Galio odorati-Fagetum*, had relatively gentle slopes and deep soils. This was mainly due to their location on Keuper marl, Loess deposits and/or Pleistocene river terraces. Pine plantations also had gentle slopes, but shallow soils, due to their position on the Luxembourg sandstone plateau. In spruce plantations, slopes could be both steep or gentle, and soils both deep and shallow, depending on the parent material.

The forest communities also significantly differed with respect to the presence of lime within the soil profile, and in their humus forms (Fig. 8.5). The two associations of *Hordelymo-Fagetum* and the *Galio-Carpinetum* had mostly calcareous profiles, with lime present within 120 cm depth. This was mainly due to the lime-rich parent materials, such as Muschelkalk limestone and Keuper marls.

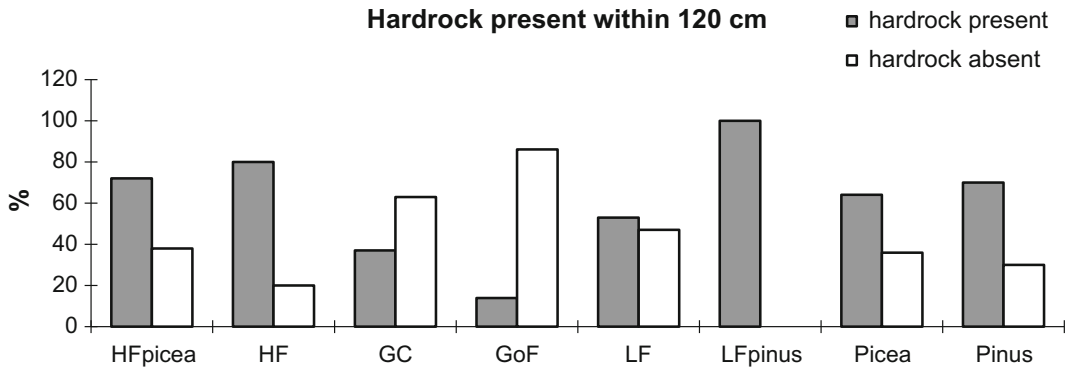


Fig. 8.4 Distribution of soils with and without hardrock, and relatively steep ($>6^\circ$) or gentle ($<6^\circ$) slopes, over different forest types in the Luxembourg cuesta landscape. *HF* Hordelymo-Fagetum, *GC* Galio-Carpinetum, *GoF* Galio odorati-Fagetum, *LF* Luzulo-Fagetum. The distribution patterns were all based on $n = 200$ and significantly different ($p < 0.05$) from expected equal distribution

Also, these communities mainly contained Mull humus forms, with only thin ectorganic horizons and rapid litter breakdown (Green et al. 1993). The forest types differed however in soil pH. In Hordelymo-Fagetum, topsoils were still calcareous, and pH values ranged from 7.1 to 7.2 (Kooijman 2010). In Galio-Carpinetum, topsoils were already decalcified, and pH values ranged from 5.0 to 5.7 (Kooijman and Cammeraat 2010). In contrast, Galio odorati-Fagetum and the two types of Luzulo-Fagetum had primarily lime-poor soils, due to lime-poor parent materials such as Loess deposits, Pleistocene river terraces and Luxembourg sandstone. In Galio odorati-Fagetum, pH of the upper 20 cm of the soil ranged from 3.6 to 3.9 in Loess deposits, and from 3.7 to 4.0 in Pleistocene river terraces (see also Chap. 6). In Luzulo-Fagetum, these pH values ranged from 4.2 to 4.4 on the oldest Pleistocene terraces and from 3.0 to 4.0 on Luxembourg sandstone (see also Chap. 6). In all the lime-poor forest associations, the organic layer often contained a distinct F-layer of more than 2 cm thickness, and was classified as Mormoder humus forms. Pine stands were also lime-poor and characterized by Mormoder humus forms, due to their plantation on the Luxembourg sandstone plateau. Spruce stands, however, could also contain lime-rich soils and Mull humus profiles, especially when planted on Muschelkalk.

As a result of the above-mentioned differences in hardrock, slope and pH regime, other soil

characteristics also significantly differed between forest associations (Fig. 8.6). Clay eluviation did not occur in the two types of Hordelymo-Fagetum, because lime content and pH were still too high to allow clay dispersion (Duchaufour 1982; van den Broek 1989). Signs of clay-eluviation were mainly found in forest communities with loamy, decalcified soils, such as Galio-Carpinetum and Galio odorati-Fagetum, and partly in the Luzulo-Fagetum, especially on Keuper marl, Loess deposits and Pleistocene river terraces. Pseudogley mottles were associated with the same forest associations. The mottling patterns point to conditions of stagnant water from time to time, which are related to the clay-rich, less permeable subsoils. The subsoil is enriched with clay due to weathering and/or clay-illuviation (van den Broek 1989), while topsoils are relatively porous, due to clay-eluviation and residual accumulation of sand and silt. Clay eluviation was not observed in Pine plantations, mainly because the Luxembourg sandstone is very poor in loam and clay. However, stagnant water conditions were found in some places, especially in the eastern part of the area, where slopes are irregular due to slumping of sandstone blocks over layers of Keuper marl. In Spruce plantations, clay eluviation and pseudogley were rare, because they were mostly planted on soils insensitive to clay dispersal, because lime content and pH are too high, or the parent material is non-clayey. Podzolization, the downward transport of iron, aluminium and

DOC, can only occur at low pH (Buurman 1984). Also, the process is stimulated by low litter quality, which leads to retarded decomposition and increased production of small organic molecules. As a result, podzolization was mainly found in forests associations with conifer trees, such as Luzulo-Fagetum with Pine, Pine plantations and the Spruce stands planted on Luxembourg sandstone.

The above-mentioned differences in soil characteristics between forest associations were further reflected in the soil classification (Table 8.5). In the two associations of Hordelymo-Fagetum, primarily occurring on Muschelkalk, soil type generally ranged from Leptosol to Leptic and Colluvic Regosol, depending on depth of the limestone hardrock. In the Galio-Carpinetum and Galio odorati-Fagetum, found on loamy Keuper marls, Loess deposits and Pleistocene river terraces, Planosols and Luvic Stagnosols predominated. These soil types are characterized by water stagnation during part of the year, due to the clay-rich subsoil. The Luzulo-Fagetum was also partly characterized by Luvic Stagnosols, especially on the oldest Plio-Pleistocene river terraces, but was dominated by Arenosols and especially Leptic Arenosols on Luxembourg sandstone. In Luzulo-Fagetum with Pine trees, Leptic Arenosols and Podzols were the main soil type, which point to sandstone hardrock within 100 cm depth, but also to increased leaching of iron, aluminium and DOC. Pine stands on top of the Luxembourg sandstone plateau were almost all characterized by Podzols. In Pine stands, pod-

zolization may have been partly stimulated by low litter quality (Swift et al. 1979; Wardenaar and Sevink 1992), but many stands were planted in former heathlands with *Calluna vulgaris*, which also has recalcitrant litter. In Spruce stands, in contrast, almost all soil types could occur, due to the variation in parent materials.

8.3.3 Parent Material Versus Litter Quality on Keuper and Muschelkalk

The above suggests that relationships between parent material and forest plant communities is indeed rather strong. A strong effect of parent material also emerged in the comparison of 60 forest plots on Keuper marl and Muschelkalk limestone, which both have base-rich, loamy soils and have many plant species in common (Tables 8.6 and 8.7). A significant effect of litter quality, tested in forest plots dominated by beech or hornbeam, could also be detected, in accordance with the literature (van Oijen et al. 2005; van Calster et al. 2008; Kooijman and Cammeraat 2010). However, the litter quality effect was secondary to the effect of parent material. In the CA-analysis, parent material was the most important factor on the first axis, with correlation values of 0.81. This suggests that parent material contributed to some 66% of the variance explained by the first species axis. Factors related to parent material such as pH of

Table 8.5 The distribution of forest types over soil types, given as percentage

	F_e	HF-Picea	HF	GC	GoF	LF	LF-Pinus	Picea	Pinus
Leptosol	12	36	34	3	–	–	–	9	–
Leptic Regosol	17	36	49	30	5	–	–	–	–
Colluvic Regosol	13	28	17	22	–	9	–	14	–
Luvic Planosol	11	–	–	41	23	9	–	9	–
Luvic/Alic Stagnosol	12	–	–	3	55	22	–	5	–
Arenosol	5	–	–	–	9	18	–	–	–
Leptic Arenosol	18	–	–	–	9	38	43	36	20
Podzol	12	–	–	–	–	4	57	27	80

The total number of relevés was 200. F_e expected frequency, based on the total number of plots for each soil type, also given as percentage. HF Hordelymo-Fagetum, GC Galio-Carpinetum, GoF Galio odorati-Fagetum, LF Luzulo-Fagetum. Picea = *Picea abies*; Pinus = *Pinus sylvestris*. The distribution over particular soil types was significantly different from the expected distribution ($p < 0.05$) for all eight forest types

Table 8.6 Correspondence of environmental parameters with the first and second axis of a CA-analysis of 60 forest plots with beech and hornbeam on Keuper marl and Muschelkalk limestone in the Luxembourg cuesta landscape

	CA-axis 1	CA-axis 2
Eigenvalues	0.58	0.40
Limestone parent material	0.81	-0.35
pH mineral topsoil	0.70	-0.27
Air-filled pore space	0.48	-0.52
Dutch red list species	0.36	-0.06
Mass organic layer	0.04	-0.50
Beech:hornbeam cover ratio	-0.09	-0.29
Ephemeral species	-0.16	0.23
Soil moisture content	-0.37	0.48
Marl parent material	-0.81	0.35

Table 8.7 Plant species composition on Keuper marl and Muschelkalk limestone, in plots dominated by beech or hornbeam

	Marl beech	Marl hornbeam	Limestone beech	Limestone hornbeam
<i>Indifferent species</i>				
<i>Hedera helix</i>	V	IV	V	V
<i>Crataegus laevigata</i>	V	IV	IV	III
<i>Rosa arvensis</i>	IV	V	III	III
<i>Viola riviniana</i>	II	IV	IV	V
<i>Viburnum opulus</i>	III	IV	III	IV
<i>Carex sylvatica</i>	II	IV	I	III
<i>Galium odoratum</i>	III	IV	II	III
<i>Polygonatum multiflorum</i>	II	III	I	IV
<i>Vicia sepium</i>	-	III	II	III
<i>Poa nemoralis</i>	II	II	II	II
<i>Milium effusum</i>	I	II	II	III
<i>Potentilla sterilis</i>	I	II	I	II
<i>Lonicera periclymenum</i>	I	I	I	II
<i>Carex flacca</i>	I	II	-	II
<i>Dryopteris filix-mas</i>	I	I	I	II
<i>Rubus caesius</i>	I	I	I	II
<i>Fragaria vesca</i>	-	II	I	II
<i>Paris quadrifolia</i>	-	II	-	II
<i>Preference for limestone</i>				
<i>Acer campestre</i>	I	II	V	V
<i>Arum maculatum</i>	I	II	V	V
<i>Corylus avellana</i>	-	I	IV	V
<i>Ribes alpinum</i>	-	-	III	V
<i>Melica uniflora</i>	I	I	IV	III

(continued)

Table 8.7 (continued)

	Marl beech	Marl hornbeam	Limestone beech	Limestone hornbeam
<i>Crataegus monogyna</i>	–	–	II	IV
<i>Cornus sanguinea</i>	–	–	III	III
<i>Daphne mezereum</i>	–	–	III	III
<i>Euonymus europaeus</i>	–	I	II	III
<i>Viburnum lantana</i>	–	–	II	III
<i>Ribes uva-crispa</i>	–	I	I	III
<i>Acer pseudoplatanus</i>	–	–	II	III
<i>Asplenium trichomanes</i>	–	–	II	II
<i>Tilia platyphyllos</i>	–	–	II	II
<i>Prunus spinosa</i>	–	I	II	II
<i>Campanula trachelium</i>	–	–	II	I
<i>Neottia nidus-avis</i>	–	–	I	II
<i>Orchis purpurea</i>	–	–	I	II
<i>Orchis mascula</i>	–	–	I	II
<i>Preference for marl</i>				
<i>Deschampsia cespitosa</i>	V	V	–	–
<i>Anemone nemorosa</i>	V	V	II	II
<i>Rubus fruticosus</i>	II	IV	–	–
<i>Circaea lutetiana</i>	II	IV	–	–
<i>Convallaria majalis</i>	II	IV	–	–
<i>Ficaria verna</i>	–	IV	I	I
<i>Phyteuma spicatum</i>	I	II	–	I

The frequency of individual species ($n = 15$) is given in classes: I = 1–20%; II = 20–40%; 3 = 40–60%; IV = 60–80% and V = 80–100%. Only species with frequency of at least II in one of the groups are listed. Preference for a particular parent material is based on double frequency or more. Data are derived from Kooijman (2010)

the mineral topsoil were also highly correlated with the first CA-axis, with mean values for beech and hornbeam plots ranging from 5.1–5.6 on Keuper, and 7.1–7.2 on limestone. The number of Dutch red-list species also pointed to parent material, and was relatively high on limestone. In contrast, litter quality parameters such as beech:hornbeam cover ratio and mass of the organic layer mainly correlated with the second CA-axis. This was also true for soil moisture content and air-filled pore space. On Keuper marl, soil moisture content at field capacity was higher under hornbeam than under beech, and air-filled pore space relatively low. This points to more water saturated conditions under hornbeam than under beech, which is consistent with other observations (Kooijman and Cammeraat 2010, see also Chap. 10). However, on limestone,

soils were as dry as beech plots on Keuper marl, and beech and hornbeam plots did not differ in soil moisture and air-filled pore space.

The findings above correspond with differences in species composition of the undergrowth. Some species were found on both parent materials, but many other species showed clear preference for Keuper marl or Muschelkalk limestone. Preference for Muschelkalk was found in species such as *Acer campestre*, *C. avellana*, *Ribes alpinum*, *C. sanguinea* and *D. mezereum*, which indicate calcareous conditions (Ellenberg et al. 1974). *Orchis mascula* and *O. purpurea*, also characteristic of calcareous conditions, were only found in limestone plots. In contrast, preference for Keuper marl was detected in species such as *Anemona nemorosa*, *D.*

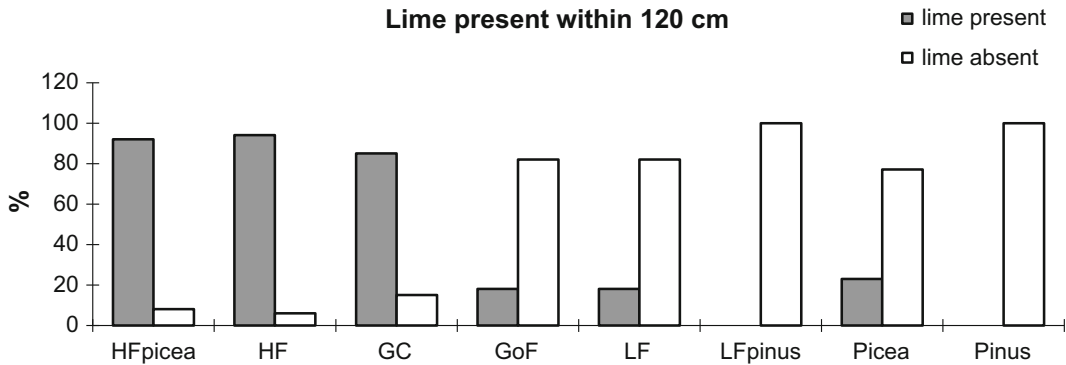


Fig. 8.5 Distribution of lime-rich and lime-poor soils, and Mull and Mormoder humus forms, over different forest types in the Luxembourg cuesta landscape. *HF* Hordelymo-Fagetum, *GC* Galio-Carpinetum, *GoF* Galio odorati-Fagetum, *LF* Luzulo-Fagetum. The distribution patterns were all based on $n = 198-200$ and significantly different ($p < 0.05$) from expected equal distribution

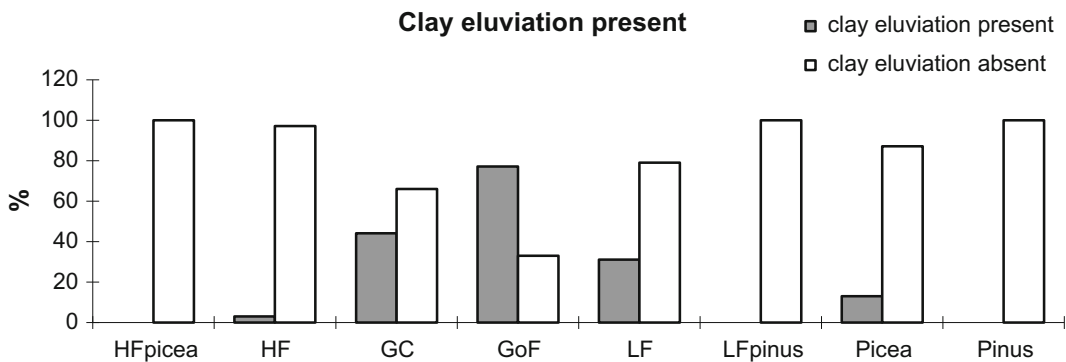


Fig. 8.6 Distribution of soils with and without clay eluviation, pseudogley mottles and podzolization over different forest types in the Luxembourg cuesta landscape. *HF* Hordelymo-Fagetum, *GC* Galio-Carpinetum, *GoF* Galio odorati-Fagetum, *LF* Luzulo-Fagetum. The distribution patterns were all based on $n = 200$ and significantly different ($p < 0.05$) from expected equal distribution

cespitosa, *C. lutetiana* and *Ficaria verna*. These are species of relatively moist habitats (Ellenberg et al. 1974). In Keuper soils, especially on relatively flat dipslope positions, the marl has become decalcified and pH has dropped. In limestone soils, clay-dispersal is restricted by high Ca-levels and pH (Duchaufour 1982; van den Broek 1989). In decalcified marl, however, clay-eluviation in the topsoil is an important process, which leads to a contrast in texture with the clay-rich subsoil, stagnant water conditions in wet periods, and relatively wet-tolerant plant species (see also Chaps. 9 and 10).

The main effect of litter quality was the reduction of general species richness under beech, probably related to much denser litter

layers than under hornbeam. Mass of the organic layer varied between 1.3 and 1.6 kg m^{-2} under beech, and between 0.5 and 0.7 kg m^{-2} under hornbeam, for limestone and marl respectively (Kooijman 2010). In general, under beech, the undergrowth contained 8–9 species less than under hornbeam. On limestone, reduction of species may be directly due to the dense beech litter, either owing to allelopathic effects (Hane et al. 2003), or because it forms a physical barrier for plants germinating in the mineral soil. On limestone, differences in habitat conditions between beech and hornbeam plots are probably small, because pH remains high as long as lime is present, and clay-dispersal does not occur at high pH (Duchaufour 1982). On Keuper marls, the

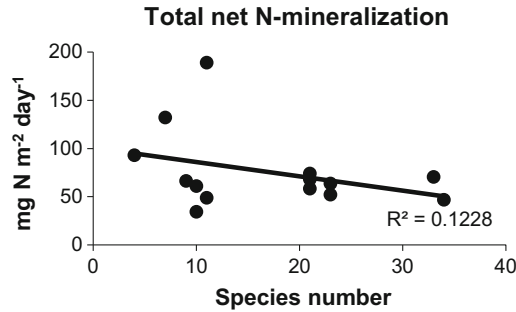


Fig. 8.7 Diversity of the undergrowth in relation to total net N-mineralization (in organic layer and mineral topsoil combined) and nitrification (in organic layer and mineral topsoil separately) in beech and hornbeam plots on Keuper marl and Muschelkalk limestone. Data are derived from Kooijman (2010)

differences in the organic layer may however lead to clearly different habitat conditions (Cammeraat and Kooijman 2009; Kooijman and Cammeraat 2010). The dense litter layer under beech may protect the soil from erosion, and ensure that leaching of base cations and clay particles can continue without interruption by bioturbation. This may explain why soils under beech are drier and more acid than under hornbeam (see also Chap. 10). On Keuper marls, under beech, species richness is thus not only be reduced by the denser litter layer, but also by lower pH and soil moisture than under hornbeam.

8.3.4 Decrease of Species Richness from Mineral-Rich to Mineral-Poor Parent Materials

The results of this study clearly suggest that plant species richness in the deciduous forests of the Luxembourg Gutland declines from calcareous to acidic soils. This seems to be a common pattern in NW-Europe (Ellenberg et al. 1974; Pärtel 2002). In NW-Europe, high pH soils have probably been the center of plant evolution, in contrast to e.g. tropical or high latitude areas, where high leaching and low pH soils prevail (Pärtel 2002). Calcareous parent materials in this region are relatively abundant, and each glacial period has led to rejuvenation of landscape and soils with often calcareous material. In

Luxembourg, the calcicole trees *C. avellana* and *Tilia* spp. were indeed common species in the early Holocene pollen records (see also Chap. 3), and calcareous soil types were probably widespread. In Luxembourg, the regional species pool for calcareous soils may thus be more abundant than for acidic soils, and may explain the general decrease in species from Muschelkalk to Keuper, Loess deposits and Pleistocene river terraces, and then to Luxembourg sandstone.

Species constraints on limestone

Nevertheless, particular species are usually associated with particular parent materials and soils (Ellenberg et al. 1974), and must have evolved adaptations to particular habitat conditions. Limestone soils, which remain calcareous in the topsoil due to the steep slopes and high rates of erosion, may be problematic with respect to Ca-toxicity and P-availability (Tyler 2003; Zohlen and Tyler 2004). Many calcicole plants may be able to live in acidic soil, but calcifuge species are generally unable to grow in calcareous soil, due to high Ca-levels (Gigon 1987). Also, in calcareous soils, P is usually a limiting factor, due to chemical precipitation with calcium at high pH (Lindsay and Moreno 1966; Kooijman et al. 1998; Tyler 2003; Zohlen and Tyler 2004; Shen et al. 2011). Calcicole plants have evolved ways to avoid this, by e.g. excretion of citric acid to dissolve calcium phosphates (Marschner 1995). Also, many calcicole plant species are associated with VA-mycorrhiza, which increase P-uptake by large hyphal surface areas and local acidification (Read and

Perez-Moreno 2003). Calcifuge species may however be unable to avoid excessive uptake of Ca, and also have problems with P-uptake in calcareous soil.

In addition to Ca and P, different forms of inorganic N may play a role. Calcareous soil are usually dominated by nitrate, as the ammonium produced during the decomposition process is rapidly transformed by nitrifying bacteria (Verhagen et al. 1992). Many calcicole plant species prefer nitrate to ammonium as primary N-source (Falkengren-Grerup 1995; Bijlsma et al. 2000; Diekman and Falkengren-Grerup 2003). Also, nitrate can stimulate germination of undergrowth species (Jobidon 1993; Vandeloos et al. 2008). Nitrate may even stimulate infection with VA-mycorrhiza (Hepper 1983; Johnson et al. 1984), which in turn stimulates P-uptake. In the study area, plant diversity indeed increased with higher nitrate availability, but only if the increase took place in the mineral soil (Fig. 8.7). With high nitrification in the organic layer, diversity of the undergrowth actually decreased. High nitrification in the organic layer is associated with higher mass of this layer, and usually with low pH. In calcareous soil, plant species richness thus increased at low rather than high total net N-mineralization. However, low total net N-mineralization may be favourable to undergrowth species, due to reduced growth of trees, which leads to increased light levels at the forest floor.

Species constraints on Keuper marl and Pleistocene deposits

On Keuper marls, Loess deposits and Pleistocene river terraces, soils have generally become decalcified during the Holocene, or even earlier interglacial periods. The associated decrease in pH not only led to decrease in calcicole species, but also to changes in moisture regime. In decalcified loamy soils, clay-eluviation from the topsoil leads to water stagnant conditions during wet periods on the clay-rich subsoil (Duchaufour 1982; van den Broek 1989, see also Chap. 9). Many characteristic species are therefore tolerant to wet conditions, such as *D. cespitosa* and *C. lutetiana*. Such species may actually profit from high soil moisture, because stomata can be kept

open for longer periods, which is an advantage when photosynthesis at the forest floor is already limited by low light. In summer, light availability on the forest floor is even lower. Many species solve this problem with a spring ephemeral life history strategy, such as the geophytes *A. nemorosa* and *F. verna*.

Species constraints on Luxembourg sandstone

On Luxembourg sandstone, soils are usually rather acidic, except for small areas where the sandstone is relatively calcareous. As pH values in the sandstone soils range from 3 to 4 (see also Chap. 6), one of the major problems is Al-toxicity (van den Berg et al. 2005; Zvereva et al. 2007; Abedi et al. 2012), due to dissolution of aluminium compounds at low pH. On acid sandy soil, beech and hornbeam leaves showed 2.1–3.7 times higher Al:Ca ratios than on calcareous soil (A.M. Kooijman and A. Smit, unpublished records). Also, Al-uptake was generally 2.0–4.5 times higher in hornbeam leaves than in beech, which may be a reason why hornbeam does not occur on the most acid soils. In addition to Al-toxicity, sandstone soils have a relatively coarse texture with high drainage, and may rapidly dry out. On the forest floor, where light availability is low for most of the growing season, dry soils form an extra problem, because closure of the stomata, to prevent water loss, reduces photosynthesis even further. Also, dense organic layers, due to low biological activity and retarded decomposition at low pH, may become a problem for undergrowth species. The organic layer may form a barrier for species germinating in the mineral soil. Also, tree species such as beech may exert phytotoxic effects by the production of particular chemical components (Hane et al. 2003). In addition, in acidic soil, the main form of inorganic nitrogen may be ammonium rather than nitrate. Beech can use both ammonium and nitrate (Gessler et al. 1998; Leberecht et al. 2016), but high ammonium concentrations are toxic to many species from base-rich habitats (de Graaf et al. 1998). Also, low nitrate concentrations may lead to lower germination of undergrowth species, which is stimulated by nitrate (Jobidon 1993; Vandeloos et al. 2008).

8.4 Conclusions

In the cuesta landscape of central Luxembourg, natural relations between forest vegetation, parent material and soil development still exist, evidenced by the distinct gradient in plant communities, associated with the gradient from acidic to calcareous soils. Even in planted conifer stands, undergrowth species point to particular parent materials and soil development. The species-poor Luzulo-Fagetum is mainly found on Luxembourg sandstone and the oldest Pleistocene river terraces, with Leptic Arenosols, Podzols and Alic Stagnosols, and pH values around or below 4. Tolerance to high Al-concentrations is probably the main factor explaining differences with other forest types. The slightly more species-rich Galio odorati-Fagetum is found on Loess deposits, Pleistocene river terraces and Keuper marls in the upper part of the cuesta. In this forest type, pH is still around or below 4, but soils are more loamy, and some of them have water stagnation during part of the year. Soil types vary from Luvic Stagnosols to Colluvic Regosols. The species-rich Galio-Carpinetum is mainly found on Keuper marls in the rolling dipslope landscape. Soil pH has increased to 5–6, and soil types vary from Luvic Stagnosols to Planosols, all characterized by temporary water stagnation. Tolerance to wet conditions is probably the main factor explaining differences with other forest types. Forest communities with calcicole species, such as Carici-Fagetum and Hordelymo-Fagetum, mainly occur on Muschelkalk, with Leptosols and Leptic Regosols, and pH values around 7. Undergrowth species have adapted to high Ca-concentrations, low P-availability and use of nitrate rather than ammonium. In general, species richness of the undergrowth increases over the geosequence from Luxembourg sandstone to Muschelkalk, because the regional species pool is higher for calcareous than for acidic soil.

Acknowledgements The authors would like to thank Mark Bokhorst, Ricardo van Dijk, Martijn Heuff, Gertrud Houkes, Vincent Kalkman, Robert Kuiper, Christiaan Kwakkestein, Maartje van Meteren, Marieke Nonhebel, Inka de Pijper, Ceciel Rip, Kasper de Rooy,

Vincent Simons, Jeroen Timmers, Femke Tonneijck, Floris van der Valk, Mirjam Vriend†, Riekje Wiersma and Sybren Ydema for collecting the student dataset. Bas van Dalen, Greet Kooijman-Schouten and Benito Martinez-Hernandez helped with fieldwork and data collection in other parts of the study, and Leo Hoitinga, Leen de Lange and Piet Wartenbergh supported us in the laboratory. Photographs were made by Jan van Arkel.

References

- Abedi M, Bartelheimer M, Poschod P (2012) Aluminium toxic effects on seedling root survival affect plant composition along soil reaction gradients—a case study in dry sandy grasslands. *J Veg Sci* 24:1074–1085
- Aubert M, Hedde M, Decaens T, Bureau F, Margerie P, Alard D (2003) Effects of tree canopy composition on earthworms and other macro-invertebrates in beech forests of Upper Normandy (France). *Pedobiologia* 47:904–912
- Bijlsma RJ, Lambers H, Kooijman SALM (2000) A dynamic whole-plant model of integrated metabolism of nitrogen and carbon. 1. Comparative ecological implications of ammonium-nitrate interactions. *Plant Soil* 220:49–69
- Bolte A, Czajkowski T, Kompa T (2007) The north-eastern distribution range of European beech—a review. *Forestry* 80:413–429
- Braak CJF ter (1988) CANOCO—a FORTRAN program for canonical community ordination by partial detrended canonical correspondence analysis, principal component analysis and redundancy analysis. Technical report: LWA 88-02, Wageningen
- Broek TMW van den (1989). Clay dispersion and pedogenesis of soils with an abrupt contrast in texture: a hydro-pedological approach on subcatchment scale. Ph.D.-thesis University of Amsterdam, 109 pp
- Bossuyt B, Hermy M, Deckers J (1999) Migration of herbaceous plant species across ancient-recent forest ecotones in central Belgium. *J Ecol* 87:628–638
- Buurman P (1984) Podzols. Van Nostrand Reinhold, Soil Science Series, 450 pp
- Cammeraat LH (1992) Hydro-geomorphological processes in a small forested sub-catchment: preferred flow-paths of water. Ph.D.-thesis University of Amsterdam, 158 pp
- Cammeraat LH (2002) A review of two strongly contrasting geomorphological systems within the context of scale. *Earth Surf Proc Land* 27:1201–1222
- Cammeraat LH, Kooijman AM (2009) Biological control of pedological and hydro-geomorphological processes in a deciduous forest ecosystem. *Biologia* 64:428–432
- Cody RP, Smith JK (1987) Applied statistics and the SAS programming language. Elsevier Science Publishers Co. Int., Amsterdam, p 280

- de Graaf MCC, Bobbink R, Roelofs JGM, Verbeek PJM (1998) *Plant Ecol* 135:185–196
- Diekmann M, Falkengren-Grerup U (2003) A new species index for forest vascular plants: development of functional indices based on mineralization rates of various forms of soil nitrogen. *J Ecol* 86:269–283
- Duchaufour P (1982) *Pedology, Pedogenesis and classification*. Translated by T.R. Paton. George Allen & Unwin, London, p 448
- Ellenberg H, Weeber HE, Düll R, Wirth V, Werner W (1974) *Zeigerwerte von Pflanzen in Mitteleuropa*. Verlag Erich Goltze GmbH & Co, Göttingen
- Ellenberg H (1988) *Vegetation Ecology of Central Europe*, 4th edn. Cambridge University Press, Cambridge
- Falkengren-Grerup U (1995) Interspecies differences in the preference of ammonium and nitrate in vascular plants. *Oecologia* 102:305–311
- Ferraris le Comte de (1777) Reissued in 1965–1970. *Carte de Cabinet des Pays-Bas Autrichiens*. Bibliothèque Royale de Belgique, Bruxelles
- Gessler A, Schneider S, Von Sengbusch D, Weber P, Hanemann U, Huber C, Rothe A, Kreuzer K, Rennenberg H (1998) Field and laboratory experiments on net uptake of nitrate and ammonium by the roots of spruce (*Picea abies*) and beech (*Fagus sylvatica*) trees. *New Phytol* 138:275–285
- Gigon A (1987) A hierarchic approach in causal ecosystem analysis. The Calcifuge-Calcicole problem in Alpine grasslands. In: *Ecological studies*, Springer 61:228–244
- Graae BJ, Sunde PB, Fritzboøger B (2003) Vegetation and soil differences in ancient opposed to new forests. *For Ecol Manage* 177:179–190
- Green RN, Trowbridge RL, Klinka K (1993) Towards a taxonomic classification of humus forms. *Supplement to Forest Science*, vol 39
- Hane EN, Hamburg SP, Barber AL, Plaut JA (2003) Phytotoxicity of American beech leaf leachate to sugar maple seedlings in a greenhouse experiment. *Can J For Res* 33:814–821
- Hill MO (1979) *TWINSPAN manual ecology and systematics*, New York
- Hepper CM (1983) The effect of nitrate and phosphate on the vesicular-arbuscular mycorrhizal infection of lettuce. *New Phytol* 92:389–399
- IUSS (2015) *World Reference Base for Soil Resources 2014, update 2015*. International soil classification system for naming soils and creating legends for soil maps. *World Soil Resources Reports No. 106*. FAO, Rome
- Jobidon R (1993) Nitrate fertilization stimulates emergence of red raspberry (*Rubus idaeus* L.) under forest canopy. *Nutr Cycl Agroecosyst* 36:91–94
- Johnson CR, Jarrell WM, Menge JA (1984) Influence of ammonium: nitrate ratio and solution pH on mycorrhizal infection, growth and nutrient composition of *Chrysanthemum morifolium* var. *Circus*. *Plant Soil* 77:151–157
- Kooijman AM (2010) Litter quality effects on undergrowth species diversity by mass of the organic layer, pH, soil moisture and N-dynamics in Luxembourg beech and hornbeam forests. *J Veg Sci* 21:248–261
- Kooijman AM, Cammeraat LH (2010) Biological control of beech and hornbeam on species richness via changes in the organic layer, pH and soil moisture characteristics. *Funct Ecol* 24:469–477
- Kooijman AM, Martinez-Hernandez GB (2009) Effects of litter quality and parent material on organic matter characteristics and N-dynamics in Luxembourg beech and hornbeam forests. *For Ecol Manage* 257:1732–1739
- Kooijman AM, Dopheide J, Sevink J, Takken I, Verstraten JM (1998) Nutrient limitation and their implications for the effects of atmospheric deposition in lime-poor and lime-rich coastal dunes in the Netherlands. *J Ecol* 86:511–526
- Laskowski R, Niklinska M, Maryanski M (1995) The dynamics of chemical elements in forest litter. *Ecology* 76:1393–1406
- Leberrecht M, Dannemann M, Tejedor J, Simon J, Rennenberg H, Polle A (2016) Segregation of nitrogen use between ammonium and nitrate of ectomycorrhizas and beech trees. *Plant, Cell Environ* 39:2691–2700
- Lindsay WL, Moreno EC (1966) Phosphate phase equilibria in soils. *Proceedings of the SSSA* 24:177–182
- Marschner H (1995) *Mineral nutrition of higher plants*. Academic press London, 889 pp
- Niemeyer T, Ries C, Härdtle W (2010) *Die Waldgesellschaften Luxemburgs*. Vegetation, Standort, Vorkommen und Gefährdung. *Ferrantia* 57, Musée national d'histoire naturelle, Luxembourg, 122 pp
- van Oijen D, Feijen M, Hommel P, den Ouden J, de Waal R (2005) Effects of tree species composition on within-forest distribution of understorey species. *Appl Veg Sci* 8:155–166
- Pärtel M (2002) Local plant diversity patterns and evolutionary history at the regional scale. *Ecology* 83:2361–2366
- Read DJ, Perez-Moreno J (2003) Mycorrhizas and nutrient cycling in ecosystems—a journey towards relevance? *New Phytol* 157:475–492
- Shen J, Yuan L, Zhang J, Li H, Bai Z, Chen X, Zhang W, Zhang Z (2011) Phosphorus dynamics: from soil to plant. *Plant Physiol* 156:997–1005
- Swift MJ, Heal OW, Anderson JM (1979) *Decomposition in terrestrial ecosystems*. University of California Press, Berkeley
- Tooren BF van, Sparrius LB (2007) *Voorlopige verspreidingsatlas van de Nederlandse mossen*. Bryologische en Lichenologische Werkgroep van de KNNV, 350 pp
- Tyler G (2003) Some ecophysiological approaches to species richness and calcicole/calcifuge behaviour—contribution to a debate. *Folia Geobotanica* 38:419–428
- van der Meijden R (2005) *Heukels Flora van Nederland, drieëntwintigste druk*. Wolters-Noordhoff, Groningen
- Vandelook F, van de Moer D, van Assche JA (2008) Environmental signals for seed germination reflect

- habitat adaptations in four temperate Caryophyllaceae. *Funct Ecol* 22:470–478
- van den Berg LJJ, Dorland E, Vergeer P, Hart M, Bobbink R, Roelofs JGM (2005) Decline of acid-sensitive plant species in heathland can be attributed to ammonium toxicity in combination with low pH. *New Phytol* 166:551–564
- van Calster H, Baeten L, Verheyen K, de Keersmaecker L, Dekeyser S, Rogister JE, Hermy M (2008) Diverging effects of overstorey conversion scenarios on the understorey vegetation in a former coppice-with-standards forest. *For Ecol Manage* 256:519–528
- Verhagen JM, Duyts H, Laanbroek HJ (1992) Competition for ammonium between nitrifying and heterotrophic bacteria in continuously percolated soil columns. *Appl Environ Microbiol* 58:3303–3311
- Verhoef P (1966) Geomorphological and pedological investigations in the Redange-sur-Attert area (Grand Duchy of Luxemburg). Ph.D.-thesis University of Amsterdam, 531 pp
- Wardenaar ECP, Sevink J (1992) A comparative study of soil formation in primary stands of Scots pine (planted) and poplar (natural) on calcareous dune sands in the Netherlands. *Plant Soil* 140:109–120
- Werf S van der (1991) Bosgemeenschappen; Natuurbeheer in Nederland deel 5. Pudoc Wageningen
- Zohlen A, Tyler G (2004) soluble inorganic tissue phosphorus and Calcicole-Calcifuge behaviour of plants. *Ann Bot* 94:427–432
- Zvereva EL, Toivonen E, Kozlov MV (2007) Changes in species richness of vascular plants under the impact of air pollution: a global perspective. *Glob Ecol Biogeogr* 17:305–319

Steinmergelkeuper Forest Soils in Luxembourg: Properties and Pedogenesis of Soils with an Abrupt Textural Contrast

9

L.H. Cammeraat, T.M.W. van den Broek and
J.M. Verstraten

Abstract

The process of clay dispersion and soil formation is investigated for an ‘in situ’ soil under semi-natural deciduous forest in Luxembourg on Steinmergelkeuper marls. We studied the genesis of these soils with a characteristic abrupt textural contrast between the topsoil and the subsurface soil. During and after rainfall, subsurface flow is generated, laterally transporting and exporting dispersed clay downslope at the interface between the silty topsoil and the clayey Bg horizon. This process resulted in a relative coarse silty and shallow topsoil, directly on a clayey Bg horizon. On hillslope positions, the clay content increased from 23% clay in the topsoil to 50% in the subsurface horizons. This abrupt textural contrast was less pronounced in soils on water divides and the colluvial valley bottom. The non-calcareous soils had an AEh–EAh–Bg–Bw–C horizon sequence, a near neutral pH, a very high base saturation (>96%) dominated by Ca and Mg, and a relative organic matter rich topsoil. They are classified as Luvic Planosols. The main mechanism involved in the development of the textural contrast in the soil was the swelling and dispersion of (fine) clay from the top of the Bg horizon, and its lateral transport in macropores downslope over the almost impervious Bg horizon. The high macroporosity and hydraulic conductivity finds its origin in bioturbation, and swelling and shrinking of the topsoil. The laterally transported (fine) clay was dispersed from the top of the Bg horizon, as indicated by the similarity in the clay mineralogy of clay of the Bg horizon and dispersed clay sampled in subsurface flow and stream. The absence of stabilizing agents in the Bg horizon, such as organic matter, carbonates and pedogenic sesquioxides, allowed slaking of

L.H. Cammeraat (✉) · J.M. Verstraten
IBED Earth Surface Science, University
of Amsterdam, Science Park 904, 1098 XH
Amsterdam, The Netherlands
e-mail: l.h.cammeraat@uva.nl

Present Address:
T.M.W. van den Broek
Hoevelmanweg 2, 7431 RB Diepenveen
The Netherlands

macro-aggregates, followed by the swelling of micro-aggregated clay. This swelling was caused due to the very low electrolyte content of the soil solution, which was always below the flocculation value of the clay of the Bg horizon. In addition, the dispersion domain of this soil material was enlarged by soluble humic substances, which were adsorbed at the clay particles. This lateral eluviation process of clays, or subsurface erosion of the Bg horizon, was the main process explaining the sharp abrupt textural contrast in these soils.

9.1 Introduction

The soils under semi-natural forest on the Steinmergelkeuper in the Luxembourg Lias Cuesta landscape exhibit a very characteristic and distinct textural difference between the A and B horizon. The origin of this abrupt textural change will be unraveled and discussed in this chapter. Textural differences between parent material, subsoil and topsoil occur in soils of all climates and are often an eye-catching feature. Beside inheritance from the substrate, e.g. textural variations in sediments and weathered sedimentary rocks, these textural differences can be due to soil forming processes. Textural differentiation mostly leads to topsoils and subsoils that are either finer or coarser than the parent material, and has a strong effect on soil hydrology and conditions for plant growth.

At least seven soil processes can result in textural differentiation, such as lithological discontinuities, pervection, hydrolysis of clay, ferralization, selective ejection, bioturbation and impoverishment of clay (Blume et al. 2016; IUSS 2015; Soil Survey Staff 2014; Van Breemen and Buurman 2002). In soil classification systems, downward transport of clay suspended in percolating soil water is emphasized.

In this chapter, the soils on the forested Steinmergelkeuper marls and their properties will be discussed. Special attention is given to the processes and conditions relevant for the impoverishment of the topsoil, e.g. the formation

of the abrupt textural contrast between mineral topsoil and subsurface soil, and its consequences for the hydrology in the forested Schrondeweilerbach catchment, Luxembourg. The aim of this chapter is to illustrate the specific soil chemical and physical properties of the Steinmergelkeuper soils (Sects. 9.2–9.4), and to explain the genesis of the abrupt textural change (Sect. 9.5). This chapter is mainly based on the monograph type Ph.D.-theses of van den Broek (1989) and Cammeraat (1992) on forested Steinmergelkeuper catchments, from which previously unpublished data and sections have been incorporated. Their combined findings are important for specific soil formation processes. For this study area, some erosion data are adapted and incorporated from Duijsings (1985), Poeteray et al. (1984) and Chap. 3 in this book. In addition, many other papers, based on work in the same region by researchers from the University of Amsterdam team, are referred to in this chapter (Bonell et al. 1984; Cammeraat 2002, 2006; Cammeraat and Kooijman 2009; Duijsings 1985, 1986, 1987a, b; Hazelhoff et al. 1981; Hendriks and Imeson 1984; Hendriks 1993; Imeson and Jungerius 1977; Imeson and Vis 1984a, b; Imeson 1986; van Hooff 1983; van Hooff and Jungerius 1984; Jungerius 1980; Jungerius and Mucher 1970; Jungerius and van Zon 1982; Jungerius et al. 1989; Kooijman and Cammeraat 2010; Chap. 10, this book). Also data collected by students for their internal and unpublished M.Sc.-theses were used.

9.2 Description of the Research Area

9.2.1 The Field Site: Climate, Geology, Geomorphology, Hydrology and Vegetation

The area of study is located within the semi-natural, completely forested part of the Schrondeweilerbaach catchment (Fig. 9.1), with a rolling landscape and slopes up to 6° in the Gutland region of Luxembourg (south of Diekirch), which has been studied in detail since the 1970s. The climate is mesic, with mean temperatures of 0.8 °C in January and 17.2 °C in July, a mean annual temperature of 9.1 °C, and an average yearly rainfall of 788 mm (Ettelbruck meteo station). Generally, July (local storms), November and December (frontal storms) are slightly wetter, and April and September somewhat drier, but the coefficient of variation in monthly precipitation amounts is large (9.0–15.3%). High rainfall intensities are rare (0.9% of the total storms), and 85% of the storms have lower intensities than 10 mm per hour (Duijsings 1985). Interception loss, the difference between gross rainfall and throughfall, was about 65% of the gross rainfall, and was similar throughout the subcatchment (Cammeraat 1992).

The field site studied is situated in a subcatchment of about 4 ha, underlain by the Steinmergelkeuper Formation (km³). This formation consists of a horizontally layered variegated marl with thin layers of dolomite (max. 5 cm), with a total thickness of 40–60 m (Lucius 1948). Near the surface, weathered marl is found with a heavy texture, with up to 50–60% of clay. The weathered upper part of the marl is non-calcareous and shows a blocky structure. The subcatchment is situated near the head of the divide, and has now a combined natural and artificial drainage network (Fig. 9.2). The subcatchment can be divided into four geomorphological main units, which are relevant for the differences in soil profile

development and hydrological processes (Cammeraat 1992) and which are indicated with four different colours in Fig. 9.2:

- (1) The broad watershed areas (green in Fig. 9.2) with closed depressions of 20–50 cm depth, poor drainage and frequent water stagnation. On top of the in situ soil profile in the depressions, a very thin layer of colluvium of a few centimetres was often present. The soil had a textural contrast between topsoil and subsurface soil, although less clear when compared to the surrounding sloping areas.
- (2) The gentle watershed slopes (3–6°) (darker blue in Fig. 9.2). This unit had the steepest slopes of the subcatchment, with wetter soil conditions at the concave transition between these slopes, and at the foot slopes. Soils were well developed, with a clear abrupt textural change. On the slopes, depressions occur as well, which are important for the generation of runoff (partial areas).
- (3) The very gentle sloping (<3°) areas (light blue in Fig. 9.2). These areas were similar in soil development and micro-topography as unit (2), but had more gentle sloping surfaces with shallower depressions.
- (4) The valley bottom (pink in Fig. 9.2). This part of the subcatchment has very low slope angles (0.5–2.0°). The valley bottom was developed in colluvial deposits lying on the weathered Steinmergelkeuper marls, and never exceeded a thickness of 40 cm, with an average of 20 cm. The textural contrast was less clear in comparison to the sloping units. Discontinuous channel-like depressions were present with a depth of up to 30 cm. Flowpaths of overlandflow have eroded through the colluvium and the topsoil of the Steinmergelkeuper soil material, and the surroundings of the channels were very moist. The pattern of natural depressions (brown in Fig. 9.2) and natural drainage system was overprinted by a partly artificial drainage system dug in the 1930s.

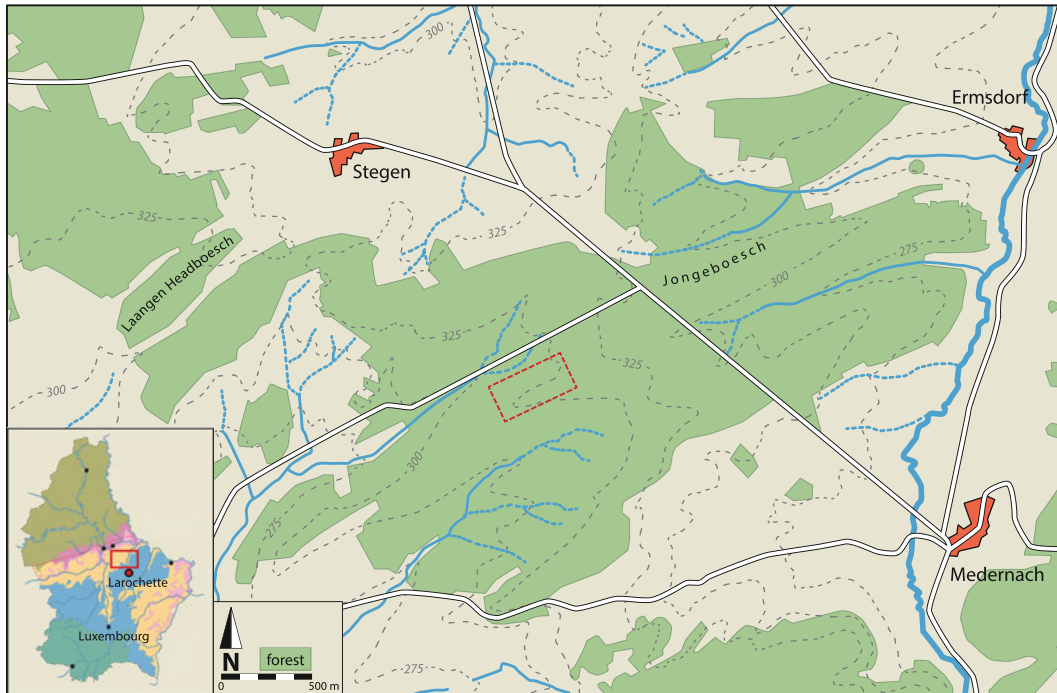


Fig. 9.1 Location of the research area. The *rectangle* indicates the instrumented subcatchment (Cammeraat 1992)

The subcatchment is covered by a semi-natural forest, consisting of oak (*Quercus robur* L.), hornbeam (*Carpinus betulus* L.), beech (*Fagus sylvatica* L.) forest, with locally shrubby undergrowth of mainly hawthorn (*Crataegus leavigata* L.) and ash (*Fraxinus excelsior* L.). Hornbeam was found in the wetter locations, whereas the drier parts were dominated by beech. The last forest thinning by selective felling of only mature trees took place in this part of the forest in the 1930s and lately around 2005, followed by natural succession (no replanting). The palynological data of Poeteray et al. (1984), van Mourik and Braekmans (2016) and as presented in Chap. 3 suggest that the forested Steinmergelkeuper catchments have had a forest cover for at least 2000 years.

For the forested Steinmergelkeuper subcatchment, current erosion rates are very low, indicated by low suspended solid outputs, which showed values of $0.765 \text{ tonne ha}^{-1} \text{ year}^{-1}$ (Duijsings 1985, 1987a, b). This equals approximately

0.05 mm of annual surface lowering, and confirms the average rates given by Poeteray et al. (1984) for the last 200 years ($0.020\text{--}0.054 \text{ mm year}^{-1}$). A more detailed discussion of soil properties related to erosion processes will be given in Chap. 10. Bonell et al. (1984) presented a relative simple hydrological model for runoff producing depressions in the forested Steinmergelkeuper subcatchment. It describes the runoff contributing process of a depression, which is generated by a combination of throughflow and saturation overlandflow, combining aspects of the variable source and partial area concepts. During storm runoff, pipeflow and macroporeflow occurred widely, related to perched water table rising into (the upper part of) the topsoil. Most important for runoff generation was the sharp decline in hydraulic conductivity with depth, at the boundary between the mineral topsoil (AEh + EAh horizons) and the subsurface (Bg horizon), which was continuously present along the slopes and watersheds. This caused temporal waterlogging of the topsoil. The

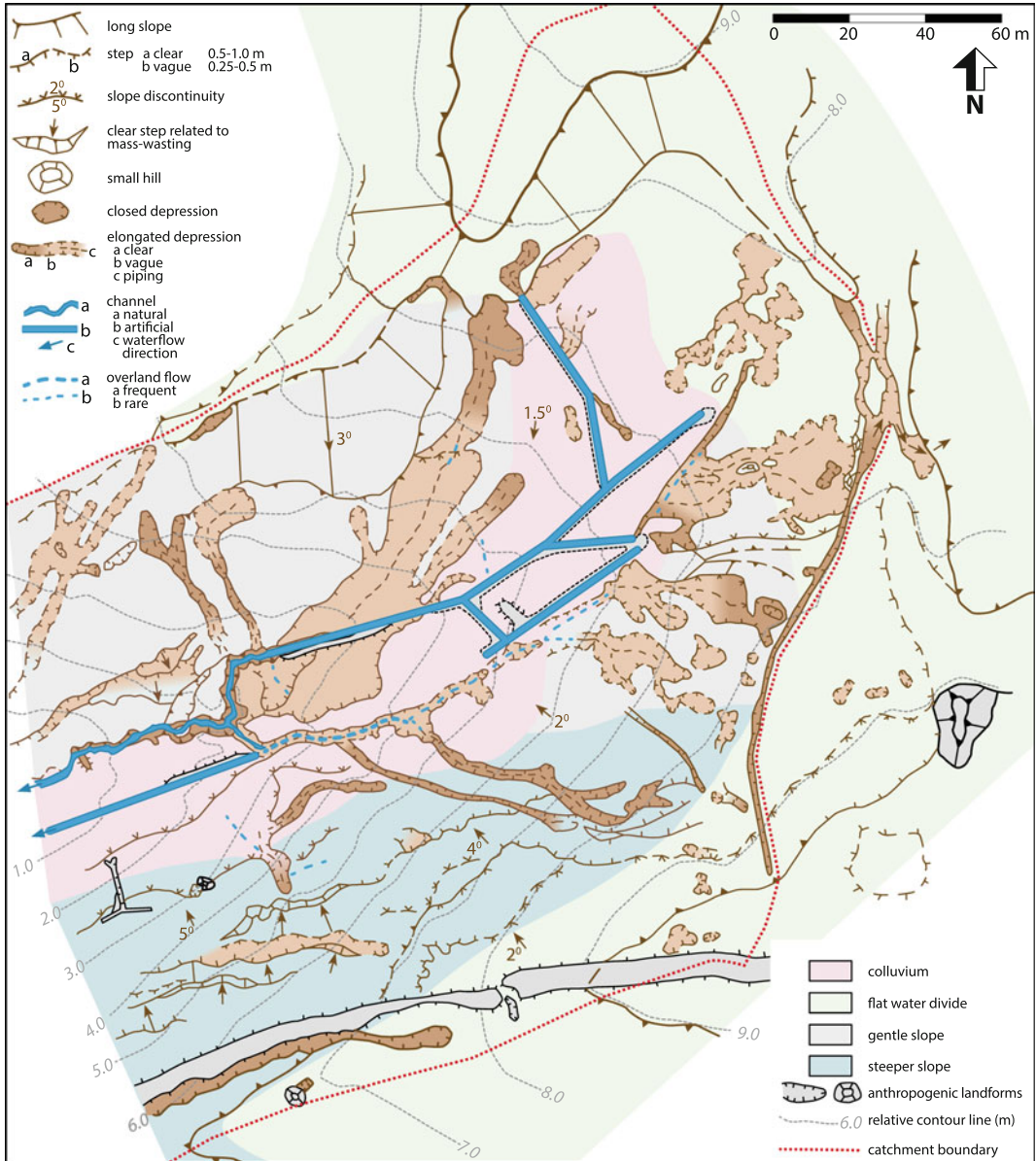


Fig. 9.2 Geomorphological map of the subcatchment (after Cammeraat 1992)

water moved laterally as throughflow (subsurface flow) through the topsoil horizons, over the Bg horizon. In periods with high rainfall and saturated topsoil conditions, saturation excess overland flow occurred. Water flowed in the topsoil dominantly through macroporosity and shrinkage cracks, and to a lesser degree, depending on wetting conditions of the soil, through the soil matrix. These soil

properties were strongly seasonal and spatial dependent, and influenced the dynamics of the lateral subsurface flow, perched water table and discharge.

Two subsystems in hydrological behaviour were distinguished, a wet and a dry subsystem (Fig. 9.3; Cammeraat 1992, 2002). Under normal meteorological conditions, the perched water table

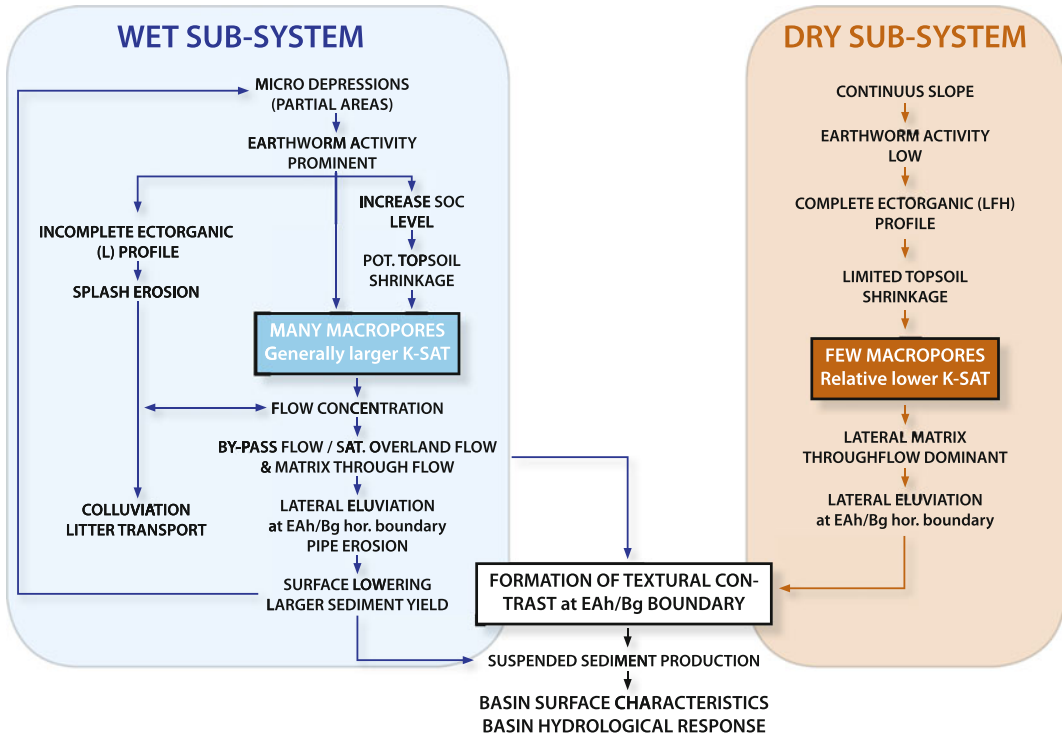


Fig. 9.3 Steinmergelkeuper forest hydro-geomorphological subsystem model (adapted from Cammeraat 1992). K-SAT = saturated hydraulic conductivity, SOC = soil organic carbon

started to develop in the wet subsystem (depressions) in mid-November or in December, and was continuously present until the end of March or April with regularly reoccurring discharge. In the summer half of the year, perched water tables occurred if the rainfall amounts and intensities were sufficient to refill the soil storage capacity, or to cause bypass flow. In this wet subsystem, bypass/pipe flow dominated the lateral matrix throughflow. In the dry subsystem (continuous slopes) however, only short periods of waterlogging occurred, even in winter months, so lateral matrix throughflow dominated in these areas (Cammeraat 1992, 2002). In Chap. 10, this process and landscape pattern relationship is further elaborated.

9.3 Soils

9.3.1 General Description of the Soils

The non-calcareous soils developed on the Steinmergelkeuper substratum under forest were characterized by a mineral topsoil (AEh and EAh horizons) with a silty loam texture, upon a strongly contrasting clayey subsurface soil (Bg, Bw, C1, C2 and C3 horizons). The boundary between the topsoil and the Bg horizon was mostly very abrupt, with the textural difference within 1 cm. Soils were classified as Aquic Dystric Eutrochrept (Soil Survey Staff 2014) or as Luvic Planosols, or when the textural change was less abrupt, as Luvic Stagnosols (IUSS

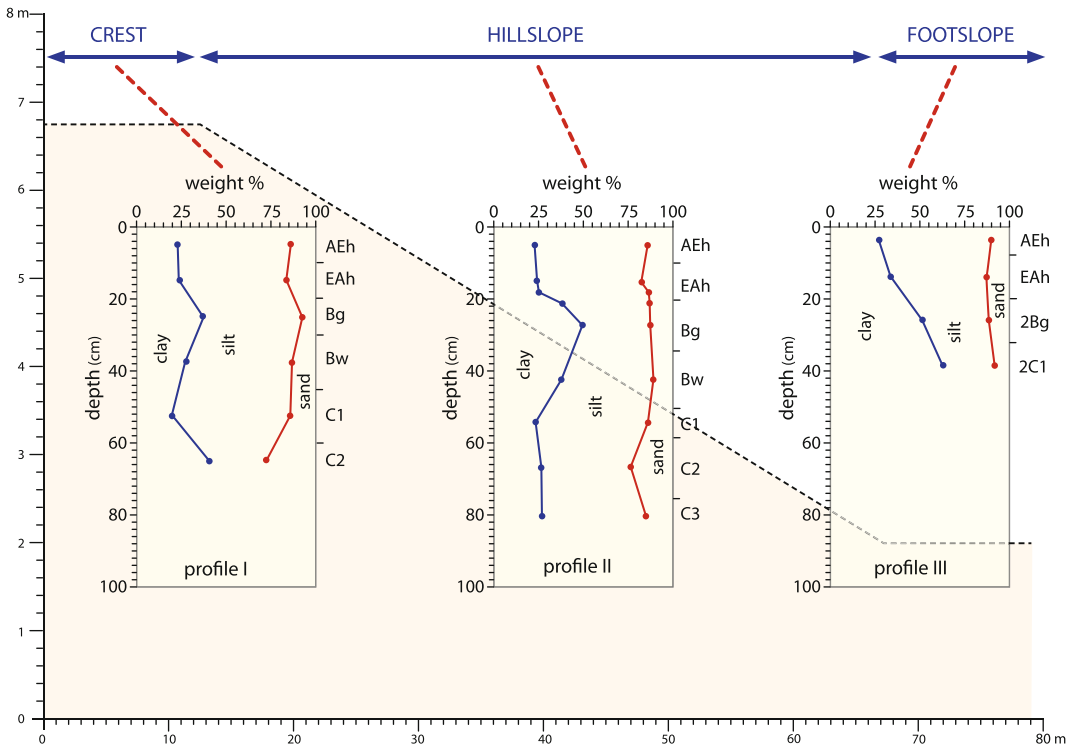


Fig. 9.4 Schematic catena of soil profiles with textural gradients in a forested Steinmergelkeuper slope; textural gradients are indicated (van den Broek 1989)

2015). Decalcification of the parent material took place to a depth of 85–90 cm.

The increase in texture, from ca. 20% clay in the topsoil to ca. 50% in the subsurface horizons, was found on all slopes in the geomorphic units (2) and (3), but much less on the geomorphic units (1) and (4) of crest and foot slopes (Fig. 9.2). Figure 9.4 gives a schematic catena with three soil profiles with their accompanying textural gradients. On the crest of the watershed, the textural gradient between topsoil and subsurface soil was more gradual (profile I in Fig. 9.4), while it became more pronounced on the mid-slopes (profile II in Fig. 9.4). The abrupt textural contrast was found everywhere on the mid-slopes, so it can be concluded that soil development at these sites was rather uniform (Dopheide 1986; van den Broek 1989). At the valley bottom in geomorphic unit (4), colluvium with 15–40 cm thickness has accumulated on the (partly truncated) Steinmergelkeuper soil, giving

rise to a similar type of soil, but with a more gradual textural change at the boundary of the EAh and the 2Bg (profile III in Fig. 9.4). The colluvial cover is deposited by splash and overland flow processes, and was found in the whole valley bottom of the subcatchment. Colluvium was also found in root cavities of fallen trees, and sometimes as apparent infillings in the EAh horizon, reminiscent of krotovina-like structures.

The AEh and EAh horizons had a (very) high biological activity and high bioturbation rates. Earthworms actively digested litter falling on the soil surface. The two topsoil horizons had a good structure, and many voids, biotic macropores and lateral shrinkage cracks occurred in dry periods. The presence and development of the ectorganic horizons (Green et al. 1993), which cover the mineral topsoil, had a strong spatial and seasonal variation. The type of litter and spatially divided activity of earthworms determined whether Litter (L), Fermentation (F) and Humus (H) horizons

were present. In the relatively wet partial areas within the geomorphic units (1), (2) and (3), ectorganic horizons were generally absent in late summer, as earthworm activity was concentrated here. During large parts of the summer and autumn, the mineral soil was directly exposed at the surface, with a litter forest floor cover of only 4% in August (Cammeraat and Kooijman 2009, see also Chap. 10). In dry areas, the humus profile was complete (LFH). Complete humus profiles were especially found under beech, located in relative dry areas. In such places, almost no litter was removed or decomposed, keeping the forest floor completely covered throughout the year with a thin, but complete ectorganic soil profile (Mormoder; Green et al. 1993). Under other types of vegetation,

especially under hornbeam, only a litter (L) horizon was present, and other ectorganic horizons were not encountered (Vermimull; Green et al. 1993).

Small differences in the thickness of the topsoil (AEh + EAh horizons) were of great importance for slope hydrology of the sub-catchment. Thickness of the AEh- and EAh horizons almost fully determined the water storage capacity of the Steinmergelkeuper soils. Due to a stronger surface lowering, the thickness of the topsoil in the wet partial areas was smaller (8–14 cm), than those of the dry subsystems (14–23 cm) on the continuous slopes (Fig. 9.3). Water storage capacity was also affected by the ectorganic horizons of the forest soils, as far as they are present. With a rainfall simulator, the

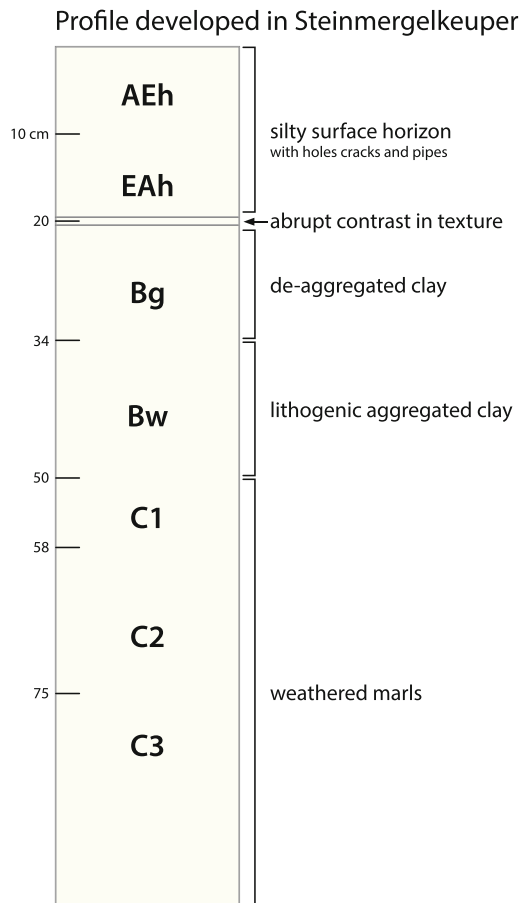


Fig. 9.5 Schematic profile of a textural contrast soil (van den Broek 1989)

water storage capacity of a fully developed L, F and H humus profile was determined as 12 mm of water, which is 9–10% of the total water storage capacity of the solum.

9.3.2 Texture and (Clay) Mineralogy

Soil profile II in Fig. 9.4, representative of the dominant soil type in the area and used as reference soil, will be presented in more detail with respect to its general properties (for detail soil description see Appendix 1). In addition, emphasis will be put on properties and features important for the pedogenesis of these forested soils. The non-calcareous soil had a dark brown silty loam-textured AEh and EAh horizons with high macroporosity (Fig. 9.5). These topsoil horizons were overlying a heavy clayey subsurface soil, consisting of Bg–Bw–C1–C2–C3 horizons. As mentioned before, the boundary between the silty loam surface horizons and the

brownish grey, clayey Bg horizon is smooth, but very abrupt. The Bg horizon has a coarse angular blocky structure, due to in situ weathering. In the underlying Bw- and C horizons, the lithogenic aggregation and structure are due to in situ weathering and/or inheritance of the structured marl parent rock (Dumbleton and West 1966). To illustrate the textural contrast between surface and subsurface horizons, the result of the standard particle size analyses are presented in Fig. 9.6. The amount of clay increased from 22% in the surface horizons to 50% in the Bg horizon.

9.3.2.1 Uniformity of the Soil Material

In order to exclude the possibility that the abrupt textural contrast was caused by lithological discontinuity in the Steinmergelkeuper, the uniformity of the parent material was tested by resistant heavy mineral indices, specific for this parent material (garnet, zircon and rutile), and relatively inert chemical element (Ti, Zr and Si) ratios (Barshad 1964). From the inert chemical element

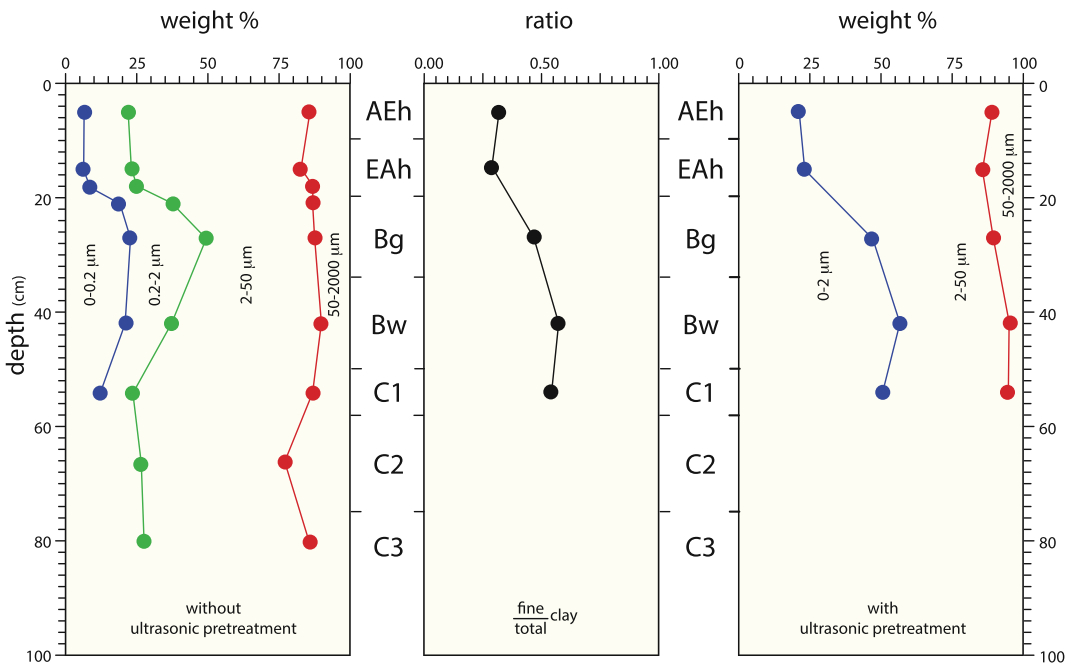


Fig. 9.6 Particle size distribution of soil profile II (on an abs. dry base): **a** classical method, without ultrasonic pretreatment; **b** ratio of fine clay to total clay, belonging to (a); **c** classical method, with very short ultrasonic pretreatment (van den Broek 1989)

ratios, and heavy minerals in the 105–150 and 32–50 μm fractions in all soil horizons, it was found that the parent material is rather uniform, without lithological discontinuities (van den Broek 1989). In addition, the Steinmergelkeuper soil contained only very small admixtures of non-Steinmergelkeuper minerals throughout the soil profile, such as epidote from loess and brown amphiboles, pyroxenes, titanite and apatite from airborne tephra of Allerød age (Lucius 1961; see also Chap. 2). The development of the textural contrast thus took place in a rather uniform parent material, originating from the Steinmergelkeuper parent rock with only very small admixtures of loess and volcanic ashes, which cannot explain the contrast between the topsoil and the subsurface soil.

9.3.2.2 Origin of Higher Clay Contents in the Bg Horizon

Deeper in the profile, in the Bw and C horizons, the clay content, measured with conventional particle size analyses, decreased compared to the Bg. At first sight, the clay bulge in the Bg horizon fits with the process of clay eluviation from the topsoil, and illuviation into the subsurface horizon. However, the trend of increasing and decreasing clay content with depth does not match with the observed ratio of fine to total clay (Fig. 9.6b). If the illuviation of clay had been important in these profiles, the ratio fine to total clay should have a maximum in the Bg horizon, and a much lower value in the C horizon. However, the ratio of fine to total clay remained almost constant for the Bg, Bw and C1 horizons, which is a strong argument against illuviation in the Bg. Also, when particle size analyses were preceded by ultrasonic pretreatment of the soil material (Fig. 9.6c), in order to destruct micro-aggregates made of clay particles (pseudo-silt), the increase in clay content from EAh to Bg horizons was still present, but the decrease in clay content towards the deeper part of the profile disappeared. From the Bg horizon on, the clay content was more or less constant with depth, due to this ultrasonic pretreatment, which destroyed the strong (lithogenic) aggregation between clay particles in the Bw and C

horizon. The more or less equal clay contents in Bg, Bw and C horizons again excludes the process of clay illuviation. In addition, micromorphological observations in these forested Steinmergelkeuper soils showed no illuvial coatings of oriented clay in the Bg horizon. On peds in the upper and lower part of the Bg horizon, (disturbed) argillans were absent, which supported the results of the adapted particle size analyses. Consequently, the higher clay content in the Bg horizon must be due to in situ weathering rather than illuviation from the topsoil.

9.3.2.3 Clay Mineralogy of the Soils

For the development of the model of the pedogenesis for the forested textural contrast soil, the relationship between the clay mineralogy of the soil profiles and the dispersed clay in runoff water was of great importance.

Together with soil chemical characteristics, the clay mineralogy of the profile determines the weathering status of the soil material, which is strongly related to the potential dispersability of the clay, as well as to the electrolyte concentration of the soil solution (Blume et al. 2016). For the mineralogical data, reference is made to diffraction patterns of the Mg-saturated, glycerol treated samples of total and fine clay fractions, as presented in Fig. 9.7. The clay mineralogy of the fine ($<0.2 \mu\text{m}$), coarse ($2\text{--}0.2 \mu\text{m}$) and total clay ($<2 \mu\text{m}$) fraction of the soil horizons is summarized in Table 9.1.

For the (lateral) transport of dispersed clay, the swelling 32 \AA interstratification is particularly important. The first-order reflection of this interstratification is very weak. Therefore, this interstratification is described by its very distinct second-order reflection at 16 \AA . In the fraction $<2 \mu\text{m}$ of the surface horizons, the swelling interstratification was almost absent. This is in contrast to the horizons below the textural contrast, in which this interstratification was clearly present. In addition, the dispersed clay transported by the subsurface flow also contained this swelling interstratification. The clay mineralogy in different clay fractions is summarized as follows (Table 9.1 and Fig. 9.7): Illite (10 \AA) and some kaolinite (7 \AA) were present throughout the

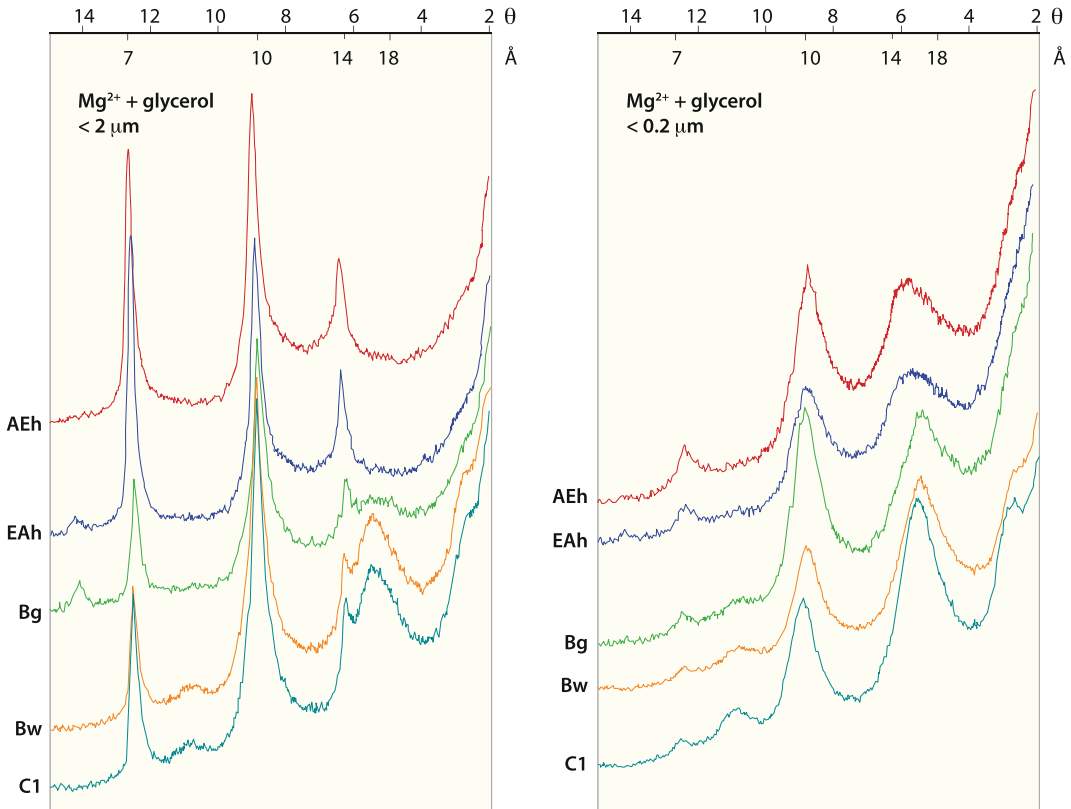


Fig. 9.7 X-ray diffraction patterns of the total clay and fine clay fractions (van den Broek 1989)

complete profile in the fine, coarse and total clay fraction. As indicated before, this was different for the swelling 16 Å interstratification. In the fine clay fraction, the swelling 16 Å interstratification was found in all horizons. In the coarse clay fraction, the swelling 16 Å interstratification was however lacking in the surface horizons. In the total clay fraction, the swelling interstratification was also not detectable in the surface horizons, but clearly present in the B- and C horizons. This swelling 16 Å interstratification is very characteristic for the Steinmergelkeuper marl. In the German Steinmergelkeuper, an interstratified mineral was found as well, and is described as corrensite, being a regular layer structure of a trioctahedral chlorite with vermiculite (Lippmann 1954, 1956, 1960). This interstratification chlorite-vermiculite was present in the fine, coarse and total clay of the complete soil profile. Chlorite was especially dominant in the

total and coarse clay fractions of the surface horizons. In our Steinmergelkeuper soil, the mineralogical composition of the fine clay was constant throughout the profile (Fig. 9.7), and consisted mainly of illite and the swelling 16 Å interstratification. The fine clay fraction in particular, showed a (060) reflection at 1.539 Å, indicating the trioctahedral status. This agrees well with the high Mg content of the fine clay fraction (Table 9.2).

Interstratified clay minerals were present in the C horizon. These minerals in the parent material of the soil are inherited from the Steinmergelkeuper marl. The interstratified 16 Å mineral in the C horizon is not liable to weathering processes, in contrast to the clay minerals in the surface soil. Therefore, the X-ray diffraction pattern of the EAh horizon in the topsoil contained less ‘crystalline’ peaks compared to the overlying AEh and underlying Bg horizon.

Table 9.1 A (semi-)quantitative interpretation of X-ray diffraction patterns and Guinier-de Wolff photographs of clays from Profile II (van den Broek 1989)

Horizon	EAh	EAh	Bg	Bw	C1
<i>Coarse clay</i>					
16 Å	–	–	–	(+)	(+)
14 Å	++	++	++	++	++
10 Å	++	++	++	++(+)	++(+)
7 Å	(+)	(+)	(+)	(+)	(+)
Feldspar %	tr	tr	tr	tr	tr
Quartz %	4–6	3–5	2–4	1–3	1–3
<i>Fine clay</i>					
16 Å	++(+)	++(+)	++(+)	++(+)	++(+)
14 Å	–	–	–	–	–
10 Å	++ (+)	++ (+)	++ (+)	++	++
7 Å	(+)	(+)	(+)	(+)	(+)
Feldspar %	0	0	0	0	0
Quartz %	≪1	≪1	≪1	≪1	≪1
<i>Total clay</i>					
16 Å	tr	tr	(+)	+	(+)
14 Å	++(+)	++(+)	(+)	(+)	+
10 Å	++(+)	++(+)	++	++	++
7 Å	(+)	(+)	(+)	(+)	(+)
Feldspar %	tr	tr	tr	tr	tr
Quartz %	4–6	3–5	1–3	ca. 1	ca. 1

The scale of relative intensities ranges from
 – absent; *tr* trace, (+) small amounts to ++(+)
 large amounts

The lower crystallinity of clay minerals agreed well with the lower cation exchange capacity in the EAh horizon (Table 9.2). The broad reflections together with the relative low CEC data of the topsoil indicated a blocking of the interlayer exchange sites by hydroxy-interlayering.

In order to assess the contribution of (strong) weathering to the development of the abrupt contrast in texture, the character of the hydroxyl-interlayering has been checked. The CEC of hydroxy-interlayered clay minerals has a wide range (Barnhisel and Bertsch 1989). The more complete the interlayer occupation, the lower the CEC value. Considering the CEC and the crystallinity of the clay of profile II (Table 9.2), hydroxy-interlayering in the topsoil has taken place. Interlayered Al/Mg/Fe(II)-hydroxy material

in the EAh, Bw and C1 horizons, and in the lateral transported dispersed clay, was removed selectively by a sodium-citrate treatment after Brinkman (1979). After destruction of the hydroxide sheets, the remaining clay should respond similar in X-ray diffraction to ionic saturation and various heat treatments as the ‘standard’ mineral. Samples with and without removal of the hydroxy-interlayering with sodium-citrate were compared. The samples with hydroxy-interlayering removal showed only a partial collapse from 16 to 14 Å, and considerable reflections still existed at 16 Å. This implies that only a small part of the hydroxide sheet has been removed. The remaining hydroxy-interlayering is probably part of the chlorite structure. This indicates that the contribution of the (sub) recent weathering processes to the

Table 9.2 General chemistry of the fine earth (<2 mm), the clay (<2 µm), the coarse clay (2–0.2 µm), and the fine clay (<0.2 µm) of Profile II on an abs. dry base (van den Broek 1989)

Horizon	Depth (cm)	Fine earth										Clay								
		pH (CaCl ₂) ^a		pH (H ₂ O) ^b	org C ^c	C/N ratio ^d	CEC ^{c-eff}	Base sat. ^f	Ca	Mg	K	Na	Al	Mn	Fe	Acidity ^h	Ca/Mg ratio	Total	Coarse	Fine
		Exchangeable cations ^g (mmol _c kg ⁻¹)																		
AEh	0–10	5.44	5.87	40.0	15.9	13.8	95.9	92	33	6.6	0.7	0.0	2.5	0.1	0.69	2.82	227	185	318	
EAh	10–20	5.14	5.75	22.0	13.6	10.4	96.3	65	31	3.8	0.4	0.0	1.8	0.0	0.58	2.13	198	158	295	
Bg	20–34	5.51	6.20	8.0	10.1	20.6	100.0	121	73	7.5	0.6	0.0	2.9	0.0	0.00	1.65	291	227	457	
Bw	34–50	5.83	6.48	4.0	nd	31.0	100.0	180	98	9.3	0.9	0.0	0.6	0.0	0.00	1.84	349	291	550	
C1	50–58	6.57	7.14	2.8	nd	29.0	100.0	202	81	8.4	0.8	0.0	0.1	0.0	0.00	2.51	345	280	559	

^apH(CaCl₂, 0.01 M), soil/solution (w/v) ratio of 1:2.5^bpH(H₂O), soil/solution (w/v) ratio of 1:2.5^cOrganic C (g kg⁻¹), based on Allison (1960)^dC/N quotient, based on organic C and total N by the Kjeldahl procedure^eEffective CEC determined by 0.01 M silver thiourea, based on Chhabra et al. (1975)^fBase saturation: $\Sigma (Ca + Mg + K + Na)/CEC_{eff} * 100\%$ ^gExchangeable cations determined in the silver thiourea centrifugate, based on Chhabra et al. (1975)^hExchangeable acidity, titration with NaOH to pH 8.3ⁱBa-clay shaken with MgSO₄ solution (Brinkman 1979)

nd = not determined

Table 9.3 Water soluble salts for the soil profile on the hillslope (reference profile), in a weight to volume ratio of 1:1, 1:2 and 1:5 extracts on an abs. dry base, Alk = alkalinity

Hor	w/v	pH	EC ₂₅ µS cm ⁻¹	K mM	Na	NH ₄	Ca	Mg	Fe	Mn	Al	Si	Alk	Cl	NO ₃	NO ₂	P _{ortho}	SO ₄	DOC ⁻¹ mgC L	Ratio Ca/Mg
	1:2	6.07	148	0.157	0.153	0.080	0.411	0.286	0.009	0.017	0.020	0.287	0.720	0.108	0.001	0.000	0.006	0.106	75	1.4
	1:5	6.10	82	0.107	0.085	0.050	0.224	0.149	0.008	0.009	0.014	0.155	0.420	0.055	0.002	0.001	0.008	0.054	43	1.5
EAh	1:1	6.03	145	0.073	0.165	0.098	0.340	0.269	0.008	0.007	0.016	0.291	0.533	0.143	0.081	0.006	0.003	0.163	111	1.3
	1:2	6.10	87	0.055	0.109	0.011	0.217	0.165	0.008	0.005	0.015	0.184	0.347	0.070	0.062	0.004	0.003	0.093	35	1.3
	1:5	6.05	48	0.038	0.048	0.009	0.122	0.089	0.008	0.003	0.012	0.101	0.210	0.027	0.026	0.002	0.002	0.060	24	1.4
Bg	1:1	6.69	124	0.035	0.111	0.016	0.289	0.232	0.002	0.001	0.000	0.240	0.467	0.100	0.036	0.003	0.001	0.191	35	1.2
	1:2	6.61	74	0.026	0.069	0.013	0.186	0.147	0.004	0.001	0.004	0.213	0.327	0.048	0.018	0.001	0.002	0.115	11	1.3
	1:5	6.63	40	0.019	0.038	0.007	0.131	0.099	0.006	0.001	0.017	0.179	0.227	0.016	0.007	0.001	0.002	0.086	8	1.3

development of the textural contrast by transformation and destruction of clay minerals by hydroxy-interlayering is only very subordinate.

The CEC of the fine, coarse and total clay fractions are given in Table 9.2. The CEC of the total clay ranged from 200 mmol_c kg⁻¹ clay for the surface horizons to 350 mmol_c kg⁻¹ clay for the C horizon. This trend of increase in CEC with increasing depth was shown for the coarse and fine clay as well. For the coarse clay, CEC in the topsoil was around 170 mmol_c kg⁻¹ coarse clay, while values amounted to almost 300 mmol_c kg⁻¹ coarse clay in the subsurface horizons. The fine clay had the highest CEC values, with values ranging from 300 to 550 mmol_c kg⁻¹ fine clay in surface and C horizon respectively. In the EAh horizon, CEC values of the fine, coarse and total clay were lower than deeper in the soil. This could be an indication of slight weathering, some hydroxy-interlayering and/or selective removal of clay minerals of the topsoil.

9.3.3 Soil Chemical Properties

In Table 9.2, the chemistry of the reference soil profile (soil profile II, Appendix 1) is summarized with regard to pH, organic carbon content, C/N ratio, cation exchange capacity, base saturation, adsorbed cations and adsorbed Ca/Mg ratio. The pH(H₂O) of the surface horizons was around 5.8, whereas it was 6.2 for the Bg horizon. Two to four percent organic carbon was found in the topsoil, but the subsurface horizons contained almost no organic matter. The Corg/N ratio of the surface horizons was around 15. Base saturation was very high, with 96–100% throughout the profile. The exchange complex was (almost) completely saturated by Ca and Mg. The adsorbed Ca/Mg ratio of these soils was around 2. It is emphasized that the Bg horizon, just below the abrupt textural contrast, had the lowest adsorbed Ca/Mg ratio (1.7), and a base saturation of 100%. The level of adsorbed K and Na ions at the exchange complex was very low, less than 10 mmol_c kg⁻¹ soil. The Steinermergelkeuper soil is thus characterized by (almost) complete base saturation of the cation

Table 9.4 Apparent charge balance (1–2) in $\text{mmol}_c \text{L}^{-1}$ and calculated organic anions according to Oliver et al. (1983) (van den Broek 1989)

Hor	w/v	(1)	(2)	(1–2)	Calculated org. anions	DOC (mgC L^{-1})
		Σ cat.	Σ inorg an.			
		$\text{mmol}_c \text{L}^{-1}$				
AEh	1:1	2.74	1.73	1.01	0.99	99
	1:2	1.78	1.05	0.73	0.75	75
	1:5	0.99	0.59	0.40	0.43	43
EAh	1:1	1.51	1.09	0.42	0.47	47
	1:2	0.94	0.67	0.27	0.35	35
	1:5	0.52	0.39	0.13	0.24	24
Bg	1:1	1.20	0.99	0.21	0.35	35
	1:2	0.77	0.63	0.14	0.11	11
	1:5	0.52	0.42	0.10	0.08	8

exchange complex, high Mg occupation, complete absence of exchangeable acidity, and a very low level of exchangeable Na and K.

Water extractable elements in the soil/water ratio (w/v) of 1:1, 1:2 and 1:5 were estimated (Table 9.3). The AEh horizon released in general twice as much water-soluble elements as the Bg horizon. Water extractable elements are strongly related to the saturation of the cation exchange complex. Overall, the concentration of Na, K and Al was again very low, with values of less than 0.23 mM for the monovalent cations, and 0.02 mM for Al. This was in contrast to the divalent cations Ca and Mg, which made up the bulk of the cations with a maximum of 0.6 and 0.5 mM respectively, and with a very low Ca/Mg ratio ranging from 1.2 to 1.5. All the extracts showed an apparent charge imbalance (Table 9.4). However, by including the pH-dependent negative charge of the organic anions, a reasonably good charge balance was achieved in the AEh and EAh horizons. In these horizons, the organic anions ranged from 30 to 50%, and contributed considerably to a negative charge. In the Bg horizon, with low organic carbon content, the apparent charge deficit was small compared to the surface horizons (<20%).

The low electrolyte level, low Na, K and Al levels and the relatively high Ca and Mg concentrations in the soil/water extracts are important with regard to clay dispersion. The

considerable contribution of the negative charged organic anions also plays a role (see Appendix 5). Based on the data given in Table 9.3, the selectivity coefficient K (Ca/Mg) for the exchange complex decreased from 2.3 to 1.9 to 1.4 for the AEh, EAh and Bg horizons respectively. This implies that the Mg ion had a higher affinity to clay in the Bg horizon than in the surface horizons. The high affinity of the clay in the Bg horizon for Mg fits in with the concept of clay dispersion at the top of this subsurface horizon, as will be explained later. As was expected for a homovalent cation exchange, the ratio of Ca and Mg in the equilibrium solution was not influenced by water dilution (Bolt and Bruggenwert 1978). The ratio Ca/Mg in the water extracts was constant for the 1:1, 1:2 and 1:5 weight to volume ratios, for each of the AEh, EAh and Bg horizons, with values of 1.4, 1.3 and 1.3 respectively. The constant Ca/Mg ratio in the equilibrium solution of the water extracts is comparable with the Ca/Mg ratios of the subsurface flow and the soil solution.

Finally, some data on the chemical (elemental) composition of the soil reference profile (profile II) will be presented. Elemental compositions of the fine earth fraction (<2 mm), total clay fraction (<2 μm) and the fine clay fraction (<0.2 μm) have been determined by X-ray fluorescence (trace) element analyses. Oxide contents of the silt fraction (2–50 μm) and coarse

Table 9.5 Major chemical elements (weight%) of the fine earth, silt, clay, coarse clay and fine clay of Profile II on an abs. dry base (fine earth, total- and fine clay) and on a LOI³-free base (silt and coarse clay) (van den Broek 1989)

	Hor	Depth	SiO ₂	Al ₂ O ₃	MgO	K ₂ O	TiO ₂	CaO	Na ₂ O	P ₂ O ₅	MnO	Fe _t (Fe ₂ O ₃)	Total	Fe ^{II} FeO	Fe ^{III} Fe ₂ O ₃	Free Fe Fe ₂ O ₃	SiO ₂ /Al ₂ O ₃	SiO ₂ /MgO
Fine earth	AEh	0-10	77.3	11.5	1.9	2.7	1.2	0.4	0.6	0.1	0.1	4.2	100	1.02	2.63	1.13	6.7	1.4
	EAh	10-20	76.9	11.6	1.9	2.8	1.2	0.3	0.5	0.1	0.1	4.6	100	0.94	3.41	1.59	6.6	0.8
	Bg	20-34	67.5	16.2	3.9	3.5	0.9	0.4	0.3	0.1	0.1	7.0	100	0.81	5.27	2.25	4.7	7.1
	Bw	34-50	63.7	17.9	5.8	4.0	0.9	0.6	0.3	0.1	0.1	6.7	100	1.12	4.81	1.37	3.6	1.0
	C1	50-58	63.6	17.5	5.7	3.8	0.9	1.1	0.3	0.1	0.1	7.0	100	1.20	4.95	1.59	3.6	1.3
Total clay		Depth	SiO ₂	Al ₂ O ₃	MgO	K ₂ O	TiO ₂	CaO	Na ₂ O	P ₂ O ₅	MnO	Fe _t (Fe ₂ O ₃)	Total	Fe ^{II} FeO	Fe ^{III} Fe ₂ O ₃	Free Fe Fe ₂ O ₃	SiO ₂ /Al ₂ O ₃	SiO ₂ /MgO
	AEh	0-10	51.7	25.9	5.4	5.0	1.5	0.1	0.3	0.2	0.1	9.8	100	1.77	6.50	2.36	2.0	9.6
	EAh	10-20	51.2	25.8	5.3	4.9	1.5	0.0	0.4	0.2	0.3	10.4	100	1.63	7.25	2.91	2.0	9.7
	Bg	20-34	52.3	24.6	6.5	4.8	0.8	0.0	0.2	0.1	0.2	10.3	100	0.90	8.10	3.30	2.1	8.0
	Bw	34-50	53.3	23.8	8.7	4.7	0.7	0.0	0.2	0.1	0.1	8.4	100	0.81	6.64	1.71	2.2	6.2
C1	50-58	52.4	23.9	8.8	4.8	0.8	0.1	0.2	0.1	0.1	8.9	100	0.97	6.76	2.15	2.2	6.0	
Fine clay		Depth	SiO ₂	Al ₂ O ₃	MgO	K ₂ O	TiO ₂	CaO	Na ₂ O	P ₂ O ₅	MnO	Fe _t (Fe ₂ O ₃)	Total	Fe ^{II} FeO	Fe ^{III} Fe ₂ O ₃	Free Fe Fe ₂ O ₃	SiO ₂ /Al ₂ O ₃	SiO ₂ /MgO
	AEh	0-10	52.6	23.4	8.3	3.7	0.4	0.0	0.1	0.3	0.1	11.1	100	1.04	8.02	3.51	2.3	6.3
	EAh	10-20	51.6	24.2	8.4	3.6	0.3	0.0	0.0	0.1	0.3	11.4	100	0.86	8.65	3.93	2.1	6.1
	Bg	20-34	53.9	23.6	8.3	4.0	0.2	0.0	0.1	0.1	0.2	9.4	100	0.64	7.41	2.63	2.3	6.5
	Bw	34-50	54.3	22.2	10.9	3.6	0.2	0.0	0.1	0.1	0.1	8.5	100	0.64	6.60	1.85	2.4	5.0
C1	50-58	53.9	21.8	11.5	3.6	0.2	0.0	0.2	0.0	0.0	8.6	100	0.66	6.78	2.14	2.5	4.7	
Silt		Depth	SiO ₂	Al ₂ O ₃	MgO	K ₂ O	TiO ₂	CaO	Na ₂ O	P ₂ O ₅	MnO	Fe _t (Fe ₂ O ₃)	Total				SiO ₂ /Al ₂ O ₃	SiO ₂ /MgO
	AEh	0-10	84.9	7.2	0.8	2.1	1.1	0.5	0.7	0.1	0.1	2.6	100				11.8	104.9
	EAh	10-20	84.7	7.4	0.9	2.1	1.0	0.4	0.5	0.1	0.1	2.9	100				11.5	97.0
	Bg	20-34	72.0	13.6	3.2	3.2	0.9	0.5	0.3	0.1	0.2	6.0	100				5.3	22.8
	Bw	34-50	66.8	16.2	5.0	3.8	0.9	0.7	0.3	0.1	0.1	6.2	100				4.1	13.4
C1	50-58	67.0	15.7	4.7	3.5	0.9	1.4	0.3	0.1	0.1	6.5	100				4.3	14.2	

(continued)

Table 9.5 (continued)

Hor	Depth	SiO ₂	Al ₂ O ₃	MgO	K ₂ O	TiO ₂	CaO	Na ₂ O	P ₂ O ₅	MnO	Fe _t (Fe ₂ O ₃)	Total	Fe ^{II} FeO	Fe ^{III} Fe ₂ O ₃	Free Fe Fe ₂ O ₃	SiO ₂ /Al ₂ O ₃	SiO ₂ /MgO
Coarse clay	AEh	51.2	27.0	4.0	5.6	2.0	0.1	0.4	0.2	0.1	9.2	100	2.59	4.92	1.65	1.9	12.7
	EAh	51.0	26.6	3.8	5.5	2.1	0.1	0.6	0.1	0.3	9.9	100	2.51	5.83	2.47	1.9	13.4
2–0.2 μm	Bg	51.6	25.1	5.7	5.2	1.1	0.0	0.2	0.1	0.2	10.7	100	1.58	8.00	4.10	2.1	9.0
	Bw	51.8	24.5	7.6	5.3	1.0	0.1	0.2	0.1	0.1	8.4	100	1.52	5.65	1.55	2.2	7.0
C1	50–58	51.6	24.9	7.5	5.4	1.0	0.1	0.3	0.1	0.1	9.0	100	1.66	6.03	2.10	2.1	6.9

^aLOI loss of ignition, material is free of (crystal) H₂O and carbon

clay fraction (2–0.2 μm) have been derived from these data and the grain size distribution (Table 9.5). The abrupt contrast in texture between the EAh and the Bg horizons showed up in the elemental composition, in particular in the fine earth and silt fraction. Here, an increase in the MgO and Al₂O₃ content from surface to subsurface horizons went along with a decrease in SiO₂. This supports the concept of impoverishment of the surface horizons of mainly fine clay, which had a high Mg content. Weathering conditions are not severe, as indicated by the constant SiO₂ and Al₂O₃ contents and ratios in the clay fractions. Also, the fine clay fraction is not subjected to strong weathering, considering the constant SiO₂/Al₂O₃ ratio and the almost constant SiO₂/MgO ratio. Slight weathering occurs, as shown by the percentages free Fe₂O₃ (Table 9.5). A maximum of free iron oxide showed up in the Bg horizon, except for the fine clay fraction (van den Broek 1989).

9.3.4 Soil Physical Properties

The key-factors in the hydraulic behaviour of the soils under forest in the Steinmergelkeuper region are the abrupt textural difference in the topsoil (AEh + EAh horizons) and the macroporosity in the topsoil (Cammeraat 1992). The first induces a sharp jump in hydraulic conductivity, and both influence the rate of drainage of these soils. Several soil physical properties of these soils are described below, as well as the character of the macroporosity of the soil. For macroporosity, biological activity by earthworms and moles is important. For the AEh and Bg horizons, pF curves are comparable with those of a silty clay loam and a clay soil respectively (Fig. 9.8). In the surface horizons, the soil matrix had a high porosity of 48–58% (Table 9.6). In the Bg horizon, the soil matrix is much denser, and had a porosity of 38%. The given porosity numbers do not include the macroporosity of larger crack and pore systems, as pF rings do not cover cracks and holes. Dry bulk density and soil moisture content of the AEh- and Bg horizons were also determined. Steinmergelkeuper soils

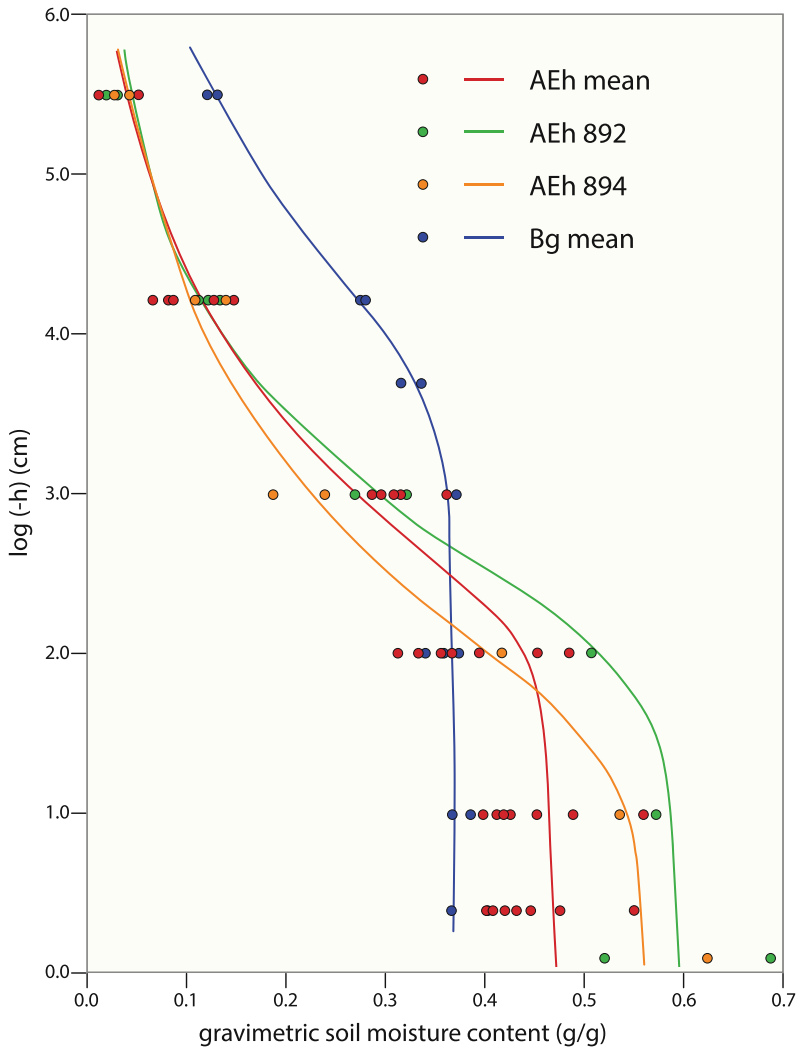


Fig. 9.8 Water retention curves of the AEh and Bg horizons (Cammeraat 1992)

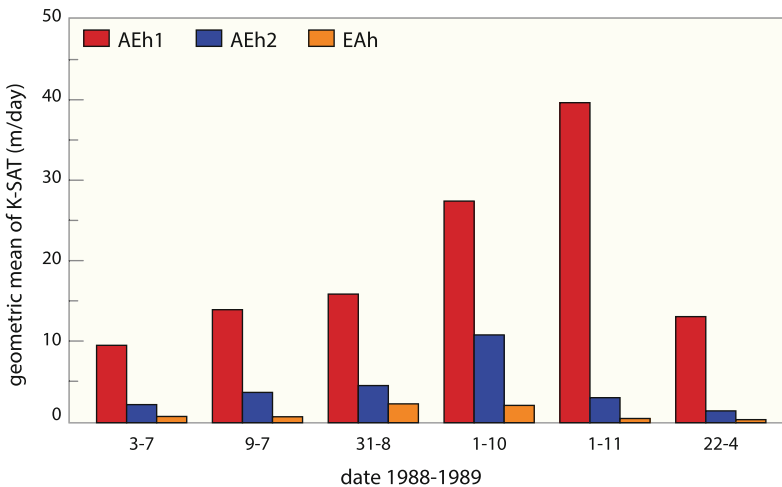
show clear shrinkage and swelling properties. Therefore, it was expected that dry bulk density would change with soil moisture content as well. The seasonality in the dry bulk density is very clear. During periods with high soil moisture content, dry bulk density was far lower than at low moisture levels. A significant correlation ($p < 0.05$) existed between the gravimetric soil moisture content and dry bulk density, although a hysteresis effect occurred between these two variables (Cammeraat 1992; Hendriks 1993). Dry bulk density of the AEh1 horizon ranged

from 773 till 1064 kg m^{-3} , while values of the Bg horizon ranged from 1278 till 1470 kg m^{-3} . Dry bulk densities of the Bw- and C horizons were between 1180 and 1470 kg m^{-3} (Cammeraat 1992; Dopheide 1986).

Both the spatial and temporal variability in macroporosity were considerable. Some soil physical properties showed a clear seasonal fluctuation due to shrinkage and swelling of the topsoil. Cracks in the surface horizons were the result of shrinking of soil material and the activity of moles. The cracks and holes

Table 9.6 Soil physical data of the forested Steinmergelkeuper soil (data adapted from Cammeraat 1992; Dopheide 1986; Hazelhoff et al. 1981; Imeson and Jungerius 1977)

	AEh horizon	Bg horizon
Texture class	Silt loam, 22% <2 μm	Clay, 50% <2 μm
Saturated hydraulic conductivity	10–40 m day^{-1}	<0.1 mm day^{-1}
Porosity	48–58%	38%
Dry bulk density	775–1110 kg m^{-3}	1280–1470 kg m^{-3}

**Fig. 9.9** Seasonal variation of K-sat for the topsoil horizons (Cammeraat 1992)

developed in particular at the contact between AEh and EAh horizons, and at the interface between EAh and Bg horizons (Fig. 10.2, in Chap. 10). The lateral cracks were interconnected and extended to the top of the Bg horizon. Due to these cracks, holes and macropores, the permeability of the topsoil was very high. The saturated hydraulic conductivity (measured by the inverse auger method) ranged from 10 to 40 m day^{-1} for the upper part, to 15–25 cm day^{-1} for the base of the surface horizon (Imeson and Jungerius 1977; Cammeraat 1992). The subsurface horizon had a clay content of approximately 50%, and the saturated hydraulic conductivity appeared to be less than 0.1 mm day^{-1} (Hazelhoff et al. 1981). Consequently, the percolation through the B and C horizons towards the stream was negligible, and according to Imeson et al. (1984), extremely localized.

Figure 9.9 shows the temporal variability in saturated hydraulic conductivity over the different seasons for the topsoil (A + E horizons) as well as the large decrease in conductivity with depth. The temporal variability in conductivity values was related to the temporal variability in the development of soil shrinkage cracks in the topsoil, which was virtually absent in the B horizons. The AEh₁ and AEh₂ horizons were significantly different with regard to the temporal variation in hydraulic conductivity if winter and summer conditions were compared (Cammeraat 1992).

Shrinkage was primarily the result of soil water depletion in the summer and autumn periods when the water balance was negative. Clay content and the 16 Å interstratification clay mineral were found to be most important for the swelling properties of the soil (van den Broek

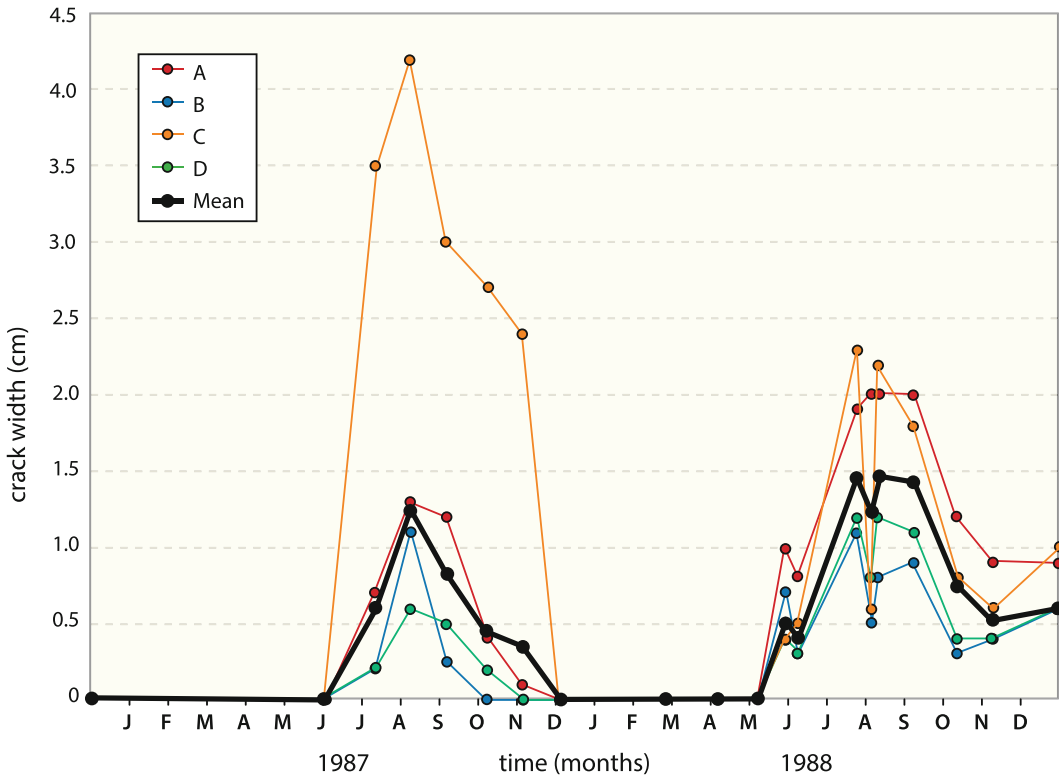


Fig. 9.10 Seasonal variation in shrinkage cracks width for four representative cracks. The thick line indicates the mean width of all measured cracks at the plot (Cammeraat 1992)

1989). However, this clay mineral was found in only very minor amounts in the topsoil, despite strong soil cracking (Table 9.1).

At the field site, large areal differences were observed in the density of cracks. Crack depth and width were greatest in the moister areas having a very high biological activity in the soil. The cracks tended to widen towards the boundary of the AEh and EAh horizons, and at the EAh/Bg horizon boundaries hollows were present in the EAh horizon. The cracks hardly penetrated into the Bg horizon, although the Bg horizon material had a higher shrinkage capacity than the two upper horizons. In general, the shrinkage cracks showed a hexagonal surface pattern. In Fig. 9.10, the seasonal change in crack width in the field is indicated. This change in width is a reflection of

the seasonal dynamics of the water balance and the physical aspects of the topsoil. The shrinkage capacity of the different soil horizons showed that the Bg horizon had the strongest shrinkage properties, followed by the C horizon. The topsoil horizons appeared to have soil shrinkage properties dependent on the organic matter content. The higher the organic matter contents of the AEh and EAh samples, the stronger the shrinkage properties were found to be, reaching similar values as those of the Bg horizon. After removal of organic matter from the soil by treatment with peroxide, the pastes of AEh material showed a considerably reduced shrinkage capacity, when compared to non-treated pastes. Material from the subsurface horizons did not show such behaviour (Cammeraat 1992).

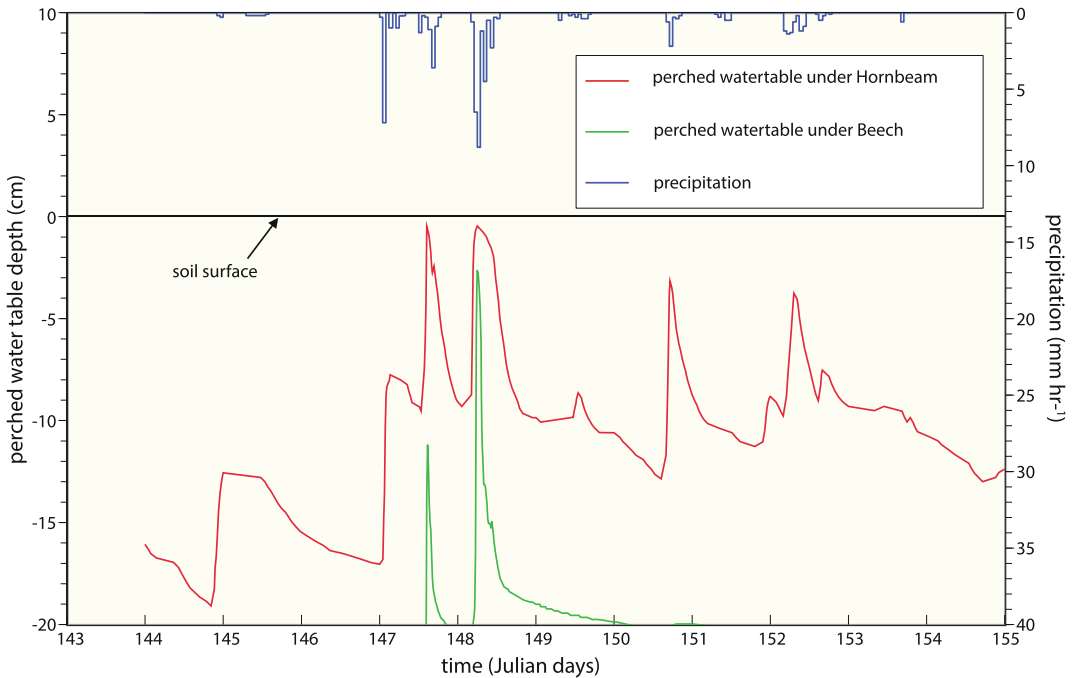


Fig. 9.11 Perched water table fluctuation as response on rainfall (reproduced with permission from: Cammeraat 2002)

9.4 Slope Hydrology and Water Characteristics

Some aspects of slope hydrology are described here in order to present the framework in which the dispersion of clay has been taken place. Slope hydrology in the subcatchment was studied in detail (Bonell et al. 1984; Duijsings 1985; Cammeraat 1992; Hendriks 1993), to investigate the hydrological discontinuities, which are characteristic for the forested Steinmergelkeuper watersheds. The low saturated hydraulic conductivity of the Bg horizon, and the high (macro)porosity in the relatively thin topsoil above, resulted in a subsurface flow or even saturation overland flow during and after rainfall (Bonell et al. 1984). Such preferential flow in pores, cracks and holes was common in soils with relative abundant macropores (e.g. Pilgrim

et al. 1978; Germann and Beven 1981; Jones 1997; Jarvis 2007). The lateral drainage pattern in the topsoil, together with the low saturated hydraulic conductivity of the Bg horizon, resulted in a low water storage capacity of these forested textural contrast soils.

In Fig. 9.11 the dynamics of water flow through and over the soil are illustrated. It shows the fast response of the perched water table to rainfall events in a very wet period in May/June. Apart from rainfall, two curves are shown, one reflecting the perched water table in a wet area, reflecting a partial area with pipe- and overland flow and hornbeam dominated vegetation, and one showing the perched water table in a nearby relative dry area under beech cover. The wet area showed many shrinkage cracks in autumn, with semi-permanent pipe systems, whereas the dry area was devoid of shrinkage cracks. At this part of the slope, no large shrinkage cracks occur, and

drainage has probably mainly taken place by matrix throughflow. At many places, pipe flow discharge was observed at the channel incision. These pipe outflow points are connected to larger pipe systems that are situated in elongated shallow depressions draining the wetter areas (see also Fig. 9.3).

At the upper hillslope, water was concentrated in pipe and crack systems present in an area with increasing perched water table height. Saturation excess overland flow was occurring at the mid slope, in the area with the highest perched water tables. Further downslope, at lower water tables, the water infiltrated diffusely and concentrates in pipe systems, leading towards the drainage ditch. The water table dropped towards the drainage ditch. The test slope discharged approximately 28% of the yearly output of the 4 ha sized sub-catchment and the partial area (20% of the slope area) delivered at least 50% of the slope discharge (Cammeraat 1992).

9.4.1 Chemical Characterization of Soil Solution and Subsurface Flow

9.4.1.1 Soil Solution

In order to obtain a chemical characterization of the soil solution on the abrupt contact between EAh and Bg horizons, porous cups were used to extract soil moisture under suction of 0.9 bar. Eighteen porous cups were installed on the 4–5° forested slope in an area of 25 * 35 m, at the contact plane between the surface and the subsurface horizons which ranged in depth from 14 to 18 cm. The soil solution chemistry over the year is given in Table 9.7. Average values together with the standard deviations are presented of pH, electrical conductivity (EC_{25}), Ca and Mg concentration, Ca/Mg ratio and Dissolved Organic Carbon (DOC). The chemistry of the soil solution sampled at relatively wet locations differed slightly from the dry locations. The EC_{25} , Ca and Mg concentration were somewhat higher at the relatively wet spots compared to the dry ones. This was in contrast to DOC, which showed the opposite trend. The average pH of

the soil solution on these wet and dry locations over the year ranged from 4.83 to 6.41. The EC_{25} had always a very low level, from 48 to 117 $\mu S\ cm^{-1}$. The ionic strength was very low, ranging in between 0.6 and 2.0 mM. The bulk of the cations in the soil solution consisted of Ca and Mg, whereas the contribution of Na and K was considerable less, around 0.1 mM (Fig. 9.12). The concentration of Ca and Mg, seen absolutely, was always low. The sum of the concentration of these divalent ions ranged from 0.16 to 0.64 mM. The Ca/Mg ratio of the soil solution was very low throughout the year, around 1.4. The concentration level of Al appeared to be always very low, less than 0.01 mM. Apart from $(HCO_3)_-$, the bulk of anions in the soil solution was made up by Cl and SO_4 of about 0.15 and 0.25 mM respectively. The $(HCO_3)_-$, important with regard to weathering, was found in a concentration up to 0.95 mM. However, the average alkalinity was very low, viz. 0.17 mM. Dissolved Organic Carbon ranged from 11 to 28 $mg\ C\ L^{-1}$. The contribution of DOC to organic anions in the soil solution was low. At an average DOC of 16.1 $mg\ C\ L^{-1}$, and a pH of 5.3, the organic anion concentration was 0.13 $mmol_c\ L^{-1}$, following Oliver et al. (1983). Considering the forest on these slopes, the DOC values were quite normal for soil solutions in surface horizons, although they were relative high for stream water (Oliver et al. 1983; van Wesemael and Verstraten 1993).

Summarizing, it can be stated that the average values of EC_{25} , Ca/Mg ratio and solute concentrations of the soil solution per sampled site, were very low and had relative low standard deviations over time (van den Broek 1989). This implies that the chemistry of the soil solution was relatively constant over the year. However, there were some differences in soil solution chemistry of the various cups, as well as a seasonal trend over the year. With regard to clay dispersion, these relative small differences are of minor importance. The most striking aspects of the soil solution chemistry over the year for clay dispersion were its very low ionic strength (0.6–2.0 mM), its low electrolyte concentration

Table 9.7 Chemical characterization of the soil solution sampled at the contact between EAh- and B-horizon, porous cups

Cup	pH			EC ₂₅ (µS cm ⁻¹)			Ca ²⁺ (mM)			Mg ²⁺ (mM)			Ratio (Ca/Mg)			DOC (mg C L ⁻¹)		
	avg	n	sd	avg	n	sd	avg	n	sd	avg	n	sd	avg	n	sd	avg	n	sd
<i>Wet location</i>																		
1	6.07	18	19	98	13	0.100	0.257	17	0.07	0.192	17	0.02	1.34	17	14.7	7.7	17	17
2	5.25	18	13	74	14	0.060	0.157	18	0.043	0.117	18	0.04	1.34	18	12.9	5.2	18	18
3	5.95	1	9	85	14	0.087	0.212	19	0.055	0.141	19	0.05	1.50	19	1.0	5.6	18	18
5	6.41	19	22	113	13	0.126	0.315	19	0.089	0.271	19	0.18	1.16	19	8.3	13.2	19	19
7	5.14	19	15	76	14	0.067	0.149	19	0.056	0.127	19	0.22	1.17	19	16.5	7.4	19	19
8	4.83	17	9	68	13	0.058	0.131	17	0.049	0.106	17	0.03	1.24	17	7.2	6.1	17	17
9	5.50	18	10	76	14	0.069	0.179	19	0.046	0.126	19	0.05	1.42	19	7.2	12.8	19	19
10	5.31	15	17	76	13	0.025	0.143	14	0.018	0.106	14	0.05	1.34	14	4.8	2.3	12	12
11	5.13	18	13	73	14	0.056	0.153	18	0.038	0.114	18	0.03	1.34	18	5.2	6.2	18	18
12	5.60	16	11	70	13	0.045	0.126	17	0.037	0.098	17	0.08	1.29	17	6.7	8.4	16	16
13	5.86	10	18	79	7	0.108	0.218	12	0.069	0.144	12	0.08	1.52	12	5.4	5.9	12	12
18	6.10	13	20	117	8	0.169	0.373	13	0.106	0.249	13	0.06	1.50	13	4.2	5.2	13	13
avg	5.38		84				0.201			0.149			1.35		15.3			
<i>Dry location</i>																		
4	5.34	15	39	73	13	0.035	0.132	15	0.019	0.078	15	0.08	1.69	15	4.9	5.3	13	13
6	5.67	14	15	61	7	0.058	0.127	10	0.050	0.109	10	0.07	1.16	10	4.7	4.6	9	9
14	4.89	13	6	56	6	0.051	0.103	12	0.053	0.090	12	0.05	0.87	12	0.0	3.9	12	12
15	5.13	15	6	48	9	0.077	0.116	11	0.051	0.092	11	0.14	1.27	11	9.1	4.5	11	11
16	5.09	15	17	56	11	0.062	0.104	14	0.043	0.071	14	0.06	1.46	14	8.9	13.3	12	12
17	4.97	13	11	57	10	0.063	0.129	11	0.037	0.077	11	0.10	1.68	11	8.7	3.3	9	9
avg	5.1		58				0.119			0.086			1.39		8.5			0.6

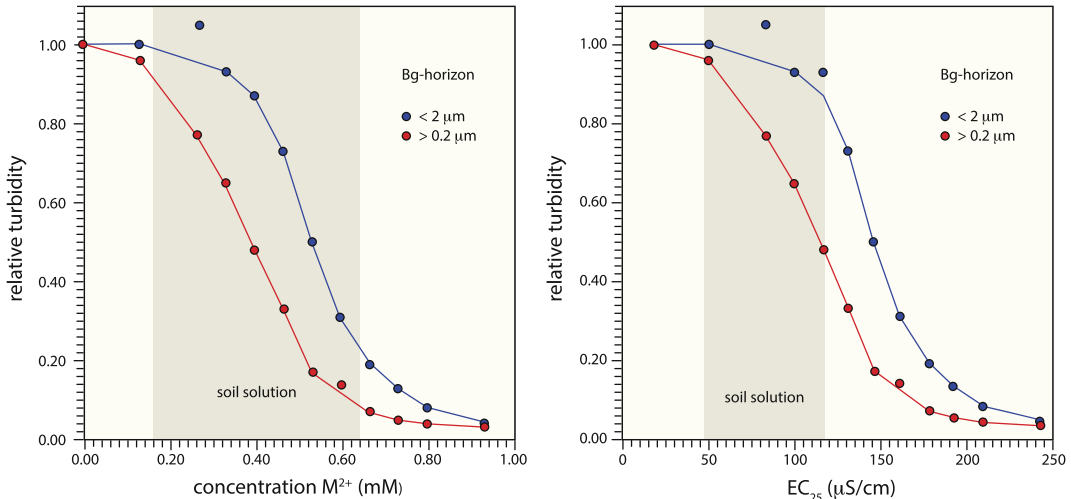


Fig. 9.12 Relative turbidity values of the two clay fractions (<2 and <0.2 μm) from the Bg horizon against increasing **a** electrolyte concentration of the used for EOE-shaking; **b** electrical conductivity (EC_{25}), measured after EOE-shaking (van den Broek 1989). The relative

turbidity is equal to the measured turbidity divided by the turbidity of the suspension in the presence of only demineralized water (see Appendix 4 Sect. “Flocculation Test”)

(ranging from 0.2 to 0.7 mM) of divalent cations, the absence of trivalent cations, and the relatively high DOC values. The low solute concentration and the water-soluble organic compounds have a direct link to clay dispersion, as depicted in Fig. 9.12. Relative turbidity values of the two clay fractions (<2 and <0.2 μm) from the Bg horizon are given against increasing (a) electrolyte concentration of the used for EOE-shaking; (b) electrical conductivity (EC_{25}), measured after EOE-shaking (van den Broek 1989). It shows that at higher electrolyte concentrations the clay start to flocculate. However the measured solute concentrations remain below the critical threshold of flocculation (see also Appendices 4 and 5).

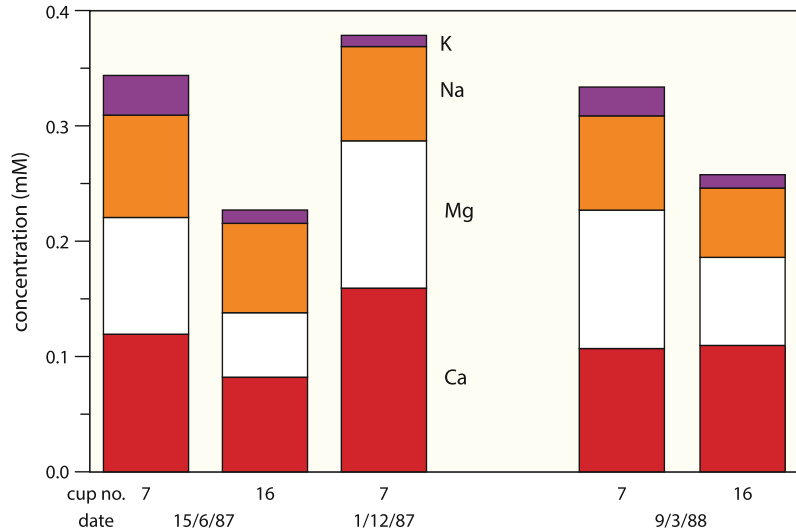
9.4.1.2 Subsurface Flow

During and after rainfall, water flowed through the many macropores, cracks and holes over the dense, waterlogged Bg horizon. Subsurface flow, flowing over the abrupt contact between the surface and subsurface horizons was sampled halfway up the slope, beneath the plot of the soil moisture cups, in trench of 7 m long and 35 cm deep. The subsurface flow chemistry was not

correlated with the discharge of the flow. For low discharges, the solute concentration of the throughflow was approximately similar to those of high discharges (van den Broek 1989). A rather constant solute concentration in throughflow with fluctuating discharge was also described by Burt (1979). The low solute concentration of the subsurface flow appeared to be a common feature in the forested Steinmergelkeuper areas, as shown by Dopheide (1986) for a comparable adjacent subcatchment.

The low solute concentration of the subsurface flow can be explained by the short residence time of the water within the soil matrix. However, in periods without subsurface flow, the soil solution at the abrupt contact between EAh and Bg horizon, must have a relatively long residence time compared to subsurface flow. Notwithstanding this relatively longer residence time, the soil solution had a low solute concentration and comparable composition (Fig. 9.13), comparable to that of subsurface flow. This implies that the soil solution rapidly equilibrated with the soil matrix, irrespective of the soil hydrological status, and independent of time. This indicates that the soluble cation chemistry is governed by the

Fig. 9.13 Contribution of Ca, Mg, Na and K in the soil solution from cup 7 and cup 16 on a wet and dry location (van den Broek 1989)



adsorption complex, and that the soil material of the Steinmergelkeuper is not very soluble under the conditions prevailing at the forested slopes. Therefore, in the context of clay dispersion, the equilibrium between soil solution and soil matrix does not depend on residence time. This relatively non-soluble character of the solid phase of the soil material is also shown by the results of the water extractable elements (Table 9.6). The water extracts of the EAh and Bg horizons, which were nearest to the soil solution and subsurface flow at the abrupt textural contrast, were low and had concentration levels which are comparable to the soil solution and subsurface flow (Table 9.3).

9.4.1.3 Dispersed Clay in the Subsurface Flow and Stream Water

During and after rainfall, a turbid subsurface flow, transporting dispersed clay, ran over the Bg horizon of the texture contrast soil. The dispersed clay finally reached the stream and was sometimes detected as a separated second sediment peak of (fine) clay in the stream water (Imeson et al. 1984). Dispersed clay in the main stream leaving the subcatchment had been sampled frequently and when possible, clay transported by the subsurface flow was also sampled. The subsurface flow, transporting dispersed clay, will

probably not only contain the fraction $<2 \mu\text{m}$, but also somewhat coarser textured material. Therefore, it is more appropriate to speak in terms of dispersed material instead of clay. The sediment concentration of the dispersed material ranged from approximately 30 to 110 mg L^{-1} (Table 9.8).

Grain size analysis of dispersed material in subsurface flow and stream was almost impossible to carry out by classical methods, because of the small amounts of sediment which were collected. Nevertheless, a particle size distribution of one sample collected in the stream leaving the subcatchment is available. It contained 15% silt ($50\text{--}2 \mu\text{m}$), 35% coarse clay ($2\text{--}0.2 \mu\text{m}$) and 50% fine clay ($<0.2 \mu\text{m}$).

The subsurface flow running over the impermeable Bg horizon cannot contain dispersed clay originating from the C horizon. However, the main stream cuts the C horizon on several locations, and it is likely that stream water might contain an admixture of dispersed C-material. Nevertheless, the clay mineralogy of the dispersed material in the stream was fully comparable to the mineralogy of the clay in the subsurface flow. This implies that the C horizon contributed only very slightly to the pool of dispersed material in the stream. Although there is a seasonal trend in drainage (Duijsings 1985; Cammeraat 1992), no clear differentiation in clay

Table 9.8 Dispersed material in stream water and subsurface flow in 1987 and 1988 (van den Broek 1989)

<i>Dispersed material in stream flow at exit subcatchment</i>			
Sampling date	Discharge (L s ⁻¹)	Sediment concentration (mg L ⁻¹)	Electrical conductivity (μS cm ⁻¹)*
12 Feb	1.97	46	76
24 Mar	1.48	66	n.d.
26 Mar	0.40	77	108
8 Sep	0.18	74	93
8 Oct	2.68	94	101
1 Dec	0.10	60	126
24 Jan	1.79	69	67
29 Feb	0.10	92	107
30 Mar	2.75	110	95
14 Apr	0.01	88	n.d.
<i>Dispersed material in subsurface flow at subsurface flow gutter</i>			
Sampling date	Discharge (mL s ⁻¹)	Sediment concentration (mg L ⁻¹)	Electrical conductivity (μS cm ⁻¹)*
8 Oct	11	34	113
24 Jan	14	42	92
30 Mar	2	79	76

n.d = not determined, * = at 25 °C

mineralogy was observed over the year. The complete pattern of X-ray diffractions of subsurface flow and stream sediment is presented in Appendix 3, and some diffraction patterns are presented in Fig. 9.14. From a clay mineralogical point of view, the dispersed material in stream and subsurface flow was comparable to the clay fraction of the Bg horizon of the soil profile (Fig. 9.14 and Appendix 3), which is explained in the following section. The clay mineralogy of the non-fractionated samples over the year showed illite, a swelling interstratification of chlorite-smectite, and an interstratification of chlorite-vermiculite. The only fractionated sample available, showed in the fine and coarse clay fraction both an illite peak (see Appendix 3). In the coarse clay, the chlorite-vermiculite interstratification was present, and in the fine clay fraction a chlorite-smectite interstratification. From the presence of the chlorite-vermiculite interstratification in the stream and subsurface flow samples, it can be concluded that this dispersed material did not only contain fine, but also

coarse clay. The fine clay of soil profile II did not contain a 14 Å peak after glycerol treatment, whereas the coarse clay did (see Fig. 9.7 and Appendix 2).

The X-ray diffraction pattern of the dispersed material in the subsurface flow and stream contained the swelling 16 Å interstratification. The same swelling 16 Å mineral was present in the (fine) clay of the Bg, Bw and C horizons, whereas it did not show up in the clay (<2 μm) of the AEh and EAh horizons (see Fig. 9.7). As the 16 Å mineral was relatively absent in the AEh and EAh horizons, the presence of it in the Bg, Bw and C horizons as well as in stream and flow material supported the concept of a lateral eluviation of clay. The lateral export of eluviated, dispersed clay was considered to be the main mechanism for the genesis of the textural contrast soil. This concept is schematically presented as

“B-horizon – dispersed material = mineral part of A + E-horizons”.

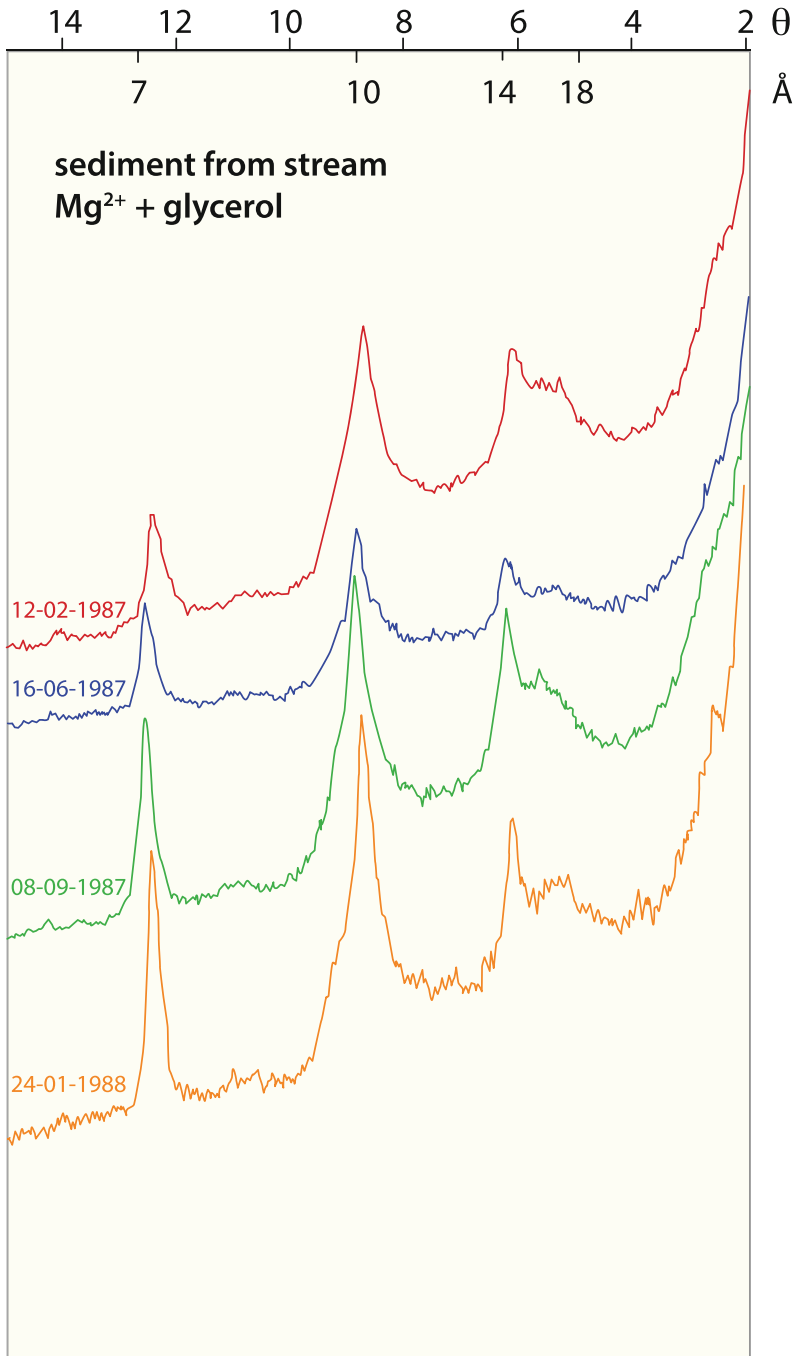


Fig. 9.14 X-ray diffraction patterns of the suspended sediment in stream water and subsurface flow (van den Broek 1989)

9.5 Discussion: Genesis of the Forested Steinmergelkeuper Soils

First an overview and discussion is given of the processes that could be relevant for the natural soil degradation in relation to the development of textural contrast soils. These processes are considered one-by-one for their relevance with regard to the development of the abrupt contrast in texture in these soils. Next, the attention is focused on physico-chemical processes and hydrological conditions responsible for the genesis of the textural contrast between the silty surface and heavy clayey subsurface horizons. For more details on the physico-chemical conditions involved see Appendices 4 and 5.

9.5.1 Discussion of Possible Soil Forming Processes Involved in the Development of the Abrupt Contrast in Texture

All the possible natural soil degradation processes with regard to the development of the abrupt contrast in texture in the soil profiles are reviewed in Table 9.9.

Although not a soil forming process, a *lithological discontinuity*, is often held responsible for the presence of a textural contrast within a soil profile. However, on the forested Steinmergelkeuper slopes such a non-pedogenic abrupt contrast in texture is ruled out. The present soil profile has developed in a rather uniform

Table 9.9 Possible soil forming processes involved in the genesis of the forested textural contrast soil

Process	Process description	Relevance	Explanation
Lithological discontinuity	Two layers lithologically and/or stratigraphically not related to each other	No	Uniform parent material with very small admixtures of loess and volcanic ashes throughout the profile
Pervection	Illuviation of suspended clay until flocculation in the B-horizon takes place	No	Ratio fine/total clay is constant with depth from Bg horizon No illuviation features in Bg horizon
Hydrolysis of clay	Mineral acids produced by soil processes (internal)	No	No congruent dissolution of minerals due to near neutral pH No output of Al (and/or Fe)
	Mineral acids due to atmospheric deposition (external)	No	Not involved in soil formation in the past
	Organic acids due to decomposition of humus	No	Low production of organic acids Produced organic acids not aggressive
	weathering effect of carbon dioxide	No	Low alkalinity Near neutral pH
Ferrollysis	Clay desintegration under alternating of conditions reduction and oxidation	No	No exchangeable Fe and Al present Base saturation of 96–100% No hydroxy-interlayering
Selective ejection	Clay accumulation in subsoil by sand ejection due to shrink and swell	No	Cracks only as deep as top of Bg horizon Regular shrink and swell cycle is prohibited
Bioturbation	Upward movement of coarse mineral particles by soil faunal activity	No	Soil fauna restricted to surface horizons (topsoil)
	Activity of worms and moles	Indirect	Soil fauna responsible for high macroporosity
Impoverishment	Selective transport of fine clay from top of Bg horizon	Yes	Discussed in this chapter

parent material. This parent material, being the weathered marls of the Steinmergelkeuper, contained only very small admixtures of loess and volcanic ash components. There was no distinct layer of silty material, e.g. a loess or colluvial layer on top of the Steinmergelkeuper parent material which is reflected today in the surface horizons of geomorphic units (1), (2) and (3).

Pervexion, the *illuviation* of suspended particles until flocculation takes place in the B horizon, is often held responsible for an increase in the texture in a soil profile. The standard particle size distribution of the forested Steinmergelkeuper profile showed a clay bulge in the Bg horizon. Therefore, clay illuviation seemed to be very likely. However, the ratio of fine to total clay ($<0.2 \mu\text{m}/<2 \mu\text{m}$) from the Bg horizon on downward in the profile, was constant with depth. Also, the increase in clay content in the Bg horizon disappeared after disaggregating the soil material by a very short ultrasonic pretreatment. The constant clay content after disaggregation, from the Bg horizon downward, supports the non-illuvial character of this subsurface horizon. This is confirmed also by the lack of any illuviation and stress features on thin sections of the Bg horizon. Clay illuviation as a main process involved in the development of the abrupt textural contrast, can therefore be excluded.

Weathering/dissolution of clay in the top soil can lead to a relative increase in clay content in the underlying Bg horizon. However, a congruent dissolution of clay minerals in the surface horizon can be excluded due to near neutral pH conditions and the lack of soluble aluminium (and iron) output by subsurface flow. In addition, the hydrolysis of clay minerals and the resulting neo-formation of secondary minerals can be excluded considering the pH, Al, Si, Mg and K concentrations of the soil solution.

The possible weathering agents on the forested Steinmergelkeuper slopes responsible for clay disintegration, are (potential) mineral acids due to the atmospheric deposition, organic acids due to the decomposition of organic matter, and dissolved carbon dioxide in the percolating soil solution and subsurface flow. The current atmospheric deposition of (potential) *mineral* acids

and their effect on the disintegration of clay is not relevant for the development of the textural contrast, which took place in the past.

Another possible factor involved in the disintegration of clay is the decomposition of organic matter, which results a.o. in the production of *organic* acids. Their presence can be estimated by the concept of Oliver et al (1983), which is based on a strong relationship between overall dissociation constant, pH and Dissolved Organic Carbon of the soil solution. Overall, the average contribution of organic anions in the soil solution sampled by the porous cups at the contact between EAh- and Bg horizons, was $0.13 \text{ mmol}_c \text{ L}^{-1}$. In addition to this low dissociated organic acid component, the humus in the surface soil had a mull type character and is not aggressive with respect to clay disintegration. Consequently, *carbon dioxide* dissolved in the percolating soil solution and subsurface flow as a weathering agent, is considered to be the last factor which could be of major importance with regard to the hydrolysis of clay in the surface horizons. However, measured alkalinity data of $0.17 \text{ mmol}_c \text{ L}^{-1}$ (average) indicated that this contribution to the disintegration/hydrolysis of the clay was also not very high, and will not result into a textural contrast soil.

Compared to hydrolysis, *ferrolysis* (Brinkman 1979; Blume et al. 2016) can play an important role for the disintegration of clay under much stronger weathering conditions. In ferrolysis, clay disintegration is always accompanied by exchangeable aluminium and/or iron at the adsorption complex, which both are absent. Furthermore, ferrolysis can, under acid conditions during the oxidation stage in the dry season, lead to the formation of hydroxy-interlayered minerals. However, the soil also has near neutral pH conditions, and clay decomposition resulting in an abrupt textural contrast caused by long continued ferrolysis does therefore not play a prominent role on the Steinmergelkeuper soils.

A texture increase with depth can be the result of *selective ejection* of sand and silt. Based on the limited depth and on the special swell and shrink behaviour of the cracks, a relative accumulation of clay by selective ejection of sand and

silt can be excluded in the texture contrast soils on the Steinmergelkeuper.

In some soils, *bioturbation* is held responsible for an increase in clay content in the profile. The soils in this study are characterized, a.o. by a high faunal activity of earthworms and moles which was restricted to the surface horizons. Spots of bare soil were liable to splash erosion during heavy rainstorms (Van Hooff 1983). Although the amount of transported material can be considerable, splash erosion together with saturation overland flow as the main mechanism responsible for the development of the abrupt contrast in texture, appears not very likely. A change in texture at 15–20 cm below surface, which was abrupt, can never be ascribed to such a mechanism. Also, the change in the fine to total clay ratio from A to Bg horizon points to a selective loss of fine clay. Rain splash will not affect the fine clay fraction selectively. However, one aspect that is important for the development of the abrupt contrast in texture is the macroporosity, due to the enormous activity of earthworms and moles. The system of macropores, cracks and holes, partly due to the high faunal activity, is essential for the generation of the lateral subsurface flow running on top of the Bg horizon in the dry and wet subsystems.

To conclude, it is evident that the contribution of the above-mentioned processes, with exception of impoverishment, is quantitatively insignificant to explain the genesis of the textural contrast soil on the forested slopes. The mechanism which plays the major role in the development of the abrupt contrast in texture is *lateral transport of dispersed clay*. This mechanism is a combination of the physico-chemical process of clay dispersion and slope hydrology (see also Appendices 4 and 5).

9.5.2 Clay Dispersion Related to the Development of the Abrupt Contrast in Texture

The subsurface flow running downslope disperses and exports clay. This lateral transport of

dispersed clay is significant for the development of the abrupt contrast in texture, and depends on a physico-chemical process in combination with the specific hydrology of the forested Steinmergelkeuper slopes. This is presented schematically in Fig. 9.15, in which the dispersion of clay is related to the genesis of the textural contrast soil.

9.5.2.1 Origin of the Lateral Transported Dispersed Clay

The clay, transported by the subsurface flow, disperses mainly from the top of the Bg horizon, and not from the overlying surface horizons. This is shown explicitly by the marked similarity in clay mineralogy between the lateral transported clay and the clay in the Bg horizon, and further supported by the special characteristics of the Bg horizon which are favorable to clay dispersion. One of the special features of this horizon is its high content of exchangeable Mg at the clay surface. This resulted in a large double layer, increasing the repulsive forces and dispersion and a low rate of hydrolysis of clay particles (Dontsova and Norton 2002; He et al. 2013; Zhang and Norton 2002). Another special feature of the Bg horizon, indicating that laterally transported clay disperses from the top of the Bg horizon, is the high potential dispersibility of this horizon compared to the surface horizons. The restraining effect of organic matter on clay dispersion in the topsoil, which is ascribed to the stable organo-mineral bonds, is clearly demonstrated. Summarizing, it is likely that at the EAh/Bg interface, the Bg material, almost without organic matter, having the highest potential dispersibility and the lowest adsorbed Ca/Mg ratio, contributes considerably to the dispersed clay.

9.5.2.2 Processes and Conditions Responsible for the Dispersion of Clay

A large difference exists between clay dispersion in a suspension and clay dispersion in a soil: “granulation is flocculation plus” (Bradfield 1936). Before clay dispersion takes place in a soil, macro-aggregates have to fall apart into

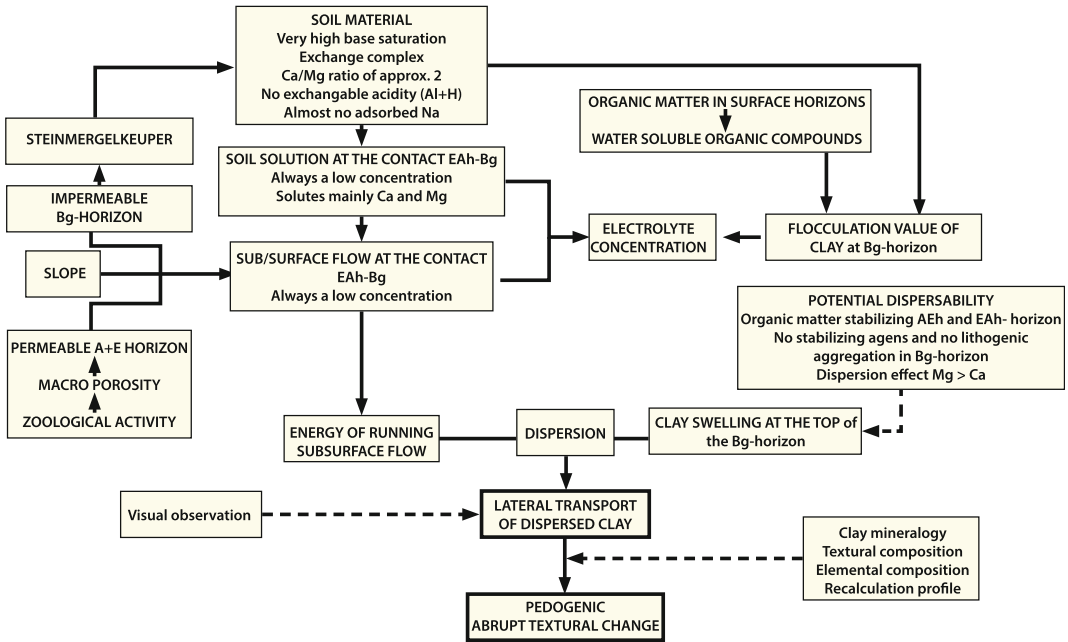


Fig. 9.15 Schematic presentation of all factors important for clay dispersion and the genesis of the textural contrast soil on the forested Steinmergelkeuper marls (adapted from van den Broek 1989)

micro-aggregates. These micro-aggregates can disperse in the absence of stabilizing agents, according to the DLVO-theory (Oades 1986; Blume et al. 2016). In the Bg horizon of the textural contrast soil, no important cementing agent is available and lithogenic aggregation is not important. The Bg horizon contains 2.25% free (pedogenic) iron (as Fe₂O₃) concentrated in “clear distinct mottles” (description of profile II, Appendix 1), and less than 1% organic carbon (Table 9.2). Consequently, the macro-aggregates at the top of the Bg horizon can slake easily into micro-aggregates. The dispersion of micro-aggregated clay is ruled completely by the competition between the attraction and repulsion forces, where the repulsion forces are the only environmental dependent variable. The physico-chemical behaviour of the clay at the top of the Bg horizon, is therefore a result of the interaction between the soil material and soil solution.

The Steinmergelkeuper soils have properties which are favorable to clay dispersion. The soil material has a near neutral pH(H₂O), around 5.8 in the Ah to 6.2 in the Bg horizon, and a base saturation above 95%. The exchange complex is characterized mainly by Ca and Mg, with an adsorbed Ca/Mg ratio of about 2. There is no Al detectable at the exchange complex, and only a very limited amount of Na (less than 10 mmol_c kg⁻¹ soil). The absence of Na and the presence of adsorbed Ca and Mg at the exchange complex do not automatically result in a stable, non-dispersable clay. Contrary to a Na-clay, divalent saturated clays show only limited swelling (Quirk and Aylmore 1971). Although a Ca or Mg-saturated clay does not disperse spontaneously in demineralized water (Rengasamy 1982), divalent saturated clays will disperse after addition of some extra energy, and this occurs either by stirring in a beaker glass (Emmerson and Chi 1977) or by the kinetic energy of water

flow in sloping soils. On the forested Steinmergelkeuper slopes, the water, running fast downslope over the contact between the EA_h and B_g horizons, supplies the energy to actually disperse the clay at the top of the B_g horizon.

The soil properties favorable to clay dispersion are indirectly caused by the low degree of weathering of the soil material. This is ascribed to the high content of exchangeable Mg at the clay surface, in combination with the structural Mg within the clay mineral structure, and leads to a high potential dispersibility of the clay and a low electrolyte concentration of the soil solution.

The other aspect related to the low degree of weathering of the soil material, and important for the physico-chemical behaviour of the clay at the top of the B_g horizon, is the concentration and composition of the soil solution at the interface between EA_h and B_g horizons. The concentration of the soil solution is, seen in the context of clay dispersion, independent of soil moisture conditions and moisture residence time. The soil solution over the year is characterized by a very low ionic strength (0.6–2 mM) and a cation composition of mainly calcium and magnesium, with a more or less constant Ca/Mg ratio of 1.4. The concentrations of monovalent ions, Na and K, are much lower on a charge base (0.1 mM), and the very low Al (and Fe) concentrations can be ignored. The composition and concentration of the subsurface flow is in good agreement with the soil solution.

The chemical conditions of the soil solution and subsurface flow were compared with the flocculation values of the clay in the AE_h, EA_h and B_g horizons. The chemical boundary condition of the soil solution was related to the dispersion properties of the soil material. As the lateral transported clay disperses mainly from the top of the B_g horizon, the soil solution was related to this flocculation value. The flocculation value of the clay in the B_g horizon is 0.8 mM of an equimolar solution of CaCl₂ and MgCl₂. Such an equimolar solution, with a Ca/Mg ratio of 1, approaches the soil solution with a Ca/Mg ratio of 1.4.

The concentration of the soil solution at the contact between EA_h and B_g horizons over the year was below the flocculation value of the clay

of the B_g horizon. This implies that suitable boundary conditions for the clay dispersion exist throughout the year. The soil solution has such a low electrolyte concentration, that the diffuse double layer surrounding the clay particles is extended. Consequently, the clay at the top of the B_g horizon will swell and its K_{sat} will be reduced. However, spontaneous dispersion of clay will not take place, as the exchange complex is saturated with divalent ions (Emmerson and Chi 1977; Rengasamy 1982, 2002) and extra energy is necessary which is supplied by the kinetic energy of the subsurface flow. This appears to be essential for the dispersion of clay at the top of the B_g horizon, and its transport downslope. Although the low electrolyte concentration of the soil solution and the subsurface flow running downslope are major keys in the mechanism, water-soluble humic substances contribute also indirectly to the dispersion of clay as shown by laboratory experiments (see Appendix 5).

9.5.2.3 The Specific Hydrological Setting of the Forested Steinmergelkeuper Slopes

The lateral transport of dispersed clay appears to be the dominant mechanism in the genesis of the texture contrast soil. In this mechanism, physico-chemical aspects of soil material and soil solution are important. In addition, the slope hydrology is essential to the lateral transport of dispersed clay. This is illustrated by the less clear abrupt textural change in profiles located at the crest of the watershed, compared to profiles at the adjacent slopes. The fast lateral subsurface flow, which has been observed many times during and after rainfall (Bonell et al. 1984; Cammeraat 1992), is due to the slope gradient and the high macroporosity in the horizons lying over the clayey subsurface horizon. The overlying surface horizons are much coarser in texture, and contain appreciable less fine clay than the underlying B_g horizon. The fine to total clay ratio changes from approximately 0.3 in the topsoil to 0.5 in the B_g, B_w and C₁ horizons.

Shortly after the start of rainfall, a lateral subsurface flow is generated in the surface

horizons and at the interface between the silty EA_h and heavy clayey B_g horizon. Subsurface flow supplies the extra energy to actually disperse the swollen clay, which is saturated with Ca and Mg and it exports the dispersed clay laterally over the B_g horizon downslope to the small stream, which drains the subcatchment, and gives the stream water a milky colour. Duijsings (1985) also demonstrated the important contribution of dispersed clay, as derived from lateral subsurface flow, in the sediment budget of Steimergelkeuper catchments. The fine clay component is exported preferentially from the top of the B_g horizon in particular. This process results in the silty topsoil (AE_h + EA_h horizons), almost lacking fine clay, abruptly overlying the B_g horizon.

In order to quantify the lateral transport of dispersed clay, the results of a global exercise are presented. The subsurface flow, e.g. the matrix throughflow, draining the surface soil on the slopes (dry subsystem), as well as the small stream leaving the subcatchment, contain 50–100 mg L⁻¹ sediment, which is mainly (fine) clay. This transport is responsible for a surface lowering of 13–26 g m⁻² year⁻¹. This implies that the present silty surface horizon has developed by lateral eluviation of clay from the clayey

(sub)surface horizon in about 4000–9000 years (van den Broek 1989).

Another hydrological feature of the Steinmergelkeuper is the marked difference in soil moisture conditions on the slopes, where partial areas are located near dry sites. These wet and dry zones differ completely in hydrology, e.g. in the presence of a perched water table and in the generation of subsurface and saturation overland flow. The thickness of the silty topsoil is different between the dry and wet subsystem, reflecting difference in process dominance: subsurface flow eluviation of fine clay (thicker topsoil) by matrix flow processes in the dry subsystem under beech, and a combination of the latter with macropore flow and pipe flow and splash erosion respectively in the wet subsystem where hornbeam dominance (Chap. 10).

Summarizing, the development of the abrupt textural contrast soil was possible due to the combination of a pedological and a hydrological process. The swelling and dispersion of clay is the dominant physico-chemical process, which is strongly related to the generation of a subsurface flow, being the essential hydrological factor in the whole mechanism. The fine clay found in the river discharge (Fig. 9.16) was found to be originating from the B_g horizon, proving that the



Fig. 9.16 Photo showing almost bankfull discharge in one of the tributaries feeding the Schrondweilerbaach. The discharge has the typical *milky colour* of dispersed (fine) clay, that is derived from the top of the B_g horizon

lateral eluviation of the clay from the top of the Bg horizon is responsible for the formation of the abrupt textural change of the forested Steinmergelkeuper soils.

9.6 Conclusions

The abrupt textural change between the surface horizons and the underlying Bg horizon is the result from impoverishment of the topsoil by lateral eluviation of the (fine) clay fraction from the top of the Bg horizon. This is supported by the following observations:

- The Steinmergelkeuper parent material in which the soil (Luvic Planosol) developed is uniform and the soil profile is relatively undisturbed by human impact through land use or forest management.
- (Recent) weathering of the parent material resulting in a textural difference between horizons can be excluded, and the impoverishment is clearly indicated by the increase of MgO and Al₂O₃ and the decrease of SiO₂ with depth.
- The continuously very low concentration of electrolytes in the soil water (<120 μS cm⁻¹) favours the dispersion of the dispersion sensitive (fine) clay.
- The clay mineralogy of the clay of the top in the Bg horizon is the same as the clay mineralogy in the dispersed clay material in the subsurface and river flow, and the eluviated clay minerals are relatively absent in the topsoil horizons.
- Fast transport of soil water through the topsoil horizons is favoured by the high macroporosity of the topsoil, due to bioturbation, swelling and shrinking and the presence of the almost impervious underlying Bg horizon.
- The abrupt textural contrast is best developed on the slopes where highest flow velocities of subsurface water are occurring.
- Luvic Planosols on the forested Steinmergelkeuper are about 4000–9000 years old,

so their formation falls well within the Holocene.

Acknowledgements We would like to thank the Direction Eaux et Forêts Luxembourg (Forest and Water Department of Luxembourg), especially J.M. Sinner and chef-forester J. Winandy for giving permission and for supporting our work in the Schrondweilerboesch. Furthermore, we would like to thank our colleagues from the Physical Geography and Soil Science laboratory (IBED-UvA) and those who did contribute to this work in one way or another, and without whom we could not have carried out this research. Finally, we would like to thank Jan van Arkel (IBED) for his graphical work.

Appendix 1

Description and particles size distribution, pH and organic carbon content of soil profile I, II and III, as presented in Fig. 9.4. The grain size distribution data are given in Table 9.10.

Description Profile I

Date of description: April 9, 1987

Author: Theo van den Broek

Classification	Aquic Dystric Eutrochrept, fine silty, mixed, over clayey, mixed, mesic (Soil Survey Staff 1975); Luvic Planosol (IUSS 2015)
Location	2 km NE of Schrondweiler, in the forest at the crest 49° 49' 16"N 6° 10' 50"E
Altitude	328 m
Relief	Gently undulating macro-relief
Slope	0° (watershed)
Drainage	Poorly to imperfectly drained
Vegetation	Oak (<i>Quercus robur</i> L), hornbeam (<i>Carpinus betulus</i> L) and beach (<i>Fagus sylvatica</i> L)
Parent rock	Steinmergelkeuper

All colours are for moist soil, according to the Munsell scale

AEh 0–10 cm	Dull yellowish brown (10 YR-5/4) wet silt loam with few, faint, fine, diffuse mottles; moderate fine to medium crumb; slightly sticky, slightly plastic; many fine, common medium and a few coarse pores; very frequent fine and common medium roots; gradual, smooth boundary to
EAh 10– 18 cm	Dull yellowish brown (10 YR-5/4) wet silt loam with few, faint, fine, diffuse mottles; moderate fine to medium crumb; slightly sticky, slightly plastic; many fine, common medium and a few coarse pores; very frequent fine and common medium roots; gradual, smooth boundary to
Bg 18–30 cm	Grayish yellow brown (10 YR-5/2) wet silty clay loam with many, medium, distinct, clear yellowish (10 YR-5/8) mottles; strong medium sub-angular blocky; slightly sticky, very plastic; common fine and few coarse pores; few fine and a very few coarse roots; gradual boundary to
Bw 30–45 cm	Grey (5 Y-6/1) wet silty clay loam with common, fine, distinct, diffuse brown (10 YR-4/4) mottles; moderate, medium, sub-angular blocky; slightly sticky, very plastic; few fine and very fine pores; few coarse roots; gradual, wavy boundary to
C1 45–60 cm	Grayish olive (5 Y-5/2) wet silt loam with no mottles; massive structure; slightly sticky, very plastic; few very fine pores; no roots; few large, hard, weathered Steinmergelkeuper fragments; gradual boundary to
C2 60–85 cm	

Grayish olive (5 Y-5/2) wet silt loam with no mottles; massive structure; slightly sticky, very plastic; few very fine pores; no roots; large, hard, weathered Steinmergelkeuper fragments

Description of Profile II. The Reference Profile

Date of description: March 24, 1987

Author: Theo van den Broek

Classification	Aquic Dystric Eutrochrept, fine silty, mixed, over clayey, mixed, mesic (Soil Survey Staff 1975); Luvic Planosol (IUSS 2015)
Location	2 km NE of Schrondweiler, in the forest halfway on the slope 49° 49' 16"N 6° 10' 50"E
Altitude	325 m
Relief	Gently undulating macro-relief
Slope	4°
Aspect	North facing
Drainage	Poorly to imperfectly drained
Vegetation	Oak (<i>Quercus robur</i> L), hornbeam (<i>Carpinus betulus</i>) and beach (<i>Fagus sylvatica</i> L)
Parent rock	Steinmergelkeuper

All colours are for moist soil, according to the Munsell scale

AEh 0–10 cm	Dark brown (10 YR-3/4) wet silt loam with few, fine, faint, diffuse mottles; moderate fine to medium crumb; slightly sticky, non-plastic; many fine, common medium and a few coarse pores; very frequent fine and common medium roots; gradual, wavy boundary to
----------------	--

EAh
10–20 cm

	Dark brown (10 YR-3/4) wet silt loam with few, fine, faint diffuse mottles; moderate medium crumb; slightly sticky, non-plastic; many fine, common medium pores; frequent, fine and common, medium roots; abrupt, smooth boundary to	Classification	Aquic Dystric Eutrochrept, fine silty, mixed, over clayey, mixed, mesic (Soil Survey Staff 1975); Luvic Planosol (IUSS 2015)
Bg 20–34 cm	Brownish grey (10 YR-5/1) wet clay with many, medium, distinct, clear yellowish brown (10 YR-5/8) mottles; strong, medium/coarse angular blocky; slightly sticky, very plastic; few very fine pores; few, very fine and very few medium roots; gradual boundary to	Location	2 km NE of Schrondweiler, in the forest at footslope, near the stream; 49° 49' 16"N, 6° 10' 50"E
Bw 34–50 cm	Brownish grey (10 YR-6/1) wet silty clay with common, fine, distinct, diffuse brown (10 YR-4/4) mottles; moderate, medium sub-angular blocky; slightly sticky, plastic; few very fine pores; few, very fine and very few medium roots, clear, irregular boundary to	Altitude	323.5 m
		Relief	Gently undulating macro-relief 2
		Slope	2°
		Aspect	North facing
		Drainage	fairly well drained
		Vegetation	Oak (<i>Quercus robur</i> L), hornbeam (<i>Carpinus betulus</i> L) and beach (<i>Fagus sylvatica</i> L)
		Parent rock	Colluvium on Steinmergelkeuper
		All colours are for moist soil, according to the Munsell scale	
Cl 50–58 cm	Dark reddish brown (5 YR-3/4) wet silt loam, no mottles; moderate, medium sub-angular blocky; slightly sticky, plastic; very few, very fine pores; no roots; clear, irregular boundary to	AEh 0–9 cm	Brown (10 YR-4/4) moist silt loam; weak fine to medium crumb; friable; many fine, medium and coarse pores; many roots, faint boundary to
C2 58–75 cm	Grayish yellow (2.5 Y-6/2) wet silt loam, no mottles; medium sub-angular blocky; slightly sticky, plastic, no pores; no roots; few weathered Steinmergelkeuper marl flakes	EAh 9–0 cm	Dull yellowish brown (10 YR-5/4) moist silty clay loam with few, fine, faint, diffuse mottles; moderate sub-angular blocky; firm; many fine, medium and coarse pores; many roots; faint boundary to
C3 75–90 cm	Grayish yellow (2.5 Y-6/2) wet silt loam, no mottles; medium sub-angular blocky; slightly sticky, plastic, no pores; no roots; weathered Steinmergelkeuper marl flakes.	2Bg 20–32 cm	Dull yellowish brown (10 YR-5/4) moist clay with common, medium, faint yellowish brown (2.5 Y-5/6) mottles; strong angular blocky; very firm; few fine pores; many fine roots; faint boundary to
		2C1 32–45 cm	Grayish yellow brown (10 YR-6/2) moist clay with common, medium, faint yellowish brown (2.5 Y-5/6) mottles; strong angular blocky; very firm; few fine pores; few fine roots.

Description of Profile III

Date of description: November 1, 1988

Author: Theo van den Broek

Table 9.10 Grain size distribution, soil pH and organic carbon content of profiles I, II and III

Profile I

Horizon	Depth (cm)	pH (H ₂ O)	pH (CaCl ₂)	org. C. (%)	Sand (%)	Silt (%)	Clay (%)
AEh	0–10	5.21	4.49	3.9	14	63	23
EAh	10–18	4.95	4.20	2.0	16	59	24
Bg	18–30	5.71	5.09	0.6	8	54	37
Bw	30–45	6.57	6.00	0.4	13	59	28
C1	45–60	7.20	6.51	0.3	24	66	20
C2	60+	7.59	6.95	0.4	27	32	41

Profile II (the reference profile)

Horizon	Depth (cm)	pH (H ₂ O)	pH (CaCl ₂)	org. C. (%)	C/N ratio	Sand (%)	Silt (%)	Clay (%)	Coarse clay	Fine clay
AEh	0–10	5.87	5.44	4.0	15.9	14	63	23	15.7	7.3
EAh	10–20	5.75	5.14	2.2	13.6	17	59	24	17.0	7.0
Bg	20–34	6.20	5.51	0.8	10.1	12	38	50	26.3	23.7
Bw	34–50	6.48	5.83	0.4	n.d.	10	52	38	16.5	21.5
C1	50–58	7.14	6.57	0.3	n.d.	13	64	24	11.1	12.9
C2	58–75	7.50	6.83	n.d.	n.d.	23	50	27	n.d.	n.d.
C3	75–90	7.72	6.98	n.d.	n.d.	14	58	28	n.d.	n.d.

Profile III

Horizon	Depth (cm)	pH (H ₂ O)	pH (CaCl ₂)	org. C. (%)	Sand (%)	Silt (%)	Clay (%)
AEh	0–9	4.75	4.19	4.2	11	62	27
EAh	9–20	5.61	5.01	1.4	13	54	33
2Bg	20–32	5.87	5.35	0.8	11	38	51
2C	32–45	6.53	6.12	0.5	7	30	63

(n.d. = not determined) (weight percentages on abs. dry base)

Appendix 2

Clay mineralogy of the total, coarse and fine clay of the reference profile (Profile II, Appendix 1):

Overall View of the Clay Mineralogy of the Soil Profile

Illite and some kaolinite is present in the whole of the profile in as well the fine, coarse as total clay fraction.

The interstratification chlorite–smectite is found in all horizons in as well the fine as well the total clay fraction. In the coarse clay fraction this swelling interstratification is lacking in the surface horizons, and is only present in the Bw

and C1 horizons (the last probably due to a non-ideal separation of the fine and coarse clay during the pretreatment of the samples, caused by lithogenic aggregation).

The interstratification chlorite–vermiculite is present in the fine, coarse and total clay fraction in the whole of the profile. Chlorite is present in particular in the surface horizons of the total and coarse clay fractions.

Total Clay (<2 µm)

Summary

Illite and some kaolinite is present in all the horizons of the profile. The interstratification chlorite–smectite is present in particular in the

Bg, Bw and Cl horizons. Chlorite is only shown in the AEh and EAh horizons, whereas the interstratification vermiculite–chlorite is present in the whole of the profile, although the most pronounced in the deeper horizons. Quartz is found in the surface horizons.

Throughout the complete profile, strong and sharp reflections show up around 10, 4.9 and 3.34 Å, being the 001, 002 and 003 reflections respectively of a good crystalline illite.

Saturation with Mg^{2+} yields for whole the profile a peak at 14 Å, which shifts after a glycerol treatment towards 16 Å for particularly the Bg, Bw and C horizons, implying a swelling, interstratified mineral. This, together with the shift of the 29–30 Å peak to a 32–34 Å peak after treatment with glycerol points towards the interstratification chlorite–smectite. The 14 Å peak is shown for the Mg as well as the K-saturation. Saturation with K^+ gives a peak at 14 Å. In the surface horizons it is a good, sharp crystalline peak, whereas deeper in the profile the peak becomes broader.

After heating to 300 °C, the peak collapses towards 10 Å the interstratification of chlorite–vermiculite. At 550 °C the 14 Å peak increases in intensity, mainly in the AEh and EAh horizons: chlorite, whereas the intensity of the 7.07, 4.7 and 3.54 Å peaks decreases. Chlorite peaks show up at 14.1, 7.07, 4.72 and 3.54 Å, being the 001, 002, 003 and 004 reflections respectively. At 550 °C the 14 Å peak of chlorite intensifies, whereas the 7 Å peak disappears: kaolinite. A Quartz peak at 4.26 Å shows up in particular in the surface horizons.

Coarse Clay (2–0.2 µm)

Summary

Illite and some kaolinite is present in all horizons, whereas the interstratification chlorite–smectite shows up mainly in the deeper (Bg), Bw and Cl horizons. The chlorite–vermiculite interstratification is shown in the complete profile, whereas chlorite is noticed particular in the upper

part of the profile. Quartz shows up in the surface horizons too.

Throughout the complete profile sharp reflections show up around 10, 4.9 and 3.34 Å, being the 001, 002 and 003 reflections respectively of a good crystalline illite.

Saturation with Mg^{2+} results in a 14 Å reflection in all the horizons. After a glycerol treatment, the 14 Å peak shifts towards 16 Å for only the Bw and Cl horizons, and in a lesser degree for the Bg horizon. It implies the presence of a swelling mineral, being the interstratification chlorite–smectite¹. Saturation with K^+ results in a 14 Å reflection in all the horizons. Compared to the Mg-peaks at 14 Å, the K-peaks are smaller: vermiculite. After heating to 300 °C, the 14 Å peak collapses, particular in the deeper horizons, towards 10 Å: the interstratification chlorite–vermiculite. At 550 °C the 14 Å peak increases in intensity especially in the surface horizons, whereas the intensity of the 7.07, 4.7 and 3.54 Å peaks decreases: chlorite, mainly in the AEh and EAh horizons. Chlorite peaks show up at 14.1, 7.07, 4.72 and 3.54 Å, being the 001, 002, 003 and 004 reflections respectively. A small Quartz peak at 4.26 Å shows up in particular in the surface horizons.

Fine Clay (<0.2 µm)

Summary

Illite and some kaolinite are present in the complete profile, even as the swelling interstratification chlorite–smectite, although the last is more pronounced in the deeper part of the profile. The interstratification chlorite–vermiculite is present

¹This interstratification occurs in the lower horizons as an artefact due to an incomplete separation of the fine and coarse clay. This incomplete separation is caused by strong lithogenic aggregation. A complete destruction of this lithogenic aggregation is caused by a 15 times repeated ultrasonic pretreatment of clay samples from the Bw and Cl horizons. After this almost complete separation in fine and coarse clay it appeared that the coarse clay fraction contained only a minor amount of the swelling interstratification.

in the whole of the profile. In the deeper horizons the chlorite component in this interstratification is larger than in the surface horizons.

Throughout the complete profile, broad reflections show up around 10, 4.9 and 3.34 Å, being the 001, 002 and 003 reflections respectively of illite. Considering the broad peaks, the illite in the fine clay has a lower degree of crystallinity compared to the illite in the total and coarse clay fractions.

Saturation with Mg^{2+} results in 14 Å peaks for whole the profile. After the glycerol treatment, these peaks shift towards 14.7 and 15 Å in the surface horizons, and to 16 Å in the deeper horizons. In the deeper horizons a clear peak shows up around 33 Å. In the Bw and C1-horizons the swelling mineral could well be the interstratification chlorite–smectite. In the surface horizons the contribution of this swelling mineral is less.

Saturation with K^+ gives a 14 Å peak in all the horizons. These peaks are lower than the Mg-peaks: vermiculite. After heating to 300 °C, the 14 Å peak shifts towards 10 Å: the interstratification chlorite–vermiculite. At 550 °C no intensified peaks show up at exactly 14 Å. In the Bw and C1-horizons the chlorite–vermiculite interstratification contains more chlorite than in the surface horizon. At 550 °C the 14 Å peak of chlorite intensifies, whereas the 7 Å peak disappears: kaolinite.

Appendix 3

Clay mineralogy of the dispersed material in stream and subsurface flow: X-ray diffraction patterns and their interpretation.

The view over the year (Fig. 9.16) of the non-fractionated samples shows illite, with reflections around 10, 4.9 and 3.34 Å. Saturation with Mg^{2+} results in a 14 Å peak. After the glycerol treatment, the 14 Å peak shifts towards 15–16 Å, whereas a peak around 29 Å shifts to 32–33 Å. This implies the presence of the interstratification chlorite–smectite. After the

glycerol treatment a reflection at 14 Å stays: a chlorite–vermiculite interstratification.

The fractionated sample ‘Lux 10’ shows in the fine as well as the coarse clay an illite peak. After Mg^{2+} saturation and a glycerol treatment, no shift of the 14 Å peak in the coarse clay fraction is shown, whereas in the fine clay a swelling is noticed to 16 Å: the interstratification chlorite–smectite. K-saturation and heating shows no chlorite, only an interstratification of chlorite–vermiculite. In other stream and subsurface flow samples a small chlorite peak shows up after K-saturation and heating to 550 °C. The peak at 7 Å disappears after heating to 550 °C: kaolinite.

The presence of a 14 Å peak in the dispersed stream and flow material implies that not only fine, but also coarse clay is transported. This conclusion is based on the absence of a 14 Å peak after glycerol treatment in the fine clay fraction of the reference profile.

Appendix 4: Dispersibility of the Soil Material

This section focusses on the dispersibility of soil material in the topsoil and subsurface Bg horizon of the forested Steinmergelkeuper soils.

In dispersion experiments, the potential dispersibility of these horizons has been compared. The effect on dispersion of the natural-, Ca-, and Mg-saturated adsorption complex was tested. In addition, tests have been carried out to determine the minimum concentration of an electrolyte which causes flocculation. This minimum is described as the flocculation value, or as the critical coagulation concentration (van Olphen 1977).

Dispersion Experiments

Soil material of AEh,EAh- and Bg horizons of soil profile II (Appendix 1) has been used for these experiments. For detailed methods of these experiments see van den Broek (1989).

Table 9.11 CEC and saturation of the exchange complex of samples used for the dispersion experiments (van den Broek 1989)

Hor	Sat.Exc. ^a	Without removal of organic matter			
		CEC	Ca	Mg	Ca/Mg ratio
		mmol _c kg ⁻¹ soil			
AEh	Ca	145	149	1	135
	Mg	143	8	129	0.1
	Nat	137	86	28	3.1
EAh	Ca	111	97	1	81
	Mg	126	4	99	0.0
	Nat	116	55	26	2.1
Bg	Ca	210	171	3	59
	Mg	211	4	178	0.0
	Nat	199	102	63	1.6

^aThe exchange complex is saturated with Ca, or with Mg, or is left in its natural (Nat) composition

AEh-, EAh- and Bg material were used with its natural adsorption complex composition. These materials were also transformed into a completely Ca- or Mg-saturated adsorption complex.

In series with increasing soil/water ratios (1–10 g fine earth with 75 ml of demineralized water) and 24 h end-over-end shaking (21 rpm) in tubes, centrifugation was carried out to give suspensions with particles <1 and <0.2 µm respectively. To measure the degree of dispersion, the nephelometric turbidity, in the clay suspensions was estimated. Also, the electrical conductivity, pH and cation- and anion concentrations were determined in the supernatant of the centrifuged clay suspensions. Cation exchange capacity (CEC), and the main exchangeable cations, Ca and Mg, have been determined Table 9.11).

In Fig. 9.17 the relation is shown between the increase in soil/water ratio and turbidity. Presented are the clay fractions <1 and <0.2 µm, originating from the AEh and Bg horizons, with a natural exchange complex composition (Nat), a Ca-saturated (Ca) and a Mg-saturated complex (Mg). For all the 12 subsamples the turbidity rises with increasing soil/water ratio. This implies that in the whole range of increasing soil/water ratio, even to 10 g fine earth in 75 ml water, the clay disperses. Flocculation would cause a decrease in turbidity, as there are less particles to scatter the incident light.

The increase in soil/water ratio implies an enhanced release of water-soluble elements, and therefore an increase in electrolyte concentration. Figure 9.17 shows that even 10 g fine earth shaken in 75 ml of demineralized water did not release enough water-soluble elements to cause flocculation, so the flocculation value is not reached.

The clay fractions from the Bg horizon show a higher turbidity than the fractions in the AEh horizon. This absolute difference is ascribed primarily to the higher clay content of the Bg horizon. It does not automatically imply that the clay in the subsurface horizon has a higher potential dispersibility compared to the clay in the surface horizon.

The low turbidity of the samples containing organic matter shows the stabilizing effect of the organic fraction on soil aggregates in the surface horizons. Here organic matter prohibits, to a certain extent, dispersion. The effect of 'free' organic matter, not linked to soil particles, is not explicitly shown by this experiment. The contribution of water-soluble organic compounds on clay dispersion is discussed in Appendix 5.

The effect of a Ca or Mg-saturated exchange complex on turbidity shows up, in particular for the fine clay fraction (Fig. 9.17). The fine clay saturated with Mg has a higher turbidity compared to the Ca-saturated material. This is in agreement with (Australian) literature. Soils with

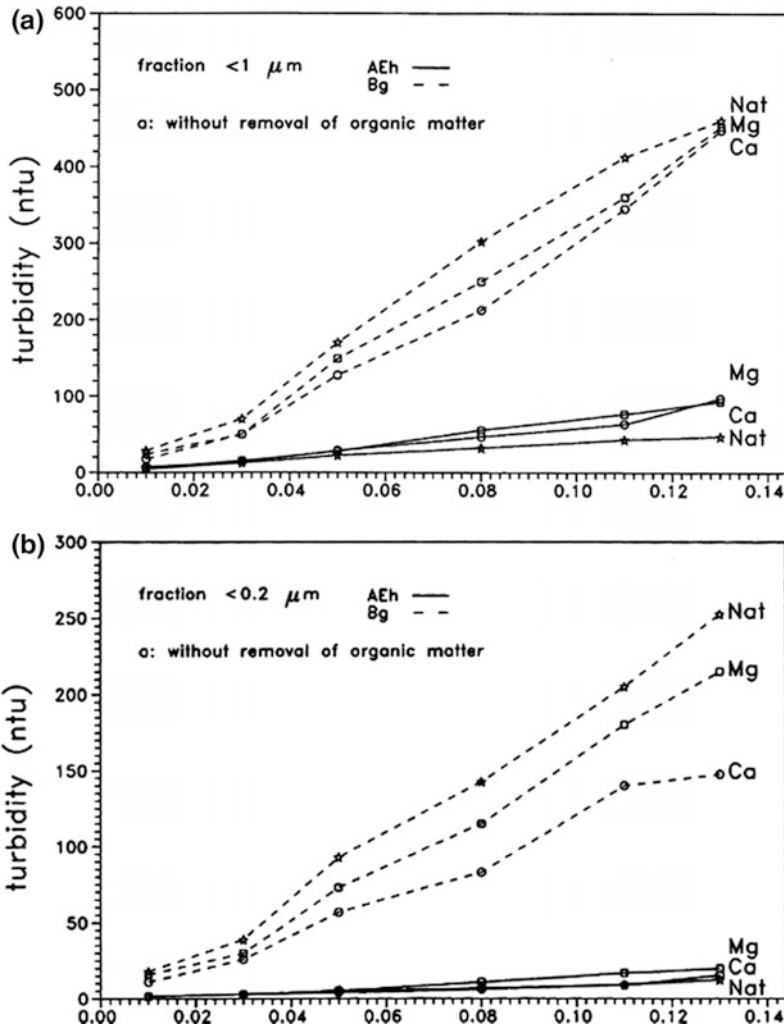


Fig. 9.17 Relationship between turbidity and soil/water ratio for **a** the clay fractions <math><1 \mu m</math>, and **b** the fine clay fractions (<math><0.2 \mu m</math>) with Ca-, Mg- or natural (Nat) exchange complex composition (van den Broek 1989)

a high magnesium content at the exchange complex were noticed for their bad physical structure and properties (Koenigs and Brinkman 1964; van Schuilenborgh and Veenbos 1951). Often the dispersive effect of magnesium was only noticed with illites, and not with montmorillonites and swelling interstratifications.

Nevertheless, Shainberg and Letey (1984), Alperovich et al. (1981), Dontsova and Norton (2002) and Zhang and Norton (2002) found that at very low electrolyte concentration magnesium has a dispersive effect on clays, especially on montmorillonites. This supports the results

of the experiment here, as the fine clay fractions composed of illite as well as of a swelling 16 Å mineral and the electrolyte concentration of the soil solution was always very low, a Ca- and Mg concentration around 0.3 mM (Table 9.8). The dispersive effect of the magnesium compared to the calcium ion can be explained by the larger diameter of the hydrated magnesium ion compared to the calcium ion, being 0.47 and 0.42 nm respectively (Stern and Amis 1959). Tucker (1985) showed that exchangeable Mg is slightly less strongly held at the clay surface than Ca.

A different effect of adsorbed Mg at the exchange complex for clay dispersion, is more indirect in nature. Kreit et al. (1982) studied the rate of hydrolysis of hectorite, a trioctahedral smectite. The rate of hydrolysis of the Mg-saturated hectorite was lower than that of its Ca equivalent. This is ascribed to the rate-reducing effect of exchangeable Mg on the hydrolysis of hectorite, so the presence of Mg, at the exchange complex stabilizes this clay mineral. Consequently, the hydrolysis of the Mg-clay also decreases, which prevents severe dissolution of the clay minerals. Due to the low rate of hydrolysis, the electrolyte concentration of the soil solution in equilibrium with the Mg clay is low, and dispersion will probably take place.

The soils in this study are characterized a.o. by a fine clay fraction which has much Mg adsorbed at the exchange complex (Table 9.2), which contains a swelling 16 Å interstratification (Table 9.5), and which is high in structural Mg. This fine clay fraction in particular is transported laterally in a dispersed state. The low electrolyte concentration of the soil solution and subsurface flow can be explained by the relatively low solubility of the Mg containing trioctahedral clay. Mg at the exchange complex prohibits severe dissolution of the clay minerals, and consequently the electrolyte concentration of the soil solution is kept at a low level, probably governed by the exchange reactions, which is favorable to clay dispersion.

Figures 9.17 and 9.18 show that even in a ratio of 10 g soil in 75 ml of demineralized water, not enough water extractable cations are released to cause flocculation of the dispersed clay. The potential dispersibility of the Bg horizon compared to the overlying topsoil is high due to the absence of aggregating agents, and its high Mg content at the adsorption complex, and the stabilizing effect of organic matter on the clay in the topsoil. The potential dispersibility of the Bg horizon exceeds the potential dispersibility of the topsoil also because of a higher fine clay content.

The adsorbed Ca/Mg ratio of the samples with a natural exchange complex (Nat) is in between the adsorbed Ca/Mg ratio of the Ca and Mg-saturated samples (Table 9.11). Figure 9.17

shows clearly that the samples with the natural exchange complex (Nat) never show a turbidity to be expected according to their Ca/Mg ratio, viz. in between the Ca and Mg-saturated samples. This “inconsistent” behaviour of the Nat-samples for turbidity and their Ca/Mg ratio is apparently due to the pretreatment of the samples and the organo-mineral bonds of the soil material. At higher organic matter levels, as in the AEh horizon (Fig. 9.17), the turbidity of the Nat-samples is the lowest. It is suggested that by saturation with Ca or Mg, the bonds between the clay, the divalent cation and the organic matter, are (partly) broken temporarily by the pretreatment. The new bonds between the freshly prepared Ca or Mg clay and the organic matter, are apparently not as strong as the bonds between the clay and the organic matter in the Nat-sample. Consequently, the Ca and Mg-saturated clays show a higher turbidity compared to the Nat-samples.

The samples with very low organic matter levels, being all horizons in Fig. 9.17 except the AEh horizons, show an opposite trend. Here the samples with a natural exchange complex have always a higher turbidity compared to the Ca and Mg-saturated clays. As is described in Appendix 5, the samples with a natural exchange complex (Nat) have been freeze-dried once, whereas the Ca and Mg-saturated clays have been freeze-dried twice. By comparing the turbidity of air dried and freeze-dried material of the Bg horizon in a separate dispersion test, it appeared that the freeze-dried samples showed a slightly lower turbidity.

Flocculation Test

In this test the minimum electrolyte concentration necessary to flocculate the clay fractions <1 and <0.2 μm of the fine earth of the AEh, EAh and Bg horizon has been determined. This minimum concentration is defined as the flocculation value, or as the critical coagulation concentration (van Olphen 1977; Sposito 1984).

The electrolyte used to determine the flocculation value is approximately equal to the soil

solution with regard to composition and concentration. Series of samples were prepared of 6.00 g fine earth in 75 ml electrolyte solution with increasing concentration, in 100 ml polyethylene tubes. The electrolyte concentration ranges from 0 to approximately 2 mM, of an equal molar solution of CaCl_2 and MgCl_2 . The soil solution contains mainly divalent cations, approximately equal amounts of Ca and Mg (Ca/Mg ratio around 1.4). The range of the electrolyte concentration in the flocculation experiment (0–2 mM) clearly exceeds the concentration of the soil solution, as the average concentration of divalent cations in the soil solution ranges from 0.15 to 0.67 mM (Table 9.8).

After 24 h End-Over-End shaking (EOE), 21 rpm, the tubes were centrifuged for the fraction <1 and $<0.2 \mu\text{m}$ to measure the nephelometric turbidity of these fractions. The separation of the clay fractions and the turbidity measurement followed procedures identical to the procedures of the dispersion experiment (van den Broek 1989). Also, the turbidity and the electrical conductivity have been determined in the centrifuged suspensions too.

In Fig. 9.18a nephelometric turbidity values are plotted against the concentration of the added electrolyte solution used for the flocculation experiment. In Fig. 9.19a the same turbidity values are presented for the electrical conductivity (EC_{25}). As the release of water extractable elements is very low, there are only very small differences between the relationship ‘turbidity-added electrolyte concentration before EOE’ and ‘turbidity-measured EC_{25} after EOE’.

The decrease of the nephelometric turbidity with increasing electrolyte concentration or EC_{25} shows up in particular in the clay fraction of the Bg horizon. Here a distinct threshold concentration is exceeded. The S-shape decrease of turbidity over a short interval of increasing electrolyte concentration agrees well with the classical DLVO-theory (van Olphen 1977). The flocculation values of the fractions <1 and $<0.2 \mu\text{m}$ are almost identical, and around an EC_{25} of $200 \mu\text{S cm}^{-1}$, or a divalent cation concentration of 0.8 mM. This critical coagulation

concentration is in the appropriate range of 0.5–2.0 mM for clays with divalent cations at the adsorption complex (van Olphen 1977).

The nephelometric turbidity of the AEh and EAh horizons decreases too with increasing electrolyte concentration. However, this decrease is not characterized by an S-shape as the fractions of the Bg horizon are. This implies that the clay in the AEh and EAh horizons behaves less according to the concept of concentration induced flocculation.

A comparison between A and B-horizons is hard to make, because of the different clay contents. To overcome this difference in texture, measured nephelometric turbidity values have been expressed relative to the turbidity of the sample containing zero CaCl_2 and MgCl_2 (Figs. 9.18b and 9.19b). This relative turbidity is equal to the measured turbidity divided by the turbidity of the suspension in the presence of only demineralized water. The relative turbidity ranges from 1.00 (dispersion due to the shaking with demineralized water) to almost 0, being the flocculated situation due to the added concentrated electrolyte solution. These relative turbidity curves show again an ‘ideal’ S-shape decrease for the clay fractions in the Bg horizon. This in contrast to the relative turbidity values of the AEh and EAh horizons. Apparently, the clay fractions in the surface horizons are not strongly affected by the increase in electrolyte concentration as the Bg horizon is. As the Bg horizon flocculates completely (relative turbidity of 0.04) at an EC_{25} of $200 \mu\text{S cm}^{-1}$ or at a concentration of 0.8 mM, the AEh and EAh horizons show more dispersion, as is indicated by their higher relative turbidity values, around 0.30, at that concentration level.

This high relative turbidity implies that the flocculating effect of the concentrated electrolyte solution is opposed. This is ascribed to the stabilizing effect of organo-mineral bonds in the surface horizons, and/or the dispersive mechanism of organic anions. The aggregation in the surface horizons due to (solid) organic matter prohibits dispersion, as is shown in Fig. 9.17. The contribution to the negative charge by organic anions in the AEh and EAh horizons is

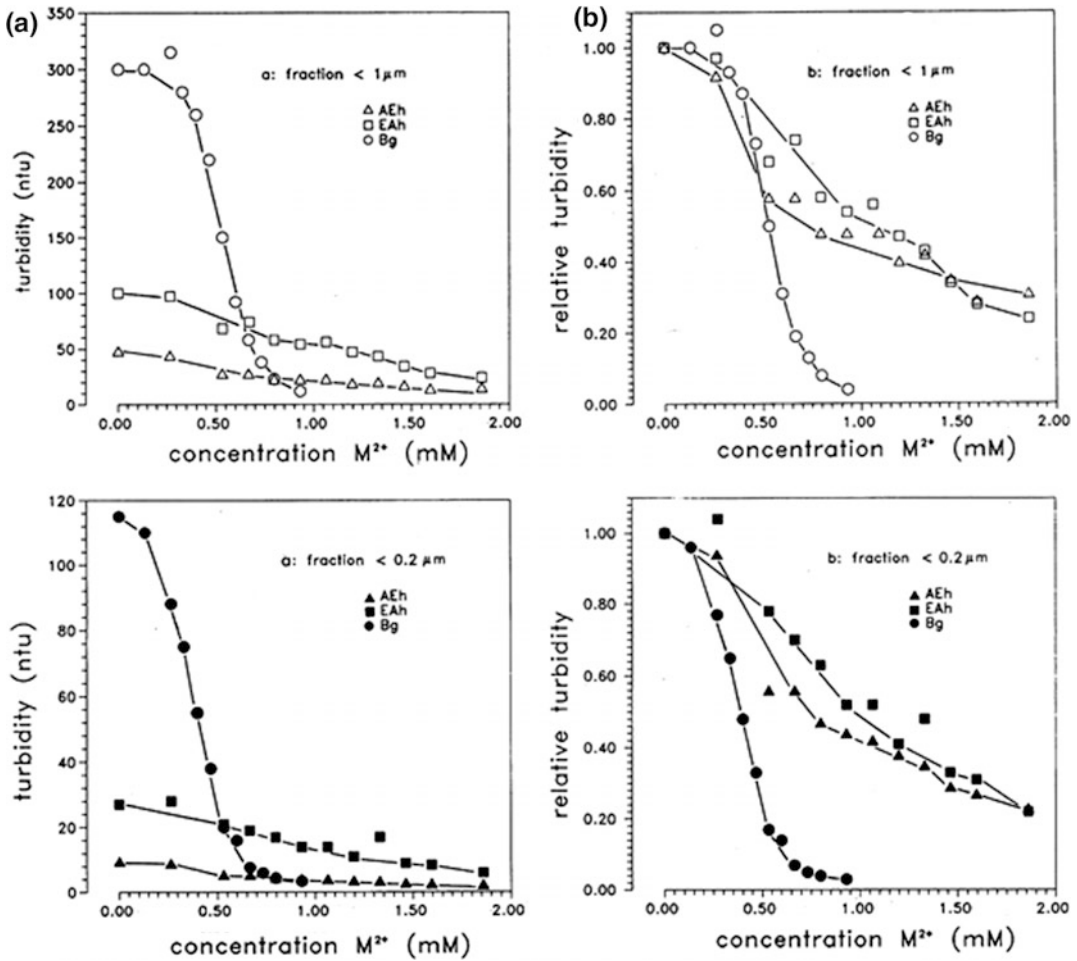


Fig. 9.18 Relationship of the concentration M^{2+} (Ca and Mg) of the solution before the start of the EOE-shaking with turbidity (a) and relative turbidity (b) of the fractions < 1 and $< 0.2 \mu\text{m}$ of the AEh, EAh and Bg horizons (van den Broek 1989)

considerable (ranging from 30 to 50%, Table 9.4). The dispersive effect, as stated by Oades (1984), of negatively charged organic compounds in the surface horizons, might play a role in prohibiting a complete flocculation. This will be discussed in Appendix 5.

Summary

The high potential dispersibility of the soil material and the flocculation values of the clay

fractions are important. The potential dispersibility of the soil material in the silty surface horizons is far below the potential dispersibility of the material in the heavy clayey Bg horizon. This is ascribed to the higher (fine) clay content in the Bg horizon, and to the stabilizing effect of (solid) organic matter in the surface horizons. The potential dispersibility of the Bg-clay is relatively high, because the low amounts of water extractable elements which are released by shaking the material in water, and its low Ca/Mg ratio at the

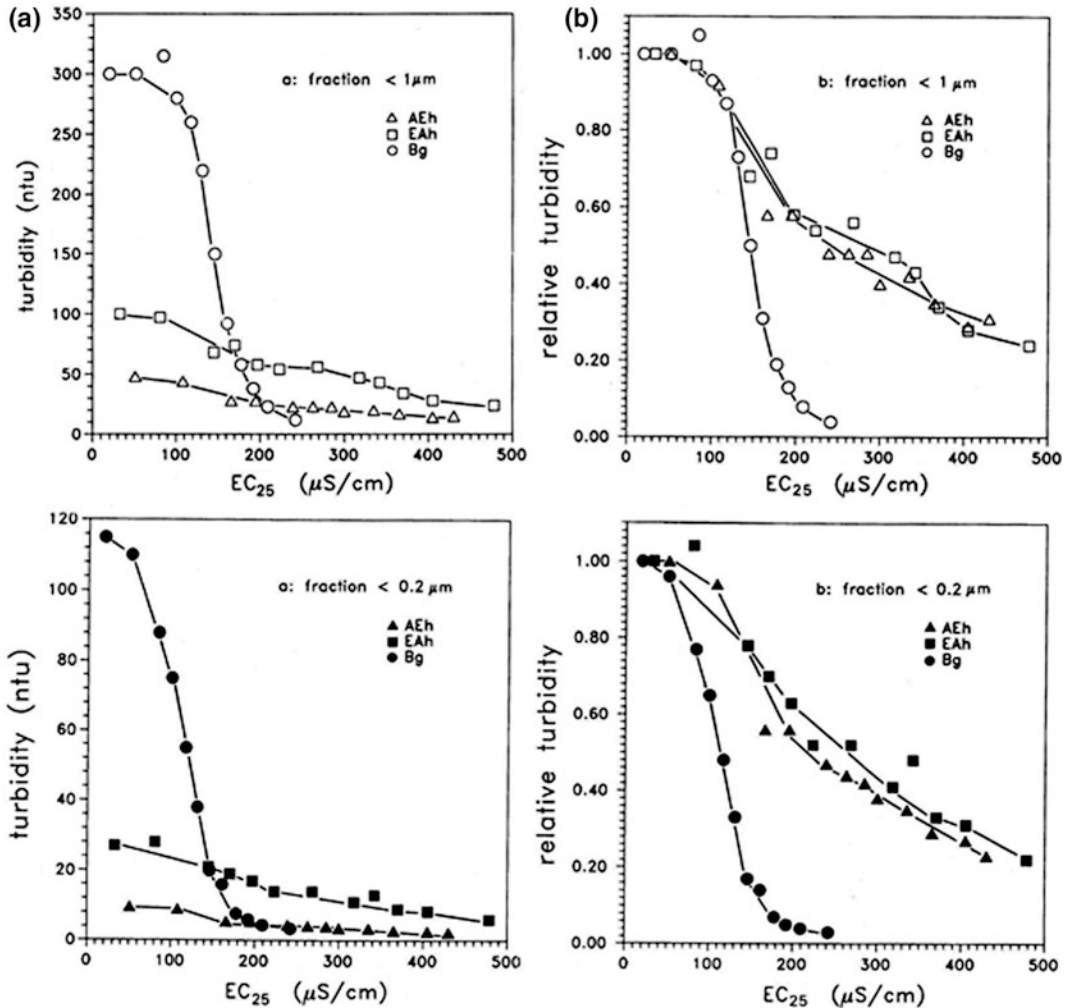


Fig. 9.19 Relationship of the electrical conductivity (EC_{25}) of the solution after EOE-shaking with turbidity (a) and the relative turbidity (b) of the fractions <math>< 1</math> and <math>< 0.2 \mu\text{m}</math> of the AEh, EAh and Bg horizons (van den Broek 1989)

adsorption complex. The positive effect of exchangeable Mg on clay dispersion of the Steinmergelkeuper soil material compared to exchangeable Ca is also shown. The flocculation value of the clay fraction <math>< 1</math> and <math>< 0.2 \mu\text{m}</math> of the Bg horizon is around 0.8 mM CaCl_2 and MgCl_2 . These values are above the highest concentration of the subsurface flow and soil solution at the contact between EAh and Bg horizons, as sampled on the forested Steinmergelkeuper slopes (Table 9.8).

Appendix 5: Effects of Water-Soluble Organic Compounds on Clay Dispersion

Dispersion/Flocculation Experiments with Water-Soluble Organic Compounds Additions

Data in Table 9.4 show that the relative contribution of organic anions in various soil/water extracts to the charge balance, is considerable.

These relative high concentrations of organic anions, and the DOC values of soil solution and subsurface flow, are all of a concentration level which appears to increase the resistance of clay against flocculation considerably. Based on the results and data of the laboratory experiment, an indirect effect on the dispersion of clay is ascribed to water-soluble humic substances in soil solution and subsurface flow (see also Appendix 5, as well as Bloomfield 1956; Durgin and Chaney 1984; Oades 1984). A mechanism which is likely to contribute to the dispersion domain of clay is the adsorption of soluble humic substances at clay particles. This causes steric stabilization of clay particles, which resists flocculation to a certain extent.

During wetting, forces developed inside and outside the "specific structural units" of the soil material. Soil aggregates which do not fall apart when wetted are regarded as "water stable". In mineral soils, most of the humified material is associated with inorganic materials, particularly clays. Cementing agents, like free sesquioxides and calcium carbonate, and organic bindings are held responsible for this water stability. However, the first two cementing agents are unimportant in the solum of the Steimergerkeuper soils and only organic matter plays a role in the topsoil.

Unfortunately, up until now, no detailed research was carried out on the stabilizing effect of (solid) organic matter, e.g. on the interactions of organic compounds, with mineral (clay) material, in our Steinmergelkeuper soils.

Moreover, the destabilizing effect of water-soluble organic matter on soil aggregates and especially on dispersion of clays is not completely understood. There are some indications that these humic substances are involved in the process of clay dispersion. If bonds between clay and organic matter are destroyed by mechanical forces, for example by the kinetic impact of a heavy rainstorm, organic matter becomes attached to one simple clay particle only. This creates an extra negative charge and therefore more repulsion, so organic matter will

act as a dispersant (Emmerson 1968). The dispersive effect due to adsorption of organic anions on positively charged edges of clay minerals is well known (Bloomfield 1956; Gilman 1974; Durgin and Chaney 1984; Oades 1984). Dispersion is increased due to blocking of the positively charged mineral sites by negative organic anions (Shanmuganathan and Oades 1983). In addition, complexation or chelation of polyvalent cations in the soil solution by dissolved organic matter might occur, reducing the activities of these cations and resulting in a more extended diffuse double layer around clay particles and they will disperse more easily.

In this section, the results of some experiments with natural and synthetic water-soluble organic compounds on the dispersion and flocculation on 2:1 clays with a divalent cation occupation will be discussed. In addition, a link to field conditions was made by using water extracts of forest litter, collected in autumn in the subcatchment in the experiments.

A dispersion/flocculation experiment with increasing salt level was carried out with the addition of various water-soluble organic compounds. The clay used in the experiments originated from the Bg-horizon of the reference profile (profile II, Appendix 1), and was saturated with Ca.

A fulvic acid extracted from a spodosol, and a synthetic citric, salicylic or p-hydroxybenzoic acid were added in various concentrations to the clay suspensions. Flocculation curves of the Ca-clay with these organic compounds in various concentrations, were determined. A range of 50 ml polyethylene tubes with the Ca-clay was prepared, containing an increasing concentration of CaCl₂ (0.1–2 mM). The tubes, with a final volume of 40 ml and a clay concentration of 1 g L⁻¹, were shaken end-over-end. After a certain settling time, the fraction <2 μm has been pipetted from the tubes in a cuvet. The nephelometric turbidity of the suspension in the cuvet was measured.

By plotting the measured turbidity data against the increasing electrolyte concentration in the tubes, flocculation curves of the Ca-clay have been determined, with and without the water-soluble organic compounds mentioned above.

In Fig. 9.20 flocculation curves of the Ca-clay are presented for relevant levels of fulvic acids. The curves show the expected S-shaped relationship between increasing salt concentration and turbidity, corresponding to the flocculation curves of the clay from the Bg horizon (Fig. 9.18). In the absence of fulvic acid the flocculation value of the Ca-clay is 1.0 mM CaCl_2 which is in agreement with earlier results (Appendix 4) and other findings (van Olphen 1977; Sposito 1984). In the presence of fulvic acid, a higher salt concentration is required to flocculate the Ca-clay compared to the clay suspensions without fulvic acid. Addition of fulvic acid to the Ca-clay causes an increase in turbidity and dispersion. From these results, it can be concluded that in this experimental design the natural water-soluble organic compounds have a dispersive effect on the Ca-clay.

When a small amount of organic polyelectrolyte is added to a clay suspension, the salt tolerance of that clay suspension is considerably increased, even to the extent that the clay remains in dispersion in a concentrated salt solution.

The synthetic low molecular water-soluble organic compounds have, in contrast with fulvic acids, not only a dispersive, for the carboxylic (citric) acid, but also a flocculating effect on the clay suspensions for the aromatic acids, e.g. salicylic and parahydroxybenzoic acids. In Fig. 9.21 the flocculation curves of the Ca-clay in presence of the various synthetic organic acids are shown.

In Fig. 9.22 the relation between added acids and the turbidity of the clay suspension is presented. A small amount of fulvic and citric acid added to the clay suspension is responsible for a large increase in turbidity, e.g. the dispersive domain, whereas aromatic acids additions cause

flocculation for the complete concentration range. Light absorbance by the brown coloured fulvic acid solution (without clay) is held responsible for the somewhat decreasing turbidity at high fulvic acid concentrations, as resulted from a separate test.

The two aromatic acids, salicylic and p-hydroxybenzoic acid, have a distinct flocculating effect. This in contrast to the citric acid, which shows an increase in dispersion of the Ca-clay for low concentrations. The dispersive whether flocculating effect of a water-soluble organic compound on clay depends on the interaction of the humic substance with the solution in which clay dispersion takes place, and on the bond between the humic substance and the clay mineral. The limited set of data, the complexity of humic substances and the many possible interactions between clay and organic compounds, exclude hard conclusions about the dispersive mechanism of humic substances. Therefore, the interpretation of the experimental data concerning the mechanism of humic substances involved in the dispersion of clay, has just a tentative character and will be summarized.

With regard to the increased dispersion of the Ca-clay caused by addition of fulvic and citric acid, cation complexation and ion-dipole interaction cannot be excluded beforehand. However, the similar response of the Na-clay (data not presented) compared to the Ca-clay on citric and fulvic acid rules out complexation and ion-dipole interaction as major mechanisms involved in the dispersion of the (Na as well as the) Ca-clay.

Another mechanism which can be involved in the interaction between water-soluble organic compounds and clay minerals is the adsorption of humic substances at the clay surface. Well known is the charge reversal at the edges of clay minerals by adsorption of small amounts of (organic) anions by ionization of the carboxylic groups (Shanmuganathan and Oades 1983). The results of the experiments here agree well with this model, as small amounts of citric and fulvic

acid give a considerable increase in the dispersion domain of the clay (Fig. 9.23). However, the clay mineralogy of the soil material from the Bg horizon (Table 9.1) points towards a relatively small edge charge. Therefore, another adsorption mechanism than charge reversal is worthwhile considering. Results of the experiments show that the dispersive effect of the low molecular citric acid holds only for low concentrations (Figs. 9.21 and 9.22). On the contrary, fulvic acids (Figs. 9.20 and 9.21), which are high in molecular weight, have also a dispersive effect at high concentrations. A bond between the clay mineral and the relatively high molecular fulvic acid is likely.

In addition to this mechanism of surface adsorption, the intercalation of uncharged parts of the fulvic acid in the interlayer of the clay mineral has also to be considered, as the pH of the solution in the experiments was around 4. The optimum pH for interlayering fulvic acids in Na-montmorillonite is around 2.5 (Schnitzer and Kodama 1966), at the prevailing pH conditions in the experiments interlayer adsorption cannot be ruled out on forehand. Notwithstanding that, no differences in X-ray diffraction patterns showed up between clay samples shaken with fulvic acids and those that were not. This implies that intercalation of fulvic acids in the soil material from the Bg horizon, can be excluded.

Summarizing, it is very likely that high molecular fulvic acids are adsorbed at the external surface of the clay. The non-flexible tails of the fulvic acid extend into the solution, and prevent the mutual attraction of particles. In this way, steric stabilization resists flocculation and contributes indirectly to the dispersion of the Ca-clay.

Adsorption of organic acids at the clay is supported by the data presented in Table 9.12. Fulvic and citric acid was added to the Ca-clay suspensions. After shaking, the water-soluble organic compounds were determined, and expressed as dissolved organic carbon (DOC). The clay suspensions with added fulvic acid contain approximately 5 mg C L^{-1} (DOC), whereas the clay suspensions with added citric acid contain approximately 7 mg C L^{-1} (DOC). From this data and the blank, containing about 8.5 and 9.0 mg C L^{-1} (DOC), it is concluded that a relative considerable amount of the high molecular fulvic acid is adsorbed at the clay surface. The adsorption of the small citric acid at the clay is less (see also Oades 1984).

Dispersion/Flocculation Experiments with Forest Litter Extract Additions

The preceding experiments show a.o. the positive effect of a fulvic acid extracted from a spodosol, on the dispersion of clay from the Bg horizon. In addition, clay dispersion under so-called field conditions was also carried out. Therefore, beech-oak litter lying on the forest floor at the experimental field site was collected and used also in a similar dispersion experiment.

Litter collected in autumn, was extracted with water in a ratio of 1:10 (w/v). This litter extract was diluted and contained 100 mg C L^{-1} (DOC).

Chromatographic separation by gel filtration of this extract with a Cu(II) solution as eluent, in order to get also information on the complexation capacity, was carried out to separate the water-soluble organic compounds on molecular

Table 9.12 DOC in the Ca-clay suspensions after EOE-shaking (van den Broek 1989)

	Fulvic acids: 25 mg L^{-1}		Citric acid: 25 mg L^{-1}	
	Concentration	DOC (mg C L^{-1})	Concentration	DOC (mg C L^{-1})
Ca-clay	1.0 mM CaCl_2	5.5	0.5 mM CaCl_2	8.9
	1.5	5.5	1.5	7.6
	2.0	5.4	2.5	7.0
Blank (without soil material)		8.5		9.0

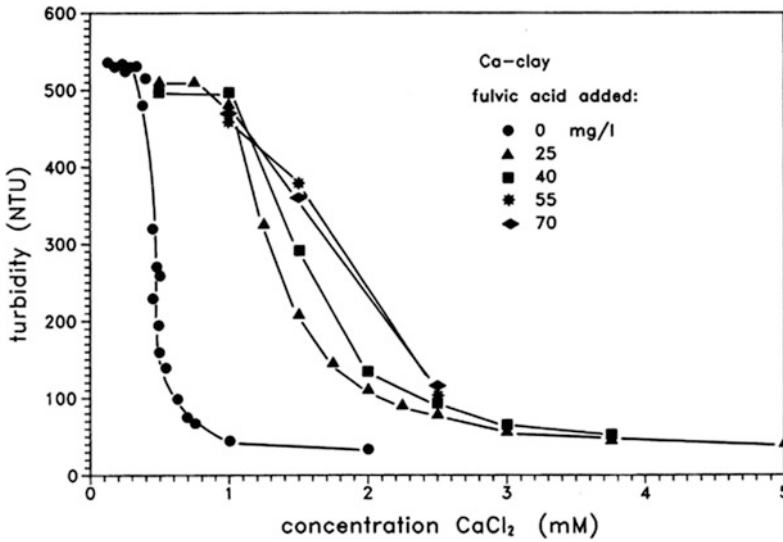


Fig. 9.20 Flocculation curves of the Ca-clay in presence of fulvic acid (van den Broek 1989)

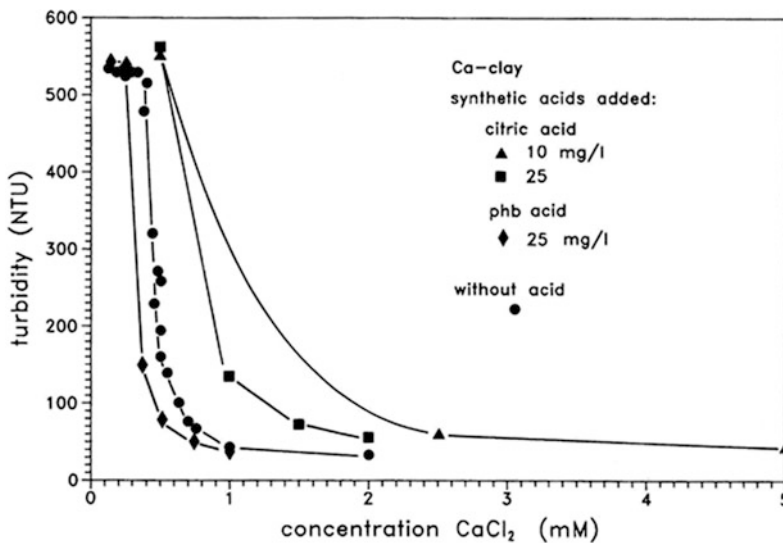


Fig. 9.21 Flocculation curves of the Ca-clay in presence of synthetic acids (phb acid = p-hydroxybenzoic acid) (van den Broek 1989)

weight. The fraction eluted first contained the relatively large molecules ($M > 5000$ D). The second fraction contained the smaller molecules with a non-aromatic character ($M < 5000$ D). To this last group the category of a.o. fulvic, citric and oxalic acid belongs. Large amounts of Cu(II)

were complexed by the small as well as the large water-soluble humic substances.

Gel filtration of an extract of soil material from the AEh horizon in a soil/water ratio of 1:2 (w/v), showed only minor amounts of small and large organic molecules, with a small

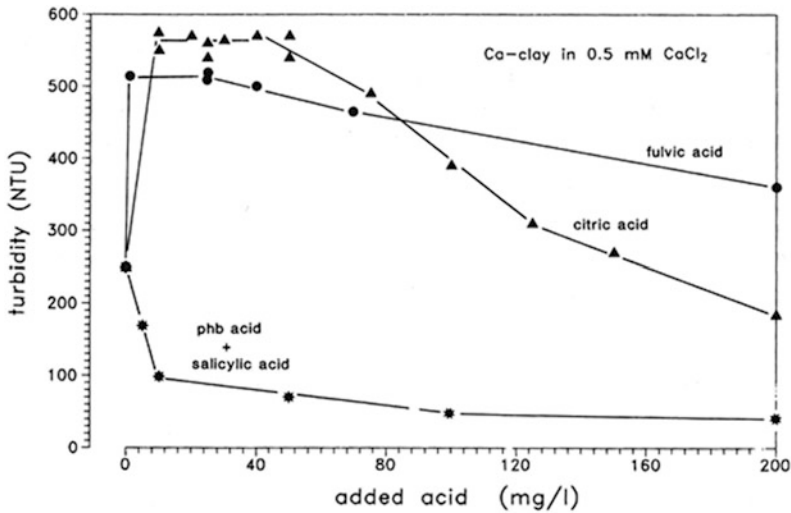


Fig. 9.22 The influence of the water soluble organic acids on the dispersion of the Ca-clay, at a concentration of 0.5 mM CaCl_2 (van den Broek 1989)

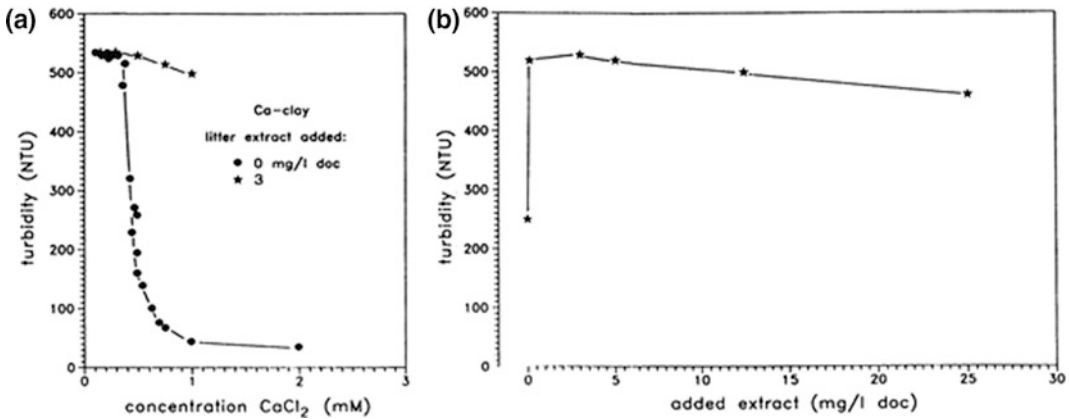


Fig. 9.23 **a** Flocculation curve of the Ca-clay in the presence of the diluted litter extract; **b** the influence of this diluted litter extract on the dispersion of the Ca-clay at 0.5 mM CaCl_2 (van den Broek 1989)

complexation of Cu(II). Gel filtration of the soil solution, sampled by means of a porous cup at the interface between EA_h and B_g horizons, did not show organic molecules at all. Consequently, the soil solution did not contain Cu-complexing water-soluble organic compounds.

Considering the DOC values of the extract of the soil material of the surface horizon and the soil solution, 34 and 20 mg C L⁻¹ respectively, it is not so surprising that gel filtration comes up with small amounts of water-soluble organic compounds and low values of Cu-complexation.

In addition, part of the humic substances is probably already complexed or adsorbed at the clay surface.

Anyway, the litter extract was considered as a kind of concentrated soil solution with regard to the composition of water-soluble organic compounds. Chromatographic separation showed that the litter extract contained Cu-complexing water-soluble organic compounds with a low as well as with a high molecular weight. Therefore, it was assumed that the litter extract has a similar effect on the dispersion of clay as the soluble

organic compounds used in the preceding experiments. These experiments showed that relatively large natural organic compounds and small, synthetic organic molecules with charged carboxyl groups, contribute considerably at the prevailing pH conditions to the dispersion of the Ca-clay (Figs. 9.20, 9.21 and 9.22). The litter extract contributes to the dispersion of clay, which is confirmed indeed by results of the additional dispersion experiment.

In Fig. 9.23a the dispersive effect of a diluted litter extract is clearly shown.

Even at the flocculation value of the Ca-clay, 1 mM CaCl_2 , a low concentration of humic substances (3 mg C L^{-1} DOC) causes a considerable increase in clay dispersion. Figure 9.23b shows even more clearly that very small amounts of litter extract cause a considerable increase in the dispersion of clay. The content of dissolved organic carbon in the soil solution ranges from 11 to 20 mg C L^{-1} (Table 9.8). In Figs. 9.22 and 9.23 it is shown that humic substances in such a concentration range contribute to the dispersion of clay. Based on these results, a positive (indirect) contribution to the dispersion of clay is ascribed to water-soluble organic compounds with charged carboxylic groups under near neutral pH conditions.

References

- Allison LE (1960) Wet combustion apparatus and procedure for organic and inorganic carbon in soils. Organic soil carbon reduction of chromic acid. *Soil Sc Soc Am J* 24:36–40
- Alperovich N, Shainberg I, Keren R (1981) Specific effect of magnesium on the hydraulic conductivity of sodic soils. *J Soil Sci* 32:543–554
- Barshad I (1964) Criteria for establishing uniformity of parent material. In: Bear FE (ed) *Chemistry of the Soil*, Reinhold Publication Corporation, New York, p 4–29
- Barnhisel RI, Bertsch PM (1989) Chlorite and hydroxy-interlayered vermiculite and smectite. In: Dixon JB, Weed SB (eds) *Mineral in soil environments*. Soil Science Society of America, Madison, Wisconsin, pp 729–788
- Bloomfield C (1956) The deflocculation of kaolinite by aqueous leaf extracts: the role of certain constituents of their extracts. *Trans 6th Int Cong Soil Sci, Paris, B*, 27–32
- Blume HP, Brümmer GW, Horn R, Kandeler E, Kögel-Knabner I, Kretschmar R, Stahr R, Wilke B-M (2016) *Scheffer/Schachtschabel soil science*, 16th edn. Springer, Berlin
- Bolt GH, Bruggenwert MGM (eds) (1978) *Soil chemistry: a basic elements*. Elsevier, Amsterdam
- Bonell M, Hendriks MR, Imeson AC, Hazelhoff L (1984) The generation of storm runoff in a for a forested clayey drainage basin in Luxembourg. *J Hydrol* 71:53–77
- Bradfield R (1936) The value and limitation of calcium in soil structure. *Am Soil Surv Assoc Bull* 17:31–32
- Brinkman R (1979) Ferrolysis, a soil-forming process in hydromorphic conditions. *Agricultural Research Reports* 699, PUDOC, Wageningen
- Burt TP (1979) The relationship between through flow generation and the solute concentration of soil and stream water. *Earth Surf Proc* 4:257–266
- Cammeraat LH (1992) Hydro-geomorphological processes in a small forested catchment: preferred flow-paths of water. Ph.D. thesis, University of Amsterdam, Amsterdam
- Cammeraat LH (2002) A review of two strongly contrasting geomorphological systems within the context of scale. *Earth Surf Proc Land* 27:1201–1222
- Cammeraat LH (2006) Luxembourg. In: Boardman J, Poesen J (eds) *Soil erosion in Europe*. Wiley, New York, pp 427–438
- Cammeraat LH, Kooijman AM (2009) Biological control of pedological and hydro-geomorphological processes in a deciduous forest ecosystem. *Biologia* 64:428–432
- Chhabra R, Pleysier J, Cremers J (1975) The measurement of the cation exchange capacity and exchangeable cations in soil: a new method. *Proc Intern Clay Conf*, 439–449
- Dontsova KM, Norton LD (2002) Clay dispersion, infiltration, and erosion as influenced by exchangeable Ca and Mg. *Soil Sci* 167:184–193
- Dopheide JCR (1986) *Verzuring van een Keuper bos-ecosystem*. Internal Report Lab of Phys Geogr and Soil Sci, University of Amsterdam, Amsterdam
- Duijsings JJHM (1985) Streambank contribution to the sediment budget of a forest stream. Ph.D. thesis, University of Amsterdam, Amsterdam
- Duijsings JJHM (1986) Seasonal variation in the sediment delivery ratio of a forested drainage basin in Luxembourg. In: Hadley RF (ed) *Drainage basin sediment delivery*. IAHS Publ 159, Wallingford, pp 153–164
- Duijsings JJHM (1987a) Runoff and sediment output from a Luxembourg Keuper catchment. *Publ Serv Geol Luxembourg Bul* 14:23–38
- Duijsings JJHM (1987b) A sediment budget for a forested catchment in Luxembourg and its implications for

- channel development. *Earth Surf Proc Land* 12:173–184
- Dumbleton MJ, West G (1966) Studies of the Keuper marl: stability of aggregation under weathering. Min of Transport, Road Res Lab, Rep 85, Crowthorne
- Durgin PB, Chaney JG (1984) Dispersion of kaolinite by dissolved organic matter from douglas-fir roots. *Can J Soil Sci* 64:445–455
- Emmerson WW (1968) The dispersion of clay from soil aggregates. *Trans 9th Int Congr Soil Sci* 1:617–626
- Emmerson WW, Chi CL (1977) Physical properties and structure. In: Russell JE, Greacen EL (eds) *Soil factors in crop production in a semi-arid environment*. University of Queensland Press, Queensland, pp p78–p104
- Germain P, Beven K (1981) Water flow in soil macropores I. An experimental approach. *J Soil Sci* 32:1–13
- Gilman GP (1974) The influence of net charge on water dispersible clay and sorbed sulphate. *Austr J Soil Res* 12:173–176
- Green RN, Towbridge RL, Klinka K (1993) Towards a taxonomic classification of humus forms. *Soc Amer Foresters Monogr*. 29, Bethesda MD
- Hazelhoff L, Van Hooff P, Imeson AC, Kwaad FJPM (1981) The exposure of forest soil to erosion by earthworms. *Earth Surf Proc Land* 6:235–250
- He Y, DeSutter TM, Clay DE (2013) Dispersion of pure clay minerals as influenced by calcium/magnesium ratios, sodium adsorption ratio, and electrical conductivity. *Soil Sci Soc Am J* 77:2014–2019
- Hendriks MR (1993) Effects of lithology and land use on storm run-off in East Luxembourg. *Hydrol Process* 7:213–226
- Hendriks MR, Imeson AC (1984) Non-channel storm period sediment supply from a topographical depression under forest in the Keuper region of Luxembourg. *Zeitschr Geomorph NF Suppl* 49:51–58
- Imeson AC (1986) Investigating volumetric changes in clayey soils related to subsurface water movement and piping. *Zeitschr Geomorph NF* 60:115–130
- Imeson AC, Jungerius PD (1977) The widening of valley incisions by soil fall in a forested Keuper area, Luxembourg. *Earth Surf Proc Land* 2:141–152
- Imeson AC, Vis M (1984a) The output of sediments and solutes from forested and cultivated clayey drainage basins in Luxembourg. *Earth Surf Proc Land* 9:585–594
- Imeson AC, Vis M (1984b) Seasonal variation in soil erodibility under different land-use types in Luxembourg. *J of Soil Sci* 35:323–331
- Imeson AC, Vis M, Duijsings JJHM (1984) Surface and subsurface sources of solids in forested drainage basins in the Keuper region of Luxembourg. In: Burt TP, Walling DE (eds) *Catchment experiments in fluvial geomorphology*. GeoBooks, Norwich
- IUSS Working Group WRB (2015). *World Reference Base for Soil Resources 2014, update 2015*. International soil classification system for naming soils and creating legends for soil maps. *World Soil Resources Reports No. 106*. FAO, Rome
- Jarvis NJ (2007) A review of non-equilibrium water flow and solute transport in soil macropores: principles, controlling factors and consequences for water quality. *Eur J Soil Sci* 58(3):523–546
- Jones JAA (1997) Subsurface flow and subsurface erosion. In: Stoddart DR (ed) *Process and form in geomorphology*. Routledge, London, pp p74–p120
- Jungerius PD (1980) Holocene surface lowering in the Lias Cuesta area of Luxembourg as calculated from the amount of volcanic minerals of Allerod age remaining on residual soils. *Zeitschr Geomorph NF* 242:192–199
- Jungerius PD, Mucher HJ (1970) Holocene slope development in the Lias Cuesta area, Luxembourg, as shown by the distribution of volcanic minerals. *Zeitschr Geomorph NF* 14:127–136
- Jungerius PD, Van Zon HJM (1982) The formation of the Lias Cuesta (Luxembourg) in the light of present day erosion processes operating on forest soils. *Geogr Ann* 64A:127–140
- Jungerius PD, Van den Ancker JAM, Van Zon HJM (1989) Long term measurement of forest soil exposure and creep in Luxembourg. *CATENA* 16:437–447
- Koenigs FFR, Brinkman R (1964) Influence of partial sodium and magnesium saturation on the structural stability of clay soils. *Trans 8th Int Congr Soil Sci, Bucharest, vol II*, pp 219–226
- Kooijman AM, Cammeraat LH (2010) Biological control of beech and hornbeam affects species richness via changes in the organic layer, pH and soil moisture characteristics. *Functional Ecol* 24:469–477
- Kreit JF, Shainberg I, Herbillon AJ (1982) Hydrolysis and decomposition of hectorite in dilute salt solutions. *Clays Clay Min* 30:223–231
- Lippmann F (1954) Über einen Keuper von Zaiserweiher bei Maulbronn. *Heidelberg Beitr Mineral Petrograf* 4:130–134
- Lippmann F (1956) Clay minerals from the Rot Member of the Triassic near Gottingen, Germany. *J Sed Petrol* 26:125–139
- Lippmann F (1960) Corrensit. In: Hintze C (ed) *Handbuch der Mineralogie, Ergänzungsband II, Neue Mineralen und Neue Mineralnamen* by Chudoba KF(ed) Teil III, pp 688–691
- Lucius M (1948) *Das Gutland: Erläuterungen zu der geologische Spezialkarte Luxemburg*. Publ Serv Geol de Luxembourg Bd V, Luxembourg
- Lucius M (1961) La presence de loess, de mineraux denses et de mineraux volcaniques dans les depots de plateaux de Norte pays. *Extr Du Bull* 1958(3):3–18
- Oades JM (1984) Soil organic matter and structural stability: mechanisms and implications for management. *Plant Soil* 76:319–337
- Oades JM (1986) Associations of colloidal materials in soils. *Trans 13th Int Congr Soil Sci, vol V. Hamburg*, 660–674
- Oliver BG, Thurman EM, Malcolm RL (1983) The contribution of humid substances to acidity of colored natural waters. *Geochim Cosmochim Acta* 47:2031–2035

- Pilgrim DM, Huff DD, Steele TD (1978) A field evaluation of subsurface and surface runoff II. Runoff processes. *J Hydrol* 38:319–341
- Poeteray FA, Riezebos PA, Slotboom RT (1984) Rates of subatlantic surface lowering calculated from marcel-trapped material (Gutland, Luxembourg). *Zeitschr Geomorph NF* 28:467–481
- Quirk JP, Aylmore LAG (1971) Domains and quasi-crystalline regions in clay systems. *Soil Sci Soc Am Proc* 35:651–654
- Rengasamy P (1982) Dispersion of Ca clay. *Austr J Soil Res* 20:153–157
- Rengasamy P (2002) Clay dispersion. In: McKenzie BM, Coughlan K, Cresswell H (eds) *Soil physical measurement and interpretation for land evaluation*. CSIRO Publishing, Melbourne, pp 200–210
- Schnitzer M, Kodama H (1966) Montmorillonite: effect of pH on its adsorption of a soil humic compound. *Science* 153:70–71
- Shainberg I, Letey J (1984) Response of soils to sodic and saline conditions. *Hilgardia* 52:1–57
- Shanmuganathan RT, Oades JM (1983) Influence of anions on dispersion and physical properties of the A-horizon of a red brown earth. *Geoderma* 29:257–277
- Soil survey Staff (1975) *Soil Taxonomy*. USDA Handbook 436, Government Printing Office, Washington, DC
- Soil Survey Staff (2014) *Keys to Soil taxonomy*, 12th edn. US Department of Agriculture, Natural Resources Conservation Service
- Sposito G (1984) Surface chemical aspects of soil colloidal stability. *The surface chemistry of soils*. Oxford University Press, New York, pp 198–228
- Stern KH, Amis ES (1959) Ionic size. *Chem Rev* 59:1–64
- Tucker BM (1985) The partitioning of exchangeable magnesium, calcium and sodium in relation to their effects on the dispersion of Australian clay subsoils. *Austr J Soil Res* 23:405–416
- Van Breemen N, Buurman P (2002) *Soil formation*, 2nd edn. Kluwer Academic Publishers, Dordrecht
- van den Broek TMW (1989) Clay dispersion and pedogenesis of soils with an abrupt contrast in texture: a hydro-pedological approach on a subcatchment scale. Ph.D. thesis, University of Amsterdam, Amsterdam
- Van Hooff P (1983) Earthworm activity as a cause of splash erosion in Luxembourg forest. *Geoderma* 31:195–204
- Van Hooff P, Jungerius PD (1984) Sediment source and storage in small watersheds on the Keuper marls in Luxembourg. *CATENA* 11:133–144
- van Mourik JM, Braekmans DJG (2016) *Mardellen*. *Geografie*, nov/dec 2016:31–43
- van Olphen H (1977) *An introduction to clay colloid chemistry*. Wiley, New York
- van Schuilenborgh J, Veenbos JS (1951) Over de invloed van Mg op de structuur van sedimenten. *Landbouwk Tijdschrift* 63:709–719
- Van Wesemael B, Verstraten JM (1993) Organic acids in a moder type humus profile under a mediterranean oak forest. *Geoderma* 59:75–88
- Zhang XC, Norton LD (2002) Effect of exchangeable Mg on saturated hydraulic conductivity, disaggregation and clay dispersion of disturbed soils. *J Hydrol* 260:194–205

Soil Animals and Litter Quality as Key Factors to Plant Species Richness, Topsoil Development and Hydrology in Forests on Decalcified Marl

10

A.M. Kooijman, L.H. Cammeraat, C. Cusell, H. Weiler and A.C. Imeson

Abstract

Animal activity and litter quality play a key role in forests on decalcified Steinmergelkeuper marls. The dominant trees hornbeam and beech clearly differ in litter quality, which affects earthworm activity and soil formation. Trees were even more important to topsoil characteristics than the subsoil. Under hornbeam, with high-palatable litter, organic layers were thinner, species richness higher and topsoils wetter and less acidic than under beech with more recalcitrant litter. In decalcified marl, lateral clay eluviation leads to differentiation in silty topsoils and clay-rich, water-impermeable Bg-horizons. Depth of the impermeable layer was shallower under hornbeam than under beech. Under hornbeam, formation of silty topsoils is probably counteracted by erosion. High animal activity leads to increased denudation of the surface, macropore systems with pipe flow in the soil, and approximately ten times higher export of soil particles than under beech. Under the low-palatable beech, leaching can continue without interruption, due to protective litter covers, low macroporosity, and throughflow with loss of base cations and clay particles rather than silt and sand. The two trees also showed habitat preferences, which extend their presence in particular habitats beyond the lifespan of individual trees. Hornbeam seedlings were only found under hornbeam, and are probably better adapted to wetness with superficial fine roots. Beech seedlings established everywhere, but further growth may be hampered in wet places due to three-dimensional fine root systems. Hornbeam and beech thus act as ecosystem engineers, with different litter quality and animal activity leading to more suitable habitat conditions for themselves, and development of wet and dry subsystems in the forest.

A.M. Kooijman (✉) · L.H. Cammeraat · C. Cusell ·
H. Weiler · A.C. Imeson
Institute for Biodiversity and Ecosystem Dynamics,
University of Amsterdam, Science Park, P.O.
Box 94062, 1090, GB Amsterdam, The Netherlands
e-mail: a.m.kooijman@uva.nl

L.H. Cammeraat
e-mail: l.h.cammeraat@uva.nl

C. Cusell
e-mail: c.cusell@witteveenbos.nl

H. Weiler
e-mail: hendrikalexanderweiler@gmail.com

C. Cusell
Witteveen+Bos, P.O. Box 233, 7400, AE Deventer,
The Netherlands

10.1 Introduction

In the Luxembourg cuesta landscape, with its clear gradient in parent materials, abiotic habitat conditions usually determine the response of biotic ecosystem components (see also Chap. 7 and 8). In the Steinmergelkeuper forests on the Keuper dipslope, it is however possible to study how biotic components affect topsoil development and habitat differentiation. In the decalcified forest soils, biological activity is significant, and the impact of earthworms on erosion processes is rather large (Hazelhoff et al. 1981; Jungerius and van Zon 1982; van Hooff 1983). The seasonal removal of litter from the soil surface by earthworms exposes the mineral soil surface to splash and overland—flow erosion processes. This includes both material derived from worm casts, as produced by *Allolobophora nocturnes* L., as well as from bare mineral soil due to litter removal by *Lumbricus terrestris* L. The latter has a burrow system which can reach more than one metre depth (Edwards and Lofty 1977), and burrowing activity is greatly stimulated when food is scarce. Earthworms also use natural cracks and pipes, such as polygonal cracks at the soil surface during dry periods (Hazelhoff et al. 1981; Cammeraat 1992). The activity of these soil animals results in strong bioturbation, as shown by Jungerius et al. (1989) who observed complete mixing of two cm thick artificial sand columns with the surrounding soil matrix within a few years. The topsoil horizons often show a strongly aggregated structure, indicating high biological activity. Earthworms are also responsible for the creation of continuous macropore systems, which are important from a hydrological point of view. In Steinmergelkeuper soils, perched water tables can be present during wet periods, when rainwater stagnates on top of the clay-rich Bg-horizon (Cammeraat 1992, see also Chap. 9). Under such conditions, water flow in wormholes was frequently observed.

Other important animals in the Steinmergelkeuper forests are wild boar (*Sus scrofa* L.) and moles (*Talpa europea* L.). Wild boars

visit the area frequently and dig in damp areas for food such as plant roots, fungi and earthworms. Their churning activity can locally lead to high erosion of freshly exposed soil. Moles are important because they create patches of bare soil in molehills, but also play a role in hydrological connectivity. They are especially common where earthworms are active (Jungerius and van Zon 1982; Cammeraat 1992). It was observed that moles were often using existing shrinkage cracks as tunnels. Shrinkage crack systems are generally disconnected, but moles can link separate segments. The moles follow the shrinkage cracks predated on the earthworms, and simultaneously change them into a continuous pipe system, which frequently conducts water.

Though animals are an important factor in Steinmergelkeuper forests, their activity is spatially heterogeneous. Patches with high earthworm activity alternate with places where no litter removal is observed. In the latter, a 3–4 cm thick organic layer is present at the soil surface, with distinct litter and fermentation and sometimes even humus horizons (Green et al. 1993). This differentiation is probably related to tree diversity. The forests consist of a mixture of tree species, such as hornbeam (*Carpinus betulus* L.) and beech (*Fagus sylvatica* L.), interspersed with summer oak (*Quercus robur* L.). Beech and hornbeam patches generally clearly differ (Fig. 10.1). Dense organic layers are usually found under (clustered) beech trees (van Hooff 1983), which has less palatable litter than hornbeam (Swift et al. 1979; Laskowski et al. 1995; Aubert et al. 2003, 2004). The more recalcitrant beech litter accumulates in dense organic layers, while the highly palatable hornbeam litter generally rapidly disappears from the forest floor (e.g., Swift et al. 1979; Berg 2000; Ponge 2003).

Differences in litter quality and animal activity may even lead to development of different habitats. Under trees with high-palatable litter, reduction of (protective) litter covers may increase erosion at the soil surface (Lee and Foster 1991; Oades 1993; Greene and Hairsine 2004). High earthworm activity also increases macroporosity and internal drainage (Lee and

Table 10.1 Differences in characteristics of organic layer and mineral topsoil between hornbeam and beech in mixed Keuper forests

	n	Species effect	Hornbeam	Beech
<i>Organic layer</i>				
Litter input (g m ⁻²)	12	ns	481 (95)	458 (67)
Beech litter input (g m ⁻²)	12	*	103 (29)	239 (51)
Hornbeam (g m ⁻²)	12	*	139 (45)	35 (27)
Summer oak (g m ⁻²)	12	*	210 (75)	159 (75)
Olson decomposition value	12	*	3.5 (2.1)	0.6 (0.3)
Organic layer previous years (g m ⁻²)	12	*	240 (70)	1085 (505)
Total mass organic layer (g m ⁻²)	21	*	644 (180)	1603 (573)
<i>Mineral topsoil</i>				
C-content (%)	9	ns	4.6 (0.6)	5.8 (1.5)
C:N ratio (g g ⁻¹)	9	*	14.0 (0.8)	16.9 (1.5)
pH-H ₂ O	18	*	5.7 (0.3)	5.0 (0.3)
Bulk density (g cm ⁻³)	12	*	0.98 (0.08)	0.84 (0.10)
Porosity (%)	12	*	63 (4)	68 (5)
Moisture content at field capacity (%)	12	*	46 (4)	36 (2)
Air-filled pore space (%)	12	*	17 (10)	32 (9)
Amount of small aggregates (%)	12	*	28 (10)	43 (12)
Depth of clay-rich B-horizon (cm)	18	*	12 (3)	19 (4)
Clay content (% soil)	6	*	28 (2)	23 (2)
Water-stable micro-aggregates (% clay)	6	*	70 (3)	68 (2)
Water-dispersible clay (mg kg ⁻¹)	6	ns	84 (13)	75 (06)
Potential clay dispersion (NTU)	12	ns	78 (25)	71 (25)

Mean values and standard deviations for both species ($n = 6-21$; each replicate is based on 5 individual measurements)

*Significant differences between species ($p < 0.05$); ns not significant

Foster 1991; Oades 1993), and can even lead to pipe flow, which is more rapid than matrix throughflow and can remove larger soil particles than clay (Cammeraat 2002). In contrast, topsoil processes such as acidification and eluviation of clay may be retarded or even counteracted by homogenization of the soil by burrowing animals (Pop 1997; Jongmans et al. 2003; Pulleman et al. 2005). Also, acidification of the topsoil may be compensated by root uptake of base cations from deeper layers, which is more common in trees with high-degradable litter (Mohr and Topp 2005).

Low-degradable litter may promote another topsoil development. Under trees with low-degradable litter, mechanical erosion is probably low, because the organic layer is present all year long, and forms a protective cover. Topsoil acidification may be relatively high, due to poor homogenization, but also to percolation of organic acids which occurs when decomposition is retarded (Hornung 1985; Neiryneck et al. 2000; Aubert et al. 2004). Lower pH values may in turn lead to increased clay eluviation in the topsoil, although this process is also regulated by other factors, such as organic carbon content, ionic



Fig. 10.1 Forest on Steinmergelkeuper showing in the foreground a Hornbeam dominated patch (with ground cover of *Anemone nemorosa*) and the slightly more

elevated Beech dominated micro-habitat (with only litter at the forest floor) in the background

strength and the amount of mono-, bi- and trivalent cations (Duchaufour 1982; van den Broek 1989). In addition, clay eluviation may be affected by lower macroporosity. When earthworm activity is low, water movement in the soil mainly occurs as matrix throughflow, rather than overland and pipe flow. In matrix throughflow, silt and sand are not transported, but clay particles can flow through the micropores (Cammeraat 2002). This leads to a relatively high loss of clay.

In the mixed forests on Steinmergelkeuper marls, habitat differentiation related to earthworm activity may thus be due to differences in litter quality between beech and hornbeam. The effects

of animal activity and litter quality are further explored in this chapter, which gives a synthesis of published and unpublished studies from the last decades. Questions discussed are: (1) how does animal activity affect litter decomposition? (2) are the litter decomposition regimes of hornbeam and beech litter really different? (3) do hornbeam and beech patches really differ in habitat conditions? (4) can habitat differentiation really be attributed to tree species, or does this merely reflect habitat preferences of beech and hornbeam? and (5) how do litter quality and animal activity affect topsoil formation and erosion?

10.2 Methods

10.2.1 Study Area

This review is based on published and unpublished results from research over the last three decades (e.g. Hazelhoff et al. 1981; Jungerius and van Zon 1982; van Hooff 1983; Cammeraat 1992; Cammeraat and Kooijman 2009; Kooijman and Cammeraat 2010). The studied forests were already indicated on the 1777 map (Ferraris le Comte de 1777), and, except for some harvesting, largely undisturbed by man (Cammeraat 2002). The forests are located on the Triassic Steinmergelkeuper and generally consist of mixed forests, dominated by hornbeam and beech, and interspersed with summer oak. They belong to the Galio-Carpinetum forest type, with transitions to Galio odorati-Fagetum (Niemeyer et al. 2010). Hornbeam and beech clearly differ in litter quality and palatability (Swift et al. 1979; Laskowski et al. 1995; Aubert et al. 2003, 2004), which may be related to differences in N-content. Initial N-content of fresh leaves did not differ between Steinmergelkeuper forests, but was $9.0 \pm 0.5 \text{ mg g}^{-1}$ for beech, and $13.3 \pm 0.6 \text{ mg g}^{-1}$ for hornbeam (Kooijman and Cammeraat 2010). Soils are mostly characterized by Mull humus forms, but under beech sometimes also by Mormoder, with distinct F-horizons (Green et al. 1993). Soil type ranged from Luvic Stagnosol, often under hornbeam, to Luvic Planosol, often under beech (IUSS 2015). Both soils had AhE-Bg-Bw-C profiles, and a clear-to-abrupt textural change between the lower part of the topsoil (AhE) and the subsoil (Bg-Bw-C), due to lateral removal of clay from the topsoil (van den Broek 1989, see also Chap. 9). After heavy rain, perched water tables may develop on top of the impermeable Bg-horizon.

10.2.2 Field Surveys

Earthworm activity was studied in the Steinmergelkeuper forest Schrondweilerbusch, mostly in oak-hornbeam patches with high biological activity. Earthworm activity was determined by

mapping the litter cover, as well as horizontal and vertical dimensions of shrinkage cracks, which can be considered as representative for the situation in early autumn (Cammeraat 1992). Apart from the surface area, five cross sections of this crack were mapped, to show the variable conditions of the shrinkage cracks. The seasonal activity of earthworms was studied by looking at litter removal patterns over time on field plots in patches of oak-hornbeam forest where earthworm activity was high (Cammeraat 1992). The plots were mapped every month at a scale of 1:10. Surface cover of litter, herbs, molehills, cracks, moss, pig activity and (fibrous rests of) litter mounds were determined. Sediment concentrations were measured during several runoff events in the Schrondweilerbusch (Cammeraat 1992). Discharge was measured continuously with V-notches during 2 consecutive years, and sediment yield was measured during 67 events which produced runoff.

In the studies dealing with litter quality and topsoil characteristics, conducted in 3 consecutive years, we concentrated on differences between well-developed $7 \times 7 \text{ m}$ beech and hornbeam plots, selected according to stratified random sampling. Studies were conducted in three Steinmergelkeuper forests, including two parts of the Schrondweilerbusch (Duijsings 1985; van den Broek 1989; Cammeraat 1992), and Jardin Napoleon near Folkendange. In each of the three forests, five beech and five hornbeam plots were selected in the forest interior. Species composition and cover was determined in the $7 \times 7 \text{ m}$ plots in May. Mass of the organic layer was sampled in $25 \times 25 \text{ cm}$ squares in May and November; litter input was only measured at the end of November. Within the squares, depth to the impermeable, clay-rich Bg-horizon was measured with an auger, and the upper 5 cm of the mineral soil sampled with standard pF-rings. If present after heavy rain, perched water tables were also measured.

The stratified random sampling of hornbeam and beech plots was expanded to a grid cell approach, with mixed forest included as well. Grids of 100 cells of $7 \times 7 \text{ m}$ were installed in two parts of the Schrondweilerbusch forests, on

characteristic slope sections from top to valley bottom. In addition to the plant and soil parameters mentioned above, soil profiles were described to a depth of 120 cm, in order to test the effect of subsoil characteristics. In addition to the auger, depth of the clay-rich Bg-horizon was also measured with a small stick, with slightly different results. However, differences between tree species were consistent in both cases. Since the grids were in the same forest area, and showed only minor differences in soil characteristics, the two datasets were combined to one set with 200 plots.

10.2.3 Laboratory Measurements

Samples of organic layer and mineral topsoil were dried for 48 h at 70 °C and weighed. Decomposition values according to Olson (1963) were calculated for autumn samples, with the amount of fresh litter and the ectorganic material remaining from the previous year(s). The pH of the mineral topsoil was determined in demineralized water with 1:2.5 weight:volume ratio. For the mineral soil samples, dry bulk density and volumetric moisture content were calculated. With dry bulk density, porosity was calculated, based on rock particle density of 2.65 g cm⁻³ (Schachtschabel et al. 1982). Air-filled pore space was calculated by subtracting volumetric moisture content from porosity. Corrections for soil organic matter were not applied, but since particle density is substantially lower than for mineral soil, this would have led to lower porosity and even lower air-filled pore space than the 10% estimated for the wettest soils. C and N content were measured with a CNS analyzer (Westerman 1990). Distribution of dry macro-aggregates was measured by sieving over 16, 8, 4.8, 4, 2, 1, 0.5, 0.25, 0.125 and 0.106 mm sieves. Because we focused on the general pattern, rather than detailed aggregate distribution, fractions smaller and larger than 4.8 mm were combined, as small and large macro-aggregates respectively. Potential clay dispersion was analyzed by measurement of turbidity after 24 h overnight shaking of 0.5 g samples in 40 ml

demineralized water (van den Broek 1989). Potential clay dispersion was expressed in nephelometric turbidity units (NTU). The more elaborate analysis of clay content was conducted on 60 spring and autumn samples. Actual clay content was measured with a Sedigraph 5100 X-ray-based particle size analyzer. The grain size distribution of the samples was measured directly after insertion into the measurement cuvette, and again after addition of Na-pyrophosphate dispersant and application of ultrasonic energy to destruct pseudo-silt clay particle assemblages. Total clay content was expressed as percentage of all soil particles <2 mm. Differences in topsoil characteristics between sampling periods were generally not significant. For statistical testing, the five replicates per species for each forest were combined to one mean value, and differences between tree species tested with one-way Anova (Cody and Smith 1987).

10.2.4 Litter Decomposition Experiment

Differences in litter breakdown between beech and hornbeam were further examined under laboratory conditions and in the field. In the laboratory, ten freshly fallen leaves of beech or hornbeam were placed in petri dishes filled with mineral soil, kept in the dark at 20 °C and constant soil moisture. Larger soil animals such as earthworms and larger insects were removed. Mineral soil was collected under both hornbeam and beech, but since there were no differences in litter breakdown between soil types, the six replicate samples for each soil type and time step were combined. Remaining litter was measured after 2, 4 and 7 months. In the field, the actual amount of beech and hornbeam litter was measured in 2 consecutive years right after leaf fall, and 5 months later. Litter bags were not used, because this would limit access of earthworms. In each sampling period, measurements were conducted in fivefold under both beech and hornbeam. For the laboratory experiment, differences between tree species were tested with two-way Anova, with species and time step as

independent factors, and post hoc *Ls*-means tests. For the field study, one-way Anova with species as independent factor was applied, as the differences between years were not significant.

10.2.5 Beech and Hornbeam Seedlings

The presence of seedlings with more than just cotyledons was counted five times during vegetation surveys in May. In 3 years, this was done in the three forests already mentioned above. In another year, seedlings were also counted in two additional Steinmergelkeuper forests in the area, south of Broderbour and north-west of Medernach, in seven beech and hornbeam plots in each forest. In addition, in the grid cell study, hornbeam and beech seedlings were counted in all of the cells dominated by one of the species. For each year, the percentage of hornbeam and beech plots with hornbeam or beech seedlings was calculated, and used as input value for statistical analysis. Two-way Anova was performed with tree plot and type of seedling as independent value, and post hoc *Ls*-means tests.

10.2.6 Pilot Study on Root Architecture

A pilot study was conducted on root architecture and differences in fine root mass, in relation to perched water table after heavy rain. In the three forests mentioned in Sect. 10.2.2, three beech and hornbeam plots were randomly selected. In each plot, fine roots were sampled in two soil blocks of 10 × 15 cm, and 10 cm depth. The roots were gently washed out by hand within a few hours after sampling, dried and weighed. To correct for differences in block size, weight of the soil blocks and dry bulk density were also measured. In all plots, perched water tables were measured directly after heavy rain.

10.2.7 Perched Water Tables After Heavy Rain

Perched water tables after heavy rain were recorded in 5 years in May or December, generally in 9–19 plots dominated by hornbeam or beech, and generally in the three forests described in Sect. 10.2.2. For each period, differences between tree species were tested with one-way Anova. In addition, mean values for hornbeam and beech plots were calculated for each period separately, and used as input values for a more general one-way Anova test of differences in perched water table between the two tree species.

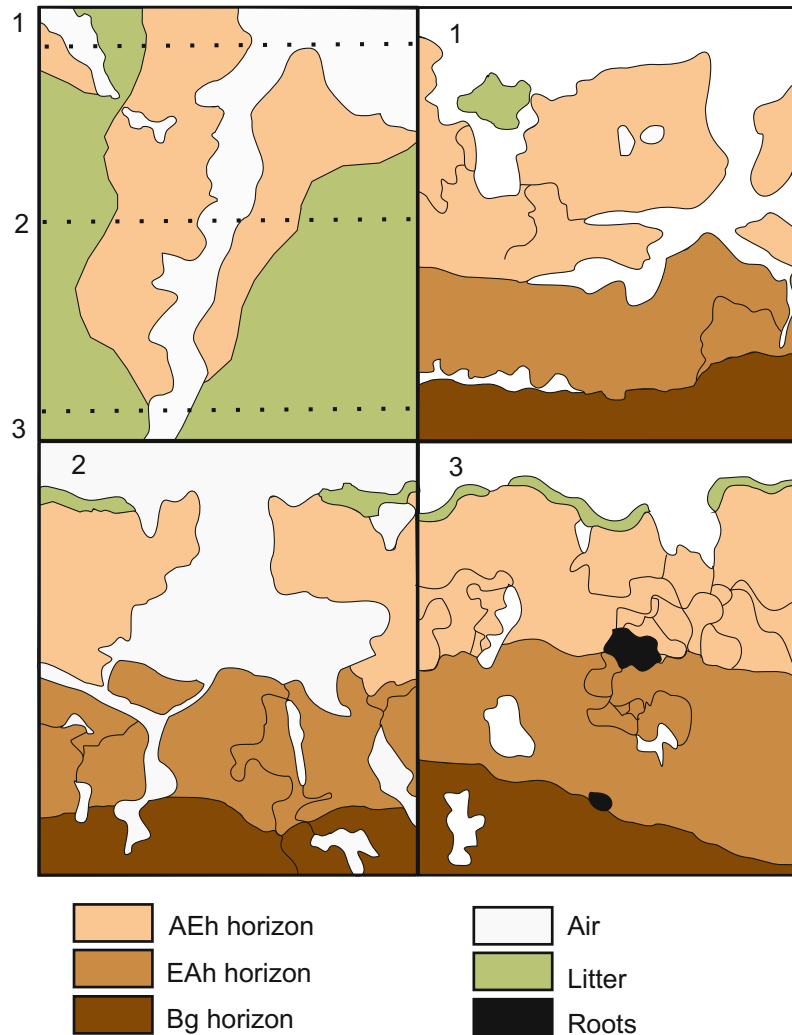
10.3 Results and Discussion

10.3.1 The Activity of Earthworms

The surface map of a shrinkage crack and surroundings showed that the soil surface was bare in early autumn especially along the crack (Fig. 10.2). Litter was however present further away from the cracks, which suggests that the litter had indeed been eaten by earthworms. In the upper part of the soil, many voids and smaller macropores were present, also indicating high faunal activity. The three cross sections further show that shrinkage cracks can be highly variable. Cracks were most abundant and largest in the AEh horizon, less wide and discontinuous in the EAh horizon, and almost absent in the clay-rich, more or less impermeable Bg-horizon. The shrinkage cracks were also not very continuous and elements of the crack polygons were often not connected, which hinders water flow through the cracks. However, moles can convert the shrinkage cracks system to a semi-permanent hydrological conduit (pipe).

Cover of the organic layer and width of the shrinkage cracks also varied seasonally (Fig. 10.3). The temporal dynamics in litter cover and width of the shrinkage crack varied

Fig. 10.2 Surface cover of forest floor (*left upper corner*) and vertical cross sections of a crack and its surroundings in a Keuper forest in early autumn. In the horizontal plan (*left upper corner*) the locations of cross sections 1–3 are indicated. The vertical-horizontal scale of cross sections is about 18 cm (based on data in Cammeraat 1992)



largely over 2 years. The plots showed almost complete removal of litter in autumn before leaf fall, similarly to observations of Hazelhoff et al. (1981) and van Hooff (1983) in nearby forests. In some cases, litter cover increased in spring or summer (arrows in Fig. 10.3), which might be attributed to transport of leaves by wind (van Zon 1980), or possibly also to overland flow processes. More or less synchronously with the litter removal, shrinkage cracks widened. This is due to the swell-shrinkage characteristics of the soil (see also Chap. 9), and shrinking in dry periods. In winter, when the soils are wetter, shrinkage cracks disappear again.

10.3.2 Differences in Litter Decomposition Between Hornbeam and Beech

Litter breakdown rates clearly differed between hornbeam and beech. Under laboratory conditions, when soil macrofauna was excluded, 42% of the hornbeam litter disappeared in 2 months, and 55% after 7 months (Fig. 10.4). However, beech litter lost only 20–24% of its mass over this period. In the field, differences between hornbeam and beech were even larger. After 5 months, approximately 86% of the hornbeam litter had disappeared, while all beech litter was

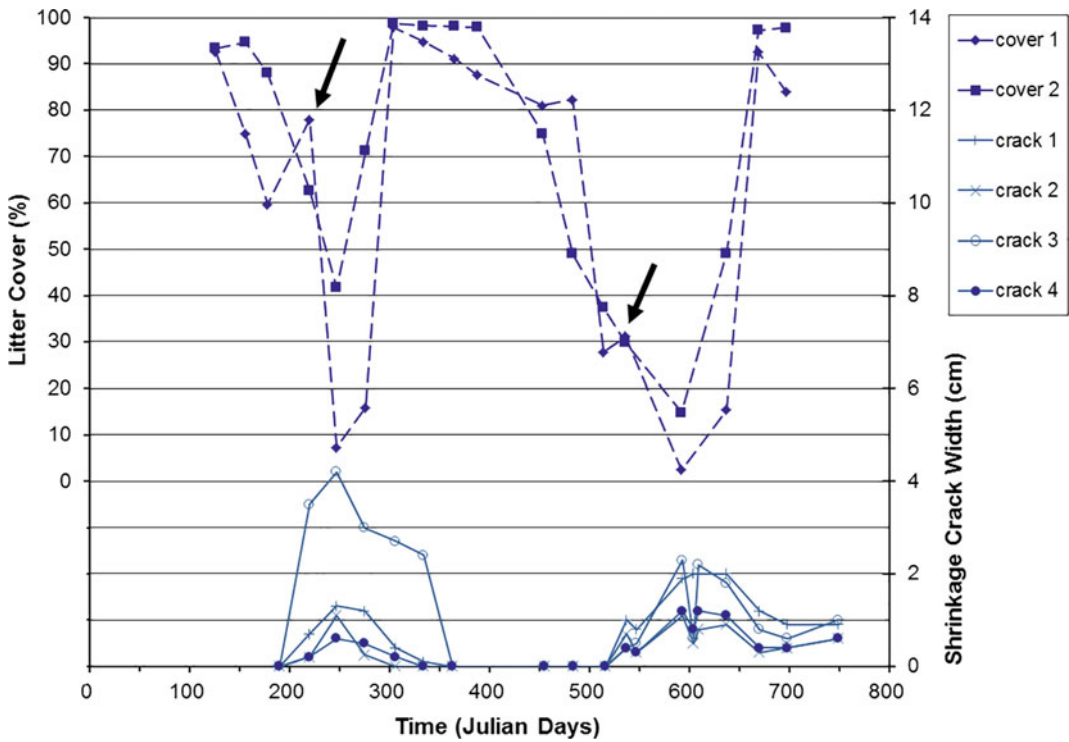


Fig. 10.3 Changes in surface litter cover (2 sites) and width of the shrinkage crack (4 plots) over 2 consecutive years, starting in late autumn. *Arrows* indicate storm periods with litter transport over the forest surface. Data are based on Cammeraat (1992)

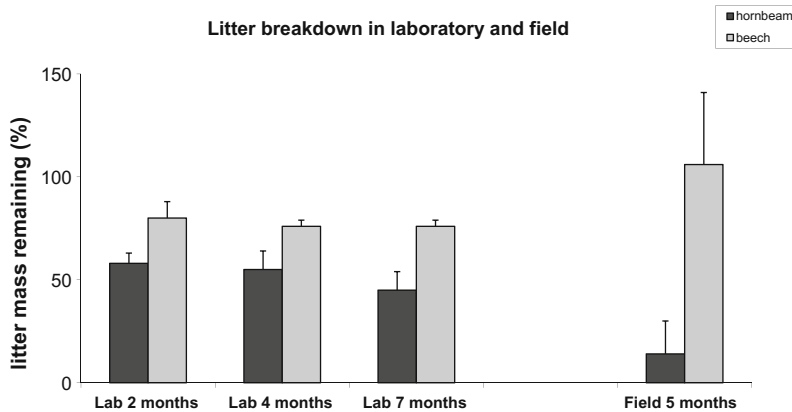
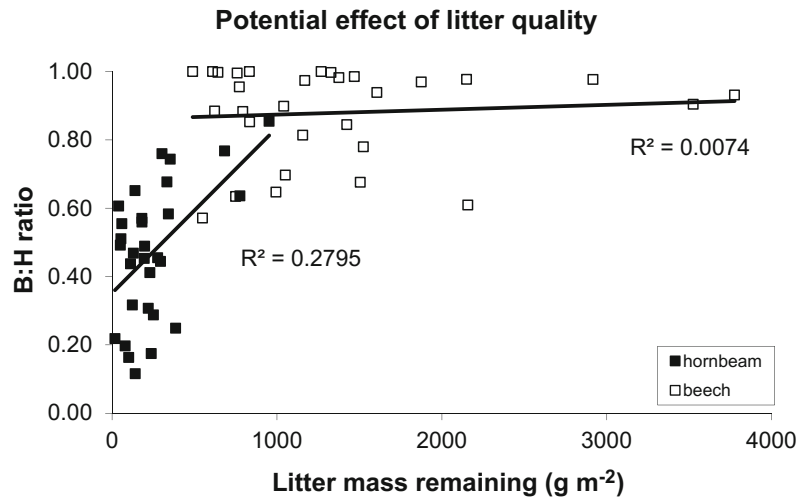


Fig. 10.4 Decomposition of hornbeam and beech litter from mixed Keuper forests under laboratory (after 2, 4 and 7 months) and field conditions (5 months). Mean values and standard deviations ($n = 12$ for laboratory and $n = 10$ for field conditions). Differences between hornbeam and beech at a particular location or time step were all significant ($p < 0.05$)

Fig. 10.5 Potential effects of the contribution of hornbeam and beech litter on the amount of litter mass remaining from previous years in mixed Keuper forests. B:H ratio = the percentage of beech litter, divided by beech + hornbeam litter. Data are based on Kooijman and Cammeraat (2010)



still there. The N-rich hornbeam litter is very palatable, and may be rapidly consumed by earthworms and other soil animals (Westernacher and Graff 1987). The more recalcitrant beech litter, however, is not very edible, and disregarded when soil animals have a choice.

These differences in animal activity and litter decomposition clearly affected the organic layer on the forest floor (Fig. 10.5). When hornbeam was the dominant tree, high earthworm activity reduced the mass of the organic layer to values around 200 g m⁻², which is not enough to cover the mineral soil completely. However, when beech was the dominant species, mass of the organic layer increased to values of (far) more than 1000 g m⁻², which is enough for a dense cover of several cm thickness.

10.3.3 Differences in Habitat Conditions Between Hornbeam and Beech

10.3.3.1 Topsoil Characteristics

Differences between hornbeam and beech in animal activity and litter breakdown rates were supported by other characteristics of the organic layer (Table 10.1). Total litter input did not differ, although the relative contribution of each species shifted between hornbeam and beech plots. However, the Olson decomposition

constant was significantly higher under hornbeam than under beech. Under hornbeam, fresh litter rapidly disappeared before the next leaf fall, while under beech, a large part of the litter would remain, in accord with the decomposition measurements. These results are in accord with earlier studies (Swift et al. 1979; Laskowski et al. 1995; Aubert et al. 2003, 2004), and support that litter quality really differs between the two tree species.

Hornbeam and beech plots also differed in the mineral topsoil. Topsoil C-content was the same, but soil C:N ratios were significantly lower for hornbeam plots, probably due to the higher N-content in hornbeam litter (Laskowski et al. 1995; Kooijman and Martinez-Hernandez 2009). Topsoil pH was significantly higher under hornbeam than under beech, with mean values of 5.7 and 5.0, respectively. The higher pH for hornbeam plots may be due to its less acidifying litter (Hornung 1985; Neiryneck et al. 2000; Aubert et al. 2004), but also due to higher earthworm activity and mixing with the mineral soil (Pop 1997; Jongmans et al. 2003; Davidson et al. 2004). Also, retrieval of base cations from deeper layers by tree roots (Mohr and Topp 2005) may increase pH under hornbeam.

Dry bulk density of the topsoil was expected to be lower under hornbeam than under beech, due to digging earthworms, which increase porosity (Lee and Foster 1991; Neiryneck et al.

Table 10.2 Plant species composition in 60 hornbeam and beech plots in mixed Keuper forests

	Hornbeam plots	Beech plots
Cover of herb layer (%)	16 (16)	5 (8)
Mean number of undergrowth species	15 (5)	7 (3)
Total number of undergrowth species	41	22
<i>Anemone nemorosa</i> L.	V	III
<i>Deschampsia cespitosa</i> (L.) P.Beauv.	V	III
<i>Arum maculatum</i> L.	V	II
<i>Crataegus laevigata</i> (Poir.) DC.	IV	IV
<i>Carex sylvatica</i> Huds.	IV	I
<i>Circaea lutetiana</i> L.	IV	I
<i>Hedera helix</i> L.	III	II
<i>Carex flacca</i> Schreb.	III	II
<i>Viola riviniana</i> Rchb.	III	I
<i>Ficaria verna</i> Huds.	III	I
<i>Rosa arvensis</i> Huds.	III	–
<i>Potentilla sterilis</i> (L.) Garcke	III	–
<i>Rubus fruticosus</i> L.	II	II
<i>Brachypodium sylvaticum</i> (Huds.) P.Beauv.	II	I
<i>Convallaria majalis</i> L.	II	I
<i>Viburnum opulus</i> L.	II	I
<i>Lamium galeobdolon</i> (L.) Ehr. & Polats	II	–
<i>Vicia sepium</i> L.	II	–

Mean cover of herb layer and number of undergrowth species are given with standard deviations. Frequency is given for characteristic plant species: *V* present in more than 80% of the plots of a particular tree species; *IV* present in 60–80%; *III* present in 40–60%; *II* present in 20–40% and *I* present in 1–20% of the plots. Only species with frequency of *II* under at least one of the trees are listed. Data are based on Kooijman and Cammeraat (2010)

2000). However, hornbeam plots showed higher dry bulk density than beech plots, although differences were relatively small. Also, soil moisture at field capacity was clearly higher under hornbeam than under beech, and air-filled pore space approximately two times lower. Lower pore space was supported by lower amounts of small soil aggregates under hornbeam than under beech, which also decreased reaction surfaces (Cammeraat 2002). The depth of the impermeable Bg-horizon was shallower under hornbeam than under beech. Under hornbeam, the impermeable layer already started within approximately 12 cm below the soil surface, but under beech only after 19 cm. As a result, clay content in the mineral topsoil was higher under

hornbeam than under beech, which may explain the higher bulk density and soil moisture content, and lower porosity. The amount of water-stable micro-aggregates in the clay was also higher for hornbeam than for beech. However, potential clay dispersion and the amount of water-dispersible clay did not differ between the two tree species, despite clear differences in clay content and depth of the clay-rich subsoil.

10.3.3.2 Undergrowth Species Composition

Species richness of the undergrowth was much higher under hornbeam than under beech (Table 10.2), which is in accord with other studies (van Oijen et al. 2005). Mean number of plant

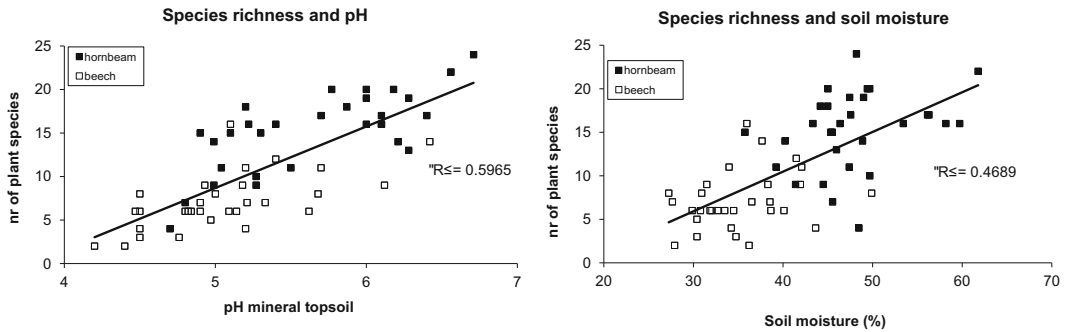


Fig. 10.6 Relationships between undergrowth species richness and pH or soil moisture in mixed Keuper forests ($n = 60$). Data are based on Kooijman and Cammeraat (2010)

species was 15 under hornbeam and 7 under beech, and total number of plant species amounted to 41 and 22 respectively. Many species would grow under both trees, such as *Anemone nemorosa* L., *Deschampsia cespitosa* (L.) P.Beauv., *Arum maculatum* L., *Carex sylvatica* Huds. and *Circaea lutetiana* L., albeit in lower numbers under beech. A few species only occurred under hornbeam, such as *Rosa arvensis* Huds. and *Potentilla sterilis* (L.) Garcke. Most species were characteristic for relatively wet conditions (Ellenberg et al. 1974; Niemeyer et al. 2010). For both tree species, species richness in the undergrowth clearly increased with pH and soil moisture (Fig. 10.6). This suggests that plant species richness is not only directly affected by tree species by thickness of the organic layer (Sydes and Grime 1981; Beatty and Sholes 1988), but also indirectly via changes in habitat conditions such as pH and soil moisture. Increase of undergrowth diversity with pH in beech and hornbeam forests corresponds with Brunet et al. (1997). In NW-Europe, species richness generally increases with pH, partly due to the higher regional species pool for soils with high pH (Pärtel 2002). Also, at low pH, species richness may decrease due to lower nitrate availability (Falkengren-Grerup 1995; Bijlsma et al. 2000; Diekmann and Falkengren-Grerup 2003), or toxic levels of ammonium or aluminium (van den Berg et al. 2005; Zvereva et al. 2007). Although pH values in the Steinmergelkeuper soils are probably not low enough for (severe) toxicity, species richness clearly decreased at lower

pH. Possibly, moisture content also plays a role, as many species are characteristic of relatively moist conditions. Under beech, where moisture content at field capacity was only 36%, undergrowth species may be restricted by drought stress in dry periods (Vincke and Celvaux 2005). Under hornbeam, drought stress is less likely, but undergrowth species have to cope with oxygen stress under wet conditions. Under hornbeam, air-filled pore space under field capacity was only 17%, which is close to the aeration limit of 10% (Zou et al. 2000), below which oxygen supply is very limited. With perched water tables after heavy rain, plants even have to survive periods of water saturation. Nevertheless, species richness clearly increased with soil moisture, which suggests that drought stress is a larger problem than oxygen stress.

10.3.4 Habitat Differentiation or Preferences

10.3.4.1 Tree Species as Active Components?

Beech and hornbeam plots clearly differed in pH values of the topsoil, but this could theoretically be due to differences in subsoil characteristics rather than litter quality. However, pH of the topsoil was uncorrelated with depth to the C-horizon, which reflects the actual depth of weathering and soil formation (Fig. 10.7). This was also the case for topsoil pH and

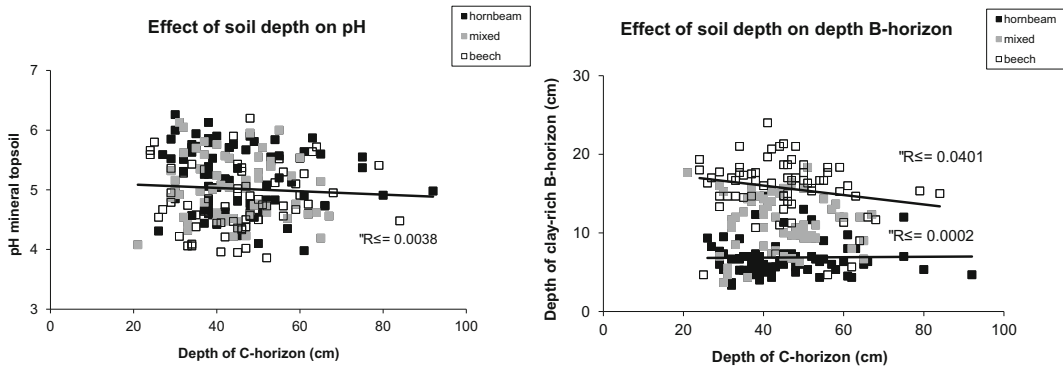


Fig. 10.7 Relationships between soil depth (depth of the C-horizon), pH of the mineral topsoil and depth of the clay-rich Bg-horizon in 200 7 × 7 m grid cells, in hornbeam, beech and mixed forests plots

decalcification depth (not shown), which was strongly correlated with depth to the C-horizon, and is normally highly relevant for pH of the topsoil. Depth to the C-horizon was also unrelated to depth of the Bg-horizon. The impermeable subsoil (Bg) was shallower under hornbeam than under beech, but was not at all correlated with depth to the C-horizon or decalcification depth. The subsoil characteristics are probably not very important for the topsoil. This is not surprising, since contact between the surface layers and the subsoil is largely prohibited by the impermeable Bg-horizon (see also Chap. 9). Most water flows laterally to the brooks, over the clay-rich Bg-horizon, rather than through it (van den Broek 1989; Cammeraat 1992). It was estimated that only 10% of the annual water surplus would reach the subsoil (Cammeraat 1992, 2002). The results thus suggest that habitat differences between hornbeam and beech are more related to the tree species than to subsoil characteristics such as depth of weathering and decalcification.

10.3.4.2 Habitat Preferences

Although habitat differentiation can actively be ascribed to tree species, habitat preference may at least play some role. In the Steinmergelkeuper forests, seedling establishment differed between years and forests, but on average, hornbeam

seedlings were found in 58% of the hornbeam plots, but in only 22% of the beech plots (Table 10.3). In contrast, beech seedlings were found in 88% of the hornbeam plots and 92% of the beech plots. This suggests that at least hornbeam seedlings have a clear habitat preference, and hardly establish under beech, perhaps due to the dense organic layer (Sydes and Grime 1981; Beatty and Sholes 1988). Beech may even be phytotoxic, as has been shown for its relative American beech (Hane et al. 2003). Also, even though both tree species occur over a wide range of pH (Niemeyer et al. 2010; Brunet et al. 1997, see also Chap. 7), in the Luxembourg study area, hornbeam is absent from the most acid soils, such as on Luxembourg sandstone. Hornbeam may have higher cation uptake than beech (Duvigneaud and Denayer-De Smet 1970). In the study area, hornbeam indeed showed two times higher Al-concentrations in fresh, mature leaves than beech (A.M. Kooijman and A. Smit unpublished data). In the most acid soils, this may lead to increased uptake of Al (Zvereva et al. 2007), although pH values in the Steinmergelkeuper soils are generally still too high for severe Al-toxicity.

In contrast to hornbeam, beech seedlings seemed to establish everywhere. This is in accord with its wide range in habitats, and tolerance to low and high pH (Wolters and Stickan 1991; Brunet et al. 1997; Niemeyer et al. 2010).

Table 10.3 Seedling establishment of hornbeam and beech in mixed Keuper forests, given as percentage of hornbeam and beech plots in which a particular seedling had established

Year	<i>n</i>	Hornbeam seedling hornbeam plot	Hornbeam seedling beech plot	Beech seedling hornbeam plot	Beech seedling beech plot
2004	15	67	7	87	100
2005	15	67	13	93	80
2009	35	57	40	83	89
2010	9	67	33	78	100
2011	140	32	15	100	90
Mean (sd)	5	58 (15) ^b	22 (14) ^a	88 (9) ^c	92 (8) ^c

Mean values and standard deviations of the five sampling years combined are also given. Different letters indicate significant differences in mean seedling establishment between hornbeam and beech ($p < 0.05$)

However, beech is generally found in relatively dry places, where soil moisture is below 40% (Bolte et al. 2007), and may be negatively affected by high soil moisture. Even though seedlings establish everywhere, it is possible that mature beech cannot grow in the wetter hornbeam plots. In these plots, soil moisture was higher than 40%, and air-filled pore space was relatively close to the aeration limit of 10% (Zou et al. 2000). Also, the shallower impermeable layer may lead to stronger water stagnation in wet periods. Perched water tables, formed on top of the impermeable Bg-horizon after severe rain storms, were almost always approximately 7–15 cm higher than under beech (Table 10.4), which roughly corresponds with the difference in depth of the impermeable layer. High water tables after heavy rain lead to water saturated

conditions during part of the year, which can lead to oxygen stress for plant roots. Moreover, high perched water tables may increase erosion, especially under hornbeam, where surface erosion and pipe flow through animal burrows are important processes (Cammeraat 1992, 2002). As a result, under hornbeam, impermeable layers come even closer to the surface, and wet conditions occur more often.

Differences in tolerance to wet conditions may be reflected in fine root biomass and architecture. In a pilot study in nine hornbeam and beech plots, beech had significantly higher fine root mass in the upper ten cm of the soil than hornbeam (Fig. 10.8). Also, fine root mass was higher at low pH. However, fine root mass decreased when perched water tables were higher, even for beech, which generally occupied drier habitats than

Table 10.4 Perched water tables (in cm below soil surface) under hornbeam and beech in mixed Keuper forests after heavy rain

Date	Rainfall	<i>n</i>	Perched water table hornbeam	Perched water table beech
<i>Measured same day</i>				
8 May 2004	31 mm	19	3 (3)	12 (7)*
6 May 2010	15 mm	9	4 (2)	11 (5)*
<i>Measured day later</i>				
15 May 2005	18 mm	15	9 (8)	22 (8)*
10 Dec 2007	8 mm	15	10 (5)	19 (6)*
16 May 2009	28 mm	14	7 (5)	22 (11)*
Mean and sd		5	7 (3)	17 (5)*

Data are mean values and standard deviations. Significant differences between hornbeam and beech are indicated with an asterisk ($p < 0.05$)

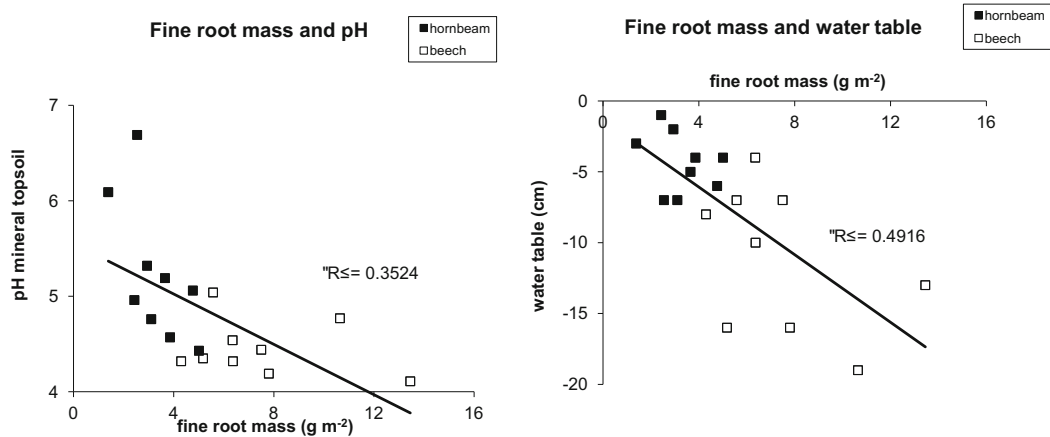


Fig. 10.8 Relationships between fine root biomass in the upper 10 cm of the mineral topsoil and pH or perched water table after heavy rain, in hornbeam and beech plots ($n = 9$) in Keuper forests

hornbeam. Root architecture may play a role (Fig. 10.9). Directly after careful washing, hornbeam roots showed a more or less two-dimensional and superficial root mat with many very fine roots. The beech root pattern was more three-dimensional, with larger and smaller roots growing in all directions, which may be hampered at high water tables. This was only a pilot study, and more research is needed, but a more superficial fine root system may explain why hornbeam can tolerate water saturated conditions better than beech. Such habitat preferences extend the presence of beech and hornbeam in particular habitats beyond the lifespan of individual trees, which enlarges their impact on habitat differentiation.

10.3.5 Impact on Topsoil Development and Erosion

10.3.5.1 Topsoil Formation

In Steinmergelkeuper soils, lateral eluviation of clay is an important soil forming process (van den Broek 1989, see also Chap. 9). As shown before, beech and hornbeam clearly differed in pH and clay content of the topsoil, and depth to the clay-rich Bg-horizon. Clay content in the topsoil also differed with pH, from approximately 20% at pH 4.2

to 30% at pH 6.8 (Fig. 10.10). In theory, differences in clay content of the topsoil could be due to differences in initial clay content of the parent material, rather than tree species or pH. However, since hornbeam and beech plots were selected in pairs close to each other, this is not very likely. However, potential clay dispersion and the amount of water-dispersible clay in the topsoil did not differ between tree species, or change with pH, which suggest that rates of clay eluviation are similar in all plots. This is probably due to compensating mechanisms. At high pH (mainly under hornbeam), clay content is high, but micro-aggregate stability is also high, which means that a large part of the clay is tied up in stable micro-aggregates. However, at low pH (mainly under beech), micro-aggregate stability is lower, which compensates for the lower clay content.

These results suggest that differences in clay content and depth of the clay-rich subsoil between hornbeam and beech are not due to different rates of clay eluviation in the topsoil, and also not to the prevailing pH. Differences in animal activity and erosion are probably more important. Under beech, the organic layer forms a permanent protective cover (Greene and Hairsine 2004), and eluviation of clay particles and base cations at the top of the Bg-horizon is not counteracted by digging earthworms and moles, nor interrupted by surface erosion

Fig. 10.9 Root architecture of beech and hornbeam in Keuper forests. Beech (*left*) had a three-dimensional fine root system, whereas the fine root system of hornbeam (*right*) was largely superficial

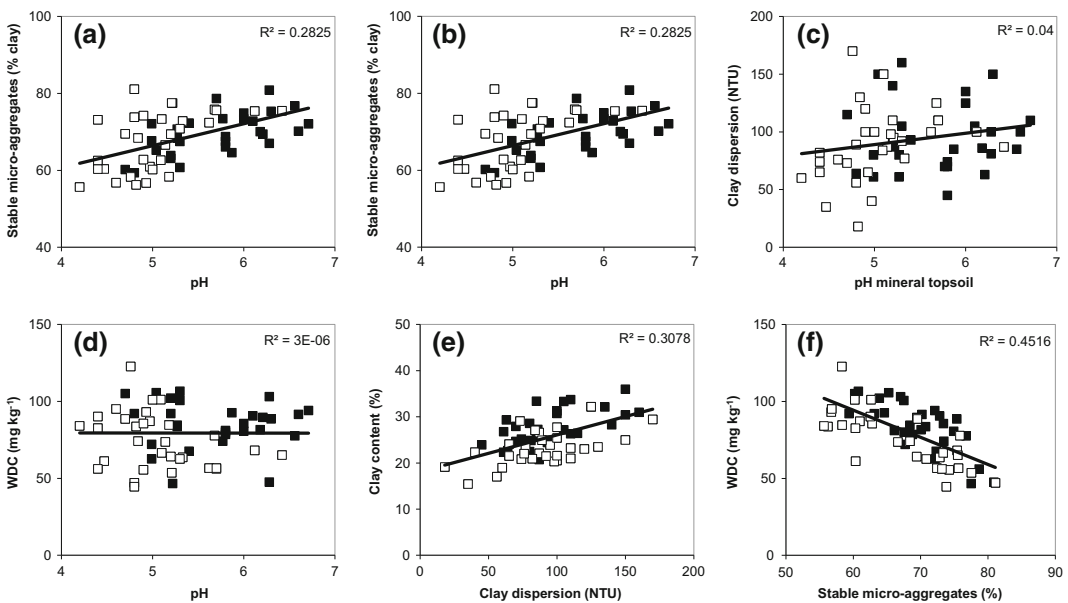
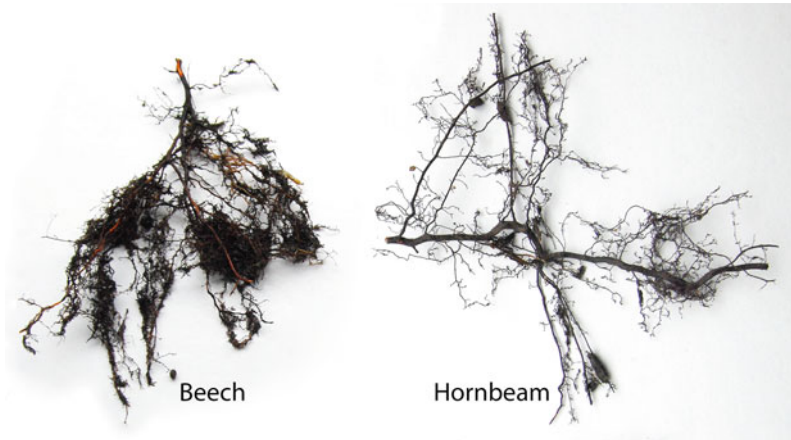


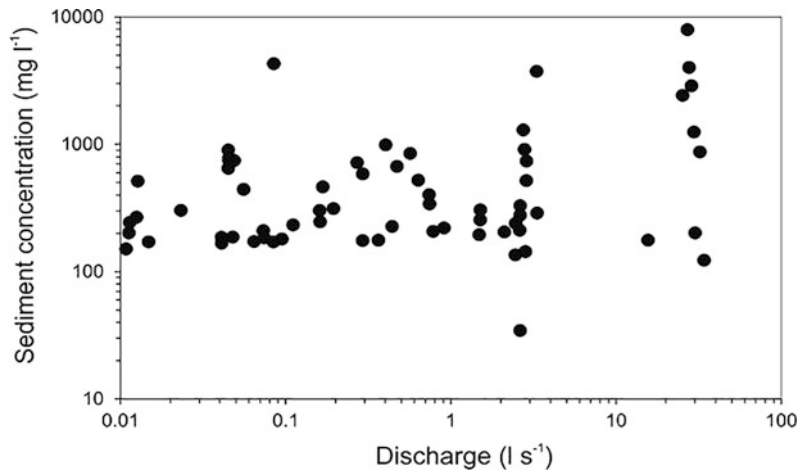
Fig. 10.10 Relationships between variables related to clay dispersion in mixed Keuper forests. **a** Clay content and pH of the mineral topsoil, **b** Stable micro-aggregates in clay and pH of the mineral topsoil, **c** Clay dispersion and pH of the mineral topsoil, **d** Water-dispersible clay

(WDC) and pH of the mineral topsoil, **e** Clay content and clay dispersion, **f** Water-dispersible clay and amount of stable micro-aggregates. Correlation coefficients are based on $n = 60$, and given in each figure separately. *Open square* beech; *closed square* hornbeam

processes. This leads to thicker AEh-horizons, and impermeable layers deeper in the soil. Under hornbeam, however, clay eluviation and acidification, and formation of AEh-horizons, may be counteracted by high biological activity, which brings back clay-rich soil material from deeper layers (Pop 1997; Jungerius et al. 1989; Jongmans et al. 2003; Davidson et al. 2004; Pulleman et al. 2005). More importantly,

surface erosion by splash erosion and overland flow transport is higher, because the soil surface is bare during a large part of the year, and worm casts are more common (van Hooff 1983; Cammeraat 1992). Overland flow may happen a few times a year, when precipitation exceeds $20\text{--}30\text{ mm day}^{-1}$ (Cammeraat 1992, 2002). Subsurface erosion by pipe flow through animal burrows also leads to export of soil particles and

Fig. 10.11 Measured sediment concentrations during several runoff events in the Schrondweilerbusch. Data are based on Cammeraat (1992)



lowering of the surface (Imeson 1986; Cammeraat 1992, 2002). An unknown factor is dissolution of primary minerals like calcite and gypsum, which may contribute to surface lowering on a catchment scale (Imeson and Vis 1984; Duijsings 1987). It is unknown whether dissolution of these primary minerals is affected by tree species. It is however possible that the lower pH under beech leads to higher dissolution values in the topsoil, which further contribute to the deeper Bg-horizons than under hornbeam.

10.3.5.2 Differences in Erosion

At the plot scale, beech and hornbeam plots probably differ in erosion, but contribution to the catchment scale may be highly variable. In hornbeam plots, soil fauna produce high amounts of sediment, which is dispersed over the soil surface by splash processes, but part of it becomes covered by litter and incorporated into the soil again by bioturbation processes (Jungerius et al. 1989). Furthermore, animal activity may be so high and unpredictable that it disturbs the normal relationship between water discharge and sediment concentrations during surface runoff events. In general, on an event base, sediment concentrations increase with higher amounts of discharge. However, in a hornbeam sub-catchment studied in the Steinmangelkeuper forest, they varied within one event, and different

events gave different results (Fig. 10.11). This variation is explained by high activity of churning wild boars, which can lead to very high, but also local erosion of freshly exposed soil. During a thunderstorm, sediment concentration of the stream originating from the area with churning activity reached an exceptional level of 9 g l^{-1} at 2 l s^{-1} discharge. This is nine times higher than sediment concentrations of the other streams without churning activity, and also much higher than the measured maximum of Duijsings (1985) of 2.35 g l^{-1} , which occurred at approximately 200 l s^{-1} discharge. The wild boar event was accidentally observed and is not frequent, but shows the local and highly variable importance of animal activity for forest soil erosion.

Despite the variability in sediment concentrations, the ecosystem response to animal activity and denudation is clearly reflected in the sediment output of different ecohydrological response units (Table 10.5). In beech forest dominated by throughflow, sediment yield was only $13\text{--}26 \text{ g m}^{-2} \text{ year}^{-1}$. In hornbeam areas with pipe flow, these values amounted to $145\text{--}200 \text{ g m}^{-2} \text{ year}^{-1}$, which is approximately ten times higher. Also, the throughflow areas mainly export (fine) dispersed clay, eroded subsurface from the top of the Bg-horizon, which leads to thicker AEh-horizons. The pipe flow areas, however, export splashed silty topsoil

Table 10.5 Rates of soil displacement by animals in Steinmergelkeuper forests compared to soil material displaced by overland flow, splash and pipe flow

Type of activity	Scale	Source	Rate
Worm cast production	Plot	Hazelhoff et al. (1981)	1.5 kg m ² year ⁻¹
Molehill production	Plot	Hazelhoff et al. (1981)*	0.3 kg m ² year ⁻¹
Bioturbation by <i>Allolobophora</i> casts	Plot	Hazelhoff et al. (1981)	1.5 mm year ⁻¹
Suspended load in pipeflow	Sub-catchment partial areas	Hendriks and Imeson (1984), Cammeraat (1992)	0.145–0.200 kg m ² year ⁻¹
Suspended load in matrix throughflow	Sub-catchment ridges	Hendriks and Imeson (1984), Cammeraat (1992)	0.013–0.026 kg m ² year ⁻¹
Splash and overlandflow erosion	Catchment	Duijsings (1987)	0.0313 kg m ² year ⁻¹
Suspended load in throughflow	Catchment	Duijsings (1987)	0.0037 kg m ² year ⁻¹

*Calculated from data given in Hazelhoff et al. (1981)

material, as well as material that is eroded from the crack and pipe-walls in the soil. This contributes to increased surface lowering, and leads to thinner AEh-horizons.

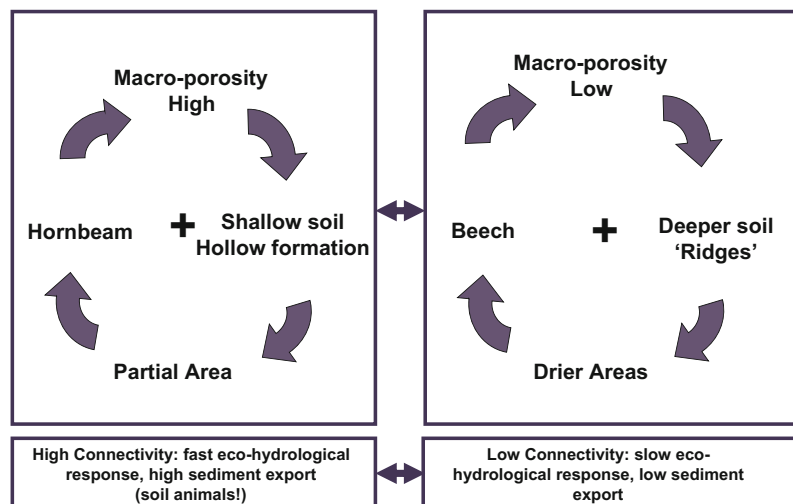
At the catchment scale, the difference between throughflow and overland flow derived sediment is still present. Duijsings (1987) made a very detailed sediment budget for a typical stream in the Steinmergelkeuper area. The catchment yields were lower than the sub-catchment yields for areas nearby (Hendriks and Imeson 1984; Cammeraat 1992), because sediment is distributed over larger surface areas. Nevertheless, erosion by splash transport and overland flow

was approximately ten times higher than erosion by throughflow.

10.4 Concluding Remarks

In the Steinmergelkeuper forests, clear relationships exist between litter quality, animal activity, topsoil formation and hydro-geomorphological response. Putting all the observations into a larger framework, we postulate a positive feedback model for the wetter areas, connecting high animal activity to the occurrence of hornbeam, preferably present in areas where increased

Fig. 10.12 Positive feedback model for different ecohydrological response units in Steinmergelkeuper forests



erosion rates prevail, and soils are wetter and have higher pH (Fig. 10.12). In contrast, a second feedback loop with far lower sediment yields is constructed for the dry areas with more acidic soil, typically at the ridges in between the shallow and damp depressions, where beech is dominant and animal activity is far less prominent. This model suggests an important linkage between geo-ecological processes driving specific ecosystem responses, but also triggering the emergence of typical abiotic landscape features, such as the further development of depressions and ridges and the development of different topsoil profiles.

Such developments require thousands of years. The time required for development of a 20 cm thick AEh-horizon, which is not uncommon under beech, is estimated four to nine thousand years (van den Broek 1989). This comes close to the time that beech has been present in the area (Slotboom 1963, see also Chap. 3). Slope denudation can be a lot faster. In mixed beech and hornbeam forests, slope denudation was estimated at 4 mm per century (Duijsings 1985), and could amount to 15 mm per century in the most active places (Cammeraat 2002). Assuming that erosion under beech is close to zero, the 7–9 cm difference in depth of the Bg-horizon found in this study between beech and hornbeam could then develop within approximately thousand years. Such time spans largely exceed the lifespan of the trees, which is approximately 150–200 years, and make habitat preference important. As suggested by the seedling surveys and the pilot study on root architecture, habitat preferences probably favour establishment of hornbeam in soil with relatively high pH, and beech in relatively dry spots. The differences in litter quality between the two species then do the rest.

At large spatial scales, the Luxemburg cuesta landscape is mainly affected by abiotic processes and factors, such as formation of parent materials and river incisions (see also Chap. 1, 2 and 5). However, within a particular geological zone, formation of soil and landscape is also controlled by biotic interactions. The conclusions described may be mainly valid for decalcified marl on

shallow slopes, which are more sensitive to changes in pH and drainage than other soils. Nevertheless, it is clear that biotic processes can change abiotic habitat conditions to a large extent. On Steinmergelkeuper marls, tree species and animal activity not only affect litter breakdown and accumulation, but also topsoil development and erosion. Tree species are probably even more important than subsoil characteristics such as depth of weathering and decalcification. Both beech and hornbeam can be considered as ecosystem engineers, which create unsuitable habitat conditions for the other species, but suitable for themselves.

Acknowledgements The authors would like to thank Bas van Dalen, Greet Kooijman-Schouten and Lex Weiler for their help in the field, and Leo Hoitinga for assistance in the laboratory. The photograph and part of the figures were made by Jan van Arkel.

References

- Aubert M, Hedde M, Decaens T, Bureau F, Margerie P, Alard D (2003) Effects of tree canopy composition on earthworms and other macro-invertebrates in beech forests of Upper Normandy (France). *Pedobiologia* 47:904–912
- Aubert M, Bureau F, Alard D, Bardat J (2004) Effect of tree mixture on the humic epipedon and vegetation diversity in managed beech forests (Normandy, France). *Can J For Res* 34:233–248
- Beatty SW, Sholes ODV (1988) Leaf litter effects on plant species composition of deciduous forest treefall pits. *Can J For Res* 18:553–559
- Berg B (2000) Litter decomposition and organic matter turnover in northern forest soils. *For Ecol Manage* 133:13–22
- Bijlsma RJ, Lambers H, Kooijman SALM (2000) A dynamic whole-plant model of integrated metabolism of nitrogen and carbon. 1. Comparative ecological implications of ammonium-nitrate interactions. *Plant Soil* 220:49–69
- Bolte A, Czajkowski T, Kompa T (2007) The north-eastern distribution range of European beech—a review. *Forestry* 80:413–429
- Brunet J, Falkengren-Grerup U, Tyler G (1997) Pattern and dynamics of the ground vegetation in south Swedish *Carpinus betulus* forests: importance of soil chemistry and management. *Ecography* 20:513–520
- Cammeraat LH (1992) Hydro-geomorphological processes in a small forested sub-catchment: preferred flow-paths of water. Ph.D. thesis University of Amsterdam, 158 p

- Cammeraat LH (2002) A review of two strongly contrasting geomorphological systems within the context of scale. *Earth Surf Proc Land* 27:1201–1222
- Cammeraat LH, Kooijman AM (2009) Biological control of pedological and hydro-geomorphological processes in a deciduous forest ecosystem. *Biologia* 64:428–432
- Cody RP, Smith JK (1987) *Applied Statistics and the SAS Programming Language*. Elsevier Science Publishers Co. Int., New York
- Davidson DA, Bruneau PMC, Grieve IC, Wilson CA (2004) Micromorphological assessment of the effect of liming on faunal excrement in an upland grassland soil. *Appl Soil Ecol* 26:169–177
- Diekmann M, Falkengren-Grerup U (2003) A new species index for forest vascular plants: development of functional indices based on mineralization rates of various forms of soil nitrogen. *J Ecol* 86:269–283
- Duijsings JJHM (1985) Streambank contribution to the sediment budget of a forest stream. Ph.D. thesis University of Amsterdam, 190 p
- Duijsings JJHM (1987) A sediment budget for a forested catchment in Luxembourg and its implications for channel development. *Earth Surf Proc Land* 12:173–184
- Duchaufour P (1982) *Pedology; pedogenesis and classification* (trans: Paton TR). George Allen & Unwin, London. 448 p
- Duvigneaud P, Denayer-De Smet S (1970) Biological cycling of minerals in temperate deciduous forests. In: Reichle DE (ed) *Analysis of temperate forest ecosystems*. Springer, Berlin, pp 199–225
- Edwards CA, Lofty JR (1977) *Biology of earthworms*. Chapman and Hall, London
- Ellenberg H, Weeber HE, Düll R, Wirth V, Werner W (1974) *Zeigerwerte von Pflanzen in Mitteleuropa*. Verlag Erich Goltze GmbH & Co, Göttingen
- Falkengren-Grerup U (1995) Interspecies differences in the preference of ammonium and nitrate in vascular plants. *Oecologia* 102:305–311
- Ferraris le Comte de (1777) Reissued in 1965–1970. *Carte de Cabinet des Pays-Bas Autrichiens*. Bibliothèque Royale de Belgique, Bruxelles
- Green RN, Trowbridge RL, Klinka K (1993) Towards a taxonomic classification of humus forms. *Suppl Forest Sci* 39
- Greene RSB, Hairsine PB (2004) Elementary processes of soil–water interaction and thresholds in soil surface dynamics: a review. *Earth Surf Proc Land* 29:1077–1091
- Hane EN, Hamburg SP, Barber AL, Plaut JA (2003) Phytotoxicity of American beech leaf leachate to sugar maple seedlings in a greenhouse experiment. *Can J For Res* 33:814–821
- Hazelhoff H, van Hooff P, Imeson AC, Kwaad FJPM (1981) The exposure of forest soil to erosion by earthworms. *Earth Surf Proc Land* 6:235–250
- Hendriks MR, Imeson AC (1984) Non-channel storm period sediment supply from a topographical depression under forest in the Keuper region of Luxembourg. *Zeitschrift für Geomorphologie N.F.Suppl.-Bd* 49:51–58
- Hornung M (1985) Acidification of soils by trees and forests. *Soil Use Manage* 1:24–28
- Imeson AC, Vis M (1984) The output of sediments and solutes from forested and cultivated clayey drainage basins in Luxembourg. *Earth Surf Proc Land* 9:585–594
- Imeson AC (1986) Investigating volumetric changes in clayey soils related to subsurface water movement and piping. *Zeitschrift für Geomorphologie N.F.Suppl.-Bd* 60:115–130
- IUSS Working Group WRB (2015) World reference base for soil resources 2014, update 2015. International soil classification system for naming soils and creating legends for soil maps. *World Soil Resources Reports* No. 106. FAO, Rome
- Jongmans AG, Pulleman MM, Balabane M, van Oort F, Marinissen JCY (2003) Soil structure and characteristics of organic matter in two orchards differing in earthworm activity. *Appl Soil Ecol* 24:219–232
- Jungerius PD, van Zon HJM (1982) The formation of the Lias cuesta (Luxembourg) in the light of present day erosion processes operating on forest soils. *Geogr Ann* 64A:127–140
- Jungerius PD, van de Ancker H, van Zon HJM (1989) Long term measurement of forest soil exposure and creep in Luxembourg. *Catena* 16:437–447
- Kooijman AM, Martinez-Hernandez GB (2009) Effects of litter quality and parent material on organic matter characteristics and N-dynamics in Luxembourg beech and hornbeam forests. *For Ecol Manage* 257:1732–1739
- Kooijman AM, Cammeraat LH (2010) Biological control of beech and hornbeam on species richness via changes in the organic layer, pH and soil moisture characteristics. *Funct Ecol* 24:469–477
- Laskowski R, Niklinska M, Maryanski M (1995) The dynamics of chemical elements in forest litter. *Ecology* 76:1393–1406
- Lee KE, Foster RC (1991) Soil fauna and soil structure. *Aust J Soil Res* 29:745–775
- Mohr R, Topp W (2005) Hazel improves soil quality of sloping oak stands in German low mountain range. *Ann For Sci* 62:23–29
- Niemeyer T, Ries C, Härdtle W (2010) Die Waldgesellschaften Luxemburgs. *Vegetation, Standort, Vorkommen und Gefährdung*. Ferrantia 57, Musée national d'histoire naturelle, Luxembourg, 122 p
- Neirynek J, Mirtcheva S, Sioen G, Lust N (2000) Impact of *Tilia platyphyllos* Scop., *Fraxinus excelsior* L., *Acer pseudoplatanus* L., *Quercus robur* L., and *Fagus sylvatica* L. on earthworm biomass and physico-chemical properties of a loamy topsoil. *For Ecol Manage* 133:275–286
- Oades JM (1993) The role of biology in the formation, stabilization and degradation of soil structure. *Geoderma* 56:377–400
- van Oijen D, Feijen M, Hommel P, den Ouden J, de Waal R (2005) Effects of tree species composition on within-forest distribution of understorey species. *Appl Veg Sci* 8:155–166

- Olson JS (1963) Energy storage and the balance of producers and decomposers in ecological systems. *Ecology* 44:322–331
- Pärtel M (2002) Local plant diversity patterns and evolutionary history at the regional scale. *Ecology* 83:2361–2366
- Ponge JF (2003) Humus forms in terrestrial ecosystems: a framework to biodiversity. *Soil Biol Biochem* 35:935–945
- Pop V (1997) Earthworm-vegetation-soil relationships in the Romanian Carpathians. *Soil Biol Biochem* 29:223–229
- Pulleman MM, Six J, van Breemen N, Jongmans AG (2005) Soil organic matter distribution and microaggregate characteristics as affected by agricultural management and earthworm activity. *Eur J Soil Sci* 56:453–467
- Schachtschabel F, Blume H, Hartge KH, Schwertmann U, Brümmer GW, Renger M (1982) Scheffer/Schachtschabel Lehrbuch der Bodenkunde, 11th edn. Enke Verlag, Stuttgart, p 442
- Slotboom RT (1963) Comparative geomorphological and palynological investigations of the Pingos (Viviers) in the Hautes Fanges (Belgium) and the Mardellen in the Gutland (Luxembourg). *Zeitschrift für Geomorphologie N.F* 7:1–41
- Swift MJ, Heal OW, Anderson JM (1979) Decomposition in terrestrial ecosystems. University of California Press, Berkeley
- Sydes C, Grime JP (1981) Effects of tree litter on herbaceous vegetation in deciduous woodland I. Field investigations. *J Ecol* 69:237–248
- van Hooff P (1983) Earthworm activity as a cause of splash erosion in Luxembourg forests. *Geoderma* 31:195–204
- Vincke C, Celvaux B (2005) Porosity and available water of temporarily waterlogged soils in a *Quercus robur* (L.) declining stand. *Plant Soil* 271:189–203
- van den Berg LJJ, Dorland E, Vergeer P, Hart M, Bobbink R, Roelofs JGM (2005) Decline of acid-sensitive plant species in heathland can be attributed to ammonium toxicity in combination with low pH. *New Phytol* 166:551–564
- van den Broek TMW (1989) Clay dispersion and pedogenesis of soils with an abrupt contrast in texture: a hydro-pedological approach on subcatchment scale. Ph.D. thesis University of Amsterdam, 109 p
- Westerman RL (1990) Soil testing and plant analysis, 3rd edn. Soil Science Society America, Madison, Wisconsin
- Westernacher E, Graff O (1987) Orientation behaviour of earthworms (Lumbricidae) towards different crops. *Biol Fertil Soils* 3:131–133
- Wolters V, Sticken W (1991) Resource allocation of beech seedlings (*Fagus sylvatica* L.)—relationship to earthworm activity and soil conditions. *Oecologia* 88:125–131
- Zou C, Sands R, Buchan G, Hudson I (2000) Least limiting water range: a potential indicator of physical quality of forest soils. *Aust J Soil Res* 38:947–958
- Zvereva EL, Toivonen E, Kozlov MV (2007) Changes in species richness of vascular plants under the impact of air pollution: a global perspective. *Glob Ecol Biogeogr* 17:305–319
- van Zon HJM (1980) The transport of leaves and sediment over a forest floor. *Catena* 7:97–110

Applications of Physiotope Mapping in the Cuesta Landscape of Luxembourg

11

A.C. Seijmonsbergen, L.H. Cammeraat
and A.M. Kooijman

Abstract

Digital physiotope maps combine multi-source abiotic information, and can be used to assess derived characteristics such as natural hazards and type of forest community. Physiotopes are spatially explicit functional landscape units that stratify landscapes into distinct units, resulting from the interplay between geological, geomorphological and soil processes. Boundaries of the physiotopes in the cuesta landscape of Luxembourg are based on geological boundaries, geomorphological processes boundaries and key indicators of soil forming processes which are supplemented by quantitative topographic land surface parameters such as slope angle. A physiotope map is presented for an area near the village of Bigelbach, which reflects the resource potential of the landscape. We present three derived applications of the physiotope map: a hazard zonation map, a forest community map and a soil erosion vulnerability map. The hazard zonation map is based on weighting and ranking of attributes of the physiotopes, such as process activity, materials, slope angle and forest cover. The derived forest community map strongly reflects the spatial distribution of geological substrate and soils of the main physiotope units along the cuesta. The soil erosion vulnerability map implements the Revised Universal Soil Loss Equation in combination with the physiotope map. The physiotope map content can be extended and updated and its derived products may support landscape conservation and restoration programs, and can be used to monitor temporal changes within a landscape.

A.C. Seijmonsbergen (✉) · L.H. Cammeraat ·
A.M. Kooijman
Institute for Biodiversity and Ecosystem Dynamics,
University of Amsterdam, Science Park, P.O. box
94062, 1090, GB Amsterdam, The Netherlands
e-mail: a.c.seijmonsbergen@uva.nl

11.1 Introduction

A landscape is not merely an environment in which people live, work and travel on a daily basis, it is also a resource which delivers many

functions, that need to be maintained. Therefore, a landscape is considered one of the key themes of policies for environmental sustainability (Peano and Casatella 2011). Science-based information is necessary to support such sustainability policies, but often comes as fragmented information of only one single component of the landscape. Moreover, long records of changes in soil quality attributes, e.g. the occurrence of erosional features, are lacking. Physiotopes are spatially explicit functional landscape units that stratify landscapes into distinct units, resulting from the interplay between geological, geomorphological and soil processes. Digital physiotope maps may overcome the problem of fragmentation in abiotic knowledge, because they combine multi-source abiotic information of a landscape. To efficiently document the abiotic status of the landscape, integration of multiple information carriers or *environmental indicators* is required.

In contrast to ecotopes (Klijn 1994), the vegetation cover is not included in the spatial delineation of natural physiotopes. Hosting vegetation communities or high biodiversity should be reflected in the resource potential of physiotopes. Resources are here defined as those properties relevant to the development and evolution of abiotic compartments of ecosystems (Parks and Mulligan 2010), as is used in geodiversity research (Gray 2004). Differences in resources are related to differences in soil quality, because contrasting lithology produces different weathering products and soils, under similar climate conditions. Differences in vulnerability to geomorphological process activity may lead to spatio-temporal differences in natural hazards, which are closely linked to physiotope variation in parent material, topographical variation, nutrient content and hydrological properties. On a fine scale, as in the cuesta landscape of Luxembourg, expert-derived inventories on geology and geomorphology can be combined and supplemented with field inventories and information on land surface parameters in a Geographical Information System (GIS).

The cuesta landscape of Luxembourg is an outstanding area for studying geology, soils and

geomorphology, due to its contrasting abiotic gradients. The cuesta landscape is the result of a complex development, due to variation in lithology (see Chap. 1), climatic change(s) and variation in soil formation (see Chap. 6), intensity of geomorphological processes (Chap. 5) and in Land Use Land Cover Change (see Chap. 3). In the present cuesta landscape the resulting abiotic patterns can be captured by mapping physiotopes.

Studying relations between the abiotic and biotic part of nature on fine scales, requires in depth representation of physiotopes and thus a transparent workflow and processing steps. Traditional field-based knowledge from geology, geomorphology and soils is the basis for the definition of physiotopes. The detailed scale demands that such fine-scaled abiotic field data has to be included to illustrate fine-scale variations between and within physiotopes. Furthermore, new techniques from the geosciences, such as expert-derived mapping and use of geomorphometric parameters (Hengl and Reuter 2008) are included and integrated in a physiotope geodatabase. For that, multiple data sources are combined, with different formats, extents, cell sizes and of varying quality. The issue of ‘scale’ should therefore be carefully addressed, so that the resulting physiotope maps are reliable.

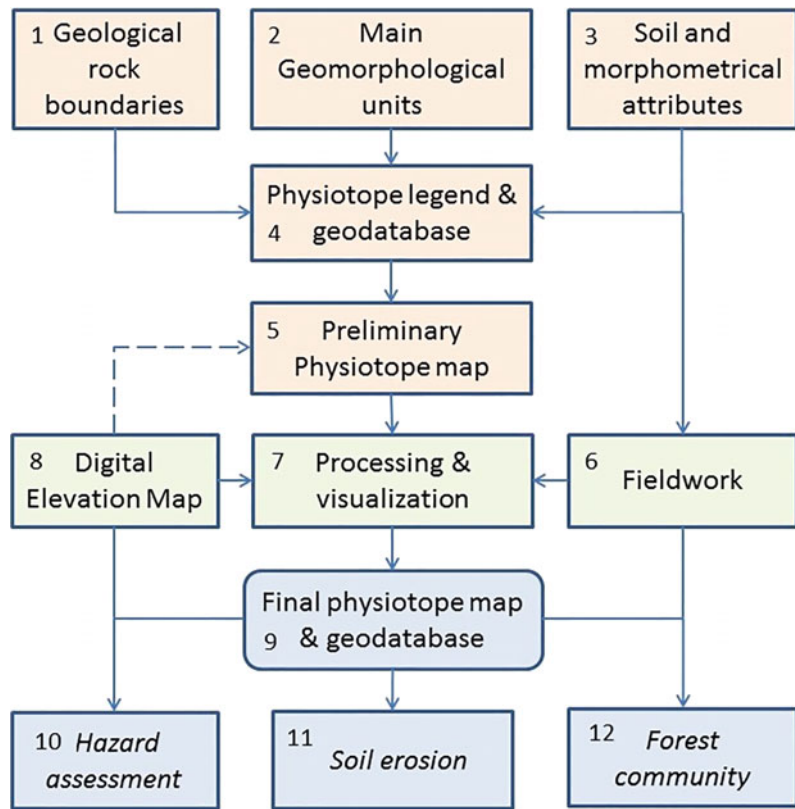
Our aim is to present a workflow for physiotope mapping and three applications that use information derived from the physiotope map and its geodatabase. A first case presents a natural hazard map, while in the second case a forest community map is compared to the physiotope map. A third example implements the Revised Universal Soil Loss Equation and an additional land use map to calculate potential annual soil loss. These examples are the results of our long-lasting experience in the cuesta landscape (see Chap. 2) and the outcome of fieldwork by staff and students (see Chap. 12).

11.2 Methods

11.2.1 Physiotope Mapping

Figure 11.1 presents a workflow for preparing the physiotope map (steps 1–9) in which three

Fig. 11.1 Workflow for physiotope mapping. In orange the preprocessing steps, in green the analyses and validation, the resulting deliverables are indicated in blue



applied maps, the natural hazard map (step 10), the erosion map (step 11) and the forest community maps (step 12) are included. On the highest level, the legend for physiotope map (step 4) is the result of a combination of the main geological units (step 1) derived from the Carte Géologique at scale 1:25.000 of Luxembourg (<http://map.geoportail.lu>), combined with the main geomorphological units (step 2), as defined by Seijmonsbergen and de Graaff (see Chap. 5), which results in 7 main units: (A) Sandstone Plateau, (B) Sandstone Cuesta, (C) Marl underlain landscape, (D) Dolomite underlain landscape, (E) Fluvial landscape, (F) Aeolian landscape, (G) Colluvial landscape and (H) Other. On a lower legend level, each main unit has been subdivided into smaller units, which are characterized by combinations of geomorphometric, morphodynamic and soil attributes (step 3), which are mainly based on field descriptions. The combination of main legend units and lower level attributes is summarized in

Table 11.1. The most important attributes hold information on relative drainage properties, soil type and soil depth, slope form and slope angle, material composition and relative age. This selection has been, during fieldwork experience of over 25 years, recognized as a set of key indicators for physiotope characterization. Many of these parameters can nowadays be calculated from high resolution elevations models, which enhances transferability to other regions, while others, such as soil and material properties, need fieldwork.

In the preprocessing steps (steps 1–5) data are collected (1–3), and a legend and a physiotope geodatabase (step 4) are designed in which a preliminary physiotope map (step 5) is compiled. This pre-field physiotope map contains all the individual map boundaries as well as the supplementary attributes. This allows flexibility to adapt physiotope boundaries and extensions with additional attributes. For the analyses and validation steps (steps 6–9), a hand drilling

Table 11.1 Main and subunits of the phytotope map and the summary of key point observations

	1	2	3	4	5	6	7
(A) Sandstone Plateau	Shallow, well-drained soils in loamy sandy weathered li2, with a Bw (Brunic Arenosol)	Deep, well-drained soils in loamy sandy weathered li2 with a Bw horizon (Brunic Arenosol)	Well-drained acid soils on li2 with an E and a cambic or spodic B (Brunic Arenosol, Podzols)	Shallow (4.1) or deep (4.2) soils having a loamy to clayey B wit pseudo-gley within 30 cm and a texture transition within 50 cm (Stagnosols)	Poorly drained soils with peaty surface layers and/or Histosols		
(B) Sandstone Cuesta	Convex to straight slopes in li2, well-drained shallow stony colluvial cover (Arenosols)	Stepped slopes of varying slope angle in li2 with stony and loamy sandy soils, local colluvial cover (Leptosols, Arenosols)	Slope segments with sandy colluvial deposits of sandstone scree, overlying marls, with intermediate to deep well-drained humus-rich sandy soils (Arenosols)	Strongly dissected slopes, varying thickness of overlying colluvial cover (complex of Leptosols and Arenosols)	Steep, straight and concave foot slopes, predominantly in marl, shallow, well-drained loamy to clayey soils (Regosols)	Irregular landslide topography with cover of large sandstone blocks, characteristic wet areas	Similar to B6, (initial podsolization)
(C) Landscape underlain by marls	Faint ridges with duplex soils or silty upper soil (Planosol, Stagnosol, Luvisol, A-B-C profiles)	Low-angle to medium steep, well-drained straight and concave slopes underlain by marls with or without a shallow colluvial cover (Regosols, A-C profiles)	Faint ridges or straight slopes underlain by marls intercalated with conglomerates, shallow loamy to clayey soils, varying in moisture conditions (Regosol)	Steep fluvial valley slopes, often underlain by conglomerate and sandstone layers. Well-drained clayey to loamy, often gravel-rich stony soils (Regosols)	Faint ridges underlain by Psilonotenschichten (Regosols, Cambisols)	Deep, V-shaped incision underlain by marl (Regosols)	
(D) Dolomite landscape	Horizontal or low angle upper levels underlain by alternating dolomite/marl. Shallow, stony. Loamy to clayey or sandy, well-drained soils (Leptosols and Regosols)	Horizontal or low-angle upper levels of low-angles upper slopes with high silt containing horizons at or close to the surface. Clayey to loamy or sandy, moderately-drained soils (Regosols)	Intermediate steep, instable slopes with intercalated marl layers. Medium to well-drained shallow, loamy to clayey or sandy soils (Regosols)	Intermediate steep stable slopes with intercalated marl layers. Medium to well-drained shallow, loamy to clayey or sandy soils (Luvisols)	Steep upper valley slopes with shallow soils. Stony, well-drained soils (Regosols, Leptosols)	Similar to D4, with mass movement	Deeply incised, steep V-shaped valley slopes

(continued)

Table 11.1 (continued)

(E) Fluvial landscape	1	Older terraces, deeply weathered soils, distinct Bt horizon. Gravel-rich silty topsoil on clay-rich substrate (C-material >1 m deep), moderately drained (complete Luvisols/Alisols) (A + E + Bt > 1 m) (E1.1)	2	Older terraces, partly truncated weathered soils. Gravel-rich silty topsoil on clayey substrate (C material). Truncated soil profiles without an E and/or (eroded) Bt. Moderate to well-drained (Regosols, Luvisols, Alisols)	3	Recent, loamy alluvial soils. Deeply drained soils, with loamy topsoil and local clayey substrate (Fluvisols, Regosols)	4	Recent, coarse-grained, well-drained sandy to loamy alluvial soils Occasional sedimentary lime-containing layered soils (Arenosols, Fluvisols)	5	Recent, loamy alluvial and/or recent colluvial alluvial and/or colluvial valley floor. This cover of recent alluvial material overlying poorly drained marls (Gleysol, Regosol)	6	7	Older terrace, on Sandstone Plateau
(F) Aeolian landscape		Löss (at least 50 cm thick). Silty grey to brown, well-drained soils (Luvisols)											
(G) Colluvial landscape		Colluvial valley bottom and soils >0.5 m thick (Regosols)	Colluvial foot slopes, including alluvial fans. Deep, well-drained silty to sandy humic soils (Regosol, Cambisols, even Phaeozems), <1 m thick.	Colluvial foot slopes, including alluvial fans. Deep, well-drained silty to sandy humic soils (Luvisols, Gleysols near streams), >1 m thick	Faint ridges, wide divides or shallow valley floors with duplex soils, or with silty topsoil developed in colluvium (Planosol, Stagnosol, Luvisol) underlain by Steimmergelkeuper	Colluvium on slopes, >0.5 m thick							
(H) Other	Built-up area, infrastructure	Excavated, levelled terrain											

campaign is executed in step 6, during which several soil catenas are investigated using standard soil investigation equipment (IUSS 2015). A field form is used to determine additional geomorphometric and soil parameters, which are added to a point feature class, that contains all the point-based observational information. Physiotope field boundaries are updated during fieldwork with the use of a DEM (step 8) and its derivatives, such as a slope map and land use information (land use map, Fig. 11.2). If necessary, small mapping units are aggregated into major units to maintain readability of the final physiotope map. The input of steps 6 and 8 is

then processed and visualized in step 7, which results in the final physiotope map (Fig. 11.3) and related geodatabase (step 9). For example, the point observation data are linked to the polygon-based physiotope boundaries. The digital elevation model at 5 m resolution is used to verify homogeneity of physiotope classes, by adding zonal statistical information on e.g. slope angle variations to the physiotope geodatabase.

Applications, such as a hazard zonation assessment, a soil erosion vulnerability and forest community map (steps 10–12), are examples of deliverables derived from data analysis, originally stored in the physiotope map.

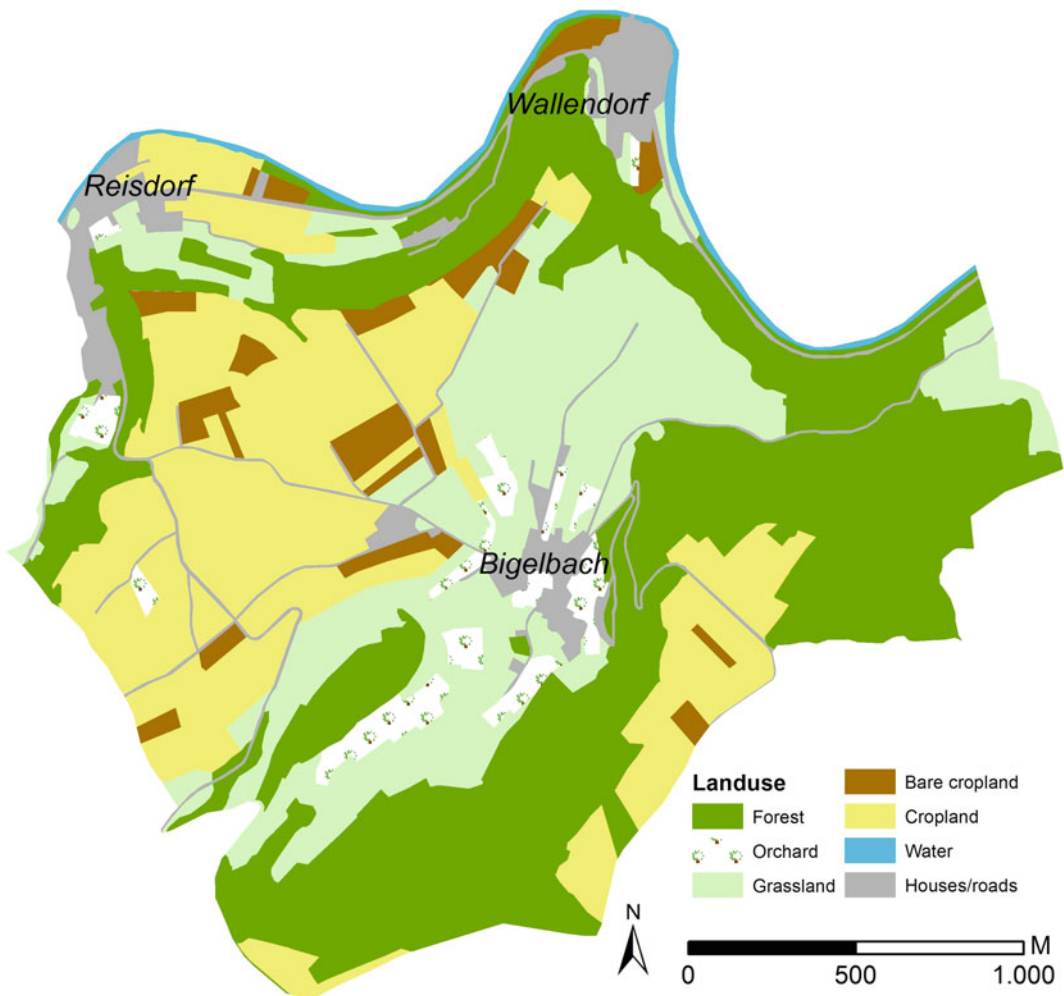


Fig. 11.2 Land use map

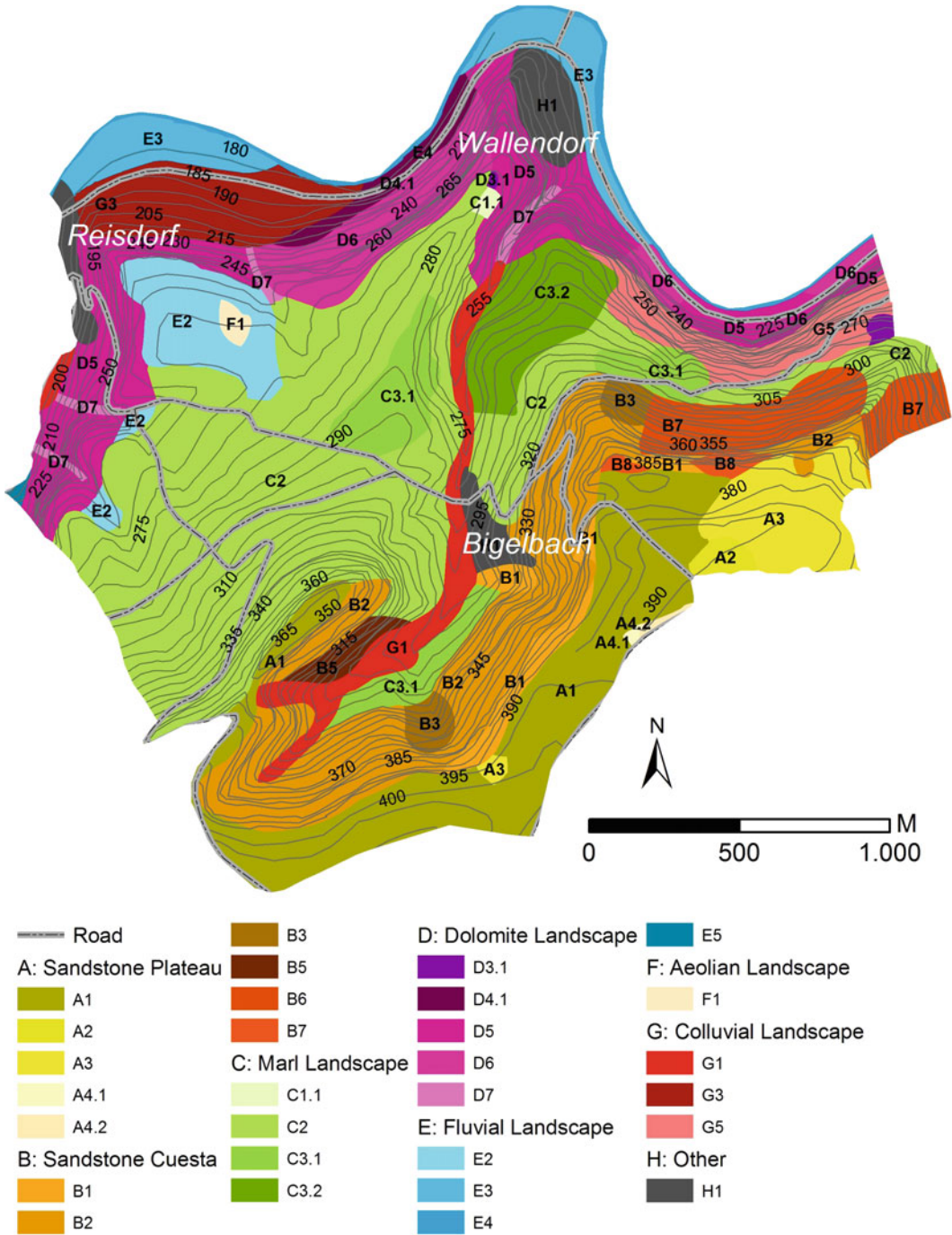


Fig. 11.3 Physiotope map in the surroundings of Bigelbach (after Koene 2012). The explanation and a summary of attribute information of the legend codes is provided in Table 11.1

11.2.2 Hazard Zonation Mapping

A natural hazard zonation map shows the spatial distribution of all hazards in an area, divided into different types of hazards, such as flooding, erosion and mass movements, and their potential impact. Procedures to produce hazard maps are described by e.g. Guzzetti et al. (2012). These techniques can be divided into inventory, heuristic, statistical and deterministic approaches (Soeters and van Westen 1996). Here we follow a combination of an inventory and heuristic approach using a weighted overlay approach. The physiotope map contains information on the spatial distribution of geomorphological processes as well as soil depth. In the heuristic approach, qualitative map combinations are made, in which expert knowledge is used to assign individual weights to a series of parameter maps that can be grouped into hazard classes.

The physiotope map (Fig. 11.2) holds attribute information on material and activity, and is supplemented with land surface parameters calculated from a 5 m resolution DEM. In this example, the physiotope units have been used in a weighted overlay to reclassify the area into zones that are equally endangered by the occurrence of natural hazards. In a weighted overlay procedure, raster maps are weighted and ranked according to their relative importance, which results in a categorization from very low hazard to very high hazard probability. The procedure works well in areas with relative fine-scale, expert-derived spatial information, in combination with quantitative Land Surface Parameters derived from a digital elevation model and field information.

First, from the 5 m DEM, a slope angle map was calculated and reclassified into 7 slope angle classes. Each class has been given a relative importance value (in brackets): $<2^\circ$ (1), 2° – 5° (2), 5° – 10° (3), 10° – 20° (4), 20° – 30° (5), 30° – 40° (6), $>40^\circ$ (7). The physiotope map was reclassified into forest (1) and non-forested area (7). The process attributes of the geomorphological map were weighted as follows: weathering (1), flow (2), erosion (3), fall (4), slide (5) and flooding (6). The geomorphological

processes were weighted 50%, the slopes angle classes 30%, and the forest map 20%. The weighting and rating system is thus based on the relative importance of various causative factors derived from field knowledge and depends on characteristics of the study area. The resulting outcome is then scaled into 5 classes: very low, low, moderate and high and very high hazard classes. This procedure was done using spatial analyst tools available in ArcGIS10.2(ESRI@).

11.2.3 Forest Community Mapping

Forest community maps subdivide the present forest land cover in homogeneous forests, according to their dominating type of plant community, which has, in general terms, clear correlations with the abiotic habitat factors (see Chap. 8). The physiotope map provides the abiotic basis for mapping forest communities. For forest community mapping, additional information is necessary on forest boundaries and forest composition. The present forest boundaries are dictated by two important factors: slope angle and land-use and land cover practice. Most forest boundaries are the same as in 1777 (Ferraris LeComte 1777). The recent forest boundaries, or changes in forest type, such as planted pine trees, have been mapped by a combination of image classification (Google Earth imagery) and topographic map interpretation (1:20.000 scale topographical maps), in combination with field checks, which offers a thorough basis for the forest community maps. The point observation data provided sufficient supplementary data to classify the forest cover into forest communities, in accordance to Niemeyer et al. (2010), van der Werf (1991) and Kooijman and Smit (Chap. 8).

At each site, plant species presence and abundance was counted in a standard grid of $10\text{ m} \times 10\text{ m}$, so that statistical analysis between vegetation and the abiotic parameters assigned to the physiotope map could be made. A first clustering based on species presence was made using TWINSpan (Hill 1979). A series of additional attributes was distinguished and assigned to forest communities. For this, tree

cover, shrub cover, herb cover, moss cover, litter cover, bare soil cover, thickness of the ectorganic layer, the F, H and Ah/Ap horizons, humus type (mor, moder, mull) and rooting depth were estimated at each point observation site. Borders between forest communities have been checked in the field.

11.2.4 Soil Erosion Mapping

Physiotope maps hold information on soil texture, organic matter content, structure and permeability. Together with additional rainfall and land use information, an erosion assessment was made. The Revised Universal Soil Loss Equation (RUSLE: Wischmeier and Smith 1978, and Renard 1997) was applied to calculate annual soil loss, according to:

$$A = R * K * LS * C * P \quad (11.1)$$

where A = annual soil loss in tons $\text{ha}^{-1} \text{year}^{-1}$, R = rainfall-runoff erosivity in $\text{MJ mm ha}^{-1} \text{h}^{-1} \text{year}^{-1}$, K = erosion sensitivity factor based on texture and organic matter (Renard et al. 1997; Panagos et al. 2014), LS = Slope length factor (unitless), C = crop factor (based on Morgan 2005) and P = supporting practice, which was in this case set constant to 1.

For each input parameter, a map was constructed showing the spatial distribution of the variables. Processing was done with an ArcMap toolbox, which used 10 m cell size raster maps as input.

Rainfall erosivity data are derived from Panagos et al (2014) for Luxembourg at $645 \text{ MJ mm ha}^{-1} \text{h}^{-1} \text{year}^{-1}$. The K-factor was determined for each of the physiotope units, by using data taken from Cammeraat et al. (2009), van den Broek (1989) and Van Zon (1980), the slope factor LS was calculated from a 10 m DEM, which was originally digitized from the topographical maps 1:5.000, while C values are taken from literature (Morgan 2005). Since the K factor also depend on organic content of the soils and the C factor is based on land use, a detailed land use map was prepared by using the

1:20.000 topographical map, Google Earth air photo information, and field checks. The land use map (Fig. 11.2) and physiotope map (Fig. 11.3) and were intersected in ArcMap, and the newly resulting units were assigned the appropriate K and C -values in the attribute (Table 11.2). The toolbox then combined the maps into calculated soil loss.

11.3 Results

11.3.1 The Physiotope Map

The physiotope map (Fig. 11.3) presents the spatial distribution of physiotopes around the village of Bigelbaach. The uppermost zone at approximately 400 m altitude is the Sandstone Plateau (A-units), which is here dominated by physiotopes A1 and A2, respectively shallow and deep well-drained soils developed in loamy to sandy weathered Luxembourg Sandstone Formation (li2), and characterized by Brunic Arenosols. Locally, loamy weathering residues of former river deposits are present, which have been indicated as A4. In other places, well-drained sandy soils have developed on the li2 with a B horizon with brunic or spodic qualities, classified as either brunic Arenosol or Podzol and are indicated as A3.

The Sandstone Cuesta (B-units) is, in its upper part, dominated by convex to straight slopes developed in li2 mostly with well-drained Arenosols in a stone-rich colluvial cover. In places, landslides have caused major slope instability, causing fast alternating fine-scale patterns of irregular topography, with wet areas (unit B6) and initial soil forming processes. The green colors are indicative for marl underlain landscapes, mostly developed on low ridges (C1) on which Planosols or Stagnosols may have developed under forest (not present in the area depicted by Fig. 11.3). On low angle or medium steep slopes (C2/3-units), mostly under agriculture, Regosols are commonly developed. The transition towards the dolomite underlain landscape (D-units) shows a transition in physiotopes characterized by steep slopes and alternations of

Table 11.2 Metadata of parameters used for the RUSLE model

RUSLE factor	Unit	Arable	Grass	Forest	Average Luxemb.
R	MJ mm ha ⁻¹ h ⁻¹ year ⁻¹	674.5	674.5	674.5	674.5
C	(-)	0.25–0.38 (0.215)*	0.162 (0.091)*	0.001 (0.0011)*	–
K	Mg h ha ha ⁻¹ MJ ⁻¹	0.012–0.073	0.009–0.058	0.006–0.031	(0.0392)*

In (*) the national average values as given by Panagos et al. (2015a, b)

marl layers, in general with well-drained clayey to sandy Leptosols and Regosols.

The fluvial landscape (E-units) include depositional fluvial landforms which can be separated into older terraces, such as the E2 unit of the Eebierg (see also Chap. 5) on which Regosols, Stagnosols, Luvisols and Alisols occur in gravel-rich silty topsoil on a clayey substrate, and younger fluvial deposits, mainly younger recent alluvium, on which clayey to loamy alluvial soils have developed (Fluvisols, Arenosols and Regosols).

Local remnants of loess are present on the old terrace of Eebierg (unit F), while the colluvial landscape (G-units) predominate in the smaller tributary valleys such as those of the Bigelbach stream (G1), indicating that deposition of colluvial material from surrounding slopes has been relatively important, and could not be transported by the fluvial system. The soils are mostly well-drained silty to sandy-loamy humic soils (Regosols).

11.3.2 The Natural Hazard Map

The natural hazard map is shown in Fig. 11.4. Very high hazards do not occur in this area, but high hazard activity may occur along the steep cuesta and valley slopes. Especially the area of the Hansche Schlaff with steep slopes and high mass movement (see Chap. 5 for detailed geomorphological descriptions) stands out as a hot-spot of high hazard. Along the valley slopes of the Sauer River distinct zones of high hazard (flooding) occur. The relatively steep slide area of the Schaedbiert is depicted as a local high risk area as well. Most of the area however, has been

classified as very low to low and moderate hazard, mainly reflecting a combination of low-angle slopes and flow-type processes on agricultural land. Although the resulting hazard map does reflect a choice on relative weighting and ranking of the input parameters, boundaries are not likely to change a lot when applying different settings.

11.3.3 The Forest Community Map

Seven forest typologies have been mapped in the area around Bigelbach (Fig. 11.5). In broad terms, the forest types follow the major subdivisions of the physiotope, and the zones of relative steep slopes, although some deviations occur. The physiotope on the Luxembourg sandstone plateau are dominated by Fago-Quercetum forests and fragments of former production forests (Leucobryo-Pinetum; van de Werf 1991). The N to NE facing slopes of the sandstone cuesta are covered by Luzulo-Fagetum forests in the upper parts, and Galio odorati-Fagetum in the lower parts (Niemeyer et al. 2010). The larger part of the marl underlain landscape is here non-forested, due to the low angle slopes on which farm and cropland is present. The physiotope developed in the dolomite underlain landscape (D-units) are dominated by the Carici-Fagetum (steeper slopes) and the Hordelymo-Fagetum forests, as well as local patches of planted pine and spruce. The correspondence between physiotope and forest communities in this area is so good, because especially the deciduous forests are relative undisturbed. After selective thinning of the forest every approximately 30 years, natural succession takes over without further management. This

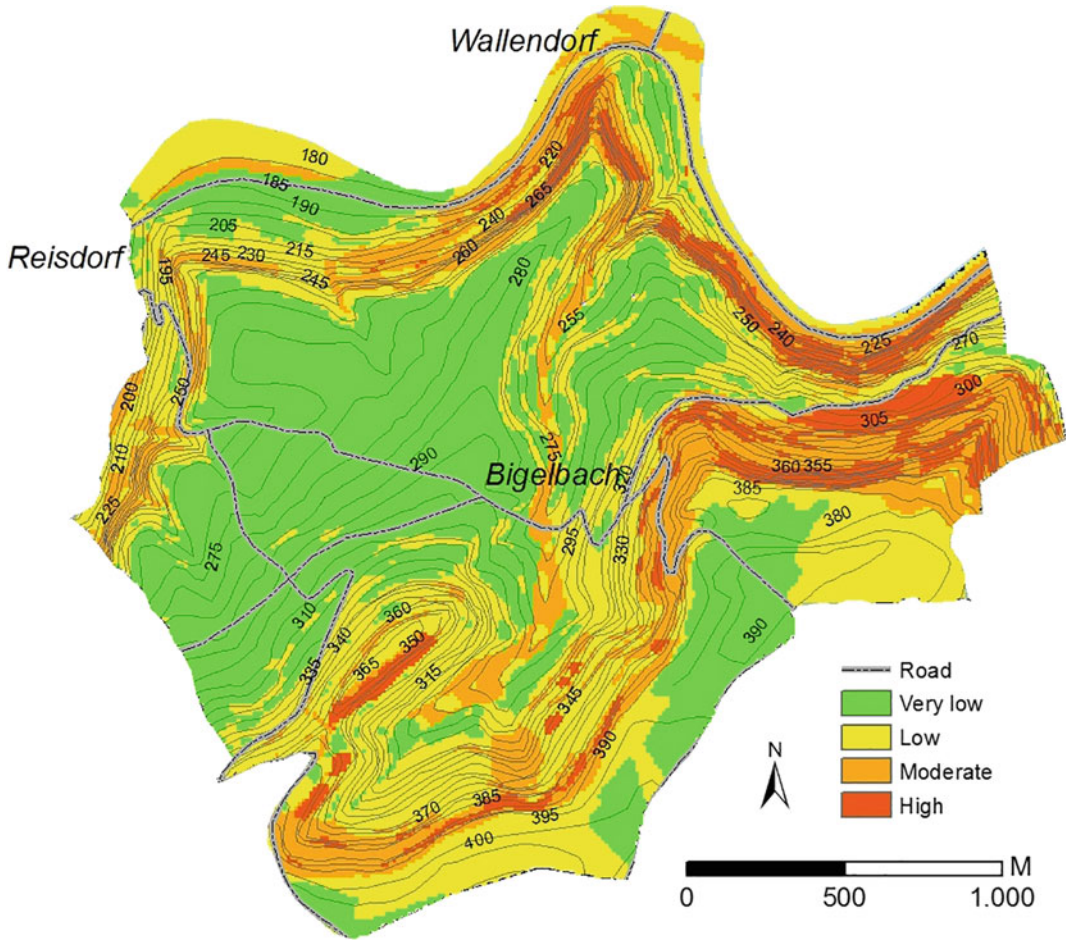


Fig. 11.4 Hazard map of the Bigelbach area, after field data provided by Brock (2012)

promotes the development of vegetation communities that are strongly related to the physical and chemical properties of the soils (physiotopes) of the forested areas.

11.3.4 The Soil Erosion Vulnerability Map

The soil erosion vulnerability map as shown in Fig. 11.6 has been classified into six units from very low to extreme erosion vulnerability. It basically shows that most of the studied area has a (very) low erosion vulnerability. The dark green areas on the map are mainly forests on the steep cuesta front and the deep river incision of

the Sauer river, and forests protect the soil relatively well. For the arable soils, vulnerability levels are much higher, especially on sloping areas. The meadow areas show mostly low to moderate vulnerabilities. It is not possible to give actual soil erosion values, as the model is not validated, but the actual erosion levels can more or less be deduced from literature. Under agricultural practice on Keuper substratum, the water erosion rates on a catchment scale are in the order of $1.5\text{--}2.5\text{ ton ha}^{-1}\text{ year}^{-1}$ (e.g. Imeson and Vis 1984; Van Hooff and Jungerius 1984). This is in accord with recent modelling work of Panagos et al. (2015c) for the whole of Europe with a spatial resolution of $500\text{ m} \times 500\text{ m}$, who showed an average rate of $2.07\text{ ton ha}^{-1}\text{ year}^{-1}$

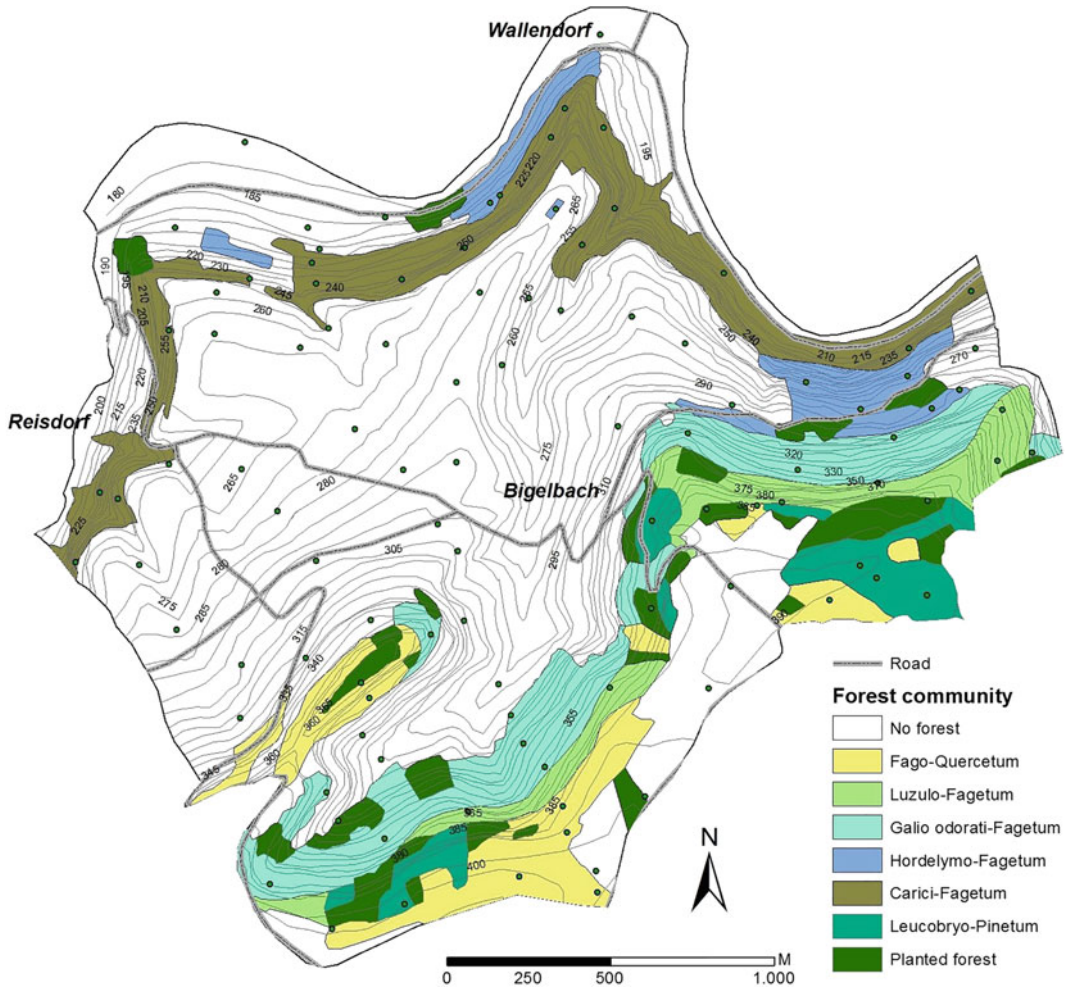


Fig. 11.5 Forest community map in the surroundings of Bigelbach (after field data by Oosterhuis 2012)

for the whole of Luxembourg, and a mean of $4.54 \text{ ton ha}^{-1} \text{ year}^{-1}$ for arable fields and even higher values ($6.19 \text{ ton ha}^{-1} \text{ year}^{-1}$) in Luxembourg for areas which are managed without ‘good environmental condition practices’. For forest, values are generally lower, but also depend on the substratum. For Luxembourg Sandstone hillslopes on the cuesta front Van Zon (1980) measured soil loss of $0.010 \text{ ton ha}^{-1} \text{ year}^{-1}$, but this was much higher for the Keuper substratum, where values ranged between 0.30 and $0.77 \text{ ton ha}^{-1} \text{ year}^{-1}$ (Imeson and Vis 1984; Duijsings 1987 respectively).

At a finer scale, erosion rates can be much higher or lower than at a $500 \text{ m} \times 500 \text{ m}$ or a catchment scale. The combination of GIS and high resolution DEMs and land use information, as shown here, makes it possible to give estimates of erosion at much finer scales, e.g., to pinpoint erosion hotspots, where the chance is high that rill or gully erosion might occur (see red areas on Fig. 11.6). The prediction of erosion hotspots can be further improved by also including high spatial resolution data of organic matter in the RUSLE models, as organic matter is one of the important factors determining erodibility (K-factor; see f.i.

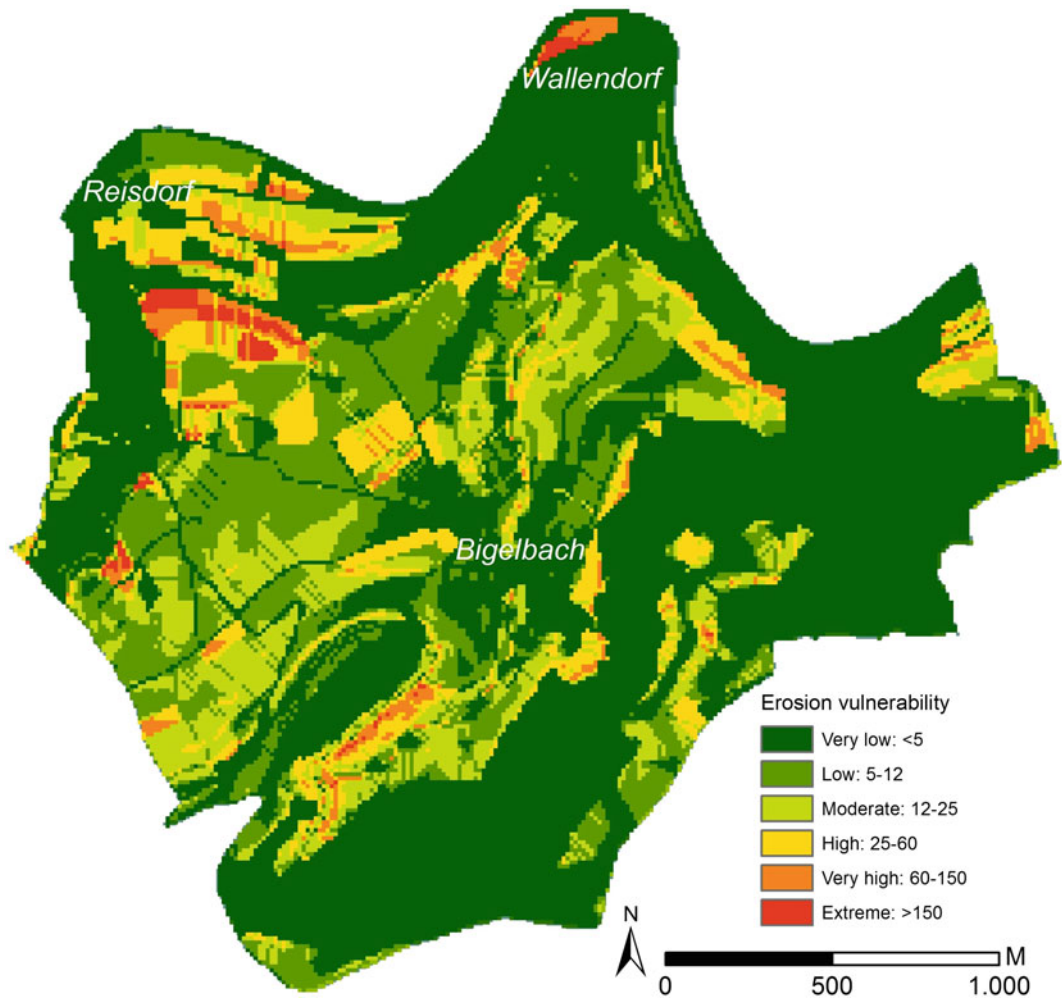


Fig. 11.6 Modelled RUSLE-based erosion vulnerability classes

Panagos et al. 2014). Recent work shows that air-borne spectrometry can be successfully used to predict organic matter in bare soils, which was also tested in Luxembourg (Denis et al. 2014). The combination of high resolution physiotope maps derived from fieldwork, remote sensing data on land use and organic matter, high resolution DEMs derived from LIDAR data and high resolution GIS based modelling is an important and rapidly expanding field that can contribute to predict erosion hotspots. This can help to design improved management practices or to implement mitigation measures at exactly at the location where it is needed.

11.4 Conclusions and Outlook

We presented a workflow for digital physiotope mapping, based on integration of multiple data sources and together forming spatially explicit functional landscape units. These landscape units are characterized by a set of key abiotic parameters from geology, soil, geomorphology and topography, which can be extended according to need, data availability and fieldwork effort. The Bigelbach area has currently no very high hazards. However, if land management changes, deforestation on currently moderate and high

hazard areas may increase the hazard class to very high hazard. The selection and the weighing and ranking thresholds remain the full choice of the earth scientist and is closely related to the landscape type, in this case the Luxembourg cuesta. Therefore, attention should be given when applying the workflow to other environments.

We further conclude that, on a fine-scale, physiotope mapping is a powerful means to represent integrated qualities of the cuesta landscape. The physiotope map is not only a solid basis for generating natural hazards and erosion maps with little additional information, but may better explain the distribution of forest community maps in the light of geological substratum, geomorphological development and soil quality potential.

The physiotope has grown from an initial, hand-drawn interpretation of a landscape unit to a digital GIS-based landscape unit, that contains a wide variety of abiotic information layers and measurements, which can be used in a wide variety of applications upon the end-user's request. The data processing workflow is mainly based on GIS-based procedures and can therefore be automated, in order to monitor changes in the status of physiotope boundaries and its content. In this way, conservation measures can be supported or validated, or the effect of disturbances in a landscape studied. The popularity and availability of high detailed LiDAR-based elevation data will further improve the physiotope mapping, not only promoting more accurate delineation of mapping units, but also offering more statistical insight in fine scale variations of the landscape. For example, the mean or standard deviation in slope angle for a certain physiotope unit of a 1 m slope angle map can easily be calculated using zonal statistics and may add to discriminate physiotopes and their properties on finer scales. The integrated character of physiotopes enables also new possibilities to study the impact of climate change and land use change, especially with regard to agriculture, and to predict hazard zones with regard to slope stability and soil degradation. High resolution multi- or hyper-spectral orthophoto imagery may reveal

better spatial information of soil chemical properties such as mineral content. Through remote sensing imagery and automated workflows, upscaling of fine-scale information to larger areas will become common practice.

Combining the physiotope maps with high resolution DEM's, and remote sensing data on land use and organic matter contents opens up a field where soil erosion hazards can be pinpointed to the real problem areas. This has important implications for land use management and mitigation of soil erosion.

Acknowledgements We thank Henk Jan Oosterhuis, Olaf Brock and Erik Koene for their important fieldwork data and maps near Bigelbach. The GIS-studio (www.GIS-studio.nl) of IBED is thanked for computational and software support. The work builds on decades of mapping in the region by students of the University of Amsterdam.

References

- Brock O (2012) Geomorfologische analyse van Bigelbach, Luxemburg. Unpublished student report, University of Amsterdam
- Cammeraat LH, Kooijman AM, Seijmonsbergen AC (2009) Syllabus Luxemburg. Veldpraktikum Luxemburg, Opleiding Aardwetenschappen-Fysische Geografie, Universiteit van Amsterdam
- Carte Géologique 1:25.000, Diekirch. <http://map.geoportail.lu>. Accessed 11 Nov 2015
- Denis A, Stevens A, van Wesemael B, Udelhoven T, Tychon B (2014) Soil organic carbon assessment by field and airborne spectrometry in bare croplands: accounting for soil surface roughness. *Geoderma* 226–227:94–102. doi:10.1016/j.geoderma.2014.02.015
- Duijsings JJHM (1987) A sediment budget for a forested catchment in Luxembourg and its implications for channel development. *Earth Surf Proc Land* 12:173–184
- Ferraris LeComte (1777, reissued in 1965–1970) Carte de Cabinet des Pays-Bas Autrichens. *Bibl Royale de Belgique, Bruxelles*
- Gray M (2004) *Geodiversity: valuing and conserving abiotic nature*. Wiley, Chichester
- Guzzetti F, Mondini AC, Cardinali M, Fiorucci F, Santangelo M, Chang K-T (2012) Landslide inventory maps: new tools for an old problem. *Earth Sci Rev* 112:42–66. doi:10.1016/j.earscirev.2012.02.001
- Hengl T, Reuter HI (eds) (2008) *Geomorphometry: concepts, software, applications*. *Developments in Soil Science*, vol 33. Elsevier
- Hill MO (1979) TWINSPLAN A FORTRAN program for arranging multivariate data in an ordered two-way

- table by classification of the individuals and attributes. Cornell University, Ithaca, New York
- Imeson AC, Vis M (1984) The output of sediments and solutes from forested and cultivated clayey drainage basins in Luxembourg. *Earth Surf Proc* 9:585–594
- IUSS Working Group WRB (2015) World Reference base for soil resources. *World Soil Resources Reports* 106. FAO, Rome
- Klijn F, Udo De Haes HA (1994) A hierarchical approach to ecosystems and its implications for ecological land classification. *Landscape Ecol* 9:89–104
- Koene E (2012) Veldrapportage Bigelbach—Fysiotopenverslag. Unpublished student report. University of Amsterdam, 47 p
- Morgan RPC (2005) *Soil erosion and conservation*, 3rd edn. Blackwell, Malden
- Niemeyer T, Ries C, Härdtle W (2010) Die Waldgesellschaften Luxemburgs: Vegetation, Standort, Vorkommen und Gefährdung. *Ferrantia* 57. Musée national d'histoire naturelle, Luxembourg
- Oosterhuis HJ (2012) Onderzoek naar vegetatie en standplaatsfactoren in Bigelbach, Luxemburg. Unpublished student report, University of Amsterdam, 29 p
- Panagos P, Meusburger K, Ballabio C, Borrelli P, Alewell C (2014) Soil erodibility in Europe: a high-resolution dataset based on LUCAS. *Sci Total Environ* 479&480:189–200. doi:[10.1016/j.scitotenv.2014.02.010](https://doi.org/10.1016/j.scitotenv.2014.02.010)
- Panagos P, Borrelli P, Meusburger K, Alewell C, Lugato E, Montanarella L (2015a) Estimating the soil erosion cover-management factor at the European scale. *Land Use Policy* 48:38–50. doi:[10.1016/j.landusepol.2015.05.021](https://doi.org/10.1016/j.landusepol.2015.05.021)
- Panagos P, Ballabio C, Borrelli P, Meusburger K, Klik A, Rousseva S, Percec-Tadic M, Michaelides S, Hrabalíková M, Olsen P, Aalto J, Lakatos Mn, Rymaszewicz A, Dumitrescu A, Beguería S, Alewell C (2015b) Rainfall erosivity in Europe. *Sci Total Environ* 511:801–814. doi:[10.1016/j.scitotenv.2015.01.008](https://doi.org/10.1016/j.scitotenv.2015.01.008)
- Panagos P, Borrelli P, Poesen J, Ballabio C, Lugato E, Meusburger K, Montanarella L, Alewell C (2015c) The new assessment of soil loss by water erosion in Europe. *Environ Sci Policy* 54:438–447. doi:[10.1016/j.envsci.2015.08.012](https://doi.org/10.1016/j.envsci.2015.08.012)
- Parks KE, Mulligan M (2010) On the relationship between a resource based measure of geodiversity and broad scale biodiversity patterns. *Biodivers Conserv* 19(9):2751–2766
- Peano A, Casatella C (2011) Landscape assessment and monitoring. In: Cassatella C, Peano A (eds) *Landscape indicators—assessing and monitoring landscape quality*, Springer, pp 1–14
- Renard KG, Foster GR, Weessies GA, McCool DK (1997) Predicting soil erosion by water: a guide to conservation planning with the Revised Universal Soil Loss Equation (RUSLE). In: Yoder DC (ed) *Agriculture handbook* 703, U.S. Department of Agriculture
- Soeters R, Westen CJV (1996) Slope instability recognition, analysis, and zonation. In: Turner AK, Schuster RL (eds) *Landslides—investigation and mitigation*. Special report 247. Transportation research Board, National Research Council, Washington, U.S. pp 129–177
- van den Broek TMW (1989) Clay dispersion and paedogenesis of soils with an abrupt contrast in texture. Unpublished Ph.D. thesis, University of Amsterdam, Amsterdam
- van Hooff P, Jungerius PD (1984) Sediment source and storage in small watersheds on the Keuper marls in Luxembourg. *Catena* 11:133–144
- Van der Werf S (1991) *Bosgemeenschappen; Natuurbeheer in Nederland*, deel 5. PUDOC Wageningen
- Van Zon H (1980) The transport of leaves and sediment over a forest floor. *Catena* 7:97–110
- Wischmeier WH, Smith DD (1978) *Predicting rainfall erosion losses—a guide to conservation planning*. Agriculture Handbook No. 537, Washington, US Department of Agriculture Science and Education Administration

Annemieke Smit, Luuk Dorren, Hans van Noord,
Josja Veraart, Casper Cusell and Henk Pieter Sterk

Abstract

For 25 years, Physical Geography students of the University of Amsterdam have experienced a 6-week field training in the cuesta landscape in Luxembourg around Diekirch. They studied the geology of the Gutland and surrounding areas, such as Ardennes and Eiffel. They mapped geomorphological patterns, studied soil development and looked at relationships between forest vegetation and the landscape in their particular area of approximately five square km, with many steep slopes. They also learned to overcome the physical and social challenges of such a fieldwork. A number of former students of different generations will give their opinion on what they learned and how this period in life helped them shape their current and future careers.

12.1 1988: The Quest for the Cuesta by Hans van Noord

The Luxemburg fieldwork marked an important shift for the study program in the mid-eighties. It envisaged bringing together the key disciplines

of the Institute in an integrated manner and replaced the pure geomorphological fieldwork in Austria. For some, this meant disappointment as they thought that the Luxemburg landscape was utterly boring compared to the Alps. My experience though was very positive. We were the

A. Smit (✉)
Alterra-Wageningen UR, Wageningen
The Netherlands
e-mail: annemieke.smit@wur.nl

L. Dorren
Berne University for Applied Sciences,
Bern, Switzerland
e-mail: luuk.dorren@bfh.ch

H. van Noord
VAN NOORD GeoConsult Environmental
Consulting, Heteren, The Netherlands
e-mail: info@noordgeoconsult.nl

J. Veraart
Natuur en Milieufederatie Utrecht, Utrecht
The Netherlands
e-mail: j.veraart@nmu.nl

C. Cusell
Witteveen+Bos, Deventer, The Netherlands
e-mail: c.cusell@witteveenbos.nl

H.P. Sterk
University of Amsterdam, Amsterdam
The Netherlands
e-mail: henk.sterk@student.uva.nl

second group that were let loose “in quest of the Cuesta” in 1988 and benefited from the guinea pig experience of the first batch. It turned out to be a milestone in our studies and helped shape our appreciation, or lack of it, of what physical geography is all about.

As an enthusiastic rock climber, I was familiar with Luxemburg, as I had visited the cliffs of Berdorf before, and was thrilled to stay for a longer period so close to a climbing spot. Several evenings and in the weekends, I cycled to Berdorf to make good use of the opportunity the Luxembourg sandstone offered. Our field work period was a bit different, as it had been decided to produce a short movie as promotional material for aspiring students Physical Geography. Initial scenes were shot in the lab, but the core of the film, named “De Wereldwachter”, was filmed on location in Luxemburg. I played one of the characters in the film and spent some days with the crew, acting typical field work activities. It was just a lot of fun to do! Just as the whole field work. I remember having a marvelous time that convinced me that I had definitely made the right study selection. Besides the mapping and field experience, it was the social dimension that made it so much fun. Being forced to work and live together in our small dwellings with a group of diverse characters proved to be a profound learning experience. Besides the obligatory work, I remember most the amount of fun we had and the many party evenings “up the hill” in a hilarious discotheque, that became a favourite hang-out.

Later I became “AIO” and was involved as staff member, responsible for the geology introduction and the geomorphology part of the field work. It brought me back a number of years to the fieldwork area and gave me the strange opportunity to visit all field work areas and help students with the basics of mapping and landscape interpretation. The initial goal of creating an integrated fieldwork has certainly been reached in my opinion and in my professional career, that brought me for extended periods to Indonesia, Nepal, Brazil and Bhutan, I have undoubtedly benefited from this holistic

landscape perspective we were exposed to initially in Luxemburg.

12.2 1990: A Social Experience in the Field by Annemieke Smit

I heard about Luxembourg even before I started studying Physical Geography. It seemed that all information about the curriculum, either presented by students or study coordinators, was about Luxembourg. I also watched the movie, starring some of the senior students including Hans van Noord. I, therefore, expected a lot of it and when I finally was in Luxembourg, I enjoyed those six weeks a lot. During the first two weeks, we focussed on geomorphology and we had to map geomorphological features. During those weeks, finding our way in ‘our area’ was already quite challenging and the moment we had to draw lines was confronting. It turned out that we sometimes had no clue where we were exactly or how we had to get somewhere. After a few days, our focus came to the geomorphology and it turned out that all those text book examples are not always easy to recognize in the field. The second part, about soil science, brought new challenges. We learned that soil classification in the field is different from the examples in the text book and describing soil profiles in the pouring rain is a muddy experience.

In 1990, the three parts (geomorphology, soil science and ecology) were unfortunately not integrated at all, they were even separated by a long weekend off. Later, when I was coming back as a Ph.D. student, coaching the new students in the field, geomorphology, soil science and landscape ecology were much more integrated. I think that focus was much more interesting. It led to a complete understanding of the area, something I didn’t understand during the 1990 field trip. I’m glad that I had the opportunity to visit Luxembourg several times. To be there as a student and later also as a teacher, gave me more insight in how the landscape was formed, how the separate courses came together. For me, Luxemburg is the fundamental under my

Fig. 12.1 Impression of the living room during the student fieldwork of 1990, after a lengthy rainy period



ability to think in a landscape system and to integrate knowledge from all aspects.

The fieldtrip was also a social experiment. During the 1990 field trip, we spent 6 weeks in very small and noisy holiday cabins. It felt like we were sleeping in closets and actually heard everything from each other. During the soil science weeks we had a lot of rain, which added a serious amount of wet clothes dripping in our ‘living room’, leaving even less space for ourselves (Fig. 12.1). Daytime work in a small group, not only on sunny days, but also in the rain, not only when everyone was happy, but also when tension in the group grew, it all contributed to a lifetime experience. And despite all these hardships we survived with a lot of humour. It taught me how to deal with these situations and I use those lessons in my current work. As a project leader and process facilitator I have to motivate people, make them feel useful to the project and sometimes I have to resolve conflicts within the (project) teams.

12.3 1994: Drawing the Line on a Map by Luuk Dorren

It was sunny, but the wind was freezing cold in subarea 2, during ‘fieldwork Luxembourg’ in the spring of 1994. After a short search on Google Earth, I note that it must have been north of

Beaufort, where our ‘base camp’ was situated, somewhere on the line between Bigelbach and Eppeldorf. Too optimistic, of course, I was dressed in a thin, yellow PVC raincoat. A nice and dry Gore-Tex jacket with a warm fleece vest did not fit in the student budget anyway. The goal of the first two weeks of this fieldwork was to complete a geomorphological map, which would show where and which materials occur in the landscape and how the different forms in the landscape have been created. Google Earth was far from its existence and aerial photographs were almost exclusively viewed through a stereoscope. Geographic information systems were still considered as scary things, and therefore not very widespread. All we had in the field was a black and white copy of a contour map, scale 1:10,000, which also contained some information on the wooded areas, as well as on the location of the main roads and villages. In addition, next we had a set of stereographic aerial photographs and a field stereoscope. Therefore, the challenge of the first days in the field was trying to figure out where we were on our map. Along the asphalt roads this was no problem (Fig. 12.2), but somewhere in the middle of a corn field or on a wooded slope, it was difficult.

Then came the hard part. Capturing the first lines on the map. For example, where you draw the line on the map indicating the boundary between

Fig. 12.2 Students trying to find their way during the fieldwork of 1994



the steep and a flatter part of a grassy slope. Identifying the top of a cliff is a lot easier. The first step was to recognize a virtual line in the field and then this line had to be drawn on the map in its correct position. In addition, the drawn map is a model of reality, for which the degree of detail is determined by the map scale. To produce a good readable map, it must constantly be decided what information will be recorded and what is left out. In other words, which line has to be put where on the map. It sounds weird, but if you do this for the first time, it takes courage to dare drawing the first line. In my current job I still put lines on a map, albeit for making hazard maps for roads and residential areas in the Alps, which then serve as input for quantitative risk assessments. Mapping is nowadays a lot easier due to the available detailed field maps produced with digital topographic models from laser scanning data and high-resolution aerial photographs. The digital mapping and global positioning possibilities have nothing to do with our exercise in Luxembourg. However, despite all these technological advances, any sophisticated analysis that is based on maps, which we perform today, starts with simple lines on a map that someone drew somewhere, hopefully based on some observations of the real situation. The basis

for doing such mapping work in a more or less correct manner, I have been given during fieldwork in Luxembourg.

12.4 1996: The ‘Echternach Procession’ and the Real Story of the Origin of the Chocolate Disaster by Josja Veraart

The ‘Echternach Procession’: 2 Steps Forwards, 1 Step Back

Spring 1996, many years ago, we went with a small car with ‘*only within the Netherlands assistance assurance*’ from Amsterdam to Luxembourg, near Echternach. The parents of Lokien were so kind to bring us all the way. We were very thankful, bringing a lot of luggage. The car passed the Belgian border and that was all it wanted to do. The Belgian hills were too much for this old vehicle. We went back to the Netherlands and waited for the ANWB, who solved the problem. Fortunately, we could still continue and only a bit later than planned we arrived at the park where we would stay during the fieldwork.

The region was divided into parts for each group. Our area was from up the hills, nearby our

Fig. 12.3 Soil description during the student fieldwork of 1996



cabin, until a little village, were we could get an ice cream at the campsite. We made a lot of quite dangerous downhill trips on our bikes overlooking the scenery. From up the hills, we could get a nice overview and this helped us a lot to understand the shapes and the way the landscape had been formed. It was great to oversee the area and trying to read it. Suddenly, all the book information came alive.

We climbed into gullies, made a lot of drillings by hand (Fig. 12.3), determined the plants and with the help of Professor Sevink discovered some stone hand axes of the Stone Age. In the evening, we went up the hill again to cook dinner and work on our results. Or rather: trying to decipher our handwriting in our soaked notebooks. This wasn't easy at all, since we soon noticed that what seemed quite obvious in the field, is very difficult to project on a two dimensional map. Are we really sure about what we wrote down? It might seem odd nowadays, but laptops weren't a common good, nor were digital cameras or don't even mention the mobile phones. So we could only rely on our own perception, memory and handwriting. We soon discovered, we weren't always agreeing with each other. Furthermore, our own uncertainty played a role. So the next day we had to go back

to the same location to check the results and try to describe it again. Later, during a fieldwork in Kenya, a biologist taught me, and I can still hear him telling me, that it is better to rely on the faintest pencil than on the best memory. Nowadays, I think, I should add a digital photo.

Charlie and the Chocolate Factory

After 4 weeks of rain, suddenly the sun appeared. We had become very capable of protecting all the things we carried inside our bags to the outside threat of rain. Now, we were facing the welcome warmth of the sun. Nothing could go wrong anymore... Until I opened my bag and screamed: Oh no, this is what you call a real chocolate disaster... The whole herbarium, a collection of 4 weeks of different plant species... was covered with a dark brown and sticky layer. Until today there are still people I meet in my professional work who remind me of this accident.

When I wrote this, I worked at Royal Haskoning, strategy and management consultants as a process- and knowledge manager. Although I am not doing any fieldwork comparable to 'Luxembourg', the things I learned during the Luxembourg period still help me in my daily work. First of all, the integral way of

approaching the system. In Luxembourg we both focused at the origin of the landscape, the soil, the vegetation, etc. When I started working as soil policy advisor, I was surprised that everything was split up into separate divisions: water, soil, air, etc. Specialists of the different areas didn't even know each other. A problem was most of the time tackled in a real sectoral way, just focusing at one medium instead of at the complete interactive system. The way we were taught to approach the system, helped me a lot during the start-up of the 'initiative of sustainable soil use' (Initiatief Bewust Bodemgebruik), where we started to increase the awareness of approaching the soil as one integral soil–water system and trying to combine and bring together specialists of different areas.

Also the analytical experience and the systematic way to start a research is very helpful. Not literally, but I still try to understand a 'landscape' (problem) and develop a long strategy vision by climbing up the highest peak and looking down (taking some distance). One of the essences of my work is to get an overview of the problem and develop a strategy, by trying to take some distance of the details.

But most of all, I learned not to stay behind my desk and trying to understand the world from the safe

environment of my office. I still prefer to go outside, look around and talk to the people in the field to experience and better understand the problem.

12.5 2002: Two Years of Theoretical Knowledge Came to Life During Five Weeks of Fieldwork by Casper Cusell

During the first two years of study, I tried to skip as many field trips as possible. I liked the theoretical part of the BSc 'Aardwetenschappen' a lot, but fieldwork was not my thing. This completely changed during the fieldwork in Luxembourg. During this course, theoretical knowledge about geology, geomorphology and soil science came alive (Fig. 12.4), and I even learned to recognize some plants. We not only saw several beautiful geological formations, soil profiles and vegetation types, but they also got connected to each other. This holistic approach, in which much attention was also paid to spatial differences and different time scales, is presumably the utmost important thing I learned during my study.

I agree with the other former students that the Luxembourg-fieldwork was not only interesting

Fig. 12.4 Examination of the humus profile during the student fieldwork of 2002



Fig. 12.5 Students on geology excursion in the Berdorf area during the fieldwork of 2012



due to its content, but it was also a nice social event. It was challenging to be isolated in small cottages in Beaufort for five weeks without family, girlfriend and ‘normal’ non-Aardwetenschappen friends. In combination with the physical challenges, e.g. long working days and cycling on those steep hills, this is an ideal mix for social tensions. However, eventually, I especially remember the fun and evenings with beer, and it was the start of some friendships.

Some years later (2009–2012), I was really happy to come back to Luxembourg. This time not as a student on a bike anymore, but as one of the teachers in a car. During these years, I assisted as a Ph.D. student in the ecology and soil science part of the fieldwork. Although I got more appreciation for plants in the meantime, since wetland plants became a crucial part of my Ph.D. study, I forgot all forest species. Fortunately, two days of private lessons from Annemieke Kooijman helped a lot, although I still picked some orchids in the first year. SORRY! I really liked those teaching weeks in Luxembourg, since you really get to know the students, and there was lots of time for individual questions. In addition to the teaching, Annemieke and I also used these weeks to study the Keuper-forests in more detail.

All those extra working hours in the weekend and evenings were inspiring and useful. To me, it is really a pity that I cannot assist this fieldwork anymore due to a new job. I am, however, sure that all experiences in Luxembourg (as a student and teacher) will be of help during my future work.

12.6 2012: Bringing Theory to Life by Henk Pieter Sterk

Everybody was excited for the fieldwork in Luxembourg, after weeks of planning and digitizing data, no one was feeling bad about going on a short ‘holiday’. This proved to be a misunderstanding: the fieldwork course given by our dearest professors at the UvA was all about working hard, from dawn till dusk. But everybody still thought of it to be a nice five weeks from home with your best friends from the Bachelor Earth Sciences and some new Future Planet Study students.

We all stayed at the camping-site Op der Sauer, in rather luxurious mobile homes and bungalows. The adventure started as soon as everybody arrived with his or her luggage, field gear, bikes and happy faces. The first few days

were all about excursions in Luxembourg, the Vosges in France and the Eiffel-region in Germany. This was the first time we were brought to places we only knew of in theory; beautiful sandstone deposits, anticlines, fossils in shale, rare plant species, caves in limestone, perilous quarry visits, olivine bombs in volcanic ash deposits, a fossilized coral reef and many other magnificent features that our surroundings had to offer (Fig. 12.5). Our bus driver was very kind and he was happy with some of the routes Kenneth Rijdsdijk tried to take; for instance going up a 3 m wide mountain road to our place in the middle of nowhere. Another trip that took longer than expected up the Grand Ballon resulted in questioning Kenneth's and Joris Haftka's ability to guide us somewhere. Furthermore, everybody's stamina was put to the test on the extended hike. But in the end, when we went crawling through an ancient mine, this was all forgotten and everybody had the time of their lives.

The fieldwork itself was all about drawing new lines on prepared and printed maps, figuring out soil-properties, and of course contemplating and raging on that one plant species that no one (except Annemieke Kooijman) could figure out. Another cool feature that we were able to play with, was the Trimble handheld: the portable

GIS-device that let us pinpoint the exact spot, or a few metres next to it, where we described the landscape, vegetation or soil. It is difficult to tell all of the stories and name all the people involved, but I would like to point out that I had a fantastic time in the field along with my group (Jouke, Marloes and Maarten). The most fun came out of finalizing the individual maps, where each of us had one specific topic. Helping each other out, and, with help of Casper Cusell and Boris Jansen, determining for instance the soil-type, brought a lot of enthusiasm in the group. Also debating with the fellow students on geomorphologic features; their origin and the processes involved on the spot, helped bringing the theory alive. To understand the whole of a diverse landscape such as the one we had to map around Diekirch, Bettendorf and Reisdorf helped understanding other concepts in the earth sciences: thinking beyond prehistoric times, the power of water and the influence of man.

The Luxembourg course has given me a lot of knowledge on how to plan, conduct and complete fieldwork. This knowhow comes in handy for the Master program Earth Sciences, where I hope to obtain my degree in at the University of Amsterdam before the end of 2015. Luxembourg along with the pleasant memories will stay dear to me for the years to come.